Mechanics of Viscoelastic Materials and Wave Dispersion

@Seismicisolation

Mechanics of Viscoelastic Materials and Wave Dispersion

Edited by
Yvon Chevalier
Jean Tuong Vinh

iSTE WILEY

@Seismicisolation

First published 2010 in Great Britain and the United States by ISTE Ltd and John Wiley & Sons, Inc.

Apart from any fair dealing for the purposes of research or private study, or criticism or review, as permitted under the Copyright, Designs and Patents Act 1988, this publication may only be reproduced, stored or transmitted, in any form or by any means, with the prior permission in writing of the publishers, or in the case of reprographic reproduction in accordance with the terms and licenses issued by the CLA. Enquiries concerning reproduction outside these terms should be sent to the publishers at the undermentioned address:

ISTE Ltd
27-37 St George's Road
London SW19 4EU
UK

www.iste.co.uk

John Wiley & Sons, Inc.
111 River Street
Hoboken, NJ 07030
USA

www.wiley.com

© ISTE Ltd 2010

The rights of Yvon Chevalier and Jean Tuong Vinh to be identified as the authors of this work have been asserted by them in accordance with the Copyright, Designs and Patents Act 1988.

Library of Congress Cataloging-in-Publication Data

Chevalier, Yvon.
Mechanics of viscoelastic materials and wave dispersion / Yvon Chevalier, Jean Tuong Vinh.
p. cm.
Includes bibliographical references and index.
ISBN 978-1-84821-077-6
1. Viscoelastic materials--Mechanical properties--Mathematical models. 2. Flexible structures--Vibration--Mathematical models. 3. Structural engineering--Materials--Mathematical models. 4. Wave motion, Theory of--Mathematics. 5. Dispersion--Mathematical models. 6. Wave equation. I. Tuong, Jean Vinh. II. Title.
TA418.2.C466 2010
620.1'1232--dc22

2009044248

British Library Cataloguing-in-Publication Data
A CIP record for this book is available from the British Library
ISBN 978-1-84821-077-6

Printed and bound in Great Britain by CPI Antony Rowe, Chippenham and Eastbourne

FSC
Mixed Sources
Product group from well-managed forests and other controlled sources
Cert no. SGS-COC-2953
www.fsc.org
© 1996 Forest Stewardship Council

@Seismicisolation

Table of Contents

Preface xix

Acknowledgements xxix

PART A. CONSTITUTIVE EQUATIONS OF MATERIALS 1

Chapter 1. Elements of Anisotropic Elasticity and Complements on Previsional Calculations 3
Yvon CHEVALIER

1.1. Constitutive equations in a linear elastic regime 4
1.1.1. Symmetry applied to tensors s_{ijkl} and c_{ijkl} 4
1.1.2. Constitutive equations under matrix form 5
1.2. Technical elastic moduli 7
1.2.1. Tension tests with one normal stress component σ 7
1.2.2. Shear test 9
1.3. Real materials with special symmetries 10
1.3.1. Change of reference axes 11
1.3.2. Orthotropic materials possess two orthogonal planes of symmetry 16
1.3.3. Quasi-isotropic transverse (tetragonal) material 19
1.3.4. Transverse isotropic materials (hexagonal system) 20
1.3.5. Quasi-isotropic material (cubic system). 21
1.3.6. Isotropic materials 22
1.4. Relationship between compliance S_{ij} and stiffness C_{ij} for orthotropic materials 23
1.5. Useful inequalities between elastic moduli 24
1.5.1. Orthotropic materials. 25
1.5.2. Quasi transverse isotropic materials 26
1.5.3. Transverse isotropic, quasi-isotropic, and isotropic materials 26

@Seismicisolation

1.6. Transformation of reference axes is necessary in many circumstances . . . 27
1.6.1. Practical examples . . . 27
1.6.2. Components of stiffness and compliance after transformation . . . 27
1.6.3. Remarks on shear elastic moduli G_{ii} (ij = 23, 31, 12) and stiffness constants C_{ii} (with i = 4, 5, 6) . . . 28
1.6.4. The practical consequence of a transformation of reference axes. . 28
1.7. Invariants and their applications in the evaluation of elastic constants . . . 28
1.7.1. Elastic constants versus invariants . . . 32
1.7.2. Practical utilization of invariants in the evaluation of elastic constants . . . 35
1.8. Plane elasticity . . . 35
1.8.1. Expression of plane stress stiffness versus compliance matrix . . . 35
1.8.2. Plane stress stiffness components versus three-dimensional stiffness components . . . 38
1.9. Elastic previsional calculations for anisotropic composite materials . . 38
1.9.1. Long fibers regularly distributed in the matrix . . . 39
1.9.2. Stratified composite materials . . . 44
1.9.3. Reinforced fabric composite materials . . . 46
1.10. Bibliography . . . 51
1.11. Appendix . . . 52
Appendix 1.A. Overview on methods used in previsional calculation of fiber-reinforced composite materials. . . . 52

Chapter 2. Elements of Linear Viscoelasticity . . . 57
Yvon CHEVALIER

2.1. Time delay between sinusoidal stress and strain . . . 59
2.2. Creep and relaxation tests . . . 60
2.2.1. Creep test. . . . 60
2.2.2. Relaxation test. . . . 61
2.2.3. Ageing and non-ageing viscoelastic materials . . . 62
2.2.4. Viscoelastic materials with fading memory . . . 63
2.3. Mathematical formulation of linear viscoelasticity . . . 63
2.3.1. Linear system . . . 63
2.3.2. Superposition (or Boltzmann's) principle. . . . 64
2.3.3. Creep function in a functional constitutive equation . . . 67
2.3.4. Relaxation function in functional constitutive equations. . . . 68
2.3.5. Properties of relaxation and creep functions . . . 68
2.4. Generalization of creep and relaxation functions to tridimensional constitutive equations . . . 71
2.4.1. Relaxation function as components in a stiffness matrix . . . 71

@Seismicisolation

2.4.2. Creep function as components in a compliance matrix 73
2.4.3. Some remarks on the mathematical formulation of linear viscoelatic behavior of materials 74
2.5. Principle of correspondence and Carson-Laplace transform for transient viscoelastic problems 74
2.5.1. Carson-Laplace's transform 76
2.5.2. Complex moduli 78
2.5.3. Properties of the complex relaxation and creep components matrix versus circular frequency 80
2.6. Correspondence principle and the solution of the harmonic viscoelastic system 82
2.7. Inter-relationship between harmonic and transient regimes 83
2.8. Modeling of creep and relaxation functions: example 87
2.8.1. Basic rheological cells 88
2.8.2. General parametric modeling 89
2.8.3. Modeling with three rheological parameters: examples 93
2.8.4. Modeling with four rheological parameters: fractional derivative 98
2.9. Conclusion 100
2.10. Bibliography 100

Chapter 3. Two Useful Topics in Applied Viscoelasticity: Constitutive Equations for Viscoelastic Materials 103
Yvon CHEVALIER and Jean Tuong VINH

3.1. Williams-Landel-Ferry's method 104
3.1.1. The effect of temperature change 104
3.1.2. Williams-Landel-Ferry's formulation 105
3.1.3. Experimental procedure to obtain the master curve 107
3.1.4. Examples of master curves 108
3.1.5. Applicability of the method of reduced variables 109
3.1.6. Utilization of another representation of complex moduli (or compliances) 111
3.1.7. Extension of Williams-Landel-Ferry's methods to composite materials 112
3.2. Viscoelastic time function obtained directly from a closed-form expression of complex modulus or complex compliance 112
3.2.1. Overview of state-of-the-art in viscoelasticity and structural dynamics 112
3.2.2. Polynomial functions of frequency used to express complex moduli 116
3.2.3. Fractional derivatives 124

@Seismicisolation

3.2.4. Use of inverse Carson-Laplace transform to obtain a closed-form expression of transient response . . . 130
3.2.5. Applications . . . 133
3.3. Concluding remarks . . . 136
3.3.1. Williams-Landel-Ferry's method . . . 136
3.3.2. Polynomial quotient and fractional derivatives are used to mathematically express the dynamic response of viscoelastic materials . . . 136
3.4. Bibliography . . . 137
3.5. Appendices . . . 139
Appendix 3.A. Inversion of Laplace transform . . . 139
Appendix 3.B. Sutton's method for long time response . . . 143

Chapter 4. Formulation of Equations of Motion and Overview of their Solutions by Various Methods . . . 145
Jean Tuong VINH

4.1. D'Alembert's principle . . . 146
4.1.1. Generalized coordinates . . . 146
4.1.2. Principle of virtual work . . . 147
4.1.3. Equation of motion by D'Alembert's principle . . . 148
4.2. Lagrange's equation . . . 149
4.2.1. System subjected to r holonomic geometric constraints . . . 149
4.2.2. Generalized forces . . . 151
4.2.3. Introduction to kinetic energy . . . 151
4.2.4. Lagrange's equation . . . 152
4.2.5. Potential function . . . 154
4.2.6. Lagrangian function with Rayleigh dissipation function . . . 155
4.3. Hamilton's principle . . . 157
4.4. Practical considerations concerning the choice of equations of motion and related solutions . . . 159
4.4.1. Boundary conditions and approximate equations of motion . . . 160
4.4.2. Choice of equations of motion . . . 160
4.4.3. The degree of approximation . . . 161
4.5. Three-, two- or one-dimensional equations of motion? . . . 162
4.5.1. Three-dimensional equations of motion . . . 162
4.5.2. Two- or one-dimensional equations of motion . . . 163
4.5.3. Wave dispersion . . . 163
4.6. Closed-form solutions to equations of motion . . . 163
4.6.1. Degree of differential equations of six or less . . . 163
4.6.2. Degree of differential equations exceeding six . . . 163
4.7. Bibliography . . . 164

@Seismicisolation

4.8. Appendices 165
Appendix 4.A. Equations of motion in elastic medium deduced from Love's variational principle. 165
Appendix 4.B. Lagrange's equations of motion deduced from Hamilton's principle 167

PART B. ROD VIBRATIONS 173

Chapter 5. Torsional Vibration of Rods 175
Yvon CHEVALIER, Michel NUGUES and James ONOBIONO

5.1. Introduction. 175
5.1.1. Short bibliography of the torsion problem 176
5.1.2. Survey of solving methods for torsion problems 176
5.1.3. Extension of equations of motion to a larger frequency range . . . 179
5.2. Static torsion of an anisotropic beam with rectangular section without bending – Saint Venant, Lekhnitskii's formulation 180
5.2.1. Airy's function and field of displacement ψ 181
5.2.2. Solution of equation [5.10] with Airy's function 184
5.2.3. Expressions of torsion moment M_t versus torsion angle α and stiffness C_T 186
5.2.4. Approximate formulae for M_T and C_T. 189
5.2.5. Dynamic torsion of a rod with rectangular section using the elementary equation of motion. 189
5.2.6. Pure dynamic torsion of a rod with rectangular cross-section using first-degree approximation 194
5.3. Torsional vibration of a rod with finite length 199
5.3.1. Closed-form solution of θ (z, t). 200
5.3.2. Evaluation of spatial solution $\Theta(z)$ 202
5.3.3. Evaluation of coefficients θ (z, t) and ζ (z, t). 203
5.4. Simplified boundary conditions associated with higher approximation equations of motion [5.49]. 204
5.5. Higher approximation equations of motion 205
5.5.1. Slenderness 205
5.5.2. Ratio E/G_{ij} 205
5.5.3. Flatness ratio s = width/thickness = b/h. 207
5.5.4. Saint Venant's theory versus higher approximation theory 207
5.6. Extension of Engström's theory to the anisotropic theory of dynamic torsion of a rod with rectangular cross-section. 207
5.7. Equations of motion. 212
5.7.1. Matricial form. 212
5.7.2. Decoupled equation of motion and correcting coefficient 214

@Seismicisolation

5.8. Torsion wave dispersion 215
5.8.1. Expressions of angular displacement α (z, t) and axial displacement ψ (z, t) 215
5.8.2. Phase velocity for the two first elastodynamic modes 217
5.9. Presentation of dispersion curves 219
5.9.1. Isotropic rod with circular section 219
5.9.2. Isotropic steel rod with rectangular section. 219
5.9.3. Anisotropic composite rods 219
5.9.4. Some remarks 223
5.9.5. Practical remark. 225
5.9.6. Comparison with other theories (Barr and Engström) 225
5.10. Torsion vibrations of an off-axis anisotropic rod 225
5.10.1. Displacement field 226
5.10.2. Equations of motion 229
5.10.3. Eigenfrequency equations of motion. 229
5.10.4. Solutions of decoupled equations. 233
5.10.5. For a very long rod 234
5.11. Dispersion of deviated torsional waves in off-axis anisotropic rods with rectangular cross-section 235
5.12. Dispersion curve of torsional phase velocities of an off-axis anisotropic rod. 240
5.13. Concluding remarks 241
5.13.1. Characterization of shear moduli and non-diagonal coefficients of a compliance matrix 241
5.13.2. Dispersion of torsional phase velocity 241
5.13.3. Saint Venant's warping theory 241
5.13.4. A more elaborate warping theory. 242
5.13.5. Dispersion of torsional phase velocity 242
5.13.6. Nugue's theory 242
5.13.7. Dispersion of phase and group velocities 242
5.14. Bibliography 242
5.15. Table of symbols 244
5.16. Appendices 246
Appendix 5.A. Approximate formulae for torsion stiffness 246
Appendix 5.B. Equations of torsional motion obtained from Hamilton's variational principle 250
Appendix 5.C. Extension of Barr's correcting coefficient in equations of motion 257
Appendix 5.D. Details on coefficient calculations for θ (z, t) and ζ (z, t) . . 258
Appendix 5.E. A simpler solution to the problem analyzed in Appendix 5.D 263

@Seismicisolation

Appendix 5.F. Onobiono's and Zienkievics' solutions using finite element method for warping function ϕ 265
Appendix 5.G. Formulation of equations of motion for an off-axis anisotropic rod submitted to coupled torsion and bending vibrations 273
Appendix 5.H. Relative group velocity versus relative wave number 279

Chapter 6. Bending Vibration of a Rod 291
Dominique LE NIZHERY

6.1. Introduction 291
6.1.1. Short bibliography of dynamic bending of a beam 292
6.2. Bending vibration of straight beam by elementary theory 293
6.2.1. Bernoulli-Euler's equation of motion 293
6.2.2. Solutions of Bernoulli-Euler's equations 296
6.3. Higher approximation theory of bending vibration 299
6.3.1. Formulation of the equations of motion 299
6.3.2. Coupled equations of motion 302
6.3.3. Decoupled equation of motion 303
6.3.4. Solution to the practical problem 305
6.3.5. Stationary bending vibration 305
6.3.6. Non-dimensional equation of motion 305
6.3.7. Equation of motion with reduced variables 306
6.3.8. Expression of flexural displacement and shear φ 307
6.3.9. Coefficient calculations 308
6.3.10. Evaluation of Young's modulus by solution of Timoshenko's equation 309
6.3.11. Dispersion curves related to various theories of bending waves in a rod 311
6.3.12. Influence of rotational inertia and transverse shear 312
6.4. Bending vibration of an off-axis anisotropic rod 313
6.4.1. Preliminary considerations 313
6.4.2. Flexural vibration of an off-axis rod 313
6.4.3. Equations of motion 314
6.4.4. Reduced variables and characteristic frequency equations for stationary waves 317
6.4.5. Computer program using trial and error method to evaluate Poisson's number 324
6.5. Concluding remarks 324
6.5.1. Choice of equations of motion 324
6.5.2. Test sample slenderness and influence of shear effect 325
6.5.3. Strong influence of shear effect for composite materials: accuracy of Young's modulus and non-diagonal technical modulus evaluation . . . 326

@Seismicisolation

6.5.4. Comments on computational effort to evaluate Young's modulus for off-axis samples . . . 326
6.6. Bibliography . . . 326
6.7. Table of symbols. . . . 327
6.8. Appendices . . . 328
Appendix 6.A. Timoshenko's correcting coefficients for anisotropic and isotropic materials. . . . 328
Appendix 6.B. Correcting coefficient using Mindlin's method. . . . 333
Appendix 6.C. Dispersion curves for various equations of motion. . . . 334
Appendix 6.D. Change of reference axes and elastic coefficients for an anisotropic rod . . . 337

Chapter 7. Longitudinal Vibration of a Rod . . . 339
Yvon CHEVALIER and Maurice TOURATIER

7.1. Presentation. . . . 339
7.1.1. Elementary equation of motion. . . . 340
7.1.2. Boundary conditions . . . 342
7.2. Bishop's equations of motion . . . 343
7.2.1. Isotropic material . . . 343
7.2.2. Transversely isotropic material. . . . 343
7.2.3. Longitudinal wave dispersion. . . . 344
7.3. Improved Bishop's equation of motion . . . 345
7.4. Bishop's equation for orthotropic materials. . . . 346
7.5. Eigenfrequency equations for a free-free rod . . . 346
7.5.1. Harmonic solution for dimensionless Bishop's equation. . . . 346
7.5.2. Boundary conditions and eigenvalue equations . . . 348
7.6. Touratier's equations of motion of longitudinal waves . . . 350
7.6.1. General considerations. . . . 350
7.6.2. Dispersion curves according to various theories. . . . 350
7.6.3. Displacement field and boundary conditions. . . . 353
7.6.4. Strain and stress components . . . 357
7.6.5. Energy functionals and Hamilton's principle . . . 361
7.6.6. Equations of motion . . . 366
7.6.7. Boundary equations . . . 367
7.7. Wave dispersion relationships. . . . 367
7.7.1. Phase velocity in composite materials. . . . 369
7.7.2. Extensional waves in an anisotropic composite rod with rectangular cross-section – dispersion curves . . . 372
7.7.3. Natural boundary conditions . . . 385
7.7.4. Various types of solutions for the equations of motion. . . . 386

@Seismicisolation

7.8. Short rod and boundary conditions 393
7.8.1. Elementary theory 393
7.8.2. Boundary conditions 394
7.9. Concluding remarks about Touratier's theory 395
7.10. Bibliography 396
7.11. List of symbols 397
7.12. Appendices 399
Appendix 7.A. an outline of some studies on longitudinal vibration of rods with rectangular cross-section 399
Appendix 7.B. Formulation of Bishop's equation by Hamilton's principle by Rao and Rao 401
Appendix 7.C. Dimensionless Bishop's equations of motion and dimensionless boundary conditions 405
Appendix 7.D. Touratier's equations of motion by variational calculus . 408
Appendix 7.E. Calculation of correcting factor q (C_{ijkl}) 409
Appendix 7.F. Stationarity of functional $\tilde{J}$ and boundary equations. . . . 419
Appendix 7.G. On the possible solutions of eigenvalue equations 419

Chapter 8. Very Low Frequency Vibration of a Rod by Le Rolland-Sorin's Double Pendulum 425
Mostefa ARCHI and Jean-Baptiste CASIMIR

8.1. Introduction. 425
8.1.1. Frequency range 425
8.1.2. Simplicity and ease 426
8.2. Short bibliography. 427
8.3. Flexural vibrations of a rod using coupled pendulums 427
8.3.1. Lagrange equations of motion 428
8.3.2. Eigenvalue equation 430
8.3.3. Solutions for pendulum oscillations 431
8.3.4. Relationship between beating period and sample stiffness k 431
8.4. Torsional vibration of a beam by double pendulum 434
8.4.1. Equations of torsional motions 434
8.5. Complex compliance coefficient of viscoelastic materials 436
8.5.1. General consideration 436
8.5.2. Expression of (ω_1-ω_2) 439
8.5.3. Utilization of correspondence principle to obtain complex sample rigidity 441
8.6. Elastic stiffness of an off-axis rod 443
8.6.1. Elementary equations of motion 444
8.6.2. Higher approximation equations of motion. 448

@Seismicisolation

8.7. Bibliography 449
8.8. List of symbols 450
8.9. Appendices 452
Appendix 8.A. Closed-form expression of θ_1 or θ_2 oscillation angles of the pendulums and practical considerations 452
Appendix 8.B. Influence of the highest eigenfrequency ω_3 on the pendulum oscillations in the expression of θ_1 (t) 457
Appendix 8.C. Coefficients a of compliance matrix after a change of axes for transverse isotropic material 458
Appendix 8.D. Mathematical formulation of the simultaneous bending and torsion of an off-axis rectangular rod 460
Appendix 8.E. Details on calculations of s_{35} and υ_{13} of transverse isotropic materials 486

Chapter 9. Vibrations of a Ring and Hollow Cylinder 493
Jean Tuong VINH

9.1. Introduction 493
9.2. Equations of motion of a circular ring with rectangular cross-section 494
9.2.1. Generalized displacement and force 494
9.2.2. Bending equations 495
9.2.3. Strain components 496
9.2.4. Force components 497
9.2.5. Equations of motion 498
9.2.6. Eigenvalue equations 498
9.2.7. Solution of characteristics equation 499
9.2.8. Equations of motion of the ring submitted to in plane forced vibrations 500
9.2.9. Expression of Young's modulus versus Q 501
9.3. Bibliography 502
9.4. Appendices 503
Appendix 9.A. Expression u (θ) in the three subintervals delimited by the roots λ of equation [9.33] 503

Chapter 10. Characterization of Isotropic and Anisotropic Materials by Progressive Ultrasonic Waves 513
Patrick GARCEAU

10.1. Presentation of the method 513
10.1.1. Use of ultrasonic waves 513
10.1.2. Practical considerations of ultrasonic waves 514
10.2. Propagation of elastic waves in an infinite medium 515

@Seismicisolation

10.3. Progressive plane waves 516
10.3.1. Christoffel tensor 517
10.3.2. Christoffel's equation. 517
10.3.3. Eigenvalues of Γ_{ik} are real 518
10.3.4. Eigenvectors of Γ_{ik} are mutually orthogonal 518
10.4. Polarization of three kinds of waves 518
10.4.1. Longitudinal wave 518
10.4.2. Transverse or shear wave 518
10.4.3. Quasi transverse (QT) wave 519
10.5. Propagation in privileged directions and phase velocity calculations . 519
10.5.1. Wave propagation along material symmetry axes 520
10.5.2. Elastic constants obtained with $\vec{p}$ colinear with one of the three material directions of symmetry 525
10.5.3. Wave propagation along a non-privileged direction. 525
10.6. Slowness surface and wave propagation through a separation surface 528
10.6.1. Slowness surface representation 529
10.6.2. Slowness surfaces for transverse isotropic composite material . . 533
10.7. Propagation of an elastic wave through an anisotropic blade with two parallel faces 535
10.7.1. Direct transducer couplings with sample 536
10.7.2. Water immersion bench 537
10.8. Concluding remarks 542
10.9. Bibliography 543
10.10. List of Symbols 544
10.11. Appendices 546
Appendix 10.A. Energy velocity, group velocity, Poynting vector 546
Appendix 10.B. Slowness surface and energy velocity 553

Chapter 11. Viscoelastic Moduli of Materials Deduced from Harmonic Responses of Beams 555
Tibi BEDA, Christine ESTEOULE, Mohamed SOULA and Jean Tuong VINH

11.1. Introduction 555
11.1.1. Trial and error method 555
11.1.2. Are wave dispersion phenomena to be taken into account or not? 556
11.1.3. Williams-Landel-Ferry's method. 556
11.1.4. Validity of elementary equations of motion 556
11.1.5. Choice of equations of motion without recourse to Williams-Landel-Ferry's method 556
11.2. Guidelines for practicians. 557
11.2.1. Viscoelastic complex moduli and frequency range 557

@Seismicisolation

11.3. Solution of a viscoelastic problem using the principle of correspondence 558
11.3.1. First step: elastic solution 559
11.3.2. Second step: estimation of dispersion curves 560
11.3.3. Searching for a solution to viscoelastic moduli using characteristic functions 561
11.4. Viscoelastic solution of equation of motions 564
11.4.1. Experimental dynamic responses must be available 564
11.4.2. Elementary equations of motion and closed-form expression for the transmissibility function for an extensional wave 566
11.4.3. Torsional vibration of a viscoelastic rod 572
11.4.4. Bending vibration of a viscoelastic rod 575
11.5. Viscoelastic moduli using equations of higher approximation degree. 579
11.5.1. Inertia and shear effects 580
11.5.2. Torsional vibration 581
11.5.3. Bending vibration of a rod (higher order approximation). 582
11.6. Bibliography 588
11.7. Appendices 589
Appendix 11.A. Transmissibility function of a rod submitted to longitudinal vibration (elementary equation of motion) 589
Appendix 11.B. Newton-Raphson's method applied to a couple of functions of two real variables β_1 and β_2 components of β. 590
Appendix 11.C. Transmissibility function of a clamped-free Bernoulli's rod submitted to bending vibration 591
Appendix 11.D. Complex transmissibility function of a clamped-free Bernoulli's rod and its decomposition into two functions of real variables β_1, β_2 593
Appendix 11.E. Eigenvalue equation of clamped-free Timoshenko's rod 594
Appendix 11.F. Transmissibility function of clamped-free Timoshenko's rod 595

Chapter 12. Continuous Element Method Utilized as a Solution to Inverse Problems in Elasticity and Viscoelasticity 599
Jean-Baptiste CASIMIR

12.1. Introduction 599
12.2. Overview of the continuous element method 601
12.2.1. Equilibrium equations and the force-displacement relationship 601
12.2.2. Explicit continuous element 603
12.2.3. State vector and dynamic transfer matrix 605

@Seismicisolation

12.2.4. Transfer matrix and dynamic stiffness presented in suitable form for matrix calculation 606
12.2.5. Eigenvalues and eigenvectors of dynamic stiffness. 607
12.3. Boundary conditions and their implications in the transfer matrix. . . 608
12.4. Extensional vibration of straight beams (elementary theory) 609
12.5. The direct problem of beams submitted to bending vibration. 612
12.5.1. Euler-Bernoulli's transfer matrix and dynamic stiffness matrix . . 612
12.5.2. Numerical simulation for a free-free Bernoulli's rod 614
12.5.3. Bending vibration of a free-free Timoshenko's beam. 614
12.5.4. Dynamic transfer matrix for Timoshenko's beam 616
12.6. Successive calculation steps to obtain a transfer matrix and simple displacement transfer function 620
12.6.1. Eigenvalue calculations 620
12.6.2. Eigenvector calculation of [Dω] 622
12.7. Continuous element method adapted for solving an inverse problem in elasticity and viscoelasticity. 622
12.8. Bibliography 624
12.9. Appendices 624
Appendix 12.A. Wavenumbers β_1, β_2 deduced from Timoshenko's equation 624

List of Authors 629

Index 631

@Seismicisolation

Preface

The mechanical testing of material is an important activity in research and industry. Scientists, engineers and technicians in a large range of domains (such as chemistry, metallurgy, mechanics, physics, polymer science, the rubber industry, aerospace and aeronautical industries, etc.) are interested in the technology used to investigate the mechanical properties of materials.

Static and dynamic tests are complementary and used concurrently. Static tests are often used in industry. Dynamic tests, however, are becoming more popular and, surprisingly, in many cases are easier to use than static ones, at least at lower frequencies. Let us take an example concerning the measurement of elastic Young's modulus or the shear modulus of a steel rod. In (nearly) static tests, glued strain gauges or special micro-displacement transducers are used to measure, the displacement of the sample in two or three directions at once, which enable us to evaluate the strains. With the measurement of applied force or torque, these two moduli are deduced from the basic definitions relating to stress and strain. There are a succession of measurements and calculations from the stress *versus* strain curves.

To obtain such elastic moduli using dynamic tests, evaluation of resonance frequencies only is required; dimensions and geometry of the sample and its weight, as well as boundary conditions, being known.

The main interest in dynamic testing, however, resides in characterization of the viscoelastic properties of materials, i.e. the dependency of technical moduli (or relaxation, creep functions) *versus* the frequency (or time).

@Seismicisolation

Growing interest in dynamic tests

In industrially advanced countries, societies for material testing regularly publish recommendations concerning mechanical tests with indications on methods and test procedures. Over the last five decades, the methods of investigating dynamic mechanical properties have made significant progress. In the scientific and technical literature devoted to this problem, various viewpoints have been adopted. For example, the dynamic tests that interpret materials at a molecular level, i.e. structural factors, molecular weight, cross-linking, crystallinity, etc., constitute tools in the chemistry and physics of polymers. The science of rheology is being more frequently adopted in order to obtain technical moduli (or time functions) which serve in viscoelastic constitutive equations relating stress components to strain components.

Composite materials cover a large domain including laminated plastics and panels for the building industry. Special composite materials were initially designed and fabricated for advanced applications in the aeronautical and aerospace industries in the 1970s. The anisotropic properties of such materials are obtained by the appropriate arrangement of high-strength fibers in metallic or non-metallic matrices of the layers or by the orientation of the layers in the structural composite. The mechanical characterization of such anisotropic materials consequently requires special testing procedures which are more elaborate than the ones devoted to isotropic materials.

Characterization of metallic and non-metallic material damping capacities is of interest to specialists in chemistry and physics as well as in mechanics.

Measuring damping

The measurement of damping coefficients of mechanical structures gives rise to a large variety of methods in structural dynamics that deserve the attention of specialists in material testing. The transposition of those methods into rheology, however, requires some caution and adaptations. The damping of a mechanical structure depends on damping of the materials used in the structure and the geometry of the structure itself. Consequently it is necessary to have this distinction in mind. Material damping can be deduced from structural damping on the condition that the relationship between these two kinds of damping is known.

Damping capacities of materials cover a much larger range than structural damping. Globally, damping capacities of materials (defined as the quotient of the imaginary to real part of a complex modulus) can be divided into three classes:

@Seismicisolation

a) low damping – $\tan \delta < 10^{-3}$;

b) medium damping – $10^{-3} < \tan\delta < 5.10^{-2}$;

c) high damping – $5.10^{-2} < \tan\delta < 10$.

Mechanical structural damping, in the majority of cases, concerns class (b) and no caution concerning measurement technique is needed. Class (a) concerns steel or special metals and requires special caution when taking measurements in order to eliminate the predominant influence of air damping on the sample. Class (c) concerns some rubbers or special blends of polymers and metal powders. The usual methods adopted in structural dynamics require special adaptations.

Size and shape of the sample

In many circumstances, analysts have to deal with samples with special or unusual shapes and sizes. The sample cut off from a hollow cylinder is curved and necessitates a special sample holder. The sample can be very small and therefore commercially available apparatus cannot be used. This is the case in biomechanics, for example, where the sample is a cut-off from a small bone. Analysts then have to come up with and devise a special set up.

Appropriate knowledge on the elastodynamics of bounded media

Let us begin with some remarks about currently available instruments. In some apparatuses, the mechanical part and adopted loading system are designed in such a way that vibrations imposed on the sample are far from simple. It eventually gives rise to different kinds of vibrations (extensional, bending, torsion) which are coupled in the sample itself. Coupling of such vibrations is often neglected in proposed formulae giving the moduli. The last formulae are deduced from the elementary theory of vibration using localized mechanical parameters that are not necessarily valid for short and thick samples. Mechanical effects (such as shear and inertia effects) are not taken into account. When experiments are conducted in higher frequency ranges, wave dispersion phenomenon (which describes the variation of the wave velocity in the sample *versus* the frequency) is rarely taken into account.

Attachment of the sample by clamping, gluing or screw tightening creates zones where there is a three-dimensional state of stress that can be localized in the sample submitted to compression forces and also beyond the contact zone between the sample and holder system. This effect is particularly pronounced for a short sample.

@Seismicisolation

These remarks, among others, show that confidence granted to an apparatus must not exclude critical thought and a mechanical background.

The book

I will now present and comment on the chapters in this book.

The authors have intentionally situated dynamic testing of materials in the context of bounded medium elastodynamics. The measurements of dynamic responses of the sample in a large range of frequencies are interesting for analysts who want to obtain viscoelastic complex moduli. Rheologists[1] are interested in the relationship between various resonance peaks of dynamic responses *versus* frequency and micromechanisms of the polymer being tested. Mechanical engineers wish to obtain the curves of complex moduli at low and high frequencies so as to include them in calculation of the dynamic responses of the mechanical structure.

The motion equations of the sample must be carefully chosen, taking into account the frequency range. The upper frequency guides the choice of degree of approximation, which is related to the set of motion equations in view of *wave dispersion* characterization at the chosen upper frequency range. Wave dispersion is not the only effect we need to account for. There is another dispersion phenomenon: the *viscoelastic dispersion*, which is also frequency dependent.

These two effects sometimes act in the same sense with respect to frequency, and *vice versa* regarding sample responses, depending on the type of stationary wave in the sample and the working frequency. This is the reason main wave dispersion should be taken into account and raises the delicate problem of reasoned choice of appropriate equations of motion, compatible with tractable numerical exploitation of experimental results.

Recently, specialists in structural computing science have focused on the *continuous element method* which permits structure calculation even in the ultrasonic frequency range. This method presents advantages and constitutes a serious competitor for *classical finite element method*. The elastodynamics of bounded media precisely furnishes theoretical foundations, particularly in the domain of wave dispersion. Consequently, this last topic is treated in detail for various wave types adopted in samples.

---

1 Rheology designates the science which studies the flow (Greek radical *Rheos*) of solid or liquid materials.

@Seismicisolation

One of the new methods of treating viscoelastic material characterization is to use continuous elements as a tool to numerically solve an inverse problem without recourse to closed-form eigenvalue solutions of boundary equations.

We try to bridge the gap between theoretical academic works on wave dispersion and practical applications that do not yet sufficiently exploit the literature. Many significant theoretical contributions concerning wave dispersion in bounded media during the last three decades merit being brought together, classified and examined in view of applications.

Part A is devoted to continuum mechanics (constitutive equations of materials including *anisotropic materials*). Chapter 1 covers linear and applied viscoelasticity. Chapter 2 looks at the principle of correspondence that permits the conversion of elastic equations of motion into viscoelastic ones, with the condition that boundary conditions and sample geometry remain the same.

Chapter 3 is devoted to Williams-Landel-Ferry's (WLF) method, which is very popular in the field of polymer chemistry and deserves the attention of mechanical engineers. It permits artificial enlargement of the modulus (or compliance) curve in an unusually large frequency range (often more than eight decades) on the condition that *the superposition principle temperature-frequency is applicable.*

Serious limitations of WLF's method must be taken into account when dealing with anisotropic artificial composite materials. The superposition principle may not be valid for such materials. The remaining possibility is to directly evaluate complex modulus (or compliance) over a large frequency range. This is the main reason to resort to appropriate wave dispersion theories for these materials.

The closed-form expression of viscoelastic modulus (or compliance) is often necessary in computer codes to evaluate the damping responses of structures. Examining this problem from a practical point of view, we notice that analog models, usually proposed in textbooks and publications, with a reduced number of springs and dashpots cleverly arranged in series and/or in parallel, indeed help the reader "visualize" the material.

For a given experimental dynamic curve, however, we do not know in advance how many associated mechanical elements (springs and dashpots) will be adopted, particularly when the frequency range is large. The appropriate model is often more complicated than the simple academic models indicated above. This unknown model

@Seismicisolation

belongs to the "*black box*" constituted by the material in the usual mechanical inverse problem to be solved![2]

Some methods are then proposed to obtain a closed-form expression of modulus (or compliance) *versus* frequency by quotient of polynomials of the same degree (without *a priori* assumption of its degree) or by fractional derivatives whose interest resides in the condensed mathematical expression.

In Chapter 4, various formulations of equations of motion are presented. As we have to deal with bounded medium and finite sample length, no exact equations are available: approximate equations of motion are to be found. The main question is: *what is the degree of approximation we must adopt*? This question raises a subsidiary question: how many generalized displacement components and generalized force components are to be adopted to fully cover the mechanical behavior of the sample?

All the methods presented in dynamics textbooks can be utilized. D'Alembert's principle and Lagrange's equations constitute the first group of methods. The second group includes Hamilton's variational principle using simple displacement field. Love's variational principle can be considered as derived from Hamilton's one.[3] Mixed field Reissner's principle is, in some cases, useful for correctly portraying the dispersion curve of the sample. This variational method is referred to in an accurate analysis of vibrations of an anisotropic rod.

Part B concerns various types of rod vibration: extension, bending and torsion. Vibration modes are a source of vocabulary confusion for analysts. Let us clarify some different definitions.

Vibration modes might concern the *nature of the vibration* as mentioned above. The nature of the vibration is related to the predominant strain in the sample, i.e. the extensional strain along the rod axis in longitudinal motion, shear strain in rod torsion, and axial strain in bending test.

---

2 Recently in electrical engineering, as well as in mechanical engineering, attention has focused on distributed models in a ladder using linear elementary models (springs and dashpots) or fractional derivatives which constitute an elegant method to characterize materials in a large frequency range with minimum parameters.

3 Using variational principles and integrating by parts, we directly obtain equations of motion and natural boundary conditions as well.

@Seismicisolation

In structural dynamics, vibration mode is related to *eigenfrequencies* and *eigenvectors,* which are portrayed by nodal lines on the sample surface whose density increases with frequency.

Elastodynamic vocabulary: attention is focused not only on the representation of nodal lines on the lateral surface of the sample, but also on the sample thickness itself. Let us take an example: the bending test on a rod with a rectangular cross-section. There is a neutral line in the thickness whose motion is representative of bending motion in the first elastodynamic mode. Higher elastodynamic modes correspond to discontinuous or undulating neutral lines in the cross-section. To create such modes, a special array of small piezoelectric exciters can be used. For the usual characterization of material, higher elastodynamic modes are rarely used, although they might constitute a good tool in fracture mechanics. To avoid confusion on the signification of vibration mode, additional indications between brackets will be used: (nature), (eigenfrequency or eigenvalue), (elastodynamics).

In some chapters, theoretical works are presented with proofs so as to facilitate the reader's consultation. Intentionally, Part B is presented with details in the theoretical formulation so as to facilitate the reader's work and reduce his/her burden in the search of scientific papers sometime published some centuries ago! Appendixes presented at the end of each chapter might help researchers to find the demonstration of formulae. For each kind of wave a collection of theories from elementary to sophisticated may present difficulties and a profusion of theories to a reader who approaches the problem for the first time. We have presented a set of theories as a toolbox: practitioners and researchers have to choose the appropriate tool for special applications themselves.

Some readers might be surprised by the unusual length of the chapters in Part B compared to a classical book devoted to the same topics. The authors' intention is to gather together all the possible groups of theories with various degrees of approximations, so the reader does not need to search elsewhere. The contributions of our research team are naturally presented with the intention of completing existing literature on the vibration of rods with finite and infinite lengths.

Coupled vibrations highlight the effect of non-diagonal elastic coefficients in the equations of motion. Coupled vibrations are intentionally used with an *off-axis anisotropic* rod. Matricial diagonal coefficients being known, such coupled vibrations permit us to evaluate *non-diagonal terms*.

Coupled vibrations exist even in an isotropic rod submitted to various vibration types, even for a closed section. In elementary theories these vibrations are neglected at lower frequencies. Shear effect in longitudinal and bending vibrations,

@Seismicisolation

however, occurs in equations of motion with higher degrees of approximation. Torsional rod vibration gives rise to axial strain and extensional vibration occurs. Consequently, two or more elastic (or viscoelastic) moduli are present in equations of motion.

The extensive utilization of rods in this book, instead of plates, necessitates explanation. In some technical and scientific publications, plate is indeed used to evaluate elastic (and/or viscoelastic) moduli. The objective of such works is to determine the whole set of elastic moduli. Elastic vibrations of plates necessitate measurements of vibration amplitude at many points and eventually for a certain number of (eigenfrequency) modes. On grounds of numerical calculation, optimization algorithms are referred to. The degree of complexity is considerably increased with respect to that concerning a rod. The challenge of adopting plate equations of motion is prohibitive compared to the one-dimensional equation for a rod with one, two or three displacement variables. The results obtained from plates in the scientific literature are unfortunately far from convincing, with the objective of solving an inverse problem to find moduli or stiffness coefficients of material[4].

Chapters 5, 6 and 7 present torsional, bending and extensional vibrations. In Chapter 5, a rod with rectangular cross-section is adopted, taking into account the ease of obtaining such a section. Warping of the cross-section is examined for isotropic and anisotropic materials. Saint Venant's dynamic equations of motion are presented as are the higher approximation equations of motion corresponding to more complex section warping.

Bending vibration in Chapter 6 concerns the elementary Bernoulli-Euler's equation of motion. Timoshenko's equation with a higher degree of approximation is preferred when working at a higher frequency. The bending vibration of an off-axis rod is also presented in order to evaluate the compliance a non-diagonal coefficient of anisotropic materials.

Extensional vibrations in a rod are presented in detail in Chapter 7. The longitudinal wave dispersion is surprisingly more difficult to apprehend than the one concerning the two aforementioned vibrations and requires a more elaborate displacement field. For application at higher frequency, the fourth-degree Bishop's equation of motion is not capable of correctly portraying the wave dispersion curve at higher frequencies. Touratier's formulation using internal constraints extends Volterra's work to anisotropic rods.

4 In Chapter 10, however, progressive waves are used in plates to obtain material stiffness coefficients at ultrasonic frequency range

@Seismicisolation

Chapter 8 is devoted to Le Rolland-Sorin's double pendulum working at very low frequency. This inventive, artful and simple method is practically unknown in English-speaking countries and deserves practicians' attention in the sense it requires so few measuring instruments compared to other test methods. The functioning principle is unusual compared to existing methods used in dynamic tests.

Chapter 9 examines vibrations in rings and hollow cylinders. In many situations we have to deal with a curved rod or straight rod with curved cross-section.

Chapter 10 is devoted to the propagation of ultrasonic waves in thick plates. Ultrasonic progressive dilatational (and/or shear) wave can be chosen in advance as can the wave direction. The second-order equation of motion is simple to handle and, surprisingly, the interpretation of experimental results is much easier to obtain than rod vibrations at lower frequencies. Plate samples with a large thickness compared to wavelength are used to equate the plate with a semi-infinite medium. Progressive waves are used for this purpose.

Chapter 11 concerns evaluation of the viscoelastic complex modulus using characteristic (trigonometric and hyperbolic) functions to express displacement components. Transmissibility function (which relates output displacement to input displacement) is used in the framework of an inverse problem to evaluate complex moduli (or compliance). Methods using some special mathematical algorithms are presented in the framework of research of solutions to the important mathematical inverse problems.

Finally, Chapter 12 complements the preceding chapter, using so-called continuous elements. This method is interesting because it offers us the chance to obtain a response curve in a very large frequency range by numerical computation which takes much less time than the finite element method. In our opinion, the matricial formulation of the problem and integration of elastodynamic equations of motion constitute one of the best ways of tackling the inverse viscoelastic problem.

Yvon Chevalier and Jean Tuong Vinh

February 2010

@Seismicisolation

Acknowledgements

This book has been written by the two coordinators and authors. Contributions from the team of researchers in our laboratories have been rewritten in a concise manner for readers. The results were obtained over more than 30 years of research in the laboratory of rheology and vibroacoustics of the ISMEP (Institut Supérieur de Mécanique de Paris). The contributions of our colleagues and researchers were important. Technical reports, PhD theses, reports prepared by scholars on short or long stays in our laboratory as well as fruitful contacts with aerospace and aeronautical industries in France and abroad, via many contracts, have enabled the coordinators to present the scientific and technical contributions of the whole laboratory. Thanks are also due to our students and researchers, whose remarks on our courses and practical experiments were very useful.

Mrs Nadège Reisky, our technical secretary, who two years ago patiently typed long chapters with lengthy equations full of mathematical signs and Greek symbols over months and months, is gratefully acknowledged. Without her precious work, this book would never have been published. Anne Vinh, editor and expert in computer layout, was a great help in assisting the coordinators in presenting this book in acceptable form. Her cooperation with Ms Cécile Rault, assistant editor at ISTE, was very fruitful.

Elhadi Brahimi, specialist in technical and scientific design on computers, accepted the difficult task of redrawing nearly all of the innumerable figures, including complicated charts with multiple parameters in intricate interlacing networks! Time and patience were applied by him, over a whole year, in order to present the drawings in an acceptable form.

@Seismicisolation

Jean Baptiste Casimir, assistant professor at ISMEP, was the author of Chapter 12. He also had the knack of creating complementary calculations and experiments over the last months of the university year. He is gratefully acknowledged.

Maurice Touratier, professor at laboratory of materials and structure of the high school ENSAM Paris, our old research fellow and author of Chapter 7, is acknowledged for providing the coordinators with his doctorate and diploma theses.

Finally, last but not least, Ms Cécile Rault is gratefully acknowledged for her advice and useful recommendations to our technical team. Without her help, we wouldn't have reached the deadline we initially promised her.

The last phase of our work consisted in the correction of type-written chapters. All the authors of this book heartily thank several proofreaders in ISTE staff for the extremely efficient way in which they coped with successive versions of galleys. In spite of our effort to present chapters in a comprehensive manner, inevitably the English sentences were often either confusing in their length or too short to be understood by the readers. Their questions and proposals to modify or change the sentences are necessary to us to clarify our ideas.

@Seismicisolation

PART A

Constitutive Equations of Materials

A lot of theories, yes, but in view of applications

Henri Bouasse
French physicist, 1920

@Seismicisolation

Chapter 1

Elements of Anisotropic Elasticity and Complements on Previsional Calculations

The objective of this chapter is to present in a concise form the constitutive equations that relate stresses to strains. Previsional calculations especially adapted for composite materials are succinctly approached in the second part of this chapter. Through experience, we are convinced that this constitutes a useful and practical tool with which to tackle the problem of artificial composite materials that are used in industrial applications.

When we have to deal with isotropic materials, the mathematical formulation of those relationships is reduced to simple expressions. The number of independent elastic constants is reduced to two, from a choice of five. The three remaining constants can be expressed against the two retained. Adoption of a given couple of elastic constants is dependent on various practical considerations, e.g. the shape and size of the sample, available method of testing (static or dynamic), nature of waves (stationary or progressive), etc.

Composite materials, whose utilization is becoming more widespread, are anisotropic in most cases. The formulation of constitutive equations requires more than two elastic constants. Symmetry considerations permit us to adopt the number of constants. Experimenters who want to mechanically characterize these materials cannot avoid these preliminary considerations.

Chapter written by Yvon CHEVALIER.

Mechanics of Viscoelastic Materials and Wave Dispersion Edited by Yvon Chevalier and Jean Tuong Vinh
© 2010 ISTE Ltd. Published 2010 by ISTE Ltd.

@Seismicisolation

1.1. Constitutive equations in a linear elastic regime

Small (infinitesimal) strains are defined from displacements, with $\vec{u} = (u_i)^{(1)}$ and $\vec{x} = (x_i)$ being coordinates:

$$\varepsilon_{ij} = \frac{1}{2}\left[\frac{\partial u_i}{\partial x_j} + \frac{\partial u_j}{\partial x_i}\right] \quad i, j = 1, 2, 3 \qquad [1.1]$$

General Hooke's law expresses the proportionality between stress tensor σ_{ij} and strain tensor ε_{ij}:

$$\sigma_{ij} = c_{ijkl}\, \varepsilon_{kl} \qquad [1.2]$$

Equation [1.2] can be inverted and rewritten as:

$$\varepsilon_{ij} = s_{ijkl}\, \sigma_{kl} \qquad [1.3]$$

Equation [1.3] is used in static tests in which forces are input signals and consequently stresses, and output signals (responses) are displacements or strains. In wave propagation in an elastic medium, the strains are input signals whereas the stresses are responses. Equation [1.2] is then adopted.

Stress and strain tensors each have nine components. Symmetry consideration reduces the number of components to six.

1.1.1. *Symmetry applied to tensors s_{ijkl} and c_{ijkl}*

If the deformation energy is evaluated with the assumption that an elastic potential w (deformation energy density) exists so as:

$$\sigma_{ij} = \frac{\partial w}{\partial \varepsilon_{ij}} \qquad [1.4]$$

or:

$$w(B) - w(A) = \int_A^B \sigma_{ij}\, d\,\varepsilon_{ij} \qquad [1.5]$$

@Seismicisolation

taking into account equation [1.2], [1.4] shows that:

$$w = \frac{1}{2}\, c_{ijkl}\, \varepsilon_{ij}\, \varepsilon_{kl} = \frac{1}{2}\, \sigma_{ij}\varepsilon_{ij} \qquad [1.6]$$

The deformation energy density w can be evaluated either from strains or stresses:

$$\left.\begin{aligned} w_{\varepsilon}(\varepsilon) &= \frac{1}{2} c_{ijkl}\, \varepsilon_{ij}\, \varepsilon_{kl} \\ w_{\sigma}(\varepsilon) &= \frac{1}{2} s_{ijkl}\, \sigma_{ij}\, \sigma_{kl} \end{aligned}\right\} \qquad [1.7]$$

Energy density being a scalar, in relation [1.7] symmetry of stiffness and compliance tensors are obtained:

$$\left.\begin{aligned} C_{iikl} &= C_{klii} \\ S_{ijkl} &= S_{klij} \end{aligned}\right\} \qquad [1.8]$$

1.1.2. *Constitutive equations under matrix form*

In practical calculations, it is convenient to adopt a matrix representation. Stress and strain tensors are represented by six components instead of nine. Only three components of shear strains and shear stresses are retained.

$$\{\sigma\} = \{C\}\ \{\varepsilon\} \qquad [1.9a]$$

$$\{\varepsilon\} = \{S\}\ \{\sigma\} \qquad [1.9b]$$

The following notations are adopted here[1]:

$$\{\sigma\} = \{\sigma_{11}, \sigma_{22}, \sigma_{33}, \sigma_{23}, \sigma_{31}, \sigma_{12}\}^{T} \qquad [1.10]$$

$$\{\varepsilon\} = \{\varepsilon_{11}, \varepsilon_{22}, \varepsilon_{33}, 2\varepsilon_{33}, 2\varepsilon_{31}, 2\varepsilon_{12}\}^{T} \qquad [1.11]$$

1 $\{\sigma\} = \{\sigma_{11}, \sigma_{22}, \sigma_{33}, \sigma_{23}, \sigma_{31}, \sigma_{12}\}^{T}$ column matrix notation.

@Seismicisolation

Factor 2 is introduced in [1.11] for shear strains.

The indexes adopted in [1.10] and [1.11] for the three last components are (23), (31) and (12). That is a convention. In other publications, this convention can be replaced by another one. However, the aforementioned convention is the prevalent one.

REMARK ON TENSORIAL WRITING: going from tensorial writing to matrix writing, there is a kind of contraction of indexes. It is difficult to find the meaning of indexes such as 4, 5 and 6. In the study of wave propagation, the adoption of matrix writing gives rise to difficulties in the interpretation of wave characteristics, e.g. polarization of wave plane and direction of wave propagation. In this respect tensorial notations are preferred.

$C_{11} = c_{1111}$	$C_{12} = c_{1122}$	$C_{13} = c_{1133}$	$C_{14} = c_{1123}$	$C_{15} = c_{1131}$	$C_{16} = c_{1112}$
$C_{21} = c_{2211}$	$C_{22} = c_{2222}$	$C_{23} = c_{2233}$	$C_{24} = c_{2223}$	$C_{25} = c_{2231}$	$C_{26} = c_{2212}$
$C_{31} = c_{3311}$	$C_{32} = c_{3322}$	$C_{33} = c_{3333}$	$C_{34} = c_{3323}$	$C_{35} = c_{3331}$	$C_{36} = c_{3312}$
$C_{41} = c_{2311}$	$C_{42} = c_{2322}$	$C_{43} = c_{2333}$	$C_{44} = c_{2323}$	$C_{45} = c_{2331}$	$C_{46} = c_{2312}$
$C_{51} = c_{3111}$	$C_{52} = c_{3122}$	$C_{53} = c_{3133}$	$C_{54} = c_{3123}$	$C_{55} = c_{3131}$	$C_{56} = c_{3112}$
$C_{61} = c_{1211}$	$C_{62} = c_{1222}$	$C_{63} = c_{1233}$	$C_{64} = c_{1223}$	$C_{65} = c_{1231}$	$C_{66} = c_{1212}$

Table 1.1. *Matrix and tensor components of stiffness*

$S_{11} = s_{1111}$	$S_{12} = s_{1122}$	$S_{13} = s_{1133}$	$S_{14} = 2s_{1123}$	$S_{15} = 2s_{1131}$	$S_{16} = 2s_{1112}$
$S_{21} = s_{2211}$	$S_{22} = s_{2222}$	$S_{23} = s_{2233}$	$S_{24} = 2s_{2233}$	$S_{25} = 2s_{2231}$	$S_{26} = 2s_{2212}$
$S_{31} = s_{3311}$	$S_{32} = s_{3322}$	$S_{33} = s_{3333}$	$S_{34} = 4s_{3323}$	$S_{35} = 2s_{3331}$	$S_{36} = 2s_{3312}$
$S_{41} = 2s_{2311}$	$S_{42} = 2s_{2322}$	$S_{43} = 2s_{2333}$	$S_{44} = 4s_{2323}$	$S_{45} = 4s_{2331}$	$S_{46} = 4s_{2312}$
$S_{51} = 2s_{3111}$	$S_{52} = 2s_{3122}$	$S_{53} = 2s_{3133}$	$S_{54} = 4s_{3123}$	$S_{55} = 4s_{3131}$	$S_{56} = 4s_{3112}$
$S_{61} = 2s_{1211}$	$S_{62} = 2s_{1222}$	$S_{63} = 2s_{1233}$	$S_{64} = 4s_{1223}$	$S_{65} = 4s_{3112}$	$S_{66} = 4s_{1212}$

Table 1.2. *Matrix and tensor components of compliance – appearance of coefficient 2 or 4 is due to the adoption of definition of shear strains in equation [1.11]*

@Seismicisolation

1.2. Technical elastic moduli

These are obtained by industrial tests which are often nearly static ones.

1.2.1. *Tension tests with one normal stress component σ*

$$\{\sigma\} = \{\sigma, 0, 0, 0, 0, 0\}^T \qquad [1.12]$$

is applied in direction 1. The stress state is supposed to be uniaxial and uniform in any sample section.

Bringing [1.12] into [1.9b], the following equations are obtained:

$$\varepsilon_{11} = S_{11}\,\sigma = \frac{\sigma}{E_1} \qquad [1.13a]$$

$$\varepsilon_{22} = S_{21}\,\sigma = -\frac{\nu_{21}}{E_2}\,\sigma \qquad [1.13b]$$

$$\varepsilon_{33} = S_{31}\,\sigma = -\frac{\nu_{31}}{E_3}\,\sigma \qquad [1.13c]$$

$$2\,\varepsilon_{23} = S_{41}\,\sigma = \frac{\eta_{1,23}}{G_{23}}\,\sigma \qquad [1.13d]$$

$$2\,\varepsilon_{13} = S_{51}\,\sigma = \frac{\eta_{1,13}}{G_{13}}\,\sigma \qquad [1.13e]$$

$$2\,\varepsilon_{12} = S_{61}\,\sigma = \frac{\eta_{1,12}}{G_{12}}\,\sigma \qquad [1.13f]$$

1.2.1.1. *Young's modulus E_1*

In such tension tests, a straight sample presented as a rod with uniform section is used for Young's modulus calculation. The lateral boundaries must be free surfaces without applied normal stresses [1.12]:[2]

2 Attempt to transform a tension test into a compression test with normal stress applied to lateral boundaries (so as to prevent buckling) may give rise to false measurement of E_1.

@Seismicisolation

$$\sigma_{22} = \sigma_{33} = 0$$

No shear stresses:

$$\sigma_{23} = \sigma_{31} = \sigma_{12} = 0.$$

1.2.1.2. *Poisson's coefficients*

In equations [1.13b] and [1.13c], ν_{21} and ν_{31} are Poisson's numbers. Symmetry of the compliance matrix implies:

$$\frac{\nu_{ij}}{E_i} = \frac{\nu_{ji}}{E_j} \qquad [1.14]$$

In general ν_{ij} with $i \neq j$ represents the contraction of the thickness in direction j with a normal stress applied in direction i:

$$\varepsilon_{22}/\varepsilon_{11} = -\nu_{21}\frac{E_1}{E_2} = -\nu_{12}.$$

1.2.1.3. *Shear moduli*

G_{ij} with $i \neq j$ are used in the last three equations of [1.13]. They are directly evaluated by other tests.

1.2.1.4. *Lekhnitskii's coefficients $\eta_{i,ij}$ with $i \neq j$*

In [1.13d] rewritten here:

$$2\varepsilon_{23} = \frac{\eta_{1,23}}{G_{23}},$$

coefficient $\eta_{1,23}$ describes a shear strain in the plane (2, 3): $2\varepsilon_{23}$ when a normal stress $\sigma_{11} = \sigma$ is applied in the direction 1.

It describes a coupling (tension shear) which happens in a special direction of anisotropic material.

This direction does not coincide with a direction of symmetry.

@Seismicisolation

1.2.2. *Shear test*

Appropriate loading is applied so the following simple state of stress is obtained:

$$\{\sigma\} = \{0, 0, 0, 0, 0, \tau\}^T \qquad [1.15]$$

Bringing [1.15] into [1.9b]:

$$\varepsilon_{11} = S_{16}\tau = \frac{\eta_{12,1}\tau}{E_1} \qquad [1.16a]$$

$$\varepsilon_{22} = S_{26}\tau = \frac{\eta_{12,2}\tau}{E_2} \qquad [1.16b]$$

$$\varepsilon_{33} = S_{36}\tau = \frac{\eta_{12,3}\tau}{E_3} \qquad [1.16c]$$

$$2\varepsilon_{23} = S_{46}\tau = \frac{\mu_{12,23}\tau}{G_{23}} \qquad [1.16d]$$

$$2\varepsilon_{13} = S_{56}\tau = \frac{\mu_{12,13}\tau}{G_{13}} \qquad [1.16e]$$

$$2\varepsilon_{12} = S_{66}\tau = \frac{\tau}{G_{12}} \qquad [1.16f]$$

1.2.2.1. *Shear or Coulomb's moduli*

Equation [1.16f] permits the evaluation of shear modulus. Shear stress $\sigma_{12} = \tau$ is applied in the plane (1, 2) and strains $2\varepsilon_{12}$ are evaluated in the same plane.

The three shear moduli G_{23}, G_{31}, G_{12} are the inverse of the last three diagonal components of a compliance matrix in the case of orthotropic materials.

@Seismicisolation

$$G_{ij} = \frac{1}{C_{pp}}, i \neq j, \; p = 9 - (i + j) \qquad [1.17]$$

Let us mention that for anisotropic material, two indexes ij ($i \neq j$) are used to describe the plane in which shear stress is applied[3].

1.2.2.2. *The Chentsov coefficient*

$\mu_{ij,\,kl}$ is the mutual influence coefficient describing shear strain appearing in the plane (k, l) when a shear stress is applied in the plane (i, j).

1.2.2.3. *Mutual influence coefficient of the first kind*

$\eta_{\,ij,\,k}$ describes the appearance of normal strain ε_{kk} when a shear stress $\tau = \tau_{ij}$ is applied in the plane (i, j) (relationship [1.16a, b and c]).

1.2.2.4. *Mutual influence coefficient of the second kind*

$\eta_{i,\,jk}$ describes the appearance of a shear strain ε_{jk} when a normal stress σ_{ii} is applied in the direction i (relationship [1.13d, e and f]).

Chentsov's and Lekhnitskii's coefficients are not zero where reference axes are not coincident with the symmetry axes of the material. Tables 1.1 and 1.2 provide the tensorial and matricial definitions of elastic coefficients.

1.3. Real materials with special symmetries

Real natural or artificial materials have some specific symmetries that reduce the number of independent elastic coefficients. Wood is a natural anisotropic material which is orthotropic. It possesses two orthogonal planes of symmetry. Changing reference axes and taking into account those symmetry planes, we must obtain the same elastic coefficients in the representation of compliance matrix {S} or stiffness matrix {C}, see Figure 1.1.

Artificial composite fabricated from a thick layer of unidirectional fibers, which are regularly distributed in the thickness, may be considered as a transverse isotropic material.

The number of elastic constants defined along a symmetry axes is five.

A quasi-transverse isotropic material exists with 90° of rotation around an axis. It possesses six elastic moduli, see Figure 1.2.

3 For isotropic materials, the two indexes are suppressed.

@Seismicisolation

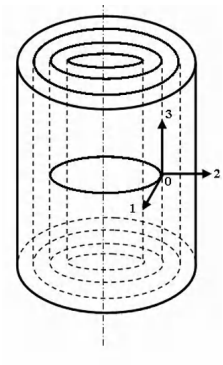

Figure 1.1. *Wood is a natural orthotropic material. It has three orthogonal symmetry planes (1, 3) and (2, 3)*

To define the elastic constants of such materials, we shall take general matrices {S} or {C} and by using an appropriate conversion matrix with specific degree of degree, we will obtain new matrices in which the components must be invariant. In what follows, thanks to the change of reference axes, we shall sweep all the possible symmetries that can exist in the materials. We shall successively define various materials in the mechanical classification framework[4].

1.3.1. *Change of reference axes*

Let the material initially be characterized in reference axes (x, y, z). Let us adopt new reference axes (x′, y′, z′) which are more appropriate for calculations. In Figure 1.3, a flat unidirectional fiber composite and cylindrical shell obtained by filament helicoidal winding is represented with old and new reference axes.

1.3.1.1. *Transformation tensors*

S and C are of fourth order. Change of reference axes applied to C tensor requires the use of direction cosines P_{ij}. The new component c'_{ijkl} is expressed *versus* the old components c_{pqrs} as:

$$\left.\begin{aligned} c'_{ijkl} &= c_{pqrs}\, P_{pi}\, P_{qj}\, P_{rk}\, P_{sl} \\ c_{ijkl} &= c'_{pqrs}\, P_{ip}\, P_{jq}\, P_{kr}\, P_{ls} \end{aligned}\right] \qquad [1.18]$$

4 Another classification exists in crystallography using another vocabulary.

@Seismicisolation

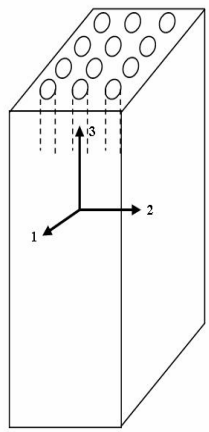

Figure 1.2. *Artificial composite made with unidirectional fibers regularly distributed in the plane (1, 2). It has a symmetry axis (0, 3). In the plane (1, 2) orthogonal to the symmetry axis, the material is isotropic. The material is a transverse isotropic one*

In spite of its apparent simplicity, equation [1.18] requires attention and in the second member there is a sum of terms. Often in the calculation some of the terms are omitted. In practice, using matrices is easier when carrying out manual calculation as well as computer code calculation.

1.3.1.2. *Passage matrices for stress and strain*

Stress and strain are second-order tensors. Changing reference axes, new stresses σ'_{ij} and new strains ε'_{ij} are:

$$\sigma'_{ij} = P_{ki}\, P_{lj}\, \sigma_{kl}\,,\ \sigma_{ij} = P_{ik}\, P_{jl}\, \sigma'_{kl} \qquad [1.19a]$$

$$\varepsilon'_{ij} = P_{ki}\, P_{lj}\, \varepsilon_{kl}\,,\ \varepsilon_{ij} = P_{ik}\, P_{jl}\, \sigma'_{kl} \qquad [1.19b]$$

The following transformation matrix is used:

$$[\,P\,] = \begin{array}{c} \\ x' \\ y' \\ z' \end{array} \begin{bmatrix} x & y & z \\ P_{11} & P_{12} & P_{13} \\ P_{21} & P_{22} & P_{23} \\ P_{31} & P_{32} & P_{33} \end{bmatrix} \qquad [1.20]$$

@Seismicisolation

to go from references (x, y, z) to new references (x′, y′, z′). Rotation is with angle α around axis z.

The transformation matrix is:

$$[\,P\,] = \begin{bmatrix} \cos\alpha & -\sin\alpha & 0 \\ \sin\alpha & \cos\alpha & 0 \\ 0 & 0 & 0 \end{bmatrix} \qquad [1.21]$$

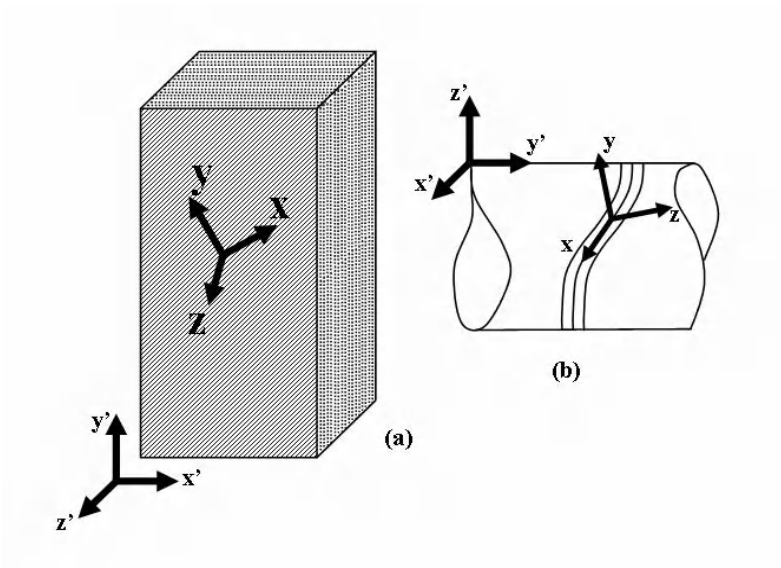

Figure 1.3. *a) Off-axis rod with unidirectional fibers;*
b) Cylindrical shell with helicoidal winding

Matrix [P] is orthogonal, which means that the column vectors (or line vectors) are orthonormal: $[P]^T$ = transpose of [P] with an interchange of lines and columns.

$$[\,P\,]^{-1} = [\,P\,]^{T} \Rightarrow [\,P^{-1}\,]_{ij} = P_{ji} \qquad [1.22]$$

1.3.1.3. *Change of axes for second-order tensors*

$$[\,\sigma\,]' = [\,P\,]^{-1}\,[\,\sigma\,]\,[\,P\,] \qquad [1.23]$$

@Seismicisolation

$$[\varepsilon]' = [P]^{t} [\varepsilon] [P] \qquad [1.24]$$

and then:

$$\{\sigma'\} = \{M_\sigma\} \{\sigma\} \qquad [1.25]$$

$$\{\varepsilon'\} = \{M_\varepsilon\} \{\varepsilon\} \qquad [1.26]$$

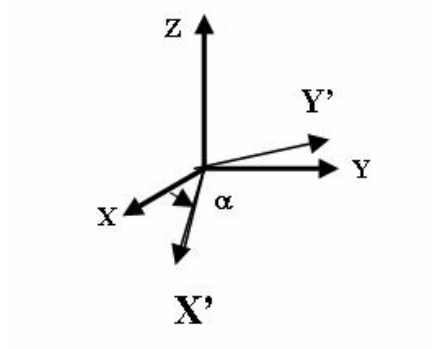

Figure 1.4. *Rotation around z axis*

The 6 x 6 matrices $\{M_\sigma\}$ and $\{M_\varepsilon\}$ are defined as follows:

$$\{M_\sigma\} = \begin{bmatrix} [D_1] & 2[A] \\ [B] & [D_2] \end{bmatrix}, \{M_\varepsilon\} = \begin{bmatrix} [D_1] & [A] \\ 2[B] & [D_2] \end{bmatrix} \qquad [1.27]$$

In equation [1.27], square sub-matrices are defined as:

$$[A] = \begin{bmatrix} P_{21}\ P_{31} & P_{11}P_{31} & P_{11}P_{21} \\ P_{22}\ P_{32} & P_{12}\ P_{32} & P_{12}P_{22} \\ P_{23}\ P_{33} & P_{13}\ P_{33} & P_{13}\ P_{23} \end{bmatrix},$$

$$[B] = \begin{bmatrix} P_{12}\ P_{13} & P_{22}\ P_{23} & P_{32}\ P_{33} \\ P_{11}\ P_{13} & P_{21}\ P_{23} & P_{31}\ P_{33} \\ P_{11}\ P_{12} & P_{21}\ P_{22} & P_{31}\ P_{32} \end{bmatrix}, \qquad [1.28]$$

@Seismicisolation

$$[D_1] = \begin{bmatrix} P_{11}^2 & P_{21}^2 & P_{31}^2 \\ P_{12}^2 & P_{22}^2 & P_{32}^2 \\ P_{13}^2 & P_{23}^2 & P_{33}^2 \end{bmatrix},$$

$$[D_2] = \begin{bmatrix} P_{22}P_{33}+P_{32}P_{23} & P_{12}P_{33}+P_{32}P_{13} & P_{12}P_{23}+P_{22}P_{13} \\ P_{21}P_{33}+P_{31}P_{23} & P_{11}P_{33}+P_{31}P_{13} & P_{11}P_{23}+P_{21}P_{13} \\ P_{21}P_{32}+P_{31}P_{22} & P_{11}P_{32}+P_{31}P_{12} & P_{11}P_{22}+P_{21}P_{12} \end{bmatrix},$$

Equations [1.19a] and [1.19b] show that:

$$\{M_\sigma\}^{-1} = \{M_\varepsilon\}^T = \begin{bmatrix} [D_1]^T & 2[B]^T \\ [A]^T & [D_2]^T \end{bmatrix}$$

[1.29]

$$\{M_\varepsilon\}^{-1} = \{M_\sigma\}^T = \begin{bmatrix} [D_1]^T & [B]^T \\ 2[A]^T & [D_2]^T \end{bmatrix}$$

Matrices $\{M_\sigma\}$ and $\{M_\varepsilon\}$ are not identical because of the adopted definition of the strain vector (equation [1.11]). In the last three components, factor 2 is introduced to describe shear strains.

Rewriting [1.25], [1.26] and [1.27] is accounted for:

$$\{\sigma'\} = \{M_\sigma\}\{\sigma\}, \qquad \{\sigma\} = \{M_\varepsilon\}^T\{\sigma'\}$$

[1.30]

$$\{\varepsilon'\} = \{M_\varepsilon\}\{\varepsilon\}, \qquad \{\varepsilon\} = \{M_\sigma\}^T\{\varepsilon'\}$$

1.3.1.4. *Change of reference axes for {C} and {S} matrices*

$$\{\sigma\} = \{C\}\{\varepsilon\} \qquad \{\varepsilon\} = \{S\}\{\sigma\}$$

$$\{\sigma'\} = \{C'\}\{\varepsilon'\} \qquad \{\varepsilon'\} = \{S'\}\{\sigma'\} \qquad [1.31]$$

@Seismicisolation

Bringing [1.30] into [1.31], we get:

$$\{C'\} = \{M_\sigma\}\ \{C\}\ \{M_\sigma\}^T$$

$$\{S'\} = \{M_\varepsilon\}\ \{C\}\ \{M_\varepsilon\}^T \qquad [1.32]$$

Matricial equalities in [1.32] portray tensorial laws defined in equations [1.19a] and [1.19b].

1.3.1.5. *Rotation around axis z*

Equation [1.21] gives the [P] matrix, from which submatrices [A] [B] [D] and [D_2] are evaluated, see Figure 1.4.

$$[A] = \begin{bmatrix} 0 & 0 & \sin\alpha\cos\alpha \\ 0 & 0 & -\sin\alpha\cos\alpha \\ 0 & 0 & 0 \end{bmatrix}$$

$$[B] = \begin{bmatrix} 0 & 0 & 0 \\ 0 & 0 & 0 \\ -\sin\alpha\cos\alpha & \sin\alpha\cos\alpha & 0 \end{bmatrix} \qquad [1.33]$$

$$[D_1] = \begin{bmatrix} \cos^2\alpha & \sin^2\alpha & 0 \\ \sin^2\alpha & \cos^2\alpha & 0 \\ 0 & 0 & 1 \end{bmatrix}$$

$$[D_2] = \begin{bmatrix} \cos\alpha & -\sin\alpha & 0 \\ \sin\alpha & \cos\alpha & 0 \\ 0 & 0 & \cos 2\alpha \end{bmatrix}$$

1.3.2. *Orthotropic materials possess two orthogonal planes of symmetry*

Passage matrix has diagonal form (see Figure 1.1):

$$[P] = \begin{bmatrix} 1 & 0 & 0 \\ 0 & 1 & 0 \\ 0 & 0 & -1 \end{bmatrix} \qquad [1.34]$$

@Seismicisolation

$\{M_\sigma\}$ and $\{M_\varepsilon\}$ defined in equation [1.27] are diagonal and identical, with the exception of the fourth and fifth terms, where it is equal to -1. Post multiplication of the stiffness matrix by $\{M_\sigma\}^T$ changes the signs of the fourth and fifth columns of this last matrix. Pre-multiplication $[M_\sigma]$, however, changes the sign of the fourth and fifth lines:

$$\{C'\} = \begin{bmatrix} C_{11} & C_{12} & C_{13} & -C_{14} & -C_{15} & C_{16} \\ & C_{22} & C_{23} & -C_{24} & -C_{25} & C_{26} \\ & & C_{33} & -C_{34} & -C_{35} & C_{36} \\ \text{sym} & & & C_{44} & C_{45} & -C_{46} \\ & & & & C_{55} & -C_{56} \\ & & & & & C_{66} \end{bmatrix}, \qquad [1.35]$$

the plane (1, 2) being symmetric $\{C'\} = \{C\}$.

Comparing original matrix $\{C\}$ with equation [1.34], we must set components that change sign to zero.

$$[C] = \begin{bmatrix} C_{11} & C_{12} & C_{13} & 0 & 0 & C_{16} \\ & C_{22} & C_{23} & 0 & 0 & C_{26} \\ & & C_{33} & 0 & 0 & C_{36} \\ \text{sym} & & & C_{44} & C_{45} & 0 \\ & & & & C_{55} & 0 \\ & & & & & C_{66} \end{bmatrix} \qquad [1.36]$$

A second symmetry with respect to plane (2, 3) or (y, z) with similar reasoning gives rise to the following matrix:

$$\{C\} = \begin{bmatrix} C_{11} & C_{12} & C_{13} & 0 & 0 & 0 \\ & C_{22} & C_{23} & 0 & 0 & 0 \\ & & C_{33} & 0 & 0 & 0 \\ \text{sym} & & & C_{44} & 0 & 0 \\ & & & & C_{55} & 0 \\ & & & & & C_{66} \end{bmatrix} \qquad [1.37]$$

@Seismicisolation

Orthotropic material has three orthogonal planes of symmetry and is characterized by nine independent moduli, nine stiffness [1.37], or nine technical moduli [1.38]:

$$\{S\}=\{C\}^{-1} = \begin{bmatrix} \frac{1}{E_1} & -\frac{\nu_{12}}{E_1} & -\frac{\nu_{13}}{E_1} & 0 & 0 & 0 \\ & \frac{1}{E_2} & -\frac{\nu_{23}}{E_2} & 0 & 0 & 0 \\ & & \frac{1}{E_3} & 0 & 0 & 0 \\ & & & \frac{1}{G_{23}} & 0 & 0 \\ \text{sym} & & & & \frac{1}{G_{13}} & 0 \\ & & & & & \frac{1}{G_{12}} \end{bmatrix} \qquad [1.38]$$

An example of a natural orthotropic material is Douglas pinewood.

Samples are taken far from the axes of the trunk body. The stiffness matrix was evaluated and components of {C} are expressed in MPa.

$$\{C\}_{MPa} = \begin{bmatrix} 17{,}000 & 2{,}950 & 1{,}500 & 0 & 0 & 0 \\ 2{,}950 & 2{,}350 & 1{,}100 & 0 & 0 & 0 \\ 1{,}500 & 1{,}100 & 2{,}800 & 0 & 0 & 0 \\ 0 & 0 & 0 & 250 & 0 & 0 \\ 0 & 0 & 0 & 0 & 1{,}100 & 0 \\ 0 & 0 & 0 & 0 & 0 & 1{,}550 \end{bmatrix} \qquad [1.39]$$

Technical elastic moduli were experimentally evaluated, from which rigidity matrix [1.39] is deduced.

E_1 = 13,300 MPa E_2 = 1,550 MPa E_3 = 2,280 MPa

ν_{12} = 1.23 ν_{13} = 0.052 ν_{23} = 0.314

@Seismicisolation

$\nu_{21} = 0.145$ $\nu_{31} = 0.009$ $\nu_{32} = 0.456$

$G_{23} = 250$ MPa $G_{13} = 1{,}100$ MPa $G_{12} = 1{,}350$ MPa

1.3.3. *Quasi-isotropic transverse (tetragonal) material*

In Figure 1.3a (the off-axis rod with unidirectional fibers) the plane of the unidirectional layers are superposed respectively at 0° and 90°. This geometry concerns orthotropic material that remains invariant with 90° rotation around an axis perpendicular to the layers (axis 3). We start with matrix {C} in [1.36] for an orthotropic material. Axis 3 being used for $\pi/2$ rotation, we must obtain six independent elastic moduli.

$$\{C\} = \begin{bmatrix} C_{11} & C_{12} & C_{13} & 0 & 0 & 0 \\ & C_{11} & C_{13} & 0 & 0 & 0 \\ & & C_{33} & 0 & 0 & 0 \\ \text{sym} & & & C_{44} & 0 & 0 \\ & & & & C_{44} & 0 \\ & & & & & C_{66} \end{bmatrix} \qquad [1.40]$$

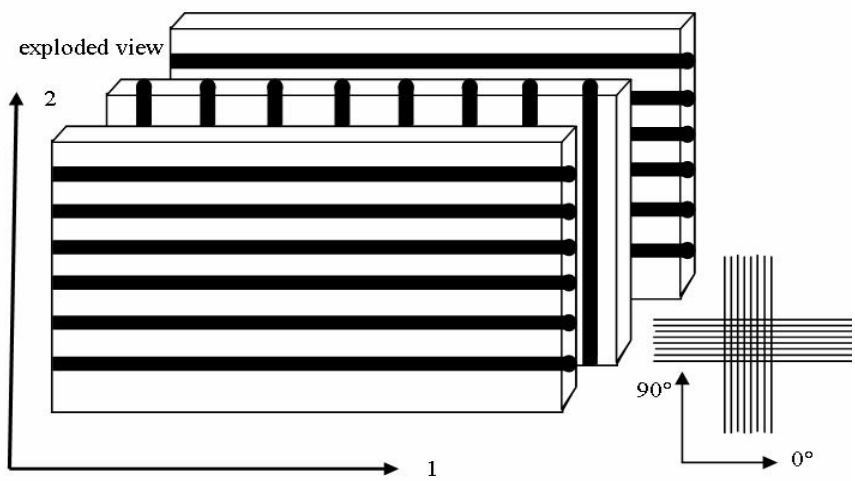

Figure 1.5. *Quasi-isotropic transverse artificial material made with successive layers at 0° and 90°*

@Seismicisolation

An example of this is a multilayered composite made with taffeta tissues – carbon-epoxy with high-strength fibers being 56 % in volume.

$E_1 = E_2 = 57.8$ GPa, $E_3 = 6.9$ GPa

$\nu_{12} = \nu_{21} = 0.025$ $\nu_{13} = \nu_{23} = 0.585$

$\nu_{31} = \nu_{32} = 0.070$

$G_{23} = G_{13} = 3.3$ GPa $G_{13} = 18.0$ GPa

1.3.4. *Transverse isotropic materials (hexagonal system)*

Figure 1.6 represents such an artificial material.

The plane representing a section is a plane of symmetry.

We can consider this to be a special orthotropic material, such that a rotation around z axis with any angle does not modify the elastic constants.

That is:

$$C_{11} = C_{22} \qquad [1.41]$$

and:

$$C_{66} = 2\,(C_{11} - C_{12} - 2\,C_{66})\,\sin^2\alpha\,\cos^2\alpha + C_{66} \qquad [1.42]$$

If we make the bracket equal to zero:

$$C_{66} = \frac{C_{11} - C_{12}}{2} \qquad [1.43]$$

we get the transverse isotropic relationship.

An example of this is a glass-epoxy transverse isotropic composite, 65% of fiber in volume.

@Seismicisolation

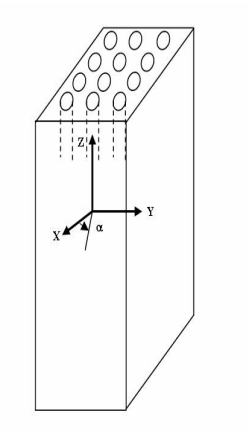

Figure 1.6. *Transverse isotropic material. z is the fiber axis*

$$\{C\} = \begin{bmatrix} C_{11} & C_{12} & C_{13} & 0 & 0 & 0 \\ & C_{11} & C_{13} & 0 & 0 & 0 \\ & & C_{33} & 0 & 0 & 0 \\ \text{sym} & & & C_{44} & 0 & 0 \\ & & & & C_{44} & 0 \\ & & & & & C_{66} = \dfrac{C_{11} - C_{12}}{2} \end{bmatrix} \qquad [1.44]$$

Elastic moduli:

$E_1 = E_2 = 18.5$ GPa $\qquad E_3 = 58.9$ GPa

$v_{12} = v_{12} = 0.425, \qquad v_{13} = v_{23} = 0.038, \qquad v_{31} = v_{32} = 0.122$

$G_{23} = G_{13} = 7.25$ GPa $\qquad G_{12} = 6.5$ GPa

1.3.5. *Quasi-isotropic material (cubic system)*

Such a material has three principal orthogonal axes of symmetry. A rotation with any angle around one of those axes must give rise to the same material. We take an orthotropic material and operate rotation:

@Seismicisolation

$$\{C\} = \begin{bmatrix} C_{11} & C_{12} & C_{12} & 0 & 0 & 0 \\ & C_{11} & C_{12} & 0 & 0 & 0 \\ & & C_{11} & 0 & 0 & 0 \\ \text{sym} & & & C_{44} & 0 & 0 \\ & & & & C_{44} & 0 \\ & & & & & C_{44} \end{bmatrix} \qquad [1.45]$$

Such a material has three independent elastic moduli. A three-dimensional composite with reinforcement in three orthogonal directions has special application in aeronautics.

1.3.6. *Isotropic materials*

We start with [1.45] concerning a quasi-isotropic material and we apply the transverse isotropic relationship [1.41] in order to get sheer stiffness coefficients.

$$\{C\} = \begin{bmatrix} C_{11} & C_{12} & C_{12} & 0 & 0 & 0 \\ & C_{11} & C_{12} & 0 & 0 & 0 \\ & & C_{11} & 0 & 0 & 0 \\ \text{sym} & & & \frac{C_{11}-C_{12}}{2} = C_{44} & 0 & 0 \\ & & & & \frac{C_{11}-C_{12}}{2} = C_{55} & 0 \\ & & & & & \frac{C_{11}-C_{12}}{2} = C_{66} \end{bmatrix}$$

Two independent elastic constants C_{11} and C_{12} are used – stiffness matrix components *versus* Lamé's coefficients. Lamé proposed the two independent elastic constants λ and μ:

$$C_{11} = \lambda + 2\,\mu$$

$$C_{12} = \lambda$$

Then when $C_{ii} = \mu = G$ with $i \geq 4$, $\mu = G$, the shear modulus is called Coulomb's modulus.

@Seismicisolation

Compliance matrix [S] is:

$$[S] = \begin{bmatrix} \frac{1}{E} & -\frac{\nu}{E} & -\frac{\nu}{E} & 0 & 0 & 0 \\ & \frac{1}{E} & -\frac{\nu}{E} & 0 & 0 & 0 \\ & & \frac{1}{E} & 0 & 0 & 0 \\ & & & \left(\frac{2(1+\nu)}{E} = \frac{1}{G}\right) & 0 & 0 \\ & & & & \left(\frac{2(1+\nu)}{E} = \frac{1}{G}\right) & 0 \\ & & & & & \left(\frac{2(1+\nu)}{E} = \frac{1}{G}\right) \end{bmatrix}$$

Usually the components of a compliance matrix are written *versus* the two independent elastic moduli, E and *v* being the Poisson's number.

1.4. Relationship between compliance S_{ij} and stiffness C_{ij} for orthotropic materials

Matrix inversion permits the calculation of compliances:

$$S_{11} = \frac{C_{22}C_{33} - C_{23}^2}{\Delta C} = \frac{1}{E_1}, S_{12} = \frac{C_{23}C_{13} - C_{33}C_{12}}{\Delta C} = -\frac{\nu_{12}}{E_1}$$

$$S_{22} = \frac{C_{33}C_{11} - C_{13}^2}{\Delta C} = \frac{1}{E_2}, S_{13} = \frac{C_{12}C_{23} - C_{22}C_{13}}{\Delta C} = -\frac{\nu_{13}}{E_1}$$

$$S_{33} = \frac{C_{11}C_{22} - C_{12}^2}{\Delta C} = \frac{1}{E_3}, S_{23} = \frac{C_{13}C_{12} - C_{11}C_{23}}{\Delta C} = -\frac{\nu_{23}}{E_1}$$

$$S_{44} = \frac{1}{C_{44}} = \frac{1}{G_{23}}, \quad S_{55} = \frac{1}{C_{55}} = \frac{1}{G_{31}}, \quad S_{66} = \frac{1}{C_{66}} = \frac{1}{G_{12}}$$

@Seismicisolation

with

$$\Delta C = C_{11}C_{22}C_{33} + 2\,C_{12}C_{23}C_{31} - C_{12}^2C_{33} - C^2_{23}C_{11} - C_{13}^2C_{22} \qquad [1.46]$$

Permutation of symbols S and C in [1.42] enables us to obtain the rigidity (or stiffness) matrix *versus* compliance matrix:

$$C_{11} = \frac{1 - \nu_{23}\,\upsilon_{32}}{E_2\,E_3\,\Delta S}, \qquad C_{12} = \frac{\nu_{21} + \nu_{23}\,\nu_{31}}{E_2\,E_3\,\Delta S}$$

$$C_{22} = \frac{1 - \nu_{31}\,\upsilon_{13}}{E_3\,E_1\,\Delta S}, \qquad C_{13} = \frac{\nu_{13} + \nu_{12}\,\nu_{23}}{E_1\,E_2\,\Delta S}$$

$$C_{23} = \frac{1 - \nu_{12}\,\nu_{21}}{E_1\,E_2\,\Delta S}, \qquad C_{23} = \frac{\nu_{32} + \nu_{31}\,\nu_{12}}{E_3\,E_1\,\Delta S}$$

$$C_{44} = \frac{1}{S_{44}} = G_{23}, \; C_{55} = \frac{1}{S_{55}} = G_{13}, \; C_{66} = \frac{1}{S_{66}} = G_{12}$$

$$\Delta S = \frac{1 - \nu_{12}\,\nu_{21} - \nu_{23}\,\nu_{32} - \nu_{31}\,\nu_{13} - 2\nu_{21}\,\nu_{13}\,\nu_{32}}{E_1\,E_2\,E_3} \qquad [1.47]$$

with:

$\nu_{12}\,\nu_{23}\,\nu_{31} = \nu_{21}\,\nu_{13}\,\nu_{32}.$

1.5. Useful inequalities between elastic moduli

Elastic systems are stable. This means that the deformation energy of such systems in order to change from natural state to deformed state must be positive. Consequently, the stiffness matrix as well as the compliance matrix must be positive.

These considerations, presented below, are useful for practitians when checking the calculations of components of stiffness and compliance matrices.

@Seismicisolation

1.5.1. *Orthotropic materials*

In [1.37] and [1.38], the following inequalities are obtained:

$$C_{ij}^2 < C_{ii}\ C_{jj}$$

$$S_{ij}^2 < S_{ii}\ S_{jj} \quad i, j = 1, 2, \ldots, 5, 6 \qquad [1.48]$$

From [1.48] and [1.14] we must obtain:

$$1 - \nu ij\ \nu ji > 0 \quad i, j = 1, 2, 3 \qquad [1.49]$$

and also:

$$\frac{1}{E_i\ E_j} > \frac{\nu_{ij}\ \nu_{ji}}{E_i\ E_j} = \frac{\nu_{ij}^2}{E_i^2}$$

or:

$$\nu_{ij}^2 < \frac{E_i}{E_j} \qquad i, j = 1, 2, 3 \qquad [1.50]$$

Matrix S is positive if and only if its eigenvalues are positive.

Determinants Δ C and Δ S in [1.46] and [1.47], being respectively the products of eigenvalues of stiffness and compliances, are positive:

$$1 - \nu_{12} - \nu_{21} - \nu_{23} - \nu_{32} - \nu_{31} - \nu_{13} - 2\ \nu_{12}\ \nu_{32}\ \nu_{13} > 0$$

This equation can be rearranged as p – p:

$$\nu_{12}\ \nu_{13}\ \nu_{32} < \frac{1 - \nu_{12}\ \nu_{21} - \nu_{23}\ \nu_{32} - \nu_{31}\nu_{13}}{2} < \frac{1}{2}$$

@Seismicisolation

Poisson's number being positive, and finally:

$$\nu_{12}\ \nu_{23}\ \nu_{31} = \nu_{21}\ \nu_{13}\ \nu_{32} < \frac{1}{2} \qquad [1.51]$$

1.5.2. *Quasi-transverse isotropic materials*

If the plane (1, 2) is the quasi-isotropic one, the first three eigenvalues of the stiffness matrix are the solution of the third-degree equation:

$$(C_{11} - C_{12} - \lambda)\left\{\lambda^2 - (C_{11} + C_{12} + C_{33})\lambda + C_{33}(C_{11} + C_{12}) - 2C_{13}^2\right\}$$

The eigenvalues are positive if and only if:

$$\begin{aligned} &C_{11} > C_{12} \\ &C_{44} = C_{55} > 0 \\ &C_{11} + C_{12} + C_{33} > 0 \\ &C_{11} + C_{12} > \frac{2C_{13}^2}{C_{33}} \end{aligned} \qquad [1.52]$$

A similar relationship can be obtained for the compliance matrix by substituting symbol S for C. The last two inequalities of [1.52] give rise to the following inequalities:

$$\begin{aligned} &\nu_{12} < 1 + \frac{E_1}{E_3} \\ &\nu_{13}\ \nu_{31} < \frac{1 - \nu_{12}}{2} \end{aligned} \qquad [1.53]$$

1.5.3. *Transverse isotropic, quasi-isotropic, and isotropic materials*

Equations [1.47] and [1.48] are satisfied for the three classes of materials, taking into account components of matrices C and S for each type of material.

For isotropic and quasi-isotropic materials, the second part of equation [1.48] shows that $v < 0.5$.

@Seismicisolation

1.6. Transformation of reference axes is necessary in many circumstances

1.6.1. *Practical examples*

Samples of composite materials are intentionally tailored in such a way that the axes of the samples do not coincide with the natural axes of the material. Stiffness or compliance matrices are consequently evaluated with sample reference axes.

Multilayered artificial composites for aerospace applications are made with superposition of a certain number of layers glued together. Each layer has its own orientation of reinforced fibers. In the calculation of global stiffness or compliance of the composites, transformation of the reference axis in each layer is necessary for the computation, using finite elements of the structure.

In a mechanical structure using multilayered composite materials, some components of the elastic compliance matrix of the materials are required. The problem is finding an optimized multilayered composite with the relevant number of layers and orientation of fibers in each layer.

In the framework of matrix calculations, this problem is presented in section 1.3.1, equations [1.17] and [1.24]. It is detailed in equations [1.26] to [1.30].

1.6.2. *Components of stiffness and compliance after transformation*

We often have to deal with the problem of rotation around an axis. Below are three tables that will be useful in Chapters 6 to 12 of this book.

If we compare Table 1.3 with Table 1.4, we see that components of new matrix {C} after transformation do not necessarily have the same coefficients. The reason is, if we refer to transformation matrices, that equations [1.24] and [1.25], $\{M_\sigma\}$ and $\{M_\varepsilon\}$ are not the same. We recall that this is due to the definition or technical shear strains in equation [1.11].

However, for the purposes of computation, in the fabrication of codes the following remarks permit the utilization of a unique computer code. Equation [1.53] points out a connection between stiffness and compliance.

If three rotations are effected around three principal axes of an orthotropic material, the problem is reduced to index permutation, a rotation around z axis, the inverse permutation being effected in the next operation.

@Seismicisolation

Table 1.5. concerns elastic technical constants.

$$\left\{\begin{array}{ll} S_{ij} = C_{ij} & i, j = 1, 2, 3 \\ S_{pp} = 4\, C_{pp} & p = 4, 5, 6 \\ S'_{ij} = C'_{ij} & i, j = 1, 2, 3 \\ S'_{pp} = 4\, C'_{pp} & p = 4, 5, 6 \\ S'_{45} = 4\, C'_{45} & \\ S'_{i6} = 2\, C'_{i6} & i = 1, 2, 3 \end{array}\right\} \qquad [1.54]$$

1.6.3. *Remarks on shear elastic moduli G_{ii} (ij = 23, 31, 12) and stiffness constants C_{ii} (with i = 4, 5, 6)*

Comparing Table 1.5 to Table 1.3, we notice that:

$$G'_{23} \neq C'_{44}, \quad G'_{31} \neq C'_{55}, \quad G'_{12} \neq C'_{12}$$

1.6.4. *The practical consequence of a transformation of reference axes*

This problem concerns only anisotropic materials. Compliance and stiffness tensors are of fourth order:

$$c'_{ijkl} = P_{pi} \,.\, P_{qj} \,.\, P_{rk} \,.\, P_{sl} \,.\, c_{pqrs} \qquad [1.55]$$

$P_{\alpha\beta}$ being direction cosine.

In Tables 1.3, 1.4 and 1.5 the consequence of the rank of those tensors is that the power of coefficients in each tensor component is 4. This raises the problem of accuracy and errors in measurements of the new components. Any error in angle α has a strong influence on the evaluated components of the two matrices. In some circumstances, before fabrication of the sample, the angle α has to be optimized.

1.7. Invariants and their applications in the evaluation of elastic constants

In textbooks devoted to continuum mechanics, invariants are extensively used in the study of stress and strain tensors. By definition, invariants are scalars obtained by a combination of matrix (or tensor) elements that remain constant by transformation of the reference axes. For second-order tensors concerning stress and strain, the three invariants are the coefficients of characteristic equation:

$$\det([\sigma] - \lambda\,[I]) = 0 \qquad [1.56]$$

@Seismicisolation

Matrix of rigidity

$$\{C'\} = \{M_\sigma\}\ \{C\}\ \{M_\sigma\}^t$$

$$C'_{11} = C_{11}\cos^4\alpha + 2\left(C_{12} + 2C_{66}\right)\sin^2\alpha\cos^2\alpha + C_{22}\sin^4\alpha$$

$$C'_{12} = \left(C_{11} + C_{12} - 4C_{66} - 2C_{12}\right)\sin^2\alpha\cos^2\alpha + C_{12}$$

$$C'_{13} = C_{13}\cos^2\alpha + C_{23}\sin^2\alpha$$

$$C'_{14} = C'_{15} = 0$$

$$C'_{16} = \left[C_{22}\sin^2\alpha - C_{11}\cos^2\alpha + \left(C_{12} + 2C_{66}\right)\left(\cos^2\alpha - \sin^2\alpha\right)\right]\sin\alpha\cos\alpha$$

- -

$$C'_{22} = C_{11}\sin^4\alpha + 2\left(C_{12} + 2C_{66}\right)\sin^2\alpha\cos^2\alpha + C_{22}\cos^4\alpha$$

$$C'_{23} = C_{13}\sin^2\alpha + C_{23}\cos^2\alpha$$

$$C'_{24} = C'_{25} = 0$$

$$C'_{26} = \left[C_{22}\cos^2\alpha - C_{11}\sin^2\alpha - \left(C_{12} + 2C_{66}\right)\left(\cos^2\alpha - \sin^2\alpha\right)\right]\sin\alpha\cos\alpha$$

- -

$$C'_{33} = C_{33}$$

$$C'_{34} = C'_{35} = 0$$

$$C'_{36} = \left(C_{23} - C_{13}\right)\sin\alpha\cos\alpha$$

- -

$$C'_{44} = C_{44}\cos^2\alpha + C_{55}\sin^2\alpha$$

$$C'_{45} = \left(C_{44} - C_{55}\right)\sin\alpha\cos\alpha$$

$$C'_{46} = 0$$

- -

$$C'_{55} = C_{44}\sin^2\alpha + C_{55}\cos^2\alpha$$

$$C'_{56} = 0$$

- -

$$C'_{66} = \left(C_{11} + C_{12} - 2C_{12} - 4C_{66}\right)\sin^2\alpha\cos^2\alpha + C_{66}$$

Table 1.3. *Rotation with an angle α around z axis and its influence on stiffness matrix {C} of an orthotropic material*

@Seismicisolation

Compliance matrix

$$\{S'\} = \{M_\varepsilon\}\{S\}\{M_\varepsilon\}^t$$

$$S'_{11} = S_{11}\cos^4\alpha + (S_{66} + 2S_{12})\sin^2\alpha\cos^2\alpha + S_{22}\sin^4\alpha$$

$$S'_{12} = (S_{11} + S_{22} - S_{66} - 2S_{12})\sin^2\alpha\cos^2\alpha + S_{12}$$

$$S'_{13} = S_{13}\cos^2\alpha + S_{23}\sin^2\alpha$$

$$S'_{14} = S'_{15} = 0$$

$$S'_{16} = 2\left[S_{22}\sin^2\alpha - S_{11}\cos^2\alpha + \left[S_{12} + \frac{S_{66}}{2}\right](\cos^2\alpha - \sin^2\alpha)\right]\sin\alpha\cos\alpha$$

- -

$$S'_{22} = S_{11}\sin^4\alpha + (S_{66} + 2S_{12})\sin^2\alpha\cos^2\alpha + S_{22}\cos^4\alpha$$

$$S'_{23} = S_{13}\sin^2\alpha + S_{23}\cos^2\alpha$$

$$S'_{12} = S'_{25} = 0$$

$$S'_{26} = 2\left[S_{22}\cos^2\alpha - S_{11}\sin^2\alpha - \left[S_{12} + \frac{S_{66}}{2}\right](\cos^2\alpha - \sin^2\alpha)\right]\sin\alpha\cos\alpha$$

- -

$$S'_{33} = S_{33}$$

$$S'_{34} = S'_{35} = 0$$

$$S'_{36} = 2(S_{23} - S_{13})\sin\alpha\cos\alpha$$

- -

$$S'_{44} = S_{44}\cos^2\alpha + S_{55}\sin^2\alpha$$

$$S'_{45} = (S_{44} - S_{55})\sin\alpha\cos\alpha$$

$$S'_{46} = 0$$

- -

$$S'_{55} = S_{44}\sin^2\alpha + S_{55}\cos^2\alpha$$

$$S'_{56} = 0$$

- -

$$S'_{66} = 4(S_{11} + S_{22} - 2S_{12} - S_{66})\sin^2\alpha\cos^2\alpha + S_{66}$$

Table 1.4. *Rotation with an angle α around z axis and its influence on compliance matrix {S} of an orthotropic material*

@Seismicisolation

Technical elastic moduli

$$\frac{1}{E_1'} = S_{11}' = \left(\frac{\cos^4\alpha}{E_1}\right) + \frac{\sin^4\alpha}{E_2} + \frac{\sin^2\alpha\,\cos^2\alpha}{G_{12}} - \frac{2\,\nu_{12}}{E_1}\sin^2\alpha\,\cos^2\alpha$$

$$\frac{1}{E_2'} = S_{22}' = \frac{\sin^4\alpha}{E_1} + \frac{\cos^4\alpha}{E_2} + \frac{\sin^2\alpha\,\cos^2\alpha}{G_{12}} - \frac{2\,\nu_{12}}{E_1}\sin^2\alpha\,\cos^2\alpha$$

$$E_3' = E_3$$

- - - -

[I] being the identity matrix:

$$[\,I\,] = \begin{bmatrix} 1 & 0 & 0 \\ 0 & 1 & 0 \\ 0 & 0 & 1 \end{bmatrix}$$

For the stress matrix we have[5]:

$$I(\sigma) = \frac{\sigma_{11} + \sigma_{22} + \sigma_{33}}{3} \quad \text{linear invariant}$$

$$II(\sigma) = \frac{1}{2}\left(\sigma_{ij}\,\sigma_{ji} - \sigma_{ij}\,\sigma_{ij}\right) \quad \text{quadratic invariant}$$

$$III(\sigma) = \det[\sigma] \quad \text{cubic invariant (determinant)}$$

In a plane stress state, the two first invariants are graphically represented by the Mohr circle [TSA 80]. This representation is convenient for the experimental evaluation of strains by strain gauges.

For fourth rank tensors, calculation of invariants is similar to that which is presented above. The number of invariants is higher. There are five invariants of the first order, two invariants of the second order, and one of the third order.

Details of the calculation can be found in [CHE 96, JON 75, LEK 60, TSA 80].

1.7.1. *Elastic constants versus invariants*

Table 1.6 collects the invariants of the three-species material, which when examined are orthotropic. It is easy to convert the expressions for another type of material (quasi-isotropic transverse, isotropic transverse or cubic ones).

---

5 Developing $II(\sigma)$, $III(\sigma)$ we obtain:

$$II(\sigma) = \sigma_{11}\,\sigma_{22} + \sigma_{22}\,\sigma_{33} + \sigma_{33}\,\sigma_{11} - \sigma_{13}^2 - \sigma_{21}^2 - \sigma_{32}^2$$

$$III(\sigma) = \sigma_{11}\,\sigma_{22}\,\sigma_{33} + 2\,\sigma_{12}\,\sigma_{13}\,\sigma_{23} - \sigma_{22}\,\sigma_{13}^2 - \sigma_{33}\,\sigma_{12}^2 - \sigma_{11}\,\sigma_{23}^2$$

@Seismicisolation

Components of stiffness matrix {C} are expressed against the invariants as follows:

$$C'_{11} = U_1 + U_2 \cos 2\alpha + U_3 \cos 4\alpha$$

$$C'_{12} = U_4 - U_3 \cos 4\alpha$$

$$C'_{13} = V_1 + V_2 \cos 2\alpha$$

$$C'_{16} = -\frac{U_2}{2} \sin 2\alpha - U_3 \sin 4\alpha$$

$$C'_{22} = U_1 - U_2 \cos 2\alpha + U_3 \cos 4\alpha$$

$$C'_{23} = V_1 - V_2 \cos 2\alpha \qquad [1.57]$$

$$C'_{26} = -\frac{U_2}{2} \sin 2\alpha + U_3 \sin 4\alpha$$

$$C'_{36} = -\frac{V_2}{2} \sin 2\alpha$$

$$C'_{44} = W_1 + W_2 \cos 2\alpha$$

$$C'_{45} = W_2 \sin 2\alpha$$

$$C'_{55} = W_1 - W_2 \cos 2\alpha$$

$$C'_{66} = U_5 - U_3 \cos 4\alpha$$

with:

$$U_1 = \frac{3C_{11} + 3C_{22} + 2C_{12} + 4C_{66}}{8}$$

$$U_2 = \frac{C_{11} - C_{22}}{2}$$

@Seismicisolation

$$U_3 = \frac{C_{11} + C_{22} - 2\,C_{12} - 4\,C_{66}}{8}$$

$$U_4 = \frac{C_{11} + C_{22} + 6\,C_{12} - 4\,C_{66}}{8}$$

$$U_5 = \frac{C_{11} + C_{22} - 6\,C_{12} - 4\,C_{66}}{8} \qquad [1.58]$$

$$V_1 = \frac{C_{13} + C_{23}}{2}$$

$$V_2 = \frac{C_{13} - C_{23}}{2}$$

$$W_1 = \frac{C_{44} + C_{55}}{2}$$

$$W_2 = \frac{C_{44} - C_{55}}{2}$$

The invariants presented in Table 1.6 are independent. By combination, other families of invariants can be obtained.

U_1, U_2, U_3 and U_4 in [1.58] can be considered to be a linear combination of invariants or power of invariants.

$$\frac{3\,C'_{11} + 3\,C'_{22} + 2\,C'_{12} + 4\,C'_{66}}{8} = \frac{I_1(C) + 2\,I_2(C)}{8} = U_1$$

$$\frac{C'_{11} + C'_{22} + 6\,C'_{12} - 4\,C'_{66}}{8} = \frac{3\,I_1(C) - 2\,I_2(C)}{8} = U_4 \qquad [1.59]$$

$$\frac{C'_{11} + C'_{22} - 2\,C'_{12} + 4\,C'_{66}}{8} = \frac{2\,I_1(C) - 2\,I_2(C)}{8} = U_5 = \frac{U_1 - U_4}{2}$$

$$C'_{11}C'_{22} + 2\,C'_{66}\left(C'_{11} + C'_{22}\right) - C'^2_{12} - 2C'^2_{16} - 2C'^2_{26} = U_1^2 - U_2^2 - U_4^2 - 4U_3^2$$

@Seismicisolation

1.7.2. *Practical utilization of invariants in the evaluation of elastic constants*

Measurements of elastic constants are subject to errors of different kinds:

– error of angle α due to the fabrication of a sample's dimension error;

– dimension errors of the samples;

– errors in measurement during static or dynamics tests.

Evaluation of elastic constants cannot be reduced to a restricted number of measurements. We have to deal with an optimization problem with α as a parameter.

The first stage concerns evaluation of elastic constants (C_{ij} or S_{ij}). Each set of experimental results corresponds to an angle α in equations [1.57] to [1.58].

In the second stage, the calculation of invariants in Table 1.6 is carried out. Optimization of invariants constitutes the third step. From optimized invariants, elastic constants are calculated from [1.57].

1.8. Plane elasticity

In many mechanical structures, plate and/or shell elements are used. In such elements, the thickness is small compared to other dimensions. For plates, the number of stress and strain components is reduced to three.

In Figure 1.7, axis 3 is directed through the thickness.

1.8.1. *Expression of plane stress stiffness versus compliance matrix*

Components S_{ij}:

$$\{\sigma\}^T = (\sigma_{11} \;\; \sigma_{22} \;\; 0 \;\; 0 \;\; 0 \;\; \sigma_{12}) \qquad [1.60]$$

is the plane stress vector applied in plane (1, 2), then for orthotropic material:

$$\{\varepsilon\}^T = (\varepsilon_{11} \;\; \varepsilon_{22} \;\; \varepsilon_{33} \;\; 0 \;\; 0 \;\; 2\varepsilon_{12})$$

@Seismicisolation

Constitutive equations in matrix forms are:

$$\begin{Bmatrix} \varepsilon_{11} \\ \varepsilon_{22} \\ 2\varepsilon_{12} \end{Bmatrix} = \begin{bmatrix} S_{11} & S_{12} & 0 \\ 0 & S_{22} & 0 \\ 0 & 0 & S_{66} \end{bmatrix} \begin{Bmatrix} \sigma_{11} \\ \sigma_{22} \\ \sigma_{12} \end{Bmatrix} \qquad [1.61]$$

Stiffness matrix

Compliance matrix	
Linear invariants	
$I_1(C) = C'_{11} + C'_{22} + 2C'_{12} = 2(U_1 + U_4)$ $I_2(C) = C'_{11} + C'_{22} + 2C'_{66} = 2(U_1 + U_5)$ $I_3(C) = C'_{66} - C'_{12} = U_5 - U_4$ $I_4(C) = C'_{13} + C'_{23} = 2V_1$ $I_5(C) = C'_{44} + C'_{55} = 2W_1$	$I_1(S) = S'_{11} + S'_{22} + 2S'_{12}$ $I_2(S) = S'_{11} + S'_{22} + \frac{S'_{66}}{2}$ $I_3(S) = \frac{(S'_{66} - 4S'_{12})}{4}$ $I_4(S) = S'_{13} + S'_{23}$ $I_5(S) = S'_{44} + S'_{55}$
Quadratic invariants	
$II_1^2(C) = \frac{(C'_{11} - C'_{22})^2 + 4(C'_{16} + C'_{26})^2}{4} = U_2^2$ $II_2^2(C) = \left\{ \begin{matrix} (C'_{11} - C'_{22} - 2C'_{12} - 4C'_{66})^2 \\ +16(C'_{26} - C'_{16})^2 \end{matrix} \right\} / 16 = 4U_3^2$	$II_1^2(S) = (S'_{11} - S'_{22})^2 + (S'_{16} - S'_{26})^2$ $II_2^2(S) = \left\{ \begin{matrix} (S'_{11} - S'_{22} - 2S'_{12} - S'_{66})^2 \\ +4(S'_{26} - S'_{16})^2 \end{matrix} \right\} / 16$
Cubic invariants	
$III_1(C) = \det(C)$	$III_2(S) = \det(S)$

Table 1.6. *Expressions of invariants* versus *components of stiffness matrix {C'} components or compliance matrix {S'}*

@Seismicisolation

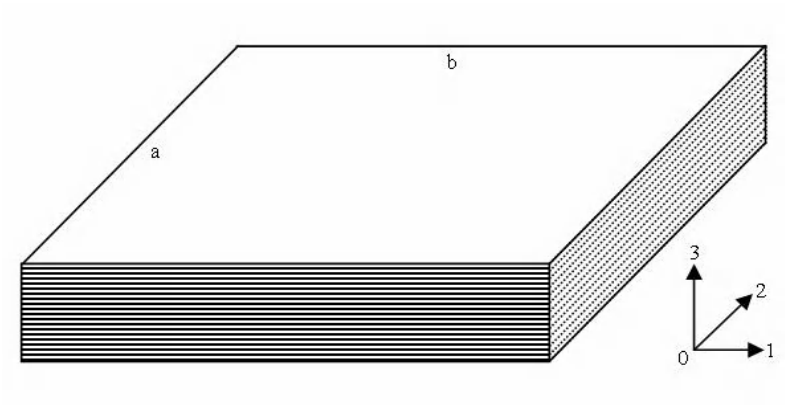

Figure 1.7. *Plate element with reference axes*

and then:

$$\begin{Bmatrix} \sigma_{11} \\ \sigma_{22} \\ \sigma_{12} \end{Bmatrix} = \begin{bmatrix} Q_{11} & Q_{12} & 0 \\ Q_{12} & Q_{22} & 0 \\ 0 & 0 & Q_{66} \end{bmatrix} \begin{Bmatrix} \varepsilon_{11} \\ \varepsilon_{22} \\ 2\varepsilon_{12} \end{Bmatrix} \qquad [1.62]$$

In [1.61], components of the stiffness matrix are not equal to those of the [C] matrix.

Inversion of reduced matrix [S] in [1.56] to obtain [Q] matrix is straight forward.

$$Q_{11} = \frac{S_{22}}{S_{11}\ S_{22} - S_{12}^2} = \frac{E_1}{1 - \nu_{12}\ \nu_{21}}$$

$$Q_{22} = \frac{S_{11}}{S_{11}\ S_{22} - S_{12}^2} = \frac{E_2}{1 - \nu_{12}\ \nu_{21}} \qquad [1.63]$$

$$Q_{12} = \frac{S_{12}}{S_{11}\ S_{22} - S_{12}^2} = \frac{\nu_{12}\ E_2}{1 - \nu_{12}\ \nu_{21}} = \frac{\nu_{21}\ E_1}{1 - \nu_{12}\ \nu_{21}}$$

$$Q_{66} = \frac{1}{S_{66}} = C_{66} = G_{12}$$

@Seismicisolation

In plane stresses, the stiffnesses of Q_{ij} are different from C_{ij}, which appears in the three-dimensional constitutive equation.

1.8.2. *Plane stress stiffness components versus three-dimensional stiffness components*

Setting normal stress in the plate thickness to zero, from [1.9], we obtain:

$$\varepsilon_{33} = -\frac{C_{13}\ \varepsilon_{11} + C_{23}\ \varepsilon_{22}}{C_{33}} \qquad [1.64]$$

Substituting in σ_{212} the value of ε_{33} in [1.64]:

$$Q_{11} = C_{11} - \frac{C_{13}^2}{C_{33}}, \qquad Q_{22} = C_{22} - \frac{C_{23}^2}{C_{33}} \qquad [1.65]$$

$$Q_{12} = C_{12} - \frac{C_{13}\ C_{23}}{C_{33}}$$

or in a general manner:

$$Q_{ij} = C_{ij} - C_{i3}\ \frac{C_{j3}}{C_{33}} \qquad [1.66]$$

Equation [1.66] shows that $Q_{ij} \leq C_{ij}$. In the case of isotropic material, $\nu_{ij} = \nu$ and the Young's modulus for plane stress is:

$$E_{\text{plane stress}} = \frac{E}{1-\nu^2} > E$$

E being Young's modulus for a three-dimensional stress state.

1.9. Elastic previsional calculations for anisotropic composite materials

Isotropic elastic materials have two elastic moduli (or stiffness coefficients). Their order of magnitude for a given material is known. The choice of experimental method and instrumentation are not difficult to determine. For anisotropic materials,

@Seismicisolation

particularly artificial composite materials, there are a variety of materials whose elastic moduli are not necessarily known in advance. The global material properties of such materials depend on a certain number of factors[6], which depend on the geometrical disposition of reinforced fibers in the matrix.

1.9.1. *Long fibers regularly distributed in the matrix*

This material is extensively used in the aerospace and aeronautical industries. Its applications are extended to the automobile and sailing ship industry. This material is considered as a transverse isotropic one.

Figure 1.8 shows a transverse cross-section in which fibers are regularly disposed in quincunx in the matrix.

Instead of studying the whole distribution of fibers in the section, let us consider the *representative elementary volume* (REV), which is the minimum volume of material that is supposed to possess the complete properties of the material. If this hypothesis is acceptable, the problem is reduced to that concerning the REV.

The second hypothesis, illustrated in Figure 1.9, is to replace the hexagonal cross-section of REV by a circular cross-section on the condition that the volume percentage of fiber in the REV is the same for the whole composite. For this purpose, the hexagonal frontier is replaced by a circular boundary. By using cylindrical coordinates, the new problem is simpler. Appendix 1.A presents some complements concerning the mathematical formulation of the problem.

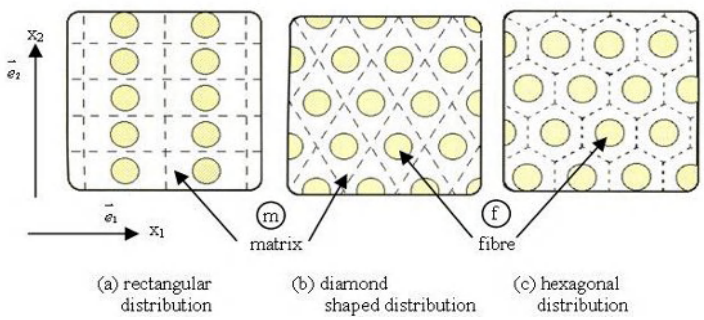

Figure 1.8. *The three possible periodic distributions of fibers in the matrix: a) orthotropic material (nine independent elastic constants); b) diamond-shaped distribution (six independent elastic constants); and c) hexagonal distribution (E elastic constants)*

6 This section is helpful for the reader when choosing appropriate experimental set-ups. Space limitation has led us to limit the presentation to some useful previsional calculation formulae.

@Seismicisolation

The homogenousequivalent material has the following effective stiffness coefficients $C_{ij}^{(e)} = \overline{C}_{ij}$ (index m is related to matrix, index f is related to fiber and exponent (e) is related to composite material) [CHE 73]:

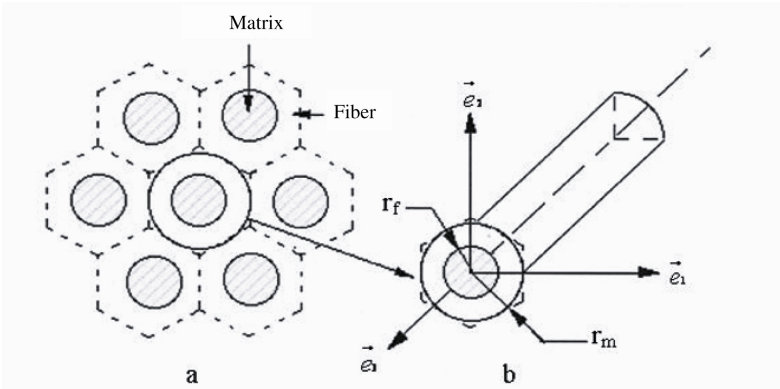

Figure 1.9. *Hexagonal distribution retained for the provisional calculation: a) in a cross-section, the hexagon is retained as the elementary representative volume (REV); b) replacement of hexagonal REV by circular cylinder, r_m and r_f being radii of the fiber matrix*

$$\left.\begin{aligned}
\overline{C}_{11} &= \overline{C}_{22} = \mu_m \left(T_0 + T_2 \right) \\
\overline{C}_{12} &= \mu_m \left(T_0 - T_2 \right) \\
\overline{C}_{13} &= \overline{C}_{23} = 4\,\mu_m \left[v_f\, \nu_f\, Q\, f_0 + \nu_m\, c_0 \left(1 - v_f\right) \right] \\
\overline{C}_{44} &= \overline{C}_{55} = \mu_m \frac{\left(1+Q\right) + \left(Q-1\right) v_f}{\left(1+Q\right) - \left(Q-1\right) v_f} \\
\overline{C}_{33} &= v_f \left(E_f - E_m \right) + E_m + \overline{C}_{13}^{2} / \mu_m T_0
\end{aligned}\right\} \qquad [1.67]$$

in which Q, T_0 and T_2 are given by:

$$Q = \frac{\mu_f}{\mu_m} \qquad [1.68]$$

the ratio of shear modulus of fiber (index f) on shear modulus of matrix (index m):

@Seismicisolation

$$T_0 = 4\,C_0\left(1-\nu_m\right)-1 \qquad [1.69]$$

$$T_2 = 1 + 8\left(1-\nu_m\right)\left[b_2 v_f^2 + C_2\left(1-2\,\nu_m\right)/v_f\right] \qquad [1.70]$$

$$C_0 = \frac{Q + 1-\nu_f}{2\left(1-2\,\nu_m\right)\left(1-v_f\right)Q + \left(1-2\,\nu_f\right)\left(1-2\,\nu_f + v_f\right)} \qquad [1.71]$$

$$f_0 = \frac{1-\nu_2}{2\left(1-2\,\nu_m\right)\left(1-v_f\right)Q + \left(1-2\,\nu_f\right)\left(1-2\,\nu_f + v_f\right)} \qquad [1.72]$$

with ν_m and ν_f as the Poisson's coefficients of matrix and fiber respectively.

$$b_2 = \frac{3(1-Q)}{2\,\Delta_1}\left\{\left[3-4\,\nu_f + Q\right]\begin{bmatrix} v_f^2 - v_f^3 + \left(1-v_f^3\right)\left(3-4\,\nu_m\right) \\ +4\left(\nu_m - 1\right)v_f^2\left[\left(4\nu_f - 3\right) + Q\left(1-v_f\right)\right]\end{bmatrix}\right\}$$

[1.73]

$$c_2 = \frac{3\,v_f^2(1-Q)\left(1-v_f\right)(3-4\,\nu_f + Q)}{\Delta_1} \qquad [1.74]$$

with:

$$\Delta_1 = \left\{\begin{matrix} \left\{(4\,v_1 - 3)\left[v_f + Q(1-v_f)\right]-1\right\} \\ \left\{3(3-4v_f+Q)(3-4v_m)(1-v_f^2) + 12v_f^2(v_m-1)(4v_f-3\right\} - \\ -9v_f(1-Q)(3-4v_f+Q)(1-v_f)^2 \end{matrix}\right\}$$

$$v_f = \frac{r_m^2}{r_f^2} = \frac{\text{square of matrix radius}}{\text{square of fiber radius}} \text{ (see Figure 1.8)} \qquad [1.75]$$

where E_f is Young's modulus of the fiber and E_m matrix is Young's modulus. In [1.67], the material components (fiber and matrix) are supposed to be isotropic. The

@Seismicisolation

formulae in [1.67] give the stiffness matrix coefficients *versus* the volume percentage of fiber [1.75] and the elastic moduli (E_f, E_m), (ν_f, ν_m) of fiber and matrix.

Fiber	**Graphite**	**Boron**	**Carbon**	**Glass**	**Glass**	**Kevlar 49**
Matrix	*Epoxy*	*Epoxy*	*Epoxy*	*Polyester*	*Epoxy*	*Epoxy*
Composite's mass density (kg/m^3)	1,200	2,600	1,485	2,010	1,870	1,100
$\bar{C}_{11} = \bar{C}_{22}$ (GPa)	9.4	26.5	8.9	17.25	18.42	8.85
$\bar{C}_{33}$ (GPa)	124.1	260	130	42.5	47.24	44.5
$\bar{C}_{44} = \bar{C}_{55}$ (GPa)	4.14	5.2	2.62	5.02	7.7	3
$\bar{C}_{66}$ (GPa)	2.54	7.3	2.26	3.81	4.12	2.68
$\bar{C}_{12}$, [1.42] (GPa)	4.32	11.9	4.38	9.63	10.18	3.5
$\bar{C}_{33} / \bar{C}_{44}$	30	50	49.38	8.47	6.14	14.88

Table 1.7. *Elastic stiffness concerning some (unidirectional fiber-matrix) long fiber composite, fiber direction: 3*

REMARKS:

Accuracy of previsional calculations depends on the accuracy of the volumic percentage. It also depends on the accuracy obtained for the elastic constants of the two components (fiber and matrix).

Percentage of void is the consequence of imperfection. The void is the third constituent. If the void percentage is known, for the first estimation of composite elastic coefficients we suggest calculation of a matrix with voids assumed to be regularly distributed in the mass.

@Seismicisolation

Imperfection of fiber distribution in the matrix gives rise to the enlargement of the ranges inside which the elastic coefficients of a composite material are situated. There are at least three methods of calculation [BEH 69, PIC 68].

$\bar{C}_{ij}$	Chevalier-Vinh's solution [CHE 73, 75]	Pickett's solution [PIC 68]	Behrens's solution [BEH 69]	Vinh's ultrasonic measurements
$\bar{C}_{11}$ (GPa)	16.16	16.84	16.51	17.40 ± 0.30
$\bar{C}_{12}$ (GPa)	7.18	6.67	6.83	7.56 ± 0.50
$\bar{C}_{13}$ (GPa)	5.69	5.71	5.69	6.80 ± 0.80
$\bar{C}_{33}$ (GPa)	51.40	51.41	51.42	42.0 ± 1.0
$\bar{C}_{44}$ (GPa)	5.15	5.19	5.15	5.70 ± 0.12
$\bar{C}_{66}$ (GPa)	4.49	5.09	4.83	4.92 ± 0.10

Table 1.8. *Long-fiber reinforced composite silicon-phenolic resin. Ultrasonic measurements must be considered as the upper bounds of stiffness coefficients, the material being viscoelastic*

Figure 1.10 presents the outcomes of the three methods that give similar results. Discrepancies between methods globally do not exceed 5%, see Figure 1.11:

– fiber: $E_f = 75.0$ MPa, $\nu_f = 0.2$;

– matrix: $E_m = 3.71$ MPa, $\nu_m = 0.34$;

– volumic percentage of fibers: 63%;

– fiber: $E_f = 75.0$ GPa, $\nu_f = 0.2$;

– matrix: $E_m = 3.71$GPa, $\nu_m = 0.34$, previsional.

The general idea adopted in previsional calculation methods is homogenization theory, which substitutes the REV containing of all the constituents with a homogenized one.

@Seismicisolation

In the application of this idea, we can adopt various methods that can be different in principle. Pickett [PIC 68] and Chevalier [CHE 73, CHE 75] adopt an elastostatic method. Behrens used an elastodymanic method with plane wave propagation in heterogeneous and periodic media, the wavelength being large with respect to the dimension of mechanical network.

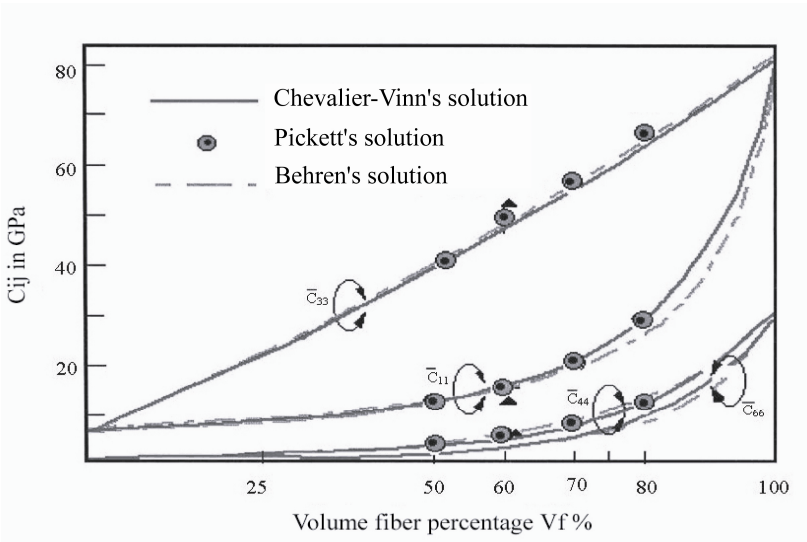

Figure 1.10. *Elastic constant* $\overline{C}_{ij}$ *of a composite with hexagonal symmetry. Comparison between three existing methods of previsional calculations*

1.9.2. *Stratified composite materials*

Stratified composite materials consist of a set of isotropic or anisotropic layers and, as shown in Figure 1.11, there is a large variety of lamellar composite materials. The difference between stratified composite, sandwich and composite laminates resides in the following characteristics.

In stratified material, there are a great number of layers (at least a dozen). Stratified material is seen as quasi-homogenous and anisotropic. The position of each layer is consequently not important.

Sandwich materials consist of three layers. The stiffness of the external layers is outstanding in comparison with those of the internal layer. Sandwich composites are light-weight materials.

@Seismicisolation

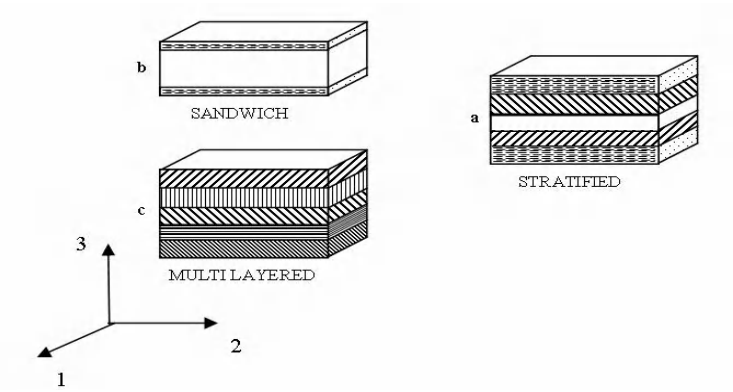

Figure 1.11. *Various types of lamellar composite materials: a) stratified; b) sandwich; c) composite laminates*

Composite laminates are structures made of a set of unidirectional laminates. The geometry and position of each layer are important in the global strength of the composite. Since lamina orientation varies across thickness, the stiffness for each orientation can be expressed in terms of a material's stiffness and orientation angle α.

Stratified composite materials are periodic in direction 3. The periodic REV is an infinite plate (directions 1 and 2) with typical configuration. The homogenous equivalent material has the following tensorial stiffness coefficients [BEH 69]:

$$\boxed{\bar{c}_{ijkl} = \langle c_{ijkl} \rangle + \sum_{p,q=1,2,3} \langle c_{ijp3}\, g^{-1}_{pq} \left[\sum_{p,q=1,2,3} \langle g^{-1} \rangle^{-1}_{qs} \langle g^{-1}_{sr}\, c_{r3kl} \rangle - c_{q3kl} \right] \rangle} \qquad [1.76]$$

In equation [1.76], the average stiffness component value in the REV, for example, is:

$$\bar{c}_{ijkl} = \frac{\int_0^e c_{ijkl}(z)\, dz}{e}$$

where e is the thickness of REV.

$[g] = (g_{ij}) = (c_{i3j3})$ 3 x 3 symmetrical matrix.

@Seismicisolation

The matrix representation of stiffness coefficients is given in Table 1.1. When every N layer of REV consists of an orthotropic material in coordinate system (1, 2, 3), the set of equations [1.75] becomes:

$$\bar{C}_{ij} = \sum_{n=1}^{n=N} v_n \left(C_{ij}^{(n)} - \frac{C_{i3}^{(n)} C_{j3}^{(n)}}{C_{33}^{(n)}} \right) + \left(\sum_{n=1}^{n=N} v_n \frac{C_{i3}^{(n)}}{C_{33}^{(n)}} \right) \left(\sum_{n=1}^{n=N} v_n \frac{C_{j3}^{(n)}}{C_{33}^{(n)}} \right) \left(\sum_{n=1}^{n=N} \frac{v_n}{C_{33}^{(n)}} \right)^{-1}$$

i= 1, 2, 3 ; j= 1, 2, 3

$$\bar{C}_{ii} = \left(\sum_{n=1}^{n=N} \frac{v_n}{C_{33}^{(n)}} \right)^{-1} \qquad i = 4, 5 \qquad [1.77]$$

$$\bar{C}_{66} = \sum_{n=1}^{n=N} v_n C_{66}^{(n)}$$

where $\left[C^{(n)} \right] = (C_{ij}^{(n)})$ is the stiffness matrix and v_n the volume fraction of nth layer in the REV.

1.9.3. *Reinforced fabric composite materials*

Fabrics with periodically arranged warp and weft are largely used in reinforced composites. In the application of such fabric immersed in a resin matrix, there is a variety of lamellar fabric composite materials.

1.9.3.1. *Presentation of the three kinds of fabric composites*

Figure 1.12 shows the three kinds of fabric composite materials:

– taffeta;

– serge; and

– satin.

The weaving is characterized by the weaving parameter or frame ratio n_t, which is the number of yarns in a period:

– $e_b = \frac{l - l_0}{l}$ is the shortening of warp yarns in weaving (it is of the order 0.05);

– v_f is the volumic percentage of fibers (50% to 55%);

@Seismicisolation

– v1 is the volumic percentage impregnation of tuft (70% to 80%);

– R is the rate of recovery (0.7–0.8) related to weight of tissue per square meter.

In Figure 1.12, the value of n_l is given for each kind of tissue.

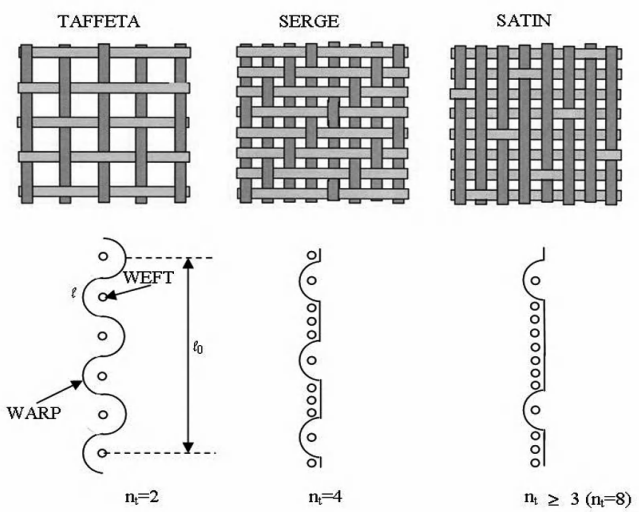

Figure 1.12. *The three kinds of fabrics*

1.9.3.2. *Modeling of a taffeta fabric*

Figure 1.13 presents a schematic decomposition of a taffeta fabric. Part a shows two continuous elements. The crosses represent the fiber elements (warp and weft) in the REV. In part b, the left REV is decomposed into three horizontal layers and the right REV is decomposed into three vertical layers. In part c the assembly of the two continuous REVs is shown.

1.9.3.3. *Elastic behavior of a hybrid taffeta: wavy tuft*

The behavior of the wavy tufts in hybrid taffeta must be modeled. Figure 1.14 shows the section of weft. The warp tuft is periodically fixed with respect to the wefts. The distance between two wefts does not correspond to the effective length of the warp. The following parameter α is introduced; α representing the angle between the axis of the tuft and x axis:

$$\alpha = \frac{\lambda x}{\ell_0} \qquad [1.78]$$

@Seismicisolation

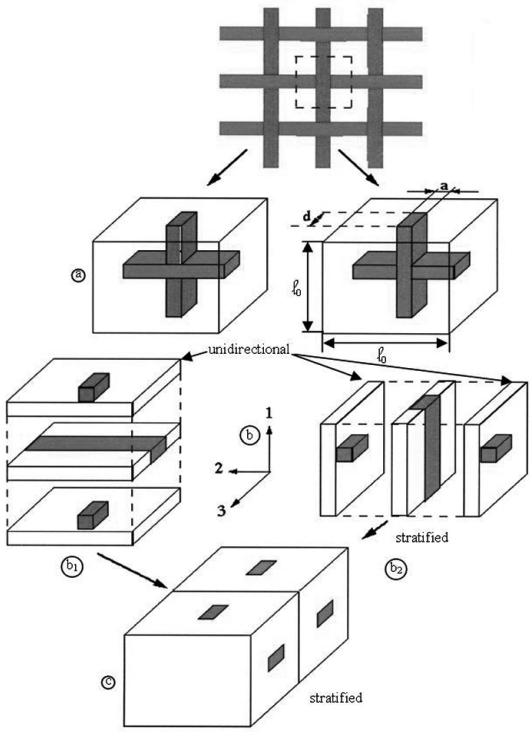

Figure 1.13. *Schematic representation of a taffeta fabric. Decomposition of the elementary cell constitutes the first step in a previsional calculation*

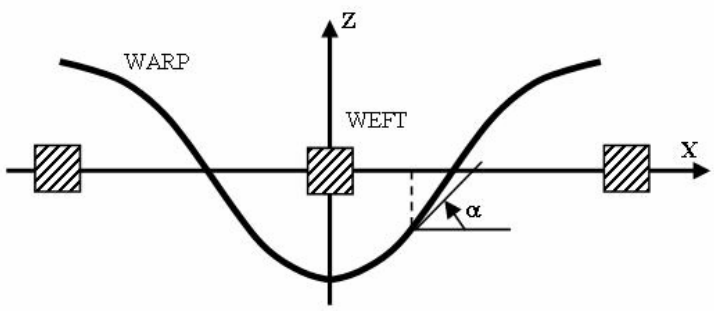

Figure 1.14. *Parameters permitting the inclusion of waviness of the tuft in taffeta tissue*

@Seismicisolation

in which ℓ_0 is the length of the elementary cell, see Figure 1.13. The differential equation giving shape z (x) to tissue 8 tuft is:

$$\frac{dz}{dx} = \text{tg}\,\alpha = \text{tg}\left(\frac{\lambda x}{\ell_0}\right) \qquad [1.79]$$

where λ is a parameter introduced to represent the shape of the tuft. Equation [1.79] has the solution:

$$z(x) = -\frac{\ell_0}{\lambda}\log\left\{\cos\frac{\lambda x}{\ell_0}\right\} - A_0 \qquad [1.80]$$

The tuft element length has the value:

$$ds^2 = dx^2 + dz^2 = \frac{dx^2}{\omega^2\left(\frac{\lambda x}{\ell_0}\right)} \qquad [1.81]$$

Then the length of the tuft is expressed *versus* l_0, the tissue length:

$$\ell = \int_{\frac{\ell_0}{2}}^{\frac{\ell_0}{2}} \frac{dx}{\cos\left(\frac{\lambda x}{\ell_0}\right)} = \frac{2\ell_0}{\lambda}\,\text{Arc tan h}\left(\sin\left(\frac{\lambda}{2}\right)\right) \qquad [1.82]$$

and [1.82] shows that the length ℓ_0 is related to l of the tuft by the relationship:

$$\tan h\,(\ell)\left[\frac{\lambda\ell}{2\ell_0}\right] = \sin\left(\frac{\lambda}{2}\right) \qquad [1.83]$$

The shortening parameter $e_b = \frac{\ell - \ell_0}{\ell}$ defined above is introduced in [I-].

@Seismicisolation

$$\sin\frac{\lambda}{2} = \tanh\left(\frac{\lambda}{2\left(1-e_b\right)}\right) \qquad [1.84]$$

Solving equation [1.84] permits us to evaluate parameter λ *versus* e_b. The method adopted for a numerical solution can be Newton's or simply a manual one. The dichotomy method is presented in Figure 1.15.

1.9.3.4. *Tuft stiffness coefficient calculation*

Taking into account the waviness of the tuft, the stiffness calculation must be calculated along x axis:

$$\overline{C}_{ij}^{(b)} = \frac{1}{\ell_0}\int_{-\frac{\ell_0}{2}}^{\frac{\ell_0}{2}} C'^{(b)}_{ij}\left(\frac{\lambda x}{\ell_0}\right) dx = \int_{-\frac{\lambda}{2}}^{\frac{\lambda}{2}} C_{ij}^{(b)}(\alpha)\, d\alpha \qquad [1.85]$$

where:

– $C'^{(b)}_{ij}$ designates mean value of stiffness coefficient (in matricial notation) and $C'^{(b)}_{ij}$ the stiffness coefficient of the tuft at each point of coordinate x.

– $C'^{(b)}_{ij}$ is obtained from C'^{b}_{ij}, defined with distinct coordinates in symmetry material axes and after changing reference axes.

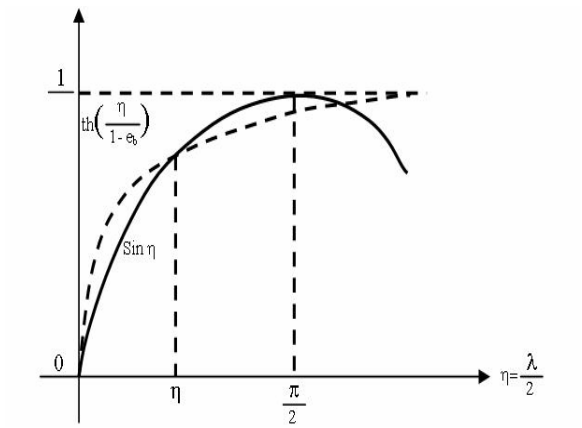

Figure 1.15. *Graphical solution to equation [1.84]. Abscissa* $\eta = \frac{\lambda}{2}$ *is between 0 and* $\frac{\pi}{2}$

@Seismicisolation

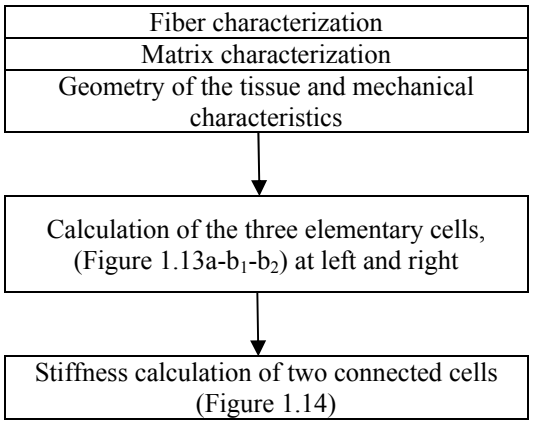

Figure 1.16. *Successive calculation steps to obtain tissue stiffness calculations*

1.10. Bibliography

[BEH 69] BEHRENS E., "Elastic constants of composite materials", *J Acoustic Soc Am*, vol. 45, no. 1, p. 102-108, 1969.

[CHE 71] CHEVALIER Y., VINH T., "Calcul de prévision des constantes élastiques d'un composite à fibres unidirectionnelles – comptes rendus", *Académie des Sciences*, vol. 271, p. 1268-1271, 1971.

[CHE 73] CHEVALIER Y., "Previsional calculation of unidirectional reinforced viscoelastic materials*", Mécanique Matériaux Electricité*, no. 280, p. 38-43, 1973.

[CHE 75] CHEVALIER Y., "Various methods of previsional calculations of composite materials*"*, *Sciences et Techniques de l'Armement*, 3rd edition, p. 417-476, 1975.

[CHE 89] CHEVALIER Y., "Mechanics of materials - elastic and viscoelastic behaviour of anisotropic materials", *Techniques de l'Ingenieur*, vol. AM5, A7 750 and A7 751, 1989.

[CHE 90] CHEVALIER Y., NOUAMANI M., "Presentation and utilization of various computer codes evaluation previsional calculations (Application to tissue reinforced composite)", *Mécanique Matériaux Electricité*, no. 433, p. 14-24, 1990.

[HAS 62] HASHIN Z., STRICKMAN S., "A variational approach to the theory of elastic behaviour of polycrystals", *J Mech Phys Solids*, vol. 11, no. 2, p. 127-140, 1962.

[HAS 62] HASHIN Z., STRICKMAN S. "On some variational approach in anisotropic and non homogenouselasticity", *J Mech Phys Solids*, vol. 10, p. 335-342, 1962.

[HAS 64] HASHIN Z., ROSEN W., "The elastic moduli of fibre reinforced materials*"*, *J Applied Mechanics*, vol. 31, no. 2, p. 223-232, 1964.

@Seismicisolation

[JON 75] JONES R. M., *Mechanics of Composite Materials*, McGraw Hill, New York, 1975.

[LEK 60] S. G. LEKHNITSKII S. G., *Theory of Elasticity of an Anisotropic Elastic Body*, Holden Day, San Francisco, California, 1960.

[PIC 68] PICKETT G., *Elastic Moduli of Fibre Reinforced Plastic Composites – Fundamental Aspects*, Interscience, 1968.

[TSA 80] TSAI S. W., HAHN H. T., *Introduction to Composite Materials*, Technomic, West Port Connecticut, 1980.

[VIN 77] VINH T., CHEVALIER Y., LE NIZERHY D., *Mechanics of Composite Materials and Dynamics of Anisotropic Bounded Media*, 1977 (Lectures at ISMCM Saint-Ouen in French), not published.

1.11. Appendix

Appendix 1.A. Overview on methods used in previsional calculation of fiber-reinforced composite materials

This appendix constitutes an overview. The length of this book does not permit the authors to go into the details of the theoretical aspects of this problem.

1.A.1. *Bounds of elastic coefficients of composite materials*

Hashin, Shtrikman and Rosen [HAS 62] have proposed variational principles that furnish the upper and lower bounds for elastic coefficients.

1.A.2. *Elastic coefficients with replacement of the boundary surface of the cross-section by circular boundary [CHE 71]*

This method is applicable to transverse isotropic materials. The circular boundary permits the simplification of calculations (see Figure 1.A.1).

1.A.2.1. *Plane strain field in cross-section* $\left(\vec{e}_1, \vec{e}_2\right)$ *permits calculation via the Airy functions* ϕ

$$\sigma_{ij} = e_{ip}\, e_{jq} \frac{\partial^2 \phi}{\partial x^p\, \partial x^q} \qquad [1.A.1]$$

with

$$e_{11} = e_{22} = 0\,, \quad e_{12} = -e_{21} = 1$$

@Seismicisolation

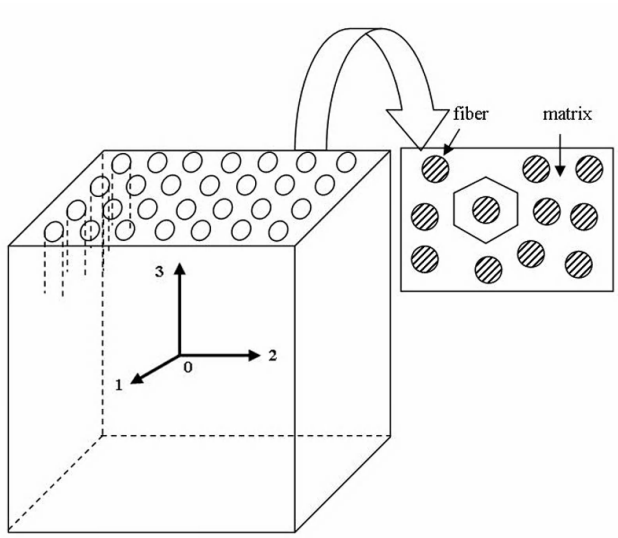

Figure 1.A.1. *Hexagonal distribution. The hexagon is retained as REV*

In polar coordinates (r, θ), the symmetry of stress shows that φ can be represented by:

$$\phi(r,\theta) = \sum_{n=1}^{\infty} \alpha_{2n}(r)\cos(2n\theta) + \frac{1}{2}\alpha_0(r) \qquad [1.A.2]$$

with (index m) for the matrix and (index f) for the fiber respectively.

$$2\alpha_0 = \mu_m\left(a_0 + b_0 \operatorname{Ln} r + c_0 r^2 + d_0 r^2 \operatorname{Ln} r\right) \qquad [1.A.3]$$

$$\alpha_{2n} = \mu_m\left(a_{2n} r^{2n} + b_{2n} r^{-2n} + C_{2n} r^{2n+2} + d_{2n} r^{-2n+2}\right)$$

$$2\alpha_0 = \mu_f\left(e_0 + f_0 r^2\right)$$

$$\alpha_{2n} = \mu_f\left(e_{2n} r^{2n} + f_{2n} r^{2n+2}\right) \qquad [1.A.4]$$

1.A.2.2. *Field of plane shearing in the plane* $(\vec{e}_2, \vec{e}_3)$

Under the Fourier series components u^3 (r, θ), this plane permits us to calculate:

$$u^3(r,\theta) = \alpha_0(r) + \sum_{n=1}^{\infty} \alpha_{2n-1}(r)\sin(2n-1)\theta \qquad [1.A.5]$$

@Seismicisolation

As u^3 (r, θ) is harmonic, we obtain:

$$\begin{cases} \alpha_0(r) = A_0 \log r + B_0 \\ \alpha_{2n-1} r^{2n-1} = A_{2n-1} r^{2n-1} + B_{2n-1} r^{-2n+1} \end{cases} \quad \text{(matrix)} \qquad [1.A.6]$$

$$\alpha_0(r) = C_0$$

$$\alpha_{2n-1} = C_{2n-1} r^{2n-1} \quad \text{(fiber)} \qquad [1.A.7]$$

1.A.2.3. *Field of pure tension in direction* $\vec{e}_3$

This field enables the calculation of $\vec{C}_{3333}$.

1.A.3. *Pickett's elastostatic method [PIC 68]*

The section retained is presented in Figure 1.8b. The calculation concerns a long-fiber reinforced composite, see Figure 1.A.1.

The fields presented in Figure 1.A.1 are to be evaluated for a couple variables (r, θ). Discretization of the surface by sectors with variables θ is effected. Equality of displacements in (ξ) is adopted:

$$u_i = \varepsilon_{ij} x_j$$

and the equality of strains and displacements on the interface fiber-matrix (with perfect contact) permit us to obtain a set of linear equations with coefficients α_{2n}, α_0 as variables. The number of points on $\mathcal{S}$ can be important and the number of equations exceeds that of unknowns. Solving by least-squares method is referred to. This numerical method permits us to solve a variety of problems in which the fiber cross-section can be elliptic.

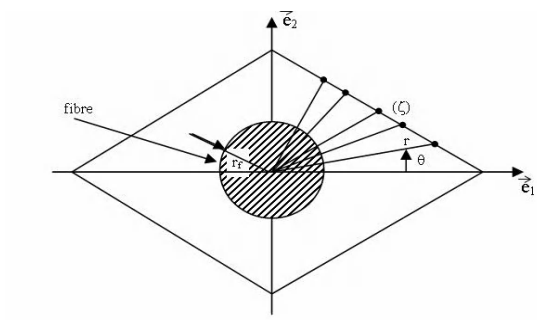

Figure 1.A.2. *In the plane* $(\vec{e}_1, \vec{e}_2)$ *the REV is a lozenge*

@Seismicisolation

1.A.4. *Chevalier's method [CHE 71]*

The hexagonal distribution in the cross-section is retained, see Figure 1.8c. The second step in the calculation consists of replacing the hexagonal section by a circular section, the percentage volume of fiber being the same (see Figure 1.9).

In equations [1.A.2] and [1.A.5], angle θ is no longer a variable. The series has a finite number of terms and the system of linear equations is of sixth order, which results in the writing of boundary conditions. The final result after calculations is presented in the set of equations [1.69] to [1.75].

@Seismicisolation

Chapter 2

Elements of Linear Viscoelasticity

The behavior of materials depends on the type and intensity of loading[1]. In what follows we exclude plastic loading, which creates irreversible deformation. All materials display viscoelastic behavior, which means that elastic and viscous deformations occur.

Let us impose a rod of material to a tension test with cycles of loading and unloading. In the curves of force *versus* displacement, closed loops are obtained and their areas represent the energy absorption of the sample (see Figure 2.1). It is often difficult to separate elastic from viscous behavior.

The elastic modulus, for example Young's modulus, is related to the mean slope of the loop. Viscous effect is time dependent. If we submit the sample to a sinusoidal force, the displacement response is harmonic. If the response is purely sinusoidal, the sample behavior is said to be linear viscoelastic. If the displacement response is composed of a component at the same frequency and harmonic, the sample behavior response is non-linear viscoelastic. In Figure 2.2a, a harmonic test is conducted with a sinusoidal force applied to a viscoelastic sample. An ellipse is obtained. It describes the delay of displacement response with respect to sinusoidal force applied. In Figure 2.2b, the closed loop is no longer elliptic and the response is non-linear.

Chapter written by Yvon CHEVALIER.

1 In this chapter, we do not mention the plastic regime of loading in which irreversible permanent elongation of the sample occurs.

Mechanics of Viscoelastic Materials and Wave Dispersion Edited by Yvon Chevalier and Jean Tuong Vinh
© 2010 ISTE Ltd. Published 2010 by ISTE Ltd.

@Seismicisolation

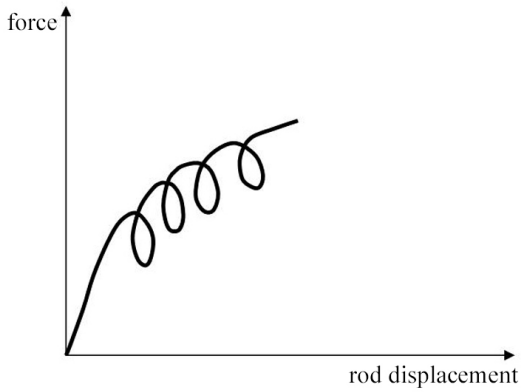

Figure 2.1. *Loop obtained on the curve of force* versus *displacement. Areas of the loops are related to viscous effect*

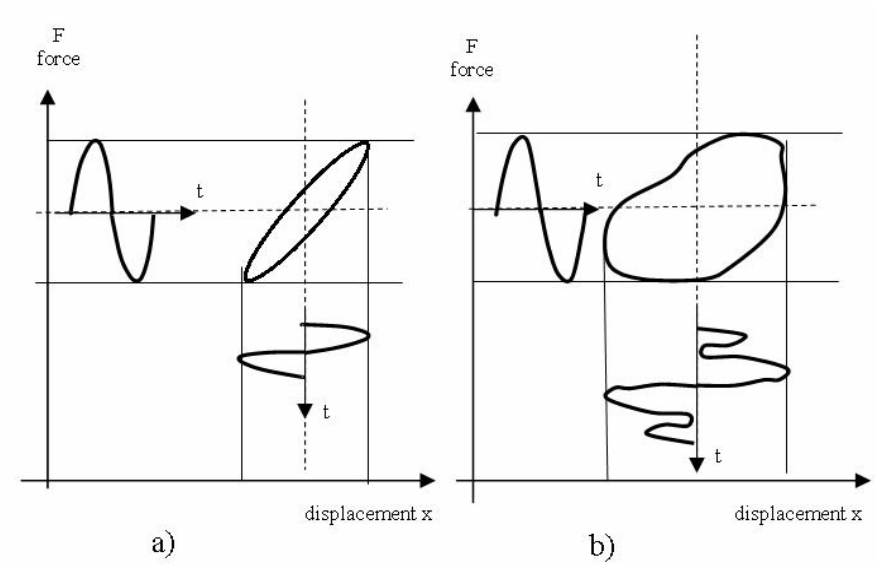

Figure 2.2. *a) In a linear viscoelastic regimen, force and displacement are purely sinusoidal; b) in a non-linear viscoelastic regimen, a sinusoidal force with large amplitude creates non-linear displacement with the presence of harmonics*

@Seismicisolation

In this chapter, we will examine linear viscoelasticity, which obeys Boltzmann's superposition principle. Non-linear viscoelasticity has a larger mathematical framework in which linear components of strain (or stress) are the firm term of the Volterra series [SAA 03, SCH 80].

Viscoelastic material response is decomposed into components of various orders, in which the first one portrays linear behavior. Other approaches exist, but the corresponding framework supposes an *a priori* knowledge of the material and it is difficult to obtain a certain degree of generality in the mathematical formulation (see [KNA 81, MUL 69, ODO 95, SCH 99]).

In this chapter, attention is focused on linear viscoelasticity. In simple examples adopted force and displacement are uniaxial. We will now further discuss generalization to multiaxial loading.

2.1. Time delay between sinusoidal stress and strain

If a sinusoidal axial stress is applied to a viscoelastic rod sample:

$$\sigma = \sigma_0 \sin \omega t \qquad [2.1]$$

the strain response is:

$$\varepsilon = \varepsilon_0 \sin (\omega t + \delta) \qquad [2.2]$$

in which δ represents the phase angle. In Figure 2.3, δ corresponds to a time delay τ, ω being circular frequency:

$$\tau = \frac{\delta}{\omega} \qquad [2.3]$$

When varying the frequency $f = \frac{\omega}{2\pi}$, the loop area changes shape. We can say that δ is frequency dependant.

$$\delta = \delta (\omega) \qquad [2.4]$$

@Seismicisolation

The loop areas in Figure 2.1 represent energy absorption by the material.

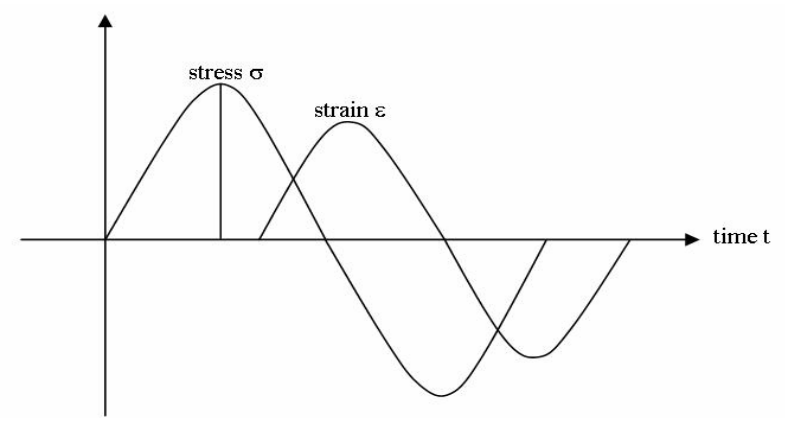

Figure 2.3. *Strain is time-delayed with respect to stress for viscoelastic rod*

2.2. Creep and relaxation tests

These two transient tests are popular in viscoelasticity and are very convenient when using Boltzmann's principle.

2.2.1. *Creep test*

Let us adopt a simple uniaxial loading history, defined as follows. Stress represented as a step (see Figure 2.4a) applied at the instant $t = t_0$.

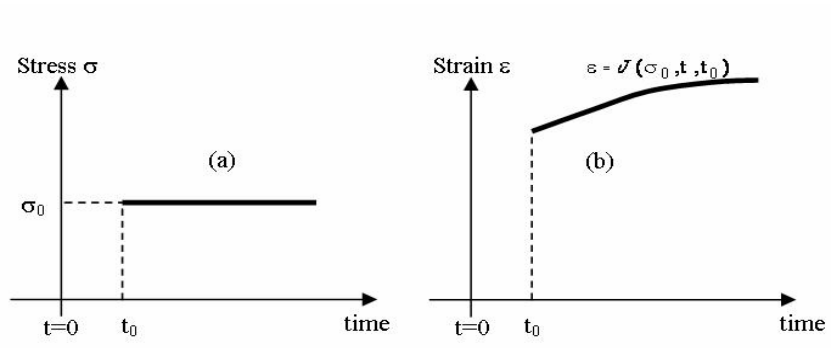

Figure 2.4. *Simple uniaxial creep test: a) applied step stress; b) response strain*

@Seismicisolation

$$\sigma(t) = \sigma_0 H(t - t_0) \quad [2.5]$$

H(t) is Heaviside step function (H(t) = 0 if t < 0). The recorded strain (see Figure 2.4b) also has a discontinuity at $t = t_0$. This is due to the instantaneous elasticity of the sample. For $t > t_0$, the strain response is represented by the creep function $J(\sigma_0, t, t_0)$:

$$\varepsilon(t) = J(\sigma_0, t, t_0) \quad [2.6]$$

where:

$$\text{for } t < t_0 \quad J(\sigma_0, t, t_0) = 0 \quad [2.7]$$

for $t > t_0$ $J(\sigma_0, t, t_0)$ is an increasing function of time t.

The creep function[2] presented in equation [2.6] concerns a general creep test including non-linear viscoelastic behavior. For linear viscoelastic behavior in [2.7], the creep function has a linear dependence of applied stress:

$$J(\sigma_0, t, t_0) = \sigma_0 J(t, t_0)$$

so we have:

$$\text{for } t < t_0 \; J(t, t_0) = 0 \quad [2.8]$$

for $t > t_0$ $J(t, t_0)$ increases with time t.

2.2.2. *Relaxation test*

This is a dual test compared to the creep test; the input signal is a strain that has the shape of a Heaviside step function:

$$\varepsilon(t) = \varepsilon_0 H(t - t_0) \quad [2.9]$$

2 Creep test is currently applied to materials such as steel at high temperature. The test is a non-linear viscoelastic and plastic one.

@Seismicisolation

For linear viscoelastic material, the response is:

$$\sigma(t) = \mathcal{R}(\varepsilon_0, t, t_0) = \varepsilon_0 \mathcal{R}(t, t_0) \qquad [2.10]$$

such as:

$$\text{for } t < t_0 \ \mathcal{R}(t, t_0) = 0 \qquad [2.11]$$

for $t > t_0$ $\mathcal{R}(t, t_0)$ decreases with time t.

2.2.3. *Ageing and non-ageing viscoelastic materials*

Non-ageing material has responses independent of time t_0 at which experiments are conducted. Let Q(t) be the input signal (which can be stress σ(t) or strain (ε(t)) and q(t) the output signal (which can be strain ε(t) or stress σ(t)).

$$\left.\begin{array}{r} Q(t) \text{ gives rise to } q(t) \text{ then} \\ Q(t+t_0) \textit{ corresponds to } q(t+t_0) \end{array}\right\} \qquad [2.12]$$

Such behavior is described by linear *time invariance*. In other words, time does not change the response. Equations [2.8] and [2.11], for non-ageing materials, become:

$$J(t, t_0) = J(t - t_0) \qquad [2.13]$$

$$\mathcal{R}(t, t_0) = \mathcal{R}(t - t_0) \qquad [2.14]$$

The properties of J and R are summarized in Table 2.1.

Creep function	J (θ)	J (θ) = 0 if θ < 0, causal function J (θ) continuous if θ > 0 J (θ) increases with θ
Relaxation function	R(θ)	R (θ) = 0 if θ < 0, causal function R (θ) continuous if θ > 0 R (θ) decreases with θ

Table 2.1. *Properties of creep and relaxation functions for non-ageing linear viscoelastic materials*

@Seismicisolation

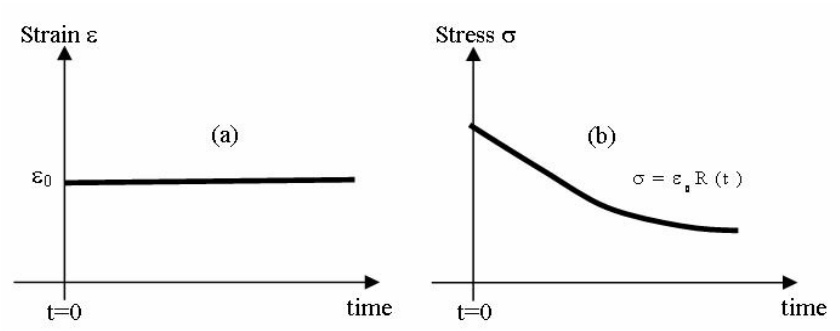

Figure 2.5. *Simple uniaxial relaxation test applied to a non-ageing linear viscoelastic material: a) applied step strain; b) response stress, relaxation function R(t)*

Ageing material is not described by [2.12]. The response of such materials depends both on varying time t (actual time) during experiments and instant t_0 (historical time or date) at which experiments are carried out. $Q(t, t_0)$ gives rise to the response $q(t, t_0)$. The date t_0 can be century, year, month or day.

2.2.4. *Viscoelastic materials with fading memory*

These materials can be considered to be *non-ageing materials*. They retain recent events in their responses; they have no memory of old events. In this condition $Q(t, t_0)$ gives rise to q(t). The date t_0 is therefore not necessary to characterize the response q(t). Many materials are characterized as fading memory materials in this case.

2.3. Mathematical formulation of linear viscoelasticity

2.3.1. *Linear system*

A system is said to be linear if the input signal, or excitation, Q(t) is a linear combination of signals $Q_1(t)$ and $Q_2(t)$:

$$Q(t) = \lambda_1 Q_1(t) + \lambda_2 Q_2(t) \qquad [2.15]$$

λ_1 and λ_2 are non-zero constants. The response q(t) is then:

$$q(t) = \lambda_1 q_1(t) + \lambda_2 q_2(t) \qquad [2.16]$$

@Seismicisolation

where $q_1(t)$ and $q_2(t)$ are responses of $Q_1(t)$ and $Q_1(t)$ respectively. Equations [2.13] and [2.14] concern the linear system in general, see Figure 2.6.

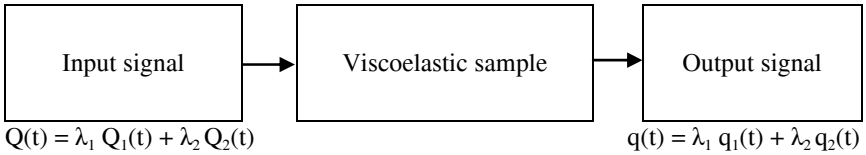

Figure 2.6. *Definition of a general linear system*

2.3.2. *Superposition (or Boltzmann's) principle*

When a material has a response that depends on the entire history of an input signal, the response is mathematically expressed as a functional. In the linear case, the functional is an integral defined in the time interval in which the experiment is conducted:

$$q(t) = F\left[\int_{-\infty}^{t} Q(\tau)\right] \qquad [2.17]$$

Viscoelastic materials define causal systems. This means a causal input signal Q(t), (Q(t) = 0 if t < 0) gives rise to causal output signal and equation [2.17] becomes:

$$q(t) = F\left[\int_{0}^{t} Q(\tau)\right] \text{ if } t > 0 \qquad [2.18]$$

$$q(t) = 0 \text{ if } t < 0$$

In Figure 2.7, the causal input and output signals are decomposed into a sum of Heaviside step functions delayed in time increment Δt:

$$\Delta t = \tau_i - \tau_{i-1} \quad i = 1,2,....,n$$

$$\tau_0 = 0, \qquad \tau_n = t$$

@Seismicisolation

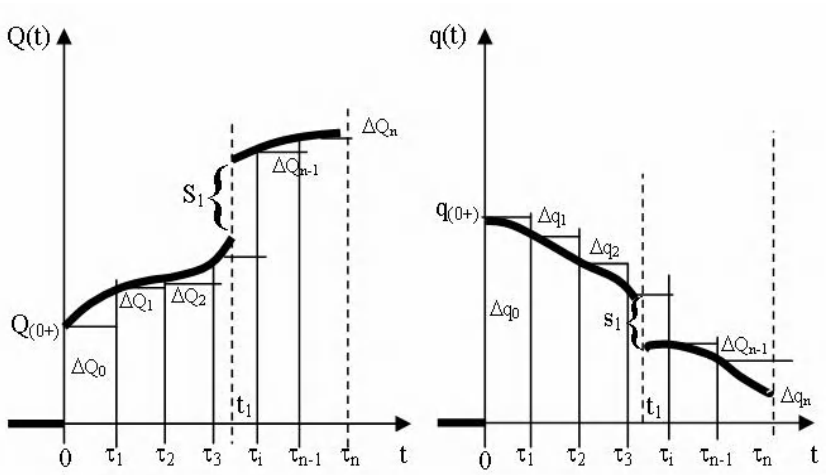

Figure 2.7. *Input and output signals are a sum of Heaviside functions decomposed into increments ΔQ and Δq functions of time increments Δτ*

In equations [2.19] and [2.20], input and output signals are considered to be a sum of primary signals, which are Heaviside step functions delayed in time τ_i:

$$Q(t) = \sum_{i=1}^{n} \Delta Q_i \; H\left(t - \tau_i\right) + S_1 \; H(t - t_1) + Q(0^+) \qquad [2.19]$$

$$q(t) = \sum_{i=1}^{n} \Delta q_i \; H\left(t - \tau_i\right) + s_1 \; H(t - t_1) + q(0^+) \qquad [2.20]$$

where:

$$Q\,(0^+) = \Delta Q_0 \;,\; S_1 = Q(t_1^+) - Q(t_1^-)$$

and:

$$q\,(0^+) = \Delta q_0 \;,\; s_1 = q(t_1^+) - q(t_1^-)$$

@Seismicisolation

are jumps at t = 0 and at $t = t_1$ of input and output signals respectively. According to the behavior of linear non-ageing viscoelastic materials (equations [2.8] and [2.10] and Table 2.1), magnitudes of step functions are related by the relationship:

$$\Delta q_i \; H\left(t-\tau_i\right) = \xi\left(t-\tau_i\right) \Delta Q_i \; H\left(t-\tau_i\right)$$

where $\xi\left(t-\tau_i\right)$ is a causal function, continuous for t > 0, which can be a creep or relaxation function. Then:

$$q(t) = \sum_{i=1}^{n} \xi\left(t-\tau_i\right) \Delta Q_i \; H\left(t-\tau_i\right) + S_1 \; \xi(t-t_1) + Q(0^+) \; \xi(t) \qquad [2.21]$$

Function $\xi\left(t\right)$ is the factor of proportionality in equations [2.13] and [2.14]. It is easy to transform [2.21] into an integral with $\Delta Q_i \rightarrow 0$, written as a Stieljes convolution:

$$q\left(t\right) = \int_0^t \xi\left(t-\tau\right) dQ\left(\tau\right) + Q(0^+) \; \xi(t) + \sum_{j=1}^{n} S_j \; \xi(t-t_j) \qquad [2.22]$$

where $S_j = Q(t_j^+) - Q(t_j^-)$, with j = 1, 2,…., n, are a jump of input signal at $t = t_j$. Equation [2.20] can also be rewritten under the Riemann convolution:

$$q\left(t\right) = \int_0^t \xi\left(t-\tau\right) \frac{\partial Q}{\partial \tau} d\tau + Q(0^+) \; \xi(t) + \sum_{j=1}^{n} S_j \; \xi(t-t_j) \qquad [2.23]$$

or (see also[3]),

$$q(t) = \xi(t) * \left[\frac{\partial Q}{\partial \tau} + Q(0^+) \; \delta(t) + \sum_{j=1}^{n} Q(t) \; \delta(t-t_j)\right] = \xi(t) * \frac{DQ}{Dt} \qquad [2.24]$$

---

3 Convolution of two causal functions f(t) and g(t): $f(t) * g(t) = \int_0^t f\left(t-\tau\right) g\left(\tau\right) d\tau$ for t > 0.

Differentiation of a distribution f(t) which is both continuous and has derivatives by steps: $\frac{Df}{Dt} = \frac{df}{dt} + \sum_{i=1}^{i=n} f_i \; \delta(t-t_i)$ where $f_i = f(t_i^+ - t_i^-)$ is the jump of f(t) at $t = t_i$, $\delta(t - t_i)$ is the Dirac distribution at $t = t_i$, and $\delta(t)$ is the unit convolution: $\delta(t - t_i) * f(t) = f(t - t_i)$.

@Seismicisolation

In equation [2.24], the step discontinuities give rise to a Dirac mass distribution in the differentiation of distribution Q(t), [SCH 78, ZEM 65], where star designates convolution. After integration by parts, equation [2.23] becomes:

$$q\,(\,t\,) = \xi(0^{+})\,Q(t) + \int_0^t \dot{\xi}(\,t - \tau\,)\;\;Q(\tau)\,d\tau \qquad [2.25]$$

where $\dot{\xi}(\theta)$ is the derivative of function ξ *versus* θ. In equation [2.25] the first part of the equation is instantaneous elastic behavior of the material while the second part is the memory effect due to viscosity. Note that discontinuities of input signal Q(t) do not interfere in constitutive viscoelastic law. Equivalent equations [2.23] and [2.25] can be rewritten in the following concise equation [2.26]:

$$\boxed{q\,(t) = \frac{\partial}{\partial t}\int_0^t \xi\,(t-\tau)\;Q(\tau)\,d\tau} \qquad [2.26]$$

2.3.3. *Creep function in a functional constitutive equation*

In equations [2.19] to [2.26] for the input and output signals, we take:

$$Q(t) = \sigma(t) \qquad [2.27]$$

$$q(t) = \varepsilon(t)$$

Then function $\xi(t) = J(t)$ is the creep function and [2.27] is rewritten as:

$$\boxed{q\,(t) = \varepsilon\,(t) = \frac{d}{dt}\int_0^t J\,(t-\tau)\;\sigma(\tau)\;\;d\tau} \qquad [2.28]$$

Creep function J(t) is currently evaluated for metals, particularly at high temperatures. In applied rheology, viscoelastic materials are submitted to such a test (see section 2.2.1).

@Seismicisolation

2.3.4. *Relaxation function in functional constitutive equations*

In equations [2.19] to [2.26], for the input and output signal we take:

$$Q(t) = \varepsilon(\mathrm{t}) \qquad [2.29]$$

$$q(t) = \varepsilon(\mathrm{t})$$

Then function $\xi(t) = \mathrm{R(t)}$ is the creep function and [2.30] is rewritten as:

$$\boxed{q\ (\mathrm{t}) = \sigma\ (\mathrm{t}) = \frac{\mathrm{d}}{\mathrm{d\,t}}\int_0^{\mathrm{t}} \mathrm{R}\ (\mathrm{t}-\tau)\ \varepsilon(\tau)\ \mathrm{d}\tau} \qquad [2.30]$$

Creep function J(t) is currently evaluated for metals, particularly at high temperatures. In applied rheology, viscoelastic materials are submitted to such a test (see section 2.2.3).

2.3.5. *Properties of relaxation and creep functions*

It is interesting to note the following characteristics of these time functions.

2.3.5.1. *Thermodynamic limitation of kernel functions R(t), J(t)*

The viscoelastic power absorbed by a material is non-negative:

$$\int \sigma_{\mathrm{ij}}\ (\tau)\ \frac{\partial\ \varepsilon}{\partial\ \tau}\ \mathrm{d}\ \tau\ \geq\ 0 \qquad [2.31]$$

In this condition, R(t) and J(t) are always positive.

2.3.5.2. *Thermodynamic limitation of kernel functions R(t), J(t)*

Thermodynamic considerations using the second principle of thermodynamics permits us to ascertain [CHE 89] for the relaxation function that if:

@Seismicisolation

$$\frac{d\,R(t)}{d\,t} < 0\,, \qquad [2.32]$$

then R(t) decreases with time and consequently J(t) increases with time. It is important to notice that R(t) is not the reverse function of J(t):

$$R(t) \neq \frac{1}{J(t)}$$

2.3.5.3. *Material with short memory*

Material is strongly dependent on recent history. The effect of these two functions on the slope decreases with time:

$$\left|\frac{d\,R}{d\,t}\right|_{t=t_1} \leq \left|\frac{d\,R}{d\,t}\right|_{t=t_2} \quad \text{with } t_1 > t_2 > 0 \qquad [2.33]$$

$$\left|\frac{d\,J}{d\,t}\right|_{t=t_1} \leq \left|\frac{d\,J}{d\,t}\right|_{t=t_2} \quad \text{with } t_1 > t_2 > 0 \qquad [2.34]$$

The slope of R is negative in equation [2.32], but its absolute value decreases with time.

2.3.5.4. *Isothermal kernel functions*

The above are isothermal tests. For some tests of creep and relaxation, strain can be large and heat is produced. At temperature T_0, if such an event occurs we must add a second term that takes temperature variation into account $\Delta T = T - T_0$ [CHE 89], so for the relaxation test:

$$\sigma(t) = \frac{\partial}{\partial\,t}\int_0^t R\,(T_0\,, t-\tau)\;\varepsilon\;(\tau)\;d\,\tau - \frac{\partial}{\partial\,t}\int_0^t a\,(T_0, t-\tau)\;\Delta\,T\;(\tau)\;d\,\tau$$

[2.35]

in which a(t) represents a kernel thermal-stress function.

@Seismicisolation

Creep and relaxation functions are related by the following convolution, [SCH 78, ZEM 65]:

$$\frac{DJ}{Dt} * \frac{DR}{Dt} = \delta(t) \qquad [2.36]$$

while thermal expansion coefficient α and thermal stress function a are linked by equation [2.37].

$$\frac{D\alpha}{Dt} = \frac{DJ}{Dt} * \frac{Da}{Dt} \Leftrightarrow \frac{Da}{Dt} = \frac{DR}{Dt} * \frac{Da}{Dt} \qquad [2.37]$$

$\delta(t)$ is the Dirac distribution.

	Boltzmann's representation [2.24]	**Mechanical representation [2.25]**	**Concise representation [2.27]**
Creep	$\varepsilon(t) = J(T_0, t) * \frac{D\sigma}{Dt} + \alpha(T_0, t) * \frac{D\Delta T}{Dt}$	$\varepsilon(t) = \frac{D\,J(T_0, t)}{Dt} * \sigma(t) + \frac{D\,\alpha(T_0, t)}{Dt} * \Delta T$	$\varepsilon(t) = \frac{D\left[J(T_0, t) * \sigma(t)\right]}{Dt} + \frac{D\left[\alpha(T_0, t) * \Delta T\right]}{Dt}$
Relaxa -tion	$\sigma(t) = R(T_0, t) * \frac{D\varepsilon}{Dt} - a(T_0, t) * \frac{D\,\Delta T}{Dt}$	$\sigma(t) = \frac{D\,R(T_0, t)}{Dt} * \varepsilon(t) - \frac{D\,a(T_0, t)}{Dt} * \Delta T$	$\sigma(t) = \frac{D\left[R(T_0, t) * \varepsilon(t)\right]}{Dt} - \frac{D\left[a(T_0, t) * \Delta T\right]}{Dt}$

Table 2.2. *Various representations of thermo-mechanical constitutive equations for non-ageing viscoelastic materials in terms of convolutions designated by star $\Delta T = T - T_0$. Star represents a convolution*

@Seismicisolation

2.4. Generalization of creep and relaxation functions to tridimensional constitutive equations

In the simple uniaxial loading already presented (equations [2.28] and [2.30]), Stieljes or Riemann convolution replaces simple multiplication (devoted to elastic material) to portray the viscoelastic material.

2.4.1. *Relaxation function as components in a stiffness matrix*

Let us recall the constitutive equations under matricial presentation for elastic materials. The constitutive equation here is:

$$\{\sigma\} = \{C\}\{\varepsilon\} \qquad [2.38]$$

The following notations are adopted[4]:

$$\{\sigma\} = \{\sigma_{11}, \sigma_{22}, \sigma_{33}, \sigma_{23}, \sigma_{31}, \sigma_{12}\}^T$$

$$\{\varepsilon\} = \{\varepsilon_{11}, \varepsilon_{22}, \varepsilon_{33}, 2\varepsilon_{23}, 2\varepsilon_{31}, 2\varepsilon_{12}\}^T$$

and the 6 x 6 stiffness matrix {C} is symmetric (see Chapter 1, equations [1.9], [1.10] and [1.11]).

Going from an elastic to viscoelastic regimen, stress and strain components are time-dependent functions as well as components of stiffness matrix {C}. Equation [2.30] and Table 2.1 are used for generalization.

$$\boxed{\begin{aligned}\{\sigma(t)\} &= \left\{\frac{D\,C(t)}{Dt}\right\} * \{\varepsilon(t)\} \\ &= \{C(t)\} * \left\{\frac{D\,\varepsilon(t)}{Dt}\right\} \\ &= \frac{D\left[\{C(t)\} * \{\varepsilon(t)\}\right]}{Dt} = \frac{d}{dt}\int_0^t \{C(t-\tau)\}\{\varepsilon(\tau)\}\,d\tau\end{aligned}} \qquad [2.39]$$

4 $\{\sigma\} = \{\sigma_{11}, \sigma_{22}, \sigma_{33}, \sigma_{23}, \sigma_{31}, \sigma_{12}\}^T$: column matrix notation.

@Seismicisolation

The star symbol designates convolution. The reader should note that the column vector representing strains in elasticity is replaced by the column vector of time differentiation of the distribution components of strains (see equation [2.39], line 2). Using tensor writing:

$$\sigma_{ij}(t) = \frac{d}{dt}\int_0^t c_{ijkl}\,(t-\tau)\,\varepsilon_{kl}(\tau)\,d\tau \qquad [2.40]$$

the 6 x 6 relaxation stiffness matrix {C(t)} is symmetric (Onsager's principle [CHR 71]). The necessary number of relaxation functions $C_{ij}(t)$ to be evaluated (21 maximum) depends on the nature of the material itself and on its symmetries.

For relaxation functions of a stiffness matrix, Heaviside step function is usually used for each strain component as the input signal:

$$\varepsilon_{ij}(t) = \varepsilon_{ij}^{0}\,H(t) \qquad [2.41]$$

The corresponding relaxation functions are recorded. In a tension test, with a normal component of stress σ in direction 1, the relaxation Young's modulus $E_1(t)$ in direction 1 is defined by the following equation:

$$\sigma_{11}(t) = \frac{d}{dt}\int_0^t E_1(t-\tau)\,\varepsilon_{11}(\tau)\,d\tau \qquad [2.42]$$

In this tension test the Poisson's ratio ν_{12} is defined from the axial $\varepsilon_{11}(t)$ and transverse strain $\varepsilon_{22}(t)$.

$$\varepsilon_{22}(t) = -\frac{d}{dt}\int_0^t \nu_{12}(t-\tau)\,\varepsilon_{11}(\tau)\,d\tau \qquad [2.43]$$

If input signal $\varepsilon_{11}(t)$ is adopted, equations [2.36], [2.37] and [2.38] lead to the following equations:

@Seismicisolation

$$E_1\ (\mathrm{t}) = \frac{\sigma(t)}{\varepsilon_{11}^0}$$

$$\nu_{12}(\mathrm{t}) = -\frac{\varepsilon_{22}(t)}{\varepsilon_{11}^0}$$

2.4.2. *Creep function as components in a compliance matrix*

Similar to equation [2.33], we can write[5]:

$$\{\ \varepsilon\ \} = \{\ \mathrm{S}\ \}\ \{\ \sigma\ \} \qquad [2.44]$$

Stress and strain column vectors compliance matrix components of a viscoelastic material are time-dependent functions. Equation [2.28] and Table 2.1 are used for generalization.

$$\boxed{\begin{aligned}\{\varepsilon(t)\} &= \left\{\frac{\mathrm{D\ S(t)}}{Dt}\right\} * \{\sigma(t)\} \\ &= \{S(t)\} * \left\{\frac{\mathrm{D}\ \sigma(\mathrm{t})}{Dt}\right\} \\ &= \frac{\mathrm{D}\left[\{\mathrm{S(t)}\} * \{\ \sigma(t)\ \}\right]}{Dt} \\ &= \frac{\mathrm{d}}{\mathrm{d\,t}}\int_0^{\mathrm{t}} \{S(\mathrm{t}-\tau)\}\ \{\sigma(\tau)\}\ \ \mathrm{d}\tau\end{aligned}} \qquad [2.45]$$

The star symbol represents convolution. Using tensor writing:

$$\varepsilon_{ij}(\mathrm{t}) = \frac{\mathrm{d}}{\mathrm{d\,t}}\int_0^{\mathrm{t}} s_{\mathrm{ijkl}}\ (\mathrm{t}-\tau)\ \sigma_{kl}(\tau)\ \ \mathrm{d}\tau \qquad [2.46]$$

5 In section 2.3.3, J(t) is a creep function. This convention is currently adopted by specialists in rheology. In equations [2.44] to [2.46], {S} square matrix is used instead of {J}, conforming to the convention adopted in continuum mechanics. This is the same for {C} and {R}.

@Seismicisolation

diagonal components of the matrix {S} give rise to classical uniaxial tests for viscoelastic composite materials (see section 1.2). As for non-diagonal components of {S}, there is difficulty in carrying out experiments in which coupling phenomena occur. This needs to be taken into account.

2.4.3. *Some remarks on the mathematical formulation of linear viscoelatic behavior of materials*

2.4.3.1. *Variation of relaxation and creep components matrix with time*

Thermodynamic considerations (see section 2.3.5.2 [CHE 89]) permit us to check that:

– only diagonal components $C_{ii}(t)$, i= 1,…,6, of the relaxation stiffness matrix and relaxation Young's moduli $E_i(t)$, i = 1, 2, 3, decrease with time;

– only diagonal components $S_{ii}(t)$, i = 1,…,6, of the creep compliance matrix increase with time.

2.4.3.2. *Mathematical functions and distributions*

Objections concerning utilization of functionals in the presence of discontinuities from material response and the unconditional use of mathematical distributions are beyond the scope of this book. Some ideas relating to those problems are succinctly demonstrated in section 2.3.5.4.

2.5. Principle of correspondence and Carson-Laplace transform for transient viscoelastic problems

There are two ways a viscoelastic problem can be solved:

– direct formulation using relaxation stiffnesses or creep compliances, presented above, with the search for equations of motion and related solutions generally obtained by numerical methods;

– indirect formulation by first solving the elastic problem *with the same geometry* for the bounded medium and *same loading force system*. The second step is to use integral transforms and assume that the solution of the viscoelastic problem, in the space of integral transforms, is similar to the solution of the elastic problem: *integral transforms of creep and relaxation functions have taken the place of elastic moduli*. We use the so-called principle of correspondence in order to directly write the solution to the viscoelastic problem.

@Seismicisolation

The second method, in the majority of cases, is easier to use, although it is indirect and requires knowledge of the elastic solution. Vibrations of viscoelastic media can be considered a companion to elastic media, particularly in the field of dynamic harmonic testing. The principle of correspondence used in conjunction with the Carson-Laplace transform permits this extension. Fourier transform replaces the Carson-Laplace transform where there is a harmonic regime. Figure 2.8 presents the main ideas concerning correspondence principle.

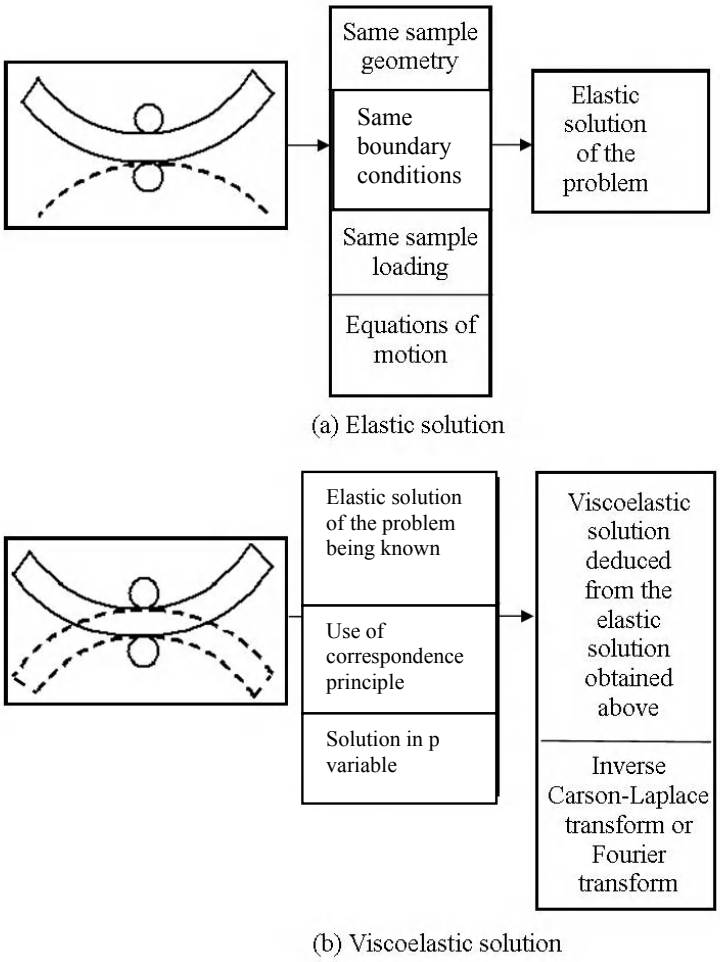

Figure 2.8. *Use of the principle of correspondence to deduce the desired viscoelastic solution to the dynamic problem of flexural vibrations of a viscoelastic beam taken as an example*

@Seismicisolation

The only restriction on some viscoelastic solutions concerns transient tests, in which boundary conditions imposed on the sample may vary simultaneously with space and time[6]. This is the case, for example, when indenting a viscoelastic half-space with a hard steel sphere. During the indentation, displacement varies with time. The boundary conditions consequently change with time. The direct viscoelastic solution deduced from the corresponding elastic solution is not possible.

2.5.1. *Carson-Laplace's transform*

For simplification, let us examine first the uniaxial test in which one stress and one strain component are non-zero. This is the case with the creep function presented in section 2.3.3 and relaxation function presented in section 2.3.4. Equations [2.28] and [2.30] are rewritten here.

$$\varepsilon\left(t\right) = \frac{d}{dt}\int_0^t J\left(t-\tau\right)\sigma(\tau)\ d\tau \qquad [2.28]$$

$$\sigma\left(t\right) = \frac{d}{dt}\int_0^t R\left(t-\tau\right)\varepsilon(\tau)\ d\tau \qquad [2.30]$$

Here we use the Carson-Laplace transform, defined as:

$$\mathscr{C}\left[f\left(t\right)\right] = \tilde{f}(p) = p\int_0^\infty e^{-pt}\ f\left(t\right)\ dt, \qquad p \in \mathbb{C} \qquad [2.47]$$

in which f(t) is a causal time function[7]. p is a complex variable:

$$p = \xi + j\omega \qquad j^2 = -1 \qquad [2.48]$$

6 $U_i(x_j,t)$ is the value of displacement $u_i(x_j,t)$ on the boundary. If the boundary condition is $U_i(x_j,t) = X_i(x_i)g(t)$, the principle of correspondence can be used. The condition is the same with all forces.

7 The difference between the Carson-Laplace transform and Laplace transform resides in factor p in equation [2.47].

@Seismicisolation

where ξ is damping coefficient, ω a circular frequency and j the imaginary number. One remarkable property of the convolution is that the Carson-Laplace transform gives rise to a transform expressed as a simple product (Duhamel's theorem).

Applying [2.47] to [2.28] and [2.30] we obtain:

$$\tilde{\varepsilon}\ (\mathrm{p}) = \tilde{\mathrm{J}}\ (\mathrm{p})\ \cdot\ \tilde{\sigma}\ (\mathrm{p}) \qquad [2.49]$$

$$\tilde{\sigma}\ (\mathrm{p}) = \tilde{\mathrm{R}}\ (\mathrm{p})\ \cdot\ \tilde{\varepsilon}\ (\mathrm{p}) \qquad [2.50]$$

The tildae notation ~ represents the Carson-Laplace transform of various terms. We see that in the second members of equations [2.49] and [2.50] we only have simple products. These are similar to classical elastic equations [2.38] and [2.44] in tridimensional representation:

$$\begin{aligned} \{\ \tilde{\varepsilon}(\mathrm{p})\ \} &= \{\ \tilde{\mathrm{S}}(\mathrm{p})\ \} \bullet \{\ \tilde{\sigma}(p)\ \} \\ \{\ \tilde{\sigma}(\mathrm{p})\ \} &= \{\ \tilde{\mathrm{C}}(\mathrm{p})\ \} \bullet \{\ \tilde{\varepsilon}(p)\ \} \end{aligned} \qquad [2.51]$$

The difference is that *equations for viscoelastic materials are presented in the space transform and the time variable is replaced by complex variable p*. Notice that the 6 x 6 matrix is reversed:

$$\{\ \tilde{\mathrm{S}}(\mathrm{p})\ \} = \{\ \tilde{\mathrm{C}}(\mathrm{p})\ \}^{-1} \quad \Leftrightarrow \quad \{\ \tilde{\mathrm{C}}(\mathrm{p})\ \} = \{\ \tilde{\mathrm{S}}(\mathrm{p})\ \}^{-1} \qquad [2.52]$$

The solution to a viscoelastic problem can be found using the Carson-Laplace transform. The algebraic solution of an elastic problem can be used and, with the principle of correspondence, algebraic calculus is applied to find the solution (see Figure 2.8). It is worth bearing in mind that calculations are made in Carson-Laplace's space. To obtain real-time solutions it is necessary to use the inverse Carson-Laplace transform [ROB 66]. Figure 2.9 includes various steps in the solution of the problem.

For transient problems, the search for a solution using this method is not easy, in the sense that the application of inverse Carson-Laplace transform requires

@Seismicisolation

integration in the complex plane with an appropriate contour in order to obtain the inside of the domain. It is therefore delimited by the contour and the complex variable function is analytic [VIN 66].

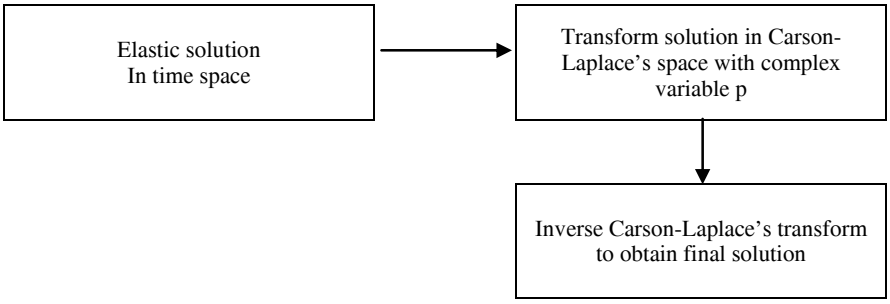

Figure 2.9. *Various steps required to arrive at the final solution to the viscoelastic problem*

Fortunately, a class of problem exists in which there is no need to evaluate the inverse Carson-Laplace transform for a bounded medium under harmonic excitation.

2.5.2. *Complex moduli*

Carson transform simplifies the writing of constitutive equations in linear viscoelasticity. In practical applications, Fourier transform is more appropriate for tackling viscoelastic problems. By definition, the Fourier transform of time function f(t) is defined as:

$$\mathscr{F}\left[f(t)\right] = \int_{-\infty}^{+\infty} f(t)\ e^{-j\omega t}\ dt = \hat{f}(\omega) \qquad [2.53]$$

where ω is the circular frequency. Applying equations [2.53] to [2.28] and [2.30] we obtain:

$$\mathscr{F}\left[\varepsilon(t)\right] = \hat{\varepsilon}\ (\omega) = \left[j\ \omega\ \hat{J}\ (\omega)\right]\ \hat{\sigma}\ (\omega) \qquad [2.54]$$

$$\mathscr{F}\left[\sigma(t)\right] = \hat{\sigma}\ (\omega) = \left[j\ \omega\ \hat{R}\ (\omega)\right]\ \hat{\varepsilon}\ (\omega) \qquad [2.55]$$

@Seismicisolation

In the second members of equations [2.54] and [2.55], between the brackets, we obtain:

$$j\,\omega\,\hat{J}\,(\omega) = \tilde{S}\,(\omega) \text{ complex compliance} \qquad [2.56]$$

$$j\,\omega\,\hat{R}\,(\omega) = \tilde{C}\,(\omega) \text{ complex stiffness} \qquad [2.57]$$

Generalization of equations [2.56] and [2.57] to tridimensional constitutive equations using complex compliances and stiffness are (see also equation [2.51]):

$$\begin{aligned} \{\,\hat{\varepsilon}(\omega)\,\} &= \{\,\tilde{S}(\omega)\,\} \bullet \{\,\hat{\sigma}(\omega)\,\} \\ \{\,\hat{\sigma}(\omega)\,\} &= \{\,\tilde{C}(\omega)\,\} \bullet \{\,\hat{\varepsilon}(\omega)\,\} \end{aligned} \qquad [2.58]$$

in which:

$$\tilde{S}_{pq}\,(\omega) = S'_{pq}(\omega) + j\,S''_{pq}(\omega) = j\,\omega\,\hat{J}_{pq}\,(\omega) \qquad p=1,2,...,6,\ q=1,2,...,6$$

$$\tilde{C}_{pq}\,(\omega) = C'_{pq}(\omega) + j\,C''_{pq}(\omega) = j\,\omega\,\hat{J}_{pq}\,(\omega) \qquad p=1,2,...,6,\ q=1,2,...,6$$

Table 2.3 presents various ways of writing complex moduli.

	Complex stiffness	**Complex compliance**	**Diagram**
Storage modulus	$C'_{pq}\,(\omega)$	$S'_{pq}(\omega)$	Cole-Cole [COL 41]
Loss modulus	$C''_{pq}(\omega)$	$S''_{pq}(\omega)$	
Storage modulus	$C'_{pq}\,(\omega)$	$S'_{pq}(\omega)$	Structural approach
Loss factor	$\text{tg}\,\delta^{C}_{pq}(\omega) = C''_{pq}/C'_{pq}$	$\text{tg}\,\delta^{S}_{pq}(\omega) = S''_{pq}/S'_{pq}$	
Magnitude	$\lvert\tilde{C}_{pq}(\omega)\rvert = \sqrt{\left(C'_{pq}\right)^2 + \left(C''_{pq}\right)^2}$	$\lvert\tilde{S}_{pq}(\omega)\rvert = \sqrt{\left(S'_{pq}\right)^2 + \left(S''_{pq}\right)^2}$	Bode or Argand represent-tation
Loss angle	$\delta^{C}_{pq/}(\omega) = \text{Arc tan}\left(C_{pq}''/C'_{pq}\right)$	$\delta^{S}_{pq}(\omega) = \text{Arc tan}\left(S_{pq}''/S'_{pq}\right)$	

Table 2.3. *Various representations of complex stiffness*

@Seismicisolation

Complex stiffness and the compliance 6 x 6 matrix have the same properties as stiffness and the compliance matrix in elasticity at each circular frequency ω, see Chapter 1. Technical complex moduli, complex Young's moduli and complex Poisson's ratio are defined by the following relations:

$$\tilde{E}_p(\omega) = \frac{1}{\tilde{S}_{p\,p}(\omega)}; \qquad \tilde{\nu}_{pq}(\omega) = \tilde{S}_{pq}(\omega)\,\tilde{E}_p(\omega)$$

with p = 1,2,3, q = 1,2,3 $p \neq q$

Notice that the 6 x 6 complex compliance and stiffness matrix are reversed when circular frequency ω is set:

$$\left\{ \tilde{S}(\omega) \right\} = \left\{ \tilde{C}(\omega) \right\}^{-1} \quad \Leftrightarrow \quad \left\{ \tilde{C}(\omega) \right\} = \left\{ \tilde{S}(\omega) \right\}^{-1} \qquad [2.59]$$

The Cole-Cole diagram [COL 41] and Nyquist diagram in viscoelastic materials are referred to.

2.5.3. *Properties of the complex relaxation and creep components matrix versus circular frequency*

Mathematical properties are necessary for understanding the behavior of viscoelastic materials, but researchers' reasoning is taken into account.

2.5.3.1. *Theoretical results*

We can prove that the variation of the real part of a complex modulus *versus* frequency is opposite to the variation of the same modulus *versus* time [CHE 89]. Keeping section 2.4.3.1 in mind, we can underscore the following properties of complex moduli $\tilde{C}_{pp}(\omega)$ and $\tilde{S}_{pp}(\omega)$:

- $C'_{pp}(\omega)$ increases with circular frequency ω, p = 1,2,…,6;
- $C''_{pp}(\omega) > 0$ stress is ahead of strain in the field of phase;
- $S'_{pp}(\omega)$ decreases with circular frequency ω, p = 1,2,…,6;

@Seismicisolation

– $S''_{pp}(\omega) < 0$ strain is behind stress in the field of phase.

The real part of the Fourier transform of real function is an even function of circular frequency ω. The imaginary part is an odd function of circular frequency ω.

The Kramer-Krönig relationship was initially developed in optics in the framework of the dispersion theory of X-rays and physics of scattering light scattering in radiation and optics [SHE 05]. It results from the causality[8] principle applied to the component of relaxation or creep matrix {C(t)} and {S(t)}, i.e. ({C(t)}= 0 and {S(t)}=0 if t < 0). These mathematical results give rise to *inter-relationships between components of complex stiffness and compliance matrix*. The results are summarized in Table 2.4. Notice that complex Young's moduli $\tilde{E}_p(\omega)$, p=1,2,3 have the same properties as $\tilde{C}_{pp}(\omega)$.

Component	*Variation*	*Sign*	*Parity*	*Kramers-Krönig relation*[8]
$C'_{pq}(\omega)$	Increase with ω when p=q	Positive, > 0 when p=q	Even with ω	$C'_{pq}(\omega) = \frac{\omega}{\pi}\,\text{v.p}\int_{-\infty}^{+\infty} \frac{C''_{pq}(\xi)}{\xi(\omega-\xi)}\,d\xi$
$C''_{pq}(\omega)$	?	Positive, > 0 when p=q	Odd with ω	$C''_{pq}(\omega) = -\frac{\omega}{\pi}\,\text{v.p}\int_{-\infty}^{+\infty} \frac{C'_{pq}(\xi)}{\xi(\omega-\xi)}\,d\xi$
$S'_{pq}(\omega)$	Decrease with ω when p=q	Negative, < 0 when p=q	Even with ω	$S'_{pq}(\omega) = \frac{\omega}{\pi}\,\text{v.p}\int_{-\infty}^{+\infty} \frac{S''_{pq}(\xi)}{\xi(\omega-\xi)}\,d\xi$
$S''_{pq}(\omega)$	?	Negative, < 0 when p=q	Odd with ω	$S''_{pq}(\omega) = -\frac{\omega}{\pi}\,\text{v.p}\int_{-\infty}^{+\infty} \frac{S'_{pq}(\xi)}{\xi(\omega-\xi)}\,d\xi$

Table 2.4. *Mathematical properties of complex stiffness and compliance components, p = 1,2,…,6 , q = 1,2,…,6. v.p designates principal value*

8 If f(t) is a causal function, then f (t)=f(t) H(t) where H(t) is the step Heaviside function. In Fourier transform space, the previous relation becomes $\hat{f}(\omega) = \frac{1}{j\pi}\,\text{V.p}\int_{-\infty}^{+\infty} \frac{\hat{f}(\xi)}{\omega-\xi}\,d\xi$. V.p denotes the Cauchy principal value.

@Seismicisolation

2.5.3.2. *Practical results*

Table 2.5 presents a rough estimation of the Young's modulus of classical viscoelastic materials at ambient temperature (T = 20°C). In the design of polymer and rubber structures, frequencies and temperature must be taken into account.

Engineers have a familiar routine in material representations, depending on their professional specialties:

– metallurgists only consider only real part of modulus E'. Damping is neglected except for special alloys (Fe-Cr-X alloys) [PUL 01, YIN 01];

– chemical engineers in the polymers field are fond of "structure representation" (see Table 2.3) and usually mix the magnitude and real part of complex moduli (see Figure 2.10), the material loss angle being very low;

– chemical engineers working on rubbers use both the real and imaginary parts of moduli that are comparable in order of magnitude.

Materials	**Real part of Young's modulus E'**	**Damping of Young's modulus $\eta = \tan\delta = E''/E'$**
Metallic materials	80 GPa – 220 GPa	10^{-4}–10^{-1}%
Polymers materials	2 GPa – 8 GPa	1–5%
Rubber materials	10 MPa – 100 MPa	10–60%

Table 2.5. *Rough estimations of various complex Young's moduli of classical materials at ambient temperature (T= 20°C)*

2.6. Correspondence principle and the solution of the harmonic viscoelastic system

A simple and convenient approach consists of assimilating the Laplace transform into the Fourier transform with p = j ω. Mathematically speaking, this approach lacks mathematical rigor [ZEM 65]: the Laplace transform is defined on right side, or causal mathematical distributions, while the Fourier transform is defined on the mathematical distribution of slow growth, for example.

The second remark concerns the permanent regime of vibration of a bounded medium. Solutions to the structure's harmonic responses are only obtained after the transient responses disappear. In other parts of this book, applications of this method will be extensively used.

@Seismicisolation

2.7. Inter-relationship between harmonic and transient regimes

Transient and harmonic tests are the two families of tests used in viscoelasticity. The inter-relationship concerns the constitutive equations of materials. During the second half of the 20th century, research was carried out in this area. Readers who would like further details on this problem might consult Ferry [FER 70].

Let us recall the two ways of writing constitutive equations. In a transient regime (equations [2.39] and [2.45]):

$$\begin{aligned} \{\sigma(t)\} &= \frac{d}{dt}\int_0^t \{C(t-\tau)\}\,\{\varepsilon(\tau)\}\,d\tau \\ \{\varepsilon(t)\} &= \frac{d}{dt}\int_0^t \{S(t-\tau)\}\,\{\sigma(\tau)\}\,d\tau \end{aligned} \qquad [2.60]$$

With a harmonic regime [2.58]:

$$\begin{aligned} \{\hat{\varepsilon}(\omega)\} &= \{\tilde{S}(\omega)\}\,\{\hat{\sigma}(\omega)\} \\ \{\hat{\sigma}(\omega)\} &= \{\tilde{C}(\omega)\}\,\{\hat{\varepsilon}(\omega)\} \end{aligned} \qquad [2.61]$$

Circumflex designates the Fourier transform (equation [2.56]). Let us try to obtain a relation between the stiffness relaxation matrix {C(t)} and the complex stiffness matrix $\{\tilde{C}(\omega)\}$ on one hand and the compliance matrix {S(t)} and complex compliances matrix $\{\tilde{S}(\omega)\}$ on the other hand.

Applying the Fourier transform to equation [2.60], equation [2.61] being taken into account, we obtain:

$$\{\tilde{C}(\omega)\} = \{C'(\omega)\} + j\,\{C''(\omega)\} = j\omega\int_0^{+\infty}\left[\{C_0(t)\}-\{C_e\}\right] e^{-j\omega t}\,dt \qquad [2.62]$$

$$\{\tilde{S}(\omega)\} = \{S'(\omega)\} + j\,\{S''(\omega)\} = j\omega\int_0^{+\infty}\left[\{S_0(t)\}-\{S_e\}\right] e^{-j\omega t}\,dt \qquad [2.63]$$

@Seismicisolation

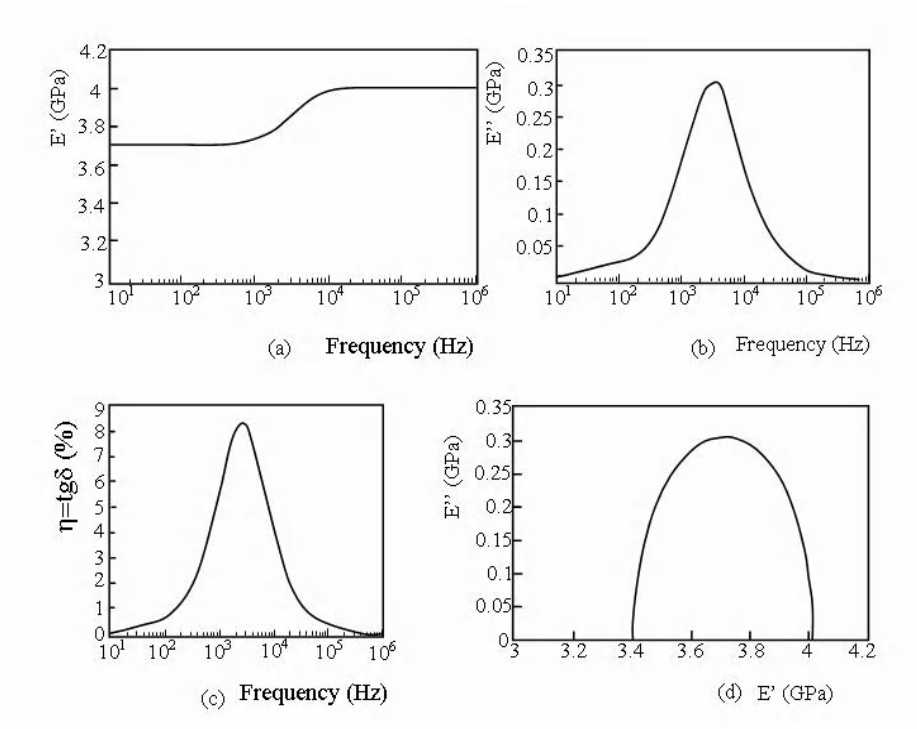

Figure 2.10. *Complex Young's modulus of epoxy resin* versus *frequency: a) real part; b) imaginary part; c) damping factor (tg δ); d) Cole-Cole diagram*

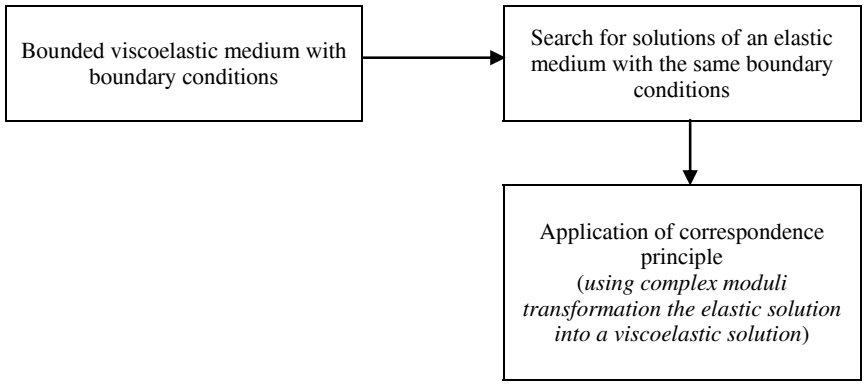

Figure 2.11. *Solution of harmonic response of a viscoelastic bounded medium*

@Seismicisolation

where $\{C_e\}$ designates the equilibrium stiffness matrix and $\{S_e\}$ the equilibrium compliance matrix[9]. In equation [2.62], by identification of real and imaginary terms on both equation members we get:

$$\begin{aligned}\{C'(\omega)\} &= \omega \int_0^{+\infty} \left[\{C_0(t)\} - \{C_e\}\right] \sin \omega t \, dt \\ \{C''(\omega)\} &= \omega \int_0^{+\infty} \left[\{C_0(t)\} - \{C_e\}\right] \cos \omega t \, dt\end{aligned} \qquad [2.64]$$

In [2.64], the lower bound of the integral is taken to equal zero because the relaxation stiffness matrix $\{C(t)\}$ is a causal or right-sided matrix ($\{C(t)\} = 0$ if $t<0$). In the past ($t<0$) the material has been at rest (neutral).

If we apply inverse Fourier transform to [2.62] we get:

$$\{C(t)\} \begin{cases} = \dfrac{1}{\pi\,\omega} \displaystyle\int_0^{+\infty} \left(\left[\{C'(\omega)\} - \{C_e\}\right] \sin \omega t + \{C''(\omega)\} \cos \omega t\right) dt & \text{if } t > 0 \\ = 0 & \text{if } t < 0 \end{cases}$$

[2.65]

where $\{C_e\}$ is the equilibrium stiffness matrix. The inter-relationships for the compliance matrix are similar to [2.64] and [2.65].

In spite of their apparent simplicity, the inter-relationships presented above and in Table 2.4 are not practically tractable. The main reason is that complex stiffness and compliance are known to be in a large range of circular frequency from zero to infinity because the integral runs from zero to infinity. Practically speaking this is not the case. The relaxation function is not known in the whole range of time from zero to infinity: it covers no more than six or eight decades. The same remarks are valid for inter-relationships between relaxation and creep functions.

To circumvent these difficulties of calculation, approximate equations have been proposed in detail [FER 70]. One example of the approximate method is given below [NIN 59]. First- and second-time derivatives of stiffness relaxation and creep

9 This way of writing permits to us obtain only components that vary with time in equations [2.62] and [2.63].

@Seismicisolation

compliance matrix are evaluated at three values of circular frequency. For example, in a tension test, ( )° and ( )°° designate first- and second-time derivatives respectively:

$$R(t) = E(t) = \mathrm{E}'(\omega) - 0.40\ \mathrm{E}''(0.40\omega) + 0.014\ \mathrm{E}''(10\omega)$$

$$J(t) = \mathrm{S}(t) = \mathrm{S}'(\omega) - 0.40\ \mathrm{S}''(0.40\omega) + 0.014\ S''(10\omega)$$

where $\omega = \frac{1}{t}$ and $\tilde{R}(\omega) = \tilde{\mathrm{E}}(\omega) = \frac{1}{\tilde{\mathrm{J}}(\omega)} = \frac{1}{\tilde{\mathrm{E}}(\omega)}$.

Another method can be found in [FER 70]. Taking the Laplace transform asymptotic properties into account[10], we arrive at the asymptotic behavior of viscoelastic materials. For stiffness relaxation matrix:

$$\lim_{t\to 0^+}\{C(t)\} = \lim_{\omega\to\infty}\left\{\tilde{\mathrm{C}}(\omega)\right\} = \{C_0\}, \qquad \{C_0\} = \left\{C(0^+)\right\}$$

transient regime [2.66]

$$\lim_{t\to\infty}\{C(t)\} = \lim_{\omega\to 0}\left\{\tilde{\mathrm{C}}(\omega)\right\} = \{C_\infty\}, \qquad \left\{C_{oo}\right\} = \lim_{t\to\infty}\{C(t)\}$$

harmonic regime

and for creep compliance matrix:

$$\lim_{t\to 0^+}\{S(t)\} = \lim_{\omega\to\infty}\left\{\tilde{\mathrm{S}}(\omega)\right\} = \{S_0\}, \qquad \{S_0\} = \left\{S(0^+)\right\}$$

---

10 Assume that f(t) is a causal function with a limit f_0 as $t \to 0$ and f_∞ as $t \to \infty$, and $\tilde{f}(p)$ Carson-Laplace transform of f is:

- $\lim_{t\to 0^+} f(t) = \lim_{p\to\infty} \tilde{f}(p) = f_0$, $f_0 = f(0^+)$ it f continuous when t >0
- $\lim_{t\to\infty} f(t) = \lim_{p\to 0^+} \tilde{f}(p) = f_\infty$, $f_\infty = \lim_{t\to\infty} f(t)$ it f continuous when t >0

@Seismicisolation

transient regime [2.67]

$$\lim_{t\to\infty}\{S(t)\} = \lim_{\omega\to 0}\left\{\tilde{S}(\omega)\right\} = \{S_\infty\}, \quad \{S_\infty\} = \lim_{t\to\infty}\{S(t)\}$$

harmonic regime

Equations [2.66] and [2.67] imply that the imaginary part of the complex stiffness matrix coefficients and compliance matrix coefficients vanish for large and small values of circular frequency ω.

2.8. Modeling of creep and relaxation functions: example

The purpose of this example is to express creep and relaxation functions as a combination of a finite number of parameters in mathematical functions of time. Functions of time are known (generally exponential functions) and parameters are particular to viscoelastic materials.

The relevance of this approach is to obtain convenient constitutive viscoelastic laws in a large range of time or frequency. A simple way to achieve this is to consider rheological schemes that are made of springs and dashpots [NOV 65], with the following notation:

R(t) = C(t): scalar relaxation function

J(t) = S(t): scalar creep function

In Carson Laplace space $\tilde{R}(p)$ and $\tilde{J}(p)$ are joined up by equation [2.68], p = j ω in Fourier space transform:

$$\tilde{R}(p) = \frac{1}{\tilde{S}(p)} \qquad [2.68]$$

We see that in the expression of tridimensional constitutive equations, see [2.52] and [2.59], equation [2.59] is not true when considering the components of complex stiffness and compliance matrix [MAR 05]. However, equation [2.68] can be used in tridimensional continuum mechanics in the special case of a tension

@Seismicisolation

test ($\tilde{R}(p) = \tilde{E}_i(p) = \frac{1}{\tilde{S}_{ii}(p)}$, Young's modulus in direction i and shear test $\tilde{R}(p) = \tilde{G}_{kl}(p) = \frac{1}{\tilde{S}_{mm}(p)}$, m=9-(k + l) in equation [2.17] and Coulomb's modulus in plane (k,l)).

Both types of formulae [2.68] are sufficient to characterize the viscoelastic behavior of isotropic materials:

– for Young's modulus $\tilde{R}(p) = \tilde{E}(p)$;

– for Coulomb's modulus $\tilde{R}(p) = \tilde{G}(p)$.

2.8.1. *Basic rheological cells*

Let us consider basic cells, the viscoelastic behavior of which depend on one or two parameters (see Figure 2.12).

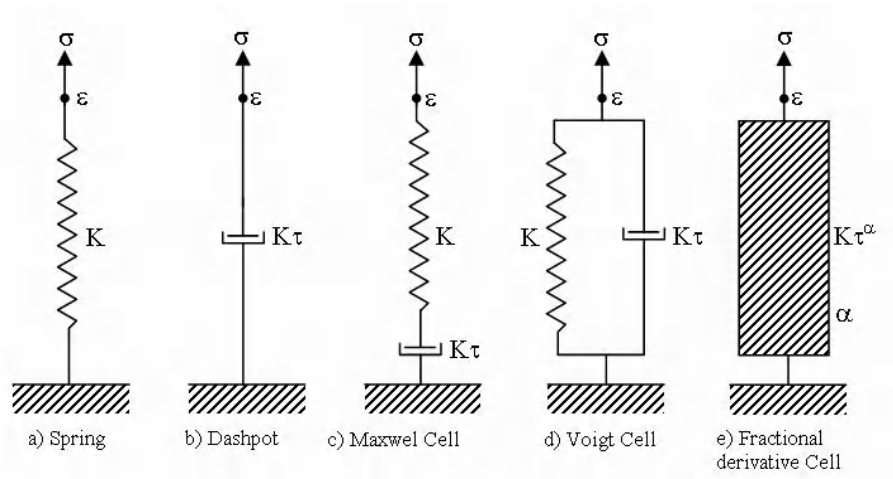

Figure 2.12. *Rheological schemes of basic viscoelastic cells: a) and b) one parameter modeling; c), d) and e) two parameter modeling*

Basic viscoelastic cells can be put together to achieve full viscoelastic modeling, characterized by resultant creep or relaxation functions. The rule is that:

@Seismicisolation

– *series assembling of basic cells*: the resultant creep function is the sum of basic creep functions;

– *parallel assembling of basic cells*: the resultant relaxation function is the sum basic relaxation functions.

The results are summarized in Table 2.4, in which:

– H(t) is the Heaviside step function;

– δ(t) is the Dirac distribution;

– j is the imaginary complex number,

$$(\mathrm{j}\omega\tau)^{\alpha} = (\omega\tau)^{\alpha} e^{j\alpha\pi/2} = (\omega\tau)^{\alpha}\left(\cos\frac{\alpha\pi}{2} + \mathrm{j}\ \sin\frac{\alpha\pi}{2}\right);$$

– Γ(z) is the factorial gamma function, $\Gamma(z) = \int_0^{+\infty} \mathrm{x}^{\mathrm{z}-1} e^{-x}\ \mathrm{dx}$;– $\frac{\mathrm{D}^{\alpha} f(t)}{\mathrm{D\,t}^{\alpha}}$ is the fractional derivative of causal distribution f(t) [BAG 83], which is defined by the following mathematical formulae: $\frac{\mathrm{D}^{\alpha} f(t)}{\mathrm{D\,t}^{\alpha}} = \frac{1}{\Gamma(1-\alpha)} \frac{d}{dt} \int_0^t \frac{\mathrm{f}(\xi)}{(\mathrm{t}-\xi)^{\alpha}}\ \mathrm{d}\xi$, and p^{α} is the Laplace transform of the above fractional derivative.

The fractional derivative cell is a continuum between spring and dashpot: $\alpha = 0$ (spring), $\alpha = 1$ (dashpot). The use of a fractional derivative permits us to reduce the number of rheological parameters characterizing the viscoelastic behavior of materials [BED 04].

2.8.2. *General parametric modeling*

Looking at Table 2.6, the Carson-Laplace transform of relaxation and creep functions can be considered a quotient of two polynomial expressions. P(p) and Q(p) are functions of complex variable p.

$$\tilde{\mathrm{R}}(\mathrm{p}) = \mathrm{K}_{\infty} \frac{Q(p)}{P(p)} = \mathrm{K}_{\infty} \frac{\left(1 + \sum_{i=1}^{i=n} b_i p^i\right)}{\left(1 + \sum_{i=1}^{i=n} a_i p^i\right)} \qquad [2.69]$$

@Seismicisolation

The Carson Laplace transform of a creep function is then also expressed as a quotient of two polynomial functions:

$$\tilde{J}(p) = \frac{1}{K_\infty}\frac{P(p)}{Q(p)} = \frac{1}{K_\infty}\frac{\left(1+\sum_{i=1}^{i=n} a_i p^i\right)}{\left(1+\sum_{i=1}^{i=n} b_i p^i\right)} \qquad [2.70]$$

According to equations [2.69] and [2.70], stress and strain are related by the following expression:

$$\sigma(t) + \sum_{i=1}^{i=n} a_i \frac{D^i\sigma}{Dt^i} = K_\infty\left(\varepsilon(t) + \sum_{i=1}^{i=n} b_i \frac{D^i\varepsilon}{Dt^i}\right) \qquad [2.71]$$

The stress-strain relationship [2.71] can be brought into a general expression including fractional derivatives (see Table 2.6):

$$\sigma(t) + \sum_{i=1}^{i=n} a_i \frac{D^{\alpha_i}\sigma}{Dt^{\alpha_i}} = K_\infty\left(\varepsilon(t) + \sum_{i=1}^{i=n} b_i \frac{D^{\alpha_i}\varepsilon}{Dt^{\alpha_i}}\right) \qquad [2.72]$$

Polynomial function in equation [2.71] can be rewritten as a product of linear functions:

$$P(p) = \frac{p+\mu_1}{\mu_1}.\frac{p+\mu_2}{\mu_2}.....\frac{p+\mu_n}{\mu_n},$$

$$Q(p) = \frac{p+\gamma_1}{\gamma_1}.\frac{p+\gamma_2}{\gamma_2}.....\frac{p+\gamma_n}{\gamma_n}$$

in which $-\mu_i$ and $-\gamma_i$ are respectively the roots of polynomials P(p) and Q(p) ($\mu_\iota > 0$, $\gamma_\iota > 0$, I = 1, 2,…..;n). This polynomial approach, characterized by 2n + 1 parameters, has the advantage of providing simple expressions[11] for creep and relaxation functions [NOV 65].

11 Equations [2.73] come from the analysis of expressions:

$$P^2(p)\ \frac{d}{dp}\left\{\frac{Q(p)}{pP(p)}\right\}\Bigg|_{p=-\mu_i} \quad \textit{and} \quad Q^2(p)\ \frac{d}{dp}\left\{\frac{P(p)}{pQ(p)}\right\}\Bigg|_{p=-\gamma_i} \qquad i= 1,2,....,n$$

@Seismicisolation

$$\boxed{\begin{aligned} R(t) &= \mathrm{K}_\infty \left(1 - \sum_{i=1}^{i=n} \frac{Q(-\mu_i)}{\mu_i \ \mathrm{P}'(-\mu_i)} \ e^{-\mu_i t} \right) \\ J(t) &= \frac{1}{\mathrm{K}_\infty} \left(1 - \sum_{i=1}^{i=n} \frac{P(-\gamma_i)}{\gamma_i \ \mathrm{Q}'(-\gamma_i)} \ e^{-\gamma_i t} \right) \end{aligned}} \qquad [2.73]$$

$$\mathrm{P}'(-\mu_i) = \left. \frac{\mathrm{dP}}{\mathrm{dp}} \right|_{p = -\mu_i},$$

$$\mathrm{Q}'(-\gamma_i) = \left. \frac{\mathrm{dQ}}{\mathrm{dp}} \right|_{p = -\gamma_i} \qquad \mathrm{i} = 1,2,....,\mathrm{n}$$

If R(t) increases and J(t) decreases with time $\frac{Q(-\mu_i)}{\mathrm{P}'(-\mu_i)} < 0$ and $\frac{P(-\gamma_i)}{\mathrm{Q}'(-\gamma_i)} > 0$, then [BLA 60] the roots of P(p) and Q(p) are arranged in alternate order:

$$0 < \gamma_1 < \mu_1 < \gamma_2 < \mu_2 < .....< \gamma_n < \mu_\mathrm{n} \qquad [2.74]$$

According to equations [2.66] and [2.67], we may rewrite the asymptotic behavior of creep and relaxation functions in the following way:

– relaxation function:

$$\lim_{t \to 0^+} R(t) = \lim_{\omega \to \infty} \tilde{\mathrm{R}}(\omega) = \mathrm{K}_\infty \frac{\mathrm{b_n}}{\mathrm{a_n}} = \mathrm{K}_\infty \frac{\mu_1.\mu_2....\mu_\mathrm{n}}{\gamma_1.\gamma_2....\gamma_\mathrm{n}}$$

$$\lim_{t \to \infty} R(t) = \lim_{\omega \to 0^+} \tilde{\mathrm{R}}(\omega) = \mathrm{K}_\infty$$

– creep function:

$$\lim_{t \to 0^+} J(t) = \lim_{\omega \to \infty} \tilde{\mathrm{J}}(\omega) = \frac{1}{\mathrm{K}_\infty} \frac{a_\mathrm{n}}{b_\mathrm{n}} = \frac{1}{\mathrm{K}_\infty} \frac{\gamma_1.\gamma_2....\gamma_\mathrm{n}}{\mu_1.\mu_2....\mu_\mathrm{n}}$$

$$\lim_{t \to \infty} J(t) = \lim_{\omega \to 0^+} \tilde{\mathrm{J}}(\omega) = \frac{1}{\mathrm{K}_\infty}$$

@Seismicisolation

where μ_i and γ_i are commensurate with frequency so specialists in rheology adopt the convention $\mu_i = \omega_{R_i} = \dfrac{1}{\tau_{R_i}}$ and $\gamma_i = \omega_{J_i} = \dfrac{1}{\tau_{J_i}}$ where τ_{R_i} and τ_{J_i} are respectively relaxation times and creep times for i= 1,2,…,n.

Basic cell / Function	Spring Figure 2.12a	Dashpot Figure 2.12b	Maxwell cell Figure 2.12c	Voigt cell Figure 2.12d	Fractional derivative cell Figure 2.12e $0 < \alpha < 1$
$\tilde{R}(p)$ Relaxation	K	$K\ \tau\, p$	$\dfrac{K\tau p}{1+\tau p}$	$K(1+\tau p)$	$K(\tau p)^{\alpha}$
$\tilde{J}(p)$ Compliance	$\dfrac{1}{K}$	$\dfrac{1}{K\tau p}$	$\dfrac{1+\tau\, p}{K\tau\, p}$	$\dfrac{1}{K(1+\tau p)}$	$\dfrac{1}{K(\tau p)^{\alpha}}$
R(t) Relaxation	$K\mathrm{H}(t)$	$K\tau\delta(t)$	$H(t)K\mathrm{e}^{-t/\tau}$	$K\left[\mathrm{H}(t)+\tau\delta(t)\right]$	$\dfrac{\mathrm{D}^{\alpha-1}\delta(t)}{\mathrm{D}\,t^{\alpha-1}}$
J(t) Compliance	$\dfrac{1}{K}H(t)$	$\dfrac{t}{K\tau}H(t)$	$\dfrac{H(t)}{K}(1+\dfrac{t}{\tau})$	$\dfrac{H(t)}{K}(1-\mathrm{e}^{-t/\tau})$	$\dfrac{H(t)t^{\alpha}}{K\tau^{\alpha}\Gamma(\alpha+1)}$
$\tilde{R}(\omega)$ Relaxation	K	$j\,K\omega\tau$	$\dfrac{jK\omega\tau}{1+\mathrm{j}\omega\tau}$	$K(1+j\omega\tau)$	$K(\mathrm{j}\omega\tau)^{\alpha}$
$\tilde{J}(\omega)$ Compliance	$\dfrac{1}{K}$	$-\dfrac{j}{K\omega\tau}$	$-j\dfrac{1+\mathrm{j}\omega\tau}{K\omega\tau}$	$\dfrac{1}{K(1+j\omega\tau)}$	$\dfrac{1}{K(\mathrm{j}\omega\tau)^{\alpha}}$

Table 2.6. *Features of basic rheological cells: creep, relaxation and complex moduli*

A very simple approach to general modeling is to put together basic cells (see Table 2.16) as described in Figure 2.13. Let us consider the three following modeling options:

– *general Voigt modeling*: series assembling of Voigt cells;

– *general Maxwell modeling*: parallel assembling of Maxwell cells;

– *waterfall modeling*: parallel alternate of springs and dashpots.

@Seismicisolation

The macro-rheological properties are listed in Table 2.7.

Practically speaking, the problem of evaluating complex viscoelastic functions of a material resorts to an inverse problem. In Chapter 3, the solutions to such classes of problems are presented.

2.8.3. *Modeling with three rheological parameters: examples*

Engineers and theoreticians have to compare modeling and experimental data. A suitable compromise using both modeling and data is to fit data with three-parameter modeling and, for example, assemble basic cells (see Figure 2.13 and Table 2.7) with N = 1.

Rheological parameters are described in Figure 2.14. Mathematically speaking, the rheological functions of three parameters are the same but in practice it is more convenient to fit creep tests with Pointing-Thompson modeling and to fit vibration tests with Zener modeling.

– relaxation function R(t):

$$R(t) = \mathrm{K}_\infty \left(1 + \mathrm{k}_\mathrm{R} e^{-\frac{t}{\tau_R}} \right) \mathrm{H(t)} \qquad [2.75]$$

– creep function J(t):

$$J(t) = \mathrm{J}_\infty \left(1 - \mathrm{k}_\mathrm{J} e^{-\frac{t}{\tau_J}} \right) \mathrm{H(t)} \qquad [2.76]$$

– complex stiffness $\tilde{R}(\omega) = \tilde{C}(\omega)$:

$$\tilde{R}(\omega) = \tilde{C}(\omega) = \mathrm{K}_\infty \left(1 + \mathrm{k}_\mathrm{R} \frac{\mathrm{j}\omega\tau_R}{1 + \mathrm{j}\,\omega\tau_R} \right) \qquad [2.77]$$

– complex compliance $\tilde{J}(\omega) = \tilde{S}(\omega)$:

$$\tilde{J}(\omega) = \tilde{S}(\omega) = \mathrm{J}_\infty \left(1 - \mathrm{k}_\mathrm{J} \frac{\mathrm{j}\omega\tau_J}{1 + \mathrm{j}\,\omega\tau_J} \right) \qquad [2.78]$$

@Seismicisolation

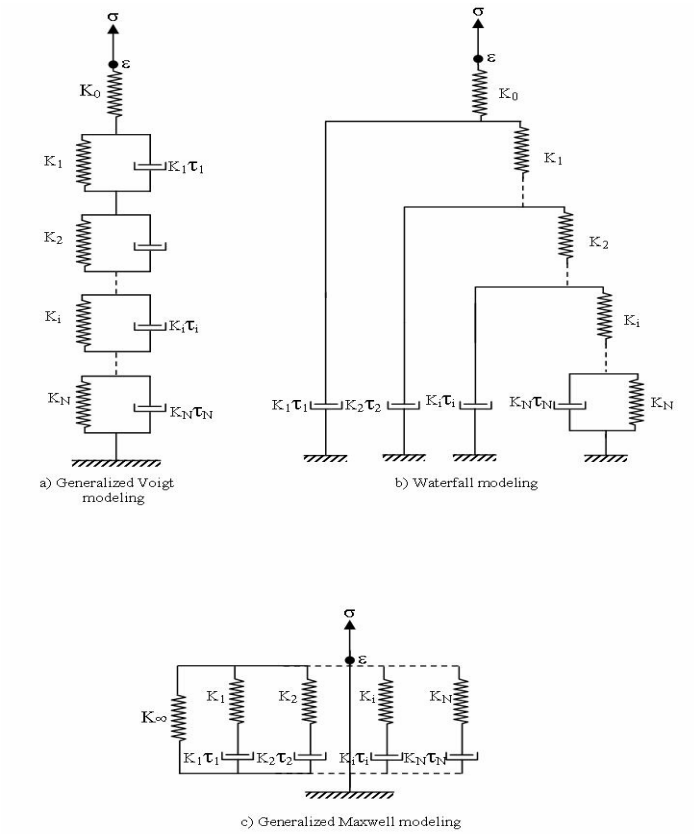

Figure 2.13. *Creep and relaxation function specific to general Maxwell's modeling*

Viscoelastic rheological parameters are related by the following equations:

$$\boxed{\begin{aligned} & J_\infty \bullet K_\infty = 1 \\ & J(0) \bullet K(0) = 1 \\ & (1 + k_R)(1 - k_J) = 1, \ k_R \geq 0, \ 0 \leq k_J \leq 1 \end{aligned}} \qquad [2.79]$$

and then:

$$\tau_J = (1 + k_R)\,\tau_R\,, \quad \tau_R = (1 - k_J)\,\tau_J \qquad [2.80]$$

@Seismicisolation

Modeling	Rheological function	Complex modulus
General Voigt, Figure 2.13a, creep function J	$J_N(t) = \frac{1}{K_0}\left(1 + \sum_{i=1}^{i=N} q_i (1 - e^{-\frac{t}{\tau_i}})\right) H(t)$ with $q_i = \frac{K_0}{K_i}$	$\tilde{J}_N(\omega) = \frac{1}{K_\infty}\left(1 - \frac{K_\infty}{K_0}\sum_{i=1}^{i=N} q_i \frac{j\omega\tau_i}{1 + j\,\omega\tau_i}\right)$ with $K_0 = K_\infty\left(1 + \sum_{i=1}^{i=N} q_i\right)$
General Maxwell, Figure 2.13c, relaxation function R	$R_N(t) = K_\infty\left(1 + \sum_{i=1}^{i=N} k_i e^{-\frac{t}{\tau_i}}\right) H(t)$ with $k_i = \frac{K_i}{K_\infty}$	$\tilde{R}_N(\omega) = K_\infty\left(1 + \sum_{i=1}^{i=N} k_i \frac{j\omega\tau_i}{1 + j\omega\tau_i}\right)$
Waterfall, Figure 2.13b, creep function J		$\tilde{J}_N(\omega) = \frac{1}{K_0}\left(1 + \sum_{i=1}^{i=N} \frac{k_i}{(1 + j\,\omega\tau_1).....(1 + j\,\omega\tau_i)}\right)$ $k_i = \frac{K_0}{K_i}$

Table 2.7. *Creep and relaxation function specific to Figure 2.13 modeling*

According to equation [2.71], stress and strain fulfill the behavior law:

$$\sigma(t) + \tau_R \frac{D\sigma}{Dt} = K_\infty\left(\varepsilon(t) + (1 + k_R)\frac{D\varepsilon}{Dt}\right) \qquad [2.81]$$

Looking at popular rheological modeling (see Figure 2.14), rheological parameters are listed in Table 2.8.

In the case of three-parameter modeling, the Bode and Cole-Cole diagrams (see Table 2.3) of complex relaxation functions are very simple geometrical figures (see Figure 2.15). The Cole-Cole diagram is a semicircle in the quarter-plane fixed by positive coordinates. Looking at the real part, imaginary part and loss factor of complex relaxations function:

@Seismicisolation

$$R'(\omega) = K_\infty \left(\frac{1 + (1 + k_R)\omega^2 \tau_R^2}{1 + \omega^2 \tau_R^2} \right)$$

$$R''(\omega) = K_\infty \left(\frac{k_R \omega \tau_R}{1 + \omega^2 \tau_R^2} \right) \qquad [2.82]$$

$$\text{tg}\ \delta^R(\omega) = \frac{k_R \omega \tau_R}{1 + (1 + k_R)\omega^2 \tau_R^2}$$

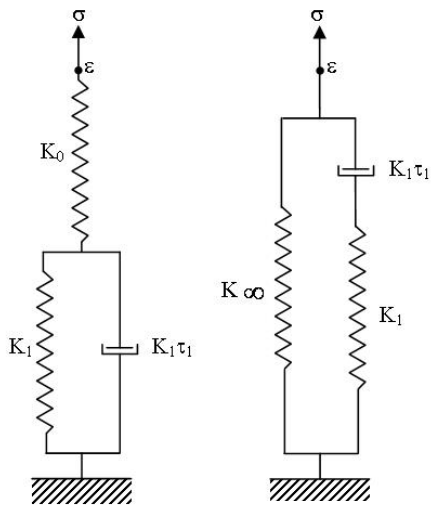

a - Pointing-Thompson modeling

b - Zener modeling

Figure 2.14. *Three-parameter modeling: a) Poynting-Thompson modeling (generalized Voigt or waterfall modeling, N=1); b) Zener modeling (generalized Maxwell, N=1)*

It is easy to show, analyzing the variation of functions *versus* non-dimensional variable $X = \omega\tau_R$, that:

– the imaginary part is maximum when $\omega = \omega_M = \frac{1}{\tau_R}$ and $R''(\omega_M) = \frac{K_\infty k_R}{2}$,

@Seismicisolation

– the loss factor is maximum when $\omega=\omega_m=\dfrac{1}{\tau_R\sqrt{1+k_R}}$ and $\mathrm{tg}\,\delta^R(\omega_m)=\dfrac{k_R}{2\sqrt{1+k_R}}$.

Modeling	K_∞	J_∞	k_R	k_J	τ_R	τ_J
Poynting-Thompson	$\dfrac{K_0K_1}{K_0+K_1}$	$\dfrac{1}{K_0}+\dfrac{1}{K_1}$	$\dfrac{K_0}{K_1}$	$\dfrac{K_0}{K_0+K_1}$	$\tau_1\dfrac{K_1}{K_0+K_1}$	τ_1
Zener	K_∞	$\dfrac{1}{K_\infty}$	$\dfrac{K_1}{K_\infty}$	$\dfrac{K_1}{K_1+K_\infty}$	τ_1	$\tau_1\dfrac{K_1+K_\infty}{K_\infty}$

Table 2.8. *Parameters of Poynting-Thomson and Zener modeling*

In the case of complex creep function, Bode and Cole-Cole diagrams are the same, just changing K_∞ into J_∞, k_R into $-k_J$ and τ_R into τ_J. Notice that $J'(\omega)$ decreases with frequency. The loss factor and imaginary part $J''(\omega)$ are negative.

Numerical values of three rheological parameter modeling of isotropic polymers are given in Table 2.9. The reader will notice that coefficient k_E and k_G and relaxation times τ_E and τ_Γ are similar. This means that for this kind of material the Poisson's ratio does not depend on time (and frequency) and remains constant, as in elasticity.

Material	**Young's modulus E**			**Coulomb's modulus G**		
	E_∞ (MPa)	k_E	τ_E (Sec)	G_∞ (MPa)	k_G	τ_G (Sec)
Epoxy resin	3,400	0.182	58.5×10^{-6}	1,290	0.185	44.6×10^{-6}
PVC	19.5	0.483	70×10^{3}	6.5	0.480	73×10^{3}

Table 2.9. *Numerical values of three-parameter modeling of epoxy resin and PVC which are the results of harmonic vibration tests (tension and torsion) and of ultrasonic tests*

@Seismicisolation

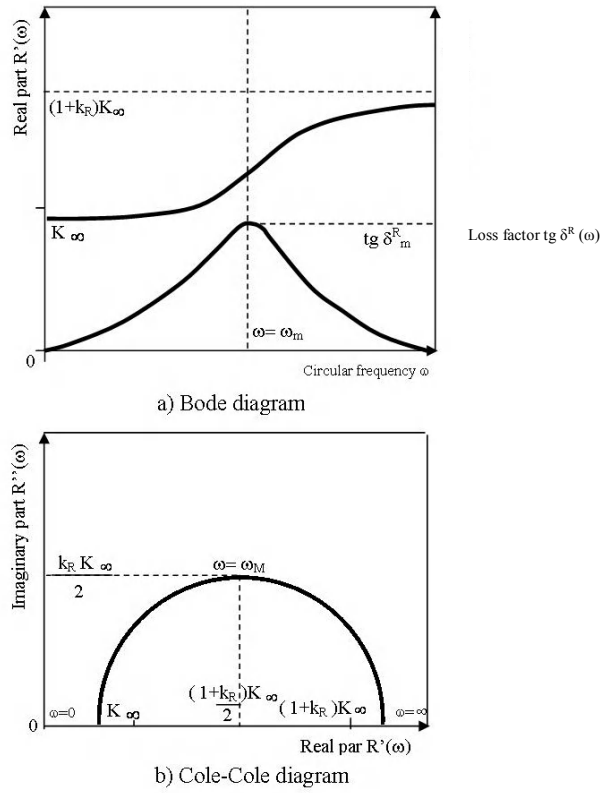

Figure 2.15. *Representations of complex relaxation functions with three-parameter modeling*

2.8.4. *Modeling with four rheological parameters: fractional derivative*

Instead of gathering a large number of basic Maxwell or Voigt cells with a large number of rheological parameters to fit experimental curves with modeling we can reduce number of parameters in putting together spring, dashpot and fractional derivative basic cells (Figure 2.16), see also section 3.2.

The Carson-Laplace transform of rheological modeling drawn in Figure 2.16 gives rise to following behavior law (equation [2.47] and Table 2.6):

@Seismicisolation

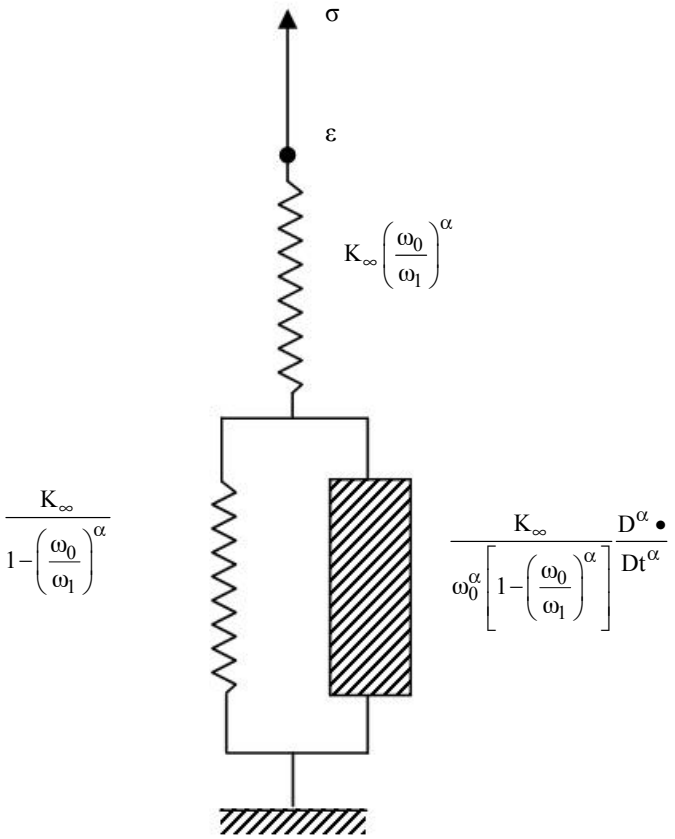

Figure 2.16. *Four-parameter modeling (K_∞, ω_0, ω_1, α) using fractional derivatives*

$$\tilde{R}(p) = K_\infty \left(\frac{1 + (p/\omega_0)^\alpha}{1 + (p/\omega_1)^\alpha} \right) \qquad [2.83]$$

and then the stress-strain relation is written in terms of fractional derivatives:

$$\sigma(t) + \frac{1}{\omega_1^\alpha}\frac{D^\alpha \sigma}{Dt^\alpha} = K_\infty \left(\varepsilon(t) + \frac{1}{\omega_0^\alpha}\frac{D^\alpha \varepsilon}{Dt^\alpha} \right)$$

Equation [2.83] leads, for example, to complex Young's modulus of materials. In the case of polyisobutylene materials [BED 04] and [NAS 75]:

@Seismicisolation

$$\tilde{E}(\omega) = E_\infty \left(\frac{1 + (j\omega/\omega_0)^\alpha}{1 + (j\omega/\omega_1)^\alpha} \right) \qquad [2.84]$$

in which E_∞ = 147 Psi, ω_0 = 40 Hz, ω_1 = 2.5 x 10 ^{6} Hz, α = 0.666.

2.9. Conclusion

What we have presented above concerns modeling in the *framework of a direct problem*. Unfortunately, a practical experimental problem in viscoelasticity requires an inverse problem, which is more difficult to tackle. We cannot know the *appropriate rheological model* or *number of elements to be assembled*. Consequently, the appropriate methods have yet to be found. The second part of Chapter 3 is devoted to this problem.

We must only use experimental curves describing the response of the material considered as a black box system, the input and output signals being known. The unicity of the solution is not guaranteed. The choice between the two methods presented in Chapter 3 – the ratio of two polynomials or fractional derivatives – is a matter of personal convenience. It also resorts to the adopted optimization technique.

2.10. Bibliography

[BAG 83] BAGLEY R. L. & TORVIK P. J., "Fractional calculus - A different approach to the analysis of viscoelastic damped structures", *AIAAJ*, vol. 21, no. 5, p. 741-748, 1983.

[BED 04] BEDA T. & CHEVALIER Y., "New method for identifying rheological parameter for fractional derivative modelling of viscoelastic behavior", *Mechanics of Time Dependent Materials*, vol. 8, p.105-118, 2004.

[BLA 60] BLAND D., *The Theory of Linear Viscoelasticity*. London, Pergamon Press, 1960.

[CHE 89] CHEVALIER Y., *Mechanics of Materials - Elastic and Viscoelastic Behavior of Anisotropic Materials*, *Techniques de l'Ingénieur*, vol. AM5, A7 750 and A7 751, 1989.

[CHR 71] CHRISTENSEN R. M., *Theory of Viscoelasticity, an Introduction*. New York, Academic Press, 1971.

[COL 41] COLE K. S. & COLE R. H., *Journal of Chemical Physics*, vol. 9, p.341, 1981.

[FER 70] FERRY J. D., *Viscoelastic Properties of Polymers*, John Wiley & Sons, 1970.

@Seismicisolation

[KNA 81] KNAUSS W. G. & EMRI I. J., "Non-linear viscoelasticity based on free volume consideration", *Computers & Structures*, vol. 13, p.123-128, 1981.

[MAR 05] MARINOVA S., POPOVA M., CHEVALIER Y., "Friction between warp and weft in viscoelastic behavior of pliable fabric composites", *Scientific Engineering of Composite Materials*, vol. 12, no. 1-2, p.109-116, 2005.

[MUL 69] MULLINS L., "Softening of rubber by deformation", *Rubber Chem Technol*, vol. 42, p. 339-362, 1969.

[NAS 75] NASHIF A. H., JONES D. I. G., HANDERSON J. P., *Vibration Damping*. New York, John Wiley & Son, 1975.

[NIN 59] NINOMYA K., FERRY J. D., *Journal of Colloidal Science,* vol. 14, p. 417-476, 1959.

[NOV 65] NOVACKI W., *Théorie du Fluage*, Paris, Editions Eyrolles, 1965.

[O'DO 95] O'DOWD N. P., KNAUSS W. G., "Time dependent large principal deformation of polymers*", J Mech Phys Solids*, vol. 43, p. 771-792, 1995.

[PUL 01] PULINO-SAGRADI D., SAGRADI M., MARTIN J. L. "Noise and vibration damping of Fe-Cr-X alloys"*, Journal of Brazilian Society of Science*, vol. 23, no. 2, p. 115-122, 2001.

[ROB 66] ROBERTS G. E., KAUFMAN H., *Table of Laplace Transform*, W. B. Saunders Company, Philadelphia, London, 1966.

[SAD 03] SAAD P., "Modélisation du comportement viscoélastique non linéaire des élastomères autour d'une précharge", *Mécanique & Industries*, vol. 4, p. 133-142, 2003.

[SCHA 99] SCHAPERY R. A., "Non linear viscoelastic and viscoplastic constitutive-equations with growing damage", *International Journal of Fracture*, vol. 97, p. 33-66, 1999.

[SCHE 80] SCHETZEN M., *The Volterra and Wiener Theories of Nonlinear Systems*, New York, John Wiley & Sons, 1980.

[SCH 78] SCHWARTZ L., *Théorie des Distributions*, Hermann, Paris, 1978.

[SHE 05] SHEIK-BAHAE M., Nonlinear optics basics: Kramers-Kronig relations in nonlinear optics, R. D. (ed.), in: *Encyclopaedia of Modern Optics*, Academic Press, Amsterdam, 2005.

[VIN 67] VINH T., Sur le passage du régime harmonique au régime transitoire*,* in: *Mémorial de l'Artillerie Française*, 3rd edition, p. 725-776,1967

[YIN 01] YIN F., TAKAMORI Y., OSHAWA A., Sato A., KAWAHARA K., *The Damping Behavior and Practical Application of the M2052 Damping Alloy*, Presentation at the 2001 International Congress and Exhibition on Noise Control Engineering, La Hague, 27-30 August 2001.

[ZEM 65] ZEMANIAN A. H., *Distribution Theory and Transform Analysis*, New York, McGraw-Hill, 1965.

@Seismicisolation

Chapter 3

Two Useful Topics in Applied Viscoelasticity: Constitutive Equations for Viscoelastic Materials

In this chapter we present two useful methods for practical characterization of viscoelastic materials[1]. Since the Second World War, theoretical and practical methods have been proposed in order to obtain complex modulus (or compliance) curves in a very large frequency range. These methods deserve the attention of practicians and researchers in this field.

The first method is well known: it concerns the artificial enlargement of the frequency (or time) range of viscoelastic responses of materials. In rheology, the frequency (or time) range is unusually large – often more than eight decades. This width is necessary for the microscopic interpretation of viscoelastic behavior at the macromolecular level. No experiment permits us obtain such curves – this large frequency (or time) range is unmeasurable with available apparatus. Its combination with temperature (considered as an adjustable parameter) permits enlargement of the response. That is Williams Landel and Ferry's main idea [FER70].

The second method permits us to obtain closed-form expressions for harmonic responses of viscoelastic samples even in a very large frequency range. By inverse

---

Chapter written by Yvon CHEVALIER and Jean Tuong VINH.

1 The second part of this chapter reproduces large extracts from French publications by [VIN 67]. Application examples are extracted from theses by Beda [BED 90] and Soula [SOU 96].

Mechanics of Viscoelastic Materials and Wave Dispersion Edited by Yvon Chevalier and Jean Tuong Vinh
© 2010 ISTE Ltd. Published 2010 by ISTE Ltd.

@Seismicisolation

Fourier transform, expressions for transient responses are obtained either by special series expansion or by sum-of-time exponentials.

3.1. Williams-Landel-Ferry's method

This method suggests the use of reduced variables (time or frequency). At the beginning, it was an empirical method that permitted us to take both temperature and time (or frequency) variables into account in the interpretation of the behavior of dilute viscoelastic polymer solutions. The temperature is used as a second parameter. The researcher obtains a collection of curves; each curve corresponds to a given temperature. There is a correspondence between temperature and frequency. By clever translation of curves obtained at different temperatures, we can finally obtain a curve with an extraordinarily large frequency range at a chosen reference temperature T_0.

Attempts to extend this method to more concentrated solutions and in undiluted polymers were conducted with success by Ferry [FER 70]. Applications of molecular theory give theoretical support to this method in a variety of situations. This is particularly interesting for high polymers.

3.1.1. *The effect of temperature change*

For a thermo-rheological simple material, a correction of time scales is necessary to take account of the variation in temperature. The relaxation function R(t) can be rewritten as a function of two variables R(t, T), with T being the temperature and t the time variable. We can attempt to write this function [MAN 78] with R(t, T) being a relaxation function, which is the product of two factors, as follows:

$$R(t, T) = h(T) \bullet \hat{R}\left[t / k(T)\right] \qquad [3.1]$$

where k (T) is a scale factor for the time variable and h(T) is a function of temperature. This function can be a constant.

If a Fourier's transform is applied to equation [3.1] we get:

$$R^*(j\omega) = h(T)\,\hat{R}^*\left[j\omega\, k(T)\right]^2 \qquad [3.2]$$

2 Star in superscript designates Fourier's transform.

@Seismicisolation

For creep function, we write:

$$J\left(t, T\right) = \frac{1}{h\left(T\right)} \bullet J\left[t/k'(T)\right] \text{ with } k'(T) < 0 \qquad [3.3a]$$

If a variable change is operated as:

$$x = \log t \text{ (or } \log \omega) \qquad [3.3b]$$

ω being the circular frequency, the relaxation curve (or complex modulus) after a change of ordinates by the factor h(T) simply undergoes translation parallel to the x axis when the temperature changes.

A reference temperature T can be adopted. All the curves (relaxation or complex modulus) undergo a translation as previously presented so as to obtain a unique curve, called the master curve. The translation can be mathematically represented by a homographic function:

$$k\left(T\right) = A \exp\left(\frac{\alpha}{\beta + T}\right) \alpha > 0 \qquad [3.4]$$

where α and β are two material constants. The interesting thing about equation [3.4] is that the reference temperature is not necessary[3].

3.1.2. *Williams-Landel-Ferry's formulation*

Ferry *et al*. [FER 70] suggested taking temperature T and material density ρ into account. So the relaxation function is written at reference temperature T_0 with $\rho = \rho_0$.

$$R_p(t) = R(t)\,(T_0\rho_0 / T\rho) \qquad [3.5]$$

3 This exponential representation is often used in the constitutive equation of material in an adiabatic regime. It is applicable to materials that are thermally activated. Unfortunately this mechanism for real materials is complex and often requires more than one term, as in equation [3.4].

@Seismicisolation

and the corresponding time variable is t/a_τ. a_τ is the shift factor that depends on temperature. ρ and ρ_0, are the densities depending on temperature T and T_0 respectively. Variation of the density can be small.

The complex stiffness is:

$$C_p(\omega) = C'_p(\omega) + j\, C''_p(\omega) \qquad [3.6]$$

$$C_p'(\omega) = [C'(\omega)]\,[T_0\,\rho_0 / T\rho] \qquad [3.7]$$

$$C''_p(\omega) = [C''(\omega)]\,[T_0\,\rho_0 / T\,\rho], \qquad [3.8]$$

where T_0 and ρ_0 refer to the curve at the reference temperature.

For creep function, the following equation is proposed:

$$J_p(t) = J(t)\,(T\,\rho / T_0\,\rho_0) \qquad [3.9]$$

In equation [3.9], factor ($T\,\rho/T_0\,\rho_0$) is the inverse ($T_0\,\rho_0/T\,\rho$) of that used in equations [3.7] and [3.8]. The corresponding complex compliance, with indexes 0 and T corresponding to reference temperature and ambient temperature respectively[4], is:

$$S_p(\omega)=S'_p(\omega)+S''_p(\omega) \qquad [3.10]$$

$$S_p'(\omega) = S'_o(\omega)[T\rho/T_0\rho_0] \qquad [3.11]$$

$$S_p''(\omega)=S''_o(\omega)[T\rho/T_0\rho_0] \qquad [3.12]$$

$$S_0(\omega)= S'_0(\omega) + jS''_0(\omega) \qquad [3.13]$$

4 Mathematical formulation of constitutive equations of material usually concerns an isothermal regime. In experiments with temperature changes, these equations have to be completed with additional terms that depend on temperature and time variables. Two tensors – thermal compressibility tensor and thermal dilatation tensor – are used.

@Seismicisolation

The relaxation function is:

$$R_0(t) = R(t)\ (T\rho/T_0\rho_0)\rho/T_0\rho_0) \qquad [3.14]$$

3.1.3. *Experimental procedure to obtain the master curve*

Figure 3.1 shows curves of the real part E^* of a complex Young's modulus *versus* circular frequency ω, T_0 being the reference temperature. The curve corresponding to temperature T, in the left of the curve referenced T_0=30ºC is to be shifted to the right.

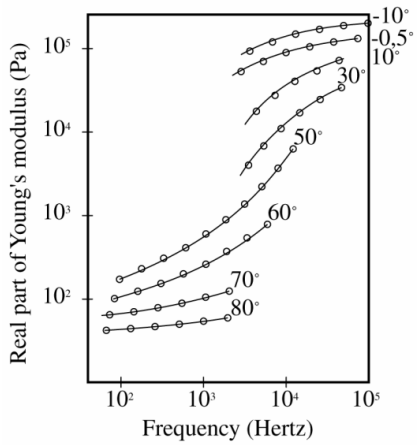

Figure 3.1. *Example of curve translation. Two translations are to be made. Abscissa shift a_T, (ordinate shift is generally weak). This figure concerns the real part of Young's modulus* versus *frequency f. After translation, a portion of the curve at T_0 coincides with a portion at T*

There is abscissa translation factor (with adjective "*reduced" as subscript,* which means circular frequency at reference temperature T_0). Another ordinate translation takes the variation in density into account. This translation is usually weak compared to the abscissa translation.

$$\omega_{reduced} = a_T\ \omega \qquad [3.15]$$

Logarithmic scales being adopted for both coordinates, we obtain:

$$\log \omega_{reduced} = \log a_T + \log \omega$$

@Seismicisolation

Factor a_T in equation [3.15] is to be evaluated for various temperatures $a_T = a_T$ (T). This function will be useful later on to obtain the extended curve at any temperature T.

The other translation concerns the ordinates. For example, in Figure 3.1 equation [3.7] is used. The vertical translation, in the logarithmic scales, is generally smaller than the horizontal translation. A knowledge of density variation with temperature ρ (T) is then necessary.

Direction for the use of Williams-Landel-Ferry's method is indicated below:

– the first step concerns choice of experimental apparatus, depending on the kind of test adopted (transient or harmonic);

– the second step is choice of temperature interval in which tests are to be conducted. Often the transition zone of the viscoelastic material is the most interesting one:

$$T_g < T < T_r \qquad [3.16]$$

when T_g corresponds to the glassy zone and T_r to the rubber-like zone ($T_g < 0$, $T_r > 0$);

– the third step concerns choice of reference temperature T_0 in the interval indicated in equation [3.17]. Often this temperature is chosen at an inflexion point in the experimental curve. Another choice, however, can be adopted for T_0;

– draw the experimental curves in logarithmic scales for the ordinates as well as the abscissas;

– draw the translation log a_T against log t (or log ω);

– evaluate factor ($T_0\,\rho_o/T\rho$) or the inverse ($T\rho/T_0\,\rho_o$) – see equations [3.5] to [3.8] or equations [3.9] to [3.14]. Multiply the ordinate by this factor. Using curves with logarithmic coordinates, this operation reduces to a coordinate addition;

– operate the curve translation (see Figure 3.1).

3.1.4. *Examples of master curves*

Figure 3.2 represents the storage modulus (real part) in the transition zone, plotted in logarithmic scale against frequency at various temperatures. Figure 3.3 is the master curve with reduced variables ωa_T, which might cover 12 decades of

@Seismicisolation

frequency. In Figure 3.3, the temperature dependence of shift factor a_T is represented.

At the beginning, Williams-Landel-Ferry's method was essentially empirical. Ferry *et al*. extended their method and incorporated many other parameters: some are physical parameters, such as pressure, others are internal variables of the polymers, such as molecular weight, free volume and molecular mobility. This method then becomes a useful tool for rheologists who want to study the physical and chemical properties of polymers in a variety of situations.

3.1.5. *Applicability of the method of reduced variables*

Practical considerations about matching the shapes of adjacent curves are helpful for practitioners of the method where:

– the same value for the shift factor a_T must superpose the viscoelastic functions i.e. real part and imaginary part of complex moduli (or compliances) must have the same factor a_T at the same temperature;

– the temperature dependence of a_T must have reasonable form consistent with experience.

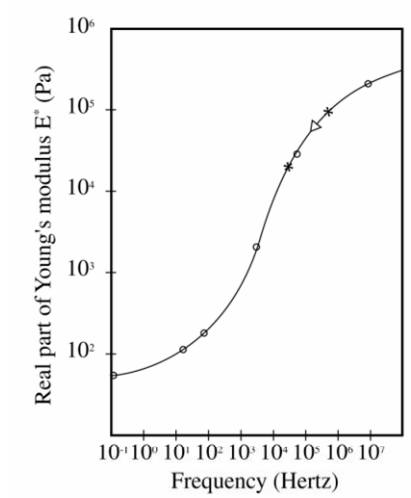

Figure 3.2. *Storage modulus curve in the transition zone between glass-like and rubber-like zones, plotted logarithmically against frequency at reference temperature: 30°C*

@Seismicisolation

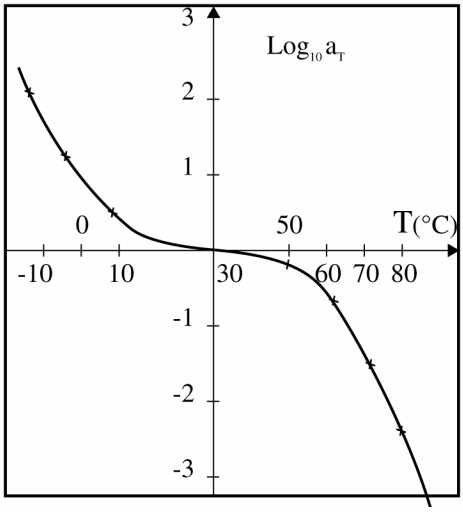

Figure 3.3. *Effect of temperature change on the curve factor of translation a_T versus temperature. The reference temperature is 30°C*

The master curve we try to obtain must cover an extremely large frequency range of seven or eight decades, while each experimental curve does not cover three frequency decades. Ferry suggested using the temperature parameter to obtain such extension. A series of testing temperatures is then adopted and a collection of isothermal curves is obtained.

The construction of the master curve at reference temperature T_0 is obtained as follows.

– In Figure 3.1, reference temperature is chosen at the middle of the transition zone where the absolute value of the complex modulus shows a drastic change of slope and radius curvature change of sign (T_0=30°C).

– If we examine the curve corresponding to $10^{\circ C}$ which is above the curve at $30^{\circ C}$, we notice that these two curves have partly a common shape and slope.

– If we horizontally translate the 10º curve at right we can partly obtain a partial superposition of the two curves; except a portion of the upper curve (at 10°C) at the right, which its contribution to the extension of the master curve at higher frequency, up to the frequency range 10^5 to 10^6 Hertz.

– There is a horizontal translation factor a_T to be evaluated.

@Seismicisolation

The same process method successively is then applied to the curve at negative temperatures -0.5°C and -10°C. Extension of the master curve to higher frequency is obtained by using negative temperatures. In rheology that corresponds to glassy zone.

The next step is the extension of the master curve at lower frequency by using experimental curves obtained at high and positive temperatures. The curve translation is operated this time at the left, at lower frequency range corresponding to the rubber zone. The master curve is then obtained in Figure 3.2 in a frequency range covering eight decades by using 8 experimental curves in Figure 3.1.

Figure 3.3 shows the curve of the translation factor a_T *versus* the temperature. It is used when we want to obtain the curve at a given temperature in the range of adopted tested temperatures from the master curve.

This method must be applied to another complex modulus component i.e. imaginary component or $\tan\delta_E$.; the translation factor must be the same as in Figure 3.3. If the two values obtained for a_T are too different, the method of reduced variables is not applicable. In this situation, the researcher must check their measurements. Errors due to transducers, non-linearity of the material responses, etc., need to be detected and the practical experiment needs to be improved. Details about cautions to be taken when applying methods can be found in [FER 70].

3.1.6. *Utilization of another representation of complex moduli (or compliances)*

In books devoted to viscoelasticity, representation of harmonic curves uses real and imaginary parts *versus* frequency. Here, the representation, using absolute value and loss angle, might be useful:

$$\left| C^* (\omega) \right| = \left\{ \left[\text{Real } C^* (\omega) \right]^2 + \left[\text{Imag } C^* (\omega) \right]^2 \right\}^{1/2} \qquad [3.17]$$

$$\delta = \text{Arc tan} \left[\frac{\text{Imag. } C^* (\omega)}{\text{Real } C^* (\omega)} \right] \qquad [3.18]$$

Equation [3.17] shows that, at a given temperature, addition of the square of the two parts of $C^*(\omega)$ is a kind of mean square average.

@Seismicisolation

3.1.7. *Extension of Williams-Landel-Ferry's methods to composite materials*

Viscoelastic properties of composite materials have given rise to research over the last five decades. Many composite materials, largely used in industry, have one polymer component. Attention is focused on their viscoelastic properties over time (or the frequency).

For advanced application in the aerospace industry, high-strength fibers such as carbon fibers in one, two or three dimensions are used. If the thermal behavior of such fibers is taken into account, we can say that such composite materials cannot be classified among simple thermal rheological materials.

Previsional calculations of viscoelastic composite materials have been successfully made by [CHE 85] among others. However, the damping properties of such materials cannot be completely predicted, although the viscoelastic properties of each component of the materials are known, because it is not possible to include important factors, such as friction between layers, friction between fibers and matrix in viscoelastic previsional calculations.

The damping properties of such materials might depend on *non-linear phenomena* that occur at the boundaries between fibers and matrix and between layers. The elastic modulus of carbon fibers increases with increasing temperature. The reduced variable method cannot be used for composites with such components.

Additional applicability conditions presented in detail in [FER 70] are valid for the extension of Williams-Landel-Ferry's method of analyzing viscoelastic composite materials.

3.2. Viscoelastic time function obtained directly from a closed-form expression of complex modulus or complex compliance

3.2.1. *Overview of state-of-the-art in viscoelasticity and structural dynamics*

The inter-relationship between the frequency response of viscoelastic material (complex modulus or compliance) and corresponding time of function (retardation or creep function) has given rise to intense investigations since the 1960s.

3.2.1.1. *Use of intermediary functions*

In the early period of research in this domain, analogical models of springs and dashpots are frequently referred to, so as to describe elastic and damping responses respectively. Unfortunately, attempts to generalize this in order to portray the

@Seismicisolation

behavior of real materials requires knowledge of the exact number of branches constituted by the aforementioned models. This is a seemingly insurmountable task.

One attempt was made to consider the time to be constant, with a spring and dashpot couple being a continuous variable varying from zero to infinity, and to use the spectra functions defined here:

$$r(t) = \int_0^\infty e^{-t/\tau_c} H(\tau_c)\, d(\ln \tau_c),$$

$$f(t) = \int_0^\infty \left(1 - e^{-t/\tau_c}\right) L(\tau_c)\, d(\ln \tau_c) \qquad [3.19]$$

where r(t) and f(t) are the relaxation and the creep functions of time t respectively.

In equations [3.20], $H(\tau_c)$ and $L(\tau_c)$ are the so-called retardation and relaxation spectra that allow generalization of a finite number N of Maxwell models to continuous spectra, with N going to infinity.

The Neperian logarithm Ln of the relaxation (or retardation) time τ_c is used to evaluate, in a convenient manner, a very large range of time variables.

Such intermediary functions are obtained from harmonic responses and require calculation of derivatives of these last functions with respect to circular frequency ω. A great variety of approximate formulae have been proposed, in which derivatives of various orders are used to evaluate $H(\tau_c)$ and $L(\tau_c)$ [NIN 59]. Some approximate direct formulae have been proposed in which intermediary viscoelastic spectra are not used [FER 70].

The difficulty that specialists in numerical calculations encountered in the early 1960s can be explained by the fact that computers were not freely available and numerical programs for calculating special series and algorithms for fast Fourier transforms were not tractable.

@Seismicisolation

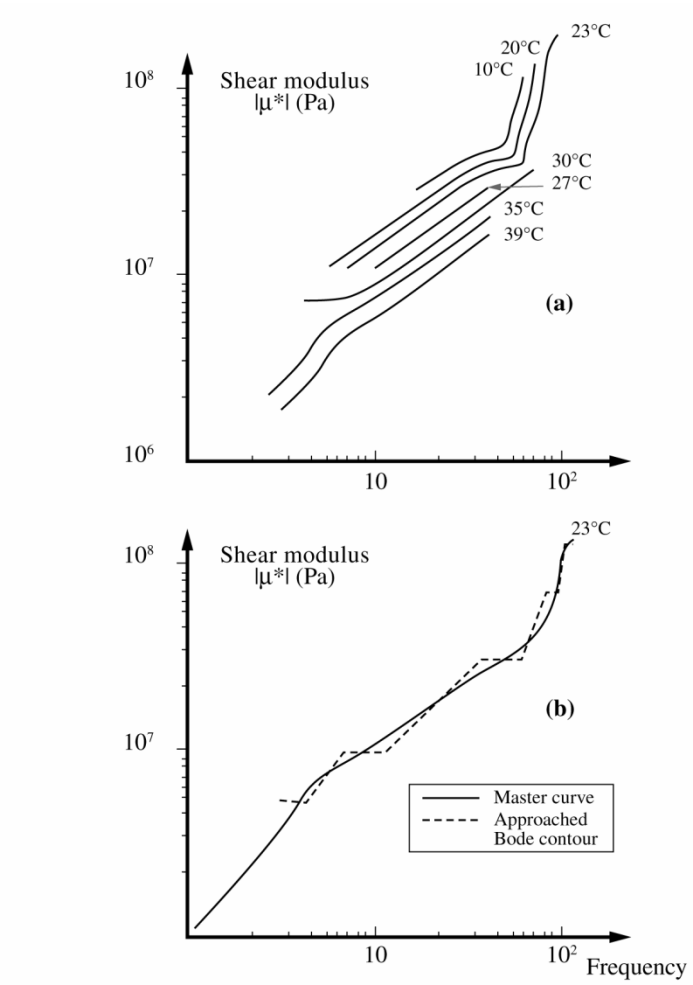

Figure 3.4. *Effect of change in temperature T = 19.8°C to T_0 = 100°C for $|\mu^*|$ (curve at 19.8°C, reference temperature). Tested material: solid propellant*

3.2.1.2. *The necessity of obtaining relaxation or retardation time functions*

In the field of structural dynamics over the past 20 years, new viscoelastic high damping materials have been introduced in the construction of mechanical structures whose dynamic responses have to be calculated using finite element methods. Appropriate constitutive equations of viscoelastic materials must be provided so as to predict the dynamic behavior of the structure.

@Seismicisolation

One of the straightforward methods in viscoelasticity is to use linear functionals to portray viscoelactic material behavior (see Chapter 2) with the aforementioned time functions as the functional kernels.

3.2.1.3. *Two possible mathematical formulations of harmonic viscoelastic responses*

This must be treated in the framework of an *inverse problem* in which we do not know the rheological models or number of elements at the beginning. What we have at our disposal is the "*gray box"* representing the sample whose response is known.

Exponential time function is apparently straightforward. In what follows, we will show that it is possible to use the decimal logarithms of ordinate and abscissa as well. The second option is to adopt fractional derivatives in order to portray harmonic responses with the minimum number of coefficients.

Fractional derivatives have given rise, over the past 15 years, to a lot of theoretical as well as practical research applications. This mathematical formulation is in complete agreement with the microstructural molecular theory of polymers proposed in the 1950s by Rouse [ROU 53] and improved by Ferry [FER 70]. Padovan [PAD 87] and Kennedy and Padovan [KEN 87] adopted such a method to express the constitutive equation of rubber and applied this to the calculation of dynamic responses of automobile tires. Bagley and Torvik [BAG 86] have made important contributions and presented thermodynamic considerations so as to obtain consistent values of fractional powers in the constitutive equation. Morgenthaler [MOR 91] examined the problem of calculating eigenvalues concerning structures incorporating a viscoelastic material described by fractional derivatives, using a frequency-dependent complex stiffness matrix. One of the authors of this book wrote an exhaustive paper on this topic in 1967 [VIN 67] covering the practical utilization of fractional derivatives and quotients of polynomials of higher degree for a variety of polymers.

Gibson *et al*. [GIB 90] used discrete inverse Fourier transformation and numerical integration to solve the problem using frequency/time integration valid over a long period of time. The difference between Gibson's work and what is presented below resides in the fact that the relaxation functions are obtained here in closed-form expressions. Long or short time ranges can be considered as special cases deduced from general formulae.

Indeed, fractional derivatives constitute the most convenient way of describing the behavior of realistic viscoelastic materials over a very large frequency range, with a restricted number of parameters.

@Seismicisolation

Evidently, the problem of interest here concerns materials science, but it may also be of interest in dynamic engineering, in the three following respects:

– Calculations of the structural responses require knowledge of the dynamic mechanical characteristics of viscoelastic materials used in a structure.

– Often, the dependency of the complex moduli (i.e. Young's and shear moduli for example) of the material on the frequency is evaluated using various methods. In rheology, the problem is finding the relaxation (or creep) functions from those complex quantities.

– Relaxation time functions are directly obtained by conventional methods in rheology using excitation as constant strains applied as a (Heaviside) step function. The stress responses are valid for times exceeding one minute. Dynamic tests, however, permit us to obtain the material response for a shorter time. For this purpose, transient responses are deduced from harmonic ones that do not suffer from the inertia of a mechanical test system as they do in direct transient tests.

– Exponential time function presents graphical and numerical methods. The graphical method enables us to evaluate poles and zeros of the quotient of two polynomials representing the complex modulus *versus* frequency. The numerical method enables us to evaluate the coefficients of closed-form expressions for complex moduli by using fractional derivatives.

– The fractional derivatives section presents inversion techniques via the inverse Fourier transform to obtain closed-form expressions for transient responses of viscoelastic materials.

3.2.2. *Polynomial functions of frequency used to express complex moduli*

3.2.2.1. *Closed-form expressions*

3.2.2.1.1. Required shape of harmonic responses

Differential operators are used to relate stress σ to strain ε:

$$P\sigma = Q\varepsilon, \quad P = \sum_{k=0}^{N} a_k \frac{d^k}{d\,t^k} \text{ and } Q = \sum_{l=0}^{M} b_l \frac{d^l}{d\,t^l} \qquad [3.20]$$

Here, P and Q are sums of differential operators. N and M are the degrees of the operators. For solid materials, using asymptotic considerations in the frequency

@Seismicisolation

domain, it can be shown that the degrees N and M must be equal, so as to obtain horizontal asymptotes when the abscissa variable (frequency) goes to zero and infinity.

Physically, that means that the stiffness or compliance of realistic materials must remain finite when the frequency goes to infinity.

The practical problem is to evaluate the degree N = M, which determines the number of terms in the series [3.20] and the 2N + 2 coefficients a_p and b_q in the differential equation. N must not be arbitrarily fixed in advance. It must only take into account the features of the experimental complex modulus curve against frequency.

The equality N = M takes into account the behavior of any viscoelastic material itself, for example *when frequency goes to zero or infinity, damping capacity must go to zero.*

3.2.2.1.2. Transfer function expressed as quotient of polynomials

If we take the Fourier transform of each term in equation [3.20], we get:

$$P(\omega) \bullet \sigma^*(\omega) = Q(\omega) \bullet \varepsilon^*(\omega) \qquad [3.21]$$

where P (ω) and Q (ω) are two polynomials against the angular frequency ω, with the same degree N.

$$P(\omega) = \sum_{p=0}^{N} a_p (j\,\omega)^p, Q(\omega) = \sum_{q=0}^{N} b_q (j\,\omega)^q \qquad [3.22]$$

Substituting [3.22] into equation [3.21] yields an expression for the complex modulus as the quotient of two polynomials:

$$E^*(j\,\omega) = \frac{\sigma^*(\omega)}{\varepsilon^*(\omega)} = \frac{Q(\omega)}{P(\omega)} = \sum_{q=0}^{N} b_q (j\,\omega)^q \Big/ \sum_{p=0}^{N} a_p (j\,\omega)^p \qquad [3.23]$$

Written in terms of its poles, $-p_{i\,i} = p_i$, and zeros, $-z_{ii} = z_i$, the equations in [3.23] become:

@Seismicisolation

$$E^*(j\,\omega) = A \prod_{i=j}^{N} (j\,\omega + z_{ii}) \Big/ \prod_{i=1}^{N} (j\,\omega + p_{ii}) \qquad [3.24]$$

where A is a constant. In the complex plane $\rho = \sigma + j\omega$, the poles and zeros are all real and negative. Due to the properties of viscoelastic materials, $E^*(\omega)$ is a monotonically increasing function of ω and must not possess any extrema (z_i, p_i real) because of stability considerations. They must be localized on the left half-plane P with $\sigma < 0$. σ designates the damping coefficient.

These complex frequency domain considerations are corroborated by theoretical considerations in the time domain [CHR 71], i.e. viscoelastic time functions (creep or relaxation function) must be monotonous continuous ones: decreasing for creep function; and increasing for relaxation function.

3.2.2.1.3. Poles and zeros are alternate

This property demonstrated by Bland [BLA 60] is:

$$z_1 < p_1 < z_2 < p_2 < z_3 < p_3 < z_i < p_i \qquad [3.25]$$

We can write equation [3.25] in the form:

$$E^*(j\,\omega) = A\,\frac{(j\,\omega + z_{11})(j\,\omega + z_{22})}{(j\,\omega + p_{11})(j\,\omega + p_{22})} \cdots \frac{(j\,\omega + z_{NN})}{(j\,\omega + p_{NN})} \qquad [3.26]$$

In equation [3.26] the factors in the numerator and denominator are assembled two by two.

Each quotient describes the behavior of $E^*(\omega)$ in the interval $z_{ii} < \omega < p_{ii}$.

The ratio $k_i = p_{ii}/z_{ii}$ determines the slope of $|E^*(\omega)|$ as well as the phase angle in the interval.

The main point of interest of this graphical representation is that, in a given frequency interval, combined action of the pair of pole and zero is predominant.

Outside the interval, the influence of the pair of pole and zero is reduced.

@Seismicisolation

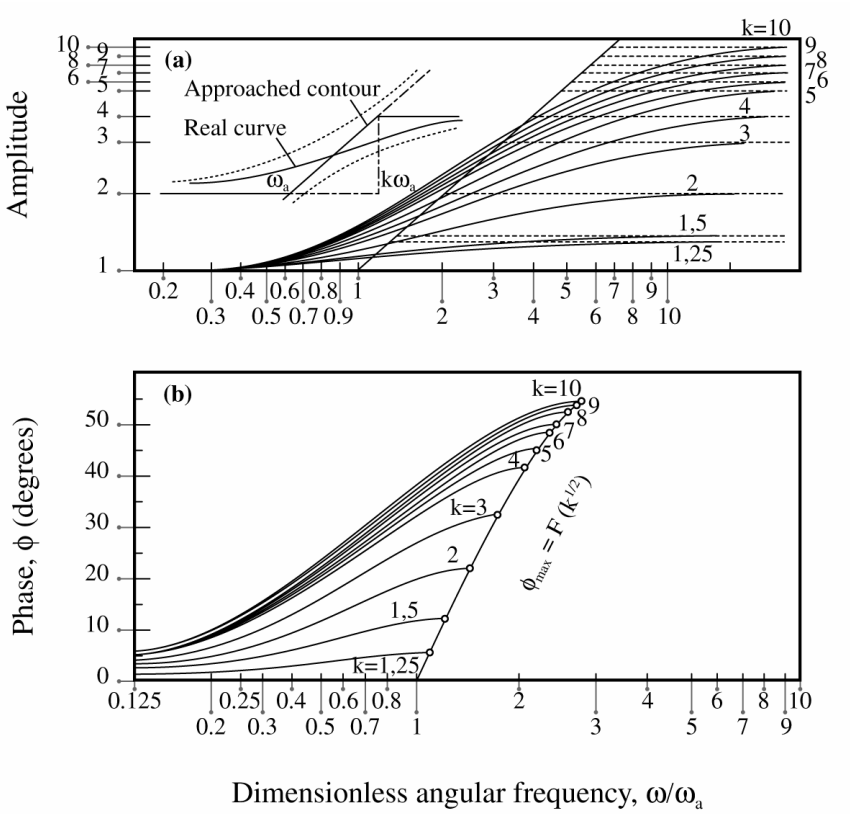

Figure 3.5. *Amplitude and phase of the ratio in equation [3.27]. Curves are symmetric with respect to point $\omega = \kappa^{0.5}\,\omega_\alpha$; k is the ratio of the two cut-off frequencies. The curve slopes in (a) depend essentially on parameter k*

3.2.2.1.4. Slope of response curve in a narrow frequency interval

If the slope is weak, this ratio varies slowly and the frequency interval is narrow. Figure 3.4 shows, in terms of the dimensionless frequency variable ω/ω_{ii}, the quotient:

$$k\,\frac{(j\,\omega + z_i)}{(j\,\omega + p_i)} = \frac{k\,z_i\,(j\,\omega/\,z_i + 1)}{p_i\,(j\,\omega/p_i + 1)} = \frac{(j\,\omega/\omega_a + 1)}{(j\,\omega/k\,\omega_a + 1)} \qquad [3.27]$$

It can be shown [BAG 86] that the slope s of curve $\left|E^*(\omega)\right|$ at the inflexion point $\omega = k^{0\text{-}5}\,\omega_a$ is related to the ratio $k = p_i/z_i$ by:

@Seismicisolation

$$k = (s + 1)/(1 - s) \qquad [3.28]$$

Consequently, equation [3.28] allows us to determine frequency interval k as a function of the slope s. Values of k are shown in Table 3.1.

If we take the decimal logarithm of equation [3.26]:

$$\left|E^*(\omega)\right|_{dB} = 20 \log_{10} A + \sum_{i=0}^{N} 20 \log_{10}\left(j\,\omega + z_{ii}\right)$$

$$- \sum_{i=0}^{N} 20 \log_{10}\left(j\,\omega + p_{ii}\right)$$

$$\varphi = \sum_{i=0}^{N} \text{arc tan}\,\frac{\omega}{z_{ii}} - \sum_{i=0}^{N} \text{arc tan}\,\frac{\omega}{p_{ii}} \qquad [3.29]$$

the graphical construction of Bode's plot is simple, in view of [3.29]. Gains in decibels as well as phases φ in degrees or grades are additive with appropriate signs.

We have shown that it is theoretically possible to *decompose a harmonic curve into intervals in which the slope remains constant*. The next problem to be solved is that of evaluating the corresponding quotient of linear functions of circular frequency ω.

3.2.2.2. *Graphical and numerical evaluation of poles and zeros*

Let us take a simple example of a harmonic test response, as follows, with $p = j\omega$:

$$E^*(p) = \frac{10\,(p + 50)\,(p + 150)\,(p + 500)\,(p + 1{,}000)\,(p + 3{,}100)}{(p + 100)\,(p + 200)\,(p + 800)\,(p + 1{,}500)\,(p + 5{,}000)} \qquad [3.30]$$

E*(p) covers four decades of frequency with five poles and five zeros.

@Seismicisolation

This test function is directly invertible after decomposition into simple elements:

$$E(t)/10 = 0.96875 - 0.0730945\,[1 - \exp(-100t)]$$

$$- 0.091346\,[(1 - \exp(-200t)] - 0.094752\,[1 - \exp(-800t)]$$

$$- 0.03658\,[1 - \exp(-1500t)] - 0.5544\,[1 - \exp(-5{,}000t)] \qquad [3.31]$$

Equations [3.30] and [3.31] will serve to test the validity of various inversion methods. The graphical curves |E* (f)| in the frequency domain and E(t) in the time domain are shown, respectively, in Figure 3.4.

Consider now evaluation of the poles and zeros of E*(p) from only curve |E* (f)| in Figure 3.5. (The various steps of the calculation are presented in Figure 3.11.)

3.2.2.3. *Curve slope in a frequency interval and utilization of asymptotic curves to approach an experimental curve*

First we need to localize the first frequency interval including the inflexion point (region I) in Figure 3.5 from the slopes at this point, where k defining the interval after equation [3.28] is evaluated. The first pole and zero pair (p_i, z_i) is then fixed. The upper and lower adjacent frequency intervals (see Figure 3.5) are evaluated in a similar manner. The process is continued until the two horizontal upper and lower asymptotes are reached.

The number N of poles and zeros is then experimentally determined. This graphical construction is followed by a numerical optimization which improves the pole and zero localization by minimizing the quadratic errors.

We obtain 10 poles and 10 zeros, as follows, with p = jω:

$$\bullet\,.\frac{(p+130)\,(p+230)\,(p+420)\,(p+960)}{(p+160)\,(p+270)\,(p+500)\,(p+1{,}150)} \qquad [3.32]$$

Then, by decomposition into simple elements, it is easy to obtain the relaxation function by using the inverse Laplace transform:

@Seismicisolation

$$E_a(t) = E_0 \left[a_0 + \sum_{i=0}^{q} a_i \, e^{-p_i t_i} \right] \qquad [3.33]$$

$$a_0 = \frac{z_1 z_2 \cdots z_n}{p_1 p_2 \cdots p_n}, \; a_i = P_n(-p_{ii})[p\, Q_{q,i}(-p_i)]^{-1}$$

$$\text{with } Q_{q,i}(-p_{ii}) = \frac{Q_p(p)}{p + p_{ii}} \qquad [3.34]$$

where $-p_{ii}$ are the poles of E_a in equation [3.32].

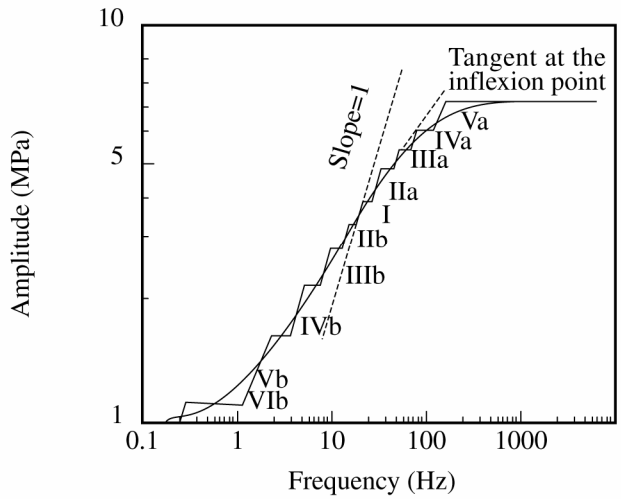

Figure 3.6. *Determination of poles and zeros from the amplitude curve of the test function in equation [3.31]. I, IIa, IIb, IIIa, and IIIb designate the successive frequency intervals*

$$E_f(t) = E'(\omega) - 0.4\, E''(\omega) + 0.014\, E''(10\,\omega) \qquad [3.35]$$

In Figure 3.8 the three relaxation functions are shown:

– the exact one (equations [3.33]);

– the numerically approximated function $E_0(t)$ equation [3.35]; and

– function $E_f(t)$ obtained by the Ninomiya-Ferry method [NIN 59].

@Seismicisolation

Here time t = l/ω, and E′ and E″ are the real and imaginary parts of the complex modulus curves deduced from the curves shown in Figures 3.7a and b.

The relaxation function curve produced by using equation [3.18] has large errors for short times in the transition regions and also for long times.

The discrepancy between $E_0(t)$ and the exact curve E(t) is small, although the poles and zeros are different in number and values.

s	k	s	k
0.50	3	0.38	2.2258
0.48	2.846	0.36	2.125
0.46	2.7037	0.34	2.03
0.44	2.5715	0.32	1.94
0.42	2.4482	0.30	1.857
0.40	2.3330	0.25	1.666
		0.20	1.5

Table 3.1. *The value of dimensionless frequency interval k* versus *slope s at the inflexion point, in Figure 3.1*

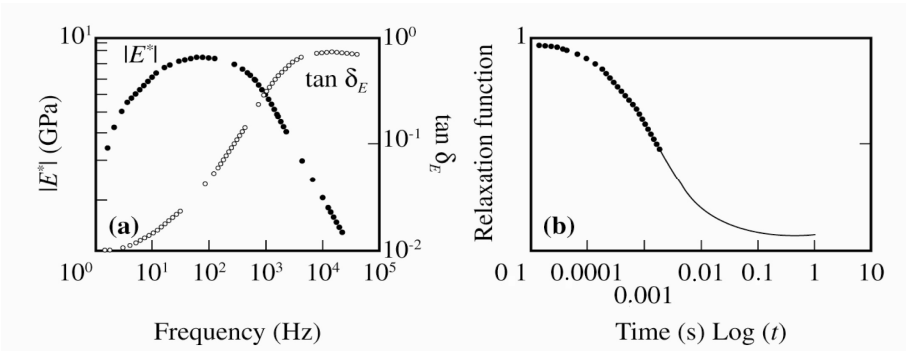

Figure 3.7. *The test function, equation [3.31], used to compare various methods:*
a) absolute value |E| (curve ooo) and damping tan δ_E (•••);*
b) relaxation function e(t) obtained by direct inversion of equation [3.31]

@Seismicisolation

3.2.3. *Fractional derivatives*

3.2.3.1. *Short survey*

Fractional derivatives find their mathematical origin as early as the beginning of the 19th century, with the pioneering works of mathematicians such as Laplace, Liouville, Riemann, Abel and Cauchy, who generalized derivation and integration of an entire order to fractional order Riemann-Liouville's integral.

Physicists noticed that diffusion phenomena in various domains of sciences cannot be portrayed only by time integration and time derivation of integer order. Physical systems with distributed elements only gave rise to fractional derivative applications in the second half of the 20th century. Vinh [VIN 67] presented the first work on viscoelasticity in 1967.

Since then, in spite of the considerable literature devoted to the applications of fractional derivatives in viscoelasticity, to the authors' knowledge, engineers even in advanced industries are unfamiliar with such a formulation. Consequently, it is not included in computer codes for finite element calculations. One of the reasons for this is that the inverse Fourier transform of the transfer function in terms of fractional derivatives does not use time exponential series but rather hypergeometric series [VIN 67]. A second reason might be the fact that the direct numerical computation of fractional derivatives in the constitutive equation is not familiar to specialists in finite elements, although it has been utilized elsewhere since 1967.

3.2.3.2. *Expression of complex modulus*

For linear viscoelastic solids, the complex modulus *versus* circular frequency ω is written in its general form as:

$$E^*(p) = A \prod_{i=1}^{n} \left[\left(1 + (T_i\ p)^{+\alpha_i}\right)\right]^{\pm 1} \qquad [3.36]$$

with $p = j\omega$. A is the static modulus and α_i are non-integer exponents of less than 1. The condition imposed on the exponents α_i is that when ω goes to infinity, modulus $|E^*(\omega)|$ *must be finite for a solid viscoelastic material.*

Equation [3.36] can be written in an explicit form as a product of many factors:

$$E^*(p) = A\{[1+(T_1p)^{\alpha 1}]/[1+(T_2p)^{\alpha 2}]\}\{[1+(T_3p)^{\alpha 3}]/[1+(T_4p)^{\alpha 4}]\} \qquad [3.37]$$

The condition on the α'_i s implies that when ω going to infinity:

@Seismicisolation

$$\underset{\omega \to \infty}{E^*(p)} = A \frac{(T_1\ p)^{\alpha_1}\ (T_3\ p)^{\alpha_3}}{(T_2\ p)^{\alpha_2}\ (T_4\ p)^{\alpha_4}} \cdots \qquad [3.38]$$

With $p = j\,\omega$ we must have:

$$\alpha_1 = \alpha_4,\ \ \alpha_2 = \alpha_3 \qquad [3.39]$$

and with the classification, T_j being time constants:

$$1/T_1 < 1/T_2 < 1/T_3 < 1/T_4 \ldots, \qquad [3.40]$$

$$\underset{\omega \to \infty}{E^*}(j\,\omega) = A \frac{T_1^{\alpha_1}}{T_2^{\alpha_2}} \frac{T_3^{\alpha_3}}{T_4^{\alpha_4}} \cdots = A \left(\frac{T_1}{T_4}\right)^{\alpha_1} \left(\frac{T_3}{T_2}\right)^{\alpha_2} \cdots, \qquad [3.41]$$

the presence of the product of more than one quotient in equation [3.41] can be explained by the microstructure of the material itself. Many polymers and elastomers are made of a blend of many constituents which creates many transition zones in the curve of complex modulus.

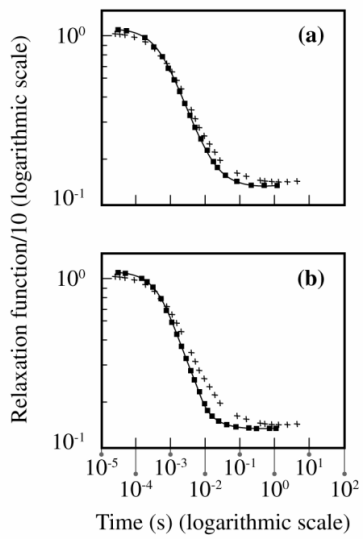

Figure 3.8. *A comparison of various inversion methods using test function (15): a) ___ , exact function , + + + (Ninomiya-Ferry's method [NIN59]), ▪▪▪▪▪▪ present method based on decomposition into frequency intervals; b) + + + + (Ninomiya –Ferry's method) ___ , exact function , ▪▪▪▪▪▪ present method based on fractional derivatives*

@Seismicisolation

In Figure 3.9a the complex Young's modulus of a special elastomer with carbon black is presented. Clearly, the gain and phase curves present the changes of slopes and many maxima, respectively.

For a great number of viscoelastic materials, the complex modulus is presented as:

$$E^*(p) = A\,\frac{\left[1 + (T_1\,p)^{\alpha_1}\right]}{\left[1 + (T_2\,p)^{\alpha_1}\right]} \qquad [3.42]$$

Four coefficients, A, T_1, T_2 and α_1, are necessary to characterize such a material.

3.2.3.3. *Evaluation of the four coefficients of complex modulus*

We can write equation [3.42] in the form:

$$E^*(p) = E_0\left[1 + \frac{1}{z}\left(\frac{p}{\omega_0}\right)^{\alpha}\right] \Big/ \left[1 + \left(\frac{p}{\omega_0}\right)^{\alpha}\right] \qquad [3.43]$$

with:

$$\omega_0 = 1/T_0,\ z^{1/\alpha}\,\omega_0 = 1/T_1,\ \alpha = \alpha_1,\ E_0 = A \qquad [3.44]$$

Parameter z is the ratio of Young's modulus evaluated at zero frequency to the same modulus at infinite frequency:

$$z = E_0/E_g,\quad E_g = \lim_{\omega \to \infty} \left| E^*(j\omega) \right| \qquad [3.45]$$

The first two parameters in equation [3.43], E_0 and z, are easily evaluated. The two remaining parameters are the exponent α and the higher cut-off circular frequency ω_0.

@Seismicisolation

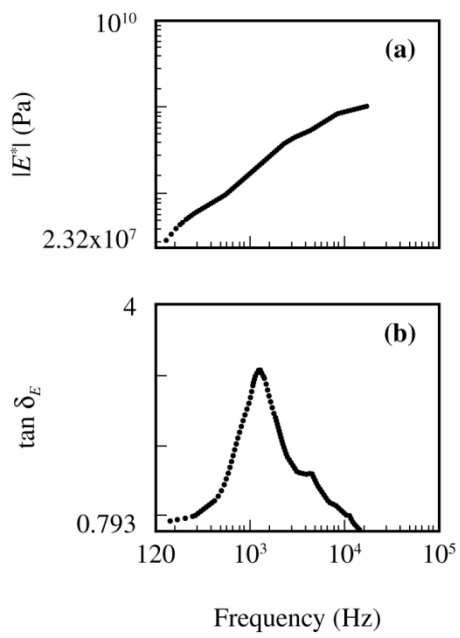

Figure 3.9. *Young's modulus of a high damping elastomer (absolute value and damping): a) change of slope; b) presence of many maxima of damping coefficient*

In the transition zone, the maximum of the damping coefficient η_{M2}, defined as the quotient of the imaginary part to the real part of the complex modulus:

$$\eta_M = \text{Im}\,[E^*] / \text{Re}\,[E^*] \qquad [3.46]$$

is localized at frequency ω corresponding to the inflexion point of the amplitude curve (absolute value).

$$\alpha = \frac{2}{\pi} \arcsin \frac{\eta_M \left[2\,(1-Z)\,Z^{1/2} + (1-Z)^2 \left(1+\eta_M^2\right)^{1/2} \right]}{\eta_M^2\,(1+Z)^2\,(1-Z)^2} \qquad [3.47]$$

Figure 3.10 shows the graphical representation of parameters E_0, E_g and η_M, which are used to evaluate α in equation [3.30].

@Seismicisolation

The evaluation of the cut-off frequency ω_0 is effected by the Newton-Raphson method as follows. The problem to be solved can be formulated as the minimization of quadratic errors between theoretical and experimental values of the complex modulus:

$$\text{minimize } \varepsilon^2 = \sum_{i=1}^{N} \left[\left| E^*_{exp} \right| - \left| E^*_{th} \left(\omega_0, \alpha \right) \right| \right]^2 \qquad [3.48]$$

ω_0 is taken here as the variable. By differentiation of expression [3.49] with respect to ω_0, we get:

$$g = \sum_{i=1}^{N} \left[\left| E^*_{exp} \right| - \left| E^*_{th} \left(\omega_0 , \alpha \right) \right| \right] \frac{\partial \left| E^*_{th} \left(\omega_0, \alpha \right) \right|}{\partial \omega_0} = 0 \qquad [3.49]$$

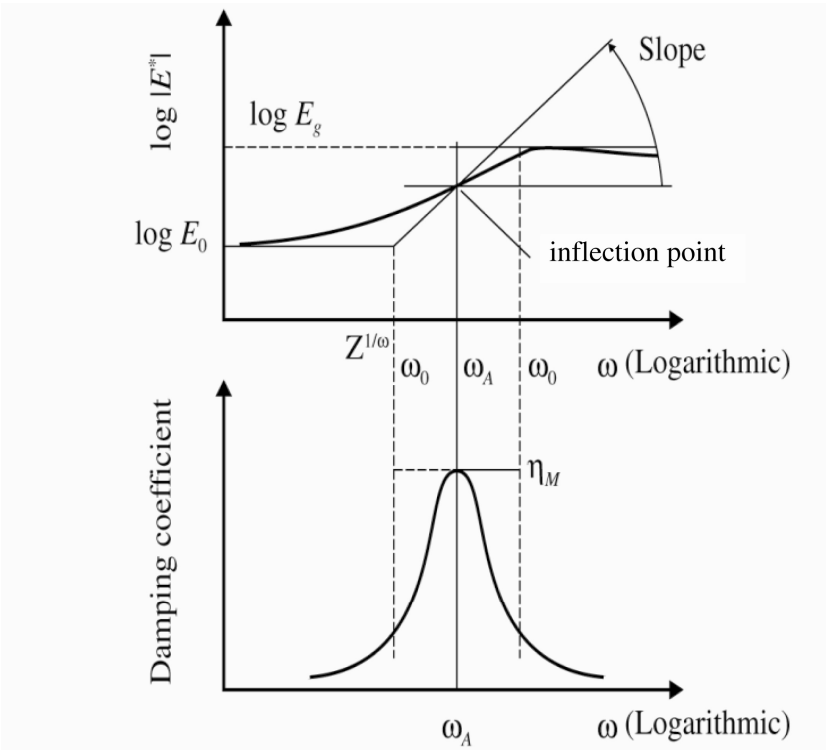

Figure 3.10. *Exponent α evaluated from η_M, the maximum value of damping*

@Seismicisolation

ω_0 is then evaluated using the Newton-Raphson formula [3.49], which yields:

$$\omega_0^{k+1} = \omega_0^k + g\left(\omega_0^k\right) / \left(\partial\, g\left(\omega_0^k\right) / \partial\, \omega_0^k\right) \qquad [3.50]$$

where superscript k designates the kth iteration.

In section 3.2.3.5, application of the method to the evaluation of a closed-form expression of the complex modulus will be presented.

A flowchart, in which the successive steps of the calculation are explained, is presented in Figure 3.11.

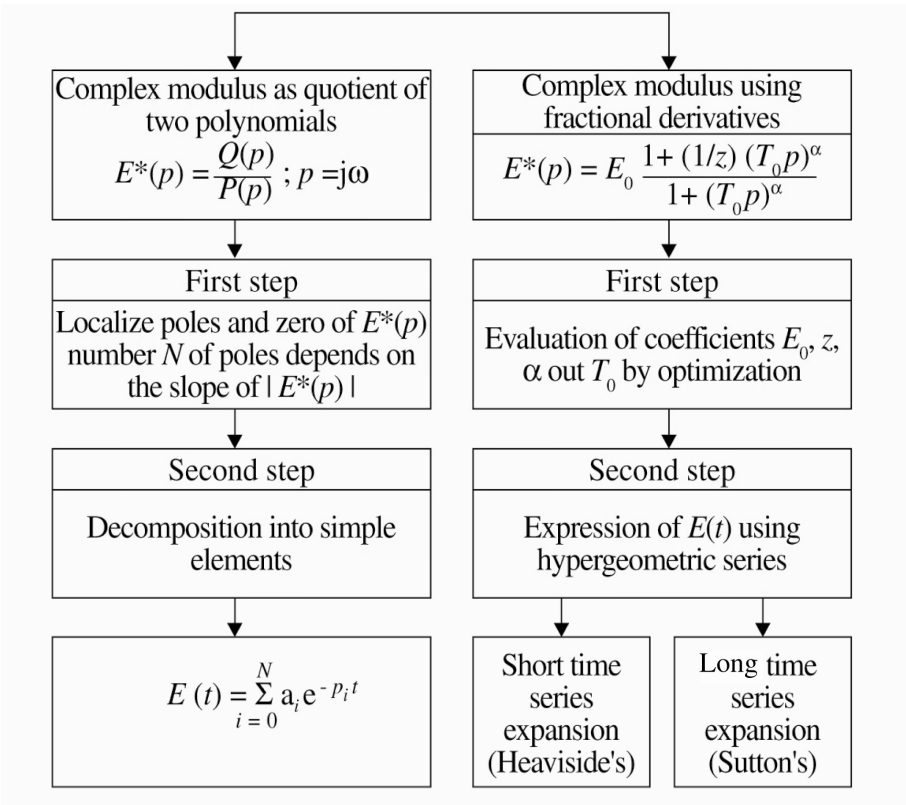

Figure 3.11. *The two classes of methods using polynomials and fractional derivatives respectively*

@Seismicisolation

3.2.4. *Use of inverse Carson-Laplace transform to obtain a closed-form expression of transient response*

In this section, two methods of inversion are presented. The first is relevant to the complex modulus defined in equation [3.26] as the quotient is of two polynomials of the same order. The second concerns the constitutive equation in terms of fractional derivatives. The first method requires decomposition into simple elements after evaluating the poles and zeros of the complex modulus. The inversion is straightforward. In the second method a series expansion of the complex modulus is used and a hypergeometric series in the time domain is adopted for the transient response.

In what follows, the original time function corresponding to the Carson-Laplace transform is presented first. Then the inverse Laplace transform of the complex modulus in the form [3.53] is presented.

3.2.4.1. *Time function, whose Carson transform is of the form* $\left(\left(1 + (T_1\ p)^{\alpha_1}\right)^{-1}\right)$

In Appendix 3.A, details are given in the calculation of the time function f(t):

$$f(t) = \frac{1}{2\pi j}\int_{c-j\infty}^{c+\infty} e^{tp}\ \frac{1}{p\left[1 + (T_0\ p)^{\alpha}\right]}\ dp \qquad [3.51]$$

A Bromwich-Wagner contour is used with a slit from $-\infty$ to 0 on the real axis of the complex variable $p = \sigma + j\omega$, so as to obtain a holomorphic (analytic) function inside the contour. The three non-zero integrals are evaluated along the real axis and around a small circle surrounding the origin (see Figure 3.A.1, Appendix 3.A.1). We thus have:

$$f(t)1 + \frac{1}{2\pi j}\left[\int_{-\infty}^{0} \frac{e^{-pt}\ dp}{\rho\left[1 + (\tau\rho)^{\alpha} e^{-j\pi\alpha}\right]} + \int_{0}^{+\infty} \frac{e^{-pt}\ dp}{\rho\left[1 + (\tau\rho)^{\alpha}\ e^{-j\pi\alpha}\right]}\right] \qquad [3.52]$$

using polar coordinates, with $p = \rho \exp(j\ \varphi) = \pm\ \pi$ along the real axis $\sigma < 0$. To evaluate the two integrals in equation [3.52] we have to expand the two denominators into series. The final result is:

@Seismicisolation

$$E_1(t) = E_0 \left\{ e^{-t/T_0} \sum_{r=0}^{\infty} (-1)^r \frac{\sin \pi r\alpha}{r\alpha} \left[\begin{array}{l} {}_1F_1\left(1, 1+\alpha r, \frac{t}{T_0}\right) \exp(-t/T_0) \\ + {}_1F_1\left(1, 1-\alpha r-\alpha, \frac{t}{T_0}\right) \\ -\left(\frac{T_0}{t}\right)^{\alpha r+\alpha} \bullet \exp\left(\frac{t}{T_0}\right) \Gamma(1-\alpha r-\alpha) \end{array} \right] \right\}$$

[3.53]

In equation [3.53], the following hypergeometric series is used [VIN 67]:

$${}_1F_1(\alpha, \beta, \chi) = \sum_{r=0}^{\infty} \frac{\Gamma(\alpha + r)}{\Gamma(\alpha)} \frac{\Gamma(\beta)}{\Gamma(\beta + r)} \frac{\chi^r}{r!} \qquad [3.54]$$

where Γ denotes the gamma function.

Note that the hypergeometric series is the necessary mathematical companion of calculus when using fractional derivatives [OLD 74]. In the past, voluminous books devoted to numerical calculations have been published with double-entry tables [SLA 60]; their utilization is cumbersome. Things have changed, however. Now convenient programs for calculating hypergeometric series, such as Mathematica or Jeandel Scientific, are available for computers.

3.2.4.2. *Inversion of the expression for complex modulus*

The expression to be inverted is:

$$E_0 \frac{\left[\left(1 + (1/z)\ (T_0\, p)^{\alpha}\right)\right]}{p\left(1 + (T_0\, p)^{\alpha}\right)} = \frac{E_0}{p\left[1 + (T_0\, p)^{\alpha}\right]} + \frac{E_0 (1/z)\ (T_0 p)^{\alpha}}{p\left[1 + (T_0 p)^{\alpha}\right]} \qquad [3.55]$$

Equation [3.55] is composed of two terms. The first one gives rise to the expression for the relaxation function in equation [3.53]. It remains to us to find the original function corresponding to the second term in equation [3.55], which is recognized as the product of two Carson-Laplace transforms. The corresponding time function is then a convolution:

@Seismicisolation

$$E_2(t) = L^{-1}\left[\frac{T_0^{\alpha}}{z}\, p^{\alpha}\, E_1(p)\right] = \frac{T_0^{\alpha}}{z}\frac{1}{\Gamma(-\alpha)}\int_0^t (t-\tau)^{-\alpha-1} E_1(\tau)\, d\tau \qquad [3.56a]$$

where L^{-1} designates the inverse Laplace transform,

$$E(t) = E_1(t) + E_2(t) \qquad [3.56b]$$

3.2.4.3. *Asymptotic series expansion of transient response*

Equations [3.56], [3.57] and [3.58] give a general expression for the transient response E(t) in the whole range of time intervals. In practical applications for mechanical structural transient responses, interest is focused on a short time interval.

In rheology, however, long time responses are often used, for example with creep function. For this purpose two asymptotic series expansions are utilized.

3.2.4.4. *Short time response*

The Laplace transform of the transient response is:

$$\frac{\left(1 + (1/z)(T_0\, p)^{\alpha}\right)}{p\,\left(1+(T_0\, p)^{\alpha}\right)} = E^*(p) \qquad [3.57]$$

The Heaviside expansion is used with condition $|T_0\ p| > 1$ to obtain the series:

$$E^*(p) = \sum_{r=0}^{\infty} (-1)^r\, T_0^{-\alpha r-\alpha}\, p^{-\alpha r-\alpha-1} + \frac{1}{z}\sum_{r=0}^{\infty} (-1)^r\, T_0^{-\alpha r}\, p^{-\alpha r-1} \qquad [3.58]$$

This series is absolutely convergent and we evaluate, term-by-term, and the corresponding time response is:

$$E(t) = \sum_{r=0}^{\infty} (-1)^r \left(\frac{t}{T_0}\right)^{\alpha r-\alpha} \frac{1}{\Gamma(\alpha r+\alpha+1)} + \frac{1}{z}\sum_{r=0}^{\infty} (-1)^r \left(\frac{t}{T_0}\right)^{\alpha r} \frac{1}{\Gamma(\alpha r+1)} \qquad [3.59]$$

@Seismicisolation

3.2.4.5. *Long time response*

Sutton's method [CAR 21] is used here (see details in Appendix 3.B). The expansion of expression [3.57] is effected with condition $|T_0\,p| < 1$. Sutton's contour is used to obtain:

$$E^*(t) = \sum_{r=0}^{\infty} (-1)^r (T_0\,p)^{\alpha r} + \frac{1}{z}\sum_{r=0}^{\infty} (-1)^r (T_0\,p)^{\alpha r + \alpha} \qquad [3.60]$$

Inversion of the convergent series [3.61] term-by-term gives:

$$E(t) = \sum_{r=0}^{\infty} (-1)^r \frac{(T_0)^{\alpha r}\, t^{-\alpha r-1}}{\Gamma(-\alpha r)} + \frac{1}{z}\sum_{r=0}^{\infty} (-1)^r \frac{(T_0)^{\alpha t+\alpha}\, t^{-\alpha r-\alpha-1}}{\Gamma(-\alpha r-\alpha)} \qquad [3.61]$$

The two asymptotic expansions [3.59] and [3.61] are cases of general formulae given in equations [3.53] and [3.54], in which the variation of time t is restricted to interval $t/T_0 < 1$ for short time periods and $t/T_0 < 1$ for long time periods. The two classes of methods are summarized in Figure 3.11.

3.2.5. *Applications*

3.2.5.1. *Comparison of transient responses obtained by various inversion methods*

With the same test function, equation [3.30], and using fractional derivatives we obtain the complex modulus:

$$E^*(j\,\omega) = \left[1 + \frac{1}{8}\left(j\,\frac{\omega}{3{,}800}\right)^{0-584}\right] \Big/ \left[1 + \left(j\,\frac{\omega}{3{,}800}\right)^{0-584}\right]$$

Inversions based on hypergeometric series, short-time Heaviside's expansion and long-time Sutton's expansion successively give rise to the three curves presented in Figure 3.7b.

The two asymptotic methods give satisfactory results in the time interval of interest. The exact hypergeometric series method gives very good results over the whole time range.

@Seismicisolation

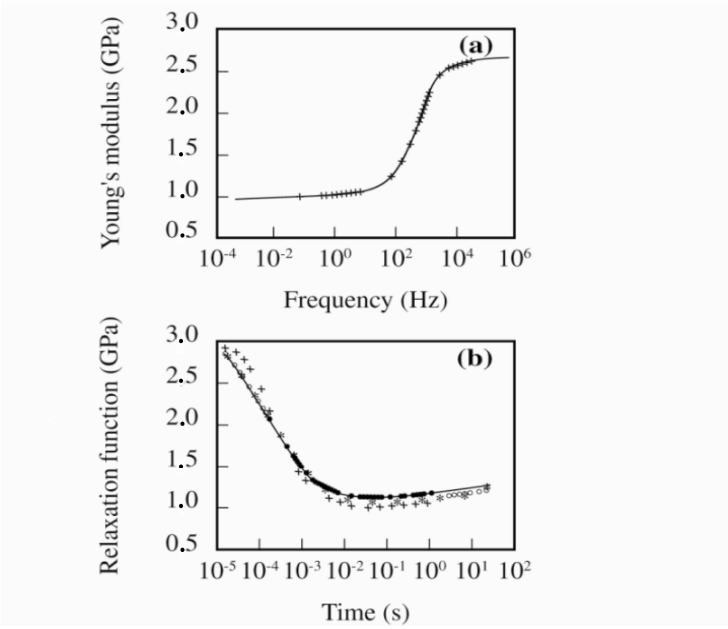

Figure 3.12. *a) Material polyamide 6; Young's modulus: + + + + +: experimental: ____ quotient of two polynomials; b) relaxation functions obtained by various methods: + + + + +, Ninomiya-Ferry; ..... quotient of polynomials and exponential series; *****, fractional derivatives and hypergeometric series; ooo, asymptotic expansions*

3.2.5.2. *Relaxation functions of polyamide 6 (PA6)*

Young's modulus curves are shown against frequency in Figure 3.12a. From the experimental curves, the poles and zeros of the quotient of the polynomials are numerically evaluated:

$$E^*_p(p) = \frac{2864\ (p+250)(p+800)(p+1{,}600)(p+2{,}400\ )(p+3{,}600)}{(p+300)(p+1{,}000)(p+2{,}000)(p+2{,}600)(p+5{,}500)}(\text{GPa})$$

[3.62]

$$E_{fd}^*(\omega) = \{\ E_0 + E_g\ (j\omega/\omega_0)^{\alpha}\} \ /\ \{1+(j\omega/\omega_0)^{\alpha}\} \qquad [3.63]$$

$\alpha = 0.54$, $\omega 0 = 4{,}200$ rad/s, $E0 = 0.923$ GPa, $Eg = 2.864$ GPa

Subscripts p and fd in [3.62] and [3.63] refer to the polynomial method and fractional derivative method, respectively.

@Seismicisolation

Figure 3.11b shows three relaxation functions obtained by various methods. The Ninomiya-Ferry method gives a curve with large discrepancies compared to those of the other methods, even in the transition zone.

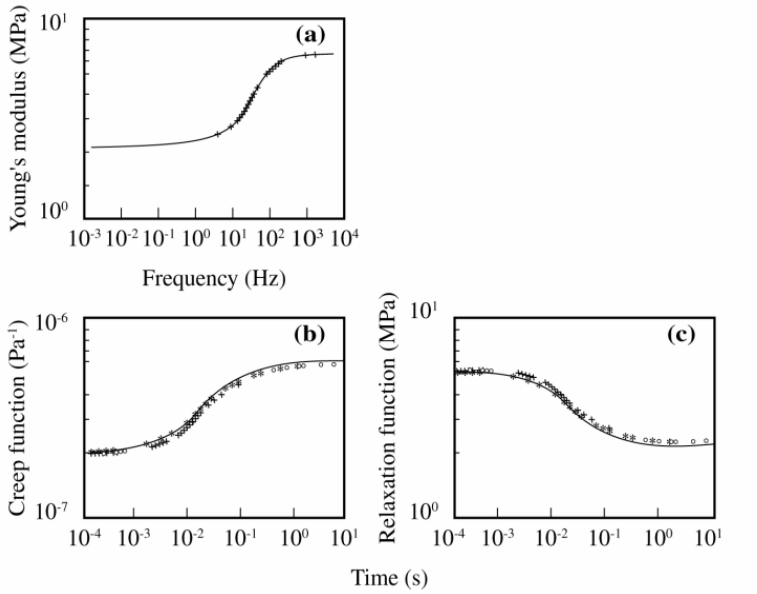

Figure 3.13. *a) Material: elastomer; Young's modulus (absolute value)**---**(continuous line) experimental curve; + + + + +, fractional derivatives;**ooo**: quotient of two polynomials; b) creep functions obtained by various methods; + + + + +, Ninomiya-Ferry:**ooo;** quotient of polynomials and exponential series; *********, fractional derivatives and hypergeometric series; **oooo**, asymptotic expansions; c) Relaxation functions; key as (b)*

3.2.5.3. *Relaxation function of elastomer*

From the experimental curve for Young's modulus in Figure 3.13a, the method of a quotient of polynomials gives the expression:

$$\frac{E^*(p)}{5.1456} = \frac{(p+15)(p+42)(p+80)(p+330)(p+1{,}800)}{(p+16.5)(p+50)(p+100)(p+420)(p+2{,}000)} \ (\text{GPa}) \qquad [3.64]$$

and the functional derivative method gives the set of coefficients:

@Seismicisolation

$$E^*(\omega) = \frac{E_0 + E_g \left(j\,\omega/\omega_0\right)^{\alpha}}{1 + \left(j\,\omega/\omega_0\right)^{\alpha}} \qquad [3.65]$$

$\alpha = 0.66069$, $\omega_0 = 820$ rad/s, $E_0 = 2.235$ MPa, $E_g = 5.156$ MPa,

where E_0 and E_g are respectively Young's moduli in glass-like and in rubber-like zones. By using various methods of inversion, we get the creep (Figure 3.13b) and relaxation (Figure 3.13c) functions. Here again, Ninomiya-Ferry's method furnishes curves with large discrepancies compared to those obtained by other methods.

3.3. Concluding remarks

During the first reading of the theoretical presentation of the second part of this chapter, practicians and engineers will be surprised by the mathematical deployment in our contributions. We are convinced, however, that the practical utilization of this part is not so difficult when we use appropriate mathematical computer codes. The following remarks may help practicians.

3.3.1. *Williams-Landel-Ferry's method*

This method is essentially a practical tool researchers can use to devise a practical experiment, prepare the campaign and interpret their results so as to obtain complex moduli (or compliances) over a very large frequency range:

– The main interest of this method resides in *the artificial enlargement of the frequency range without recourse to special apparatus for direct measurements over a very large frequency range by using temperature as a parameter.* The limitation of this method is presented with details.

– In spite of the approximation adopted in the Ninomiya-Ferry relationship, the global trend of time functions (relaxation or creep) can be used with the restriction concerning its accuracy.

3.3.2. *Polynomial quotient and fractional derivatives are used to mathematically express the dynamic response of viscoelastic materials*

The experimental complex modulus must be obtained over a large frequency range to include the static E_0 and high frequency (asymptotic) modulus E_g.

@Seismicisolation

A quotient of polynomials constitutes an efficient method for finding roots and poles by using appropriate numerical calculations. The degree of the polynomials is not arbitrarily fixed in advance but is closely dependent on experimental frequency response curves. Fractional derivatives can be used to characterize viscoelastic materials. The reduced set of coefficients is obtained using a special optimization method.

These two methods are well adapted to describe the linear behavior of material, particularly when the frequency range is wide (more than four decades).

Fractional derivative is a tool that deserves rheologists' attention. For practicians, it requires a restricted number of coefficients in constitutive equations. The corresponding relaxation function is obtained either in a closed-form expression or a numerical one.

By using hypergeometric series, transient responses are obtained using a fractional derivative over the whole frequency range. Its utilization is facilitated by the availability of special computer codes. The functional kernel is obtained in a closed-form expression. It can be conveniently used to relate input and output signals and be numerically evaluated.

Two asymptotic series expansions have been presented to obtain transient responses over short and long time periods. The methods presented above do not use intermediary functions, such as viscoelastic spectra, that require derivatives of relaxation (or creep) functions. They can be expressed under either closed-form expressions or by means of numerical computations using special functions (i.e. hypergeometric series). For this purpose, it is possible to use the computer codes available.

3.4. Bibliography

[BAG 86] BAGLEY R. L., TORVIK P. J., "On the fractional calculus model of viscoelastic behaviour", *Journal of Rheology,* vol. 30, no. 1, p. 133-155, 1986.

[BLA 69] BLAND D., *The Theory of Linear Viscoelasticity*, London Pergamon, 1960.

[CAR 63] CARSLAW H. S., JAEGER J. C., *Operational Methods in Applied Mathematics*, New York Dover, Chapter 13, p. 271-285, 1963.

[CHE 85] CHEVALIER Y., "Previsional calculations of some composite materials", *Mécanique - Matériaux - Journal du GAMI*, Paris, no. 412, p. 28-35, 1985.

@Seismicisolation

[CHR 71] CHRISTENSEN R.P., *Theory of Viscoelasticity - An Introduction*, Academic Press, New York, London, 1971.

[FER 70] FERRY J. D., *Viscoelastic Properties of Polymers,* John Wiley and sons Inc, New York, 1970, Chapter 9, p. 195-246; Chapter 10, p. 247-351; Chapter 11, p. 292-347.

[GIB 90] GIBSON R. F., HWANG S. J., SHEPPARD C. H., "Characterization of creep in polymer composites by the use of frequency-time transformations", *Journal of Composite Materials*, vol. 24, p. 441-453, 1990.

[KEN 87] KENNEDY R., PADOVAN G. W., "Finite elements analysis of steady and transiently moving/rolling non-linear viscoelastic structure I: theory", *Computers and Structures*, vol. 27, pp. 249-257, 1987.

[MAN 78] MANDEL J., *Propriétés Mécaniques des Matériaux,* Eyrolles Editor Paris, Chapter IV, p. 47, 1978.

[MOR 91] MORGENTHALER D. R., *Proceeding of Damping Practical Design and Analysis of Systems with Fractional Derivatives Materials and Active Control, I BCA1-BCA 28*, Proceedings of Damping, Edited by Wright Patterson Laboratory Flight Dynamics Directorate, February 13-15, 1991.

[NIN 59] NINOMIYA K., FERRY J. D., "Some approximate equations useful in the phenomonological treatment of linear viscoelastic data", *Journal of Colloïd Science*, vol. 14, p. 36-48, 1959.

[OLD74] OLDHAM J. B., SPANIER J., *The Fractional Calculus – Theory and Application of Differentiation and Integration of Arbitrary Order,* San Diego, Academic Press, 1974.

[PAD 87] PADOVAN J., "Finite element analysis of steady and transiently moving and rolling non linear viscoelastic structure in shell and three dimensional simulations", *Computers and Structures*, vol 27, no.2, p. 249-257, 1987.

[ROU 53] ROUSE P. E., "A theory of the linear viscoelastic properties of dilute solution of coiling polymers", *Journal of Chemical Physics* vol. 21, no. 7, p. 1212-1277, 1953.

[SLA 60] SLATER L., *The Confluent Hypergeometric Function*, Cambridge University Press, 1960.

[SOU 96] SOULA M., Etude du comportement mécanique des matériaux viscoélastiques par les dérivées fractionnaires, PhD thesis, CNAM, Paris, 1996.

[SOU 97] SOULA M., VINH T., CHEVALIER Y., "Transient responses of polymers and elastomers deduced from harmonic responses", *Journal of Sound and Vibrations*, vol. 205, p. 185-203, 1997.

[STA 56] STAVERMAN A. J., SCHWARTZ J., *Die Physik der Hochpolymeren*, H. A. Stuart, ed., vol. IV, Chapter I, Springer-Verlag, Berlin, 1956.

@Seismicisolation

[TSC 89] TSCHOEGL N. W., *The Theory of Linear Viscoelastic Behavior,* Springer-Verlag, New York, 1989.

[VIN 67] VINH N. P. T., "On the interrelation between harmonic and transient viscoelastic responses", *Mémorial de l'Artillerie Française*, vol. III, p. 725-776, 1967.

[VIN 87] VINH T., CHENOUIL J., ESTEOULE C., "Impact testing on solid propellant", *Mémorial de l'Artillerie Française,* vol 61, no. 3, p. 201-296, 1987.

3.5. Appendices

Appendix 3.A. Inversion of Laplace transform[5]

$1/p\,[1 + (T_0 p)\,\alpha]$

The Mellin-Fourier integral associated with the Bromwich-Wagner contour in the complex domain permits us to evaluate the corresponding transient response f(t) (see Figure 3.A.1):

$$f(t) = \frac{1}{2\pi j} \int_{c-j\infty}^{c+j\infty} e^{tp} \frac{1}{p\left[1 + (T_0\, p)^{\alpha}\right]}\, dp \qquad [3.A.1]$$

Function $1/p\,[1 + (T_0\, p)^{\alpha}]$ is multi-valued and has a critical point at the origin in complex plane $p = j\omega + \sigma$. The contour must include a slit for negative values of σ, $-\infty < \sigma < 0$, and a small circle C_2 around the origin. The contour, with appropriate directions for each portion, is shown in Figure 3.A.1. This is decomposed into four integrals: C_1, and C_2 are a partial contour along oriented circles; DC and BA refer to the linear integral along real axis σ.

$$E(t) = \frac{1}{2\pi j}\left[\int_{C_1} + \int_{DC} + \int_{BA} + \int_{C_2}\right] \qquad [3.A.2]$$

When the radius of C_1 goes to infinity, the first integral in equation [3.A.2] tends to zero. When the radius of C_2 goes to zero, the fourth integral tends to +1.

5 The presence of complex variable p can be explained by the definition of the Carson transform itself with respect to the Laplace transform.

@Seismicisolation

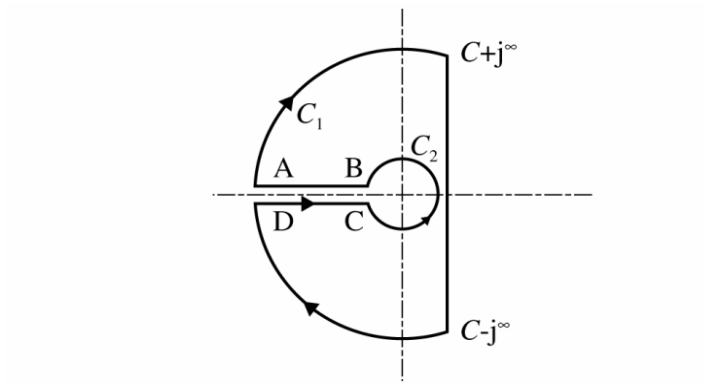

Figure 3.A.1. *Bromwich-Wagner integration contour in the complex plan $p = j\omega + \sigma$ to evaluate the relaxation function $E_r(t)$*

The two remaining integrals in equation [3.A.2] are:

$$I_2 = \frac{1}{2\pi j} \quad J_2 = \frac{1}{2\pi j} \int_{DC} e^{tp} \frac{1}{p\left(1 + (T_0\, p)\right)^{\alpha}} \, dp \qquad [3.A.3]$$

$$J_2 = \int_{-\infty}^{0} \frac{e^{-pt}\, e^{-j\pi} d\rho}{-\rho\left[1 + (\rho\, T_0)^{\alpha}\, e^{-j\alpha\pi}\right]} \quad \text{with } p = \rho\, e^{-j\pi} \qquad [3.A.4]$$

$$I_1 = \frac{1}{2\pi j} \quad J_1 = \frac{1}{2\pi j} \int_{BA} e^{pt} \frac{1}{p\left(1 + (T_0\, p)\right)^{\alpha}} dp$$

$$J_1 = \int_{0}^{\infty} \frac{e^{-pt}\, e^{j\pi} d\rho}{-\rho\left[1 + (\rho\, T_0)^{\alpha}\, e^{j\alpha\pi}\right]} \quad \text{with } p = \rho\, e^{j\pi} \qquad [3.A.5]$$

To evaluate J_2, we have to expand the function $1/p\,(1 + (T_0\, p)^{\alpha})$ into a series as follows:

@Seismicisolation

$$\frac{1}{p\left(1+(T_0\ p)^{\alpha}\right)} = \sum\ (-1)^r\ A^r\ u^{-\alpha r-1}\ \text{ for } |\,u\,| < \frac{t}{T_0} \qquad [3.A.6]$$

With $A = (T_0/t)^{\alpha}\ e^{-j\alpha\pi}$, and the change of variables $p\ t = u$, expansion into a series gives:

$$\frac{1}{p\left(1+(T_0\ p)^{\alpha}\right)} = \sum\ (-1)^r\ A^{-r-1}\ u^{-\alpha r-\alpha-1}\ \text{ for } |\,u\,| > \frac{t}{T_0} \qquad [3.A.7]$$

Equation [3.A.4] is now written as the sum of three integrals, with:

$A = e^{-j\pi\alpha}\,(T/t)^{\alpha}$ [6]

$$J_2 = \sum_{r=0}^{\infty} \int_0^{t/T-\varepsilon} (-1)^r\ u^{\alpha\ r-1} \exp(-u)\,du + \sum_{r=0}^{\infty} \int_{t/T+\varepsilon}^{+\infty} (-1)\ A^{-r-1} u^{-\alpha r-\alpha-1}$$
$$\exp\ (-u)\,du \int_{t/T-\varepsilon}^{t/T+\varepsilon} + \frac{\exp\ (-u)\ du}{u\left[\ 1+\left(\ Au^{\alpha}\right)^{\alpha}\right]} \qquad [3.A.8]$$

When $\varepsilon \rightarrow 0$, the last integral tends towards zero. In equation [3.A.8] two integrals remain. The first integral is easily identified as a confluent hypergeometric series [SLA 60]:

$$\int_0^{t/T_0} (-1)^r\ A^{-r-1}\ u^{-\alpha r-\alpha-1} \exp(-u)\ du =$$
$$(-1)^r\ A^r \left(\frac{t}{T}\right)^{\alpha r} B\ (\alpha t,\ 1)_1\ F_1\left(\alpha r,\ \alpha r+1,\ -\frac{t}{T}\right) \qquad [3.A.9]$$

6 ρ designates circle radius and must not be confused with density.

@Seismicisolation

The hypergeometric series ${}_1F_1$ (a, b, x) is defined in equation [3.37] and B (x, y) is Euler's function defined with gamma function Γ:

$$B(x, y) = \frac{\Gamma(x)\,\Gamma(y)}{\Gamma(x, y)}, \quad x > 0, \quad y > 0 \qquad [3.A.10]$$

The second integral in [3.A.8] is identified as the Kummer series [SLA 60], U (a, b, x):

$$\int_{t/T_0}^{+\infty} u^{-\alpha r-\alpha-1} \exp(-u)\,du = \exp\left(-\frac{t}{T_0}\right)\left(\frac{T_0}{t}\right)^{\alpha r+\alpha} U\left(1, 1-\alpha r-\alpha, \frac{t}{T_0}\right) \qquad [3.A.11]$$

$$U(a; b, x) = \frac{e^{x}}{\Gamma(a)} \int_{1}^{+\infty} w^{a-b-1}\, w^{a-1} \exp(-x\,w)\,dw \qquad [3.A.12]$$

In equation [3.A.11], U (a, b, x) is again identified as a hypergeometric series [SLA 15].

The evaluation of J_1 in [3.A.5] follow a similar procedure as above.

Assembling the three integrals in equation [3.A.2], we get:

$$f(t) = e^{-t/T_0} \sum_{r=0}^{\infty} (-1)^r \frac{\sin \pi r\alpha}{\pi r\alpha} \left[{}_1F_1\left(1, 1+\alpha r, \frac{t}{T_0}\right) + {}_1F_1\left(1, 1-\alpha r-\alpha, \frac{t}{T_0}\right) - \exp\left(\frac{t}{T_0}\right)\left(\frac{T_0}{t}\right)^{\alpha r+\alpha} \Gamma(1-\alpha r-\alpha) \right] \qquad [3.A.13]$$

This equation is valid over the whole range of time $0 < t < \infty$.

@Seismicisolation

Appendix 3.B. Sutton's method for long time response

The Laplace transform is expanded into a series [CAR 63] (see Figure 3.B.1):

$$L\left[f(t)\right] = \sum_{n=0}^{\infty} a_n (p-p_0)^{n-1} + (p-p_0)^{\alpha-1} \sum_{n=0}^{\infty} b_n (p-p_0)^n \qquad [3.B.1]$$

Where $0 < \alpha < 1$, p_0 is the singular point, the real part of which is nearest to the origin.

If the condition $| p - p_0 | < 1$ is satisfied, f(t) has an asymptotic expansion:

$$f(t) \approx e^{p_0 t}\left[a_0 + \frac{\sin \pi \alpha}{\pi} \sum_{n=0}^{\infty} (-1)^n b_n \Gamma(\alpha + n) t^{-\alpha-1}\right] \qquad [3.B.2]$$

$$f(t) \approx \left[a_0 + \frac{\sin \pi \alpha}{\pi} \sum_{n=0}^{\infty} (-1)^n b_n \Gamma(\alpha + n) t^{-\alpha-1}\right] \qquad [3.B.3]$$

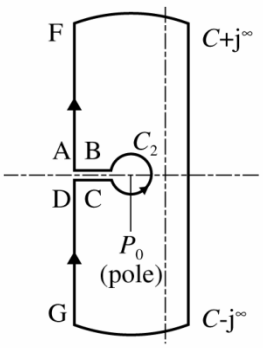

Figure 3.B.1. *Sutton's contour in the complex plane $p = j\omega + \sigma$ to evaluate relaxation function $E_r(t)$ for a long time. $0 > Re\, p_0 > Re\, p_1 \ldots > Re\, p_n$*

@Seismicisolation

Chapter 4

Formulation of Equations of Motion and Overview of their Solutions by Various Methods

This chapter aims to accurately present the principal methods that permit us to obtain the equations of motion of a bounded continuous elastic medium. It presents a guideline for obtaining solutions to the equations, either in closed-form expressions or directly by numerical calculation.

For an infinite or semi-infinite medium, such as a rod with circular cross-section, it is possible to find exact equations of motion where there are no boundary conditions at either end (infinite length) except the free lateral boundary.

In the majority of problems concerning a bounded medium, the boundary conditions must be satisfied. The theoretical equations of motion for an infinite or semi-infinite rod that give rise to exact solutions must unfortunately be abandoned. Consequently, approximate equations of motion have to be found by adopting a field of displacement (in the case of a simple field) compatible with the boundary conditions. There are three principal methods for setting up differential equations of motion:

– D'Alembert's principle, which permits us to write symbolic equations of motion;

– Lagrange's equations; and

Chapter written by Jean Tuong VINH.

Mechanics of Viscoelastic Materials and Wave Dispersion Edited by Yvon Chevalier and Jean Tuong Vinh
© 2010 ISTE Ltd. Published 2010 by ISTE Ltd.

@Seismicisolation

– variational calculus including Hamilton's principle and Love's derived energy principle[1].

The last group utilizes variational calculus. In our opinion, the three methods must be considered practical tools for engineers, applied scientists and experimenters working on material characterization using dynamic methods. Let us also mention that variational calculus permits us to obtain the so-called natural boundary conditions by successive integration.

4.1. D'Alembert's principle

Let us consider a mechanical system composed of n particles of mass m_i (i = 1, 2, ... , n). The geometrical configuration of the system at any instant t is described by 3 n Cartesian coordinates (x_i, y_i, z_i):

$$i \in (1, 2, ..., n)$$

The system is said to be free and have 3n degrees of freedom.

Certain geometric restrictions called constraints may be imposed on the system. These constraints may limit the region of space in which the masses can move. The system can be submitted to forces acting on the masses provoking their motion, consistent with conditions of constraint, called forces of constraint. The condition of constraint can be expressed by the following equation:

$$F\,(x_1, y_1, z_1\,; \ldots, x_n, y_n, z_n\,; t) = 0 \qquad [4.1]$$

If such an equation exists, the constraint is holonomic.

4.1.1. *Generalized coordinates*

The 3n coordinates of the system are no longer independent of each other. There are r equations of the form [4.1] that are used to reduce the number of independent coordinates, r being the number of holonomic constraints:

$$p = 3\,n - r \qquad [4.2]$$

1 Reissner variational calculus, with mixed fields of stress, strain and displacements, is used with success in numerous rod vibration problems in Chapter 5 with Onobiono's work.

@Seismicisolation

The p degrees of freedom correspond to q_1, q_2, …q_p parameters, called generalized coordinates. The original coordinates are expressed as functions of generalized coordinates, t being time:

$$x_i = F_i\,(q_1, \ldots q_p, t)$$

$$y_i = G_i\,(q_1, \ldots, q_p, t) \qquad p = (1, 2, \ldots, 3n - r) \qquad [4.3]$$

$$z_i = H_i\,(q_i, \ldots, q_p, t)$$

The $3\,n - r = p$ functions $q_j = q_j\,(t)$, with $j \in (1, 2, \ldots, 3n - r)$ need to be determined. Bringing these functions q_j into equation [4.3], the original coordinates can then be evaluated.

4.1.2. *Principle of virtual work*

The principle of virtual work makes it possible to write the equilibrium equations of a mechanical system where the forces of constraint do not appear. This is convenient, since the reactions are not known in advance. Moreover, if the system is in motion, the reactions are not constant but depend on the motion of the system.

Virtual displacement is a displacement with components $\delta\,x_i$, $\delta\,y_i$ and $\delta\,z_i$, which are compatible with the constraints imposed on the system but are otherwise arbitrary. The work done in a *virtual displacement* by forces acting on the system is called *virtual work.*

Let X_i, Y_i and Z_i be the components resulting from applied forces acting on the mass m_i, and let X_i^c, Y_i^c and Z_i^c be components of the resultant of forces of constraint acting on m_i.

The system equilibrium is portrayed by:

$$X_i + X_i^c = 0\,,\ Y_i + Y_i^c = 0\,,\ Z_i + Z_i^c = 0 \qquad [4.4]$$

The work done is expressed as:

@Seismicisolation

$$\sum_{i=1}^{n} \left[\left(X_i + X_i^c \right) \delta x_i + \left(Y_i + Y_i^c \right) \delta y_i \ \left(Z_i + Z_i^c \right) \delta z_i \right] = 0 \qquad [4.5]$$

The principal assumption is that the virtual work done by the forces of constraint is zero.

$$\sum \left(X_i^c \ \delta x_i + Y_i^c \ \delta y_i + Z_i^c \delta z_i \right) = 0 \qquad [4.6]$$

Bringing equation [4.6] into [4.5], we have:

$$\sum \left(X_i \ \delta x_i + Y_i \ \delta y_i + Z_i \ z_i \right) = 0 \qquad [4.7]$$

This is the principle of virtual work. Equation [4.7] is formulated when the virtual work of the forces of constraint is zero.

4.1.3. *Equation of motion by D'Alembert's principle*

The extension of equilibrium to a system in motion is made possible by D'Alembert's principle.

$$X_i + X_i^c = m_i \ \ddot{x}_i \ , \ Y_i + Y_i^c = m_i \ \ddot{y}_i \ , Z_i + Z_i^c = m_i \ \ddot{z}_i \qquad [4.8]$$

$$i \in \ [\ 1, 2, \ldots , n \ ]$$

If equation [4.8] is rewritten with the second member equal to zero:

$$X_i + X_i^c - m_i \ \ddot{x}_i \ = 0 \ , Y_i + Y_i^c - _i \ \ddot{y}_i \ = 0 \ , \ Z_i + Z_i^c - m_i \ \ddot{z}_i \ = 0 \qquad [4.9]$$

the last terms in the equations are *inertia forces,* having components:

@Seismicisolation

$$-m_i \ddot{x}_i, \; -m_i \ddot{y}_i, \; -m_i \ddot{z}_i.$$

D'Alembert principle asserts that, at any instant, the state of motion of a mechanical system can be considered at equilibrium provided appropriate inertia forces are introduced as the products of masses and negative accelerations.

4.2. Lagrange's equation

Equation [4.9] can be written under a symbolic equation of motion, which extends virtual work to a system in motion:

$$\sum_{i=1}^{n} \left[\left(X_i - m_i \ddot{x}_i \right) \delta x_i + \left(Y_i - m_i \ddot{y}_i \right) \delta y_i + \left(Z_i - m_i \ddot{z}_i \right) \delta z_i \right] = 0 \qquad [4.10]$$

The virtual work of the forces of constraint is zero, by virtue of equation [4.7].

From equation [4.10] a number of differential equations can be derived. This is possible in the case where geometric constraints imposed on the system are holonomic.

4.2.1. *System subjected to r holonomic geometric constraints*

As presented in equation [4.3], instead of 3n degrees of freedom, the system subjected to r holonomic geometric constraints has p = 3n – r degrees of freedom.

To derive p equations of motion, the symbolic equations of motion in [4.10] are transformed into equations in terms of p generalized coordinates and p generalized forces $Q_1, Q_2, \ldots, Q_p$.

The following equations:

$$x_i = x_i(q_1, \ldots, q_p),$$

$$y_i = y_i(q_1, \ldots, q_p), \qquad i \in (1, 2, \ldots, n),$$

$$z_i = z_i(q_1, \ldots, q_p)$$

@Seismicisolation

are expressions in terms of independent quantities;

$$\delta x_i = \sum_{i=1}^{p} \frac{\partial x_i}{\partial q_i} \delta q_i \ ,$$

$$\delta y_i = \sum_{i=1}^{p} \frac{\partial y_i}{\partial q_i} \delta q_i \ , \qquad [4.11]$$

$$\delta z_i = \sum_{i=1}^{p} \frac{\partial z_i}{\partial q_i} \delta q_i$$

and the velocity components are:

$$\dot{x}_i = \sum_{i=1}^{p} \frac{\partial x_i}{\partial q_i} \dot{q}_i + \frac{\partial x_i}{\partial t}$$

$$\dot{y}_i = \sum_{i=1}^{p} \frac{\partial y_i}{\partial q_i} \dot{q}_i + \frac{\partial y_i}{\partial t}$$

$$\dot{z}_i = \sum_{i=1}^{p} \frac{\partial z_i}{\partial q_i} \dot{q}_i + \frac{\partial z_i}{\partial t} \qquad [4.12]$$

$$\dot{x}_i = \frac{d x_i}{d t}, \qquad \dot{q}_i = \frac{d q_i}{d t}$$

From [4.12] we obtain:

$$\frac{d \dot{x}_i}{d \dot{q}_i} = \frac{\partial x_i}{\partial q_i}, \quad \frac{d \dot{y}_i}{d \dot{q}_i} = \frac{\partial y_i}{\partial q_i}, \quad \frac{d \dot{z}_i}{d \dot{q}_i} = \frac{\partial z_i}{\partial q_i} \qquad [4.13]$$

@Seismicisolation

4.2.2. *Generalized forces*

Using equation [4.11], the virtual work of applied forces in equation [4.10] becomes:

$$\sum_{i=1}^{n}\left(X_i\ \delta x_i + Y_i\ \delta y_i + z_i\ \delta z_i\right)$$

$$= \sum_{i=1}^{p}\left[\left(\sum_{k=1}^{n} X_i \frac{\partial x_i}{\partial q_k} + Y_i \frac{\partial y_i}{\partial q_k} + Z_i \frac{\partial z_i}{\partial q_k}\right)\delta q_k\right] = \sum_{k=1}^{p} Q_k\ \delta q_k \qquad [4.14]$$

The quantities:

$$Q_k = \sum_{i=1}^{n}\left(X_i \frac{\partial x_i}{\partial q_k} + Y_i \frac{\partial y_i}{\partial q_k} + Z_i \frac{\partial z_i}{\partial q_k}\right) \qquad [4.15]$$

$k \in (1, 2, \ldots, p)$

Components of *generalized forces* Q_k correspond to the generalized coordinates q_k:

– if q_k is an angle, Q_k has the dimension of a torque;

– if q_k has a dimension of a length, Q_k has the dimension of a force.

4.2.3. *Introduction to kinetic energy*

Let us introduce kinetic energy U_c:

$$U_c = \frac{1}{2}\sum m_i\left(\ddot{x}_i^2 + \ddot{y}_i^2 + \ddot{z}_i^2\right) \qquad [4.16]$$

@Seismicisolation

Differentiation of [4.16] yields:

$$\frac{\partial U_c}{\partial \dot{x}_i} = m_i \dot{x}_i, \frac{\partial U_c}{\partial \dot{y}_i} = m_i \dot{y}_i, \frac{\partial U_c}{\partial \dot{z}_i} = m_i \dot{z}_i \qquad [4.17]$$

and:

$$\frac{d}{dt}\left(\frac{\partial U_c}{\partial \dot{x}_i}\right) = m_i \ddot{x}_i, \frac{d}{dt}\left(\frac{\partial U_c}{\partial \dot{y}_i}\right) = m_i \ddot{y}_i, \frac{d}{dt}\left(\frac{\partial U_c}{\partial \dot{z}_i}\right) = m_i \ddot{z}_i \qquad [4.18]$$

Using equations [4.18] and [4.11] we obtain:

$$\sum_{i=1}^{n}\left(m_i \ddot{x}_i \delta x_i + m_i \ddot{y}_i \delta y_i + m_i \ddot{z}_i \delta z_i\right)$$

$$= \sum_{i=1}^{n}\left\{\left[\frac{d}{dt}\left(\frac{\partial U_c}{\partial \dot{x}_i}\right)\delta x_i + \frac{d}{dt}\left(\frac{\partial U_c}{\partial \dot{y}_i}\right)\delta y_i + \frac{d}{dt}\left(\frac{\partial U_c}{\partial z_i}\right)\delta z_i\right]\right\}$$

$$= \sum_{k=1}^{n}\left\{\sum_{l=1}^{n}\left[\frac{d}{dt}\left(\frac{\partial U_c}{\partial \dot{x}_i}\right)\frac{\partial x_i}{\partial q_k} + \frac{d}{dt}\left(\frac{\partial U_c}{\partial \dot{y}_i}\right)\frac{\partial y_i}{\partial q_k} + \frac{d}{dt}\left(\frac{\partial U_c}{\partial z_i}\right)\frac{\partial z_i}{\partial q_k}\right]\right\} \bullet \delta q_k \qquad [4.19]$$

since $$\frac{d}{dt}\left(\frac{\partial U_c}{\partial \dot{x}_i}\right)\frac{\partial x_i}{\partial q_k} = \frac{d}{dt}\left(\frac{\partial U_c}{\partial \dot{x}_i}\frac{\partial x_i}{\partial q_k}\right) - \frac{\partial U_c}{\partial \dot{x}_i}\frac{\partial \dot{x}_i}{\partial q_k} \qquad [4.20]$$

with similar expressions for y_i and z_i.

4.2.4. *Lagrange's equation*

The next step is to express the coefficients δq_k in equation [4.19], [4.20] being taken into account:

@Seismicisolation

$$\sum_{i=1}^{n}\left(\frac{\partial U_c}{\partial \dot{x}_i}\frac{\partial x_i}{\partial q_k}+\frac{\partial U_c}{\partial \dot{y}_i}\frac{\partial y_i}{\partial q_k}+\frac{\partial U_c}{\partial \dot{z}_i}\frac{\partial z_i}{\partial q_k}\right)$$

$$-\sum_{i=1}^{n}\left(\frac{\partial U_c}{\partial \dot{x}_i}\frac{\partial \dot{x}_i}{\partial q_k}+\frac{\partial U_c}{\partial \dot{y}_i}\frac{\partial \dot{y}_i}{\partial q_k}+\frac{\partial U_c}{\partial \dot{z}_i}\frac{\partial \dot{z}_i}{\partial q_k}\right) \qquad [4.21]$$

In [4.21] the first sum is recognized as:

$$\sum_{i=1}^{n}\frac{d}{dt}\left(\frac{\partial U_c}{\partial \dot{x}_i}\frac{\partial \dot{x}_i}{\partial q_k}+\frac{\partial U_c}{\partial \dot{y}_i}\frac{\partial \dot{y}_i}{\partial q_k}+\frac{\partial U_c}{\partial \dot{z}_i}\frac{\partial \dot{z}_i}{\partial q_k}\right)$$

$$=\frac{d}{dt}\sum_{i=1}^{n}\left(\frac{\partial U_c}{\partial \dot{q}_k}\right)$$

[4.22]

by virtue of [4.13]. Equation [4.22] is based on the fact that kinetic energy only depends on velocities $\dot{x}_i$, $\dot{y}_i$ and $\dot{z}_i$. The second sum in [4.21] is equal to $\frac{\partial U_c}{\partial q_k}$. Finally equation [4.19] is written under the form:

$$\sum_{i=1}^{n}\left(m_i\ddot{x}_i\,\delta x_i+m_i\ddot{y}_i\,\delta y_i+m_i\ddot{z}_i\,\delta z_i\right)=$$

$$\sum\left\{\frac{d}{dt}\left[\frac{\partial U_c}{\partial \dot{q}_k}\right]-\frac{\partial U_c}{\partial q_k}\right\}\delta q_k \qquad [4.23]$$

Taking into account [4.23] and [4.14], the symbolic equation of motion [4.10] is rewritten as follows:

@Seismicisolation

$$\sum_{k=1}^{p}\left[\frac{d}{dt}\left(\frac{\partial U_c}{\partial \dot{q}_k}\right)-\frac{\partial U_c}{\partial q_k}-Q_k\right]\delta q_k=0 \qquad [4.24]$$

The p generalized coordinates q_k are independent quantities. The p virtual displacements δq_k are also independent, since the left of equation [4.24] must be zero for all values δq_k. This leads to p Lagrange equations:

$$\frac{d}{dt}\left(\frac{\partial U_c}{\partial \dot{q}_q}\right)-\frac{\partial U_c}{\partial q_k}-Q_k=0 \qquad [4.25]$$

$k \in 1, 2, \ldots, p$

4.2.5. *Potential function*

For conservative systems, the potential function:

$$U_p = U_p\left(x_i, y_i, z_i, \cdots, x_n, y_n, z_n\right)$$

exists. This potential energy depends on the system coordinates alone:

$$X_i = -\frac{\partial U_p}{\partial x_i}, \quad Y_i = -\frac{\partial U_p}{\partial x_i}, \quad Z_i = -\frac{\partial U_p}{\partial x_i} \qquad [4.26]$$

Bringing [4.26] into [4.16], we get:

$$Q_k = \left(X_i\frac{\partial x_i}{\partial q_k}+Y_i\frac{\partial y_i}{\partial q_k}+Z_i\frac{\partial z_i}{\partial q_k}\right)=$$

$$-\sum_{i=1}^{n}\left(\frac{\partial U_p}{\partial x_i}\frac{\partial x_i}{\partial q_k}+\frac{\partial U_p}{\partial y_i}\frac{\partial y_i}{\partial q_k}+\frac{\partial U_p}{\partial z_i}\frac{\partial z_i}{\partial q_k}\right)$$

@Seismicisolation

or

$$Q_k = -\frac{\partial U_c}{\partial q_k} \qquad [4.27]$$

Substituting equation [4.27] into [4.25]:

$$\frac{d}{dt}\left(\frac{\partial U_c}{\partial \dot{q}_q}\right) - \frac{\partial U_c}{\partial q_k}\left(U_c - U_p\right) = 0 \quad k \in \left(1, 2, \cdots, p\right) \qquad [4.28]$$

Defining the difference:

$$U_c - U_p = L \qquad [4.29]$$

Equation [4.28] can be written in condensed form as:

$$\frac{d}{dt}\left(\frac{\partial L}{\partial \dot{q}_k}\right) - \frac{\partial L}{\partial q_k} = 0 \quad k \in \left[1, 2, \cdots, k\right] \qquad [4.30]$$

This is the Lagrangian function.

4.2.6. *Lagrangian function with Rayleigh dissipation function*

Rayleigh dissipation function is defined as:

$$D = \frac{1}{2}\sum_{i=1}^{n}\left(C_{ix}\,\dot{x}^2 + C_{ij}\,\dot{y}^2 + C_{iz}\,\dot{z}^2\right) \qquad [4.31]$$

Equation [4.31] concerns a system with n particles. From [4.31], friction forces are deduced:

@Seismicisolation

$$\left.\begin{aligned} X_i^f &= -\frac{\partial D}{\partial \dot{x}_i} = -C_{ix}\,\dot{x}_i \\ Y_i^f &= -\frac{\partial D}{\partial \dot{y}_i} = -C_{iy}\,\dot{y}_i \\ Z_i^f &= -\frac{\partial D}{\partial \dot{z}_i} = -C_{iz}\,\dot{z}_i \end{aligned}\right\} \qquad i \in (1, 2, \cdots, n) \qquad [4.32]$$

– *generalized friction forces*

$$Q_k^f = \sum_{i=1}^{n} \left(X_i^f \frac{\partial x_i}{\partial q_k} + Y_i^f \frac{\partial y_i}{\partial q_k} + Z_i^f \frac{\partial z_i}{\partial q_k} \right) \qquad [4.33]$$

$$= -\sum_{i=1}^{n} \left(\frac{\partial D}{\partial \dot{x}_i} \frac{\partial \dot{x}_i}{\partial \dot{x}_i} + Y_i^f \frac{\partial \dot{y}_i}{\partial \dot{q}_k} + Z_i^f \frac{\partial \dot{z}_i}{\partial \dot{q}_k} \right)$$

equation [4.14] being accounted for since D is function of velocity only.

$$Q_k^f = -\frac{\partial D}{\partial \dot{q}_k} \quad k \in (1, 2, \cdots, P) \qquad [4.34]$$

– *components of generalized forces*: for a system subjected to a conservative force derived from U_p and friction force derived from dissipation function D, the components of generalized force are:

$$Q_k = -\frac{\partial U_p}{\partial q_k} - \frac{\partial D}{\partial \dot{q}_k}, k \in (1, 2, \ldots, p) \qquad [4.35]$$

@Seismicisolation

Lagrange's equation is:

$$\frac{d}{dt}\left(\frac{\partial L}{\partial \dot{q}_k}\right) - \frac{\partial L}{\partial q_k} + \frac{\partial D}{\partial \dot{q}_k} = 0 \text{ , } k \in (1, 2, 3, ..., p) \qquad [4.36]$$

4.3. Hamilton's principle

The symbolic equation of motion is:

$$\sum_{i=1}^{n} \left[\left(X_i - m_i \ddot{x}_i \right) \delta x_i + \left(Y_i - m_i \ddot{y}_i \right) \delta y_i + \left(Z_i - m_i \ddot{z}_i \right) \delta z_i \right] = 0 \qquad [4.37]$$

This is rewritten as:

$$\sum_{i=1}^{n} m_i \left(\ddot{x}_i \, \delta x_i + \ddot{y}_i \, \delta y_i + \ddot{z}_i \, \delta z_i \right) = \sum \left(X_i \, \delta x_i + Y_i \, \delta y_i + Z_i \, \delta z_i \right) \qquad [4.38]$$

where δx_i, δy_i and δz_i are continuously differentiable functions of time in the interval from t_0 to t_1 during which the motion takes place.

Adding the following terms to [4.38], we get:

$$\sum_{i=1}^{n} m_i \left(\dot{x}_i \, \delta \dot{x}_i + \dot{y}_i \, \delta \dot{y}_i + \dot{z}_i \, \delta \dot{z}_i \right) = \delta \sum_{i=1}^{n} \frac{m_i}{2} \left(\dot{x}^2 + \dot{y}^2 + \dot{z}^2 \right) = \delta U_c \qquad [4.39]$$

@Seismicisolation

Where U_c is the kinetic energy of the system, we obtain:

$$\sum_{i=1}^{n} m_i\left(\ddot{x}_i\,\delta x_i + \ddot{y}_i\,\delta y_i + \ddot{z}_i\,\delta z_i + \dot{x}_i\,\delta\dot{x}_i + \dot{y}_i\,\delta\dot{y}_i + \dot{z}_i\,\delta\dot{z}_i\right) = \sum_{i=1}^{n}\left(X_i\,\delta x_i + Y_i\,\delta y_i + Z_i\,\delta z_i\right) + \delta\,\amalg_c \qquad [4.40]$$

$$\delta\,\dot{x}_i = \frac{d}{dt}\,\delta x_i\ ,\ \delta\,\dot{y}_i = \frac{d}{dt}\,\delta z_i\ ,\ \delta\,\dot{z}_i = \frac{d}{dt}\,\delta z_i$$

Then equation [4.40] is rewritten as:

$$\frac{d}{dt}\left[\sum_{i=1}^{n} m_i\left(\dot{x}_i\,\delta x_i + \dot{y}_i\,\delta y_i + \dot{z}_i\,\delta z_i\right)\right] = \sum_{i=1}^{n}\left(X_i\,\delta x_i + Y_i\,\delta y_i + Z_i\,\delta z_i\right) + \delta U_c \qquad [4.41]$$

$$V = \sum\left(X_i\,\delta x_i + Y_i\,\delta y_i + Z_i\,\delta z_i\right) \qquad [4.42]$$

Integration of equation [4.41] between times t_0 and t_1 yields:

$$\left[\sum_{i=1}^{n} m_i\left(\dot{x}_i\,\delta x_i + \dot{y}_i\,\delta y_i + \dot{z}_i\,\delta z_i\right)\right]_{t_0}^{t_1} = \left(V + \delta U_c\right)\,dt \qquad [4.43]$$

It is assumed that the variations δx_i, δy_i and δz_i are equal to zero at time t_0 and t_1, so [4.43] becomes:

$$\int_{t_0}^{t_1}\left(V + \delta U_c\right)\,dt = 0 \qquad [4.44]$$

@Seismicisolation

Equation [4.44] constitutes Hamilton's principle, which is expressed as follows with V identified as $-\delta U_p$. The motion of a system in the interval of time t_0 to t_1 occurs in a such manner that, if a virtual displacement is given to the system at each instant, equation [4.44] is satisfied provided that the virtual displacement is zero at the initial and final instants t_0 and t_1. If the forces are conservative and U_p is the initial potential, we obtain:

$$X_i = -\frac{\partial U_p}{\partial x_i}, \quad Y_i = -\frac{\partial U_p}{\partial y_i}, \quad Z_i = -\frac{\partial U_p}{\partial z_i}$$

and V is written as:

$$\sum_{i=1}^{n} \left(X_i\ \delta x_i + Y_i\ \delta y_i + Z_i\ \delta z_i\right) = \left(-\sum_{i=1}^{n} \left(\frac{\partial U_p}{\partial x_i}\ \delta x_i + \frac{\partial U_p}{\partial y_i}\ \delta y_i + \frac{\partial U_p}{\partial z_i}\ \delta z_i\right) \right) = -\delta U_p \qquad [4.45]$$

Therefore Hamilton's principle can be expressed by the following equation:

$$\int_{t_1}^{t_e} \left(\delta U_c - \delta U_p\right) d\,t = \delta \int_{t_0}^{b_1} \left(U_c - U_p\right) d\,t = 0 \qquad [4.46]$$

In Appendices 4.A and 4.B, equations of motion of an elastic solid as well as Lagrange's equations of motion are deduced from Hamilton's principle.

4.4. Practical considerations concerning the choice of equations of motion and related solutions

So far, we have presented the principal methods of obtaining equations of motion of bounded media. Here we adopt the point of view of an experimenter who wishes to study the dynamic responses of bounded media subjected to excitation, such as harmonic, white noise, random or impulse signal. In part B of this book, we discuss experimental works and the results of measurements in detail. We look at the solutions to inverse problems in order to obtain elastic and/or viscoelastic modulus (or compliance) of the material being tested. The first thing the experimenter has to

@Seismicisolation

do is choose the appropriate equations of motion for the adopted bounded medium and boundary conditions.

4.4.1. *Boundary conditions and approximate equations of motion*

In books devoted to theoretical elastodynamics (see bibliography, section 4.7) the problem of dynamic responses of infinite or semi-infinite media is discussed. The theory of elasticity used in conjunction with potential theory permits us to obtain closed-form solutions in terms of the sum of exponentials. The ease with which we obtain such solutions can be explained by the nature of waves in the medium:

– *Progressive waves* occur when there are no wave reflections. There are consequently no stationary waves. The medium being infinite or semi-infinite, particle displacements are expressed by an exponential function of time. The boundary condition for rods is often reduced to the free boundary of lateral surfaces.

– *Medium with symmetry of the section* – for an infinite length rod with circular section, various kinds of Bessel's series are successfully utilized to solve the problem of progressive wave propagation. For a semi-infinite plate, a closed-form solution of dynamic response exists.

– *Necessity of choosing approximate equations of motion* – unfortunately we do not have an ideal situation, such as an infinite or semi-infinite rod or plate. For a rod with finite length, closed-form solutions for infinite or semi-infinite length rod cannot take the boundary conditions at both ends into account.

In such a bounded medium, waves are essentially stationary and require us to search for appropriate approximate equations of motion with a set of boundary condition equations that are related to the experiment adopted by the experimenter him- or herself.

4.4.2. *Choice of equations of motion*

When considering the information presented above, the experimenter is oriented towards approximate equations. It does not mean that he or she has to adopt elementary equations of motion that do not take into account things such as shear effect (which is related to geometrical distortion of the sample, shear properties of the material) and inertia effect (which is essentially time dependent).

@Seismicisolation

4.4.3. *The degree of approximation*

The degree of approximation of the equations of motion depends on the following parameters:

– *Frequency range* – for the majority of commercially available elasticimeters, the equations of motion proposed by the apparatus builder are often of elementary nature. Often wave dispersion (which describes the dependency of phase or group velocity *versus* frequency) is not taken into account. If such apparatus is utilized, the validity of the proposed equations of motion needs to be checked within the prescribed frequency range.

– *Nature of the material* – the *low damping material* can be weakly viscoelastic, such as iron (whose damping capacity tan δ is less than 10^{-2}). The assumption of frequency independent wave dispersion is reasonable at low frequency.

– *For viscoelastic materials,* such as high polymers, complex modulus varies more or less with frequency according to the width of the transition zone between the rubber and glassy states of the material. For isothermal tests, the experimenter can adopt elementary equations of motion on the condition that he or she limits the test to the lower frequency range. The validity of adopted equations of motion in the frequency range, however, needs to be checked.

– *For high damping materials* (i.e. large tanδ in the range 10^{-2} to 10^{-1}) – complex modulus strongly varies with frequency. The elementary equations of motion must be replaced by equations with a higher degree of approximation.

– *For composite materials*, shear properties play a dominant role and wave dispersion must be taken into account in the equations of motion. The experimenter must be careful. What is valid for non-composite and isotropic materials is not necessarily applicable to composite materials. Shear effect plays a predominant role for the experimenter who has to characterize materials for the first time.

– *Williams-Landel-Ferry's principle* – this correspondence principle is presented in Chapters 2 and 3. It is very useful and permits us to artificially extend the frequency range to eight or more decades. (This unusually large range is necessary for polymer specialists who want to interpret transition phenomena in viscoelastic materials.) For anisotropic artificial material, this principle is not always applicable. Isothermal dynamic tests with a large frequency range are referred to. Consequently, equations of motion with a higher degree of approximation are adopted.

– *Boundary conditions* are closely related to the experimental set-up adopted by the experimenter him- or herself in order to maintain the sample in relation to the exciter and rigid platform of the apparatus/attachment of the transducer.

@Seismicisolation

– *Sample geometry* – in practice, sample geometry is often imposed on the experimenter. This is the case when a sample is cut from a hollow cylinder. A ring sample or curved rod is used. Equations with cylindrical coordinates are to be found in Chapter 9.

– *Multilayered samples* can be woods or artificial composite materials. There is a shear distribution through the thickness. In dynamic tests homogenized theory is referred to in order to replace the multilayered sample with an equivalent anisotropic homogeneous sample. Technical modulus, for example Young's modulus, can be different in tension and bending tests. The experimenter must consult books and papers concerning multilayered materials (see Chapter 1).

– *Off-axis sample* – to characterize anisotropic materials, non-diagonal terms of modulus (or compliance) matrix are to be evaluated. The only way to characterize them is to use an off-axis rod whose axis is not coincident with a symmetry axis of the material. Dynamic tests on such samples give rise to two (or more) waves of different nature. Wave coupling is intentionally created in the sample. Interpretation of such a test is more complex than for a test with rod axis coincident with a symmetry axis of the material. This problem is examined in Chapters 5, 6 and 7 for torsional, bending and longitudinal waves respectively.

4.5. Three-, two- or one-dimensional equations of motion?

Let us review the three possible cases. We must not lose sight of the fact that the mechanical characterization of elastic or viscoelastic materials requires an inverse problem whose solution must satisfy eventually mathematical unicity. The second difficulty resides in the computational effort, which increases with increasing dimensions of the equations of motion.

4.5.1. *Three-dimensional equations of motion*

Three-dimensional equations of motion were proposed by many researchers using finite elements. The unknowns are the number of elastic (or viscoelastic) technical moduli of the material.

Attempts to solve the problem of an isotropic material have not been convincing. The number of measuring points is high.

When dealing with anisotropic materials, the difficulties increase and no progress is seen using the method of finite elements.

@Seismicisolation

4.5.2. *Two- or one-dimensional equations of motion*

When formulating equations of motion, some insight into the benefits of reducing the number of dimensions is useful. Differential equations of motion need to be found and the maximum number of boundary conditions satisfied. The degree of approximation of these equations depends on the number of boundary conditions satisfied, including those of the rod's lateral surface.

The reduction of dimensions in equations of motion is compensated for by correcting terms introduced in the equations of motion. These correcting terms take into account various effects that occur in the bounded medium. The method, observed from this angle, is essentially physical and is capable of taking the whole problem of wave dispersion, i.e. dependency of phase (or group) velocity *versus* frequency – even at very high frequency – into account.

4.5.3. *Wave dispersion*

Wave dispersion is the cornerstone of the problem of evaluating technical moduli of a material that are evaluated via the phase velocity itself. If we do not quantitatively know this last function, evaluation of the material's moduli is subject to large errors, particularly at higher frequencies. The trend of the phase velocity curve *versus* frequency must be examined before tackling the inverse problem of moduli calculation.

4.6. Closed-form solutions to equations of motion

4.6.1. *Degree of differential equations of six or less*

For a bounded medium, when the degree of each equation does not exceed six, it is possible to appeal to the characteristic functions. These functions are the linear combination of trigonometric functions (sine and cosine) and hyperbolic functions (sinh and cosh). The boundary conditions give rise to eigenvalue equations.

4.6.2. *Degree of differential equations exceeding six*

Using closed-form eigenvalue equations and characteristic functions in equations with six degrees is approaching the limit of this method. Beyond this limit,

@Seismicisolation

calculations become cumbersome and intractable. Characteristic functions are then abandoned in favor of a linear combination of exponential functions.

Matricial treatment of the problem permits us to obtain a numerically dynamic response from the bounded medium.

Extension of the method gives rise to the so-called continuous element method, which is presented in Chapter 12.

Recently, it has been demonstrated that when exploring higher frequency domains for the same bounded medium, calculation time is far greater when using finite elements compared to continuous elements in the direct problem.

4.7. Bibliography

[ABA 72] ABACAR R. B. and CUNIFF P., "The vibration of cantilever beams of fiber reinforced materials", *Journal of Composite Materials*, vol. 6, p. 504-516, 1972.

[CAS 97] CASIMIR J. B., Rod type continuous elements (Static and dynamic formulations - Assembling of plane and out of plane rods), PhD thesis, Conservatoire des Arts et Métiers, Paris, 1997.

[DYM 73] DYM C. L. and SHAMES I. H., *Solid Mechanics – A Variational Approach*, McGraw Hill, New York, 1973.

[FLE 97] FLEURET J. S., Continuous elements method applied to plate dynamics, PhD thesis, Conservatoire des Arts et Métiers, Paris, 1997.

[GER 72] GERMAIN P., "About the application of virtual power in continuum mechanics", *Comptes Rendus de l'Académie des Sciences*, p.1051-1055, 1972.

[GOR 02] GORMAN D. J., *Free Vibration of Plates*, Elsevier, Holland, 2002.

[GRA 75] GRAFF K. F., *Wave Motions in Elastic Solids*, Clarendon Press, Oxford, 1975.

[MEI 67] MEIROVITCH L., *Analytical Methods in Vibrations,* MacMillan, USA, 1967.

[MUL 83] MULLER P. Contribution to the study of wave dispersion in uniform elastic wave guides, PhD thesis, University of Pierre and Marie Curie, Paris, 1983.

[VOL 65] VOLTERRA E., ZACHMANOGLU E. C., *Dynamics of Vibrations,* Charles E. Merrill Books, Inc. Columbus, Ohio USA, 1965.

@Seismicisolation

4.8. Appendices

Appendix 4.A. Equations of motion in elastic medium deduced from Love's variational principle

The Hamilton principle is:

$$\delta \int_{t_0}^{t_1} \left(U_c - U_p + L \right) d\,t = 0 \qquad [4.A.1]$$

where: U_c is kinetic energy; U_p potential energy; and L is work done by external force.

Kinetic energy, where $\dot{u}_1$, $\dot{u}_2$ and $\dot{u}_3$ are velocity components, is:

$$U_c = \frac{1}{2} \int \int \int \rho \left[\dot{u}_1^2 + \dot{u}_2^2 + \dot{u}_3^2 \right] dx\,dy\,dz \qquad [4.A.2]$$

$$\delta \int_{t_0}^{t_1} U_c\, d\,t = \delta \int_{t_0}^{t_1} \int \int \int \frac{\rho}{2} \left[\dot{u}_1^2 + \dot{u}_2^2 + \dot{u}_3^2 \right] dx\,dy\,dz$$

$$= \int_{t_0}^{t_1} d\,t \int \int \int \rho \left[\frac{\partial u_1}{\partial t} \frac{\partial \delta u_1}{\partial t} + \frac{\partial u_2}{\partial t} \frac{\partial \delta u_2}{\partial t} + \frac{\partial u_3}{\partial t} \frac{\partial \delta u_3}{\partial t} \right] dx\,dy\,dz \qquad [4.A.3]$$

Integration by parts of the first term in the bracket of [4.A.3] in the second member gives us:

$$\int_{t_0}^{t_1} \rho \frac{\partial u_1}{\partial t} \frac{\partial \delta u_1}{\partial t}\, d\,t$$
$$= \rho \frac{\partial u_1}{\partial t} \delta u_1 \Big|_{t_0}^{t_1} - \int_{t_0}^{t_1} \rho \frac{\partial^2 u_1}{\partial t^2} \delta u_1\, d\,t \qquad [4.A.4]$$

The first term in the second member of [4.A.4] is zero, according to Hamilton's principle. Extending [4.A.4] to all terms in [4.A.3] gives:

@Seismicisolation

$$-\int_{t_0}^{t_1} d\,t \int\int\int \rho\left[\frac{\partial^2 u_1}{\partial t^2}\,\delta u_1 + \frac{\partial^2 u_2}{\partial t_2}\,\delta u_2 + \frac{\partial^2 u_3}{\partial t^2}\,\delta u_3\right] dx\,dy\,dz$$

[4.A.5]

Potential energy is:

$$U_p = \frac{1}{2} C_{ijkl}\,\varepsilon_{kl}\,\varepsilon_{ij} = \sigma_{ij}\,\varepsilon_{ij} = \frac{1}{2}\sigma_{ij}\left(u_{i,j} + u_{j,i}\right) = \sigma_{ij}\,u_{i,j} \qquad [4.A.6]$$

Letters in subscript can be inverted $\left(\sigma_{ij} = \sigma_{ji}\right)$ so the bracket can be replaced by $2u_{i,j}$.

$$\delta\,\amalg_p = \delta\int_{t_0}^{t_1} d\,t \int\int\int \left(\sigma_{ij}\,u_{i,j}\right) dx\,dy\,dz$$

[4.A.7]

$$= \int_{t_0}^{t_1} \int\int\int \delta\left(\sigma_{ij}\,u_{i,j}\right) dx\,dy\,dz$$

In equation [4.A.7], we notice that:

$$\delta\,(\sigma_{ij}\,u_{i,j}) = \delta\,(\sigma_{ij}\,u_{i,j}) - \delta\,(\sigma_{ij,j}\,u_i) \qquad [4.A.8]$$

$$\delta\amalg_p = \int_{t_0}^{t_1} \int\int\int \left[\delta\left(\sigma_{ij}\,u_i\right)_{,j} - \delta\left(\sigma_{ij,j} \bullet u_i\right)\right] dx\,dy\,dz \qquad [4.A.9]$$

Gauss formula gives:

$$\delta\underbrace{\int\int\int \left(\sigma_{ij}\,u_i\right) dx\,dy\,dz}_{\text{volume integral}} = \delta\underbrace{\int\int \left(\sigma_{ij}\,u_i\right) u_j\,d\,S}_{\text{surface integral}} \qquad [4.A.10]$$

@Seismicisolation

Work done by external forces:

$$\delta \int_{t_0}^{t_1} L\, d\,t = \int_{t_0}^{t_1} \delta\, L\, d\,t$$

$$= \int_{t_0}^{t_1} d\,t \int \int \int \rho \left(X_1\, \delta\, u_1 + X_2\, \delta\, u_2 + X_3\, \delta\, u_3 \right) dx\, dy\, dz$$

$$= \int_{t_0}^{t_1} d\,t \int \int_S \rho \left(X_{1\,\sigma}\, \delta\, u_1 + X_{2\,\sigma}\, \delta\, u_2 + X_{3\,\sigma}\, \delta\, u_3 \right) d\,S$$

[4.A.11]

4.A.1. Expression of Hamilton's principle

Collecting equations [4.A.5], [4.A.9] and [4.A.11], we get:

$$\int_{t_0}^{t_1} d\,t \int \int_V \int \left[\rho\, X_i - \frac{\partial^2\, u_i}{\partial\, t^2} + \sigma_{i,jj} \right] \delta\, u_i\, dx\, dy\, dz \qquad [4.A.12]$$

$$+ \int_{t_0}^{t_1} d\,t \iint_s \left[-\sigma_{ij}\, u_i\, n_j + X_{j\sigma} \right] \delta\, u_i\, d\,S = 0$$

In [4.A.12], the second term represents the boundary conditions on S, which are obtained by setting the terms in brackets to zero.

[4.A.12], reduced to the first term, can be considered as a variational principle. It bears the name Love's variational formulation.

Appendix 4.B. Lagrange's equations of motion deduced from Hamilton's principle

Let 3n the number of coordinates of a set of particles of mass m_i and coordinates x_i, y_i and z_i. There are r constraint relationships of the type:

$$Fj\, [(x_1, y_1, z_1), \ldots, (x_n, y_n, z_n)] = 0,\ j \in (1, \ldots, r) \qquad [4.B.1]$$

@Seismicisolation

If the system is holonomic, the 3n coordinates can be expressed by p = 3n – r independent quantities (generalized coordinates):

$$q_1, q_2, \dots, q_p$$

$$x_i = x_i(q_1, q_2, \dots, q_p) \qquad [4.B.2]$$

$$y_i = y_i(q_1, q_2, \dots, q_p)$$

$$z_i = z_i(q_1, q_2, \dots, q_p)$$

If the system is in motion, the generalized coordinates are also a function of time. The problem to be solved consists of finding which relationships must exist during motion between variables q_i (i = 1, 2, ... , p) and their derivatives when forces that are acting on the system are known.

We can write:

$$\dot{x}_i = \sum_{s=1}^{p} \frac{\partial x_i}{\partial q_s} \dot{q}_s$$

$$\dot{y}_i = \sum_{s=1}^{p} \frac{\partial y_i}{\partial q_s} \dot{q}_s \quad i \in (1, 2, \dots, n) \qquad [4.B.3]$$

$$\dot{z}_i = \sum_{s=1}^{p} \frac{\partial z_i}{\partial q_s} \dot{q}_s \quad s \in (1, 2, \dots, p)$$

Kinetic energy:

$$\text{Ц}_c = \frac{1}{2} \sum_{i=1}^{p} m_i \left(\dot{x}_i^2 + \dot{y}_i^2 + \dot{z}_i^2 \right) \qquad [4.B.4]$$

$$= \frac{1}{2} \sum m_i \left\{ \left[\sum_{s=1}^{p} \frac{\partial x_i}{\partial q_s} \dot{q}_s \right]^2 + \left[\sum_{s=1}^{p} \frac{\partial y_i}{\partial q_s} \dot{q}_s \right]^2 + \left[\sum_{s=1}^{p} \frac{\partial z_i}{\partial q_s} \dot{q}_s \right]^2 \right\}$$

@Seismicisolation

U_c is a second degree, homogeneous function of $\dot{q}_s$:

$$U_c = \frac{1}{2} \sum_{r=1}^{p} \sum_{s=1}^{p} E_{rs} \dot{q}_r \dot{q}_s \qquad [4.B.5]$$

E_{rs} are functions of the quantities (q_1, ..., q_p) only.

For every virtual displacement of the system characterized by δq_1, ... , δq_r, we have:

$$\delta x_i = \sum_{s=1}^{p} \frac{\partial x_i}{\partial q_s} \delta q_s ;$$

$$\delta y_i = \sum_{s=1}^{p} \frac{\partial y_i}{\partial q_s} \delta q_s ; \qquad [4.B.6]$$

$$\delta z_i = \sum_{s=1}^{p} \frac{\partial z_i}{\partial q_s} \delta q_s$$

Work performed by the forces in the virtual displacement corresponding to variations δq_1, ... , δq_p, is given by:

$$U_p = \sum_{i}^{n} \left(X_i \, \delta x_i + Y_i \, \delta y_i + Z_i \, \delta z_i \right)$$

$$= \sum_{i=1}^{n} \left[X_i \left(\sum_{s=1}^{p} \frac{\partial x_i}{\partial q_s} \delta q_s \right) + Y_i \left(\sum_{s=1}^{p} \frac{\partial y_i}{\partial q_s} \delta q_s \right) + Z_i \left(\sum_{s=1}^{p} \frac{\partial z_i}{\partial q_s} \delta q_s \right) \right]$$

$$= \sum_{s=1}^{n} \left[\sum_{i=1}^{n} \left(\frac{\partial x_i}{\partial q_s} X_i + \frac{\partial y_i}{\partial q_s} Y_i + \frac{\partial z_i}{\partial q_s} Z_i \right) \right] \delta q_s \qquad [4.B.7]$$

@Seismicisolation

Letting:

$$Q = \sum_{i=1}^{n} \left(\frac{\partial x_i}{\partial q_s} X_i + \frac{\partial y_i}{\partial q_s} Y_i + \frac{\partial z_i}{\partial q_s} Z_i \right) \qquad [4.B.8]$$

equation [4.B.7] becomes:

$$U_c = \sum_{s=1}^{p} Q_s \, \delta q_s \qquad [4.B.9]$$

Quantities Q_s are completely determined if forces acting on the elements of the system are known. Kinetic energy is a function of quantities $q_1, \ldots, q_s$ and their first derivatives:

$$\dot{q}_1 , \cdots , \dot{q}_s .$$

Variation of U_c is given by:

$$\delta U_c = \sum_{s=1}^{p} \left(\frac{\partial U_c}{\partial q_s} \delta q_s \right) + \left(\frac{\partial U_c}{\partial \dot{q}_s} \delta \dot{q}_s \right) \qquad [4.B.10]$$

Bringing equations [4.B.10] and [4.B.9] into [4.B.8]:

$$\int_{t_0}^{t_1} \left(\sum_{s=1}^{p} \frac{\partial U_c}{\partial q_s} \delta q_s + \sum_{s=1}^{p} \frac{\partial U_c}{\partial \dot{q}_s} \delta \dot{q}_s + \sum_{s=1}^{p} Q \, \delta q_s \right) d\,t = 0 \qquad [4.B.11]$$

Variations $\delta x_i, \ldots, \delta y_i, \delta z_i$ are zero at t_0 and t_1 because if the variables $q_1, \ldots, q_p$ are independent then $\delta q_1, \ldots, \delta q_p$ are zero at t_0 and t_1.

@Seismicisolation

Consequently, the integral terms in equation [4.B.11] must be zero and the following equation is satisfied:

$$\int_{t_0}^{t_1} \left[\sum_{s=1}^{p} \frac{\partial U_c}{\partial q_s} - \frac{d}{dt} \left(\frac{\partial U_c}{\partial \dot{q}_s} \right) + Q_s \right] \delta q_s \, dt = 0 \qquad [4.B.12]$$

δq_s being independent, Lagrange's equations are deduced:

$$\frac{d}{dt} \left(\frac{\partial U_c}{\partial \dot{q}_s} \right) - \frac{\partial U_c}{\partial q_s} = Q_s \; s = 1, 2, ..., p \qquad [4.B.13]$$

@Seismicisolation

PART B

Rod Vibrations

@Seismicisolation

Chapter 5

Torsional Vibration of Rods[1]

5.1. Introduction

Static and dynamic torsion tests on rods with a circular section are extensively used to evaluate the shear moduli of materials. Adoption of a circular section for an isotropic rod gives rise to an exact and simple solution to the problem of shear wave propagation in a rod. Absence of distortion of the cross-section under torsion moment (a phenomenon that bears the name warping) facilitates the study of torsional vibrations for a finite or infinite length rod. On the other hand, a rod of non-circular section is more complicated to study in static or dynamic tests.

Warping phenomenon requires a special study. This is the price we pay for using samples that are easier to fabricate. On a practical level, for many materials, such as composite artificial ones, the only section that can be tested is rectangular. This is why we discuss rectangular cross-sections in this chapter.

There are a couple of exceptions to the warping phenomenon. Some three-dimensional composites with a special axial symmetry exist[2] and a circular section is possible. Wood, which is a natural orthotropic material, is an exception if the rod axis is also a symmetry material axis. Apart from these examples, rods for torsion tests are fabricated from uniform or multilayered plates.

Chapter written by Yvon CHEVALIER, Michel NUGUES and James ONOBIONO.

1 This chapter uses large extracts from Nugues's CNAM engineering degree work. Onobiono's PhD thesis concerning higher elastodynamic warping mode is partly mentioned.

2 Concerning three-dimensional carbon-carbon composites.

Mechanics of Viscoelastic Materials and Wave Dispersion Edited by Yvon Chevalier and Jean Tuong Vinh
© 2010 ISTE Ltd. Published 2010 by ISTE Ltd.

@Seismicisolation

5.1.1. *Short bibliography of the torsion problem*

As early as 1856, Saint Venant [SAI 1856] solved the problem of static torsion of an isotropic rod with rectangular section. Lekhnitskii [LEK 63] around the 1940s extended Saint Venant's theory to anisotropic materials. Recently, the static torsion problem has been revisited by many researchers. It is now possible to obtain relationships between the torsion moment and torsion angle using polynomials instead of transcendental functions [DYM 73, JOH 71, MIN 69, MIN 75, RIT 75, VOI 28].

Torsional (shear) waves in elastic rods have been examined by many researchers since 1966 [BLE 70, FRA 69, MED 66, NIG 66, TOU 77]. Higher frequency elastodynamic modes have been analyzed, with Barr [BAR 62] and Engström's work [ENG 74] holding our attention. The first author proposed improvements to Love's equation by introducing additional terms that take the axial displacement of an isotropic rectangular rod and longitudinal inertia into account. However, some simplification assumptions are adopted. The cross-section warping is that adopted by Saint Venant [SAI 1856]. The distortion of the cross-section is, however, not examined and *the plane projection of the cross-section rigidly rotates in the plane*. Engström considered the warping phenomenon to be part of the solution to the dynamic problem. Helmholtz's equation and related boundary curves permitted this author to extend warping modes beyond the first one. Higher elastodynamic modes with different section mode shapes are presented.

5.1.2. *Survey of solving methods for torsion problems*

In order to clarify the ideas and classify various assumptions, we distinguish three classes of problems:

– static torsion including Saint Venant's warping solution;

– dynamic torsion at lower frequencies using Saint Venant's theory;

– torsional wave propagation and solution for the wave dispersion problem discarding Saint Venant's theory.

For practical torsion testing, we focus our attention on the aforementioned items. Figure 5.1 gives the main ideas concerning the static torsion problem. Attention is devoted to warping phenomenon. For isotropic materials, only pure torsion is considered. For anisotropic materials, when the rod axis is not a transverse isotropic axis (off-axis rod) there is coupling between the torsion and bending of the rod. Consequently, the solutions to the problem have to take this coupling into account.

@Seismicisolation

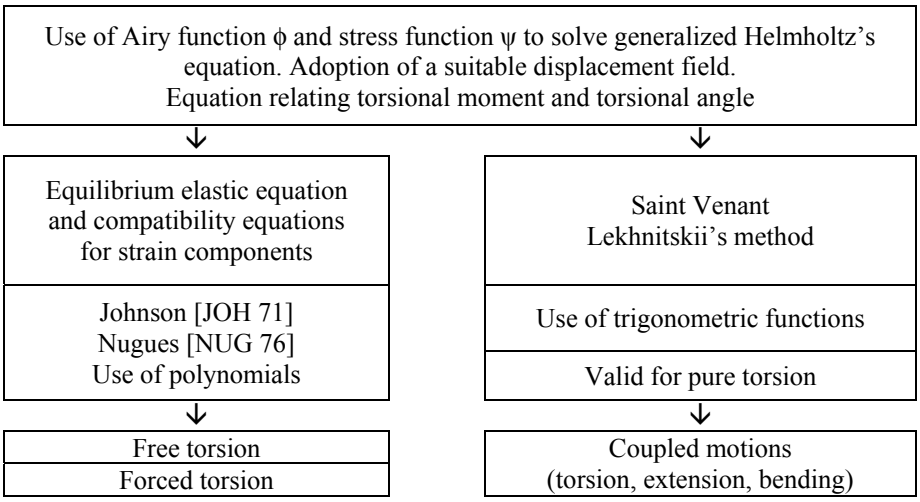

Figure 5.1. *Static torsion of a rod with rectangular section for various proposed methods*

In order to obtain tractable solutions, [JOH 71, VOI 28 and VOL 71] proposed utilization of polynomials instead of trigonometric and hyperbolic functions. To facilitate understanding of the dynamic torsion problem, we will first distinguish low-order approximation theories of torsional vibrations at lower frequencies, see Figure 5.2. Hamilton's variational principle (or Love's variational principle, which is equivalent, see Appendix 4.A) permits us to obtain equations of motion.

One of the simplest assumptions adopts the static Saint Venant's warping solution in order to relate the torsional moment to torsional angle. Elementary theory gives rise to second-order equations of motion. An off-axis rod is not utilized in order to avoid coupling between torsion and bending. The first warping mode of the cross-section is approximately valid for low frequencies.

To obtain one-dimensional equations of motion, as indicated above, and to take into account the influence of axial motion of the rod as longitudinal inertia and axial stress, additional terms are introduced in the coupled equations of motion between the torsion and extension of the rod [BAR 62, NUG 76]. The empirical coefficient introduced in the equations of motion was suggested by Barr so as to satisfy the wave dispersion curve trend at very high frequency.

If the behavior of the rod at very high frequencies is to be accounted for, Saint Venant's warping solution is abandoned for a more sophisticated warping solution with higher elastodynamic modes [ENG 74].

@Seismicisolation

Variational Hamilton's principle		**Variational Love's principle** [LOV 27]
Coupled equations of motion, Engström [ENG 74]		Coupled equations of motion, Nugues [NUG 76]

↓ ↓

One-dimensional differential equations of motion		
Elementary (second-order) equations	Higher approximation (fourth-order) equations	Higher approximation (fourth-order) equations
Warping of the section	Saint Venant's warping theory	Higher warping modes not covered by Saint Venant's theory
Longitudinal inertia neglected	Longitudinal inertia	Longitudinal inertia
Axial stress neglected	Axial stress	Axial stress
No dispersion, Nugues [NUG 76]	Isotropic material, Barr [BAR 62] Anisotropic material [NUG 76]	Isotropic material, Engström [ENG 74] Onobiono [ONO 78]

Figure 5.2. *Dynamic torsion of a rod with rectangular cross-section. The three classes of one-dimensional equations of motion*

The third class of problems concerns torsional wave propagation, see Figure 5.3 [FRA 69, MED 66 MIN 69, MIN 75].

Engström [ENG 74] shows that Barr's theory gives rise to a solution that deviates from the finite element solution at higher frequencies.

@Seismicisolation

FOURTH-ORDER EQUATION OF MOTION	FOURTH-ORDER EQUATION OF MOTION
Isotropic medium Medick [MED 66], Frazer [FRA 69], Mindlin [MIN 75, MIN 69]	Isotropic medium with complementary finite element calculation; infinite length (progressive wave); finite length (stationary wave) Engström [ENG 74]
Cross-section warping; longitudinal inertia; axial stress	
Equation with correction coefficient to satisfy asymptotic behavior at a frequency going to infinity	Anisotropic medium. Use of Reisner variational principle to find an elaborate equation of motion. Touratier [TOU 77, TOU 79] Onobiono [ONO 78]

Figure 5.3. *Torsional wave propagation in a rod with rectangular section. Attention is focused on wave dispersion*

5.1.3. *Extension of equations of motion to a larger frequency range*

In this chapter, one-dimensional equations of motion are adopted instead of three-dimensional ones. This constitutes a simplifying assumption after the reduction of a system of equations with more than one unknown variable in order to obtain an equation with one variable.

The combined influence of static and dynamic effects is presented in Figure 5.2. Are the additional terms introduced in the equations of motion sufficient to correctly portray the behavior of the rod at higher frequencies? To answer to this question, we need to examine dispersion waves.

5.1.3.1. *Dispersion of waves in an infinite length rod*

For the case of dispersion waves in a rod of infinite length, there are no boundary conditions at the tips. Progressive waves are then examined. For a given set of equations of motion, progressive waves are relatively easy to handle and the dispersion curves obtained are without boundary conditions, except at the free lateral rod surface.

@Seismicisolation

5.1.3.2. *Wave dispersion of a rod with finite length*

In practice all waves are of finite length. We have to take two sets of boundary conditions at both tips into account. It is difficult to review all the possible sets of boundary conditions. Engström [ENG 74] and Barr [BAR 62] examined the free-free boundary conditions of rods and compared the corresponding behavior to that of a rod of infinite length. The discrepancy between the two natural frequencies for various vibration modes is taken into account by adopting an appropriate empirical correction coefficient, so as to minimize the root mean square error deviation.

In conclusion, there are two steps for adopting a correction coefficient:

– Mindlin's correcting method;

– improvement of Mindlin's method for a finite length rod with appropriate boundary conditions.

5.2. Static torsion of an anisotropic beam with rectangular section without bending – Saint Venant, Lekhnitskii's formulation

The material in this situation is supposed to be transverse isotropic. The rod axis is supposed to coincide with a symmetry axis of the material, which allows pure torsion of the rod.

Figure 5.4 represents a composite material made of long fibers regularly distributed in the plate thickness. Three rods with rectangular cross-section plane (x,y) can be fabricated from the composite plate. In case 1 (Figure 5.4b), the cross-section is isotropic and the two elastic shear moduli G_{xz} and G_{yz}, are equal:

$$G_{xz} = G_{13} = G_{yz} = G_{23} \qquad [5.1]$$

For cases 2 and 3 (Figures 5.4c and 5.4d), G_{xz} and G_{yz} are different:

$$G_{xz} \neq G_{yz} \qquad [5.2]$$

Depending on the direction of the rod axis with respect to fiber direction, one or two shear moduli are used in forming the rod's torsion problem. For the three rods presented in Figure 5.4, we have to deal with pure torsion. (x, y, z) are coordinates attached to the rod. Axes (1, 2, 3) concern the material and z is the rod axis.

@Seismicisolation

5.2.1. *Airy's function and field of displacement ψ*

One Airy's function ψ is utilized so the stress components σ_{yz} and σ_{xz} are expressed against ψ[3]:

$$\sigma_{xz} = \frac{\partial \psi}{\partial y}, \qquad \sigma_{yz} = -\frac{\partial \psi}{\partial x} \qquad [5.3]$$

Notice that the equilibrium equation in z direction:

$$\frac{\partial \sigma_{xz}}{\partial x} + \frac{\partial \sigma_{yz}}{\partial y} = 0$$

is satisfied if:

$$\frac{\partial \sigma_{zz}}{\partial z} = 0$$

5.2.1.1. *Displacement field*

The choice of displacement field must take the section warping, which is introduced in the displacement field by function φ_w (x, y), into account:

$$\left.\begin{aligned} u &= -\alpha\, z\, y \\ v &= \alpha\, z\, x \\ w &= \alpha\, \phi_w\, (x, y) \end{aligned}\right\} \qquad [5.4]$$

where α is the unitary torsion angle. Oz is the axis of the beam.

---

3 $\vec{\sigma}_z = \text{rot}\, \vec{\psi}$, if $\vec{\sigma}_z = (\sigma_{xz}, \sigma_{yz}, \sigma_{zz})$ and $\vec{\psi} = (0, 0, \psi)$

@Seismicisolation

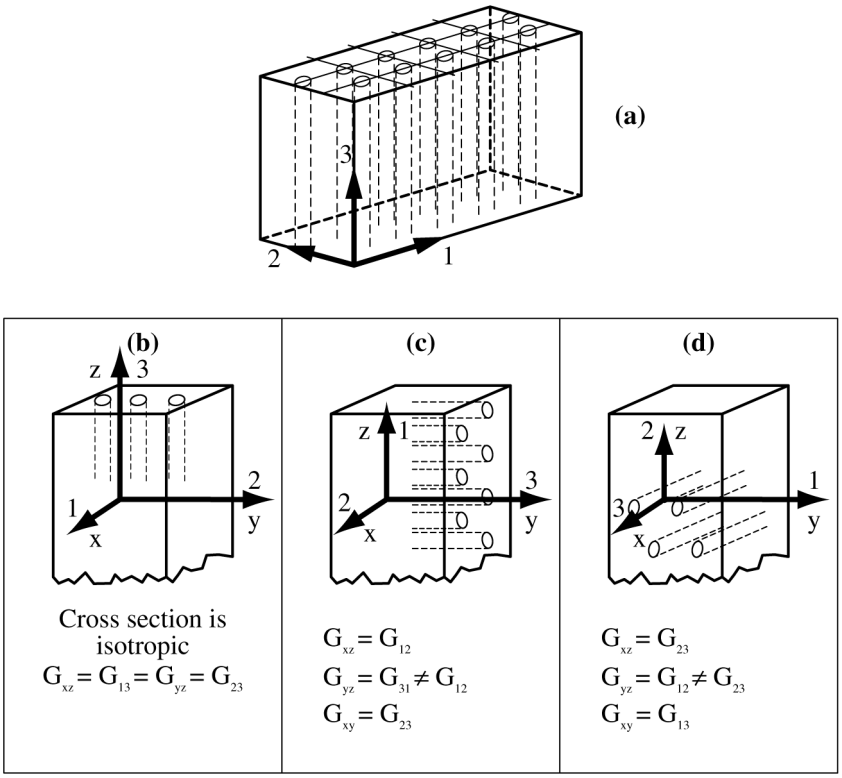

Figure 5.4. *a) Transverse isotropic material made of long fibers regularly distributed throughout the thickness of the plate; b) case 1 – the rod axis is in the same direction as the fibers. The two shear moduli G_{xz} and G_{yz} are equal; c) and d) are case 2 and 3 with G_{xz} and G_{yz}*

5.2.1.2. *Strain expressions*

From equation [5.4], strain components are calculated:

$$\varepsilon_{xx} = \varepsilon_{yy} = \varepsilon_{zz} = \varepsilon_{xy} = 0 \qquad [5.5]$$

$$\gamma_{xz} = \frac{\partial u}{\partial z} + \frac{\partial w}{\partial x} = -\alpha\, y + \alpha\, \phi_{w,x} = \alpha \left(\phi_{w,x} - y \right) \qquad [5.6]$$

@Seismicisolation

The letter after the comma in subscript indicates the derivatives with respect to the corresponding coordinate.

$$\gamma_{yz} = \alpha\,(\phi_{w,y} + x) \qquad [5.7]$$

5.2.1.3. *Constitutive equations*

Shear stress components are evaluated:

$$\sigma_{xz} = G_{xz}\,\gamma_{xz} = \alpha\,G_{xz}\left(\phi_{w,x} - y\right) = \frac{\partial\,\psi}{\partial\,y} \qquad [5.8]$$

$$\sigma_{yz} = G_{yz}\,\gamma_{yz} = \alpha\,G_{yz}\left(\phi_{w,y} + x\right) = -\frac{\partial\,\psi}{\partial\,x} \qquad [5.9]$$

5.2.1.4. *Equation in ϕ_w and ψ*

In [5.8] and [5.9] we have two equations in ψ and ϕ_w. Deriving [5.8] and [5.9] with respect to y and x successively and by subtraction we obtain:

$$\frac{1}{G_{xz}}\,\frac{\partial^2\,\psi}{\partial\,y^2} + \frac{1}{G_{yz}}\,\frac{\partial^2\,\psi}{\partial\,x^2} = -2\,\alpha \qquad [5.10]$$

In a similar manner, it is possible to obtain an equation in ϕ_w:

$$G_{xz}\,\frac{\partial^2\,\phi_w}{\partial\,x^2} + G_{yz}\,\frac{\partial^2\,\phi_w}{\partial\,y^2} = 0 \qquad [5.11]$$

5.2.1.5. *Boundary conditions for ϕ_w and ψ*

For the lateral free boundary, the stress vector $\vec{T}$ is given by:

$$T_i = \sigma_{ij}\,n_j = 0 \qquad \text{on } \mathfrak{D}$$

@Seismicisolation

where $n_1 = n_x$, $n_2 = n_y$ and $n_3 = 0$ are direction cosines of the unit vector normal to the lateral surface generated by the curve $\mathfrak{D}$ in plane (x,y):

$$dx = n_x ds, \qquad dy = n_y ds$$

where ds is the elementary length of curve.

Then for lateral free boundary:

$$T_x = T_{yj} = 0, \quad T_z = n_x \sigma_{xz} + n_y \sigma_{yz} = 0$$

So, on curve $\mathfrak{D}$:

$$n_x G_{xz} \left(\phi_{w,x} - y\right) + n_y G_{yz} \left(\phi_{w,y} + x\right) = n_x \frac{\partial \psi}{\partial y} - n_y \frac{\partial \psi}{\partial x} = 0 \qquad [5.12]$$

The second equation [5.12] states that $\vec{n} = \left(n_x, n_y, 0\right)$ is parallel to $\overrightarrow{\text{grad}}\, \psi$ and then $\psi(x,y) = \text{cste} = 0$ on curve $\mathfrak{D}$:

$$\int_{\mathfrak{D}} \left[G_{xz}\, \alpha \left(\phi_{w,x} - y\right) n_x + G_{yz}\, \alpha \left(\phi_{w,y} + x\right) n_y\right] ds = 0 \qquad [5.13]$$

concerns the overall free lateral boundary.

5.2.2. *Solution of equation [5.10] with Airy's function*

If a closed-form expression is found for ψ, torsion moment M_T and stiffness C_T can be evaluated. The variable separation method is used in what follows:

$$\psi = \sum_{k=1,3,5} Y_k\,(y) \cos \frac{k \pi x}{b} \qquad [5.14]$$

where b and h are width and thickness of the rod section respectively.

Choosing equation [5.14], ψ is automatically zero on the lateral frontier of the section; see Figure 5.5. Bringing [5.14] into [5.10]:

@Seismicisolation

$$\sum_{k=1,3,5}\left[\frac{Y''_k}{G_{xz}} - \frac{k^2\,\pi^2}{b^2\,G_{yz}}\,Y_k\right]\cos\frac{k\,\pi\,x}{b} = \varsigma(\alpha) \qquad [5.15]$$

where $\varsigma(\alpha)$ is the even 2b-periodic function of x defined as following:

$$\varsigma(\alpha) = \begin{cases} -2\alpha & \text{if } -b/2 < x < b/2 \\ 2\alpha & \text{if } -b < x < -b/2 \text{ or } b/2 < x < b \end{cases}$$

The two double primes in superscript (″) indicate the second derivative with respect to the y coordinate. Developing $\varsigma(\alpha)$ in Fourier series[4] equation [5.15] is rewritten as:

$$\frac{Y''_k}{G_{xz}} - \frac{k^2\,\pi^2}{b^2\,G_{yz}}\,Y_k = -\frac{4\,\alpha}{k\,\pi}(-1)^{\frac{k-1}{2}} \quad k = 1, 3, 5,..... \qquad [5.16]$$

A partial solution Y_k is to be obtained and then summation effected for the final solution of ψ. Let us introduce the following parameter μ:

$$\mu^2 = \frac{G_{xz}}{G_{yz}} \qquad [5.17]$$

Taking equation [5.16] into account, [5.17] is rewritten:

$$Y''_k - \frac{k^2\,\pi^2}{b^2}\,\mu^2\,Y_k = \frac{-4\,\alpha\,G_{xz}}{k\,\pi}\,(-1)^{\frac{k-1}{2}} \quad k = 1, 3, 5,.... \qquad [5.18]$$

Partial solution Y_k of [5.18] is to be obtained. The minus sign in the first member of [5.18] shows that a linear combination of hyperbolic function sin h ( )

---

4 $\varsigma(\alpha) = \sum_{k=0}^{\infty}\frac{-4\,\alpha}{k\,\pi}\sin\frac{k\,\pi}{2}\cos\frac{k\,\pi\,x}{b} = \sum_{k=1,3,5}\frac{-4\,\alpha}{k\,\pi}(-1)^{\frac{k-1}{2}}\cos\frac{k\,\pi\,x}{b}$

@Seismicisolation

and cos h ( ) is suitable for the solution of this equation and then summation effected for the final solution of ψ :

$$\psi = \sum_{k=1,3,5..} \left[A \sinh \frac{k \pi \mu y}{b} + B \cosh \frac{k \pi \mu y}{b} + \frac{4 \alpha b^2}{k^3 \pi^3} G_{yz} (-1)^{\frac{k-1}{2}} \right] \quad [5.19]$$

with k being an odd number.

Taking the boundary condition into account in equation [5.19], coefficient A must be zero, Y being an even function. Finally the following expression is obtained:

$$\boxed{\psi(x,y) = \frac{4 \alpha G_{yz}}{\pi^3} b^2 \sum_{k=1,3,5,....} \frac{(-1)^{\frac{k-1}{2}}}{k^3} \left(1 - \frac{\cosh \frac{k \pi \mu y}{b}}{\cosh \frac{k \pi \mu h}{2b}} \right) \cos \frac{k \pi x}{b}}$$

[5.20]

where ψ in equation [5.20] contains $\frac{1}{k^3}$ in the second member, so the series is quickly convergent and some first terms in the series are sufficient for practical application.

5.2.3. *Expressions of torsion moment M_t versus torsion angle α and stiffness C_T*

The resultant torsion momentum is defined by the following equation (see Figure 5.2):

$$\vec{\mathfrak{M}}_T = \iint_S \vec{OP} \wedge \vec{T} \, dx \, dy = (0, 0, M_T)$$

where S is the area of the beam's section bounded by curve $\mathfrak{D}$ and $\vec{T}$ the stress vector. By definition, with C_T being the torsion stiffness, we have:

$$M_t = C_T \alpha \quad [5.21]$$

@Seismicisolation

Expressing the first member of [5.21] *versus* the Airy's function from which stresses σ_{xz} and σ_{yz} are derived from [5.8] and [5.9]:

$$M_T = \iint_{\mathcal{S}} \left(x\,\sigma_{yz} - y\,\sigma_{xz} \right) dx\,dy = -\iint_{\mathcal{S}} \left(x\frac{\partial \psi}{\partial x} + y\frac{\partial \psi}{\partial y} \right) d\,x\,d\,y \qquad [5.22]$$

The divergence theorem applied to [5.22], on the $\psi\,(x,y) = 0$ boundary $\mathcal{D}$, shows that[5]:

$$M_T = 2\iint_{\mathcal{S}} \psi\,dx\,dy = C_T \alpha \qquad [5.23]$$

Introducing equation [5.20] into [5.23], we obtain the torsional stiffness:

$$C_T = \frac{8\,G_{yz}\,b^2}{\pi^3} \sum_{k=1,3,5,\ldots} \frac{(-1)^{\frac{k-1}{2}}}{k^3} \iint_{\mathcal{D}} \cos\frac{k\,\pi\,x}{b} \left(1 - \frac{\cos h\,\frac{k\,\pi\,\mu\,y}{b}}{\cos h\,\frac{k\,\pi\,\mu\,h}{2\,b}} \right) dx\,dy \qquad [5.24]$$

$\mathcal{S}$ designates the section whose dimensions are given in Figure 5.5.

Integration of [5.24], taking into account [5.20], gives:

$$C_T = \frac{32\,G_{yz}}{\pi^4}\,b^3\,h \sum_{k=1,3,5,\ldots} \frac{1}{k^4} \left(1 - \frac{2\,b}{k\,\pi\,\mu}\,\text{tangh}\,\frac{k\,\pi\,\mu\,h}{2\,b} \right) \qquad [5.25]$$

For a more condensed expression, μ being the ratio in equation [5.17], we suggest adopting:

---

5 If $\vec{V}(x, y)$ is a vector of plane (x, y): $\iint_{\mathcal{D}} \text{div}\,\vec{V}\,dx\,dy = \int_{\mathcal{D}} \vec{V} \cdot \vec{n}\,ds$ where $\vec{n}$ is the unit normal vector of boundary $\mathcal{D}$ of the section $\mathcal{S}$,

$$\Rightarrow -\iint_{\mathcal{S}} \left(x\frac{\partial \psi}{\partial x} + y\frac{\partial \psi}{\partial y} \right) d\,x\,d\,y = \iint_{\mathcal{D}} 2\,\psi\,d\,x\,d\,y + \int_{\mathcal{D}} \left(x\,n_x + y\,n_y \right) \psi\,ds$$

@Seismicisolation

$$c = \frac{\mu \text{ h (thickness)}}{\text{b (width)}} = \frac{h}{b}\sqrt{\frac{G_{xz}}{G_{yz}}} \qquad [5.26]$$

which includes the flatness ratio $\delta = b/h$ of the section. C_T is rewritten as:

$$C_T = G_{yz}\ h\, b^3\ \beta_T\ (c) = G_{xz}\ b\, h^3\ \beta_T\ (1/c) \qquad [5.27]$$

with

$$\beta_T(c) = \frac{32}{\pi^4} \sum_{k=1,3,5,\ldots} \frac{1}{k^4}\left(1 - \frac{2}{k\,\pi\,c}\ \text{tang h}\ (k\,\pi\,c/2)\right) \qquad [5.28]$$

In [5.28] the sum of the series with odd terms can be written as:

$$\sum_{k=1,3,5} \frac{1}{k^4} = \frac{\pi^4}{96} \quad \text{then} \quad \sum_{k=1,3,5} \frac{32}{\pi^4\ k^4} = \frac{32}{\pi^4}\ \frac{\pi^4}{96} = \frac{1}{3} \qquad [5.29]$$

So equation [5.28] is simplified as follows:

$$C_T = G_{yz}\ h\, b^3\ \beta_T\ (c) = G_{xz}\ c^2\, b\, h^3\ \beta_T\ (c)$$

in which [5.30]

$$\beta_T(c) = \left[\frac{1}{3} - \frac{64}{c\,\pi^5} \sum_{k=1,3,5,\ldots} \frac{1}{k^5}\ \text{tang h}\left(\frac{k\,\pi\,c}{2}\right)\right]$$

Numerical values of series $\beta_T(c)$ and curves β_T versus ratio c are explained in detail in Appendix 5.A. The reader should notice that for an isotropic or transverse isotropic rod (with a section considered as isotropic):

$$G_{xz} = G_{yz} = G \qquad [5.31]$$

and c is reduced to the ratio b/h in equation [5.25].

@Seismicisolation

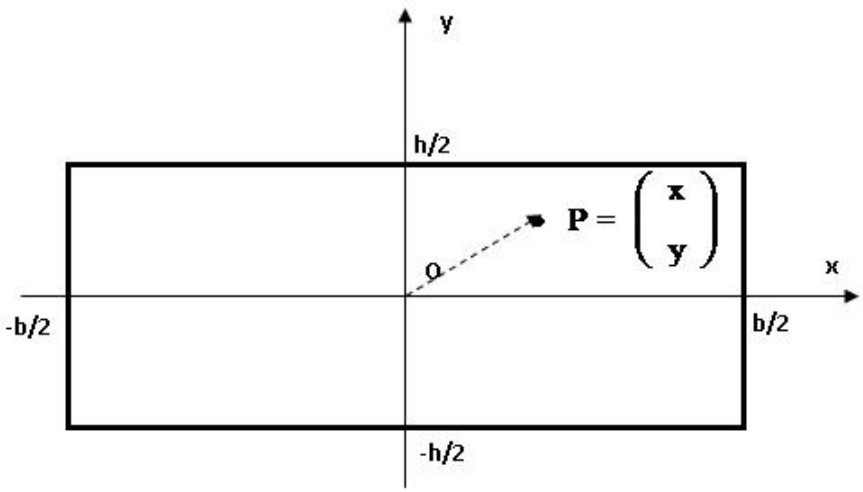

Figure 5.5. *Rectangular rod section*

5.2.4. *Approximate formulae for M_T and C_T*

We have shown above that the torsion problem of a rectangular anisotropic rod with two equal shear moduli in equation [5.31] can be solved by a hyperbolic function series, as in [5.30], which is quickly convergent. Equation [5.30] is convenient for practical applications. Approximate methods are presented with various formulae in Appendix 5.A.

5.2.5. *Dynamic torsion of a rod with rectangular section using the elementary equation of motion*

Now we will successively examine the elementary equation of motion, and the more elaborate one suggested by Barr [BAR 62] and Engström [ENG 74], taking longitudinal inertia effect into account.

5.2.5.1. *Elementary theory*

The equation of motion is obtained by writing the equilibrium in an element of the rod:

$$\left(M_T + \frac{\partial M_T}{\partial z} dz - M_T \right) S = \rho S I_p \frac{\partial^2 \theta}{\partial t^2} dz$$

@Seismicisolation

$$\frac{\partial M_T}{\partial z} = \rho I_p \frac{\partial^2 \theta}{\partial t^2} \qquad [5.32]$$

Torsion moment is related to torsion angle α:

$$M_T = C_T \frac{\partial \theta}{\partial z} \qquad [5.33]$$

In which $\frac{\partial \theta}{\partial z}$ is the unitary torsion angle (see [5.21], $\theta = \alpha z$). Bringing equation [5.33] into [5.32]:

$$C_T \frac{\partial^2 \theta}{\partial z^2} = \rho I_p \frac{\partial^2 \theta}{\partial t^2} \qquad [5.34]$$

where ρ is the mass density.

I_p is the polar surface inertia parameter with respect to z axis.

$$I_p = \int_D \left(x^2 + y^2\right) d x \, d y \qquad [5.35]$$

Phase velocity is obtained by adopting a progressive wave solution in the form:

$$\theta\left(z, t\right) = \exp j \left(\omega t - k z\right) \qquad [5.36]$$

$$\rho I_p \omega^2 = C_T k^2$$

and the phase velocity is frequency independent:

$$v_p = \frac{\omega}{k} = \sqrt{\frac{C_T}{\rho I_p}} \qquad [5.37]$$

@Seismicisolation

5.2.5.2. *Boundary conditions*

The lateral boundary conditions concern the free surface. The two ends of the rod can be submitted to various boundary conditions that depend on the type of rod excitation and transducers adopted for measuring the torsion angle.

One of the experimental set-ups adopted is represented in Figure 5.6. The sample is clamped in the middle between two rigid circular cylinders. It is submitted to forced vibration by application of a torsion couple, for reasons of convenience, to obtain equal vibrations at the rod tips. A greater vibration amplitude is easily obtained at the free ends.

A closed-form solution for rod vibration is obtained:

$$\theta\left(z, t\right) = \exp\left(j\,\omega\,t\right)\left[A\cos\frac{\zeta\,z}{L} + B\sin\frac{\zeta\,z}{L}\right] \qquad [5.38]$$

in which the wave number ζ is defined by the following equation:

For z = 0:

$$\alpha = (0, t) = 0$$

then A = 0.

For z = L:

$$\frac{\zeta^2}{L^2} = \frac{\rho\,I_p\,\omega^2}{C_T} \qquad [5.39]$$

For z = 0

$$\theta\,(0, t) = 0$$

then A = 0.

For z = L

@Seismicisolation

From equation [5.39] we obtain:

$$J_a \frac{\partial^2 \theta}{\partial t^2}(L, t) = -M_T(L, t) = -C_T \frac{\partial \theta}{\partial z} \qquad [5.40]$$

J_p is the additional torsion inertia at z = L.

5.2.5.3. *Simplifying eigenvalue equation [5.40]*

$$M_t = C_T \exp(j\omega t) \frac{B\zeta}{L} \cos\zeta = J_a \omega^2 B \exp(j\omega t) \sin\zeta \qquad [5.41]$$

J_a is the additional torsion inertia at z = L.

Eliminating ω^2 by using [5.39], we get:

$$C_T \frac{\zeta}{L} \cos\zeta = J_a \omega^2 \sin\zeta \qquad [5.42]$$

$$\boxed{\zeta \operatorname{tg}\zeta = \frac{I}{J_a} = \gamma} \qquad [5.43]$$

REMARK: In Chapter 2 of another book[6], we give details of the so called pseudo-clamping adopted in Figure 5.6, which presents some advantages with respect to classical clamping whose disadvantages are accounted for in the design of a sample with attachments.

In equation [5.43] the first member is the ratio of the inertia of half the sample $I = \rho L I_p$ of length L to the additional torsion inertia J_a at the end. Let γ be this ratio:

$$\gamma = \frac{I}{J_a} \qquad [5.44]$$

6 *Mechanical Characterization of Materials and Wave Dispersion*

@Seismicisolation

To obtain a large vibration of the rod, a larger J_a is chosen compared to rod inertia ρ L I_p:

$$\gamma << 1$$

In this case, a limited expansion of the series tan ζ *versus* ζ is adopted:

$$\text{tg}\,\zeta \approx \zeta + \frac{\zeta^3}{3} \qquad [5.45]$$

then the torsion stiffness C_T (equation [5.42]) is:

$$C_T = L\,J_a\,\omega^2\,\frac{\text{tg}\,\zeta}{\zeta}$$

$$C_T \cong L\,J_a\,\omega^2\left(1 + \frac{\zeta^2}{3}\right) \qquad [5.46]$$

Taking into account [5.43], $\zeta^2 = \gamma$:

$$C_T \cong L\,J_a\,\omega^2\left(1 + \frac{\gamma}{3}\right) \qquad [5.47]$$

Approximate equation [5.47] is only valid for the first mode of vibration. Equation [5.43] has a multiplicity or roots that consequently need to be calculated for higher modes.

However, this attempt may be controversial, because for a higher mode of vibration the elementary equation of motion may not be applicable. We now have to take longitudinal inertia effect into account.

If J_a is chosen smaller compared to rod inertia $I = \rho\,L\,I_p$, then:

@Seismicisolation

$$\gamma >> 1 \text{ tg } \zeta \cong \infty \Rightarrow \zeta_k \cong (2k - 1)\pi / 2 \quad k= 1, 2, 3,.....$$

This equation is valid for every mode of vibration.

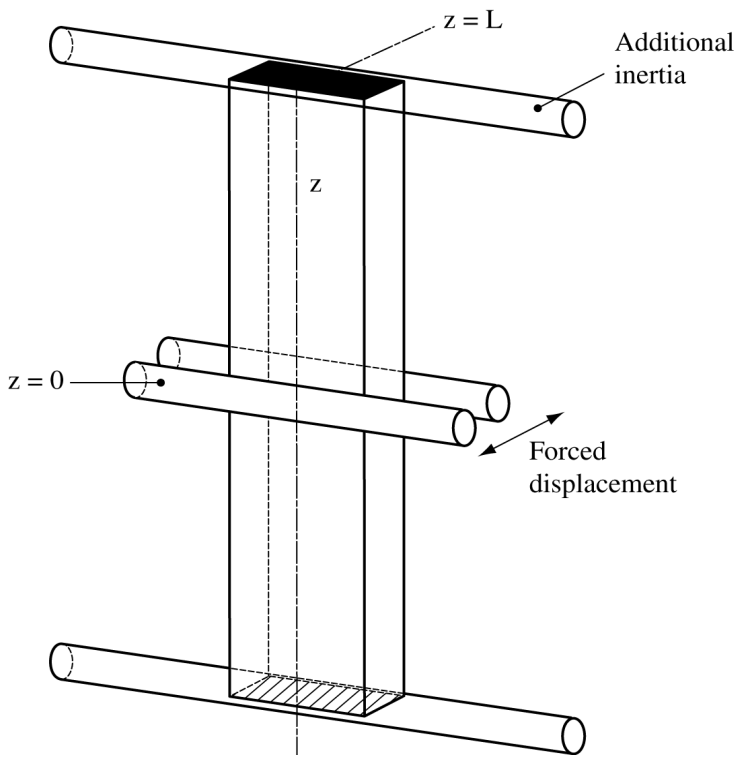

Figure 5.6. *One possible experimental set-up. Torsion is obtained in the middle of the sample, which is attached between two circular cylinders. At the free ends, two short cylinders are used as additional inertias$_a$. For drawing convenience, length is not respected*

5.2.6. *Pure dynamic torsion of a rod with rectangular cross-section using first-degree approximation*

In equation [5.4] the axial displacement is expressed as the product of two functions: the warping function ϕ_w (x , y) in Saint Venant's theory; and ζ (z, t).

@Seismicisolation

5.2.6.1. *Displacement field*[7]

$$u(z,t) = -\theta(z,t)\, y$$

$$v(z,t) = \theta(z,t)\, x$$

$$w(z,t) = \xi(z,t)\, \phi_w(x,y) \qquad [5.48]$$

where ζ (z, t) replaces the unit torsion angle α in [5.4]. We then have two functions θ (z , t) and ζ (z , t) to evaluate instead of one θ (z , t). $\phi_w(x,y)$ is the warping function, which is supposed to be identical to that of static torsion presented in [5.4].

5.2.6.2. *Equations of motion deduced from Hamilton's variational principle*

In Appendix 5.B details of Hamilton's variational principle calculations are presented. The two Euler equations are obtained:

$$\boxed{\begin{aligned} &\frac{P_1}{S_{33}}\frac{\partial^2\xi}{\partial z^2} - \rho P_1 \frac{\partial^2 \xi}{\partial t^2} - K_a\, \xi - K_a \frac{\partial \theta}{\partial z} = 0 \\ &-\rho I_p \frac{\partial^2\theta}{\partial t^2} + I_a \frac{\partial^2\theta}{\partial z^2} - K_a \frac{\partial \xi}{\partial z} = m \end{aligned}} \qquad [5.49]$$

where m designates distributed torque on the rod.

Coefficients in [5.49] are expressed in terms of warping function ϕ_w [5.11] and [5.12]. Coordinates x and y can be found in equation [5.B.10], Appendix 5.B [5.B.12] and [5.B.13] where the natural boundary conditions are:

7 The projection of the cross-section rotates rigidly in its plane. This is the simplifying assumption in the framework of Saint-Venant's theory. m designates distributed torque on the rod.

@Seismicisolation

$\frac{d\,\xi}{d\,z} = 0$ corresponds to zero warping stress.

$\delta\,\xi = 0$ concerns zero warping displacement.

Free	$\frac{\partial \xi}{\partial z} = 0$ for z = 0, L **Free end, zero warping stress**	or →	$\delta\,\xi = 0$ for z = 0, L **Zero warping displacement**	Clamped
Forced	$-K_a\,\xi + I_a\,\frac{\partial \theta}{\partial z} = T$ for z = 0, L **Prescribed torque**	or →	$\delta\,\theta = 0$ For z = 0, L **Clamping end**	Free

Table 5.1. *Four possible natural boundary conditions*

In the second line of Table 5.1, T is the prescribed torque at the end section or prescribed zero rotation. Equations [5.49] can be decoupled so as to obtain just one variable, θ or ξ, by substitution:

$$\left(\rho^2\,\frac{P_1\,I_p}{K_a}\right)\frac{\partial^4\theta}{\partial\,t^4} + \left(\frac{P_1\,I_a}{s_{33}\,K_a}\right)\frac{\partial^4\theta}{\partial\,z^4} - \left[\frac{\rho\,P_1\,I_p}{s_{33}\,K_a} + \frac{\rho\,P_1\,I_a}{K_a}\right]\frac{\partial^4\theta}{\partial\,z^2\,\partial\,t^2}$$

@Seismicisolation

$$+ \rho I_p \frac{\partial^2 \theta}{\partial t^2} - (I_a - K_a) \frac{\partial^2 \theta}{\partial z^2} = 0 \qquad [5.50]$$

Equation [5.50] is valid for zero distributed torque, m = 0. When the distributed torque m exist the second member of equation [5.50] is:

$$\frac{P_1}{K_a} \left(\rho \frac{\partial^2 m}{\partial t^2} - \frac{1}{S_{33}} \frac{\partial^2 m}{\partial z^2} \right)$$

In equation [5.50], we recognize that the two last terms are from the equation of motion in elementary Saint Venant's theory, in which $(I_a - K_a) = C_T$. This equality is demonstrated at the end of Appendix 5.B.5. The third term is called the longitudinal inertia term by Barr [BAR 62]. The two first components correspond to axial stress correcting terms.

We notice that the higher approximation equations [5.49] and [5.50] are of fourth order instead of second order in elementary theory, see equation [5.34]. This is the consequence of coupling of torsion motion (second order) and extensional axial motion (second order).

If we examine Table 5.1 again, we notice that there are four possible natural boundary conditions. Consequently, this matches the degree of equations of motion [5.50]. In Appendix 5.C Barr's correcting coefficient is introduced in equations of motion to better satisfy the dynamic behavior of rod waves at very high frequency.

5.2.6.3. *Asymptotic behavior of phase velocity at frequencies from zero to infinity*

To obtain quantitative information in such domains, three-dimensional finite element calculations need to be referred to. Engström [ENG 74] has presented such studies that were completed by experiments on rods of various lengths by Barr [BAR 62] for isotropic material.

For anisotropic material, to our knowledge, Touratier [TOU 79] was the first to use the Reissner variational principle with mixed fields of stress and displacement.

@Seismicisolation

Closed-form calculations are troublesome but convincing (see Chapter 15 of our other book[8]).

Returning to the one-dimensional equations of motion adopted in this chapter, we indicate trends of this behavior only. The difficulty of this problem resides in the presence of a great number of parameters that need to be taken into account. In Appendix 5.B we present the equations of motion [5.B.9] and parameters [5.B.10]. Warping function ϕ_w needs to be evaluated as well as various inertia moments in which the flatness ratio of the section is defined as:

$$\delta = \frac{\text{width}}{\text{thickness}} = \frac{b}{h} \qquad [5.51]$$

Using decoupled equation [5.50], the study is restrained to the first mode of warping. For higher modes, Helmholtz equations need to be written for anisotropic materials and the corresponding solutions of warping are outside the fields of application of Saint Venant's method. Figure 5.7 represents some possible warping functions at higher modes.

Figure 5.8 represents the trend of wave dispersion curves. The shear wave phase velocity is given by:

$$v_T = \sqrt{\frac{1}{\rho\, I_p}\left(\frac{I_1}{s_{44}} + \frac{I_2}{s_{55}}\right)} \qquad [5.52]$$

in which:

$$I_1 = \iint_S x^2\, dx\, dy\,, \quad I_2 = \iint_S y^2\, dx\, dy\,,$$

$$I_p = I_1 + I_2 = \iint_S \left(x^2 + y^2\right) dx\, dy$$

where ρ is material mass density.

8 *Mechanical Characterization of Materials and Wave Dispersion*

@Seismicisolation

The upper bound of torsional phase velocity is the Rayleigh surface wave v_R, which is lower than v_T torsion velocity, presented above. The lower bound (frequency going to zero) is strongly dependent on the flatness s_f equation [5.51]. One of the most interesting points is that the square section of the rod corresponds for the first elastodynamic mode and to the absence of wave dispersion.

5.3. Torsional vibration of a rod with finite length

We have examined warping function in detail in the framework of Saint Venant's theory. We will now focus our attention on torsional vibration of a rod with rectangular section. For dynamic torsion tests, the finite length of the rod gives rise to stationary waves.

We have the decoupled equation of motion [5.50]. Let us now mention the boundary conditions we adopt in the test[9].

In Figure 5.6, two additional inertias are added to the sample at both tips[10].

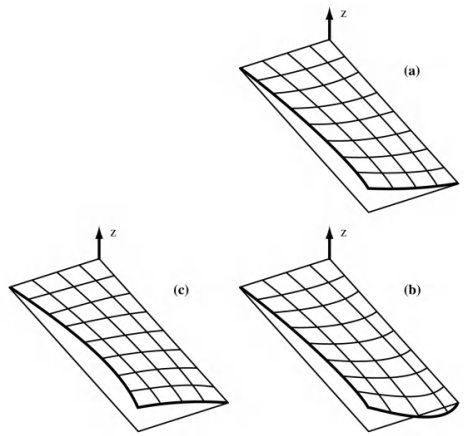

Figure 5.7. *a) Graphical representation of Saint Venant's warping function ϕ_w;*
b) first mode for warping function that is not deduced from Saint Venant's theory;
c) second mode of warping function ϕ_w that differs from Saint Venant's warping function.
One quarter of the section only is represented

9 In the second part of *Mechanical Characterization of Materials and Wave Dispersion,* which is devoted to experimental works, another kind of boundary conditions will be adopted.
10 In *Mechanical Characterization of Materials and Wave Dispersion* other kinds of boundary conditions are adopted in Chapter 15.

@Seismicisolation

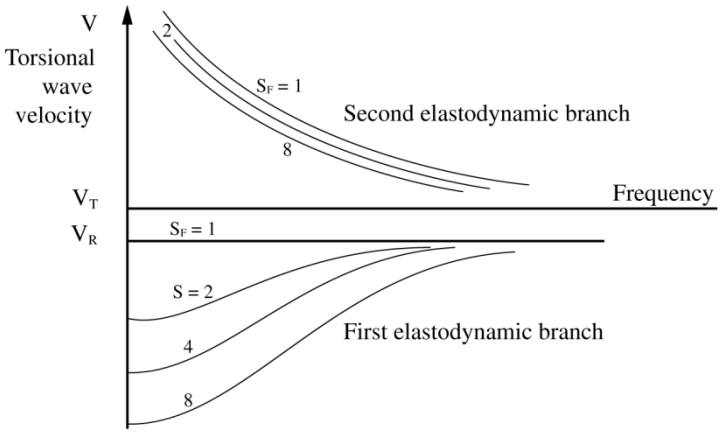

Figure 5.8. *Trend of wave dispersion curves. Parameter s = b (width)/h (thickness) is the flatness ratio. Two elastodynamic branches are represented*

The corresponding natural boundary conditions are in equation [5.B.13], Appendix 5.B, rewritten here:

$$T = I_a \frac{\partial \theta}{\partial z} - \xi K_a \qquad [5.53]$$

K_a and I_a coefficients of the equation of motion are given in equation [5.B.13], torque at the tips. T is the prescribed torque at the end section.

5.3.1. *Closed-form solution of θ (z, t)*

Equations of motion [5.50] associated with [5.53] have a harmonic solution:

$$\theta(z, t) = \Theta(z) \exp j\omega t \qquad [5.54]$$

where ω is the circular frequency. Equation [5.49] is the fourth-order differential equation. Function Θ (z) can be represented by a combination of exponentials with real or imaginary exponents:

@Seismicisolation

$$\theta\ (z\,,t) = \exp\left(\frac{\beta\, z}{L}\right) \exp\ (j\ \omega\, t) \qquad [5.55]$$

and L is the half length of the sample.

Bringing equation [5.55] into [5.50] we obtain:

$$\left(\frac{\rho^2\ P_1\ I_p}{K_a}\right)\omega^4 + \left(\frac{P_1\ I_a}{s_{33}\ K_a}\right)\frac{\beta^4}{L^4} + \left(\frac{\rho\ P_1 I_p}{s_{33}\ K_a} + \frac{\rho\ P_1\ I_a}{K_a}\right)\omega^2\,\frac{\beta^2}{L^2}$$
$$-\rho\ I_p\ \omega^2 - (I_a - K_a)\frac{\beta^2}{L^2} = 0 \qquad [5.56]$$

Let us rearrange equation [5.56] as an equation in ascending powers of β:

$$\left(\frac{P_1\ I_a}{s_{33}\ K_a\ L^4}\right)\beta^4 + \left[\left(\frac{\rho\ P_1\ I_p}{s_{33}\ K_a} + \frac{\rho\ P_1\ I_a}{K_a}\right)\frac{\omega^2}{L^2} - \frac{(I_a - K_a)}{L^2}\right]\beta^2$$
$$-\rho\ I_p\ \omega^2 + \left(\frac{\rho^2\ P_1\ I_p}{K_a}\right)\omega^4 = 0 \qquad [5.57]$$

It is convenient to adopt the following dimensionless parameters:

$$v_1 = \frac{\rho\ I_p\ \omega^2\ L^2}{C_T}\,,\ v_2 = \frac{P_1}{I_p\ L^2} \qquad [5.58]$$

$$v_3 = \frac{I_p\ \omega^2}{s_{33}\ C_T}\,,\ v_4 = \frac{I_a}{C_T}$$

C_T is the torsion rigidity relating torque to angle. It is equal to:

$$C_T = (I_a - K_a) \qquad [5.59]$$

@Seismicisolation

This equality is demonstrated in Appendix 5.B, equations [5.B.18] to [5.B.20]. Equation [5.57] is is multiplied by L^2/C_T and then rewritten with new notations in [5.58].

$$\frac{v_2\, v_3\, v_4}{v_4 - 1}\ \beta^4 + \left[\frac{v_1 v_2}{v_4 - 1}\left(v_3 + v_4\right) - 1\right]\ \beta^2 + \frac{v_1^2\ v_2}{v_4 - 1} - v_1 = 0 \qquad [5.60]$$

Equation [5.60] is rearranged in relation [5.61]:

$$\beta^4 - \left[\frac{v_4 - 1}{v_2 v_3 v_4} - \frac{v_1 v_2 (v_3 + v_4)}{v_2 v_3 v_4}\right]\beta^2 - v_1\left[\frac{v_4 - 1}{v_2 v_3 v_4} - v_1 \frac{v_2}{v_2 v_3 v_4}\right] = 0 \qquad [5.61]$$

In this bisquared equation, the sum of the roots is positive in β and their product is negative.

The solution for Θ (z) in equation [5.54] can be written as:

$$\Theta\ (z) = A_a\ \cos h\ \frac{\beta_1\ z}{L} + B_a\ \sin h\ \frac{\beta_1\ z}{L} + C_a\ \cos\ \frac{\beta_2\ z}{L} + D_a\ \sin\ \frac{\beta_2\ z}{L} \qquad [5.62]$$

A_a, B_a, C_a and D_a the set of coefficients is to be evaluated by the four boundary conditions, two at each end.

5.3.2. *Evaluation of spatial solution* $\Theta\ (z)$

Figure 5.6 represents displacement in the middle (z = 0).

The forced motion of the rod is symmetrical with respect to z = 0. We only consider the half of the sample at z = 0 and z = L, the length of the rod being 2 L.

The boundary conditions are:

– For z = 0, at the middle of the sample, there is no axial displacement. If we refer to Table 5.1 and the displacement field in equation [5.48] we must have:

@Seismicisolation

$$\delta \xi = 0 \qquad [5.63]$$

– The second boundary condition in the middle of the sample is a prescribed external torque that permits rotation of the rod around its axis z:

$$J_m \frac{\partial^2 \theta}{\partial t^2} = 2 \left[I_a \frac{\partial \theta}{\partial z} - K_a \xi \right] \qquad [5.64]$$

where J_m is the mandrel polar inertia. Coefficient 2 can be explained by the adoption of excitation in the middle of the sample. The reaction of the sample takes both its parts into account.

For $z = \pm L$, there is no warping stress at either end:

$$\frac{\partial \xi}{\partial z} = 0 \qquad [5.65]$$

The second boundary condition concerns the additional lever inertia, which corresponds to prescribed torque:

$$- J_a \frac{\partial^2 \theta}{\partial^2} = I_a \frac{\partial \theta}{\partial z} - K_a \xi \qquad [5.66]$$

5.3.3. *Evaluation of coefficients* $\theta(z, t)$ *and* $\zeta(z, t)$

The boundary conditions presented above include $\theta(z, t)$ and also the second variable ξ. Equation [5.48] is the displacement field that permits us to adopt a higher approximation for equations of motion. Consequently it is necessary to express $\zeta(z, t)$ as follows:

$$\xi(z, t) = Z(z) \exp j \omega t \qquad [5.67]$$

$$Z(z) = A_b \cos h \frac{\beta_1 z}{L} + B_b \sin h \frac{\beta_1 z}{L} + C_b \cos \frac{\beta_2 z}{L} + D_b \sin \frac{\beta_2 z}{L} \qquad [5.68]$$

@Seismicisolation

As the decoupled equation of motion for $\theta\,(z\,,t)$ and $\xi\,(z\,,t)$ is the same, we must have the same roots for β as in [5.60] and [5.61]. However, the set of coefficients A_b, B_b, C_b and D_b for Z (z, t) in equation [5.68] are different from the coefficient set A_a, B_a, C_a and D_a for Θ (z) in [5.61].

The second equation of motion in [5.49] is retained and rewritten here. It will serve to evaluate the coefficients in [5.68]:

$$-\rho\, I_p \frac{\partial^2 \theta}{\partial t^2} + I_a \frac{\partial^2 \theta}{\partial t^2} - K_a \frac{\partial \xi}{\partial z} = 0 \qquad [5.69]$$

For m = 0 there is no distributed torque on the sample. We have eight coefficients in equations [5.62] and [5.68] to evaluate coefficients and we only have four boundary conditions. The problem is not, however, undetermined. In Appendix 5.D we show that there are four additional equations relating the two sets of coefficients in [5.62] and [5.66].

5.4. Simplified boundary conditions associated with higher approximation equations of motion [5.49]

In section 5.3 we present a complete solution to the forced torsional motion of a rod in an experimental set up. Equations [5.D.9] to [5.D.11] in Appendix 5.D give details of the eigenvalue calculation.

In *Mechanical Characterization of Materials and Wave Dispersion*, practical details of the required apparatus will be given. Here we will just provide some remarks. The inertia of the mandrel in the middle of the apparatus, as well as additional inertias fixed at the free ends, give rise to two boundary conditions among the four conditions and complicate the search for a practical, tractable solution. It is possible to find a simpler solution by taking some additional points on board. If the inertia of the mandrel (associated with connection to an electric exciter) is large compared to the inertia and we can adopt the following boundary conditions:

$$\text{For } z = 0 \quad \text{or} \quad \begin{cases} \xi = 0 \\ \theta = 0 \end{cases} \qquad [5.70]$$

This corresponds to the clamping end in Figure 5.6.

@Seismicisolation

$$\text{For } z = L \qquad \left.\begin{aligned} \frac{d\,\xi}{d\,z} &= 0 \\ -J\,\frac{\partial^2\,\theta}{\partial t^2} &= J_a\,\frac{\partial\,\theta}{\partial\,z} - K_a\,\xi \end{aligned}\right\} \qquad [5.71]$$

Appendix 5.E gives details of calculations that are simpler than those presented in Appendix 5.D.

5.5. Higher approximation equations of motion

In many circumstances when we have to deal with the measurements of shear moduli of materials, the available sample length is short. This is the case with bones or high-cost composites, such as three-dimensional carbon-carbon composites.

5.5.1. *Slenderness*

This corresponds to the case of low slenderness of a thick sample, defined as the ratio of length to the largest dimension of the section (where L is half length, b width and h thickness):

$$s_d = \frac{L}{(b \text{ or } h)}$$

5.5.2. *Ratio E/G_{ij}*

The second set of parameters to take into account is the ratio of Young's modulus to the largest shear modulus of the composite material (G_{ij}). E/G_{ij} is an important parameter in the formulation of equations of motion. For an isotropic material this ratio is known as:

$$E/G_{ij} = 2\,(1 + \nu) \approx 2.6 \qquad [5.72]$$

where ν is the Poisson's number, which is less than 0.3. For some composite materials, the ratio E/G_{ij} can reach larger values (in the order of 50 for Kevlar). This coefficient in some terms of [5.57] and [5.61] may have a strong influence on the dispersion of shear wave velocity *versus* frequency.

@Seismicisolation

In Appendix 5.E, equations [5.E.5] and [5.E.6] for a higher approximation and in elementary theory respectively show that the value β_2 is not the same. For higher modes the discrepancy may be important. In Figure 5.9, curve representing the ratio:

$$\frac{\left(v_1 = \beta^2_{ha}\right)}{\beta^2_{sv}} \textit{ versus } \text{the rank of the vibration mode} \qquad [5.73]$$

β^2_{ha} corresponds to a higher approximation and β^2_{sv} is evaluated by elementary Saint Venant's theory. The parameter E_{33}/G_{13} attached to each curve corresponds to a specified material. We notice here that the discrepancy can be important.

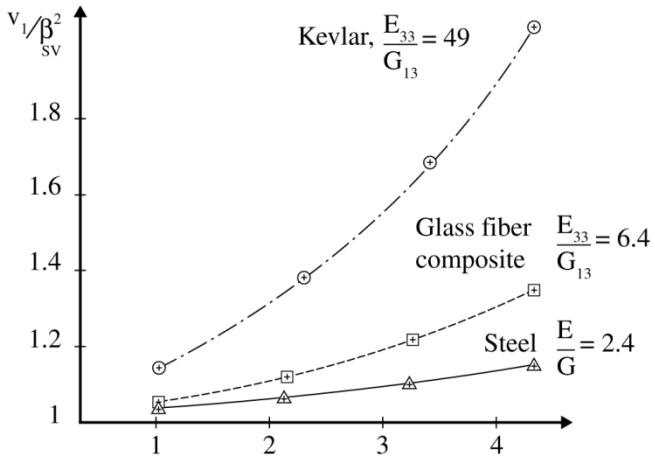

Figure 5.9. *Influence of wave dispersion on eigenfrequencies obtained by Saint Venant's theory. β^2_{sv} and $v_1 = \beta^2_{ha}$ are obtained by higher approximation. The discrepancy between the two values is described by their ratio, represented in ordinate $v_1 = \beta^2_{ha}/\beta^2_{sv}$* versus *the structural mode rank. Kevlar has the highest ratio E_{33}/G_{13} and the corresponding discrepancy is the most pronounced. Steel has a ratio of $E/G = 2.4$ and the discrepancy is less pronounced*

@Seismicisolation

5.5.3. *Flatness ratio s = width/thickness = b/h*

Section warping depends strongly on flatness. Warping has a strong influence on torsion stiffness C_T, given by equation [5.30]. Equation [5.30] is dependent on the ratio of the two shear moduli in the planes (z, x) and (z, y) in equations [5.26] to [5.30].

$$C_T = G_{yz}\ h\ b^3\ \ \beta_T(c) \ \text{ with } \quad \left(c = \frac{b}{h}\sqrt{\frac{G_{xz}}{G_{yz}}} \right) \qquad [5.74]$$

The shape of curve β_T (c) is easily obtained by the series in equation [5.30], which is quickly convergent. For a high flatness value of b/h > 1, curve β (c) tends towards a horizontal asymptote. The accuracy of the value obtained for G_{yz} may suffer if we work in this zone. From a practical point of view it is better to have a sample with a small flatness if possible. Square section is the best shape for the torsion test.

5.5.4. *Saint Venant's theory versus higher approximation theory*

The ratio $\left(v_1 = \beta_{ha}^2\right)/\beta_{sv}^2$ portrays the discrepancy between the theories of higher approximation and Saint Venant's. If the curve v_1/β_{sv}^2 is presented *versus* the sample length L for various materials, wave dispersion has a strong influence. Figure 5.10 shows that the variation of each curve is dependent on the ratio E_3/G_{13}. Figure 5.11 represents v_1/β_{sv}^2 *versus* thickness h.

5.6. Extension of Engström's theory to the anisotropic theory of dynamic torsion of a rod with rectangular cross-section[11]

In the preceding sections, attention has focused on the first elastodynamic mode, which permits the elastic characterization of shear modulus. This constitutes an improvement on Saint Venant's theory. The Helmholtz equation is solved by means of Airy's functions whose solution is applicable to anisotropic materials.

11 This section concerns the torsional wave dispersion problem in a general sense. Readers who are only interested in the characterization of shear modulus at low frequency can skip this section in the first reading.

@Seismicisolation

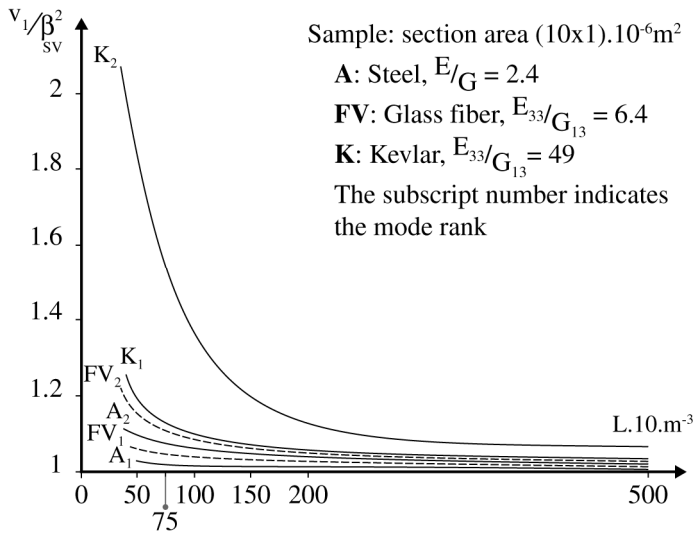

Figure 5.10. *Ratio* $\left(v_1 = \beta^2_{ha}\right)/\beta^2_{sv}$ versus *sample half length*

If we are interested in the dispersion phenomenon, not only for the first elastodynamic mode but also for higher elastodynamic modes in a large frequency range, Engström's theory [ENG 74] is a good framework. Effort is concentrated on the extension of this theory to composite materials. In his PhD thesis, Onobiono [ONO 78] did not use a simple field as Nugues did (see equation [5.48]) but a mixed field including displacement, strain and stress fields, as suggested by Reissner [REI 57]. The difference with Nugues' formulation (see Appendix 5.B) resides in the expression of potential energy. So, in equation [5.B.2] additional terms are afforded.

Potential energy U_p is written as follows:

$$U_p = \frac{1}{2}\iiint_V \left(C_{ijkl}\,\varepsilon_{ij}\,\varepsilon_{kl} - u_i\,\sigma_{ij,j} + \sigma_{ij}\,u_{i,j} - 2\,\sigma_{ij}\,\varepsilon_{ij}\;2\,u_i\,f_i\right) d\,V$$

$$+\frac{1}{2}\iint_{\partial S_\sigma} u_i\left(\sigma_{ij}\,n_j - 2\,\hat{\sigma}_{ij}\,n_j\right) d\,S - \frac{1}{2}\iint_{\partial S_u} \sigma_{ij} n_j\left(u_j - 2\,\hat{u}_j\right) d\,S \qquad [5.75]$$

@Seismicisolation

where $\hat{u}_j$ and $\hat{\sigma}_{ij}$ are prescribed displacements and stress on the boundary ∂S_u and ∂S_σ respectively, and f_i is volumic force.

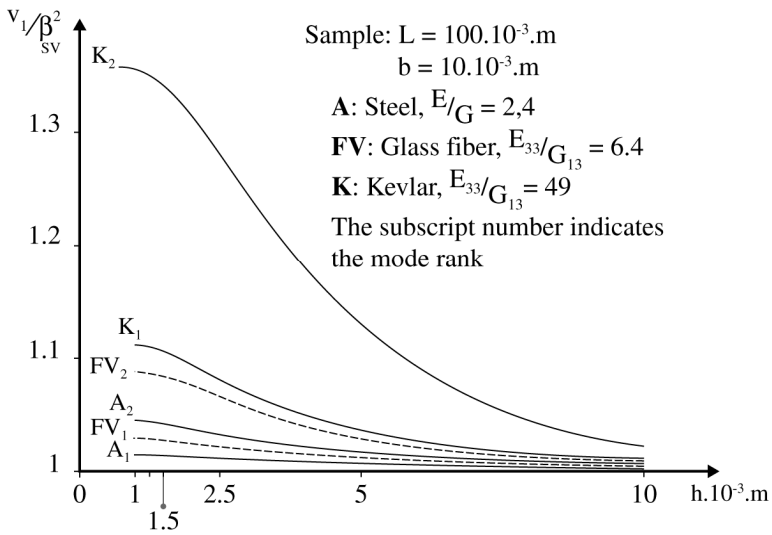

Figure 5.11. *Ratio* $\left(v_1 = \beta^2_{ha} \right) / \beta^2_{sv}$ *versus the sample thickness h*

Variations of Hamilton's principle are effected:

$$\delta \int_{t_0}^{t} \left(U_p - U_c \right) d\,t = 0 \qquad [5.76]$$

Kinetic energy U_c is:

$$U_c = \frac{1}{2} \iiint_V \rho\, \dot{u}_i\, \dot{u}_i\, d\,V \qquad [5.77]$$

@Seismicisolation

Onobiono [ONO 78] has shown that, variational calculations being effected, the following coupled equations of motions are obtained:

$$T_{\theta\theta_L} \frac{\partial^2 \theta}{\partial t^2} - S_{\theta\theta_L} \frac{\partial^2 \theta}{\partial z^2} + S_{\psi\theta_L} \frac{\partial \psi}{\partial z} = 0 \qquad [5.78]$$

$$T_{\psi\psi_L} \frac{\partial^2 \psi}{\partial t^2} - S_{\psi\psi_L} \frac{\partial^2 \psi}{\partial z^2} + S_{\psi\psi} \psi - S_{\psi\theta_L} \frac{\partial \theta}{\partial z} = 0 \qquad [5.79]$$

where:

$\phi(x, y)$ warping function, $\psi(z, t)$ axial displacement,

$\theta(z, t)$ torsional angle.

Notice that equations [5.78] and [5.79] are quite similar to equations [5.49] with coefficients of derivative depending on stiffness of material.

In equations [5.49], which are results of beam theory, coefficients of derivatives depend on compliances of material.

The two natural boundary conditions are:

$$\left\{ \left[S_{\theta\theta_L} \frac{\partial \theta}{\partial z} - S_{\psi\theta_L} \psi \right] \delta\theta \right\}_0^L = \left\{ \bar{T} \delta\theta \right\}_0^L \qquad [5.80]$$

$$\left\{ \left[S_{\psi\psi} \frac{\partial \psi}{\partial z} \right] \delta\psi \right\}_0^L = \left[\bar{M} \delta\psi \right]_0^L = 0 \qquad [5.81]$$

$\bar{T}_1$ is the prescribed or applied torsion couple and $\bar{M}$ is the prescribed moment due to longitudinal stress.

@Seismicisolation

$T_{\alpha\alpha 1}$ and $T_{\psi\psi 1}$ are coefficients in the equations of motion [5.74] and [5.75], which are defined as follows:

$$T_{\theta\theta_L} = \rho \iint_S \left(x^2 + y^2\right) d\,x\,d\,y = \rho\, I_p \qquad [5.82]$$

and I_p polar is the moment of the rod.

$$T_{\psi\psi_1} = \rho \int\int_S \phi^2\, d\,x\,d\,y \qquad [5.83]$$

where ϕ (z, t) is warping function, ψ (z, t) axial displacement, and α (z, t) torsion angle.

In equations [5.78] and [5.79], the coefficients are defined as:

$$S_{\theta\theta_L} = \iint_S \left(y^2\, C_{55} + x^2\, C_{44} \right) d\,x\,d\,y \qquad [5.84]$$

$$S_{\psi\psi} = C_{33} \int\int_S \phi^2\, d\,x\,d\,y \qquad [5.85]$$

$$S_{\psi\psi} = \iint_S \left\{ C_{55} \left(\frac{\partial\,\phi}{\partial\,x}\right)^2 + C_{44} \left(\frac{\partial\,\phi}{\partial\,y}\right)^2 \right\} d\,x\,d\,y \qquad [5.86]$$

$$S_{\psi\psi_1} = \int\int_S \left\{ C_{55} \left(\frac{\partial\,\phi}{\partial\,x}\right)^2 + C_{44} \left(\frac{\partial\,\phi}{\partial\,y}\right)^2 \right\} d\,x\,d\,y \qquad [5.87]$$

$$k_1 = \frac{\int_0^L \left\{ C_{33} \left(\frac{\partial\,\psi}{\partial\,z}\right)^2 - \rho \left(\frac{\partial\,\psi}{\partial\,t}\right)^2 \right\} d\,z}{\int_0^L \psi^2 d\,z} \qquad [5.88]$$

@Seismicisolation

$$k_3 = \frac{\int_0^L \psi \frac{\partial \theta}{\partial z} dz}{\int_0^L \psi^2 dz} \qquad [5.89]$$

For orthotropic materials in directions (1,2,3) or (x,y,z) $C_{44} = G_{yz}$ and $C_{55} = G_{xz}$ are Coulomb moduli. In Appendix 5.F, a solution for warping function ϕ is proposed by Onobiono. ϕ is not derived from the Laplace equation, as suggested by Saint Venant. It is the solution to Helmholtz equation on one hand and is frequency-dependent on the other hand.

The solution proposed by Onobiono does not contradict Nugue's solution. For a low frequency range, the difference between the two solutions is small. For a large frequency range and for the solution to the wave dispersion problem, Onobiono's proposal is more accurate. In other respects, Onobiono's solution is appropriate for higher elastodynamic modes.

The boundary conditions defined in [5.80] and [5.81] are:

– simply supported end $\left[\ \theta\ (z, t) = 0,\ \bar{M} = 0\ \right]$;

– clamped end $\left[\ \theta\ = 0\ ,\ \psi = 0\ \right]$;

– free end $\left[\bar{T}_1 = 0,\ \bar{M} = 0\right]$.

The six boundary conditions are gathered in Table 5.2. In equation [5.87], $S_{\psi\theta_L}$ represents the coupling coefficient between torsion motion and warping (or longitudinal) motion.

5.7. Equations of motion

5.7.1. *Matricial form*

Equations [5.78] and [5.79] can be written as:

$$\begin{bmatrix} D_{11} & D_{12} \\ D_{21} & D_{22} \end{bmatrix} \begin{bmatrix} \alpha \\ \psi \end{bmatrix} = 0 \qquad [5.90]$$

@Seismicisolation

Kinematic boundary conditions	**Natural boundary conditions**
θ prescribed or $\delta\theta = 0$ ψ prescribed or $\delta\psi = 0$	$\left\{ \left[S_{\theta\theta_L} \frac{\partial \theta}{\partial z} - S_{\psi\theta_L} \psi \right] \delta\theta \right\}_0^L = \left\{ \bar{T} \delta\theta \right\}_0^L =$ $\left\{ \left[S_{\psi\psi_L} \frac{\partial \psi}{\partial z} \right] \delta\psi \right\}_0^L = \left[\bar{M} \delta\psi \right]_0^L = 0$
Clamped end	$\theta = 0$ $\quad$ $\psi = 0$
Free end	$\bar{T} = 0$ $\quad$ $\bar{M} = 0$
Simply supported end	$\theta = 0$ $\quad$ $\bar{M} = 0$
Additional weight at one end	$J_a \frac{\partial \theta}{\partial z} = S_{\theta\theta_L} \frac{\partial \theta}{\partial z} - S_{\psi\theta_L} \psi$

Table 5.2. *Various boundary conditions at one end*

With mathematical operation defined as:

$$D_{11} = T_{\theta\theta_L} \frac{\partial^2}{\partial t^2} - S_{\theta\theta_L} \frac{\partial^2}{\partial z^2} \qquad [5.91]$$

$$D_{12} = S_{\psi\alpha_1} \frac{\partial}{\partial z} = D_{21}, \quad D_{22} = T_{\psi\psi_1} \frac{\partial^2}{\partial z^2} - S_{\psi\psi_1} \frac{\partial^2}{\partial z^2} + S_{\psi\psi} \qquad [5.92]$$

5.7.1.1. *Kinematic boundary conditions*

ψ prescribed or $\delta\psi = 0$.

5.7.1.2. *Natural boundary conditions*

Eliminating θ or ψ in equations [5.78] and [5.79], we obtain a decoupled equation of motion that is valid for either θ or ψ.

Let us call the variable $f = \alpha$ (or ψ).

$$-\frac{\partial^4 f}{\partial z^4} + \left(\frac{T_{\psi\psi_L}}{S_{\psi\psi_L}} + \frac{T_{\theta\theta_L}}{S_{\theta\theta_L}} \right) \frac{\partial^4 f}{\partial z^2 \partial t^2} - \left(\frac{S^2_{\psi\theta_L}}{S_{\psi\psi_L} S_{\theta\theta_L}} - \frac{S_{\psi\psi}}{S_{\psi\psi_L}} \right) \frac{\partial^2 f}{\partial z^2}$$

@Seismicisolation

$$-\frac{S_{\psi\psi}\,T_{\theta\theta_l}}{S_{\psi\psi_l}\,S_{\theta\theta_L}}\frac{\partial^2 f}{\partial t^2}-\frac{T_{\theta\theta_L}\,T_{\psi\psi_L}}{S_{\psi\psi_L}\,S_{\theta\theta_L}}\frac{\partial^4 f}{\partial t^4}=0 \qquad [5.93]$$

5.7.2. *Decoupled equation of motion and correcting coefficient*

The phase velocity v of a plane progressive wave can be evaluated from equation [5.93]. When the frequency goes to infinity, the asymptotic value of v must equal Rayleigh wave velocity v_R.

For this purpose, a correcting coefficient p is necessary and equations of motion [5.78] and [5.79] become:

$$T_{\theta\theta_L}\frac{\partial^2\theta}{\partial t^2}-S_{\theta\theta_L}\frac{\partial^2\theta}{\partial z^2}+S_{\psi\theta_L}\frac{\partial\psi}{\partial z}=0 \qquad [5.94]$$

$$T_{\psi\psi_L}\frac{\partial^2\psi}{\partial t^2}-p^2\,S_{\psi\psi_L}\frac{\partial^2\psi}{\partial z^2}+S_{\psi\psi}\,\psi-S_{\psi\theta_L}\frac{\partial\theta}{\partial z}=0 \qquad [5.95]$$

Barr [BAR 62] and Engström [ENG 74] have adopted such a correcting coefficient:

$$\lim_{\substack{k\to 0\\ \text{or } f\to\infty}} v^2=v_R^2=p^2\frac{S_{\psi\psi_l}}{T_{\psi\psi_l}} \qquad [5.96]$$

For an isotropic material, Viktorov [VIK 67] proposed an empirical formula that is suitable for all applications:

$$p^2(\gamma)=\left(\frac{0.87+1.12\,\nu}{1+\nu}\right)^2 \qquad [5.97]$$

where v is Poisson's coefficient. The ratio used in [5.96] is written as:

$$\frac{S_{\psi\psi_l}}{T_{\psi\psi_l}}=\frac{1}{A_{\psi\psi}^2} \qquad [5.98]$$

@Seismicisolation

5.8. Torsion wave dispersion

In section 5.5, wave dispersion is partly examined with a short, finite rod length. Only the relative variation of phase velocity *versus* some structural modes (eigenfrequencies) is examined. The influence of the material is represented by the ratio of Young's modulus/shear modulus, see Figure 5.7.

If we focus our attention on the torsional wave dispersion phenomenon in general, the curve phase velocity *versus* wave number k (or frequency f) must be drawn in a large range covering f or k from zero to infinity. This problem only occurs if we are dealing with a very long rod. Theoretically speaking, a progressive wave is used. In this section we have presented Onobiono's work [ONO 78], which extends Engström's [ENG 74] work to anisotropic materials.

Material	Graphite fiber	Phenolic Silicon	Glass fiber epoxy	Kevlar 49 epoxy	Carbon fiber epoxy	Glass fiber polyester
$A^2_{\psi\psi}$	0.03293	0.12596	0.13408	0.02400	0.02400	0.14600
v_R^2 (m/s)	0.02725	0.10264	0.11038	0.01475	0.01387	0.12567
p^2	0.82753	0.81488	0.82327	0.82296	0.57782	0.86077

Table 5.3. *Values of correcting coefficient p^2 for some artificial composites*[12]

5.8.1. *Expressions of angular displacement α (z, t) and axial displacement ψ (z, t)*

Angular and axial displacement are expressed by exponential functions as:

$$\theta(z,t) = \theta_0 \exp j(kz - \omega t) \qquad [5.99]$$

$$\psi(z,t) = \psi_0 \exp j(kz - \omega t) \qquad [5.100]$$

If a very long rod is considered to be of infinite length, a relationship exists between wave number k and rod length l:

12 For anisotropic materials, Touratier's work is presented in Chapter 7 with notation differences.

@Seismicisolation

$$k_{,n} = \frac{n\,\pi}{L} \qquad [5.101]$$

n integer number. Circular frequency ω_t is related to k by:

$$\omega^2_{T,n} = \left(\frac{n\,\pi}{L}\right)^2 \frac{S_{\theta\theta_L}}{T_{\theta\theta_L}} \qquad [5.102]$$

Bringing [5.99] and [5.100] into [5.94] and [5.95], taking conditions concerning a rod with infinite length into account, we obtain the following dispersion relation under matricial form:

$$\begin{vmatrix} D'_{11} & D'_{12} \\ D'_{12} & D'_{22} \end{vmatrix} = 0 \qquad [5.103]$$

with:

$$D'_{11} = \omega^2 - k^2 \frac{S_{\theta\theta_L}}{T_{\theta\theta_L}}, \quad D'_{12} = j\,k \frac{S_{\psi\,\theta_L}}{T_{\theta\theta_L}} = -D'_{21}$$

$$D'_{22} = \omega^2 - p^2 k^2 \frac{S_{\psi\psi_L}}{T_{\psi\psi_L}} + \frac{S_{\psi\psi}}{T_{\psi\psi_L}} \qquad [5.104]$$

with $\omega = kv$.

v is phase velocity. Developing equation [5.103], we obtain a linear bisquared fourth-order equation that permits us to study the two first modes.

$$v^4 - v^2 \left(p^2 \frac{S_{\psi\psi_L}}{T_{\psi\psi_L}} + \frac{S_{\theta\theta_L}}{T_{\theta\theta_L}} - \frac{S_{\psi\psi}}{k^2\, T_{\psi\psi_L}} \right) +$$

$$+ p^2 \frac{S_{\theta\theta_L}\, S_{\psi\psi_L}}{T_{\theta\theta_L}\, T_{\psi\psi_L}} - \frac{S_{\theta\theta_L}\, S_{\psi\psi} + S^2_{\psi\theta_L}}{k^2\, T_{\theta\theta_L}\, T_{\psi\psi_L}} = 0 \qquad [5.105]$$

@Seismicisolation

Using non-dimensional variables:

$$\bar{V} = \left(\frac{v}{v_T}\right)^2 \qquad [5.106]$$

$$\bar{k} = k\,h/2 \text{ where h is thickness of the rod} \qquad [5.107]$$

$$\delta = \frac{b\ (\text{width})}{h\ (\text{thickness})}, \text{ flatness ratio} \qquad [5.108]$$

v_T is the shear wave velocity deduced from ω_T, equation [5.102].

5.8.2. *Phase velocity for the two first elastodynamic modes*

The bisquared equation obtained in [5.105] is transformed as follows, using non-dimensional variables:

$$\left(\frac{v}{v_T}\right)^4 - \left(\frac{v}{v_T}\right)^2 \left(1 + p^2 \frac{S_{\psi\psi_L}\ T_{\theta\theta_L}}{S_{\theta\theta_L}\ T_{\psi\psi_L}} - \frac{S_{\psi\psi}\ T_{\theta\theta_L}}{k^2\ T_{\psi\psi_l}\ S_{\theta\theta_L}}\right)$$
$$+ p^2 \frac{S_{\psi\psi_L}\ T_{\theta\theta_L}}{S_{\theta\theta_L}\ T_{\psi\psi_L}} - \frac{\left(S_{\psi\psi}\ S_{\theta\theta_L} + S^2_{\psi\theta_L}\right)\ T_{\theta\theta_L}}{k^2\ T_{\psi\psi_L}\ S^2_{\theta\theta_L}} = 0 \qquad [5.109]$$

Adopting the convention:

$$\bar{V} = \left(\frac{v}{v_T}\right)^2 \qquad [5.110]$$

equation [5.109] becomes:

@Seismicisolation

$$\bar{V}^2 - \bar{V}\left\{1 + p^2 \frac{S_{\psi\psi_L}\ T_{\theta\theta_L}}{S_{\theta\theta_L}\ T_{\psi\psi_L}} - \frac{S_{\psi\psi}\ T_{\theta\theta_L}\ b^2}{4\delta^2\bar{k}^2\ T_{\psi\psi_L} S_{\theta\theta_L}}\right\}$$

$$+ p^2 \frac{S_{\psi\psi_L}\ T_{\theta\theta_L}}{S_{\theta\theta_L}\ T_{\psi\psi_L}} - \frac{\left(S_{\psi\psi}\ S_{\theta\theta_L} + S^2_{\psi\theta_L}\right) T_{\theta\theta_L} h^2}{4\delta^2\bar{k}^2\ T_{\psi\psi_L}\ S^2_{\theta\theta_L}} = 0 \qquad [5.111]$$

The roots of [5.111] are real and the phase velocities $\bar{v}_1$ and $\bar{v}_2$ are:

$$\bar{V}_1 = \frac{1}{2}\left\{1 + p^2 \frac{S_{\psi\psi_L}\ T_{\theta\theta_L}}{S_{\theta\theta_L}\ T_{\psi\psi_L}} - \frac{S_{\psi\psi}\ T_{\theta\theta_L}\ b^2}{4\delta^2\bar{k}^2\ T_{\psi\psi_L} S_{\theta\theta_L}} + \left[\left(1 + p^2 \frac{S_{\psi\psi_L}\ T_{\theta\theta_L}}{S_{\theta\theta_L}\ T_{\psi\psi_L}} - \frac{S_{\psi\psi}\ T_{\theta\theta_L}\ b^2}{4\delta^2\bar{k}^2\ T_{\psi\psi_L} S_{\theta\theta_L}}\right)^2 - 4\left(p^2 \frac{S_{\psi\psi_L}\ T_{\theta\theta_L}}{S_{\theta\theta_L}\ T_{\psi\psi_L}} - \frac{\left(S_{\psi\psi}\ S_{\theta\theta_L} + S^2_{\psi\theta_L}\right) T_{\theta\theta_L} b^2}{4\delta^2\bar{k}^2\ T_{\psi\psi_L}\ S^2_{\theta\theta_L}}\right)\right]^{1/2}\right\} \qquad [5.112]$$

$$\bar{V}_2 = \frac{1}{2}\left\{1 + p^2 \frac{S_{\psi\psi_L}\ T_{\theta\theta_L}}{S_{\theta\theta_L}\ T_{\psi\psi_L}} - \frac{S_{\psi\psi}\ T_{\theta\theta_L}\ b^2}{4\delta^2\bar{k}^2\ T_{\psi\psi_L} S_{\theta\theta_L}} - \left[\left(1 + p^2 \frac{S_{\psi\psi_L}\ T_{\theta\theta_L}}{S_{\theta\theta_L}\ T_{\psi\psi_L}} - \frac{S_{\psi\psi}\ T_{\theta\theta_L}\ b^2}{4\delta^2\bar{k}^2\ T_{\psi\psi_L} S_{\theta\theta_L}}\right)^2 - 4\left(p^2 \frac{S_{\psi\psi_L}\ T_{\theta\theta_L}}{S_{\theta\theta_L}\ T_{\psi\psi_L}} - \frac{\left(S_{\psi\psi}\ S_{\theta\theta_L} + S^2_{\psi\theta_L}\right) T_{\theta\theta_L} b^2}{4\delta^2\bar{k}^2\ T_{\psi\psi_L}\ S^2_{\theta\theta_L}}\right)\right]^{1/2}\right\} \qquad [5.113]$$

@Seismicisolation

5.9. Presentation of dispersion curves

5.9.1. *Isotropic rod with circular section*

Cross-sectional geometry is adopted here in order to get a set of dispersion curves as a reference. These curves are obtained from a closed-form expression of equations of motion using Bessel's function [POC 1876].

Figure 5.14 shows the dispersion curves with three branches corresponding to the first three elastodynamic modes. There is no dispersion at all for the first mode. This property is largely exploited in dynamic tests.

5.9.2. *Isotropic steel rod with rectangular section*

As we have to deal with a fourth-order bisquared equation for phase velocity, only the first two branches are available. Figure 5.12 shows the first elastodymanic mode. The dispersion is strongly dependent on flatness factor.

$$\delta = \frac{\text{b width}}{\text{h thickness}}$$

Engström's and Barr's theories are also mentioned in this figure. The discrepancy between those two theories and Onobiono's one is small.

Figure 5.13 uses the same material (steel) and the second branch. Pronounced discrepancies can be seen between Onobiono's and Engström's theories from one side and Barr's theory from the other side.

5.9.3. *Anisotropic composite rods*

Four composite materials (which are transverse isotropic) are examined:

- glass fiber-polyester resin;
- glass fiber-epoxy resin;
- carbon fiber-epoxy resin; and
- boron fiber-epoxy resin.

@Seismicisolation

Two important parameters are retained for further analysis:

– the quotient $\frac{E_z}{G_{xz}} = \frac{\text{Young's modulus in fiber direction}}{\text{Shear modulus in plane orthogonal to fiber direction}}$;

– the section flatness $\delta = b/h$.

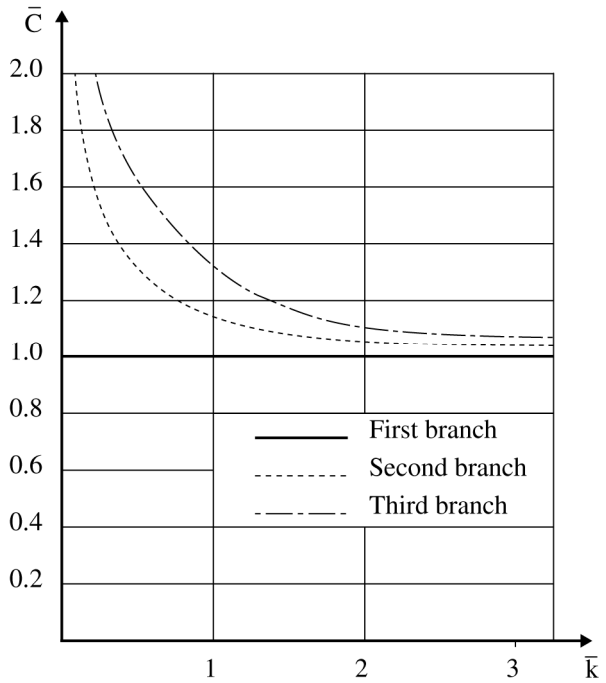

Figure 5.12. *Dispersion curve* $\bar{C} = \bar{v}\left(\bar{k}\right)$, *where* $\bar{c}$ *is the non-dimensional torsional phase velocity* $\bar{c} = v/v_T$ *(*v_T *is the asymptotic value of phase velocity with* $k \to 0$*). The material is steel,* $\gamma = 0.3$*. Radius of the circular section* $R = 0.3$*,* $\bar{k}\ kh/2$ *is the non-dimensional wave number; h is thickness. The three first branches are represented*

In Figure 5.15, the first branches of the dispersion curves are represented for the glass fiber-polyester resin composite, with various values of δ. Figure 5.16 concerns the second branch of the dispersion curve for the same composite material.

@Seismicisolation

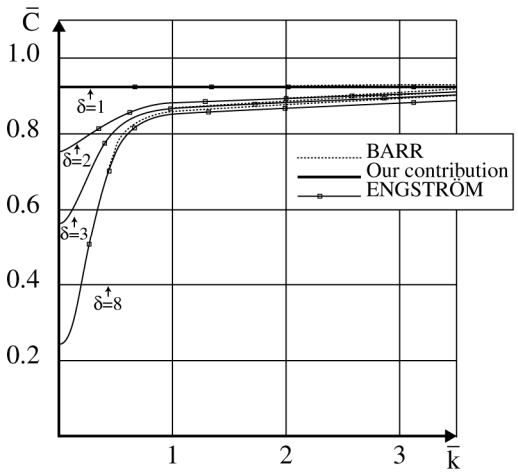

Figure 5.13. *Steel isotropic rod with various values of flatness coefficient* δ *= width/thickness. First branch of dispersion curve* $\bar{C} = \bar{C}\left(\bar{k}\right) = v/v_T$, $v_T = (\mu/\rho)^{1/2}$. *Comparison between three theories: Barr, Engström and Onobiono*

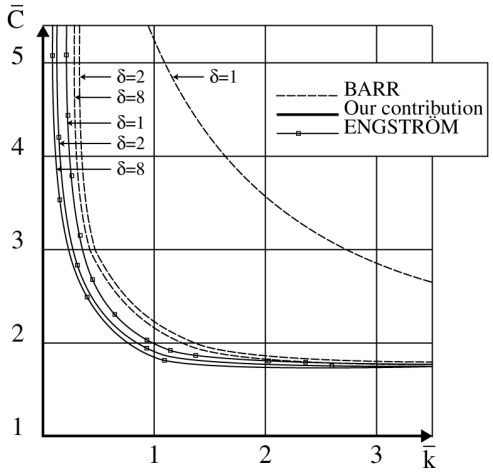

Figure 5.14. *Curves* $\bar{c} = v/v_T$ versus *non-dimensional wave number* $\bar{k} = kh/2$ *where h is thickness. The material is steel, isotropic,* $\bar{\gamma}$ *= 0.3. Second branches comparing three theories: Barr, Engström and Onobiono Discrepancies are large between Barr's theory and the two other theories for δ = width b/thickness h*

@Seismicisolation

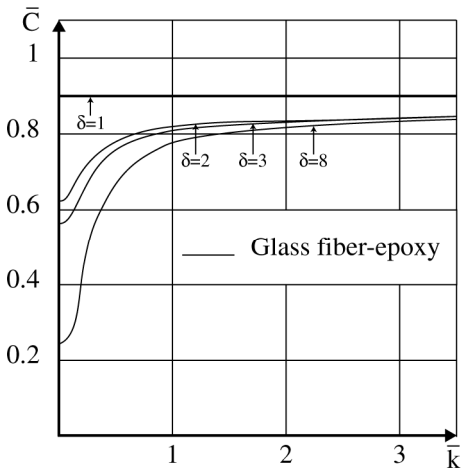

Figure 5.15. *Non-dimensional phase velocity* $\bar{c}$ versus *non-dimensional wave number* k $\bar{c} = v/v_T$ where v_T *is the asymptotic value of velocity with* $\bar{k} \to \infty \bar{k}$. *The material is composite glass fiber-polyester resin,* $\bar{\delta}$ *= width b/thickness h. For square section δ = 1, there is no dispersion for* $\bar{v}$. *The dispersion curve is strongly dependent on δ*

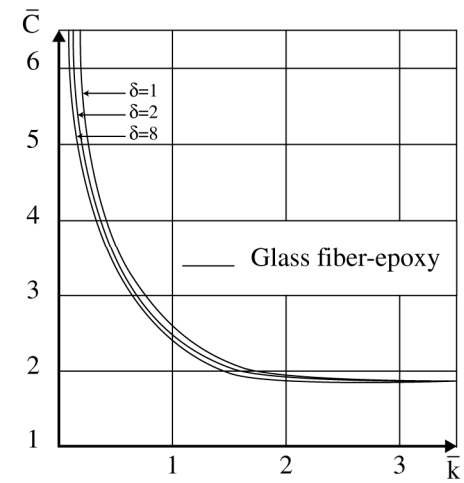

Figure 5.16. *Dispersion curve for torsional vibration* $\bar{c} = \bar{c}\left(\bar{k}\right)$, $v_T\,(\bar{c} = v/v_T, v_T)$, *is asymptotic value of velocity for* $k \to \infty$. $\bar{k} = kh/2$. *Material: fiber glass-polyester resin, δ = width b /thickness h*

@Seismicisolation

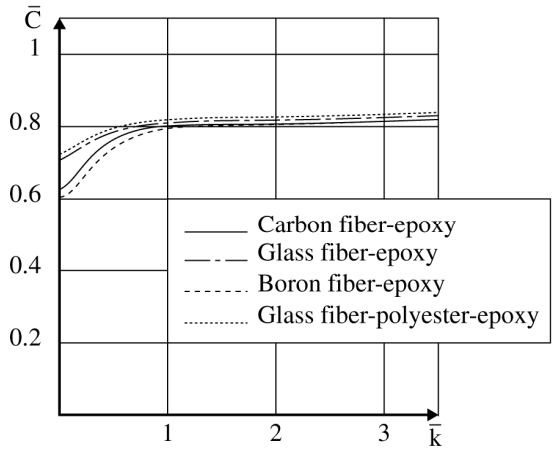

Figure 5.17. *Dispersion of torsional non-dimensional velocity ($\bar{c} = v/v_T$) versus non-dimensional wave number $\bar{k} = kh/2$ for four anisotropic composites*
First branches – δ (flatness coefficient) = $\bar{\delta}$ = width b /thickness h

In Figure 5.17 the first branches of dispersion curves are drawn for four different composite materials. The flatness coefficient $\bar{\delta} = \dfrac{\text{width b}}{\text{thickness h}}$ is 2.

5.9.4. *Some remarks*

5.9.4.1. *Asymptotic values of phase velocity for k going to infinity (zero frequency)*

Asymptotic values of phase velocity give rise to the following points:

– When the wave number goes to zero, phase velocity for the first branch is a constant and is equal to the phase velocity obtained by Saint Venant's theory in low frequency range.

– When the wave number goes to infinity, thanks to correcting coefficient p^2, the phase velocity of the first branch remains finite and its slope goes to zero. The asymptotic value is the Rayleigh surface wave.

– When k tends to infinity, the phase velocity of the second elastodynamic mode remains finite and the corresponding group velocity (the slope) tends to zero. In all the curves corresponding to the second branch, for $k \to \infty$, the velocity decreases and tends to the warping phase velocity.

@Seismicisolation

– For the second branch, the phase velocity goes to infinity when k tends to zero.

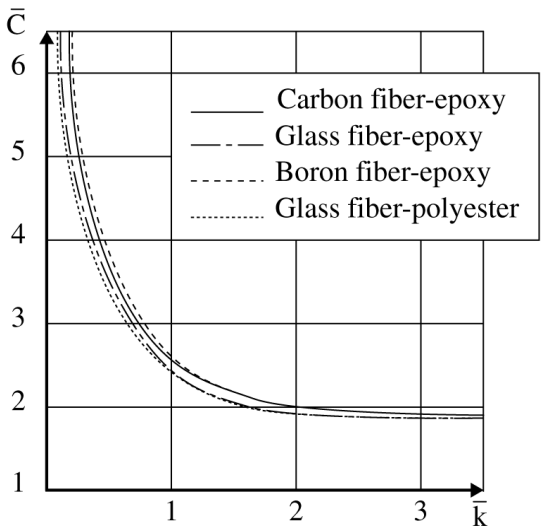

Figure 5.18. *Dispersion of torsional wave velocity* $\bar{c} = v/v_T$ versus *relative wave number* $\bar{k} = kh/2$. *Second branches of dispersion cures with* δ *= width b /thickness h = 2,* $\bar{k} = kh/2$

5.9.4.2. *Anisotropic degree characterizes ratios*

The anisotropic degree characterized ratios $\frac{S_{\theta\theta_L}}{S_{\psi\psi_1}}$ and $\frac{S_{\psi\psi_L}}{S_{\psi\psi}}$, which are equal to C_{33}/C_{44} for transverse isotropic materials, constitute an appropriate parameter for wave dispersion study.

The flatness coefficient $\delta = \frac{\text{width b}}{\text{thickness h}}$ has a strong influence on the trend of the dispersion curve.

However, for $\delta = 1$ (square section), the dispersion curve for the first branch is weak and similar to that concerning a circular section.

@Seismicisolation

5.9.5. *Practical remark*

If possible, the experimenter should choose a square section and avoid the problem of the dependency of phase velocity on the first elastodynamic mode with respect to wave number or frequency.

5.9.6. *Comparison with other theories (Barr and Engström)*

At low frequency, the phase velocity of the first branch obtained by our theory is coincident with that obtained by Barr and Engström for isotropic materials. When frequency increases, the discrepancy between the three curves obtained by our theory and the aforementioned theories becomes large, particularly for large values of flatness coefficient δ. For the second elastodynamic mode, the discrepancy between the three dispersion curves is small for both isotropic and anisotropic materials. The flatness coefficient is much less sensitive.

Barr's theory gives rise to dispersion curves that are different from curves obtained in the framework of our theory. This discrepancy can be explained by the fact that warping phenomenon cannot be correctly described by Saint Venant's theory for the second branch. Discarding this theory and adopting correcting coefficient p^2 (C_{ijkl}) for the asymptotic value of phase velocity is a reasonable hypothesis for all elastodynamic modes.

5.9.6.1. *Dependency of propagation mode on the second branch*

Dependency of propagation mode of the second branch with respect to warping is very important. This dependency is less pronounced for the first mode where torsion motion is predominant.

5.10. Torsion vibrations of an off-axis anisotropic rod

Off-axis anisotropic rods are used in material characterization using dynamic tests that permit us to evaluate the non-diagonal coefficient of a compliance matrix. These tests are interesting when dealing with natural or artificial anisotropic materials. Torsional vibrations are coupled with bending vibrations in the rod whose axis is not coincident with one of the material symmetry axes.

In Chapter 6, the bending vibration of a rod is examined. The problem of coupling vibrations (bending and torsion) is examined by means of d'Alembert's

@Seismicisolation

principle to obtain equations of motion. In this section, this problem is examined using variational Hamilton's principle.

5.10.1. *Displacement field*

Displacement $\vec{u}$ is a linear combination of two fields: one for bending motion, the other for torsional motion.

$$\left.\begin{aligned} u_1 &= u_{1F} + u_{1T} \\ u_2 &= u_{2F} + u_{2T} \\ u_3 &= u_{3F} + u_{3T} \end{aligned}\right\} \qquad [5.114]$$

The subscripts F and T are related to flexural and torsion respectively.

$$u_{1F} = w(z,t), \qquad u_{1T} = -y\,\theta(z,t)$$

$$u_{2F} = 0, \qquad u_{2T} = x\,\theta(z,t)$$

$$u_{3F} = -x\frac{\partial w}{\partial z}, \qquad u_{3T} = \phi(x,y)\,\psi(z,t) \qquad [5.115]$$

In the second line of [5.113] setting $u_{2F} = 0$, relative motion in the direction y is eliminated at the cross-section due to bending. Equation [5.115] is rewritten as:

$$u_1 = w(z,t) - y\,\theta(z,t)$$

$$u_2 = x\,\theta(z,t)$$

$$u_3 = -x\frac{\partial w}{\partial z} + \phi(x,y)\,\psi(z,t) \qquad [5.116]$$

@Seismicisolation

The field of velocity is:

$$\dot{u}_1 = \frac{\partial w}{\partial t} - y \frac{\partial \theta}{\partial t}$$

$$\dot{u}_2 = x \frac{\partial \theta}{\partial t}$$

$$\dot{u}_3 = - x \frac{\partial^2 w}{\partial z \, \partial t} + \phi \left(x , y \right) \frac{\partial \psi}{\partial t} \qquad [5.117]$$

Neglecting surface forces and volume forces, the strain energy is:

$$U_p = \int_0^L d z \iint_{dS} \frac{1}{2} C_{ijkl} \, \varepsilon_{ij} \, \varepsilon_{kl} \, dx \, dy \qquad [5.118]$$

and the kinetic energy is:

$$U_c = \int_0^L d z \iint_S \frac{1}{2} \rho \, \dot{u}_i \, \dot{u}_i \, dx \, dy \qquad [5.119]$$

The strain field is:

$$\left.\begin{array}{ll} \varepsilon_{xx} = 0 & \varepsilon_{zz} = - x \dfrac{\partial^2 w}{\partial z^2} + \phi \dfrac{\partial \psi}{\partial z} \\ \varepsilon_{yy} = 0 & \gamma_{xz} = - y \dfrac{\partial \theta}{\partial z} + \psi \dfrac{\partial \phi}{\partial x} \\ \gamma_{xy} = 0 & \gamma_{yz} = x \dfrac{\partial \theta}{\partial z} + \psi \dfrac{\partial \phi}{\partial y} \end{array}\right\} \qquad [5.120]$$

@Seismicisolation

Bringing equation [5.117] into [5.119], we get:

$$U_c = \int_0^L d\,z \iint_S \frac{1}{2}\rho \left\{ \begin{array}{l} \left(\frac{\partial w}{\partial t} - y\frac{\partial \theta}{\partial t}\right)^2 + \left(x\frac{\partial \theta}{\partial t}\right)^2 \\ + \left(\phi\frac{\partial \psi}{\partial t} - x\frac{\partial^2 w}{\partial z\,\partial t}\right)^2 \end{array} \right\} dx\,dy \qquad [5.121]$$

Bringing [5.120] into [5.118]:

$$U_p = \int_0^L dz \iint_S \frac{1}{2} \left\{ \begin{array}{l} C_{33}\left(\phi\frac{\partial \psi}{\partial z} - x\frac{\partial^2 w}{\partial z^2}\right)^2 + \\ + C_{44}\left(x\frac{\partial \theta}{\partial z} + \psi\frac{\partial \phi}{\partial y}\right)^2 + \\ + C_{55}\left(\psi\frac{\partial \phi}{\partial x} - y\frac{\partial \theta}{\partial z}\right)^2 + \\ + 2C_{34}\left(x\frac{\partial \theta}{\partial z} + \psi\frac{\partial \phi}{\partial y}\right)\left(\phi\frac{\partial \psi}{\partial z} - x\frac{\partial^2 w}{\partial z^2}\right) + \\ + 2C_{35}\left(\psi\frac{\partial \phi}{\partial x} - y\frac{\partial \theta}{\partial z}\right)\left(\phi\frac{\partial \psi}{\partial z} - x\frac{\partial^2 w}{\partial z^2}\right) + \\ + 2C_{45}\left(\psi\frac{\partial \phi}{\partial y} + x\frac{\partial \theta}{\partial z}\right)\left(\psi\frac{\partial \phi}{\partial x} - y\frac{\partial \theta}{\partial z}\right) \end{array} \right\} dx\,dy$$

[5.122]

@Seismicisolation

Hamilton's principle is applied to the functionals, which satisfies:

$$\delta \int_{t_1}^{t_2} \left(U_c - U_p \right) dt = 0 \qquad [5.123]$$

5.10.2. *Equations of motion*

Appendix 5.G presents details of calculations that give rise to the three equations of motion:

– [5.G.10];

– [5.G.11]; and

– [5.G.12].

5.10.3. *Eigenfrequency equations of motion*

Let us introduce the displacement field:

$$\left.\begin{aligned} \alpha(z, t) &= \alpha_0 Y_1(z) \sin \omega t \\ \psi(z, t) &= \psi_0 Y_2(z) \sin \omega t \\ w(z, t) &= w_0 Y_3(z) \sin \omega t \end{aligned}\right\} \qquad [5.124]$$

where α_0, ψ_0 and w_0 are the constants that represent vibration amplitudes. Yj (z) and (j = 1, 2, 3) are functions of coordinate z uniquely dependent on mode shapes.

Kinetic and potential energy are condensed as follows:

$$\left.\begin{aligned} U_c &= \frac{1}{2} \omega^2 \tilde{U}_c \cos^2 \omega t \\ U_p &= \frac{1}{2} \tilde{U}_p \sin^2 \omega t \end{aligned}\right\} \qquad [5.125]$$

@Seismicisolation

Bringing equation [5.124] into [5.121] and [5.122], for kinetic energy we obtain:

$$\tilde{U}_c = \left\{ \begin{array}{l} \theta_0^2\ T_{\theta\theta_1} \int_0^L Y_1^2\ dz + \psi_0^2\ T_{\psi\psi_1} \int_0^L Y_2^2\ dz + \\ + w_0^2 \left(T_{ww} \int_0^L Y_3^2\ dz + T_{ww_1} \int_0^L \left(\frac{d\,Y_3}{d\,z} \right)^2 d\,z \right) - \\ - 2\ \psi_0 w_0\ T_{\psi w} \int_0^L Y_2 \left(\frac{d\,Y_3}{d\,z} \right) d\,z\ - \\ -\ 2\ \theta_0 w_0\ T_{ww_2} \int_0^l (Y_1 Y_3)\ d\,z \end{array} \right\} \qquad [5.126]$$

The potential energy U_p is 0.

$$\tilde{U}_p = \left\{ \begin{array}{l} \theta_0^2\ S_{\theta\theta_1} \int_0^L \left(\frac{d\,Y_1}{dz} \right)^2 d\,z + w_0^2\ S_{ww\,L} \int_0^L \left(\frac{d^2\ Y_3}{d\,z^{\ 2}} \right)^2 d\,z\ + \\ +\psi_0^2 \left(S_{\psi\psi_L} \int_0^L \left(\frac{d\,Y_2}{d\,z} \right)^2 d\,z + 2\,S_{\psi\psi} \int_0^L Y_2^{\ 2}\ d\,z + 2\,S_{\psi\psi_2} \int_0^L Y_2 \left(\frac{d\,Y_2}{d\,z} \right) d\,z \right) + \\ +\,2\ \psi_0\ \theta_0 \left(S_{\psi\theta_1} \int_0^L Y_2 \left(\frac{d\,Y_1}{d\,z} \right) dz + S_{\psi\theta_2} \int_0^L \left(\frac{dY_1}{d\,z} \right) \left(\frac{d\,Y_2}{d\,z} \right) d\,z \right) + \\ +\,2\ w_0\ \theta_0\ S_{\theta w_L} \int_0^L \left(\frac{d\,Y_1}{d\,z} \right) \left(\frac{d^2\ Y_3}{d\,z^2} \right) d\,z\ - \\ -\,2\ w_0\ \psi_0 \left(S_{\psi w_1} \int_0^L \left(\frac{dY_2}{d\,z} \right) \left(\frac{d^2 Y_3}{dz^2} \right) d\,z + S_{\psi w_2} \int_0^L Y_2 \left(\frac{d^2 Y_3}{dz^2} \right) d\,z \right) \end{array} \right\} \qquad [5.127]$$

@Seismicisolation

Coefficients S_{xx} and T_{xx} are given in Appendix 5.G, equation [5.G.9].

Equations [5.123] and [5.124] are condensed as follows. The equality U_c max = U_p max gives:

$$\omega^2 = \frac{\tilde{U}_p}{\tilde{U}_c} \qquad [5.128]$$

Equality [5.126] contains amplitudes θ_0 , ψ_0 , w_0 for which the optimal values are those resulting from the minimum value of ω. This condition is fulfilled if and only if we have:

$$\frac{\partial}{\partial w_0}\left(\frac{\tilde{U}_p}{\tilde{U}_c}\right) = 0, \quad \frac{\partial}{\partial \psi_0}\left(\frac{\tilde{U}_p}{\tilde{U}_c}\right) = 0, \quad \frac{\partial}{\partial \theta_0}\left(\frac{\tilde{U}_p}{\tilde{U}_c}\right) = 0 \qquad [5.129]$$

Introducing [5.129] and [5.128] we obtain:

$$\left.\begin{aligned} &\frac{\partial \tilde{U}_p}{\partial \theta_0} - \omega^2 \frac{\partial \tilde{U}_c}{\partial \theta_0} = 0 \\ &\frac{\partial \tilde{U}_p}{\partial \psi_0} - \omega^2 \frac{\partial \tilde{U}_c}{\partial \psi_0} = 0 \\ &\frac{\partial \tilde{U}_p}{\partial w_0} - \omega^2 \frac{\partial \tilde{U}_c}{\partial w_0} = 0 \end{aligned}\right\} \qquad [5.130]$$

[5.130] is a set of linear equations in θ_0 , ψ_0 and w_0 with a trivial solution to $\psi_0 = w_0 = \theta_0 = 0$.

To obtain ψ_0, w_0 and α_0 different to zero, the coefficient determinant of the linear system must be equalized to zero:

@Seismicisolation

$$\left.\begin{aligned} D_{11}\alpha_0 + D_{12}\,\psi_0 + D_{13}\,w_0 &= 0 \\ D_{21}\,\alpha_0 + D_{22}\,\psi_0 + D_{23}\,w_0 &= 0 \\ D_{31}\alpha_0 + D_{32}\,\psi_0 + D_{33}\,w_0 &= 0 \end{aligned}\right\} \qquad [5.131]$$

Coefficients D_{ij} are defined as follows:

$$D_{11} = S_{\theta\theta_L} \int_0^L \left(\frac{d\,Y_1}{d\,z}\right)^2 d\,z - \omega^2\, T_{\theta\theta_L} \int_0^L Y_1^2\, d\,z$$

$$D_{12} = D_{21} = S_{\psi\theta_L} \int_0^L Y_2 \left(\frac{d\,Y_1}{d\,z}\right) d\,z + S_{\psi\theta_2} \int_0^L \left(\frac{d\,Y_1}{d\,z}\right)\left(\frac{d\,Y_2}{d\,z}\right) d\,z$$

$$D_{13} = D_{31} = S_{\theta w_L} \int_0^L \left(\frac{d\,Y_1}{d\,z}\right)\left(\frac{d^2\,Y_3}{d\,z^2}\right) d\,z + \omega^2\, T_{ww_2} \int_0^L Y_1\, Y_3\, dz$$

$$D_{22} = S_{\psi\psi_L} \int_0^L \left(\frac{d\,Y_2}{d\,z}\right)^2 d\,z + S_{\psi\psi} \int_0^L Y_2^2\, d\,z$$

$$+ S_{\psi\psi_2} \int_0^L Y_2 \left(\frac{d\,Y_2}{d\,z}\right) d\,z - \omega^2\, T_{\psi\psi_1} \int_0^L Y_2^2\, d\,z$$

$$D_{33} = S_{ww_L} \int_0^L \left(\frac{d^2\,Y_3}{d\,z^2}\right)^2 d\,z - \omega^2\, T_{ww} \int_0^L Y_3^2\, d\,z$$

$$- \omega^2\, T_{ww_L L} \int_0^L \left(\frac{d\,Y_3}{d\,z}\right)^2 d\,z \qquad [5.132]$$

@Seismicisolation

With [5.132] we obtain the eigenfrequency equations under the determinant form:

$$\begin{vmatrix} D_{11} & D_{12} & D_{13} \\ D_{21} & D_{22} & D_{23} \\ D_{31} & D_{32} & D_{33} \end{vmatrix} = 0 \qquad [5.133]$$

If the exact expressions of Y_1 (z), Y_2 (z) and Y_3 (z) are known, introducing them in [5.133] enables us to obtain exact value of ω^2.

In practice, exact expressions of Y_j (z) are not known. If expressions Y_j (z) satisfy the boundary conditions, this gives rise to a solution of eigenfrequencies. This is a well-known property of the Rayleigh-Ritz method.

5.10.4. *Solutions of decoupled equations*

In the case where torsional, bending and warping vibrations are decoupled, components D_{ij} , $i \neq j$ in [5.132] are set to zero. The determinant of the matrix $[D] = (D_{ii})$ gives the following:

– for torsional vibration $(D_{11} = 0)$:

$$\omega_T^2 = \frac{S_{\theta\theta_L} \int_0^L \left(\frac{d\,Y_1}{d\,z} \right)^2 d\,z}{T_{\theta\theta_L} \int_0^L Y_1^2 \, d\,z} \qquad [5.134]$$

– for bending vibrations $(D_{33} = 0)$:

$$\omega_F^2 = \frac{S_{ww_1} \int_0^L \left(\frac{d^2\,Y_3}{d\,z^2} \right)^2 d\,z}{T_{ww} \int_0^L Y_3^2 \, d\,z + T_{ww_L} \int_0^L \left(\frac{d\,Y_3}{d\,z} \right)^2 d\,z} \qquad [5.135]$$

@Seismicisolation

– for longitudinal motions $\left(D_{22} = 0\right)$:

$$\omega_L^2 = \frac{S_{\psi\psi_L} \int_0^L \left(\frac{d\ Y_2}{d\ z}\right)^2 d\ z + S_{\psi\psi} \int_0^L Y_2^2\ d\ z + S_{\psi\psi_2} \int_0^L Y_2\ \frac{d\ Y_2}{dz}\ d\ z}{T_{\psi\psi_L} \int_0^L Y_2^2\ d\ z} \qquad [5.136]$$

The circular frequencies obtained above are independent of the boundary conditions at the rod ends.

5.10.5. *For a very long rod*

For stationary waves:

$$Y_1\ (z) = Y_2\ (z) = Y_3\ (z)$$
$$= \sin \frac{2\ \pi\ z}{\lambda_n} \quad \text{with } \lambda_n = \frac{2\ L}{n} \qquad [5.137]$$

Bringing equation [5.137] into [5.134], [5.135] and [5.136], we obtain the following for eigenvalues for spatial mode n:

$$\omega_{T,n}^2 = \left(\frac{n\ \pi}{L}\right)^2 \frac{S_{\theta\theta_L}}{T_{\theta\theta_L}}$$

$$\omega^2{}_{F,n} = \left(\frac{n\ \pi}{L}\right)^2 \frac{\left(\frac{n\ \pi}{L}\right)^2 S_{ww_L}}{T_{ww} + \left(\frac{n\ \pi}{L}\right)^2 T_{ww_L}} \qquad [5.138]$$

$$\omega_l^2 = \left(\frac{n\ \pi}{l}\right)^2 \left(\frac{S_{\psi\psi_l}}{T_{\psi\psi_l}} + \frac{l^2}{n^2\ \pi^2}\ \frac{S_{\psi\psi_l}}{T_{\psi\psi_l}}\right) \qquad [5.139]$$

@Seismicisolation

$$\omega_{L,n}^2 = \left(\frac{n\,\pi}{L}\right)^2 \left(\frac{S_{\psi\psi_L}}{T_{\psi\psi_L}} + \frac{L^2}{n^2\pi^2}\,\frac{S_{\psi\psi}}{T_{\psi\psi_L}}\right) \qquad [5.140]$$

In equation [5.139] for bending vibrations, only rotational inertia correction is taken into account (Love's theory of bending vibration).

5.11. Dispersion of deviated torsional waves in off-axis anisotropic rods with rectangular cross-section

Here we examine the linear equation system [5.141] with the coefficients defined in [5.132] by setting the determinant of coefficients D_{ij} to zero:

$$|D_{ij}| = 0 \qquad [5.141]$$

Developing [5.133] or [5.141], a sixth order bisquared equation in ω as obtained: $\omega^6\ (1 - \alpha_5\ \alpha_8) - \omega^4\ \left(\omega_L^2 + \omega_F^2 + \omega_T^2 + \alpha_5\ \alpha_8\ \omega_L^2\right)$

$$+\,\omega^2 \left(\omega_L^2\ \omega_T^2 + \omega_F^2\ \omega_T^2 - \omega_L^2\ \omega_F^2 - \alpha_1\ \alpha_4\ \alpha_8 - \alpha_3\ \alpha_2\ \alpha_8 - \alpha_1\ \alpha_3 - \alpha_4\ \alpha_7\right)$$

$$+\,\omega_t^2\ \omega_l^2\ \omega_f^2 - \alpha_4\ \alpha_7\ \omega_T^2 - \alpha_1\ \alpha_3\ \omega_F^2 = 0 \qquad [5.142]$$

The coefficients in [5.142] are defined as below:

$$\alpha_1 = \frac{n\,\pi}{L}\ \frac{S_{\psi\theta_2}}{T_{\theta\theta_1}}$$

$$\alpha_2 = \frac{S_{\psi w_2}}{T_{\theta\theta_2}}$$

$$\alpha_3 = \left(\frac{n\,\pi}{l}\right)^3 \frac{S_{\psi\theta_2}}{T_{\psi\psi_L}}$$

@Seismicisolation

$$\alpha_4 = \left(\frac{n\,\pi}{L}\right) \frac{S_{\psi w_2}}{T_{\psi\psi_L}}$$

$$\alpha_5 = \frac{T_{\psi w_2}}{T_{\theta\theta_L}}$$

$$\alpha_6 = \left(\frac{n\,\pi}{L}\right)^3 \frac{S_{\alpha w_L}}{T_{ww} + \left(\frac{n\,\pi}{L}\right) T_{ww_L}}$$

$$\alpha_7 = \left(\frac{n\,\pi}{L}\right) \frac{S_{\psi w_2}}{T_{ww} + \left(\frac{n\,\pi}{L}\right)^2 T_{ww_L}}$$

$$\alpha_8 = \left(\frac{n\,\pi}{L}\right) \frac{T_{ww_2}}{T_{ww} + \left(\frac{n\,\pi}{L}\right)^2 T_{ww_L}} \qquad [5.143]$$

Introducing non-dimensional variables in [5.143], the following equation is obtained:

$$\left(\frac{v}{v_T}\right)^6 [1 - \alpha_5\,\alpha_8] - \left(\frac{v}{v_t}\right)^4 \left[1 + \frac{v_L^2}{v_T^2} + \frac{v_F^2}{v_T^2} + \frac{\alpha_5\,\alpha_8}{v_T^2}\right]$$

$$+ \left(\frac{v}{v_T}\right)^2 \left[\begin{array}{l} \frac{v_L^2}{v_T} - \frac{v_F^2}{v_T} - \frac{v_L^2\,v_F^2}{v_T^4} - \\ \left(\frac{\alpha_1\,\alpha_3 + \alpha_4\,\alpha_7 - \alpha_2\,\alpha_3\,\alpha_8 - \alpha_1\,\alpha_4\,\alpha_8}{v_T^4}\right) \frac{b^4}{16\bar{k}^4\delta^4} \end{array}\right]$$

@Seismicisolation

$$+\frac{v_L^2}{v_T^2}.\frac{v_F^2}{v_T^2}-\left(\frac{\alpha_4\ \alpha_7}{v_T^4}+\frac{\alpha_1\ \alpha_3\ v_F^2}{v_T^6}\right)\frac{b^4}{16\ \bar{k}^4\delta^4}=0 \qquad [5.144]$$

Dividing all the terms in equation [5.144] by $[1-\alpha_5\ \alpha_8]$, with $\bar{k}=k\ \frac{h}{2}$ (half thickness) of the rod, we get:

$$\left(\frac{v}{v_t}\right)^6-\left(\frac{v}{v_t}\right)^4\ [1-\ \alpha_5\ \alpha_8]^{-1}\left[1+\frac{v_L^2}{v_T^2}+\frac{v_F^2}{v_T^2}+\frac{\alpha_5\ \alpha_8}{v_T^2}\right]$$

$$+\left(\frac{v}{v_t}\right)^2\ [1-\ \alpha_5\ \alpha_8]^{-1}\left\{\begin{array}{l}\left[\frac{v_L^2}{v_T}-\frac{v_F^2}{v_T}-\frac{v_L^2\ v_F^2}{v_T^4}\right]-\\ -\left(\frac{\alpha_1\ \alpha_3+\alpha_4\ \alpha_7-\alpha_2\ \alpha_3\ \alpha_8-\alpha_1\ \alpha_4\ \alpha_8}{v_T^4}\right)\\ \frac{b^4}{16\bar{k}^4\delta^4}\end{array}\right\}$$

$$+[1-\alpha_5\ \alpha_8]^{-1}\left[\begin{array}{l}+\frac{v_L^2}{v_T^2}.\frac{v_F^2}{v_T^2}-\\ \left(\frac{\alpha_4\ \alpha_7}{v_T^4}+\frac{\alpha_1\ \alpha_3\ v_F^2}{v_T^6}\right)\frac{b^4}{16\ \bar{k}^4\delta^4}\end{array}\right]=0 \qquad [5.145]$$

For reasons of convenience, we adopt the following notations:

$$a_1=[1-\ \alpha_5\ \alpha_8]^{-1}\left[1+\frac{v_L^2}{v_T^2}+\frac{v_F^2}{v_T^2}+\frac{\alpha_5\ \alpha_8}{v_T^2}\right]$$

@Seismicisolation

$$a_2 = \left[1 - \alpha_5\ \alpha_8\right]^{-1} \left\{ \begin{array}{l} \left[\dfrac{v_L^2}{v_T} - \dfrac{v_F^2}{v_T} - \dfrac{v_L^2\ v_F^2}{v_T^4} \right] - \\ \\ -\left(\dfrac{\alpha_1\ \alpha_3 + \alpha_4\ \alpha_7 - \alpha_2\ \alpha_3\ \alpha_8 - \alpha_1\ \alpha_4\ \alpha_8}{v_T^4} \right) \dfrac{b^4}{16\bar{k}^4\delta^4} \end{array} \right\}$$

$$a_3 = \left[1 - \alpha_5\ \alpha_8\right]^{-1} \left[\begin{array}{l} + \dfrac{v_L^2}{v_T^2} \cdot \dfrac{v_F^2}{v_T^2} - \\ \\ \left(\dfrac{\alpha_4\ \alpha_7}{v_T^4} + \dfrac{\alpha_1\ \alpha_3\ v_F^2}{v_T^6} \right) \dfrac{b^4}{16\ \bar{k}^4\delta^4} \end{array} \right] \qquad [5.146]$$

The non-dimensional velocity is written as:

$$\left(\frac{v}{v_T}\right)^6 - a_1 \left(\frac{v}{v_T}\right)^4 + a_2 \left(\frac{v}{v_T}\right)^2 + a_3 = 0 \qquad [5.147]$$

or with non-dimensional torsional velocity[13]:

$$\bar{V} = \left(\frac{v}{v_T}\right)^2,\ v_T = \text{torsion velocity at zero frequency}$$

$$\bar{V}^3 - a_1\ \bar{V}^2 + a_2\ \bar{V} + a_3 = 0 \qquad [5.148]$$

This equation admits three real roots $\bar{V}_j$ corresponding to the phase velocity $\bar{C}'_j$ of the three first modes of propagation. A closed-form solution exists for equation [5.148] [MIN 66]. The roots of equation [5.148] are[14]:

13 $\bar{V}$ this notation designates the square of dimensionless velocity.

14 $\bar{V}'_1$, $\bar{V}'_2$, $\bar{V}'_3$ designate the square dimensionless velocities respectively.

@Seismicisolation

$$\bar{C}'_1 = \left\{ \left(\frac{a_1^2}{9} - \frac{a_2}{3} \right)^{1/2} \cos \left[\frac{1}{3} \text{ Arc cos} \left\{ - \frac{a_3 - \frac{a_1\, a_2}{3} + \frac{2\, a_1^3}{27}}{2 \sqrt{- \left[\frac{a_2}{3} - \frac{a_1^2}{9} \right]^3}} \right\} + \frac{2\,\pi}{3} \right] - \frac{a_1}{3} \right\}^{1/2}$$

$$\bar{C}'_2 = \left\{ 2 \left(\frac{a_1^2}{9} - \frac{a_2}{3} \right)^{1/2} \cos \left[\frac{1}{3} \text{ Arc cos} \left\{ - \frac{a_3 - \frac{a_1\, a_2}{3} + \frac{2\, a_1^3}{27}}{2 \sqrt{- \left[\frac{a_2}{3} - \frac{a_1^2}{9} \right]^3}} \right\} + \frac{4\,\pi}{3} \right] - \frac{a_1}{3} \right\}^{1/2}$$

$$\bar{C}'_3 = \left\{ 2 \left(\frac{a_1}{9} - \frac{a_2}{3} \right)^{1/2} \cos \left[\frac{1}{3} \text{ Arc cos} \left\{ - \frac{a_3 - \frac{a_1\, a_2}{3} + \frac{2\, a_1^3}{27}}{2 \sqrt{- \left[\frac{a_2}{3} - \frac{a_1^2}{9} \right]^3}} \right\} \right] - \frac{a_1}{3} \right\}^{1/2}$$

$$\bar{v}'_2 = \left\{ 2 \left(\frac{a_1^2}{9} - \frac{a_2}{3} \right)^{1/2} \cos \left[\frac{1}{3} \text{ Arc cos} \left\{ - \frac{a_3 - \frac{a_1\, a_2}{3} + \frac{2\, a_1^3}{27}}{2 \sqrt{- \left[\frac{a_2}{3} - \frac{a_1^2}{9} \right]^3}} \right\} + \frac{4\,\pi}{3} \right] - \frac{a_1}{3} \right\}^{1/2}$$

$$\bar{v}'_3 = \left\{ 2 \left(\frac{a_1}{9} - \frac{a_2}{3} \right)^{1/2} \cos \left[\frac{1}{3} \text{ Arc cos} \left\{ - \frac{a_3 - \frac{a_1\, a_2}{3} + \frac{2\, a_1^3}{27}}{2 \sqrt{- \left[\frac{a_2}{3} - \frac{a_1^2}{9} \right]^3}} \right\} \right] - \frac{a_1}{3} \right\}^{1/2}$$

[5.149]

@Seismicisolation

5.12. Dispersion curve of torsional phase velocities of an off-axis anisotropic rod

The two parameters retained for the presentation of dispersion curves are:

$$\left.\begin{array}{l} \bar{k} = k\,\dfrac{h}{2} \\ \delta = \dfrac{\text{width}}{\text{thickness}} \text{ flatness of the rod section} \end{array}\right\} \qquad [5.150]$$

Figure 5.19 concerns an artificial composite material (long glass fiber-phenolic resin). For the first branch (first elastodynamic mode) the difference between the dispersion curve of "pure torsion"[15] and curve corresponding to the off-axis rod is weak. The flatness *δ,* defined above, has a strong influence in both cases.

Figure 5.20 shows the second and third branches of the dispersion curves for an off-axis rod (of the same material). There are large discrepancies between the two aforementioned rods (pure torsion and deviated torsion).

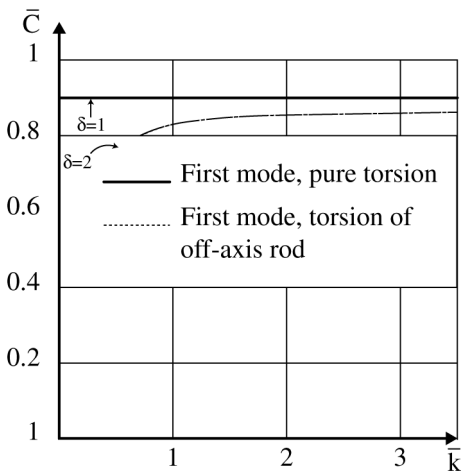

Figure 5.19. *Material: composite glass fiber-polyester resin. First branch of dispersion curves* $\bar{C} = v/v_T$ versus *relative wave number* $\bar{k} = kh/2$. *Curves are dependent on flatness coefficient δ=b/h*

In Appendix 5.H, the curves concerning group velocities are represented.

15 Material axis coincident with the rod axis.

@Seismicisolation

5.13. Concluding remarks

5.13.1. *Characterization of shear moduli and non-diagonal coefficients of a compliance matrix*

Attention is focused on tests at low frequency, for which the Saint-Venant theory of warping is applicable in two cases corresponding to Saint Venant's theory and a more elaborate, higher-order theory using Helmholtz's equation.

5.13.2. *Dispersion of torsional phase velocity*

The dispersion of torsional phase velocity is negligible if the choice of rod cross-section with flatness coefficient $\delta = \frac{\text{b width}}{\text{h thickness}}$ is approaching unity. This is the best choice.

5.13.3. *Saint Venant's warping theory*

Adopting Saint Venant's warping theory and the mechanical effect, such as longitudinal inertia, we obtain a reasonable, tractable theory.

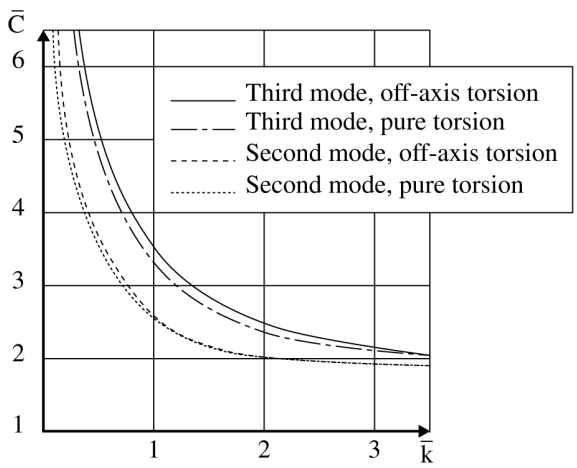

Figure 5.20. *Deviated torsional vibration of an off-axis composite rod. The second and third branches of dispersion curves are represented in comparison with "pure" torsion and deviated torsion for the same material. Flatness δ=2,* $\bar{c} = v/v_T$

@Seismicisolation

5.13.4. *A more elaborate warping theory*

The adoption of a more elaborate warping theory valid for higher elastodynamic modes gives rise to Helmhotz's equation. This equation includes dynamic effect via two coefficients, such as k_1 and k_3 [ONO 78].

5.13.5. *Dispersion of torsional phase velocity*

The dispersion of torsional phase velocity is examined in detail using Onobiono's theory.

5.13.6. *Nugue's theory*

For practical applications in material characterization, Nugue's theory proposes a simpler theory that is applicable at a lower frequency range and uses samples of finite length. The influence of some parameters is examined: flatness coefficient, Young's modulus/shear modulus ratio and rod length.

5.13.7. *Dispersion of phase and group velocities*

This problem, which is neglected in dynamic tests, was wrongfully considered to be academic and inapplicable in practice. When an experimenter wants to characterize a material in a large frequency range, the problem of wave dispersion inevitably has to be solved. The two works presented in this chapter, Nugues's and Onobiono's theories, can be applied in this situation.

For more elaborate theories with higher approximations, readers can go to Chapter 15 in *Mechanical Characterization of Materials and Wave Dispersion*, which examines Touratier's theory using Reissner variational principle with mixed fields.

5.14. Bibliography

[ABA 72] ABACARR. B., CUNIFF P. F., "The vibration of cantilever beam of fibre – reinforced materials", *Journal of Composite Materials*, vol. 6, p.504, 1972.

[BAR 62] BARR A. D. S., "Torsional waves in uniform rods of non circular section", *Journal of Mechanical Engineering Science*, vol. 4, no. 2, p.127-135, 1962.

@Seismicisolation

[BLE 70] BLEUSTEIN J. L., STANLEY R. M., "A dynamical theory of torsion", *International Journal of Solids and Structure*, vol. 6, no.5, p. 569-586, 1970.

[DYM 73] DYM C. L., SHAMES I. H., *Solid Mechanics – A Variational Approach*, McGraw-Hill, New York, 1973.

[ENG 74] ENGSTRÖM O. L., "Dispersion of torsional waves in uniform elastic rods", *Journal of Applied Mechanics*, vol. 41, p. 1041-1046, 1974.

[FRA 69] FRAZER W. B., "Stress wave propagation in rectangular bars", *International Journal of Solids and Structures,* vol. 5, p. 379-397, 1969.

[JOH 71] JOHNSON A. F., *Bending and Torsion of Anisotropic Beams,* National Laboratory England, Report DNAM, March, 1971.

[LEK 63] LEKHNITSKI S. G., *Theory of Anisotropic Body,* Holden Day, San Francisco, 1963.

[LOV 27] LOVE A. E. H., *Mathematical Theory of Elasticity,* Cambridge University Press, fourth edn, p. 171, 1927.

[MED 66] MEDICK M. A., "One dimensional theories of wave propagation and vibrations - In elastic bars of rectangular cross section", *Journal of Applied Mechanics*, vol. 33, no. 3, p. 489-495, 1966.

[MIN 69] MINDLIN R. D., HERMANN G., "A one dimensional theory of compressional waves in elastic rod", *Proc First US Nat Congress of Applied Mechanic*s, p. 187-191, 1969.

[MIN 75] MINDLIN R. D., "Solution of Saint Venant's torsion problem by power series", *International Journal of Solids and Structures*, vol. 11, p. 321-328, 1975.

[MIN 76] MINDLIN R. D., "Low frequency vibrations of elastic bars", *International Journal of Solids and Structures*, vol.12, p. 27-49, 1976.

[MIN 66] MINEUR H., *Techniques de Calcul Numérique*, Dunod, Paris, 1966.

[NIG 66] NIGRO N. J., "Steady state wave propagation in infinite bars of non circular cross section", *Journal of the Acoustical Society of America*, vol. 40, p. 1501-1508, 1966.

[NUG 76] NUGUES M., Elastostatic torsion of a beam of rectangular section in anistropic - material – Dynamic torsion of a anistropic beam with rectangular section, Masters thesis, CNAM Paris, June 29, Paris, 1976.

[ONO 78] ONOBIONO J. O., Dynamic torsion of rod with rectangular section, PhD Thesis, University of Paris (P. and M. Curie), France, 1978.

[POC 1876] POCHHAMMER L., "Über die Fortpflanzungsgeschwindigkeiten kleiner Schwingungen in einem übergrenzten isotropen Kreiszylinder", *Journal für Reine Angewandte Mathematik*, vol. 81, p. 324-336, 1976.

[REI 57] REISSNER E., "On non uniform torsion of cylindrical rods", *Journal of Mathematics and Physics*, vol. 31, p. 214-221, 1957.

@Seismicisolation

[RIT 71] RITCHIE L. G., ROSINGER H. E., "Torsional rigidity of rectangular section bars of orthotropic materials", *Journal of Composite Materials*, vol. 9, no. 2, p. 187-190, 1971.

[SAI 1853] SAINT VENANT B., "Mémoire sur la torsion des prismes", *Mémoires présentés par divers savants à l'Académie des Sciences, Sciences Math et Physique*, vol. 14, vol. 36, p1028-1031, 1853.

[TOU 79] TOURATIER M., Propagation of waves in transverse isotropic in rod with rectangular section, PhD Thesis, University of Paris VI, 1976.

[TOU 77] TOURATIER M., On the propagation of longitudinal waves on rectangular composites rods (Rayleigh waves and wave dispersion), final studies report, October 19, Conservatoire National des Arts et Métiers, Paris, 1977.

[VOI 28] VOIGT H., *Lehrbuch der Kristaphysik*, Leipzig, Berlin, Teubner, 1928.

[VOL 71] VOLTERRA E., GAINES J. H., *Advanced Strength of Materials,* Prentice Hall, New Jersey, 1971.

[VIK 67] VIKTOROV I. A., *Rayleigh and Lamb Waves*, Plenum Press, New York, 1967.

[VIN 76] VINH T., NUGUES N., "Torsional vibration of anisotropic rods with rectangular section", *Comptes Rendus Académie des Sciences*, vol. 283, Series B, p. 289-292, 1976.

[ZIE 73] ZIENKIEWICS C. C., *Finite Element Method,* Ediscience, McGraw-Hill Paris, French edition, 1973.

5.15. Table of symbols

Latin alphabet

b	sample width
$c = \frac{h}{b}\sqrt{\frac{G_{xz}}{G_{yz}}} = \frac{\text{thickness}}{\text{width}}\sqrt{\text{ratio of shear moduli}}$	
$= v/v_T$	non-dimensional torsional velocity
C_T	torsional rod stiffness relating torque T to torsional angle α
$\mathcal{D}$	curve bounding $\mathcal{S}$ area
E_{ii}	Young's modulus for anisotropic material in the direction i
E	Young's modulus of isotropic modulus
G_{ij}	shear modulus (anisotropic material)
G	shear modulus (isotropic material)

@Seismicisolation

h	sample thickness
i, j, k	indexes indicating axis direction
I_a	approximate anisotropic torsional rod stiffness
$I_p = I_1 + I_2$	polar inertia of the section
I_1	flexural quadratic momentum round x
I_2	flexural quadratic momentum round y
J	volume polar inertia of the sample
J_m , J_a	inertias of the mandrel (at the sample middle) and of additional inertia at a free end respectively
k	entire number is series or wave number
$\bar{k}$	dimensionless wave number $\bar{k} = k \frac{h}{2}$
2 L	sample length
m	prescribed torque
M_T	torsion moment
r_a, s_a	parameter introduced in [5D.4]
$\mathcal{S}$	cross-section of sample
S	cross-section of $\mathcal{S}$ area
s	surface variable
v_1, v_2, v_3, v_4	coefficients introduced in [5D.4]
v_T	torsional velocity independent of frequency (sample of circular section) = $[Gxz/\rho]^{1/2}$
v	torsional wave velocity of squared rod
v_L	longitudinal velocity (decoupled wave)
v_R	Rayleigh surface wave velocity
U_p U_c	potential and kinetic energies
u_i	displacement in the direction i
V, v	bounded volume of the sample, volume variable
x, y, z	coordinates, coordinate along rod axis

@Seismicisolation

Greek alphabet

α	unit torsional angle
θ	torsional angle
$\pm j\,\beta_2\ ,\ \beta_1$	roots of bisquared characteristic equation
β_T	parameter in warping expression [5.27] [5.28]
$\pm i\,\beta_2\ ,\ \beta_1$	roots of bisquared characteristic equation

$$\gamma\gamma = \frac{\text{volume inertia of sample}}{\text{additional inertia at free end}}$$

$$\eta_a = \frac{\text{additional inertia at free end}}{\text{volume inertia of sample}}$$

$$\eta_l = \frac{\text{additional inertia}}{\text{volume inertia of sample}}$$

$$\eta_m = \frac{\text{inertia of mandrel in the middle}}{\text{volume inertia of sample}}$$

ψ	Airy's function
ρ	density
Θ	function introduced in [5.54]
ω	circular frequency
ζ	function introduced in [5.48]
$\delta = \frac{b}{h}$	flatness coefficient
ξ	function introduced in [5.48]

5.16. Appendices

Appendix 5.A. Approximate formulae for torsion stiffness

In the technical literature, there are many publications concerning the torsion of a rod with rectangular section. Johnson [JOH 71] examined the static torsion of an anisotropic rod in various situations:

– rod axis coinciding with one symmetry axis of the material;

@Seismicisolation

– off-axis of the material;

– off-axis rod in which coupling between torsion and bending occurs.

In the majority of works, with approximate displacement fields and appropriate stress functions, static rod torsion and variational approaches permit a variety of formulae which deserve reader's attention [ABA 72, RIT 75, SAI 56, VOI 28, VOL 71].

The following formulae are applicable for isotropic materials only. Let us recall *Saint Venant's formulae,* equation [5.27]:

$$C_T = b^3\ h\ G\ \beta_T(c) = b\ h^3\ G\ \beta_T(1/c) \qquad [5.A.1]$$

where G is the shear modulus, b the width and h thickness. c=h/b is reduced to the ratio in [5.26] and β(c) is the sum of the series with odd terms (see details in this chapter):

$$\beta_T(c) = \left[\frac{1}{3} - \frac{64}{\pi^5}\ \frac{1}{c} \sum_{k=1,3,5,\ldots} \frac{1}{k^5}\ \text{tang h}\left(\frac{k\,\pi\,c}{2}\right)\right] \qquad [5.A.2]$$

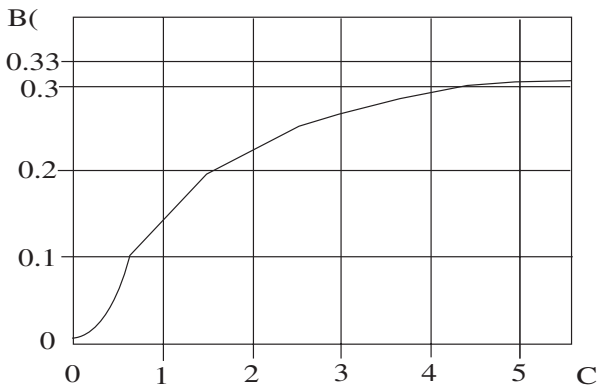

Figure 5.A.1. *Sum of series [5.A.2]* versus *the ratio c*

@Seismicisolation

c	β_T (c)	c	β_T (c)	c	β_T (c)
0	0	1.6	0.203 7	4.0	0.280 8
0.1	0.003 1	1.7	0.210 9	4.5	0.286 6
0.2	0.011 6	1.8	0.217 4	5.0	0.291 3
0.3	0.024 3	1.9	0.223 3	6.0	0.298 3
0.4	0.039 0	2.0	0.228 6	7.0	0.303 3
0.5	0.057 1	2.1	0.233 5	8.0	0.307 0
0.6	0.075 1	2.2	0.238 0	9.0	0.310 0
0.7	0.092 8	2.3	0.242 1	10	0.312 3
0.8	0.109 9	2.4	0.245 9	15	0.319 3
0.9	0.125 8	2.5	0.249 3	20	0.322 8
1.0	0.140 5	2.6	0.252 6	25	0.324 9
1.1	0.154 0	2.7	0.255 5	30	0.326 3
1.2	0.116 1	2.8	0.258 3	40	0.328 0
1.3	0177 0	2.9	0.260 9	50	0.333 3
1.4	0186 9	3.0	0.263 3	100	0.333 3
1.5	.0195 7	3.5	0.273 3	∞	0.333 3

Table 5.A.1. *Sum of series [5.A.2]*

Mindlin [MIN 75] suggested for isotropic materials the following stiffness:

$$C_T = G\,h^3\,b\,\frac{1}{12}\left[1+\lambda-\frac{\left(1-\lambda^2\right)^2\left(7+212\,\lambda^2+7\,\lambda^4\right)}{\left(1+\lambda^2\right)\left(7+121\,\lambda^2+7\,\lambda^4\right)}+7\,\lambda^2\,\frac{\left(13-25\,\lambda^2-25\,\lambda^4+13\,\lambda^6\right)}{\left(1+\lambda^2\right)^2\left(7+121\,\lambda^2+7\,\lambda^4\right)}\right] \qquad [5.A.3]$$

$$\lambda = \frac{b}{h} = 1/c$$

Johnson [JOH 71] proposed many approximations in the static torsion of an anisotropic rod:

@Seismicisolation

$$C_{T_{forced}} = \frac{h\,b^3}{4}\,\frac{M^*}{s_{33}} \text{ forced torsion stiffness} \qquad [5.A.4]$$

$$C_{T_{free}} = \frac{h\,b^3}{s_{33}}\,\frac{M^*}{s_{33}}\,\frac{1}{\left(1 + \frac{3}{4}\,A_{35}^2\,M^*\right)} \text{ free torsion stiffness} \qquad [5.A.5]$$

Forced torsion means that bending is avoided, and free torsion means that torsion and bending are produced.

$$M_1^* = \frac{10}{9}\,\frac{1}{\lambda^2\,A_{44} + B_{55}} \qquad [5.A.6]$$

$$M_3^* = \frac{56\left(9\,\lambda^4\,A_{44}^2 + 9\,B_{55}^2 + 82\,\lambda^2\,A_{44}\,B_{55}\right)}{9\left(\lambda^2\,A_{44} + B_{55}\right)\left[45\left(\lambda^4\,A_{44}^2 + B_{55}^2\right) + 464\,\lambda^2\,A_{44}\,B_{55}\right]} \qquad [5.A.7]$$

M_1^* and M_3^* designate two approximations for moments M^* in equations [5.A.4] and [5.A.5]:

$$A_{35} = \frac{s_{35}}{s_{33}}$$

$$A_{44} = \frac{s_{44}}{s_{33}}, \qquad B_{55} = \frac{s_{55}\,s_{33} - s_{53}\,s_{53}}{s_{33}^2} \qquad [5.A.8]$$

s_{ij} is the compliance component $\lambda = \frac{b}{h}$.

In equation [5.A.8], expressions of A_{44} and B_{44} concern an anistropic rod whose axis is not a symmetry axis of the material. Voigt [VOI 28] proposed:

$$C_T = \frac{h\,b^3}{3}\,\frac{(1 - 0.63\,\lambda)}{s_{55} - 0.63\,\lambda} \qquad [5.A.9]$$

@Seismicisolation

Volterra and Gaines [VOL 71]:

$$C_T = \frac{h\,b^3}{3}\,\frac{\left(1 + J\,\frac{b}{h}\right)}{s_{55} + J\,\frac{b}{h}\,\frac{s_{55}^2}{s_{33}}} \qquad [5.A.10]$$

with

$$J = -0.6274\left(\frac{s_{44}}{s_{55}}\right)^{1/2}\sum_{k=1,3,5}\frac{1}{k^5}\tan h\left[\frac{k\,\pi}{2}\,\frac{b}{h}\left(\frac{s_{55}}{s_{44}}\right)^{1/2}\right] \qquad [5.A.11]$$

Abarcar and Cunniff [ABA 72]:

$$C_T = \frac{h\,b^3}{s_{55}}\left[\frac{1}{3} - \frac{0.6274}{3}\,\frac{1}{C}\sum_{k=1,3,5}\frac{1}{k^5}\tan h\,\frac{k\,\pi\,c}{2}\right] \qquad [5.A.12]$$

$$C = \frac{b}{h}\left(\frac{s_{55}}{s_{44}}\right)^{1/2}$$

with

$$\frac{0.6274}{3} = \frac{64}{\pi^5} \qquad [5.A.13]$$

Appendix 5.B. Equations of torsional motion obtained from Hamilton's variational principle

From Hamilton's variational principle, equations of motion are deduced as Euler equations:

$$\delta\int_{t_0}^{t}\left(U_p - U_c\right)d\,t = \int_{t_0}^{t}\text{(work of applied load or virtual displacement)}\,d\,t \qquad [5.B.1]$$

@Seismicisolation

U_p is potential energy of the rod in the rod volume V:

$$U_p = \frac{1}{2} \int_V \sigma_{ij}\, \varepsilon_{ij}\, d\,v \qquad [5.B.2]$$

U_c is kinetic energy:

$$U_c = \frac{1}{2} \int_v \rho\, \dot{u}_i^2\, d\,v \qquad [5.B.3]$$

From the displacement field in equation [5.17] we obtain the following strain components:

$$\left.\begin{aligned} \varepsilon_{zz} &= \phi_w \frac{\partial \xi}{\partial z} \\ \varepsilon_{xx} &= \varepsilon_{yy} = \gamma_{xy} = 0 \\ \gamma_{zy} &= \xi \frac{\partial \phi_w}{\partial y} + x \frac{\partial \theta}{\partial z} \\ \gamma_{zx} &= \xi \frac{\partial \phi_w}{\partial x}\, \xi - y \frac{\partial \theta}{\partial z} \end{aligned}\right\} \qquad [5.B.4]$$

Adoption of equation [5.48] implies that the cross-section rotates rigidly in its plane without changing shape but is allowed to warp.

This constitutes a simplifying assumption mentioned by Reissner [REI 52], who admitted that shape distortion of the section is possible in the framework of another theory.

The three non-zero stress components, in the case of orthotropic material, are as follows:

@Seismicisolation

$$\left.\begin{aligned} \sigma_{zz} &= \frac{1}{s_{33}}\left(\frac{\partial\,\xi}{\partial\,z}\,\varphi_w\right) \\ \sigma_{yz} &= \frac{1}{s_{44}}\left(+x\,\frac{\partial\,\alpha}{\partial\,z}+\xi\,\frac{\partial\,\varphi_w}{\partial\,y}\right) \\ \sigma_{zx} &= \frac{1}{s_{55}}\left(-y\,\frac{\partial\,\alpha}{\partial\,z}+\xi\,\frac{\partial\,\varphi_w}{\partial\,x}\right) \end{aligned}\right\} \qquad [5.B.5]$$

where S_{33}, $S4_4$ and S_{55} are components of compliance matrix.

Evaluating potential and kinetic energies U_p and U_p from equations [5.B.2] and [5.B.3]:

$$U_p = \int_0^L dz \iint_S \frac{1}{2}\left(\sigma_{zz}\,\varepsilon_{zz}+\sigma_{zx}\,\gamma_{xz}+\sigma_{zy}\,\gamma_{yz}\right) d\,x\,d\,y \qquad [5.B.6]$$

$$U_c = \int_0^L d\,z \iint_S \rho\frac{1}{2}\left(\dot{u}_x^2+\dot{u}_y^2+\dot{u}_z^2\right) d\,x\,d\,y \qquad [5.B.7]$$

The dot over the letter designates the time derivative.

Performing independent variations of the variables in equation [5.48], $\delta\left[\theta\,(z\,,t)\right]$ and $\delta\left[\,\xi\,(\,z\,,t)\right]$ in [5.B.1], we then obtain the following equation of motion:

$$\begin{aligned} &\frac{1}{s_{33}}\,\frac{\partial^2\,\xi}{\partial\,z^2}\iint_S\left(\phi_w^2\,dx\,dy\right)-\rho\,\frac{\partial^2\,\xi}{\partial\,t^2}\iint_S\phi_w^2\,dx\,dy\;- \\ &-\xi\iint_S\left(\frac{1}{s_{55}}\left(\frac{\partial\,\phi_w}{\partial\,x}\right)^2+\frac{1}{s_{44}}\left(\frac{\partial\,\phi_w}{\partial\,y}\right)^2\right)dx\,dy+ \\ &+\frac{d\,\theta}{d\,z}\iint_S\left(\frac{x}{s_{44}}\,\frac{\partial\,\phi_w}{\partial\,y}-\frac{y}{s_{55}}\,\frac{\partial\,\phi_w}{\partial\,x}\right)\,dx\,dy\;=0 \end{aligned} \qquad [5.B.8]$$

@Seismicisolation

$$- \rho I_p \frac{\partial^2 \theta}{\partial t^2} + \frac{\partial^2 \theta}{\partial z^2} \iint_S \left(\frac{y^2}{s_{55}} + \frac{x^2}{s_{44}} \right) dx\, dy +$$

$$+ \frac{\partial \xi}{\partial z} \iint_S \left(\frac{x}{s_{44}} \frac{\partial \varphi_w}{\partial y} - \frac{y}{s_{55}} \frac{\partial \varphi_w}{\partial x} \right) dx\, dy = 0 \qquad [5.B.9]$$

Let us adopt following notations for writing convenience:

$$P_1 = \iint_S \phi_w^2 \, dx\, dy \;,\; P_{21} = \iint_S \left(\frac{\partial \phi_w}{\partial x} \right)^2 dx\, dy \,,$$

$$P_{22} = \iint_S \left(\frac{\partial \phi_w}{\partial y} \right)^2 dx\, dy \;,\; P_{31} = \iint_S y \frac{\partial \phi_w}{\partial x} dx\, dy \;,$$

$$P_{32} = \iint_S x \frac{\partial \phi_w}{\partial y} dx\, dy$$

$$I_p = \iint_S \left(x^2 + y^2 \right) dx\, dy = I_1 + I_2 \;,\; I_1 = \int_S \int y^2 \, dx\, dy \,,$$

$$I_a = \frac{I_2}{s_{44}} + \frac{I_1}{s_{55}} \,,\; K_a = \frac{P_{21}}{s_{55}} + \frac{P_{22}}{s_{44}}$$

$$L_a = \frac{P_{32}}{s_{44}} - \frac{P_{31}}{s_{55}} \qquad [5.B.10]$$

I_a is the approximate anisotropic torsional rod stiffness.

Bringing [5.B.10] into [5.B.9], we obtain:

$$\frac{P_1}{s_{33}} \frac{\partial^2 \xi}{\partial z^2} - \rho P_1 \frac{\partial^2 \xi}{\partial t^2} - K_a \xi + L_a \frac{\partial \theta}{\partial z} = 0$$

$$-\rho I_p \frac{\partial^2 \theta}{\partial t^2} + I_a \frac{\partial^2 \theta}{\partial z^2} - K_a \frac{\partial \xi}{\partial z} = 0 \qquad [5.B.11]$$

@Seismicisolation

The coupling terms K_a and L_a in equation [5.B.11] are defined by the warping function ϕ_w defined by equations [5.11] and boundary condition [5.12].

If we compare [5.B.11] to [5.B.9] we have to demonstrate that $K_a = -L_a$.

5.B.1. *Natural boundary conditions*

By performing independent variations $\delta\alpha$ and $\delta\xi$ in equation [5.B.1], the following natural boundary conditions are obtained:

$$\frac{\partial \xi}{\partial z} = 0 \text{ for } z=0, L \text{ or } \delta\xi = 0 \text{ for } z = 0, L \qquad [5.B.12]$$

$$\frac{\delta\alpha}{\partial z} J_a - K_a \xi = M_T \text{ or } \delta\alpha = 0 \text{ for } z=0,L \qquad [5.B.13]$$

$$K_a = \frac{P_{21}}{s_{55}} + \frac{p_{22}}{s_{44}} = -L_a = -\left(\frac{P_{32}}{s_4} - \frac{P_{31}}{s_{55}}\right)$$

T is the prescribed torque at the end section.

5.B.2. *Demonstration of relation* $K_a = \frac{P_{21}}{s_{55}} + \frac{p_{22}}{s_{44}} = -L_a = -\left(\frac{P_{32}}{s_4} - \frac{P_{31}}{s_{55}}\right)$

Using the last equation [5.B.10] the coupling term Ka, integrating by parts, is given by:

$$\left[K_a = \iint_S \frac{1}{s_{55}}\left(\frac{\partial \phi_w}{\partial x}\right)^2 + \frac{1}{s_{44}}\left(\frac{\partial \phi_w}{\partial x}\right)^2 dx\, dy\right] =$$

$$-\iint_S \phi_w \left(\frac{1}{s_{55}}\frac{\partial^2 \phi_w}{\partial x^2} + \frac{1}{s_{44}}\frac{\partial^2 \phi_w}{\partial y^2}\right) dx\, dy + \qquad [5.B.14]$$

@Seismicisolation

$$+\iint_S \left[\frac{1}{s_{55}} \left(\phi_w \frac{\partial \phi_w}{\partial x} \right)_{,x} + \frac{1}{s_{44}} \left(\phi_w \frac{\partial \phi_w}{\partial y} \right)_{,y} \right] dx\,dy$$

A comma in index followed by a letter (concerning the coordinate) designates derivative with respect to this coordinate. In [5.B.14], taking into account relation [5.11], the first term in the second member is zero; notice that in relation [5.11] for orthotropic materials $G_{xz} = \frac{1}{s_{55}}$ and $G_{yz} = \frac{1}{s_{44}}$. By divergence theorem, [5.B.14] is rewritten for both members:

$$K_a = \int_{\mathfrak{D}} \phi_w \left(\frac{\partial \phi_w}{\partial x} \frac{n_x}{s_{55}} + \frac{\partial \phi_w}{\partial y} \frac{n_y}{s_{44}} \right) ds \qquad [5.B.15]$$

where $n_1 = n_x$, $n_2 = n_y$ and $n_3 = 0$ are direction cosines of the unit vector normal to the lateral surface generated by the curve $\mathfrak{D}$ in plane (x,y) where ds is the elementary length of curve.

On the free boundary representing the lateral surface $\mathfrak{D}$, see [5.12], we have:

$$x = \pm \frac{b}{2} \qquad n_1 = \pm 1 \qquad \frac{\partial \phi_w}{\partial x} = y$$

$$y = \pm \frac{h}{2} \qquad n_2 = \pm 1 \qquad \frac{\partial \phi_w}{\partial y} = -x \qquad [5.B.16]$$

so the second member of [5.B.16] is rewritten as:

$$K_a = \int_{\mathfrak{D}} \phi_w \left(\frac{y}{s_{55}} n_x - \frac{x}{s_{44}} n_y \right) ds \qquad [5.B.17]$$

Using divergence's theorem and taking into account the last equation in [5.B.10], [5.B.16] is rewritten as:

$$K_a = \iint_S \left(\frac{y}{s_{55}} \frac{\partial \phi_w}{\partial x} - \frac{x}{s_{44}} \frac{\partial \phi_w}{\partial y} \right) ds = -L_a \qquad [5.B.18]$$

@Seismicisolation

Equality $C_T = (I_a - K_a)$ where I_a and K_a are given in last equations [5.B.10];

$$I_a = \frac{I_2}{s_{44}} + \frac{I_1}{s_{55}} = \iint_S \frac{y^2}{S_{44}}\, dx\, dy + \iint_S \frac{x^2}{S_{55}}\, dx\, dy;$$

$$K_a = \frac{P_{21}}{s_{55}} + \frac{P_{22}}{s_{44}}$$

$$= \iint_S \frac{1}{s_{55}}\left(\frac{\partial \phi_w}{\partial x}\right)^2 dx\, dy + \iint_S \frac{1}{s_{44}}\left(\frac{\partial \phi_w}{\partial y}\right)^2 dx\, dy \qquad [5.B.19]$$

With the static fields defined by equations [5.4], [5.6], [5.7], [5.8] and [5.9], let us evaluate the torque M_T around z axis defined by [5.22].

$$M_T = \iint_S \left(x\, \sigma_{yz} - y\, \sigma_{xz} \right) dx\, dy$$

$$= \alpha \iint_S \left[\frac{x}{s_{44}}\left(x + \frac{\partial \phi_w}{\partial y} \right) - \frac{y}{s_{55}}\left(-y + \frac{\partial \phi_w}{\partial x} \right) \right] dx\, dy$$

$$M_T = \alpha \left\{ \left[\begin{array}{l} \iint_S \left(\frac{x^2}{s_{44}} + \frac{y^2}{s_{55}} \right) dx\, dy + \\ \iint_S \left(\frac{x}{s_{44}} \frac{\partial \phi_w}{\partial y} - \frac{y}{s_{55}} \frac{\partial \phi_w}{\partial x} \right) dx\, dy \end{array} \right] \right\} \qquad [5.B.20]$$

in which $\alpha = \dfrac{\partial \theta}{\partial z}$ is the unitary torsion angle.

By identification we obtain using [5.B.10]

$$M_T = \alpha \left(I_a + L_a \right) \qquad [5.B.21]$$

@Seismicisolation

The equality

$$K_a = - L_a$$

is demonstrated by equations [5.B.14] to [5.B.17];

So the torque M_T is written as:

$$M_T = \alpha \left(I_a - K_a\right) = \alpha\, C_T \qquad [5.B.22]$$

Appendix 5.C. Extension of Barr's correcting coefficient in equations of motion

Barr [BAR 62] introduced coefficient η in equations of motion for isotropic materials. Here the material is supposed to be anisotropic (transverse isotropic in the section):

$$\left(\frac{\rho^2\, I_p\, P_l}{K_a}\right) \frac{\partial^4\, \theta}{\partial\, t^4} + \eta^2 \left(\frac{P_l\, I_a}{s_{33}\, K_a}\right) \frac{\partial^2\, \theta}{\partial\, z^4}$$

$$- \left[\frac{\rho\, P_l\, I_p}{s_{33}\, K_a} + \eta^2\, \frac{\rho\, P_l\, I_a}{K_a}\right] \frac{\partial^4\, \theta}{\partial\, t^2\, d\, z^2} \qquad [5.C.1]$$

$$+ \rho\, I\, \frac{\partial^2\, \theta}{\partial\, t^2} - \left(I_a - K_a\right) \frac{\partial^2\, \theta}{\partial\, z^2} = 0$$

For an isotropic material, empirical Barr's correcting coefficient $\eta^2 = 0.86$.

This permits us to calculate phase velocity tending to the Rayleigh surface wave velocity when the frequency goes to infinity.

This coefficient was proven to be valid by Engström [ENG 74]. [ENG 74] is used for a long rod.

For a given anisotropic material, coefficient η^2 must be eventually be evaluated through experiments on rods with differing lengths.

@Seismicisolation

Appendix 5.D. Details on coefficient calculations for θ (z, t) and $\xi(z,t)$

5.D.1. *Relations between two sets of coefficients*

Introducing equations [5.54] and [5.57] into [5.49] we obtain:

$$\rho\, I_p \omega^2\, \Theta + I_a \frac{\partial^2 \Theta}{\partial z^2} - K_a \frac{\partial Z}{\partial z} = 0 \qquad [5.D.1]$$

By dividing all the terms in [5.D.1] by C_T / L^2 we obtain:

$$\frac{\rho\, I_p\, \omega^2\, L^2}{C_T}\, \Theta + \frac{I_a\, L^2}{C_T} \frac{\partial^2\, \Theta}{\partial\, z^2} - \frac{K_a\, L^2}{C_T} \frac{\partial\, Z}{\partial\, z} = 0 \qquad [5.D.2]$$

with the parameters v_1, v_2, v_3 and v_4 in [5.58], equation [5.D.2] has the following form:

$$v_1\, \Theta + L^2\, v_4 \frac{\partial^2\, \Theta}{\partial\, z^2} - L^2\, (v_4 - 1) \frac{\partial\, Z}{\partial\, z} = 0 \qquad [5.D.3]$$

Equation [5.D.3] relates variable Θ to Z as follows:

$$A_b = B_a \frac{v_1 + v_4\, \beta_1^2}{\beta_1\, L\, (v_4 - 1)}, \quad B_b = A_a \frac{v_1 + v_4\, \beta_1^2}{\beta_1\, L\, (v_4 - 1)}$$

$$C_b = -D_a \frac{(v_1 - v_4\, \beta_2^2)}{\beta_2\, L\, (v_4 - 1)}, \quad D_b = C_a \frac{(v_1 - v_4\, \beta_2^2)}{\beta_2\, L\, (v_4 - 1)}$$

or:

$$A_b = r_a\, B_a, \qquad B_b = r_a\, A_a \qquad [5.D.4]$$

$$C_b = -s_a\, D_a, \qquad D_b = s_a\, C_a$$

@Seismicisolation

In [5.D.4], β_1 and β_2 are the two roots of characteristic equation [5.104].

5.D.2. *Equations in A_a, B_a, C_a and D_a deduced from the four boundary conditions*

Equation [5.D.4] has proven to be convenient for expressing coefficients with index b as functions of a coefficient with index a. The following two coefficients concern non-dimensional polar inertia at the free end of the rod and polar inertia of the mandrel in the middle.

$$\eta_a = \frac{J_a}{\rho\, I_p\, L} = \frac{1}{\gamma} \qquad \eta_m = \frac{J_m}{\rho\, I_p\, L} \qquad [5.D.5]$$

(m) (n)

The denominators of η_l and η_m in equations [5.D.5] represent the polar inertia of half the rod. γ is already used in the elementary equation of torsional motion, presented in equations [5.43] and [5.44].

For z = L the prescribed torque T in [5.B.13] at the end z =L of sample is $-J_a \dfrac{\partial^2\theta}{\partial t^2}$, so:

$$\eta_a \frac{v_1}{L\, v_4} \Theta = \left(\frac{\partial \Theta}{\partial z} - Z \frac{v_4 - 1}{v_4} \right) \text{ (prescribed torque at free end)}$$

$$\frac{\partial Z}{\partial z} = 0 \text{ (no warping stress)} \qquad [5.D.6]$$

For z = 0:

$$-\eta_m \frac{v_1}{v_4\, L} \Theta = 2 \left[\frac{\partial \Theta}{\partial z} - Z \frac{v_4 - 1}{v_4} \right] \qquad [5.D.7]$$

Bringing equations [5.62] and [5.68] into [5.D.6] and [5.D.7], the following set of equations are obtained:

@Seismicisolation

$$A_a \left[-\frac{\eta_a}{v_4} \frac{v_1}{L} \cos h\, \beta_1 + \sin h\, \beta_1 \left(\frac{\beta_1}{L} - \frac{v_4 - 1}{v_4} r_a \right) \right] +$$

$$B_a \left[-\frac{\eta_a}{v_4} \frac{v_1}{L} \sin h\, \beta_1 + \cos h\, \beta_1 \left(\frac{\beta_1}{L} - \frac{(v_4 - 1)}{v_4} r_a \right) \right] +$$

$$C_a \left[-\frac{\eta_a}{v_4} \frac{v_1}{L} \cos \beta_2 - \sin \beta_2 \left(\frac{\beta_2}{L} + \frac{v_4 - 1}{v_4} s_a \right) \right] +$$

$$D_a \left[-\frac{\eta_a}{v_4} \frac{v_1}{L} \sin \beta_2 + \cos \beta_2 \left(\frac{\beta_2}{L} + \frac{v_4 - 1}{v_4} s_a \right) \right] = 0$$

$$\begin{aligned} A_a\, r_a\, \beta_1 \cos h\, \beta_1 & \\ & + B_a\, r_a\, \beta_1 \sin h\, \beta_1 \\ & + C_a\, s_a\, \beta_2 \cos h\, \beta_2 \\ & + D_a\, s_a\, \beta_2 \sin h\, \beta_2 = 0 \end{aligned}$$

$$A_a \left[-\frac{\eta_m\, v_1}{v_4\, L} \right] - 2\, B_a \left[\frac{\beta_1}{L} - \frac{v_4 - 1}{v_4} r_a \right]$$

$$-2\, D_a \left[\frac{\beta_2}{L} + \frac{v_4 - 1}{v_4} s_a \right] + C_a \left[-\frac{\eta_m\, v_1}{v_4\, L} \right] = 0$$

$$B_a\, r_a - D_a\, s_a = 0 \qquad [5.D.8]$$

The four equations in [5.D.8] permit us to establish the determinant of coefficients of A_a, B_a, C_a and D_a, presented under matricial form.

@Seismicisolation

$$\begin{bmatrix} 0 & \dfrac{v_1 + v_4\beta_1^2}{\beta_1} & 0 & -\dfrac{v_1 - v_4\beta_2^2}{\beta_2} \\ \eta_m & -\dfrac{2}{\beta_1} & \eta_m & \dfrac{2}{\beta_2} \\ \left(v_1+v_4\beta_1^2\right)\cosh\beta_1 & \left(v_1+v_4\beta_1^2\right)\sinh\beta_1 & \left(v_1-v_4\beta_2^2\right)\cos\beta_2 & \left(v_1-v_4\beta_2^2\right)\sin\beta_2 \\ \left(\eta_a\cos h\,\beta_1 + \dfrac{\sinh\beta_1}{\beta_1}\right) & \left(\eta a\sinh\beta_1 + \dfrac{\cos h\,\beta_1}{\beta_1}\right) & \left(\eta a\cos\beta_2 + \dfrac{\sin\beta_2}{\beta_2}\right) & \left(\eta a\sin\beta_2 - \dfrac{\cos\beta_2}{\beta_2}\right) \end{bmatrix} = 0$$

[5.D.9]

By setting this determinant to zero, we obtain the characteristic equation in β_1 and β_2. There are two unknowns – β_1 and β_2 – but the sum of the squares of β_1 and β_2 in a bisquared equation is:

$$\beta_1^2 + (j\,\beta_2)^2 = \beta_1^2 - \beta_2^2 = \frac{v_4 - 1}{v_2\ v_3\ v_4} - \frac{v_1\ v_2\ (v_3 + v_4)}{v_2\ v_3\ v_4} \qquad [5.D.10]$$

and the product is:

$$\left(\beta_1^2\right)\left(j\,\beta_2^2\right) = -\,\beta_1^2\ \beta_2^2 = -\,v_1\left[\frac{v_4 - 1}{v_2\ v_3\ v_4} - \frac{v_1\ v_2}{v_2\ v_3\ v_4}\right] \qquad [5.D.11]$$

[5.D.9] [5.D.10] and [5.D.11] are three equations in β_1, β_2 and v_1. The following notations are adopted to simplify the writing of these equations:

$$S_1 = v_2\ v_3\ v_4\,,\ S_2 = \frac{v_4 - 1}{S_1}\,,\ S_3 = \frac{v_2}{S_1}\,,\ S_4 = \frac{v_2\ (v_3 + v_4)}{S_1} \qquad [5.D.12]$$

Eliminating β_1, we obtain:

$$v_1^2\ S_3 - v_1\ \left(S_2 + \beta_2^2\ S_4\right) + \left(\beta_2^4 + S_2\ \beta_2^2\right) = 0 \qquad [5.D.13]$$

Effecting [5.D.9] and eliminating β_1, a new equation in $v_1$and v_2 is obtained.

@Seismicisolation

$$\frac{-2\,\eta a}{\left[v_1\,\left(S_2 - v_1\,S_3\right)\right]^{1/2}}\left[v_1^2 + v_4\,v_1\,\left(S_2 - v_4\,v_1\right) - v_4^2\,v_1\,\left(S_2 - v_1\,S_3\right)\right]$$

$$+\sin\beta_2\,\cosh\left[\beta_2^2 + S_2 - v_1\,S_4\right]^{1/2}$$

$$\bullet v_4\sqrt{\Delta}\,\frac{\left(2 - \eta a\eta_m\beta_2^2\right)\left[v_1 + v_4\,\left(\beta_2^2 + S_2 - v_4\,S_4\right)\right]}{\beta_2\,\left[v_1\,\left(S_2 - v_1\,v_1\,S_3\right)\right]^{1/2}}$$

$$-\sin\beta_2\,\sin h\left[\beta_2^2 + S_2 - v_1\,S_4\right]^{1/2}$$

$$x\,\frac{\left[\eta a\,\left(S_2 - v_1\,S_4\right)\right]\left[v_1^2 + v_4\,v_1\,\left(S_2 - v_1\,S_4\right) - v_4^2\,v_1\,\left(S_2 - v_1\,S_4\right)\right]}{v_1\,\left(S_2 - v_1\,S_3\right)}$$

$$-\cos\,\beta_2\,\sin h\left[\beta_2^2 + S_2 - v_1\,S_4\right]^{1/2}$$

$$x\,\frac{\left(v_1 - v_4\right)\beta_2^2 \bullet \sqrt{\Delta}\,v_4\left[2 + \eta_a\,\eta_m\,\left(\beta_2^2 + S_2 - v_1\,S_4\right)\right]}{\left[v_1\,\left(S_2 - v_1\,S_3\right)\right]^{1/2}\,\left[\beta_2 - S_2 - v_1\,S_4\right]^{1/2}}$$

$$-\cos\,\beta_2\,\cos h\left[\beta_2^2 + S_2 - v_1\,S_4\right]^{1/2}$$

$$\left\{\begin{array}{l}\dfrac{2\,\eta_m\,v_4^2\,\Delta}{\left[v_1\,\left(S_2 - v_1\,S_3\right)\right]^{1/2}} \\[2ex] + \dfrac{\eta_a\left[2\,v_1^2 + v_1\,v_4\,\left(S_2 - v_1\,S_4\right) + v_4^2\,\left(\beta_2^4 + \left(\beta_2^2 + S_2 - v_1\,S_4\right)\right)^2\right]}{\left[v_1\,\left(S_2 - v_1\,S_3\right)\right]^{1/2}}\end{array}\right\} = 0$$

[5.D.14]

@Seismicisolation

Equations [5.D.14] and [5.D.13] constitute a set whose unknowns are v_1 and β_2. It is possible to solve those equations to obtain v_1 and β, however the calculations are tedious. It is better to solve them numerically.

In Chapter 7 of the other book[16], this problem will be discussed for practical applications.

Appendix 5.E. A simpler solution to the problem analyzed in Appendix 5.D

When calculating coefficients we can adopt inertia for the mandrel in which the sample is attached in the middle, that is larger than the sample inertia, see Figure 5.6. This is a simple solution that is easily satisfied so that the inequality:

$$\frac{1}{\eta_m} = \frac{\rho\, I_p\, L}{J_m} << 1 \qquad [5.E.1]$$

is satisfied.

Returning to equation [5.D.8], the third equation is reduced to:

$$A_b + C_b = 0 \qquad [5.E.2]$$

For convenience when writing, determinant [5.D.9] is rewritten with r and s, presented is in equation [5.D.4]. The first, third and fourth equations in [5.D.8] remain unchanged. Only the third equation is replaced by [5.E.2], so we obtain the following determinant governing the vector (B_a, A_a, D_a, C_a):

$$\begin{bmatrix} 1 & 0 & 1 & 0 \\ 0 & r & 0 & -s \\ \left(\eta_a \cos h\, \beta_1 + \frac{\sin h\, \beta_1}{\beta_1}\right) & \left(\eta_a \sin h\, \beta_1 + \frac{\cos h\, \beta_1}{\beta_1}\right) & \left(\eta_a \cos\, \beta_2 + \frac{\sin \beta_2}{\beta_2}\right) & \left(\eta_a \sin\, \beta_2 - \frac{\cos\, \beta_2}{\beta_2}\right) \\ r\, \beta_1 \cos h\, \beta_1 & r\, \beta_1 \sin h\, \beta_1 & s\, \beta_2 \cos \beta_2 & s\, \beta_2 \sin \beta_2 \end{bmatrix} = 0$$

[5.E.3]

16 *Characterization of Materials and Wave Dipersion.*

@Seismicisolation

Subtracting the third column from the first column term-by-term, we obtain a matrix with a second row of three zeros.

The development of this matrix then permits us to obtain a 3 x 3 matrix whose determinant is:

$$\begin{bmatrix} r & 0 & -s \\ \eta_a \sin h\, \beta_1 + \dfrac{\cos h\, \beta_1}{\beta_1} & \begin{bmatrix} (\cos \beta_2)\, \eta_1 + \dfrac{1}{\beta_2} \sin \beta_2 \\ -\eta_a \cos h\, \beta_1 - \dfrac{1}{\beta_1} \sin h\, \beta_1 \end{bmatrix} & \left[\eta_a \sin \beta_2 - \dfrac{\cos \beta_2}{\beta_2}\right] \\ r\, \beta_1 \sin h\, \beta_1 & \left[s\, \beta_2 \cos \beta_2 - r\, \beta_1 \cos h\, \beta_1\right] & s\, \beta_2 \sin \beta_2 \end{bmatrix} = 0$$

[5.E.4]

The final equation giving eigenvalues, after devising [5.E.4] by $\cos h\, \beta_1 \cos \beta_2$ is:

$$\frac{2\, s\, r}{\cos h\, \beta_1 \cos \beta_2} + \text{tang}\, \beta_2 \left[- rs\, \eta_a\, \beta_2 + rs \left(\frac{\beta_1}{\beta_2} - \frac{\beta_2}{\beta_1} \right) \text{tang}\, h\, \beta_1 + r^2\, \beta_1\, \eta_a \right]$$

$$+ \left[\left(sr\, \beta_1\, \eta_1 - s^2\, \beta_2\, \eta_a \right) \text{tang}\, h\, \beta_1 - \left(\frac{s^2\, \beta_2}{\beta_1} - \frac{r^2\, \beta_1}{\beta_2} \right) \right] = 0 \qquad [5.E.5]$$

5.E.1. ***Remarks***

Elementary Saint Venant's theory presented in section 5.2.5 can be recognized in equation [5.E.4], in which all the terms in $\cos h\, \beta_1$ and $\sin h\, \beta_1$ are suppressed.

If warping is not taken into consideration in the expression of Z (z), r and s are set to zero, we then obtain:

$$\eta_a \sin \beta_2 - \frac{\cos \beta_2}{\beta_2} = 0$$

@Seismicisolation

or $$\beta_2 \text{ tang } \beta_2 = \frac{1}{\eta_a} \qquad [5.E.6]$$

This is equation [5.43], in which we set:

$$\beta_2 = \delta \text{ and } \frac{1}{\eta} = \gamma$$

For calculations, β_1 is the principal unknown and β_2 is related to β_1 by equation [5.D.11] in Appendix 5.D.

Appendix 5.F. Onobiono's and Zienkievics' solutions using finite element method for warping function ϕ

The solution for ϕ is obtained via Hamilton's principle [5.29].

The first step in the calculation concerns the explicit expression of potential energy U_p (equation [5.28]) and kinetic energy [5.B.3] taking into account the displacement field [5.48]:

$$\begin{cases} u(z,t) = -\theta(z,t)\, y \\ v(z,t) = \theta(z,t)\, x \\ w(z,t) = \psi(z,t)\, \phi(x,y) \end{cases}$$

U_c depends on the displacement field only:

$$U_c = \int_0^L dz \iint_S \frac{1}{2} \rho \left[\left(x^2 + y^2\right) \left(\frac{\partial \theta}{\partial t}\right)^2 + \phi^2 (x, y) \left(\frac{\partial \psi}{\partial t}\right)^2 \right] dx\, dy \qquad [5.F.1]$$

For potential energy, the calculation from [5.28] is more complex:

@Seismicisolation

$$U_p = \int_0^L dz \iint_S \frac{1}{2} \left\{ \begin{array}{l} C_{33}\ \phi^2 \left(\frac{\partial \psi}{\partial z}\right)^2 + C_{44} \left(\psi \frac{\partial \phi}{\partial y} + x \frac{\partial \theta}{\partial z}\right)^2 + \\ + C_{55} \left(\psi \frac{\partial \phi}{\partial x} - y \frac{\partial \theta}{\partial z}\right)^2 + \\ + 2C_{34} \left(\phi \frac{\partial \psi}{\partial z}\right)\left(\psi \frac{\partial \phi}{\partial y} + x \frac{\partial \theta}{\partial z}\right) + \\ + 2C_{35} \left(\phi \frac{\partial \psi}{\partial z}\right)\left(\psi \frac{\partial \phi}{\partial x} - y \frac{\partial \theta}{\partial z}\right) + \\ + 2C_{45} \left(\psi \frac{\partial \phi}{\partial y} + x \frac{\partial \theta}{\partial z}\right)\left(\psi \frac{\partial \phi}{\partial x} - y \frac{\partial \theta}{\partial z}\right) \end{array} \right\} dx\, dy$$

[5.F.2]

Variational calculation effected on Hamilton's principle permits us to obtain the following Helmholtz's equation in the case of orthotropic materials or a symmetric beam:

$$C_{55} \frac{\partial^2 \phi}{\partial x^2} + C_{44} \frac{\partial^2 \phi}{\partial y^2} = k_1\ \phi \text{ in S} \qquad [5.F.3]$$

S is the cross-section area of the rod and a second equation in ϕ on the boundary ∂S is:

$$C_{55} \left(\frac{\partial \phi}{\partial x} - k_3\ y\right) n_x + C_{44} \left(\frac{\partial \phi}{\partial y} + k_3\ x\right) n_y = 0 \text{ on } \partial S \qquad [5.F.4]$$

k_1 and k_3, [5.F.3] and [5.F.4] are defined in equations [5.88] and [5.89] respectively. Notice that in general case of anisotropic materials, equations [5.F.3] and [5.F.4] become:

@Seismicisolation

$$C_{55}\ \frac{\partial^2\phi}{\partial x^2} + C_{44}\ \frac{\partial^2\phi}{\partial y^2} + 2C_{45}\ \frac{\partial^2\phi}{\partial x\partial y} = k_1\ \phi + k_4(yC_{35} + xC_{34})\ \text{ on S}$$

With boundary conditions

$$\left[C_{55}\left(\frac{\partial\phi}{\partial x} - k_3\ y\right) + k_2C_{35}\phi\right]n_x + \left[C_{44}\left(\frac{\partial\phi}{\partial y} + k_3\ x\right) + k_2C_{34}\phi\right]\ n_y = 0\ \text{ on } \partial S$$

k_2 and k_4 are defined in the following relations:

$$k_2 = \frac{\int_0^L \psi \frac{\partial\ \psi}{\partial\ z}\ d\ z}{\int_0^L \psi^2 d\ z}$$

$$k_4 = \frac{\int_0^L \frac{\partial\ \psi}{\partial\ z}\frac{\partial\ \theta}{\partial\ z}\ dz}{\int_0^L \psi^2 d\ z}$$

5.F.1. *Functionals L*

In the case of orthotropic materials or a symmetric beam, from equations [5.F.3] and [5.F.4] Onobiono suggests using a functional that is a linear combination of those equations.

$$L\ (\phi) = k_1^{'}\ S_{\psi\psi_L}\ (\phi) + S_{\psi\psi}\ (\phi) + 2\ k_3\ S_{\psi\theta_L}\ (\phi) \qquad [5.F.5]$$

in which $k_1^{'} = k_1 / C_{33}$. It can be shown that equations [5.F.3] and [5.F.4] are equivalent to the function [5.F.5] if the last one is stationary.

$$L\ (\phi) = k_1 \iint_S \phi^2\ dx\ dy + \iint_S \left[C_{55}\left(\frac{\partial\phi}{\partial x}\right)^2 + C_{44}\left(\frac{\partial\phi}{\partial y}\right)^2\right] dx\ dy$$

$$+ 2\ k_3 \iint_S \left(C_{44}\ x\ \frac{\partial\phi}{\partial y} - C_{55}\ y\ \frac{\partial\phi}{\partial x}\right) dx\ dy \qquad [5.F.6]$$

@Seismicisolation

5.F.2. *Approximate solution*

A truncated double power series is used:

$$\phi\ (x,y) = \sum_{n=0}^{N} \sum_{m=0}^{N} e_{nm}\ x^{n}\ y^{m} \qquad [5.F.7]$$

In equation [5.F.6], the expressions for ϕ^2, $\frac{\partial \phi}{\partial x}$ and $\frac{\partial \phi}{\partial y}$ must be evaluated from equation [5F.7].

With the convention:

$$\sum_{n=0}^{N} \sum_{m=0}^{N} = \sum_{n,m}^{N}$$

the following expressions are obtained:

$$\phi^2\ (x\ ,\ y) = \sum_{n,m=0}^{N} \sum_{p,q=0}^{N} e_{nm}\ e_{pq}\ x^{n+p}\ y^{m+q} \qquad [5.F.8]$$

$$\frac{\partial \phi}{\partial x} = \sum_{n,m=0}^{N} n\, e_{nm}\ x^{n-1}\ y^{m} \qquad [5.F.9]$$

$$\frac{\partial \phi}{\partial y} = \sum_{n,m=0}^{N} m\, e_{nm}\ x^{n}\ y^{m-1} \qquad [5.F.10]$$

$$\left(\frac{\partial \phi}{\partial x}\right)^2 = \sum_{n,m=0}^{N} \sum_{p,q=0}^{N} n\, p\, e_{nm}\ e_{pq}\ x^{n+p-2}\ y^{m+q}$$

$$\left(\frac{\partial \phi}{\partial y}\right)^2 = \sum_{n,m=0}^{N} \sum_{p,q=0}^{N} m\, q\, e_{nm}\ e_{pq}\ x^{n+p}\ y^{m+q-2} \qquad [5.F.11]$$

@Seismicisolation

$$\iint_S \phi^2 \, dx\, dy = \sum_{n,m=0}^{N} \sum_{p,q=0}^{N} e_{nm} \; e_{pq} \; I_{n+p,\, m+q} \qquad [5.F.12]$$

$$\iint_S \left(C_{55} \left(\frac{\partial \phi}{\partial x} \right)^2 + C_{44} \left(\frac{\partial \phi}{\partial y} \right)^2 \right) dx\, dy =$$

$$= \sum_{n,m=0}^{N} \sum_{p,q=0}^{N} n\, p\, C_{55} \; e_{nm} \; e_{pq} \; I_{n+p-2,m+q} + \sum_{n,m=0}^{N} \sum_{p,q=0}^{N} m\, q\, C_{44} \; e_{nm} \; e_{pq} \; I_{n+p,m+q-2}$$

[5.F.13]

$$\iint_S \left(C_{44} \; x \frac{\partial \phi}{\partial y} - C_{55} y \frac{\partial \phi}{\partial y} \right) dx\, dy =$$

$$= \sum_{n,m=0}^{N} \left(m \; C_{44} \; e_{nm} \; I_{n+1,m-1} - n\, C_{55} \; e_{nm} \; I_{n-1,m+1} \right) \qquad [5.F.14]$$

with:

$$I_{n,m} = \iint_S x^n y^m dx\, dy = 4 \int_0^h \int_0^b x^n y^m dx dy = \frac{4\, h^{n+1} \; b^{m+1}}{(m+1)(n+1)} \qquad [5.F.15]$$

where h and b designate the thickness and the width of the rod respectively.

Finally, function L (ϕ) is obtained as:

$$L\,(\phi) = k_1 \sum_{n,m=0}^{N} \sum_{p,q=0}^{N} e_{nm} \; e_{pq} \; I_{n+p\,,\, m+q} + \sum_{n,m=0}^{N} \sum_{p,q=0}^{N} n\, p\, C_{55} \; e_{nm} \; e_{pq} \; I_{n+p-2,m+q} +$$

$$+ \sum_{n,m=0}^{N} \sum_{p,q=0}^{N} mq\, C_{44} \; e_{nm} \; e_{pq} \; I_{n+p,\, m+q-2} +$$

$$+ 2\, k_3 \sum_{n,m=0}^{N} e_{nm} \left(m\, C_{44} \; I_{n+1,\, m-1} - n\, C_{55} \; I_{n-1,m+1} \right)$$

[5.F.16]

@Seismicisolation

I_{nm} in equation [5.F.15] is a parameter obtained by calculation of [5.F.15]. After truncating the series in [5.F.7], the number of terms being fixed, stationarity of L (ø) is effected by the variable set of coefficients e_{nm}:

$$\frac{\partial L}{\partial e_{nm}} = 0\,,\ \ m, n = 0, 1, 2, \ldots, N \qquad [5.F.17]$$

Effecting [5.F.17], we obtain a set of linear equations in e_{nm}. Solving this system, the set e_{nm} is determined.

Warping function ø (x, y) can be evaluated as a function of k_1' and k_2.

5.F.3. *Second method of Φ evaluation by finite elements*

This method is the functional minimization method was suggested by Zienkiewicz.

The calculations are made in a quadrant of cross-section S and in the whole section. Antisymmetry considerations are referred to so as to complete the curve ø.

The quadrant is divided into rectangular elements:

$$x = x_i = \frac{1}{2}\,\frac{b\,(i-1)}{n} \quad i = 1, 2, \ldots, n_1 + 1 \qquad [5.F.18]$$

$$y = y_i = \frac{1}{2}\,\frac{b\,(j-1)}{n_2} \quad j = 1, 2, \ldots, n_2 + 1 \qquad [5.F.19]$$

where n_1 and n_2 are the number of intervals in directions x and y respectively.

Each rectangle defined above is divided into two triangles by a line joining the points (x_i, y_i) (x_{i+1}, y_{+1}). $N = n_1$, where n_2 is the number of nodes. The nodes situated on the axes x and y are excluded. We then number each node in the quadrant:

$$r = r\,(x_i, y_j) = i + (n_2 + 1 - j)\,(n_1 + 1) \qquad [5.F.20]$$

@Seismicisolation

The functional $L(\phi)$ is defined as:

$$L(\phi) = 4\left\{\sum_{r=1}^{M}\sum_{s=1}^{M}\frac{1}{2}A_{rs}\,\phi_r\,\phi_s + \sum_{r=1}^{M} B_r\,\phi_r\right\} \qquad [5.F.21]$$

The stationary condition is:

$$\sum A_{rs}\,\varnothing_{s+}\,B_s = 0 \qquad [5.F.22]$$

The lines and columns corresponding to nodes on axes x and y where $\varnothing = 0$ are eliminated before solving [5.F.21] with $M = (n_1 + 1)(n_2 + 1)$. A_{rs} and B_r are defined as follows:

$$A_{rs} = k_1^{'}\,A_{rs}^{1} + A_{rs}^{2} = \sum_{e} k_1^{'}\,A_{rs}^{1e} + A_{rs}^{2e} \qquad [5.F.23]$$

$$B_r = k_3\left(\sum_{e} B_r^{e}\right) \qquad [5.F.24]$$

Sum sign $\sum$ is understood to be the sum of all elements e of the quadrant.

Let an element e be defined by node points (i, j and k):

$$B_r^e = b_r\,\overline{y} - c_r\,\overline{x} \;\text{ if } r \in (i, j, k) \qquad [5.F.25]$$

$$B_r^e = 0 \;\text{ if } r \notin (i, j, k) \qquad [5.F.26]$$

$$A_{rs}^{1e} = K_{rs} \;\text{ if } r \in (i, j, k) \qquad [5.F.27]$$

$$A_{rs}^{2e} = \left(b_s\,b_r + c_s\,c_r\right)/2\Delta \;\text{ if } (r, s) \in \{i, j, k\} \qquad [5.F.28]$$

$$A_{rs}^{1e} = A_{rs}^{2e} = 0 \;\text{ if } (r, s) \notin \{i, j, k\} \qquad [5.F.29]$$

@Seismicisolation

Let us designate K_{rs} as:

$$K_{rs} = \left\{ \begin{array}{l} \Delta \left[2\Delta \left(a_r + a_s \right) / 3 - a_r \, a_s \right] + b_2 \, b_s \, I_{xx} + c_r \, c_s \, I_{yy} \\ + \left(b_s \, c_2 + b_r \, c_s \right) I_{xy} \end{array} \right\} \Big/ 2 \, \Delta^2 \qquad [5.F.30]$$

with:

$$I_{xx} = \iint_S x^2 \, d \, S_e \, , \quad I_{yy} = \iint_S y^2 d \, S_e \, , \quad I_{xy} = \iint_S xy \, d \, S_e \qquad [5.F.31]$$

S_e is the region occupied by element e.

$$I_{xx} = \frac{\Delta}{12} X^T \, \bar{M} \, X \qquad [5.F.32]$$

$$I_{xy} = \frac{\Delta}{12} X^T \, \bar{M} \, Y \qquad [5.F.33]$$

$$I_{yy} = \frac{\Delta}{12} Y^T \, \bar{M} \, Y \qquad [5.F.34]$$

and:

$$X^T = [x_i, x_j, x_k] \qquad [5.F.35]$$

$$Y^T = [y_i, y_j, y_k] \qquad [5.F.36]$$

$$\bar{M} = \begin{bmatrix} 2 & 1 & 1 \\ 1 & 2 & 1 \\ 1 & 1 & 2 \end{bmatrix} \qquad \Delta = \begin{bmatrix} 1 & x_i & y_i \\ 1 & x_j & y_j \\ 1 & x_k & y_k \end{bmatrix} \qquad [5.F.37]$$

where Δ is the area of element e and:

@Seismicisolation

$$\overline{x} = \frac{x_i + x_j + x_k}{3} \qquad [5.F.38]$$

$$\overline{y} = \frac{y_i + y_j + y_k}{3} \qquad [5.F.39]$$

$$\left.\begin{aligned} a_i &= x_j\, x_k - x_k\, x_j \\ b_i &= x_j - y_k \\ c_i &= x_k - x_j \end{aligned}\right\} \qquad [5.F.40]$$

We then obtain values (a_j, b_j, c_j) and (a_k, b_k, c_k) by cyclic permutation on the indexes in equation [5.F.40]. Indexes i, j and k of the nodes are numbered so that the area Δ of element e is always positive. After evaluating k_1, equation [5.F.22] is calculated numerically.

Appendix 5.G. Formulation of equations of motion for an off-axis anisotropic rod submitted to coupled torsion and bending vibrations

Let us write the Hamilton's functionals [5.76] by introducing energies [5.121] and [5.122], where Φ is the static warping function:

$$-\frac{\partial^2\theta}{\partial t^2}\left\{\rho \iint_S \left(x^2 + y^2\right) dx\, dy\right\} - \frac{\partial^2 w}{\partial t^2}\left\{\rho \iint_S y\, dx\, dy\right\} + \frac{\partial^2\theta}{\partial z^2}$$

$$\left\{\iint_S \left(y^2\, C_{55} + x^2\, C_{44} - 2\, xy\, C_{45}\right) dx\, dy\right\}$$

$$-\frac{\partial\psi}{\partial z}\left\{\iint_S \left(y\, C_{55}\, \frac{\partial\phi}{\partial x} - x\, C_{44}\, \frac{\partial\phi}{\partial y} - C_{45}\left(x\, \frac{\partial\phi}{\partial x} - y\, \frac{\partial\phi}{\partial y}\right)\right) dx\, dy\right\}$$

$$-\frac{\partial^2\psi}{\partial z^2}\left\{\iint_S \left(y C_{35}\, \phi - x\, C_{34}\, \phi\right) dx\, dy\right\} - \frac{\partial^3\psi}{\partial z^3}\left\{\iint_S \left(x^2\, C_{34} - xy\, C_{35}\right) dx\, dy\right\} = 0$$

[5.G.1]

@Seismicisolation

$$-\frac{\partial^2\psi}{\partial t^2}\left\{\rho\iint_S \phi^2\,dx\,dy\right\}+\frac{\partial^3\psi}{\partial z\,\partial t^2}\left\{\rho\iint_S x\phi\,dS\right\}+\frac{\partial^2\psi}{\partial z^2}\left\{\iint_S C_{33}\,\phi^2\,dx\,dy\right\}-$$

$$-\psi\left\{\iint_S\left(C_{55}\left(\frac{\partial\phi}{\partial x}\right)^2+C_{44}\left(\frac{\partial\phi}{\partial y}\right)^2+2\,C_{45}\left(\frac{\partial\phi}{\partial x}\right)\left(\frac{\partial\phi}{\partial y}\right)\right)dx\,dy\right\}-$$

$$-\frac{\partial\theta}{\partial z}\left\{\iint_S\left((y\,C_{55}-x\,C_{45})\frac{\partial\phi}{\partial x}-(x\,C_{44}-y\,C_{45})\frac{\partial\phi}{\partial y}\right)dx\,dy\right\}-$$

$$-\frac{\partial^2\theta}{\partial z^2}\left\{\iint_S(C_{35}\,y\,\phi-C_{34}\,x\,\phi)\,dx\,dy\right\}-\frac{\partial^3 w}{\partial z^3}\iint_S x\,\phi\,C_{33}\,dx\,dy+$$

$$+\frac{\partial^2 w}{\partial z^2}\left\{\iint_S\left(x\,(C_{35}\frac{\partial\phi}{\partial x}+C_{34}\frac{\partial\phi}{\partial y})\right)dx\,dy\right\}=0$$

[5.G.2]

$$-\frac{\partial^2 w}{\partial t^2}\left\{\rho\iint_S dx\,dy\right\}-\frac{\partial^2\theta}{\partial t^2}\rho\iint_S y\,dx\,dy+\frac{\partial^4 w}{\partial z^2\,\partial t^2}\left\{\rho\iint_S x^2\,dx\,dy\right\}-$$

$$-\frac{\partial^4 w}{\partial z^4}\left\{C_{33}\iint_S x^2\,dx\,dy\right\}+\frac{\partial^3\psi}{\partial z^3}\left\{\iint_S x\,\phi\,C_{33}\,dx\,dy\right\}-$$

$$-\frac{\partial^3\psi}{\partial z\,\partial t^2}\left\{\rho\iint_S x\,\phi\,dx\,dy\right\}-\frac{\partial^2\psi}{\partial z^2}\left\{\frac{1}{2}\iint_S x\left(C_{35}\frac{\partial\phi}{\partial x}+C_{34}\frac{\partial\phi}{\partial y}\right)dx\,dy\right\}+$$

$$+\frac{1}{2}\frac{\partial^3\theta}{\partial z^3}\left\{\iint_S\left(x^2\,C_{34}-xy\,C_{35}\right)dx\,dy\right\}=0$$

[5.G.3]

@Seismicisolation

$$\left[\left(\begin{array}{l}\left(\frac{\partial\theta}{\partial z}\right)\left\{\iint_S\left(y^2\,C_{55}+x^2\,C_{44}-2\,xy\,C_{45}\right)dx\,dy\right\}+\\ +\psi\left\{\iint_S\left(x\,C_{44}\frac{\partial\phi}{\partial y}-y\,C_{55}\frac{\partial\phi}{\partial x}+C_{45}\left(x\frac{\partial\phi}{\partial x}-y\frac{\partial\phi}{\partial y}\right)dx\,dy\right\}-\\ -\frac{\partial\psi}{\partial z}\left\{\iint_S\left(\phi\left(y\,C_{35}-x\,C_{34}\phi\right)\right)dx\,dy\right\}+\\ +\frac{\partial^2 w}{\partial z^2}\left\{\iint_S\left(x^2\,C_{34}+xy\,C_{35}\right)dx\,dy\right\}\end{array}\right)\delta\,\theta\right]^L=0$$

[5.G.4]

Effecting variations on the functionals, we obtain:

$$\left[\left(\begin{array}{l}-\frac{\partial^2 w}{\partial z^2}\iint_s x\,\phi\,C_{33}\,dx\,dy+\psi\iint_S\phi\left(C_{35}\frac{\partial\phi}{\partial x}+C_{34}\frac{\partial\phi}{\partial y}\right)dx\,dy\\ +\frac{\partial\theta}{\partial z}\iint_S\phi\left(x\,C_{34}-y\,C_{35}\right)dx\,dy+\frac{\partial\psi}{\partial z}\iint_S C_{33}\,\phi^2\,dx\,dy\end{array}\right)\delta\,\psi\right]_0^L=0$$

[5.G.5]

$$\left[\left(\begin{array}{l}\frac{\partial^2\psi}{\partial t^2}\iint_S\rho\,x\,\phi\,dS-\frac{\partial^2\psi}{\partial z^2}\iint x\,\phi C_{33}\,dS-\frac{\partial^3 w}{\partial z\,\partial t^2}\iint_S\rho\,x^2\,dS\\ +\frac{\partial^3 w}{\partial z^3}\iint_S x^2\,C_{33}\,dS+\frac{\partial\psi}{\partial z}\iint_S\left(C_{35}\,x\frac{\partial\phi}{\partial x}-C_{34}\,x\frac{\partial\phi}{\partial y}\right)dS\\ -\frac{\partial^2\theta}{\partial z^2}\iint_S\left(x^2C_{34}-xy\,C_{35}\right)dS\end{array}\right)\delta w\right]_0^L=0$$

[5.G.6]

@Seismicisolation

$$\left[\left(\begin{array}{l}\dfrac{\partial\psi}{\partial z}\iint x\,\phi\,C_{33}\,dx\,dy - \psi\iint_S x\left(C_{35}\dfrac{\partial\phi}{\partial x}+C_{34}\dfrac{\partial\phi}{\partial y}\right)dx\,dy \\ \\ +\dfrac{\partial^2 w}{\partial z^2}\iint_S x^2\,C_{33}\,dx\,dy - \dfrac{\partial\theta}{\partial z}\iint_S (x^2C_{34} - xy\,C_{35})\,dx\,dy\end{array}\right)\frac{\partial(\delta w)}{\partial z}\right]_0^L = 0$$

[5.G.7]

which take into account geometrical symmetry's properties of rectangular rods.

$$T_{\theta\theta_L} = \rho\iint_S\left(x^2+y^2\right)\,dx\,dy = T_{ww_1} + T_{ww_2}$$

$$T_{\psi\psi_L} = \rho\iint_S \phi^2\,dx\,dy$$

$$T_{ww_1} = \rho\iint_S x^2\,dx\,dy,$$

$$T_{ww_2} = \rho\iint_S y^2\,dx\,dy$$

$$T_{ww} = \rho\iint_S dx\,dy,$$

$$T_{\psi w} = \rho\iint_S x\,\phi\,dx\,dy$$

$$S_{ww_L} = C_{33}\iint_S x^2\,dx\,dy$$

$$S_{\theta\theta_L} = \iint_S\left(C_{55}\,y^2+C_{44}\,x^2 - 2\,xy\,C_{45}\right)dx\,dy$$

$$= \iint_S\left(C_{55}\,y^2+C_{44}\,x^2\right)dx\,dy;$$

in case of an orthotropic material or a symmetric beam.

@Seismicisolation

$$S_{\psi\psi} = \iint_S \left\{ C_{55} \left(\frac{\partial\phi}{\partial x}\right)^2 + C_{44} \left(\frac{\partial\phi}{\partial y}\right)^2 + 2\, C_{45} \left(\frac{\partial\phi}{\partial x}\right)\left(\frac{\partial\phi}{\partial y}\right) + 2\, C_{35}\phi \right\} dx\, dy$$

$$= \iint_S \left\{ C_{55} \left(\frac{\partial\phi}{\partial x}\right)^2 + C_{44} \left(\frac{\partial\phi}{\partial y}\right)^2 \right\} dx\, dy; \text{ in case of orthotropic material}$$

$$= \iint_S \left\{ C_{55} \left(\frac{\partial\phi}{\partial x}\right)^2 + C_{44} \left(\frac{\partial\phi}{\partial y}\right)^2 + C_{35}\, \phi \right\} dx\, dy; \text{ in case of a symmetric beam}$$

$$S_{\psi\psi_L} = C_{33} \iint_S \phi^2 \; dx\, dy$$

$$S_{\psi\psi_2} = \iint_S \phi \left(C_{34} \frac{\partial\phi}{\partial y} + C_{35} \frac{\partial\phi}{\partial x} \right) dx\, dy = 0; \text{ in the case of orthotropic material}$$

$$S_{\psi\theta_L} = \iint_S \left((x\, C_{45} - y\, C_{55}) \frac{\partial\phi}{\partial x} + (x\, C_{44} - y C_{45}) \frac{\partial\phi}{\partial y} \right) dy\, dx$$

$$= \iint_S C_{45} \left(x \frac{\partial\phi}{\partial x} - y \frac{\partial\phi}{\partial y} \right) dx\, dy; \text{ in the case of a symmetric beam}$$

$$= \iint_S \left(C_{44}\, x \frac{\partial\phi}{\partial y} - C_{55}\, y \frac{\partial\phi}{\partial x} \right) dx\, dy; \text{ in the case of an orthotropic material}$$

$$S_{\psi w_L} = \iint_S C_{33}\; x\, \phi \;\; dx\, dy = 0$$

[5.G.8]

$$S_{\theta w_L} = \iint_S (xy\, C_{35} - x^2 C_{34})\, dx\, dy$$

$$= 0; \text{ in the case of an orthotropic material}$$

$$= -\iint_S x^2 C_{34} \;\; dx\, dy; \text{ in the case of a symmetric beam}$$

@Seismicisolation

$$S_{\psi w_2} = \iint_S x \left(C_{35} \frac{\partial \phi}{\partial x} - C_{34} \frac{\partial \phi}{\partial y} \right) dx\, dy$$

$= 0$; in the case of an orthotropic material

$$= \iint_S x\, C_{35} \frac{\partial \phi}{\partial x}\, d\,S; \text{ in the case of a symmetric beam}$$

$$S_{\psi\theta_2} = \iint_S \phi \left(x\, C_{34} - y\, C_{35} \right) dx\, dy = 0$$

$$k_1 = \frac{\int_0^L \left\{ C_{33} \left(\frac{\partial \psi}{\partial z} \right)^2 - \rho \left(\frac{\partial \psi}{\partial t} \right)^2 \right\} dz}{\int_0^L \psi^2\, dz}$$

$$k_2 = \frac{\int_0^L \psi \frac{\partial \psi}{\partial z}\, dz}{\int_0^L \psi^2\, dz}$$

Taking into account the zero value of the odd integral, allows us to rewrite equations [5.G.1] and [5.G.7] in following forms:

$$T_{\theta\theta_L} \frac{\partial^2 \theta}{\partial t^2} - S_{\theta\theta_L} \frac{\partial^2 \theta}{\partial z^2} + S_{\psi\theta_L} \frac{\partial \psi}{\partial z} + S_{\theta w_L} \frac{\partial^3 w}{\partial z^3} = 0 \qquad [5.G.9]$$

$$T_{\psi\psi_L} \frac{\partial^2 \psi}{\partial t^2} - S_{\psi\psi_1} \frac{\partial^2 \psi}{\partial z^2} + S_{\psi\psi}\, \psi + S_{\psi w_2} \frac{\partial^2 w}{\partial z^2} - S_{\psi\theta_L} \frac{\partial \theta}{\partial z} = 0 \qquad [5.G.10]$$

$$T_{ww} \frac{\partial^2 w}{\partial t^2} - T_{ww_L} \frac{\partial^4 w}{\partial z^2 \partial t^2} + S_{ww_L} \frac{\partial^4 w}{\partial z^4} + S_{\psi w_2} \frac{\partial^2 \psi}{\partial z^2} - S_{\theta w_L} \frac{\partial^3 \theta}{\partial z^3} = 0 \qquad [5.G.11]$$

We must add four natural boundary conditions to the three equations of motion [5.G.9], [5.G.10] and [5.G.11]:

@Seismicisolation

$$\left\{\left(S_{\theta\theta_L}\frac{\partial\theta}{\partial z} - S_{\psi\theta_L}\psi + S_{\theta w_L}\frac{\partial^2 w}{\partial z^2}\right)\delta\theta\right\}_0^L = 0$$

$$\left\{\left(-S_{\psi w_L}\frac{\partial^2 w}{\partial z^2} + S_{\psi\psi}\frac{\partial\psi}{\partial z} - S_{\psi w_2}\psi\right)\delta\psi\right\}_0^L = 0$$

$$\left\{\left(S_{ww_L}\frac{\partial^3 w}{\partial z^3} - S_{\theta w_1}\frac{\partial^2\theta}{\partial z^2} - S_{\psi w_L}\frac{\partial^2\psi}{\partial z^2} - T_{ww_L}\frac{\partial^3 w}{\partial z\partial t^2} + S_{\psi w_2}\frac{\partial w}{\partial z} + T_{\psi w}\frac{\partial^2\psi}{\partial t^2}\right)\delta w\right\}_0^L = 0$$

$$\left\{\left(S_{ww_L}\frac{\partial^2 w}{\partial z^2} + S_{\psi w_L}\frac{\partial\psi}{\partial z} + \left(S_{\psi w_2} + S_{\theta w_L}\right)\frac{\partial\theta}{\partial z}\right)\delta(w,z)\right\}_0^L = 0 \qquad [5.G.12]$$

There are also two independent equations for ϕ:

$$C_{55}\frac{\partial^2\phi}{\partial x^2} + C_{44}\frac{\partial^2\phi}{\partial y^2} = k_1\,\phi \text{ on } S \qquad [5.G.13]$$

$$C_{55}\left(\frac{\partial\phi}{\partial x} - k_3\,y\right)n_x + C_{44}\left(\frac{\partial\phi}{\partial y} + k_3\,x\right)n_y + k_2\,\phi\,C_{35}\,n_x + k_2\,\phi\,C_{34}\,n_y = 0 \quad \text{on } \partial S \qquad [5.G.14]$$

where n_x and n_y are external unit vectors normal to the boundary surface in directions x and y.

Appendix 5.H. Relative group velocity versus relative wave number

In dynamic tests for obtaining elastic moduli, phase velocity is used. The main reason is that it is closely related to the elastic moduli of the material.

Group velocity in a lossless medium, however, presents an area of interest in elastodynamics. It is equal to the propagating energy velocity.

@Seismicisolation

Chapter 10, Appendix 10.A is devoted to energy velocity, group velocity and the Poynting vector.

Group velocity is defined as:

$$v_g = \frac{d\,\omega}{d\,k} \qquad [5.H.1]$$

where ω is circular frequency and k is wave number. Equation [5.H.1] can be written as:

$$v_g = \frac{d\,(v\,k)}{d\,k} \qquad [5.H.2]$$

where v is the phase velocity. From equation [5.H.2], v_g has the expression:

$$v_g = v + k\,\frac{dv}{dk} \qquad [5.H.3]$$

Adopting a non-dimensional velocity:

$$\overline{v}_g = \overline{v} + \overline{k}\,\frac{d\overline{v}}{d\overline{k}} \qquad [5.H.4]$$

Two methods for calculating $\overline{v}_g$ are available. Both use equation [5.H.4] to evaluate $\overline{v}_g$ *versus* $\overline{v}$ the phase velocity. If the curve $\omega = \omega$ (k) is known, the phase velocity can be calculated directly.

To obtain a closed-form expression for v_g, we use equation [5.H.4].

5.H.1. *Group velocity for the two first propagation modes of an on-axis rod*[17]

Phase velocity is the root of equation [5.111] or [5.112], which depends on the first or second branch retained.

17 The rod axis is coincident with a symmetry axis of the material.

@Seismicisolation

For the first branch, the dimensionless phase velocity is:

$$\bar{v}_1 = \frac{1}{2}\left\{1 + p^2 \frac{S_{\psi\psi} S_{\alpha\alpha_1}}{S_{\alpha\alpha_1} T_{\psi\psi_1}} - \frac{1}{\bar{k}^2} \frac{S_{\psi\psi} T_{\alpha\alpha_1} \delta^2}{T_{\psi\psi_1} S_{\alpha\alpha_1}} + \left[\left(1 + p^2 \frac{S_{\psi\psi} T_{\alpha\alpha_1}}{S_{\alpha\alpha_1} T_{\psi\psi_1}} - \frac{1}{\bar{k}^2} \frac{S_{\psi\psi} T_{\alpha\alpha_1} \delta^2}{S_{\alpha\alpha_1} T_{\psi\psi_1}}\right)^2 - 4\left(\frac{p^2 S_{\psi\psi} T_{\alpha\alpha_1}}{S_{\alpha\alpha_1} T_{\psi\psi_1}} + \frac{1}{\bar{k}^2} \frac{T_{\alpha\alpha_1} S_{\psi\psi} \delta^2}{S_{\alpha\alpha_1} T_{\psi\psi_1}}\right)^{1/2}\right]^{1/2}\right\} \qquad [5.H.5]$$

For the second branch, dimensionless phase velocity is:

$$\bar{v}_2 = \frac{1}{2}\left\{1 + p^2 \frac{S_{\psi\psi} S_{\alpha\alpha_1}}{S_{\alpha\alpha_1} T_{\psi\psi_1}} - \frac{1}{\bar{k}^2} \frac{S_{\psi\psi} T_{\alpha\alpha_1} \delta^2}{T_{\psi\psi_1} S_{\alpha\alpha_1}} - \left[\left(1 + p^2 \frac{S_{\psi\psi} T_{\alpha\alpha_1}}{S_{\alpha\alpha_1} T_{\psi\psi_1}} - \frac{1}{\bar{k}^2} \frac{S_{\psi\psi} T_{\alpha\alpha_1} \delta^2}{S_{\alpha\alpha_1} T_{\psi\psi_1}}\right)^2 - 4\left(\frac{p^2 S_{\psi\psi} T_{\alpha\alpha_1}}{S_{\alpha\alpha_1} T_{\psi\psi_1}} + \frac{1}{\bar{k}^2} \frac{T_{\alpha\alpha_1} S_{\psi\psi} \delta^2}{S_{\alpha\alpha_1} T_{\psi\psi_1}}\right)^{1/2}\right]^{1/2}\right\} \qquad [5.H.6]$$

In order to simplify calculations, let us adopt the following notations:

$$\left.\begin{aligned} h_1 &= 1 + p^2 \frac{S_{\psi\psi} T_{\alpha\alpha_1}}{S_{\alpha\alpha_1} T_{\psi\psi_1}} - \frac{1}{\bar{k}^2} \frac{S_{\psi\psi} T_{\alpha\alpha_1} \delta^2}{S_{\alpha\alpha_1} T_{\psi\psi_1}} \\ h_2 &= p^2 \frac{S_{\psi\psi} T_{\alpha\alpha_1}}{S_{\alpha\alpha_1} T_{\psi\psi_1}} + \frac{1}{\bar{k}^2} \frac{S_{\psi\psi} T_{\alpha\alpha_1} \delta^2}{S_{\alpha\alpha_1} T_{\psi\psi_1}} \end{aligned}\right\} \qquad [5.H.7]$$

@Seismicisolation

Then equations [5.H.5] and [5.H.6] are reduced to:

$$\left.\begin{aligned} \bar{v}_1 &= \frac{1}{2}\left\{h_1 + \left(h_1^2 - 4\,h_2\right)^{1/2}\right\} \\ \bar{v}_2 &= \frac{1}{2}\left\{h_1 - \left(h_1^2 - 4\,h_2\right)^{1/2}\right\} \end{aligned}\right\} \qquad [5.H.8]$$

Deriving equation [5.H.8] with respect to $\bar{k}$, we get:

$$\frac{d\bar{v}_1}{d\bar{k}} = \frac{1}{2}\left\{\frac{dh_1}{d\bar{k}} + \left(h_1\,\frac{dh_1}{d\bar{k}} - 2\,\frac{dh_2}{d\bar{k}}\right)\left(h_1^2 - 4\,h_2\right)^{-1/2}\right\} \qquad [5.H.9]$$

$$\frac{d\bar{v}_2}{d\bar{k}} = \frac{1}{2}\left\{\frac{dh_1}{d\bar{k}} - \left(h_1\,\frac{dh_1}{d\bar{k}} - 2\,\frac{dh_2}{d\bar{k}}\right)\left(h_1^2 - 4\,h_2\right)^{-1/2}\right\} \qquad [5.H.10]$$

with:

$$\frac{dh_1}{d\bar{k}} = \frac{2}{\bar{k}^3}\,\frac{S_{\psi\psi}\,T_{\alpha\alpha_1}\,\delta^2}{S_{\alpha\alpha_1}\,T_{\psi\psi_1}} \qquad [5.H.11]$$

$$\frac{dh_1}{d\bar{k}} = -\,\frac{2}{\bar{k}^3}\,\frac{S_{\psi\psi}\,T_{\alpha\alpha_1}\,\delta^2}{S_{\alpha\alpha_1}\,T_{\psi\psi_1}} \qquad [5.H.12]$$

Then the dimensionless group velocity is:

$$\bar{v}_{g_1} = \frac{1}{2}\left\{\begin{aligned} &h_1 + \left(h_1^2 - 4\,h_2\right)^{1/2} + \bar{k}\,\frac{dh_1}{d\bar{k}} + \bar{k}\left(h_1\,\frac{dh_1}{d\bar{k}} - 2\,\frac{dh_2}{d\bar{k}}\right) \\ &\bullet\left(h_1^2 - 4h_2\right)^{-1/2} \end{aligned}\right\} \qquad [5.H.13]$$

$$\bar{v}_{g_2} = \frac{1}{2}\left\{\begin{aligned} &h_1 - \left(h_1^2 - 4\,h_2\right)^{1/2} \\ &+ \bar{k}\,\frac{dh_1}{d\bar{k}} - \bar{k}\left(h_1\,\frac{dh_1}{d\bar{k}} - 2\,\frac{dh_2}{d\bar{k}}\right)^{-1/2} \end{aligned}\right\}$$

@Seismicisolation

5.H.2. *Dimensionless group velocity* $\bar{C}_g$ *for on axis and off axis rod*[18]

Phase velocity $\bar{C}_1$ is one of the three roots of the sixth-order bisquared equations of motion [5.144] and [5.146].

In order to easily exploit those equations, let us adopt the notations:

$$\left.\begin{aligned} r_1 &= \left(\frac{a_1^2}{9} - \frac{a_2}{3}\right)^{1/2} \\ r_2 &= -a_3 + \frac{a_1\, a_2}{3} - \frac{2a_1^3}{27} \\ r_3 &= 2\left[-\left(\frac{a_2}{3} - \frac{a_1^2}{9}\right)^3\right]^{1/2} \end{aligned}\right\} \qquad [5.H.14]$$

Then the squares of phase velocities for the three branches [5.149] are:

$$\left.\begin{aligned} \bar{C}_1^2 &= 2\, r_1 \cos\left(\frac{1}{3}\,\text{Arc cos}\,\frac{r_2}{r_3} + \frac{2\pi}{3}\right) - \frac{a_1}{3} \\ \bar{C}_2^2 &= 2\, r_1 \cos\left(\frac{1}{3}\,\text{Arc cos}\,\frac{r_2}{r_3} + \frac{4\pi}{3}\right) - \frac{a_1}{3} \\ \bar{C}_3^2 &= 2\, r_1 \cos\left(\frac{1}{3}\,\text{Arc cos}\,\frac{r_2}{r_3}\right) - \frac{a_1}{3} \end{aligned}\right\} \qquad [5.H.15]$$

Group velocity $\bar{C}_{g_j}$ is related to phase velocity $\bar{C}_j$ by the following relation:

$$\bar{C}_{g_j} = \bar{C}_j + \bar{k}\,\frac{d\bar{C}_j}{d\bar{k}}$$

18 The rod axis is not coincident with the symmetry axis of the material.

@Seismicisolation

Deriving $\bar{C}_j^2$ with respect to $\bar{k}$ we obtain:

$$\bar{C}_{g_1} = \bar{C}_1 + \frac{\bar{k}}{2\bar{C}_1}\left\{\begin{array}{l} 2\dfrac{dr_1}{d\bar{k}}\cos\left(\dfrac{1}{2}\,\text{Arc}\cos\dfrac{r_2}{r_3} + \dfrac{2\pi}{3}\right) + \\ + \dfrac{2r_1}{3}\sin\left(\dfrac{1}{3}\,\text{Arc}\cos\dfrac{r_2}{r_3} + \dfrac{2\pi}{3}\right)\left[1 - \dfrac{r_2^2}{r_3^2}\right]^{-1/2}\dfrac{d}{d\bar{k}}\left(\dfrac{r_2}{r_3}\right) - \\ - \dfrac{1}{3}\,\dfrac{da_1}{d\bar{k}} \end{array}\right\} \quad [5.H.16]$$

$$\bar{C}_{g_2} = \bar{C}_2 + \frac{\bar{k}}{2\bar{C}_2}\left\{\begin{array}{l} 2\dfrac{dr_1}{d\bar{k}}\cos\left(\dfrac{1}{2}\,\text{Arc}\cos\dfrac{r_2}{r_3} + \dfrac{4\pi}{3}\right) + \\ + \dfrac{2r_1}{3}\sin\left(\dfrac{1}{3}\,\text{Arc}\cos\dfrac{r_2}{r_3} + \dfrac{4\pi}{3}\right)\left[1 - \dfrac{r_2^2}{r_3^2}\right]^{-1/2}\dfrac{d}{d\bar{k}}\left(\dfrac{r_2}{r_3}\right) - \\ - \dfrac{1}{3}\,\dfrac{da_1}{d\bar{k}} \end{array}\right\} \quad [5.H.17]$$

$$\bar{C}_{g_3} = \bar{C}_3 + \frac{\bar{k}}{2\bar{C}_3}\left\{\begin{array}{l} 2\,\dfrac{dr_1}{d\bar{k}}\cos\left(\dfrac{1}{3}\,\text{Arc}\cos\dfrac{r_2}{r_3}\right) + \dfrac{2r_1}{3}\sin\left(\dfrac{1}{3}\,\text{Arc}\cos\dfrac{r_2}{r_3}\right)\bullet \\ \bullet\left[1 - \dfrac{r_2^2}{r_3^2}\right]^{-1/2}\dfrac{d}{d\bar{k}}\left(\dfrac{r_2}{r_3}\right) - \dfrac{1}{3}\,\dfrac{da_1}{d\bar{k}} \end{array}\right\} \quad [5.H.18]$$

with:

$$\frac{dr_1}{d\bar{k}} = \frac{1}{3}\left(\frac{a_1^2}{9} - \frac{a_2}{3}\right)^{-1/2}\left(\frac{2a_1}{9}\,\frac{da_1}{d\bar{k}} - \frac{1}{3}\,\frac{da_2}{d\bar{k}}\right)$$

@Seismicisolation

$$\frac{dr_2}{d\bar{k}} = \frac{1}{3}\left(a_2 - \frac{2}{3}a_1^2\right)\frac{da_1}{d\bar{k}} + \frac{1}{3}a_1\frac{da_2}{d\bar{k}} - \frac{da_3}{d\bar{k}}$$

$$\frac{dr_3}{d\bar{k}} = \left\{-\left(\frac{a_2}{3} - \frac{a_1^2}{9}\right)^3\right\}^{-1/2}\left\{\left(\frac{a_2}{3} - \frac{a_1^2}{9}\right)\left(\frac{da_2}{d\bar{k}} - \frac{2a_1}{3}\frac{da_1}{d\bar{k}}\right)\right\} \qquad [5.H.19]$$

and:

$$\frac{da_1}{d\bar{k}} = -\left\{(1 - \alpha_5\ \alpha_8)^{-1}\left(\frac{\alpha_5\ \alpha_8}{v_T^2}\right)\frac{2}{\bar{k}^3}\right\}$$

$$\frac{da_3}{d\bar{k}} = \left\{(1 - \alpha_5\alpha_8)^{-1}\left[\left(\frac{\alpha_4\alpha_7}{v_T^4} + \frac{\alpha_1\alpha_3\ v_F^2}{v_t^6}\right)\frac{b^4}{4\bar{k}^5\delta^4}\right]\right\} \qquad [5.H.20]$$

In equation [5.H.20], v_F designates the phase velocity of bending, longitudinal and torsional decoupled vibrations.

5.H.3. *Torsional velocity versus wave number*

5.H.3.1. *Isotropic material – steel*

Figure 5.H.1 shows the first three branches of an isotropic material. The cross-section is rectangular with $\delta = 2$.

5.H.3.2. *Anisotropic material (composite glass fiber-polyester epoxy), rod with rectangular cross-section and flatness coefficient $\delta = 2$*

Consider a composite material (glass fiber-polyester resin) where $\delta = 2$, $\bar{c}=v/v_T$; and k=kh/2, where h is thickness.

The trends of the curves for the first mode in Figures 5.H.1 and 5.H.2 are different.

@Seismicisolation

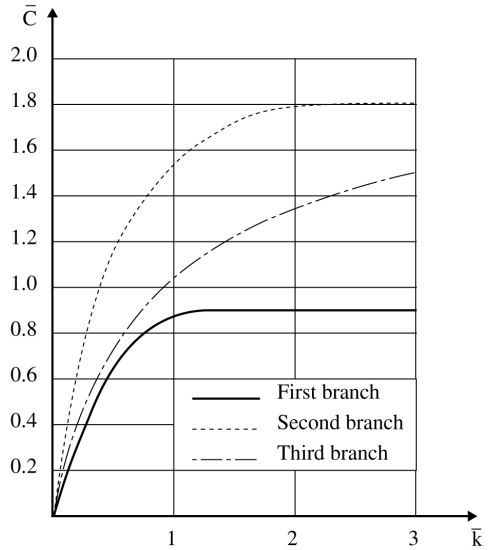

Figure 5.H.1. *Variation of dimensionless group velocity for the three first branches. The material is steel and the flatness coefficient* $\delta = 2$; $\bar{c} = v/v_T$, $\bar{k} = k\,h/2$

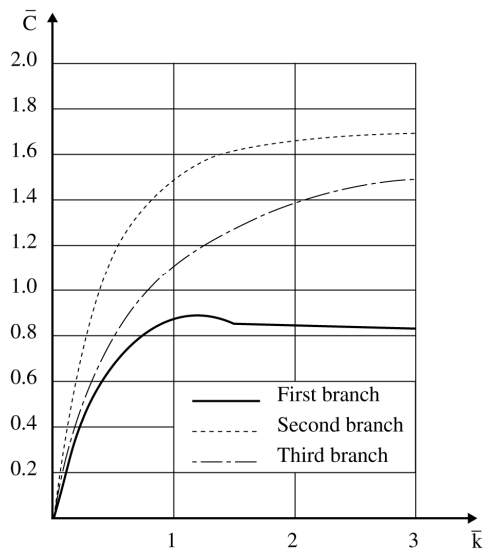

Figure 5.H.2. *Relative group velocity* versus *relative wave number*

@Seismicisolation

For the composite material, the maximum on the curve corresponding to the first branch is pronounced, flatness $\delta = 2$ being the same for both rods.

5.H.3.3. *First branches for four composite materials with flatness coefficient* $\delta = 2$

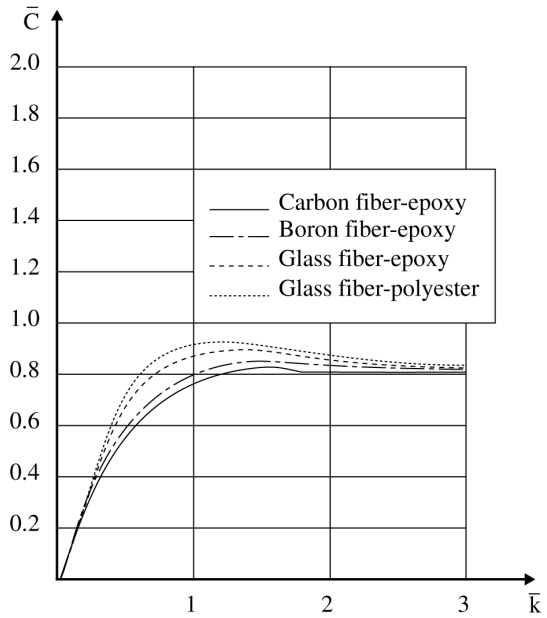

Figure 5.H.3. *First branches: relative group velocity* versus *relative wave number for four anisotropic composite materials with the same flatness* $\delta = 2$

5.H.3.4. *Second branches for four composite materials*

Figure 5.H.4 presents the second branches of the curve of relative velocity $\bar{c} = v / v_T$ *versus* relative wave number, the flatness $\delta =$ b/h = 2 of the four composite materials being the same as above.

@Seismicisolation

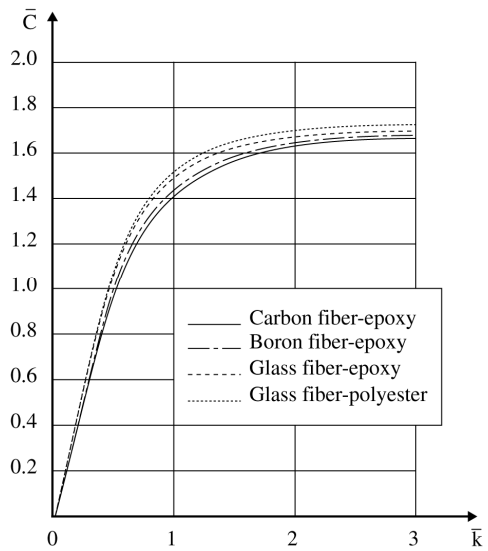

Figure 5.H.4. *Second branches for four composite materials flatness* $\delta = b/h = 2$

5.H.3.5. *Third branches for four composite materials*

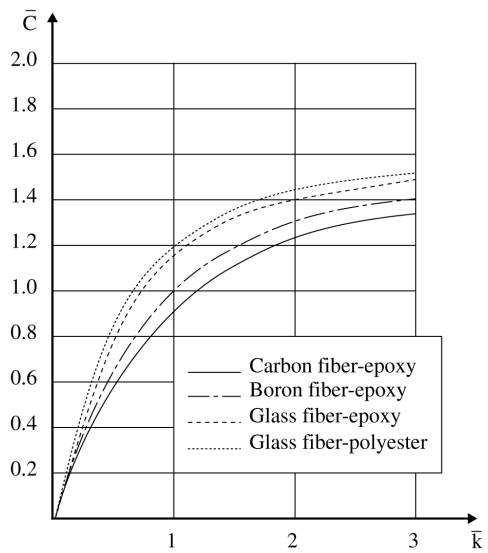

Figure 5.H.5. *Third branches of relative group velocity* $\bar{c}_g$ versus *relative wave number* $\bar{k}$ *for four composite materials, as above. Flatness coefficient* $\delta = 2$

@Seismicisolation

5.H.3.6. *General remarks*

The trends of the three branches of dispersion curves are the same. Group velocity varies continuously with increasing wave number and asymptotical value, which is the Rayleigh phase velocity. The ratio C_{44}/C_{33} is an important coefficient. Group velocities decrease with the increasing of this quotient.

@Seismicisolation

Chapter 6

Bending Vibration of a Rod

6.1. Introduction

In many industrial testing apparatuses, bending vibration is extensively used to evaluate Young's modulus. This can be explained by the ease with which we can produce stationary flexural waves in rods at low frequency and with large displacement amplitude.

This method has recently been applied to composite anisotropic materials. This extension requires additional parameters and correcting coefficients to be introduced in the equations of motion to take into account the nature of the composite material itself. Let us mention some of the additional parameters. Many composites are multilayered. Each layer can be composed of unidirectional fibers regularly distributed in a matrix. The directions of fibers are different between one layer and another. Homogenization technique is used at low frequency to study the sample, particularly when the shear effect in a section is accounted for. For many artificial anisotropic materials, the ratio E_z/G_{xz} of Young's modulus E_z along the rod axis Oz and shear modulus G_{xz} in the plane (x z) can be very high. It can exceed 40 for ansiotropic materials, however for isotropic materials this ratio cannot exceed 3. The slenderness of the sample, defined as the length/thickness ratio, is usually adopted for choosing the appropriate equations of motion. It consequently does not take unique parameters into account.

This chapter was written initially by Dominique LE NIZHERY. It was rewritten in condensed form by Jean Tuong VINH and utilizes large extracts of le Nizhery's engineering degree dissertation from Ecole Centrale Paris [LEN 73].

Mechanics of Viscoelastic Materials and Wave Dispersion Edited by Yvon Chevalier and Jean Tuong Vinh
© 2010 ISTE Ltd. Published 2010 by ISTE Ltd.

@Seismicisolation

In what follows, elementary Bernoulli-Euler's equation of motion is examined first. The more elaborate Timoshenko's equation is then presented. It is valid for material (isotropic or anisotropic) samples whose rod axis coincides with the material symmetry axis. For anisotropic materials only, in order to obtain some non-diagonal components of the compliance matrix we must refer to a special rod sample in which the rod axis does not coincide with the material symmetry axis. Timoshenko's coupled equations of motion are then presented, in which various correcting coefficients are included.

6.1.1. *Short bibliography of dynamic bending of a beam*

Euler [EUL 1744] and Bernoulli [BER 1751] separately presented the equations of motion bearing their names in 1744 and 1751 respectively. At this time, the field of differential calculus was just starting to emerge. These equations concern a straight beam.

In 1887 Love [LOV 1899] introduced the rotational inertia effect. More than 40 years elapsed until Timoshenko re-examined the equation and suggested that the shear effect in a beam section is an important phenomenon that already exists in the static bending of a beam [TIM 21]. From this, the equations of motion reach their final form. Let us mention, however, some minor modifications of Timoshenko's equations:

– Cowper [COW 66] proposed a different correcting coefficient (which did not modify those equations).

– Stephen and Levinson [STE 79] re-examined the expressions of longitudinal and shear strains in a section and proposed, instead of a unique correcting coefficient, two different correcting ones without modifying Timoshenko's equation.

– A different way of introducing a correcting coefficient was proposed by Mindlin [MIN 51]. This deserves our attention. Instead of examining the shear effect in a section in detail, Mindlin proposed to study the asymptotic behavior of a rod bending at high frequency. When the elastic bending wave velocity reaches its asymptotic value, that of a surface Rayleigh's wave velocity, it gives rise to a different value of correcting coefficient.

Recently, many researchers have examined the applicability of Timoshenko's equations to composite materials.

@Seismicisolation

– Abarcar and Cunniff [ABA 72] extended Timoshenko's equation to include composite materials and examined the bending dynamic behavior of an off-axis beam. The coupling bending-torsion in a beam is eventually taken into account.

– Le Nizerhy [LEN 73] proposed a complete study of the bending vibration of composite materials, including off-axis rods. Formulations of the problem for numerical computational purposes are proposed and presented in this chapter.

6.2. Bending vibration of straight beam by elementary theory

In this chapter, only straight beams are examined. The bending vibration of a curved beam, however, is interesting in applications for the characterization of materials. This problem will be looked at in Chapter 9.

6.2.1. *Bernoulli-Euler's equation of motion*

Elementary equations of motion do not take shear effect in the cross-section into account. These equations can be obtained directly by using the generalized force method. Let an element of the straight beam, see Figure 6.1, be subjected to bending moments at the left and right ends of a beam element. Here x is the transverse coordinate through the thickness and z the coordinate along the beam axis. q (z) is the distributed force along the beam.

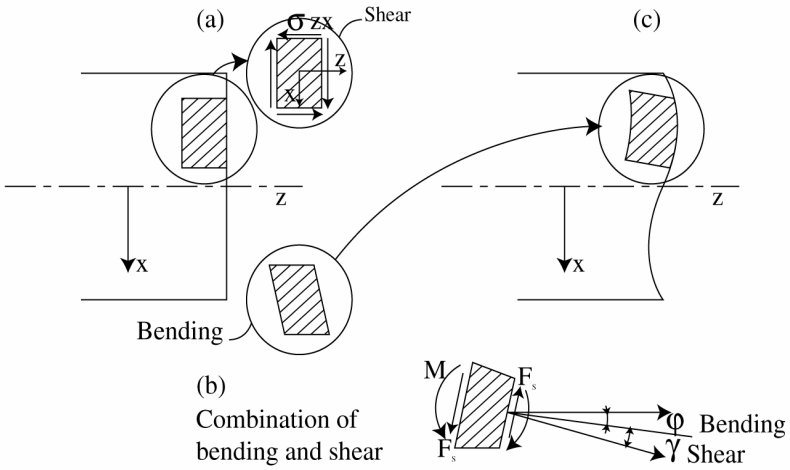

Figure 6.1. *a) An element of rod in plane x z. This element is subjected to bending and shear; b) there are two angles: one due to bending ϕ, the other due to shear γ; c) the section in plane (x y) does not remain in the plane after deformation*

@Seismicisolation

6.2.1.1. *Relationship between bending moments and shear forces*

$$-M + \left(M + \frac{\partial M}{\partial z} dz\right) + \left(2F + \frac{\partial F}{\partial z} dz\right) \frac{dz}{2} = 0 \qquad [6.1]$$

6.2.1.2. *Shear forces and inertia force*

$$-F + \left(F + \frac{\partial F}{\partial z} dz\right) + q(z)\, dz = \rho S\, dz \frac{\partial^2 w}{\partial t^2}$$

$$\frac{\partial F}{\partial z} + q(z) = \rho S \frac{\partial^2 w}{\partial t^2} \qquad [6.2]$$

where S is the cross-section's area and ρ the mass density of the material.

6.2.1.3. *Bending moment and curvature radius*

$$M = E I \frac{\partial^2 w}{\partial z^2} \qquad [6.3]$$

In the second member of equation [6.3], I is the quadratic momentum, E the Young's modulus of the material and the second derivative of displacement is assimilated to the curvature radius of the beam in the first approximation.

Combining [6.1], [6.2] and [6.3], we get the following equation of motion:

$$\rho S \frac{\partial^2 w}{\partial t^2} + E I \frac{\partial^4 w}{\partial z^4} = q(z) \qquad [6.4]$$

If there is no distributed force q (z), the second member is set to zero.

$$\rho S \frac{\partial^2 w}{\partial t^2} + E I \frac{\partial^4 w}{\partial z^4} = 0 \qquad [6.5]$$

Equations [6.4] and [6.5] are valid if the shear energy is much less than the bending energy of the whole sample.

$$\frac{U\ \text{shear}}{U\ \text{bending}} = 2(1+\nu)\left(\frac{h}{L}\right)^2 \qquad [6.6]$$

@Seismicisolation

Equation [6.6] is valid for isotropic material. h and L designate the thickness and the length of the material respectively. ν is the Poisson's coefficient.

The slenderness: h/L is the parameter that enables us to appreciate the validity of equation [6.6]. For higher modes of vibration, equation [6.6] is abandoned to the detriment of other criteria, including the distance separating the two modes of vibration along the beam.

6.2.1.4. *Boundary conditions*

With the generalized force method each kind of boundary condition has to be examined separately. If a variational principle is adopted, the natural boundary conditions are obtained directly after parts of the variational equations are integrated.

Kinematic boundary condition		**Natural boundary condition**
$\frac{\partial w}{\partial z}$ prescribed slope	or	$E I \frac{\partial^2 w}{\partial z^2} = 0$ bending moment
w prescribed	or	$\frac{\partial}{\partial z}\left(E I \frac{\partial^2 w}{\partial z^2}\right) = 0$ shear force

Table 6.1. *Boundary conditions on the bending of a beam*

Consequently there are four possible sets of boundary conditions. Let us focus our attention on the two boundary conditions written on the same line that are not compatible. The following three practical boundary conditions are:

Clamping end	$\frac{\partial w}{\partial z} = 0$ and w (z, t) prescribed
Free end	$\frac{\partial^2 w}{\partial z^2} = \frac{\partial^3 w}{\partial z^3} = 0$ bending moment and shear force equal to zero
Supported end	$w(z, t) = 0$ and $\frac{\partial^2 w}{\partial z^2} = 0$

Table 6.2. *Three practical boundary conditions*

@Seismicisolation

6.2.2. *Solutions of Bernoulli-Euler's equations*

For a beam of finite length, stationary bending waves need to be considered. By using the separate variable method, the solution for w (z, t) can be expressed as:

$$w\left(z, t\right) = A\left[\exp\left(j\,\omega\,t\right)\right]\exp\left(\frac{\beta\,z}{L}\right) \qquad [6.7]$$

Equation [6.7] means that bending displacement w (z, t) is a linear combination of exponentials of $\frac{\beta\,z}{L}$, β being a root of the characteristic equation (which is of four degrees). The root can be either real or imaginary. This means that w (z, t) can be written as:

$$w\left(z, t\right) = \exp\left(j\,\omega\,t\right)\left[A\cosh\frac{\beta\,z}{L} + B\sinh\frac{\beta\,z}{L} + C\cos\frac{\beta\,z}{L} + D\sin\frac{\beta\,z}{L}\right] \qquad [6.8]$$

in which trigonometric and hyperbolic functions are utilized. A linear combination of hyperbolic and trigonometric functions is called a characteristic function.

6.2.2.1. *Clamped-free rod*

For z = 0, where the clamped end is the Eriving equation [6.8], with respect to coordinate z we obtain:

$$\frac{\partial\,w}{\partial\,z} = A\,\frac{\beta}{L}\,\sinh\frac{\beta z}{L} + \frac{B\beta}{L}\cosh\frac{\beta z}{L} - \frac{C\beta}{L}\sin\frac{\beta z}{L} + \frac{D\beta}{L}\cos\frac{\beta z}{L} \qquad [6.9]$$

For convenience we do not mention factor exp (j ω t) in equation [6.8]. Setting z to zero in [6.8] and [6.9], we obtain:

$$\left.\begin{aligned} A + C &= 0 \\ \frac{B\beta}{L} + \frac{D\beta}{L} &= 0 \end{aligned}\right\} \qquad [6.10]$$

@Seismicisolation

The third and fourth derivatives with respect to z are presented in the following equations:

$$\frac{\partial^2 w}{\partial z^2} = A\frac{\beta^2}{L^2}\cosh\frac{\beta z}{L} + \frac{B\beta^2}{L^2}\sinh\frac{\beta z}{L} - \frac{C\beta^2}{L^2}\cos\frac{\beta z}{L} - \frac{D\beta^2}{L^2}\sin\frac{\beta z}{L} \qquad [6.11]$$

$$\frac{\partial^3 w}{\partial z^3} = A\frac{\beta^3}{L^3}\sinh\frac{\beta z}{L} + \frac{B\beta^3}{L^3}\cosh\frac{\beta z}{L} + \frac{C\beta^3}{L^3}\sin\frac{\beta z}{L} - \frac{D\beta^3}{L^3}\cos\frac{\beta z}{L} \qquad [6.12]$$

For z = L, the second members of equations [6.11] and [6.12] are set to zero:

$$\left.\begin{aligned} &A\cos h\,\beta + B\sin h\,\beta - C\cos\beta - D\sin\beta = 0 \\ &A\sin h\,\beta + B\cos h\,\beta + C\sin\beta - D\cos\beta = 0 \end{aligned}\right\} \qquad [6.13]$$

The determinant of the coefficient in equations [6.10] and [6.13] is set to zero for non-trivial solutions:

$$\begin{vmatrix} 1 & 0 & 1 & 0 \\ 0 & 1 & 0 & 1 \\ \cos h\,\beta & \sin h\,\beta & -\cos\beta & -\sin\beta \\ \sin h\,\beta & \cos h\,\beta & \sin\beta & -\cos\beta \end{vmatrix} = 0 \qquad [6.14]$$

The non-zero solution for A, B, C and D requires us to set the determinant to zero.

To facilitate calculation of equation [6.14], a new determinant is created by subtracting the first column from the third column and by subtracting the fourth column from the second column term-by-term.

@Seismicisolation

$$\begin{vmatrix} 1 & 0 & 0 & 0 \\ 0 & 1 & 0 & 0 \\ \cos\beta & \sin\beta & -(\cos\beta+\cosh\beta) & -(\sin\beta+\sin h\,\beta) \\ \sin h\,\beta & \cos h\,\beta & (\sin\beta-\sin h\,\beta) & -(\cos\beta+\cos h\,\beta) \end{vmatrix} = 0 \qquad [6.15]$$

Developing [6.15] we obtain:

$$\cos\beta\cosh\beta + 1 = 0 \qquad [6.16]$$

6.2.2.2. *Clamped-clamped rod*

Without demonstration, the eigenvalue equation is:

$$\cos h\,\beta\cos\beta - 1 = 0 \qquad [6.17]$$

6.2.2.3. *Supported-supported rod*

$$\sin\beta = 0 \qquad [6.18]$$

Equation [6.18] is an example of an application for evaluating Young's modulus.

If Bernoulli-Euler's equation of motion is valid, the boundary conditions for both ends have to be mentioned.

If a clamped-free rod is adopted, we can use the eigenvalue equation [6.16], from which value β is obtained for a given vibration mode order.

Young's modulus is derived from Bernoulli's equation. Bringing equation [6.7] into [6.4], we get:

$$-\rho\, s\, \omega^2 + EI\,\frac{\beta^4}{L^4} = 0$$

$$\text{or}\quad E = \frac{\rho\, S\, \omega^2\, L^4}{I\,\beta^4} \qquad [6.19]$$

@Seismicisolation

where I is the section's inertia moment with respect to z axis. If the cross-section is rectangular, we have:

$$I = \frac{b\,h^3}{12}, \text{ where b is width and h is thickness} \qquad [6.20]$$

Bringing equation [6.20] into [6.19], where m is rod mass and f the eigenfrequency which coincide with resonance frequency for small damping of material, we get:

$$E = \left(\frac{48\,\pi^2}{\beta^4}\right)\left(\frac{m}{b}\right)\left(\frac{L}{h}\right)^3 f^2 \qquad [6.21]$$

with $\omega^2 = 4\,\pi^2\,f^2$, ω the circular frequency and ρ rod density = M/bhL.

Vibration mode	1	2	3	4
β	1,8751	469,409	7,855	10,996

Table 6.3. *Eigenvalue β at the four first modes of a clamped-free rod*

6.3. Higher approximation theory of bending vibration

In Bernoulli-Euler's equation of motion [6.5], rotational inertia and shear effect are not accounted for in a section.

We will now present Timoshenko's equations of motion.

6.3.1. *Formulation of the equations of motion*

The method of generalized forces (force and moment) is used to formulate the equations of motion.

6.3.1.1. *Slope*

In Bernoulli's equation, the slope is entirely assimilated to the first derivative of flexural displacement with respect to coordinate z along the rod:

@Seismicisolation

$$\frac{\partial w}{\partial z} = \varphi \qquad \text{Bernoulli's theory}$$

In Timoshenko's theory, a part of the slope is due to shear effect:

$$\frac{\partial w}{\partial z} = \varphi + \gamma_0 \qquad [6.22]$$

So a new variable γ_0, the shear angle, is introduced. This variable is related to the shear force.

6.3.1.2. *Shear force and correcting coefficient K*

Knowing the shear stress σ_{xz} (x coordinate through the thickness), let us evaluate shear force:

$$F_S = \iint_S \sigma_{xz}\, dx\ dy \qquad [6.23]$$

The constitutive equation concerning σ_{xz} is:

$$\underline{\sigma}_{xz} = G_{xz}\, \gamma_{xz} \qquad [6.24]$$

Shear stress σ_{xz} in the section is not constant, see Figure 6.1. The gradient must be taken into account. As we have to deal with one-dimensional equations of motion, the space coordinate is z.

The equations we want to find concern the neutral plane. For a rectangular rod section and a material homogenous through the thickness, the neutral plane corresponds to the mid plane. Let γ_0 be the shear angle in this plane. Shear force (see Figure 6.1) is:

$$F_s = G_{xz}\, \gamma_0\, SK \qquad [6.25]$$

in which a correcting coefficient K is introduced to include the shear stress gradient, S being the area. In Appendix 6.A details of the calculation for a multilayered composite are presented. A composite of homogenous thickness is a good example. Calculation of coefficient K releases to the strength of the material (Timoshenko's

@Seismicisolation

method) or the asymptotic method suggested by Mindlin [MIN 51]. Let us remind ourselves that Timoshenko's coefficient is the same as for the static bending of a beam. With Mindlin's method, the dispersion curve of the phase velocity of a bending wave is examined against frequency. When the frequency is very high, the bending wave affects a thin external layer of the rod. The wave tends to be a Rayleigh surface wave. The velocity depends on elastic constants for an isotropic material. The coefficient also depends on the shape of the section.

For a rectangular section of isotropic material, K only depends on Poisson's coefficient ν:

$$K = \frac{10\left(1+\nu\right)}{12+11\,\nu} \qquad [6.26]$$

In Appendix 6.B values of K are presented for isotropic material and for various section shapes.

For composite material, ν is replaced by ν_{xz}, z being the coordinate along the rod's axis and x the coordinate through the thickness along which bending motion occurs.

Returning to equation [6.25], let us relate shear force F_s to the angle due to shear γ_0:

$$F_S\ G_{xz}\ SK\left(\frac{\partial\, w}{\partial\, z} - \varphi\right) \qquad [6.27]$$

with $\gamma_0 = \partial w/\partial z - \phi$. φ is the angle concerning bending. $\frac{\partial\, w}{\partial\, z}$ is the total slope expressing the angle between the section normal at the neutral plane and the normal before bending, see Figure 6.1c.

6.3.1.3. *Motion of a rod element*

The equation of motion is:

$$-F_S + F_S + \frac{\partial\, w}{\partial\, z}\, d\,z + q\left(z\right)\, d\,z = \rho\, S\, \frac{\partial^2\, w}{\partial\, t^2}\, d\,z \qquad [6.28]$$

@Seismicisolation

That is the same as [6.2]:

$$\frac{\partial F_S}{\partial z} + q(z) = \rho S \frac{\partial^2 w}{\partial t^2} \qquad [6.29]$$

6.3.1.4. *Flexural motion of the rod element*

$$- M + M + \frac{\partial M}{\partial z} dz + \frac{1}{2} F_S dz + \frac{1}{2} \left(F_S + \frac{\partial F_S}{\partial z} \right) dz = dJ \frac{\partial^2 \varphi}{\partial t^2} \qquad [6.30]$$

where J is the polar inertia of the element:

$$dJ = \rho I dz \qquad [6.31]$$

Equation [6.30] is reduced to:

$$F_S + \frac{\partial M}{\partial z} = \rho I \frac{\partial^2 \varphi}{\partial t^2} \qquad [6.32]$$

The bending moment is:

$$M = E_{zz} I \frac{\partial \varphi}{\partial z} \qquad [6.33]$$

Let us introduce equation [6.33] into [6.32]:

$$F_S + E_{zz} I \frac{\partial^2 \varphi}{\partial z^2} = \rho I \frac{\partial^2 \varphi}{\partial t^2} \qquad [6.34]$$

6.3.2. *Coupled equations of motion*

Replacing F by the value in equation [6.27], equation [6.34] becomes:

@Seismicisolation

$$G_{xz}\ SK\left(\frac{\partial\ w}{\partial\ z}\ -\ \varphi\right)+E_{zz}\ I\ \frac{\partial^2\ \varphi}{\partial\ z^2}=\rho\ I\ \frac{\partial^2\ \varphi}{\partial\ t^2} \qquad [6.35]$$

In equation [6.29], let us introduce variable φ:

$$G_{xz}\ SK\left(\frac{\partial^2\ w}{\partial\ z^2}\ -\ \frac{\partial\ \varphi}{\partial\ z}\right)+q\ (z,t)=\rho\ S\ \frac{\partial^2\ w}{\partial\ t^2} \qquad [6.36]$$

which is rearranged as:

$$-G_{xz}\ SK\left(\frac{\partial^2\ w}{\partial\ z^2}\ -\ \frac{\partial\ \varphi}{\partial\ z}\right)+\rho\ S\ \frac{\partial^2\ w}{\partial\ t^2}=q\ (z,t) \qquad [6.37]$$

6.3.3. *Decoupled equation of motion*

Equations [6.35] and [6.36] are two coupled equations in φ and w. Deriving [6.35] with respect to z, by substitution, we obtain the following equation in w:

$$\left(\rho\ S\ \frac{\partial^2\ w}{\partial\ t^2}+E_{zz}\ I\ \frac{\partial^4\ w}{\partial\ z^4}\right)+\frac{\rho^2\ I}{K\ G_{xz}}\ \frac{\partial^4\ w}{\partial\ t^4}$$
$$-\left(\rho\ I+\frac{E_{zz}\ \rho\ I}{G_{xz}\ K}\right)\frac{\partial^4\ w}{\partial\ t^4\ \partial\ z^2}= \qquad [6.38]$$
$$=\frac{\rho\ I}{K\ G_{xz}\ S}\ \frac{\partial^2\ q}{\partial\ t^2}-\frac{E_{zz}\ I}{K\ G_{xz}\ S}\ \frac{\partial^2\ q}{\partial\ z^2}+q(x,t)$$

In the decoupled equation of motion [6.38], we recognize that in the first member the first term corresponds to Bernoulli's equation.

Rotational inertia (with factor I) concerns the second and third terms.

Shear effect appears in terms including G_{xz}.

If there is no distributed force on the lateral surface, in the second member of [6.37] the term in q (z, t) is set to zero.

@Seismicisolation

6.3.3.1. *Boundary conditions*

The natural boundary conditions are given by variational calculus. Here we mention the boundary conditions obtained by the aforementioned method.

Kinematic boundary conditions	**Natural boundary conditions**
$\delta\varphi = 0$ φ prescribed angle due to flexural motion	$\dfrac{\partial \varphi}{\partial z} = 0$ Bending moment $M = 0$
$\delta w = 0$ w prescribed	$\dfrac{\partial w}{\partial z} - \varphi = \gamma = 0$ Shear force $F_s = 0$

Table 6.4. *Boundary conditions related to Timoshenko's equations of motion*

The three practical sets of boundary conditions are indicated in Table 6.5.

Clamping end	($\delta w = 0$, w prescribed) and $\begin{pmatrix} \delta\varphi = 0 \\ \varphi \text{ prescribed} \end{pmatrix}$
Free end	$\dfrac{\partial w}{\partial z} - \varphi = 0$ and $\dfrac{\partial \varphi}{\partial z} = 0$ shear force and bending moment are set to zero
Supported end	($\delta w = 0$, $w = 0$) and $\left(\dfrac{\partial \varphi}{\partial z} = 0 \text{ or } M = 0 \right)$

Table 6.5. *Practical boundary conditions*

@Seismicisolation

6.3.4. *Solution to the practical problem*

We adopt a clamped-free rod here, as we have done with Bernoulli's equation. In equation [6.37], the second member is set to zero.

6.3.5. *Stationary bending vibration*

Displacement w (z, t) is adopted as follows:

$$w\left(z, t\right) = \left(\exp j\,\omega\, t\right) \exp \frac{\beta\, z}{L} \qquad [6.39]$$

Bringing [6.38] into [6.37] we obtain:

$$\left(-\rho\, S\, \omega^2 + E_{zz}\, I\, \frac{\beta^4}{L^4}\right) + \frac{\rho^2\, I}{K G_z}\, \omega^4 - \left(\rho\, I + \frac{E_{zz}\, I\, \rho}{G_{xz}\, K}\right) \omega^2\, \frac{\beta^2}{L^2} = 0 \qquad [6.40]$$

If we want to calculate Young's modulus where circular frequency ω is known, β needs to be calculated from the boundary conditions.

6.3.6. *Non-dimensional equation of motion*

It is convenient to adopt non-dimensional parameters for the solution of β.

6.3.6.1. *Non-dimensional circular frequency*

Let us adopt:

$$T = \frac{\omega^2}{\omega_B^2} = \frac{\omega^2\, \rho\, S\, L^4}{E_{zz}\, I},$$

where ω_B comes from Bernoulli's equation [6.5].

6.3.6.2. *Inertia area moment*

$$u_1 = \frac{I}{S\, L^2} \qquad [6.41]$$

@Seismicisolation

6.3.6.3. *Transverse shear parameter*

$$u_2 = \frac{E_{zz}}{G_{xz}K}\, u_1 \qquad [6.42]$$

where u_1 and u_2 are adopted notations for inertia area moment and shear parameter. They are not to be confused with displacements u_x, u_y and u_z.

6.3.7. *Equation of motion with reduced variables*

For this purpose, let us divide all the terms in [6.39] by $E_{zz}\, I/L^4$:

$$\frac{-\rho\, S\, \omega^2\, L^4}{E_{zz}\, I} + \beta^4 + \frac{\rho^2\, I}{KG_{xz}}\, \frac{L^4\, \omega^4}{E_{zz}\, I} - \left(\rho\, I + \frac{E_{zz}\, I\, \rho}{G_{xz}\, K}\right) \frac{\omega^2\, \beta^2}{L^2}\, \frac{L^4}{E_{zz}\, I} = 0 \qquad [6.43]$$

Taking into account equations [6.40], [6.41] and [6.42], we can write equation [6.43] in the following form:

$$-T + \beta^4 + T^2\, u_1\, u_2 + T\,(u_1 + u_2)\, \beta^2 = 0\,.$$

By rearranging in increasing order of β:

$$\beta^4 + T\,(u_1 + u_2)\, \beta^2 + T\,(u_1\, u_2\, T - 1) = 0 \qquad [6.44]$$

This bisquared equation in β^2 has two roots β_1^2 and $-\beta_2^2$ with opposite signs as we can easily see in the second member of [6.45]:

$$\left.\begin{matrix}\beta_1^2 \\ -\beta_2^2\end{matrix}\right\} = \frac{1}{2}\left[\pm\left\{T^2\,(u_1 + u_2)^2 - 4T\,(u_1\, u_2\, T - 1)\right\}^{1/2} - T\,(u_1 + u_2)\right]$$

@Seismicisolation

$$\left.\begin{matrix}\beta_1^2 \\ -\beta_2^2\end{matrix}\right\} = \frac{1}{2}\left[\pm\left\{T^2\ (u_1 - u_2)^2 + 4T\right\}^{1/2} - T\ (u_1 + u_2)\right] \qquad [6.45]$$

The four roots of equation [6.44] are (β_1, -β_1, j β_2, -j β_2).

6.3.8. *Expression of flexural displacement and shear φ*

With the equations presented above, displacement is of the following form:

$$w(z, t) = (\exp j\,\omega\, t)\left[\begin{matrix} A_1 \cos h \dfrac{\beta_1\, z}{L} + B_1 \sin h \dfrac{\beta_1\, z}{L} \\ \\ + C_1 \cos \dfrac{\beta_2\, z}{L} + D_1 \sin \dfrac{\beta_2\, z}{L} \end{matrix}\right] \qquad [6.46]$$

A similar expression can be adopted for φ (z, t), however, with a different set of coefficients A_2, B_2, C_2 and D_2 :

$$\varphi(z, t) = (\exp j\,\omega\, t)\left[\begin{matrix} A_2 \cos h \dfrac{\beta_1\, z}{L} + B_2 \sin h \dfrac{\beta_1\, z}{L} + \\ \\ + C_2 \cos \dfrac{\beta_2\, z}{L} + D_2 \sin \dfrac{\beta_2\, z}{L} \end{matrix}\right] \qquad [6.47]$$

For four boundary conditions we only have four equations for solving the eight unknowns (A_1, B_1, C_1, D_1) and (A_2, B_2, C_2, D_2).

Fortunately, the two sets of coefficients can be joined up together by equation [6.29], which is rewritten with variables φ and w in [6.37]. This last equation is arranged as follows, with q (z, t) = 0:

$$\frac{\partial^2 w}{\partial z^2} - \frac{\rho}{K\, G_{xz}} \frac{\partial^2 w}{\partial t^2} = \frac{\partial \varphi}{\partial z} \qquad [6.48]$$

@Seismicisolation

In equations [6.41] and [6.42], φ (z, t) in the second member of equation [6.48] is related to w (z, t) in the first member. The following equations can thus be deduced:

$$A_2 = \frac{T\,u_2 + \beta_1^2}{L\,\beta_1}\,B_1 = r\,B_1\,;$$

$$B_2 = \frac{T\,u_2 + \beta_1^2}{L\,\beta_1}\,A_1 = r\,A_1 \qquad [6.49]$$

$$C_2 = \left(-\frac{\left(T\,u_2 - \beta_2^2\right)}{L\,\beta_2}\right)D_1 = -\,s\,D_1\,;$$

$$D_2 = \frac{T\,u_2 - \beta_2^2}{L\,\beta_2}\,C_1 = s\,C_1$$

6.3.9. *Coefficient calculations*

The two boundary conditions for a clamped-free rod are:

z = L free end: shear force and bending moment set to zero

z = 0 clamped end: w = 0 $\varphi = 0$ [6.50]

The eigenvalue equation is obtained by writing the four boundary conditions indicated above. To obtain a non-trivial solution for the coefficients, the coefficient determinant is set to zero:

$$\begin{vmatrix} 1 & 0 & 1 & 0 \\ 0 & r & 0 & -s \\ \beta_1\,r\cos h\,\beta_1 & \beta_1\,r\sin h\,\beta_1 & \beta_2\,s\cos\beta_2 & \beta_2\,s\sin\beta_2 \\ \left(\frac{\beta_1}{L}-r\right)\sin h\,\beta_1 & \left(\frac{\beta_1}{L}-r\right)\cos h\,\beta_1 & -\left(\frac{\beta_2}{L}+s\right)\sin\beta_2 & \left(\frac{\beta_2}{L}+s\right)\cos\beta_2 \end{vmatrix} = 0$$

[6.51]

@Seismicisolation

Developing [6.51], the following equation is obtained:

$$2+\left[2+\frac{T\,(u_1-u_2)^2}{1+Tu_2(u_1+u_2)}\right]\cos h\,\beta_1\,\cos\beta_2-\sin h\,\beta_1\,\sin\beta_2\,\frac{\sqrt{T}\,(u_1+u_2)}{(1-u_1\,u_2\,T)^{1/2}}=0$$

[6.52]

β_1 and β_2 are evaluated from [6.45]:

$$\left.\begin{aligned}\beta_2^2-\beta_1^2&=T\,(u_1+u_2)\\ \beta_1^2\,\beta_2^2&=T\,(1-u_1\,u_2\,T)\end{aligned}\right\}$$

[6.53]

Let us mention that the implicit equations in β_2 and β_1 are more complex than the eigenvalue equation [6.16], which is related to Bernoulli's equation [6.5]. In [6.16] the two roots are equal.

$$\beta_1=\beta_2=\beta$$

6.3.10. *Evaluation of Young's modulus by solution of Timoshenko's equation*

Using dimensionless variables, equation [6.40] gives us a dimensionless circular frequency $\omega^2/\omega_B^2=T$, with ω_B^2 being the eigenvalue in Bernouilli's theory.

Equations [6.52] and [6.53] can be solved using a computer program. In Figure 6.2, elementary theory is referred to in the first step. A value of β_2 assimilated to β_0 and equation [6.16] is adopted.

6.3.10.1. *First step:* $\beta_2=\beta_0$

$$1+\cos h\,\beta_0\,\cos\beta_0=0 \qquad [6.54]$$

6.3.10.2. *Second step: calculation of* β_2 *and* T

Equations [6.52] and [6.53] are used to evaluate the improved values of β_2 and β_1.

@Seismicisolation

6.3.10.3. *Trial and error calculation of β_2 and T using a loop*

This calculation is conduced until the accuracy for β_2, say $\Delta\beta_2/\beta_2$, reaches a prescribed value.

6.3.10.4. *Second loop calculation for Young's modulus*

In this calculation, β_1 is evaluated by equation [6.53].

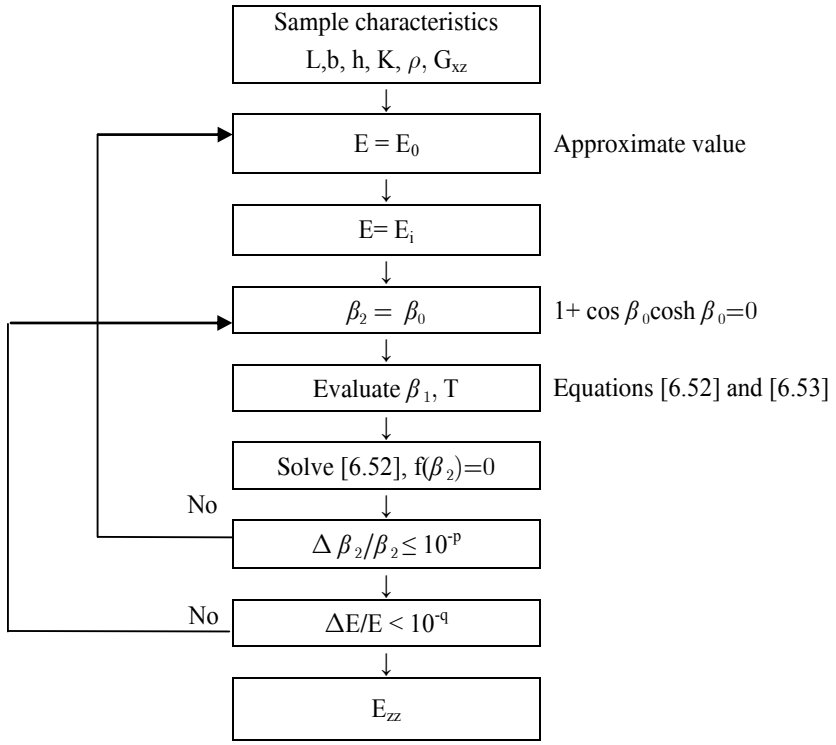

Figure 6.2. *Computer program to evaluate E_{zz} using Timoshenko's equation*

Let us focus our attention on the calculation of Young's modulus, as presented in Figure 6.2. E_{zz} is not evaluated by equation of motion [6.21], which is valid for Bernoulli-Euler's equation. There are four roots β_i. Young's modulus is evaluated from T in equation [6.40] after loop calculations that enable us to obtain the value of $E_{zz} = E_i$.

@Seismicisolation

6.3.11. *Dispersion curves related to various theories of bending waves in a rod*

Wave dispersion is an important problem in the dynamic bending of a rod, particularly at high frequency.

Figure 6.C.1 in Appendix 6.C gives the trends of three curves representing bending phase velocity v_F *versus* frequency for Bernoulli's theory, Love's theory and Timoshenko's theory. The three curves show that, at high frequency, errors in the calculation of phase velocity by Bernoulli's theory may be important.

When eigenfrequency corresponds to a higher mode, the discrepancies between calculated Young's moduli by various theories (Bernoulli, Love and Timoshenko) can be important, see Figure 6.3.

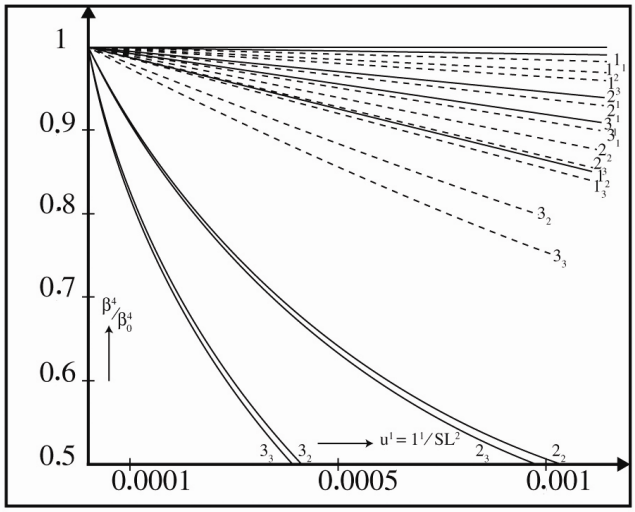

Figure 6.3. *The influence of rotational inertia and transverse shear on steel and graphite-epoxy composite materials that are free-clamped. Curves* $(\beta/\beta_0)^4$ *where* β *is the wave number for various equations of motion and* β_0 *Bernoulli's wave number* versus *slenderness* I/SL^2. *In this figure, index number 1 is related to Love's correction, 2 to shear effect, and 3 to combined influences (rotational inertia + shear) in Timoshenko's theory. For capital numbers, 1 is the first mode, 2 second mode and 3 third mode. Curves with dotted lines are steel and curves with continuous lines are a graphite-epoxy composite*

@Seismicisolation

6.3.12. *Influence of rotational inertia and transverse shear*

It is interesting to evaluate the efficiency of each equation of motion by separately examining the influence of *rotational inertia*, *transverse shear effect* and their combined influence.

The nature of the material itself is important. Comparing steel and some composite materials, we will see that shear effect is predominant for composite materials, taking into account the ratio E_{zz}/G_{xz}. This is an important factor.

In Figure 6.3, a set of curves are presented. The ratio β^4/β_0^4 represents the fourth power of the wave number quotient (or root of the equation of motion).

The wave number concerning Bernoulli's equation is represented against slenderness, defined as I/SL^2, where I is the section's inertia moment with respect to the neutral line.

The difference in wave number compared to Bernoulli's wave number is not important (curves in dotted lines) for steel, particularly at lower vibration modes.

On the contrary, for a composite material, such as the graphite-epoxy composite, the influence of shear is very pronounced and the ratio is much higher than three (for metals).

$$\frac{E_{zz}}{G_{xz}} = 40$$

Timoshenko's equation is consequently preferred to Bernoulli's and Love's equations. Love's equation ignores shear effect and only retains the effect of inertia.

As vibration mode increases, the discrepancy between Timoshenko's wave number and Bernoulli's wave number becomes very important (curves in continuous lines). The shear effect for this composite material is more important than the rotational inertia effect.

The circumstances presented above are very helpful for making the correct choice of apparatus and equation of motion.

@Seismicisolation

6.4. Bending vibration of an off-axis anisotropic rod

Off-axis anisotropic rods are adopted in flexural vibration in order to evaluate the non-diagonal elastic components of the stiffness matrix or some Poisson's coefficients of composite materials.

On-axis rods are used in order to avoid coupling between bending motion and shear motion. With such rods, diagonal coefficients of an elastic matrix are obtained, such as Young's moduli of composite materials.

It is, however, necessary to evaluate the non-diagonal component of elastic matrix wave coupling.

6.4.1. *Preliminary considerations*

In the choice of rods and equations of motion, the objective is to obtain tractable equations of motion. The equations need to be compatible with the exploitation of experimental results that are not considered insurmountable. For this purpose, where possible we want to choose a degree of equations of motion that is not too high.

Let us take an example. In coupled motions of a rod with rectangular sections, fourth-order equations of motion for torsional vibrations combine with flexural vibrations, which give rise to a fourth-order equation of motion. From this we obtain two coupled equations of motion of the fourth order.

By substitution method, an eighth-order differential equation is obtained for the decoupled equation of motion. So if we adopt a second-order equation for torsional motion and a fourth-order equation for flexural motion, the result gives rise to a sixth-order decoupled equation of motion. This method will be retained below when an appropriate sample (length, slenderness, etc.) is chosen and there is a low vibration mode for torsional motion.

6.4.2. *Flexural vibration of an off-axis rod*

Figure 6.4 represents a rod with rectangular cross-section. The symmetry axis of the anisotropic material does not coincide with the rod axis. The material is a homogenous composite with long fibers embedded in a resin matrix. The fibers are regularly distributed. α is the angle between fiber direction and rod axis.

@Seismicisolation

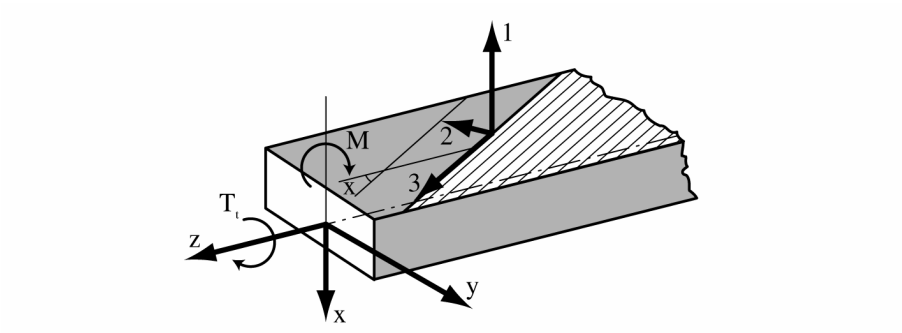

Figure 6.4. *A transverse isotropic composite material with 1, 2 and 3 symmetry axes, x, y and z rod axes with, T_t torque and M bending moment*

6.4.3. *Equations of motion*

Torsional motion is governed by Saint-Venant's theory and bending motion by Timoshenko's one. Bending and shear motion correspond to two angles, φ and γ_0, respectively:

$$\frac{\partial w}{\partial z} = \varphi + \gamma_0$$

$$\frac{\partial w}{\partial z} = \varphi + \frac{F_S}{KG_{xz}\,S} \qquad [6.55]$$

$$\frac{\partial \varphi}{\partial z} = \frac{M}{E_{zz}\,I}\,\frac{T_t}{C_{mt}} \qquad [6.56]$$

C_{mt} designates the coupling coefficient between torsion and bending, M the bending moment, T_t torque, F_s shear in a cross-section and K the shear correcting coefficient.

$$\frac{\partial \theta}{\partial z} = \frac{T_t}{C_T} - \frac{M}{C_{mt}} \qquad [6.57]$$

@Seismicisolation

θ is the torsional angle around rod axis z, and C_T is the torsional stiffness of the rod.

$$\frac{\partial M}{\partial z} + F = \rho I_z \frac{\partial^2 \varphi}{\partial t^2} \qquad [6.58]$$

$$\frac{\partial F_S}{\partial z} = \rho S \frac{\partial^2 w}{\partial t^2} \qquad [6.59]$$

$$\frac{\partial T}{\partial z} = I_{pz} \frac{\partial^2 \theta}{\partial t^2} \qquad [6.60]$$

where I_{pz} is the polar moment of the cross-section with respect to the rod axis z. Bending displacement along the y axis is supposed to be negligible.

Equations [6.56] and [6.57] show that there are linear equations connecting bending moment M and torque T_t.

$$\left.\begin{aligned} M &= a \frac{\partial \varphi}{\partial z} + b \frac{\partial \theta}{\partial z} \\ T_t &= c \frac{\partial \varphi}{\partial z} + d \frac{\partial \theta}{\partial z} \end{aligned}\right\} \qquad [6.61]$$

with:

$$a = \frac{1}{C_T \Delta}, \qquad b = \frac{1}{C_{mt} \Delta},$$

$$c = \frac{1}{C_{mt} \Delta}, \qquad d = \frac{1}{E_{zz} I \Delta}$$

$$\Delta = \frac{1}{C_T E_{zz} I} - \frac{1}{C_{mt}^2} \qquad [6.62]$$

@Seismicisolation

Equations [6.56] and [6.57] give rise to:

$$\rho\, S\, \frac{\partial^2 w}{\partial t^2} = KG_{xz}\, S \left(\frac{\partial^2 w}{\partial z^2} - \frac{\partial \varphi}{\partial z} \right)$$

$$KG_{xz} \left(\frac{\partial^2 w}{\partial z^2} - \frac{\partial \varphi}{\partial z} \right) = \rho\, \frac{\partial^2 w}{\partial t^2} \qquad [6.63]$$

Bringing [6.61] into [6.58] and [6.60], we get:

$$a\, \frac{\partial^2 \varphi}{\partial z^2} + b\, \frac{\partial^2 \theta}{\partial z^2} + KG_{xz}\, S \left(\frac{\partial w}{\partial z} - \varphi \right) = \rho\, I\, \frac{\partial^2 \varphi}{\partial t^2} \qquad [6.64]$$

$$c\, \frac{\partial^2 \varphi}{\partial z^2} + d\, \frac{\partial^2 \theta}{\partial z^2} = \rho\, I_{pz}\, \frac{\partial^2 \theta}{\partial t^2} \qquad [6.65]$$

We have three displacement variables: w, φ and θ.

We also have three coupled equations: [6.63], [6.64] and [6.65].

By successive elimination we can obtain the following sixth-order equations of motion in w:

$$-\frac{1}{\Delta \rho I_{pz}} \frac{\partial^6 w}{\partial z^6} + B \frac{\partial^6 w}{\partial z^4\, \partial t^2} - C \frac{\partial^6 w}{\partial z^2\, \partial t^4} - D \frac{\partial^6 w}{\partial z^2 \partial t^2}$$

$$+ \rho\, S \frac{\partial^4 w}{\partial t^4} + \frac{\rho\, I}{KG_{xz}} \frac{\partial^6 w}{\partial t^6} = 0 \qquad [6.66]$$

$$B = \frac{1}{\Delta\, KG_{xz}\, I_{pz}} + \frac{E_{zz}\, I}{\left(1 - \dfrac{C_T\, E_{zz}\, I}{C_{mt}^2} \right)} + \frac{I\, C_T\, C_{mt}^2}{I_{pz} \left(C_{mt}^2 - C_T\, E_{zz}\, I \right)}$$

@Seismicisolation

$$C = \frac{\rho}{KG_{xz}} \left(KG_{xz}\, I + \frac{E_{zz}\, I}{1 - \frac{C_T\, E_{zz}\, I}{C_{mt}^2}} + \frac{I\, C_T}{I_{pz}\left(1 - \frac{C_T\, E_{zz}\, I}{C_{mt}^2} \right)} \right)$$

$$D = \frac{S\, C_T\, C_{mt}^2}{I_{pz}\left(C_{mt}^2 - C_T\, E_{zz}\, I \right)} \qquad [6.67]$$

6.4.4. *Reduced variables and characteristic frequency equations for stationary waves*

Adopting variable separation:

$$w = W(\xi) \exp j\omega t,$$

$$\varphi = \Phi(\xi) \exp j\omega t,$$

$$\theta = \Theta(\xi) \exp j\omega t,$$

$$\xi = z / L \qquad [6.68]$$

Reduced coordinate ξ is adopted to simplify equation writing.

6.4.4.1. *Reduced variables and reduced coefficients*

$$T = \frac{\omega^2\, \rho\, S\, L^4}{E_{zz}\, I},\ v_1 = \frac{I}{S\, L^2},\ v_2 = \frac{E_{zz}}{KG_{xz}}$$

$$v_3 = \frac{E_{zz}\, I_{pz}}{C_T},\ v_4 = \frac{C_T\, E_{zz}\, I}{C_{mt}^2} \qquad [6.69]$$

Bringing equations [6.69] and [6.66] into [6.67], we obtain the following characteristic equation which is valid for all three displacement variables w, φ and θ with $\xi = z/L$.

@Seismicisolation

We designate s to one of the three aforementioned variables.

$$y^{(6)}(\xi)+y^{(4)}\ v_1\ T(1+v_2+v_3)+y^{(2)}\left[v_1^2\ T^2\left(v_2+v_3\ (1-v_4)+v_2\ v_3\right)-T\right]+$$

$$+\,y(\xi)\left[v_1^3\ T^3\ v_2\ v_3(1-v_4)\right]-v_1\ T^2\ v_3(1-v_4)=0 \qquad [6.70]$$

The superscript figure between parentheses designates the order of space derivative ξ.

6.4.4.2. *Relationships between the set of coefficients of* w, φ *and* θ

$$W(\xi)=A_1\ \cos h\ \alpha\ \xi+B_1\ \sin h\ \alpha\ \xi+C_1\ \cos\beta\ \xi+D_1\ \sin\beta\ \xi$$
$$+E_1\ \cos\gamma\ \xi+F_1\ \sin\gamma\ \xi$$

$$\Phi(\xi)=A_2\ \sin h\ \alpha\ \xi+B_2\ \cos h\ \alpha\xi\ +C_2\ \sin\beta\ \xi+D_2\ \cos\beta\ \xi$$
$$+E_2\ \sin\gamma\ \xi+F_2\ \cos\gamma\ \xi$$

$$\Theta(\xi)=A_3\ \sin h\ \alpha\ \xi+B_3\ \cos h\ \alpha\ \xi\ +C_3\ \xi\sin\beta\ \xi\ +D_3\ \cos\beta$$
$$+E_3\ \sin\gamma\ \xi+F_3\ \cos\gamma\ \xi \qquad [6.71]$$

The sets of coefficients in equation [6.71] are mutually dependent via two equations of motion [6.64] rewritten here:

$$\left.\begin{aligned}&\frac{\partial\varphi}{\partial z}=\frac{\partial^2 w}{\partial z^2}-\frac{\rho}{K\,G_{xz}}\ \frac{\partial^2 w}{\partial t^2}\\&c\frac{\partial^2\varphi}{\partial z^2}+d\ \frac{\partial^2\theta}{\partial z^2}-\rho\ I_{pz}\ \frac{\partial^2\theta}{\partial t^2}=0\end{aligned}\right\} \qquad [6.72]$$

Using equation [6.68], we get:

$$W^{(2)}(\xi)+T\ v_1\ v_2\ W\ (\xi)-L\ \Phi^{(1)}(\xi)=0 \qquad [6.73]$$

@Seismicisolation

$$v_5\ \Phi^{(2)}(\xi) + \Theta^{(2)}(\xi) + T\ v_1\ v_2\ (1 - v_4)\ \Theta\ (\xi) = 0$$

with

$$v_5 = \frac{c}{d} = \frac{I\ E_{zz}}{C_{mt}}.$$

Bringing [6.71] into the first equation in [6.73]:

$$\left.\begin{aligned} A_2 &= \frac{T\ v_1\ v_2 + \alpha^2}{L\ \alpha}\ A_1; \qquad B_2 = \frac{T\ v_1\ v_2 + \alpha^2}{L\ \alpha}\ B_1 \\ C_2 &= \frac{T\ v_1\ v_2 - \beta^2}{L\ \beta}\ C_1; \qquad D_2 = -\frac{T\ v_1\ v_2 - \beta^2}{L\ \beta}\ D_1 \\ E_2 &= \frac{T\ v_1\ v_2 - \gamma^2}{L\ \gamma}\ E_1; \qquad F_2 = -\frac{T\ v_1\ v_2 - \gamma^2}{L\ \gamma}\ F_1 \end{aligned}\right\} \qquad [6.74]$$

Bringing [6.71] into the second equation of [6.73]:

$$A_3 = \frac{-\alpha^2\ v_5}{\alpha^2 + T\ v_1\ v_2\ (1 - v_4)}\ A_1; \qquad B_3 = \frac{-\alpha^2\ v_5}{\alpha^2 + T\ v_1\ v_3\ (1 - v_4)}\ B_1$$

$$C_3 = \frac{\beta^2\ v_5}{-\beta^2 + T\ v_1\ v_2\ (1 - v_4)}\ C_1; \qquad D_3 = \frac{\beta^2\ v_5}{-\beta^2 + T\ v_1\ v_2\ (1 - v_4)}\ D_1 \qquad [6.75]$$

$$E_3 = \frac{\gamma^2\ v_5}{-\gamma^2 + T\ v_1\ v_3\ (1 - v_4)}\ E_1; \qquad F_3 = \frac{\gamma^2\ v_5}{-\gamma^2 + T\ v_1\ v_3\ (1 - v_4)}\ F_1$$

@Seismicisolation

For simplification, let us rewrite [6.74] and [6.75] as:

$$\left.\begin{array}{ll} A_3 = l\,A_2 = l\;i\,A_1; & B_3 = l\,B_2 = l\,i\,B_1 \\ C_3 = m\,C_2 = m\,p\,C_1; & D_3 = m\,D_2 = -m\,p\,D_1 \\ E_3 = n\,E_2 = n\,k\,E_1; & F_3 = n\,F_2 = -n\,k\;F_1 \end{array}\right\} \qquad [6.76]$$

The new set of coefficients – l, i, m, n, p and k – are easily identified.

6.4.4.3. *Boundary conditions*

The example of a (clamped-free) off-axis rod is analyzed here.

– Clamped end at z = 0:

$$\left.\begin{array}{l} w\,(0,t) = 0 \\ \varphi\,(0,t) = 0 \\ \theta\,(0,t) = 0 \end{array}\right\} \rightarrow \left.\begin{array}{l} W\,(0) = 0 \\ \Phi\,(0) = 0 \\ \Theta\,(0) = 0 \end{array}\right\} \qquad [6.77]$$

– Free end at z = L:

$$\left.\begin{array}{l} M\,(L,t) = 0 \\ F_S\,(L,t) = 0 \\ T_t\,(0,t) = 0 \end{array}\right\} \rightarrow \left.\begin{array}{l} \Phi^{(1)}(1) = 0 \\ \Theta^{(1)}(1) = 0 \\ \dfrac{W^{(1)}}{L}\,(1) - \Phi\,(1) = 0 \end{array}\right\} \qquad [6.78]$$

@Seismicisolation

By expressing equations [6.77] and [6.78] by using [6.71] for the clamped end, we get:

$$\left.\begin{aligned} A_1 + C_1 + E_1 &= 0 \\ B_2 + D_2 + F_2 &= 0 \\ B_3 + D_3 + F_3 &= 0 \end{aligned}\right\} \qquad [6.79]$$

and for the free end:

$$\left.\begin{aligned} &\alpha \cosh \alpha A_2 + \alpha \sinh \alpha B_2 + \beta \cos\beta C_2 - \beta \sin\beta D_2 \\ &+ \gamma \cos \gamma E_2 - \gamma \sin \gamma F_2 = 0 \\ &\alpha \cosh \alpha A_3 + \alpha \sinh \alpha B_3 + \beta \cos\beta C_3 - \beta \sin\beta D_3 \\ &+ \gamma \cos \gamma E_3 - \gamma \sin \gamma F_3 = 0 \\ &\frac{1}{L}\left(\begin{aligned} &\alpha \sinh \alpha A_1 + \alpha \cosh \alpha B_1 - \beta \sin\beta C_1 + \beta \cos\beta D_1 \\ &- \gamma \sin \gamma E_1 + \gamma \cos \gamma F_1 \end{aligned}\right) - \\ &-(\sinh \alpha A_2 + \cosh \alpha B_2 + \sin\beta C_2 + \cos\beta D_2 \\ &+ \sin \gamma E_2 + \cos \gamma F_2) = 0 \end{aligned}\right\} \qquad [6.80]$$

[6.80] and [6.79] constitute six homogenous equations with six unknown coefficients A_1, B_1, C_1, D_1, E_1 and F_1.

From [6.76] it is easy replace the coefficients (A_2, B_2, C_2, D_2, E_2 F_2) and (A_3, B_3, C_3, D_3, E_3, F_3) with the set of coefficients with index 1.

A non-trivial solution is obtained by setting the coefficient determinant to zero.

@Seismicisolation

6.4.4.4. *Eigenvalue equation*

$$\begin{pmatrix} 1 & 0 & 1 & 0 & 1 & 0 \\ 0 & i & 0 & -p & 0 & -k \\ 0 & li & 0 & -mp & 0 & -nk \\ (a_i \cosh\alpha) & (i\,\alpha \sinh\alpha) & (p\,\beta \cos\beta) & (p\,\beta \sin\beta) & (k\,\gamma \cos\gamma) & (k\,\gamma \sin\gamma) \\ (i\,l\,\alpha \cosh\alpha) & (i\,l\,\alpha \sinh\alpha) & (p\,m\,\beta \cos\beta) & (p\,m\,\beta \sin\beta) & (k\,n\,\gamma \cos\gamma) & (k\,n\,\gamma \cos\gamma) \\ \left(\frac{\alpha}{L}-i\right)\sinh\alpha & \left(\frac{\alpha}{L}-i\right)\cosh\alpha & \left(-\frac{\beta}{L}-p\right)\sin\beta & \left(\frac{\beta}{L}+p\right)\cos\beta & \left(-\frac{\gamma}{L}-k\right)\sin\gamma & \left(-\frac{\gamma}{L}-k\right)\cos\gamma \end{pmatrix} = 0$$

[6.81]

By developing [6.81], the characteristic equation is obtained as follows:

$$\cosh\alpha \cos\alpha \cos\gamma \left[\frac{i\,\alpha\,p\,\beta(m-l)}{k\,\gamma(n-l)(m-n)} + \frac{p\,\beta\,k\,\gamma(m-n)}{i\,\alpha(m-l)(n-l)} + \frac{k\,\gamma\,i\,\alpha(n-l)}{p\,\beta(m-l)(m-n)}\right]$$

$$-\sinh\alpha \sin\beta \cos\gamma \left[\frac{k\,\gamma}{m-l}\,\frac{\beta^2-\alpha^2}{\beta\,\alpha}\right] -2\left[\frac{i\,\alpha \cosh\alpha}{m-n} + \frac{p\,\beta \cos\beta}{n-l} - \frac{k\,\gamma \cos\gamma}{m-l}\right] = 0$$

[6.82]

To lighten the equation writing, [6.82] has a new form as follows:

$$(\cosh\alpha \cos\alpha \cos\gamma)\left(\frac{t_1\,t_2}{t_3} + \frac{t_2\,t_3}{t_1} + \frac{t_3\,t_1}{t_2}\right)$$

$$+\sin\gamma\left[\sinh\alpha \cos\beta \bullet t_2\,\frac{\alpha^2-\gamma^2}{\alpha\,\gamma}\right]-$$

$$-\cosh\alpha \sin\beta\left[t_1\,\frac{(\beta^2+\gamma^2)}{\beta\gamma}\right] + (\sinh\alpha \sin\beta \cos\gamma)\left(t_3\,\frac{\alpha^2-\beta^2}{\alpha\,\gamma}\right)$$

$$+2\,(t_1 \cos h\,\alpha + t_2 \cos\beta + t_3 \cos\gamma) = 0$$

[6.83]

@Seismicisolation

with:

$$t_1 = \frac{i\,\alpha}{m-n} = \frac{T\,v_1\,v_2 + \alpha^2}{\left[\dfrac{\beta^2}{-\beta^2 + T\,v_1\,v_3\,(1 - v_4)} - \dfrac{\gamma^2}{-\gamma^2 + T\,v_1\,v_3\,(1 - v_4)}\right]}$$

$$t_2 = \frac{p\,\beta}{n-l} = \frac{T\,v_1\,v_2 - \beta^2}{\left\{\dfrac{\gamma^2}{-\gamma^2 + T\,v_1\,v_3\,(1 - v_4)} + \dfrac{\alpha^2}{\alpha^2 + T\,v_1\,v_3\,(1 - v_4)}\right\}}$$

$$t_3 = \frac{k\,\gamma}{l-m} = \frac{T\,v_1\,v_2 - \gamma^2}{\left\{\dfrac{-\alpha^2}{\alpha^2 + T\,v_1\,v_2\,(1 - v_4)} - \dfrac{\beta^2}{-\beta^2 + T\,v_1\,v_2\,(1 - v_4)}\right\}}$$

[6.84]

Equations [6.83] and [6.82] must be associated with circular frequency equation [6.70], in which T represents the square of reduced circular frequency.

6.4.4.4.1. Relationship between the roots of a characteristic polynomial

By solving [6.70], the roots of this equation give the following relationship:

$$\alpha^2\,\beta^2\,\gamma^2 = T^2\,v_1\,v_2\,(1 - v_4) + T^3\,v_1^3\,v_2\,v_3\,(1 - v_4) \qquad [6.85a]$$

$$-\alpha^2\,\beta^2 - \alpha^2\,\gamma^2 + \beta^2\,\gamma^2 = T^2\,v_1^2\,\left(v_2\,v_3 + v_2 + v_3\,(1 - v_4)\right) - T \qquad [6.85b]$$

$$\alpha^2 - \beta^2 - \gamma^2 = -T\,v_1\,(1 + v_2 + v_3) \qquad [6.85c]$$

Taking into account the lengthy equations [6.82] and [6.84], [6.83] and [6.85], a computer program can be built to evaluate T and Poisson's number v_{31}. In Appendix 6.D, the set of elastic moduli s_{ij} (i, j = x, y, z) *versus* elastic moduli s_{ij} (i, j = 1, 2, 3) defined with the material's axis of symmetry are given. It is worth commenting on equation [6.D.1] regarding the accuracy of elastic moduli calculations using an off-axis rod.

@Seismicisolation

In [6.D.1], the diagonal coefficients of compliance matrix are G_{ij} (the shear moduli) and E_{ii} (Young's moduli) in the natural symmetry direction of the materials.

The objective of measuring Young's moduli with an off-axis rod is to evaluate the Poisson's number. The accuracy of this measurement (v_{13} from equation [6.D.1a]) depends on many factors:

– the accuracy of previous measurements of E_{11}, E_{33} and G_{13};

– the accuracy of angle α during fabrication of the off-axis rod.

Elastic compliances belong to the fourth-order tensor (see Chapter 1). The elastic constant coefficient of each compliance in the second member of [6.D.1a] is expressed as the fourth power of trigonometric functions cos α and sin α. This constitutes the main difficulty in the evaluation of v_{ij}.

6.4.5. *Computer program using trial and error method to evaluate Poisson's number*

Figure 6.5 gives the successive steps needed for calculating Poisson's number.

6.5. Concluding remarks

The following remarks are aimed at practicians.

6.5.1. *Choice of equations of motion*

Bernoulli-Euler's equation of bending is applicable on the condition that experiments are limited to a low frequency. The frequency validity range must be checked to ensure the effective dispersion wave effect can be assimilated to Bernoulli wave dispersion (see curve in Figure 6.C.1 in Appendix 6.C).

Timoshenko's equation is valid in the whole frequency range, including higher frequencies.

When we have to deal with a short sample that is very slim slenderness, Bernoulli-Euler's equation is no longer valid for evaluating Young's modulus.

@Seismicisolation

6.5.2. *Test sample slenderness and influence of shear effect*

When experimenters have to deal with a composite material they must be careful when choosing the dimensions of the sample. The thicker the sample, the more critical the influence of shear effect. In the case of a very thick sample, it is necessary to use Timoshenko's equation.

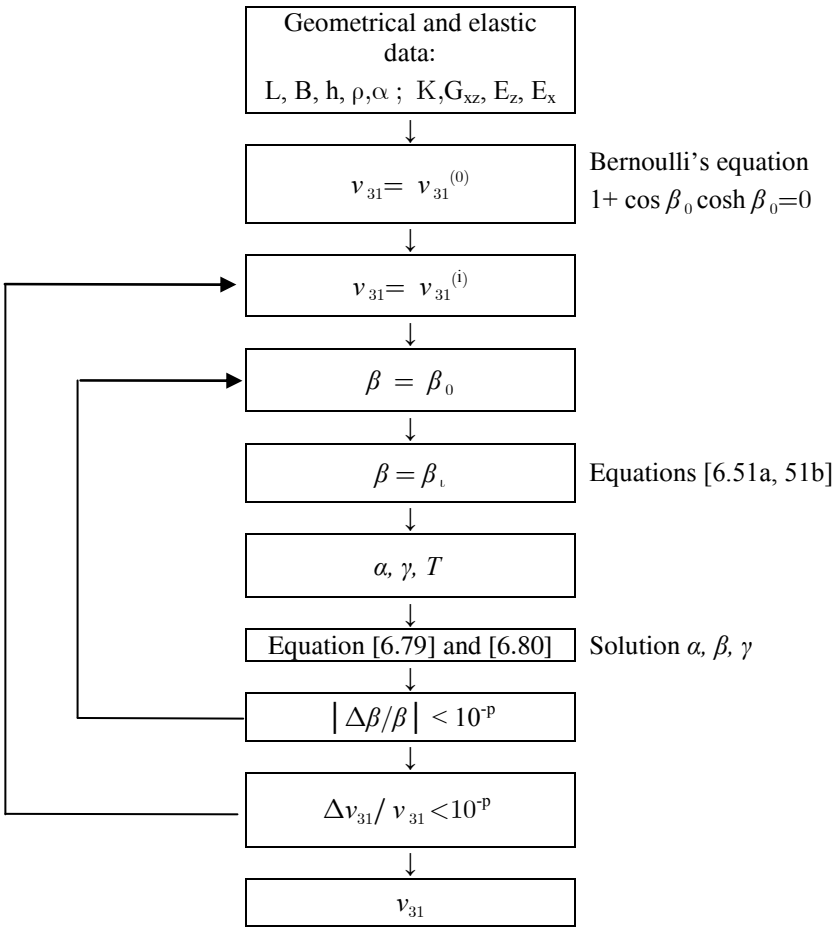

Figure 6.5. *Computer program to obtain Poisson's number ν_{31}*

@Seismicisolation

6.5.3. *Strong influence of shear effect for composite materials: accuracy of Young's modulus and non-diagonal technical modulus evaluation*

Coupled equations combining the bending and torsion of an off-axis sample are interesting for evaluating some non-diagonal components of the compliance matrix. Coupled equations are used for composite materials. The experimenter must bear in mind, however, that a change of reference axes in an off-axis rod when using Young's modulus concerns the elastic compliance tensor $S_{\alpha\beta\gamma\delta}$, which is of fourth order. This raises the problem of accuracy when measuring non-diagonal components using four direction cosines for changing a reference axis! One technique that can be used to overcome this difficulty is the utilization of invariants, which is covered in Chapter 1.

6.5.4. *Comments on computational effort to evaluate Young's modulus for off-axis samples*

This chapter systematically uses characteristic functions to evaluate eigenvalues. The calculations using characteristic functions become cumbersome when the degree of equations of motion exceeds six. This constitutes the limit beyond which it is necessary to make a numerical calculation of matrices (see Chapter 12) using the so-called continuous elements.

6.6. Bibliography

[BER 1751] BERNOULLI D., *De Vibrationibus et Sono Laminarum Elasticarum*, *de Sonis Multiferiis quos Laminae Elasticae Edunt*, Commentarii Academiae Scientarum Imperialis Petropolitanae, vol. 13, p. 105-120, 1751.

[CHO 71] CHOW T. S., "On the propagation of flexural waves hotropic laminated plate and its response to an impulsive load", *Journal of Composite Materials*, vol. 5, p.320, 1971.

[COW 66] COWPER G. R., "The shear coefficient in Timoshenko beam theory", *Journal of Applied Mechanics*, vol. 33, p. 335-340, 1966.

[DYM 73] DYM C. L., SHAMES I. H., *Solid Mechanics, a Variational Approach*, McGraw-Hill, New York, p.190, 1973.

[EUL 1744] EULER L., *Methodus Inveniendi*, Lausannae & Genavae, 1744.

[LEN 73] LE NIZERHY D., Elastic and viscoelastic properties of composite materials – Flexural motions of beams, MSc thesis, Saint-Ouen, France, 1973.

[LOV 1899] LOVE A. E. H., *Cambridge Phil Soc Trans*, vol. 18, p. 364-374, 1899.

@Seismicisolation

[LOV 34] LOVE A. E. H., *The Mathematical Theory of Elasticity,* Cambridge University Press, 1934.

[MIN 51] MINDLIN R. D., "Influence of rotary inertia and shear on flexural motion of isotropic plates", *Journal of Applied Mechanics*, vol. 18, p. 31, 1951.

[STE 79] STEPHEN N. G., LEVINSON M., "A second order beam theory", *Journal of Sound and Vibration*, vol. 67, p. 293-305, 1979.

[TIM 21] TIMOSCHENKO S. P., "On the correction for shear of the differential equation for transverse vibration of prismatic bar", *Philosophical Magazine*, vol. 41, p 744-746, 1921.

[WHI 71] WHITNEY J., "Stress analysis of thick laminated composite and sandwich plates", *Journal of Composite Materials*, vol. 5, p.320, 1971.

6.7. Table of symbols

b	beam width
C_{ij}	elastic constant
D_{ij}	bending stiffness of a composite material
E_{zz}	Young's modulus along rod axis z
F, F_{ss}	shear force
g (x)	continuous function used in the K calculation
G_{xz}	shear modulus in the plane x, z
f	frequency
h	thickness
I	section's inertia moment
I_{pz}	polar moment of the cross-section with respect to the z axis
I_z	area inertia moment
J	polar inertia moment
K	correcting shear coefficient (Timoshenko or Mindlin's theory)
L	beam length
l	coefficient
m	rod's mass
M_b	beam weight
M, M_z	bending moment

@Seismicisolation

q (z)	distributed force
S	cross-section area
T	square of non-dimensional eigenvalue
v_F	bending wave velocity
u_x	energy density
U_x	bending displacement along the x axis
β	root of Bernouilli's characteristic equation
α, β, γ	coefficients in eigenvalue equations that are the root of the characteristic Timoshenko's equation and coupled bending-torsion equation
γ_0	shear strain in plane x, z, shear strain in the neutral plane
φ	angle due to bending at coordinate x = 0
ω	circular frequency

6.8. Appendices

Appendix 6.A. Timoshenko's correcting coefficients for anisotropic and isotropic materials

Calculations are made in a static regime where inertia is neglected. Shear stress is calculated using two different methods:

– integration of the equilibrium equation of stress permits us to obtain shear stress and the corresponding shear energy;

– direct calculation of shear energy in the thickness. By equalizing the two calculated energies, coefficient K is obtained. Isotropic homogenous material is a case where this method is used.

6.A.1. *Shear energy obtained from the integration of equilibrium equation*

Flexural stiffness D_{ij} is defined as:

$$D_{ij} = \int_{-h/2}^{h/2} \overline{C}_{ij}\, x^2\, d\,x \qquad [6.A.1]$$

@Seismicisolation

where $\bar{C}_{ij}$ designates the elastic constants of layer k.

Normal axial stress is calculated from the bending moment M_z:

$$\sigma_{zz}(x) = \frac{M_z\, C_{33}\, x}{D_{33}} \qquad [6.A.2]$$

D_{33} in equation [6.A.1] is defined as:

$$D_{33} = \int_{-h/2}^{h/2} \bar{C}_{33}(x)\, x^2\, dx \qquad [6.A.3]$$

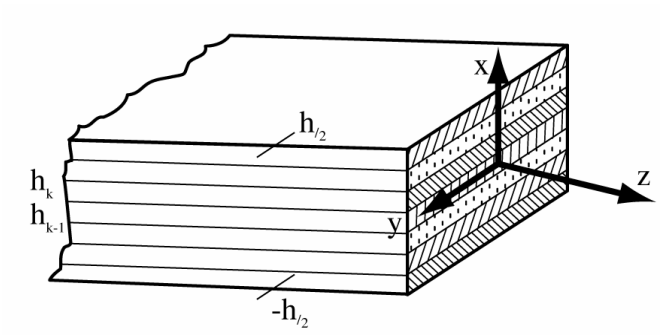

Figure 6.A.1. *Calculations of shear stress and shear energy through the thickness of a multilayered composite material*

Neglecting inertia effect, the equilibrium equation is:

$$\frac{\partial \sigma_{zz}}{\partial z} + \frac{\partial \sigma_{zx}}{\partial x} = 0 \qquad [6.A.4]$$

Integrating equation [6.A.4], we get:

$$\sigma_{zx} = \int_{-h/2}^{x} \frac{\partial \sigma_{zz}}{\partial z}\, dx \qquad [6.A.5]$$

@Seismicisolation

Bringing equation [6.A.2] into [6.A.5]:

$$\sigma_{zx}(x) = -\int_{-h/2}^{x} \frac{\partial}{\partial z}\left(\frac{M_z\, C_{33}\, \chi}{D_{33}}\right) d\chi \qquad [6.A.6]$$

In the second member of [6.A.6], M_z depends only on z:

$$\sigma_{zx}(x) = -\frac{\partial M_z}{\partial z}\,\frac{1}{D_{33}}\int_{-h/2}^{x} C_{33}(\chi)\,\chi\, d\chi \qquad [6.A.7]$$

$$g(x) = \int_{-h/2}^{x} C_{33}(\chi)\,\chi\, d\chi = \frac{1}{2}\, C_{33}^{k}\left(h_k^3 - h_{k-1}^3\right) \qquad [6.A.8]$$

In [6.A.7], $-\frac{\partial M}{\partial z}$ is recognized as shear force.

$$\sigma_{zx}(x) = \frac{F_z\, g(x)}{D_{33}} \qquad [6.A.9]$$

where g (x) is a continuous function that must satisfy the continuity condition at the layers' boundaries.

6.A.2. *Shear coefficient K from energy calculation*

Shear energy in the cross-section, with b being the width, is:

$$b\int_{-h/2}^{h/2} \sigma_{zx}\,\gamma_{zx}\, dx = b\int_{-h/2}^{h/2} \frac{\sigma_{zx}^2(x)}{G_{xz}(x)}\, dx\gamma$$

$$b\int_{-h/2}^{h/2} \sigma_{zx}\,\gamma_{zx}\, dx = \int_{-h/2}^{h/2} \frac{F_z^2\, g^2(x)\, b}{G_{xz}(x)}\, dx \qquad [6.A.10]$$

@Seismicisolation

Shear energy can be calculated by another method from equation [6.25]:

$$F_z = G_{xz}^{*} S \gamma_0 K \qquad [6.25]$$

where G* designates a global value of a material that is homogenized beforehand.

$$G^*_{xz} = \frac{1}{h} \int_{-h/2}^{h/2} G_{xz}(x)\, dx \qquad [6.A.11]$$

In equation [6.25], γ_0 designates shear strain at the neutral plane. S is the area of the section, S = b h.

$$b \int_{-h/2}^{h/2} \sigma_{zx}\, \gamma_{zx}\, dx = \frac{F_z}{h} \frac{F_z\, b}{G_{xz} \bullet K} = \frac{F_z^2\, b}{KG^*_{xz}\, h} \qquad [6.A.12]$$

Let us equalize [6A.12] to [6.A.10]:

$$b \int_{-h/2}^{h/2} \frac{\sigma^2_{zx}(x)}{G_{xz}(x)}\, dx = \frac{b\, F_z^2}{KG^*_{xz}\, h} \qquad [6.A.13]$$

K is then obtained:

$$K = \frac{D_{33}^2}{G^*_{xz}\, h \int_{-h/2}^{h/2} \frac{g^2(x)\, dx}{G_{xz}(x)}} \qquad [6.A.14]$$

6.A.3. ***Homogenous beam***

$$\underset{\text{(homogenized)}}{G^*_{xz}} = G_{xz}(x) = G_{xz} \text{ constant}$$

@Seismicisolation

$$D_{33}^2 = \left(C_{zz} \frac{h}{12} \right)^2 \qquad [6.A.15]$$

$$g^2(x) = \frac{C_{zz}^2}{4} \left(x^2 - \frac{h^2}{4} \right) = C_{zz} \frac{h^2}{16} \left[1 - \left(\frac{2x}{h} \right)^2 \right]^2 \qquad [6.A.16]$$

By changing the integrating variable, we get:

$$\int_{-h/2}^{h/2} \frac{g^2(x)\, dx}{G_{xz}(x)} = \frac{1}{G_{xz}} C_{zz}^2 \frac{h^2}{16} \int_{-1}^{+1} \left(1 - u^2\right)^2 du$$
$$= \frac{C_{zz}^2 h^5}{G_{xz}\, 2^3 \times 15} \qquad [6.A.17]$$

Equation [6A.14] is then rewritten as:

$$K = \frac{\left(C_{zz} \frac{h^3}{12} \right)^2}{\frac{G_{xz}\, h\, 4\, C_{33}^2\, h^5}{G_{xz}\, 2^5 \times 15}}$$

$$K = \frac{2^3 \bullet 15}{(12)^2} = \frac{5}{6} \qquad [6.A.18]$$

This is the value obtained by Timoshenko.

This value is also valid for an anisotropic material of homogenous thickness.

6.A.4. *Symmetrical multilayered beam*

Each beam is differently oriented with respect to the beam axis z. An example of this given by Chow [CHO 71] has fiber orientations of 0°, 90°, 90° and 0°.

@Seismicisolation

	Four symmetrical layers		Homogenous material
Material	glass-epoxy	graphite epoxy	isotropic or anisotropic
K	0.815	0.828	$\frac{5}{6} = 0.833$

Table 6.A.1. *Coefficients K for multilayered composites and homogenous material*

Appendix 6.B. Correcting coefficient using Mindlin's method

Coefficient K is obtained by examining the behavior of bending wave velocity when the frequency goes to infinity. The asymptotic limit of bending wave velocity is the Rayleigh surface velocity.

6.B.1. *Homogenous isotropic material*

For a rectangular section, we have $K = \frac{10\,(1+\nu)}{12+11\,\nu}$, where ν is the Poisson's number.

6.B.2. *Non-rectangular section – isotropic material*

Circle	$K = \frac{6\,(1+\nu)}{7+6\,\nu}$
Rectangle 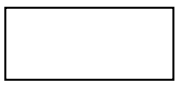	$K = \frac{10\,(1+\nu)}{12+11\,\nu}$
Semicircle 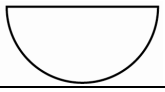	$K = \frac{1+\nu}{1{,}305+1{,}273\,\nu}$

Table 6.B.1. *Correcting shear coefficient K for various section shapes of isotropic material; ν is the Poisson's coefficient, Dym and Shame [DYM73]*

@Seismicisolation

Cowper [COW 66] determined a calculation for various beam shapes. Table 6.B.1 on the previous page gives the different values of K for each section shape.

Appendix 6.C. Dispersion curves for various equations of motion

There are three principal theories: Bernoulli-Euler, Timoshenko and Love. Love's theory is contained within Timoshenko's one, in which only rotational inertia is retained (equation [6.38]).

6.C.1. *Bernoulli-Euler's theory equation [6.4]*

For a progressive wave, bending displacement is written as:

$$w\left(z, t\right) = \exp j\left(j\,\omega\, t - k\, z\right) \qquad [6.C.1]$$

where k is the wave number. Bringing equation [6.C.1] into [6.4]:

$$-\rho\, S\, \omega^2 + E_{zz}\, I\, k^4 = 0 \qquad [6.C.2]$$

The second member of [6.4] is set to zero.

The phase velocity is defined as:

$$V_F = \omega/k$$

from [6.C.2], superscript B being related to Bernoulli's theory:

$$v^B = \left(\frac{E_{zz}\, I\, \omega^2}{\rho\, S}\right)^{1/4} \qquad [6.C.3]$$

Phase velocity increases indefinitely with circular frequency. This shows that Bernoulli-Euler's theory is valid for very low frequencies. The application of this theory is controversial at higher frequencies.

@Seismicisolation

6.C.2. *Love's theory*

Equation [6.37] is rewritten here with terms that do not only contain G_{xz}:

$$\rho\, S \frac{\partial^2 w}{\partial t^2} + E_{zz}\, I \frac{\partial^4 w}{\partial z^4} - \rho\, I \frac{\partial^4 w}{\partial t^2\, \partial z^2} = 0 \qquad [6.C.4]$$

Bringing [6.C.1] into [6.C.4], we get:

$$-\rho\, S\, \omega^2 + E_{zz}\, I\, k^4 - \rho\, I\, \omega^2\, k^2 = 0 \qquad [6.C.5]$$

Calculating k^2 *versus* ω, we obtain:

$$k^2 = \omega^2 \frac{\rho\, I}{2\, E\, I} \left(1 + \sqrt{1 + \frac{4\, S\, E}{\rho\, I\, \omega^2}} \right)$$

The phase velocity for the flexural wave is:

$$v_F^L = \frac{\omega}{k} = \sqrt{\frac{2\, E_{zz}}{\rho}} \left[-1 \pm \sqrt{1 + \frac{4\, S\, E_{zz}}{\rho\, I\, \omega^2}} \right]^{-1/2} \qquad [6.C.6]$$

The asymptotic value of v_F^L (superscript L designates Love's theory) with ω going to infinity is $\sqrt{2}$ time of the extensional wave the phase velocity. This highlights the deficiency of Love's theory at higher frequencies.

6.C.3. *Timoshenko's theory*

Equation [6.37] is rewritten with the second member set to zero and with w (z, t) given by [6.C.1]:

$$-\rho\, S\, \omega^2 + E_{zz} I\, k^4 + \frac{\rho^2\, I\, \omega^4}{K\, G_{xz}} - \left(\rho\, I + \frac{E_{zz}\, I\, \rho}{G_{xz}\, K} \right) \omega^2\, k^2 = 0 \qquad [6.C.7]$$

@Seismicisolation

Rearranging this in increasing power of k, we get:

$$E_{zz}\ I\,k^4 - \left(\rho\,I + \frac{E_{zz}\ I\,\rho}{G_{xz}\ K}\right)\omega^2\ k^2 - \left(\rho\ S\ \omega^2 - \frac{\rho^2\ I\,\omega^4}{KG_{xz}}\right) = 0 \qquad [6.C.8]$$

After solving [6.C.8] to find k^2, the square phase velocity v_F^T (superscript T designates Timoshenko theory) is obtained for the asymptotic value of v_F^T:

$$\left(v_F^T\right)^2 = \frac{\omega^2}{k^2} = \frac{2\ E_{zz}\ P}{\rho\left(1 + \dfrac{E_{zz}}{G_{xz}\ K}\right)} \qquad [6.C.9]$$

$$P = \left[1 \pm \left\{1 - \frac{4\,\rho\left(1 - \dfrac{S\ KG_{xz}}{\rho\ I\,\omega^2}\right)}{KG_{xz}\left(1 + \dfrac{E_{zz}}{KG_{xz}}\right)}\right\}^{1/2}\right]^{1/2} \qquad [6.C.10]$$

K is adopted in the framework of Mindlin's theory so that v_F^T has a Rayleigh surface wave as a asymptotic value.

Let us focus our attention on the ratio E_{zz}/G_{xz} in equation [6.C.10], which can have the value of 50 or 100 for artificial composite materials. For isotropic materials this does not exceed three.

Mindlin's coefficient for a rectangular section is:

$$K^M = \frac{10\ (1+\nu)}{12 + 11\ \nu} = \frac{13}{15.2} = 0.8496$$

Timoshenko's coefficient is:

$$K^T = \frac{5}{6} = 0.8333$$

In our opinion, for the dynamic vibration of a rod at high frequency, K^M is preferred to K^T.

@Seismicisolation

6.C.4. *Trend of dispersion curves*

It is not possible to draw dispersion curves for the bending theories mentioned above. Phase velocity depends on many geometrical factors of the rod (I inertia, ρ density) and elastic constants of the material (E_{zz}, G_{xz}). In Figure 6.C.1, trends of the three curves are presented.

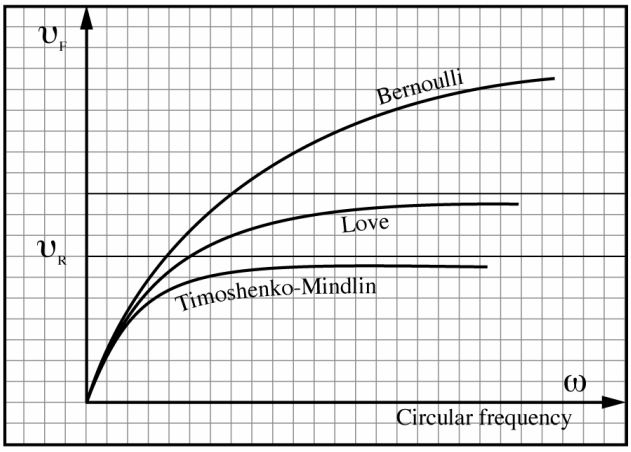

Figure 6.C.1. *Trends of dispersion curves. Timoshenko-Mindlin's theory gives a satisfactory asymptotic value for phase velocity V_F. V_R designates the Rayleigh surface wave*

Appendix 6.D. Change of reference axes and elastic coefficients for an anisotropic rod

In Figure 6.4, *α* designates the angle of fiber direction 3 and rod axis z.

$$\frac{1}{E_{zz}} = \frac{\sin^4 \alpha}{E_{11}} + \frac{\cos^4 \alpha}{E_{33}} - \frac{2\,\nu_{13}}{E_{11}} \sin^2 \alpha \cos^2 \alpha + \frac{1}{G_{13}} \sin^2 \alpha \cos^2 \alpha$$

$$\frac{1}{G_{xz}} = \frac{\sin^2 2\alpha}{E_{11}} + \frac{2 \sin^2 2\alpha}{E_{11}} \nu_{13} + \frac{\sin^2 2\alpha}{E_{33}} + \frac{\cos^2 2\alpha}{G_{13}}$$

$$s'_{35} = \sin \alpha \cos \alpha \left[\frac{2 \sin^2 \alpha}{E_{11}} - \frac{2 \cos^2 \alpha}{E_{33}} + \frac{1}{G_{13}} - \frac{2\,\nu_{31}}{E_{33}} \right] \left(\cos^2 \alpha - \sin^2 \alpha \right)$$

@Seismicisolation

$$\frac{1}{G_{xz}} = \frac{\sin^2 2\alpha}{E_{11}} + \frac{2\upsilon_{13}}{E_{11}}\sin^2 2\alpha + \frac{\sin^2 2\alpha}{E_{33}} + \frac{\cos^2 2\alpha}{G_{13}} \qquad [6.D.1]$$

Compliances in [6.D.1] are evaluated with the axes attached to the rod. Directions 1, 2 and 3 are related to the material. s′35 index refers to the third line and the fifth column of the matrix. In the first equation of [6.D.1], second member, Poisson's number υ_{13} appears. This formula serves to evaluate υ_{13}, angle α and E_{11} with E_{33} and G_{13} being known (see Chapter 1).

@Seismicisolation

Chapter 7

Longitudinal Vibration of a Rod[1]

7.1. Presentation

Longitudinal vibrations of a rod were being examined as early as 1876 by Pochhammer [POC 1876] and 1889 by Chree [CHR 1889]. These publications concern an infinite rod with circular cross-section. Since then a great number of publications concerning an infinite rod with circular, rectangular or square section have been produced. Attention is focused particularly on wave dispersion covering a large range of wave numbers k up to asymptotic behavior, with k going to infinity. Beyond the original mode, propagation of a great number of higher elastodynamic modes have been investigated.

As for a non-circular section, no exact equation of motion exists; attempts were made to create correcting terms for the elementary equation of motion. Love [LOV 44] proposed a lateral inertia correction. Bishop [BIS 52] suggested lateral inertia and shear corrections. Bishop's equation will be examined in detail in this chapter.

There are indeed elaborate equations of motion with a more or less complicated displacement field [FRA 69,MED 66, MOR 50, NIG 68, VOL 55]. One-dimensional solutions are proposed for rectangular or square sections in all of these publications.

For other arbitrary sections, readers can refer to [HER 50, MIN 60, ROS 74].

Chapter written by Yvon CHEVALIER and Maurice TOURATIER.

1 This chapter contains large extracts from Touratier's thesis [TOU 77] for his mechanical engineering degree, CNAM, Paris.

Mechanics of Viscoelastic Materials and Wave Dispersion Edited by Yvon Chevalier and Jean Tuong Vinh
© 2010 ISTE Ltd. Published 2010 by ISTE Ltd.

@Seismicisolation

Touratier [TOU 77] adopted a simple displacement field with three components of displacement. Each component is expressed as a series of x_1, x_2 coordinates of the section. The rod material is transversely isotropic[2]. His contribution is an extension of the so-called internal constraint of Volterra's method on an anisotropic rod. In his PhD thesis [TOU 79], Touratier proposed a mixed field of displacements and stresses using Reissner 's variational formulation[3].

In Appendix 7.A, a succinct bibliographical and historical review is presented. Let us focus our attention once more on the attempt to solve the inverse problem, i.e. the evaluation of elastic constants C_{3333} (axis 3 being the symmetry axis of the material and rod). Dispersion of the longitudinal wave is taken into account so that the application in a low and medium frequency range (f < 100,000 Hz) is covered.

In publications on wave dispersion, a more or less sophisticated displacement field is adopted in order to satisfy lateral boundary conditions. Complete sets of stress components are introduced. Consequently a great number of stiffness matrix coefficients are used.

This approach is tempting in the framework of a direct problem, in which all of the mechanical characteristics of the sample material are known. For an inverse problem, we have to deal with the multiple optimization parameters that rapidly become intractable, if not impossible. Our aim is to evaluate longitudinal Young's modulus. Only when we have done this will the non-diagonal matrix coefficients and shear moduli be calculated. However, the elementary equations of motion suffer from their wave dispersion-free solution. More elaborate equations of motion must be found so that the dynamic behavior of a rod covers an acceptable frequency range, as indicated above.

7.1.1. *Elementary equation of motion*

This popular equation of motion can be found in any text book devoted to the vibrations of continuous systems.

Figure 7.1 represents an element of the rod, with the simple constitutive equation:

2 Isotropic material is considered a case in which the number of elastic moduli are reduced from 5 to 2.
3 To be published in a book entitled *Mechanical Characterization of Materials and Wave Dispersion*, written be the same authors.

@Seismicisolation

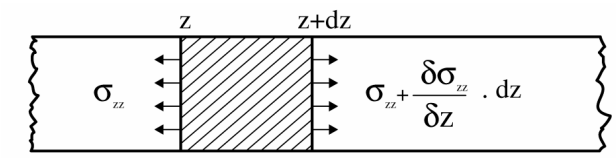

Figure 7.1. *An element of the rod is presented with at both ends of the hatched element. Axial stresses σ_{zz} and σ_{zz} + d σ_{zz} are applied*

$$\sigma_{zz} = E_z \, \varepsilon_{zz} = E_z \frac{\partial w}{\partial z} \qquad [7.1]$$

The forces acting on the faces from left to right are F and F + d F, S being the cross-section area:

$$F = \left(E_z \frac{\partial w}{\partial z} \right) S \qquad [7.2]$$

$$F + dF = \left(E_z \frac{\partial w}{\partial z} + E_z \frac{\partial^2 w}{\partial z} dz \right) S \qquad [7.3]$$

The resultant force is:

$$F + dF - F = E_z \frac{\partial^2 w}{\partial z} dz \; S \qquad [7.4]$$

The mass of element S is:

$$dm = (S \, dz) \, \rho \qquad [7.5]$$

Newton's second law is used for the equation of motion:

$$(S \, dz) \, \rho \frac{\partial^2 w}{\partial t^2} = E_z \frac{\partial^2 w}{\partial z^2} S \, dz \qquad [7.6]$$

@Seismicisolation

or

$$\frac{\partial^2 w}{\partial t^2} - \frac{E_z}{\rho}\frac{\partial^2 w}{\partial z^2} = 0 \qquad [7.7]$$

The phase velocity deduced from equation [7.7] is frequency independent:

$$v_p = \sqrt{\frac{E_z}{\rho}} \qquad [7.8]$$

7.1.2. *Boundary conditions*

7.1.2.1. *Adopted natural boundary conditions*

The natural boundary conditions adopted are:

$$\frac{\partial (z, t)}{\partial z} = 0 \qquad [7.9a]$$

$$w(z, t) = 0 \qquad [7.9b]$$

Equations [7.9a] and [7.9b] correspond to the free end (zero axial stress) and fixed end (zero displacement) respectively.

7.1.2.2. *Additional mass m*

Writing the equality between tensile force and the addition of inertia force, we have:

$$S\,E\,\frac{\partial w}{\partial x}(z, t) = -m\,\frac{\partial^2 w}{\partial t^2}(z, t) \quad \text{for } z = z_0 \qquad [7.10]$$

Equation [7.10] is often used in experiments. m can be an additional mass that represents the weight of the electric exciter or transducer (accelerometer, for example). Chapters 5, 6, 8, 9, 11 and 12 of this book present and discuss details of various boundary conditions.

@Seismicisolation

7.2. Bishop's equations of motion

7.2.1. *Isotropic material*

Love [LOV 44] was the first to introduce an additional term describing lateral inertia to equation [7.7]:

$$-\nu\, r_p^2\, \partial^4 w / \partial x^2 \partial t^2$$

where r_p is the radius of gyration and ν Poisson's number.

In 1952 Bishop [BIS 52] proposed a second term t to take into account the shear effect, G shear modulus:

$$\upsilon^2\, r_p^2\, \frac{G}{\rho}\, \frac{\partial^4 w}{\partial x^4}$$

Bishop's equation becomes.

$$\frac{\partial^2 w}{\partial t^2} - \frac{E}{\rho}\, \frac{\partial^2 w}{\partial z^2} - \upsilon^2\, r_p^2\, \frac{\partial 4 w}{\partial z^2\, \partial t^2} + \upsilon^2\, r_p^2\, \frac{G}{\rho}\, \frac{\partial^4 w}{\partial z^4} = 0 \qquad [7.11]$$

7.2.2. *Transversely isotropic material*

To extend these calculations to transversely isotropic material, with the cross-section being an isotropic plane, we can write:

$$\frac{\partial^2 w}{\partial t^2} - \frac{E_3}{\rho}\, \frac{\partial^2 w}{\partial z^2} - \upsilon_{31}^2\, r_p^2\, \frac{\partial^2 w}{\partial z^2\, \partial t^2} + \upsilon_{31}^2\, r_p^2\, \frac{G_{31}}{\rho}\, \frac{\partial^4 w}{\partial z^4} = 0 \qquad [7.12]$$

$r_p^2 = \dfrac{h^2 + b^2}{12}$ for a rectangular section where h is thickness and b width.

In equation [7.12] the material symmetry axis coincides with rod axis Oz. In [7.12] we get:

$$G_{31} = G_{32} \text{ and } \upsilon_{31} = \upsilon_{32}\,.$$

@Seismicisolation

7.2.3. *Longitudinal wave dispersion*

Let us adopt a progressive wave for axial displacement:

$$w\left(z, t\right) = w_0 \exp j\, k \left(z - v_p\, t\right) \qquad [7.13]$$

which propagates in positive direction Oz. k is the wave number and v_p the phase velocity. Introducing equation [7.13] into [7.12], we get:

$$-k^2 v_p^2 + \frac{E}{\rho} k^2 - \upsilon^2 r_p^2 k^4 v_p^2 + \upsilon^2 r_p^2 \frac{G}{\rho} k^4 = 0 \qquad [7.14]$$

The phase velocity is:

$$v_p = \left[\frac{\dfrac{E}{\rho} + \dfrac{\upsilon^2 r_p^2 G}{\rho}}{1 + \upsilon^2 r_p^2 k^2} \right]^{1/2} \qquad [7.15]$$

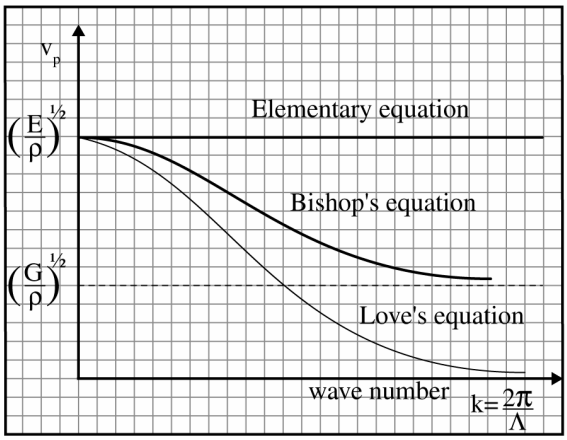

Figure 7.2. *Dispersion curve after Bishop's equation compared to dispersion curves related to elementary and Love's equations*

@Seismicisolation

The horizontal line is related to elementary equation [7.7]. Love's equation only takes inertia effect into account. The dispersion curve has an asymptotic value going to zero. Figure 7.2 shows that the asymptotic value of phase velocity with k going to infinity is the shear wave velocity after Bishop's equation:

$$v_p = v_z = \sqrt{\frac{G}{\rho}} \qquad [7.16]$$

7.3. Improved Bishop's equation of motion

As suggested by Mindlin, to improve the bending equation of a rod for the asymptotic value of phase velocity, instead of v_s as the lower bound value we suggested the following for v_p:

$$v_p = q v_s \qquad [7.17]$$

The correcting coefficient value depends on the material itself. v_p at $k \to \infty$ must have the phase velocity of a Rayleigh surface wave v_R. For isotropic material, Viktorov's formula [VIK 67] is valid:

$$q(\upsilon) = \frac{0.87 + 1.12\,\upsilon}{1 + \upsilon} \qquad [7.18]$$

For composite materials, equation [7.18] is not valid. This problem is examined below. The proposed improved Bishop's equation is:

$$\frac{\partial^2 w}{\partial t^2} - \frac{E_3}{\rho}\frac{\partial^2 w}{\partial z^2} - \upsilon_{31}^2 r_p^2 \frac{\partial^4 w}{\partial z^2\,\partial t^2} + q^2 \upsilon_{31}^2 r_p^2 \frac{G_{31}}{\rho}\frac{\partial^4 w}{\partial z^4} = 0 \qquad [7.19]$$

$$r_p^2 = \frac{\left(b h^3 + b^3 h\right)}{12\,h\,b}$$ for rectangular section, with b width, h thickness.

In Appendix 7.B, Hamilton's principle is applied to the longitudinal vibration of a rod with an appropriate displacement field that yields Bishop's equation. Homogenous boundary conditions are also presented.

@Seismicisolation

7.4. Bishop's equation for orthotropic materials

In the case where rod axis z is not a transversely isotropic axis, the rod cross-section is not an isotropic plane. In this plane, two different shear moduli G_{zx} and G_{zy}, and two different Poisson's numbers are to be used (ν_{zx} and ν_{zy}).

Equation [7.19] must be replaced by the following one:

$$\frac{\partial^2 w}{\partial t^2} - \frac{E_z}{\rho}\frac{\partial^2 w}{\partial z^2} - \left(\frac{\upsilon_{zx}^2\, b\, h^3 + \upsilon_{zy}^2\, h\, b^3}{12\, b\, h}\right) + \left(\frac{\upsilon_{zx}^2\, b\, h^3\, G_{zx} + \upsilon_{zy}^2\, h\, b^3\, G_{zy}}{12\, b\, h\, \rho}\right) q^2 \frac{\partial^4 w}{\partial z^4} = 0 \qquad [7.20]$$

This is the case in in Figure 7.3 where, the material being transversely isotropic, the rod axis coincides with axis 2. In the cross-section plane y = 3 and x = 1. Letters concern the rod axes and figures the material axes.

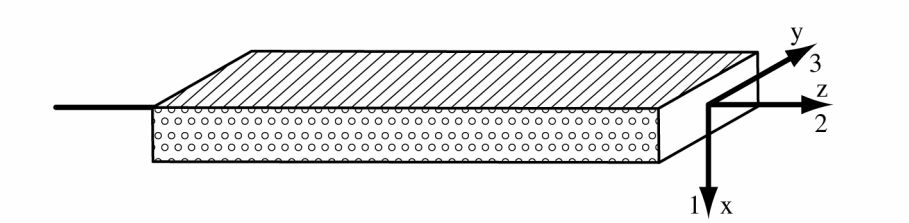

Figure 7.3. *A transversely isotropic material. Rod axis z is not a polar symmetry axis. Cross-section plane (x, y) is not an isotropic plane. Poison's numbers and shear modulus are different in planes (z.x) and (z.y)*

7.5. Eigenfrequency equations for a free-free rod

Table 7.B.1 of Appendix 7.B gives the natural boundary conditions for a free-free rod (see case A).

7.5.1. *Harmonic solution for dimensionless Bishop's equation*

In Appendix 7.C, it can be seen that the dimensionless equation of motion is:

@Seismicisolation

$$\frac{\partial^2 \bar{w}}{\partial \bar{t}^2} - \frac{\partial^2 \bar{w}}{\partial \bar{z}^2} - r_1 \frac{\partial^4 \bar{w}}{\partial \bar{z}^2 \partial \bar{t}^2} + r_2 \frac{\partial^4 \bar{w}}{\partial \bar{z}^4} = 0 \qquad [7.C.2]$$

A harmonic progressive wave is adopted for displacement:

$$\bar{w} = \bar{w}_0 \exp j \left(\bar{\omega}\, \bar{t} - \bar{k}\, \bar{z} \right) \qquad [7.21]$$

with $\bar{t} = \dfrac{t \,.\, L}{v_L}$

$$k = \bar{k}\, L \qquad [7.22]$$

Bringing equation [7.21] into [7.C.2], we have:

$$-\bar{\omega}^2 + \bar{k}^2 - r_1\, \bar{\omega}^2\, \bar{k}^2 + r_2\, \bar{k}^4 = 0 \qquad [7.23]$$

Rearranging in decreasing power of $\bar{k}$:

$$\bar{k}^4 + \frac{\left(1 - r_1\, \varpi^2\right)}{r_2} \bar{k}^2 - \frac{\bar{\omega}^2}{r_2} = 0$$

$$\bar{k}^2 = \left[\left(\frac{1 - r_1\, \varpi^2}{r_2} \right) \pm \sqrt{\frac{\left(1 - r_1\, \varpi^2\right)^2}{r_2^2} + \frac{4\, \varpi^2}{r_2}} \right]$$

Adopting Rao and Rao's [RAO 74] notation:

$$\left. \begin{aligned} d &= \left(1 - r_1 \varpi^2 \right) / r_2 \\ c &= \varpi^2 / r_2 \end{aligned} \right\} \qquad [7.24]$$

@Seismicisolation

The two roots of [7.23], a_1 and a_2, are:

$$\bar{k}^2 = \begin{cases} a_2^2 = \left[-d + \left(d^2 + 4\,c\right)^{1/2}\right] \Big/ 2 > 0 \\ a_1^2 = \left[+d + \left(d^2 + 4\,c\right)^{1/2}\right] \Big/ 2 < 0 \end{cases} \qquad [7.25]$$

a_2^2 being negative, the two roots of a_2 are imaginary and yield trigonometric function $\sin a_2\ \bar{z}$. a_1 being positive, the two corresponding roots are real and give rise to hyperbolic functions $a_1\,\bar{z}$, and $\cos h\ a_1\,\bar{z}$.

The closed-form expression for dimensionless displacement $\bar{w}\left(\bar{z}, \bar{t}\right)$ is:

$$\bar{w}\left(\bar{z}, \bar{t}\right) = \bar{w}_0\ \exp j\,\omega\,t \begin{bmatrix} A_1\ \cos a_1\bar{z} + A_2\ \sin a_1\bar{z} \\ \\ + A_3\ \cosh a_2\bar{z} + A_4 \sinh a_2\bar{z} \end{bmatrix} \qquad [7.26]$$

7.5.2. *Boundary conditions and eigenvalue equations*

Equations [7.C.6] and [7.C.7] of Appendix 7.C give the two end conditions. Substituting equation [7.26] in [7.C.6] and [7.C.7], four equations are obtained (two for each end).

7.5.2.1. *For* $\bar{z} = 0$

$$\left.\begin{aligned} A_2\left(d + a_1^2\right) a_1 + A_4\ \left(d - a_2^2\ \right) a_2 = 0 \\ A_1\ a_1^2 - A_3\ a_2^2 = 0 \end{aligned}\right\} \qquad [7.27]$$

7.5.2.2. *For* $\bar{z} = \dfrac{z}{L} = 1$

$$- A_1\ \left(d + a_1^2\right) a_1\ \sin a_1 + A_2\ \left(d + a_1^2\right) a_1\ \cos a_1 + A_3\ \left(d - a_2^2\right) a_2 +$$

$$+ A_4\ \left(d - a_2^2\right) a_2 = 0$$

@Seismicisolation

$$A_1\ a_1^2\ \cos a_1 + A_2\ a_1^2\ \sin a_1 - A_3\ a_2^2\ \cos h\ a_2 - A_4\ a_2^2\ \sin h\ a_2 = 0 \qquad [7.28]$$

Equations [7.27] and [7.28] constitute four homogenous equations whose non-trivial solution requires setting the determinant to zero:

$$\begin{vmatrix} 0 & \left(d + a_1^2\right) a_1 & 0 & \left(d - a_2^2\right) a_2 \\ a_1^2 & 0 & -a_2^2 & 0 \\ -\left[\left(d+a_1^2\right)a_1 \sin a_1\right] & \left[\left(d+a_1^2\right)a_1 \cos a_1\right] & \left[\left(d-a_2^2\right)a_2 \sin h\ a_2\right] & \left[\left(d-a_2^2\right)a_2 \cosh a_2\right] \\ a_1^2\ \cos a_1 & a_1^2\ \sin a_1 & -a_2^2\ \cos h\ a_2 & -a_2^2\ \sin h\ a_2 \end{vmatrix} = 0$$

[7.29]

Developing [7.29], the following eigenvalue equation is obtained:

$$1 + \cos a_1\ \cos h\ a_2 + \frac{1}{2}\left[\left(\frac{d + a_1^2}{d - a_1^2}\right)\frac{a_2}{a_1} + \frac{\left(d - a_2^2\right) a_1}{\left(d + a_1^2\right) a_2}\right]\sin a_1\ \sin h\ a_2 = 0$$

[7.30]

with $d = \dfrac{1 - r_1\ \omega^2}{r_2}$

$$r_1 = \frac{\upsilon^2\ r_p^2}{L^2} = \frac{\upsilon^2\ I_p}{S\ L^2}, \quad \text{where S is the cross-section area} \qquad [7.31]$$

$$r_2 = \frac{\upsilon^2\ I_p\ \alpha^2}{S^2\ L^2}, \quad \alpha^2 = \frac{G}{E} \quad \frac{\text{shear modulus}}{\text{Young's modulus}}$$

In Rao and Rao's paper [RAO 74], a series of eigenvalue equations (corresponding to 10 possible boundary conditions) can be found.

@Seismicisolation

Equation [7.30] can easily be extended to transversely isotropic material by using equation [7.12] instead of equation [7.11]. The set of dimensionless equations [7.C.2] is modified, see Appendix 7.C.

7.6. Touratier's equations of motion of longitudinal waves

7.6.1. *General considerations*

In the numerous publications since 1950 (see Appendix 7.A), attention has been focused on the adoption of a displacement field with three components, each of which is the function of polynomials of three coordinate variables or of special orthogonal polynomials (Legendre, etc.). The main reason for this is the extensional wave in a rod cannot only be portrayed by one strain component as in elementary theory. The other strain components have important contributions and cannot be neglected. The combined influence of a great number of strain components, which are in the same order of importance in the quantitative formulation of the dispersion problem, must be understood by the reader.

The second difficulty can be found in the absence of an exact theory. This means we cannot accurately compare approximate theories that have been proposed. What we have presented above concerns a direct problem in which all the elastic constants of the material are supposed to be known.

In the framework of an inverse problem, the fact that the existence of many elastic coefficients are considered to be unknown is difficult to grasp. Solutions to a set of equations of motion with many unknown parameters in the numerical analysis, with eventual instability in calculations, are another important aspect of the problem.

What we try to provide here is a compromise between tractable theories and empirical and practical considerations for users. In our presentation, practical considerations consist, for various composite anisotropic materials, of dispersion curves that permit the reader to evaluate the influence of frequency or wave number on the variation of wave velocity. Some important parameters, such as the slenderness or the flatness of the rod, are discussed.

7.6.2. *Dispersion curves according to various theories*

Here we present some elements of comparison between various theories. The objective is to examine the approximate theories applicable to extensional waves in

@Seismicisolation

a rod with rectangular cross-section. With this objective in view, the following steps are proposed.

7.6.2.1. *Conversion of Cartesian coordinates into polar coordinates*

This conversion enables us to compare the approximate with exact Pochhamner-Chree theory, which is applicable to isotropic materials. The reader will see that the majority of engineering theories give a good dispersion curve trend for the asymptotic values of phase velocity with wave number k going to zero or infinity.

Unfortunately in the range of k, applicable in practice, a great number of theories depart from exact theory. The method of internal constraints proposed by Volterra [VOL 65] seems to propose a correct dispersion curve that is not far from the one proposed by Pochhammer-Chree. Consequently, it is only possible to compare a rod with a circular cross-section.

Figure 7.4 shows five dispersion curves. The abscissas of those curves are not wave number $k = \frac{2\pi}{\Lambda}$ (Λ being the wavelength) but $\bar{k} = \frac{d}{\Lambda}$ in which d is the diameter of the cross-section.

Bishop's theory does not allow us to correctly describe the dispersion.

7.6.2.1.1. Confrontation of higher-order approximate theories for a square cross-section

Figure 7.5 shows six dispersion curves concerning an isotropic material and square cross-section.

The first-order displacement field [MED 66] gives rise to a dispersion curve that is far from the general trend of other curves obtained with higher-order displacement fields [FRA 69, HET 68].

7.6.2.1.2. Influence of the flatness coefficient[4]

Dispersion is strongly influenced by this ratio and the variation of phase velocity *versus* reduced wave number is:

$$\bar{k} = \frac{2\pi b}{\Lambda}$$

4 It is defined as the ratio h/b thickness on the width of the cross-section.

@Seismicisolation

where b is the width and the wave length Λ is more pronounced for $\bar{k} \simeq 1$. In this respect, Figure 7.5 can be compared with Figure 7.4.

7.6.2.1.3. Higher branches (of elastodynamic modes) of vibration

Figures 7.4 and 7.5 concern the first branches of a dispersion curve (*). The mode in elastodynamics devoted to rod vibration is related to the distribution of mode contours in a cross-section. The higher the mode, the higher the density of contours of modes. The higher elastodynamic mode yields a possible phase velocity higher than the upper bound of extensional velocity:

$$C_L = \sqrt{\frac{E}{\rho}}.$$

Figure 7.6 gives first and second elastodynamic modes of a rod with rectangular cross-section.

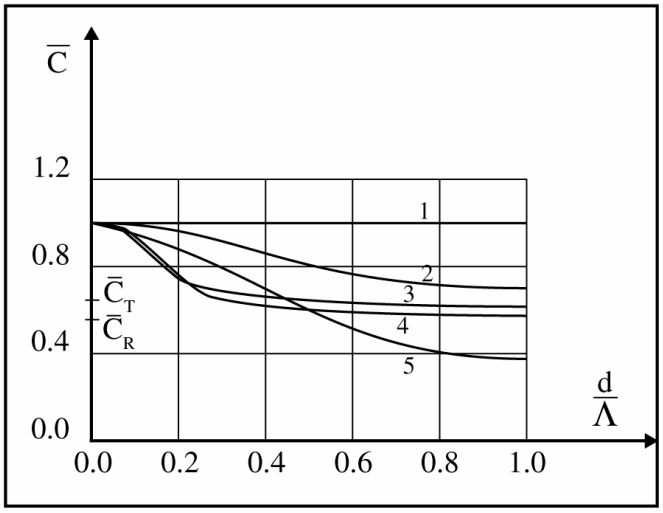

Figure 7.4. *Non-dimensional dispersion curves of extensional waves in a cylindrical rod: 1 – elementary theory; 2 – Bishop's theory; 3 – Volterra's theory (internal constraints); 4 – exact Pochammer-Chree theory; 5 – Love's theory* $= c/c_L$ *with* $c_L = (E/\rho)^{1/2}$

@Seismicisolation

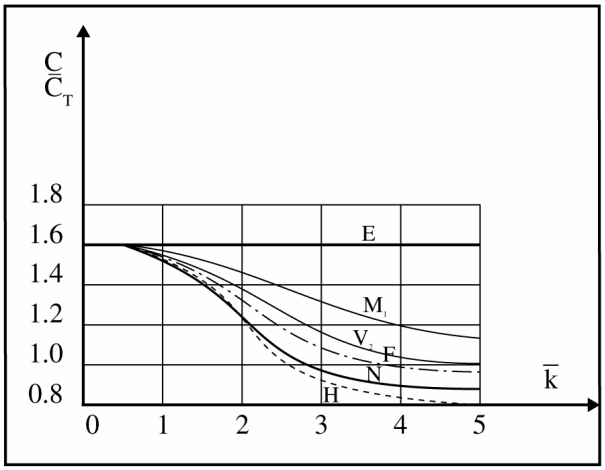

Figure 7.5. *Longitudinal waves in a rod with square cross-section. The material is isotropic with $\upsilon = 1/3$ – E (elementary theory), M_1 (Medick's theory), υ_2 (Volterra's theory), F (Fraser's theory), N (Nigro's theory) and H (Heterlendy's theory)*

In practical applications higher elastodynamic modes are not used, taking into account the difficulty of producing such waves and taking the vibration measurements.

We can introduce correction factor q in the equations of motion. For anisotropic materials, this correction factor was proposed in section 7.4, equation [7.19].

In what follows, we will see how to evaluate factor q by calculating the Rayleigh wave velocity.

7.6.3. *Displacement field and boundary conditions*

Touratier [TOU 79] adopted Volterra's method using internal constraints [VOL 55] and extended the method to transversely anisotropic material. In the plane cross-section, the axis that is initially perpendicular to $z = u_3$ remains plane and perpendicular.

The term "mode" can confuse the reader as this vocabulary is used in modal analysis with a different significance: here mode means higher eigenfrequency.

@Seismicisolation

Displacement components in a cross-section $(x_1 = x\,,\, x_2 = y)$ are such that:

$$\left.\begin{aligned} u_1\,(x_1\,,x_2\,,x_3\,,t) &= -\,u_1\,(-x_1\,,x_2\,,x_3\,,t) \\ u_2\,(x_1\,,x_2\,,x_3\,,t) &= -\,u_2\,(x_1\,,-x_2\,,x_3\,,t) \end{aligned}\right\} \qquad [7.32]$$

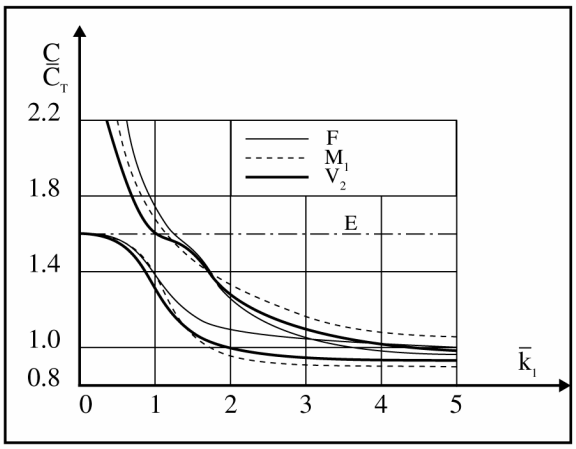

Figure 7.6. *The first two elastodynamic modes of extensional waves: isotropic material $\nu = 0.3$; flatness thickness/width = 0.555 rectangular cross-section; C_T shear wave velocity; k_1=bk, reduce wave number; E – elementary theory; F – Fraser; M_1 – Medick; V_2 – Volterra*

They are antisymmetric in the planes $(x_1 = x\,,\; x_3 = z)$ and $(x_2 = y\,, x_3 = z)$ respectively. Axial displacement component u_3 is symmetric with respect to $(x_1\,,\; x_2)$: $u_3\,(x_1\,,x_2\,,x_3) = u_3\,(x_1\,,x_2\,,-x_3)$. We follow Touratier's notation $(x_1 = x,\, x_2 = y,\, x_3 = z)$ $(x_1\,,\, x_2\,,\, x_3)$. This is possible if the following *displacement field* is adopted:

$$u_1(x_1, x_2\,, x_3\,, t) = \sum_{p=0}^{\infty}\;\sum_{q=0}^{\infty}\; x_1^{2p+1}.\, x_2^{2q}\; u_1^{(2p+1,\,2q)}\;(x_3\,,t)$$

@Seismicisolation

$$u_2(x_1, x_2, x_3, t) = \sum_{p=0}^{\infty} \sum_{q=0}^{\infty} x_1^2 \; x_2^{2q+1} \; u_2^{(2q+2p+1)}(x_3, t)$$

$$u_3(x_1, x_2, x_3, t) = \sum_{p=0}^{\infty} \sum_{q=0}^{\infty} x_1^{2p} \, . \, x_2^{2q} \; u_3^{(2p, 2q)}(x_3, t) \qquad [7.33]$$

The adopted displacement field seems complicated. The accuracy of a dispersion curve depends on the number of terms retained in equation [7.33]. In what follows, for the first version of internal constraints only three components are retained.

Boundary conditions are imposed on the lateral rod surface so that the last one is free from all applied stresses. Conditions at the end of the rod are such that the ends can receive any applied force field.

For $x_1 = \pm \dfrac{h}{2}$:

$$\left.\begin{aligned} \sigma_{11} &= \left(\pm \frac{h}{2}, x_2, x_3, t\right) = 0 \qquad \forall\, x_2 \text{ and } x_3 \\ \sigma_{21} &= \left(\pm \frac{h}{2}, x_2, x_3, t\right) = 0 \qquad \forall\, x_2 \text{ and } x_3 \\ \sigma_{31} &= \left(\pm \frac{h}{2}, x_2, x_3, t\right) = 0 \qquad \forall\, x_2 \text{ and } x_3 \end{aligned}\right\} \qquad [7.34]$$

For $x_2 = \pm \dfrac{b}{2}$:

@Seismicisolation

$$\left.\begin{aligned}
\sigma_{12} &= \left(x_1, \pm\frac{b}{2}, x_3, t\right) = 0 \qquad \forall\, x_1 \text{ and } x_3 \\
\sigma_{22} &= \left(x_1, \pm\frac{b}{2}, x_3, t\right) = 0 \qquad \forall\, x_1 \text{ and } x_3 \\
\sigma_{32} &= \left(x_1, \pm\frac{b}{2}, x_3, t\right) = 0 \qquad \forall\, x_2 \text{ and } x_3
\end{aligned}\right\} \qquad [7.35]$$

The expanded series [7.33] has the forms:

$$\begin{aligned}
u_1 &= x_1 \left[u_1^{(1,0)} + x_2^2\, u_2^{(2,1)} + x_2^4\, u_1^{(1,4)} + \bullet\bullet\bullet)\right] \\
&\quad + x_1^3 \left[u_1^{(3,0)} + x_2^2\, u_1^{(3,2)} + x_2^4\, u_1^{(3,4)} + \bullet\bullet\bullet\right. \\
&\quad + \bullet\bullet\bullet\bullet\bullet\bullet\bullet\bullet\bullet\bullet\bullet\bullet\bullet\bullet
\end{aligned} \qquad [7.36]$$

$$\begin{aligned}
u_2 &= x_2 \left[u_2^{(0,1)} + x_1^2\, u_1^{(2,1)} + x_1^4\, u_2^{(4,1)} \bullet\bullet\bullet\right] \\
&\quad + x_2^3 \left[u_2^{(0,3)} + x_1^2\, u_2^{(2,3)} + \bullet\bullet\bullet\right]
\end{aligned}$$

$$u_3 = u_3^{(0,0)} + x_2^2\, u_3^{(0,2)} + x_1^2\, u_3^{(2,0)} + \ldots$$

The series truncation must take the boundary conditions into account. Normal stresses at the boundaries are set to zero.

The second hypothesis concerns shear stress, which is neglected at the boundaries. The polynomials adopted in equations [7.32] and [7.33] permit tractable calculations when reduced to their minimum.

The three components retained are:

$$u_1^{(1,0)}, \quad u_2^{(0,1)}, \quad u_3^{(0,0)}$$

@Seismicisolation

However, normal stresses σ_{11} and σ_{22} are odd functions in x_1^2 and x_2^2, in order to satisfy equations [7.34] and [7.35]. Consequently there are seven components in the expressions of displacement. These are:

$$u_1(x_1,x_2,x_3,t) = x_1\ u_1^{(1,0)} + x_1\ x_2^2\ u_1^{(1,2)} + x_1^3\ u_1^{(3,0)}$$

$$u_2(x_1,x_2,x_3,t) = x_2\ u_2^{(0,1)} + x_1^2\ x_2\ u_1^{(2,1)} + x_2^3\ u_2^{(0,3)}$$

$$u_3(x_3,t) = u_3^{(0,0)}(x_3,t) \qquad [7.37]$$

7.6.4. *Strain and stress components*

7.6.4.1. *Strain components*

Strain components are deduced from equation [7.37]:

$$\varepsilon_{11} = u_1^{(1,0)} + 3\ x_1^2\ u_1^{(3,0)} + x_2^2\ u_1^{(1,2)}$$

$$\varepsilon_{22} = u_2^{(0,1)} + 3\ x_2^2\ u_2^{(0,3)} + x_1^2\ u_2^{(2,1)}$$

$$\varepsilon_{33} = \frac{\partial\ u^{(0,0)}{}_3}{\partial\ x_3}$$

$$\varepsilon_{12} = x_1\ x_2\ \left[u_1^{(1,2)} + u_2^{(2,1)}\right]$$

$$\varepsilon_{13} = \frac{x_1}{2}\left(\frac{\partial u_1^{(1,0)}}{\partial x_3} + x_1^2\ \frac{\partial u_1^{(3,0)}}{\partial x_3} + x_2^2\ \frac{\partial u_1^{(1,2)}}{\partial x_3}\right)$$

$$\varepsilon_{23} = \frac{x_2}{2}\left(\frac{\partial u_2^{(0,1)}}{\partial x_3} + x_2^2\ \frac{\partial u_2^{(0,3)}}{\partial x_3} + x_1^2\ \frac{\partial u_2^{(2,1)}}{\partial x_3}\right) \qquad [7.38]$$

7.6.4.2. *Stress components for transversely isotropic materials*

Five components of stiffness coefficients C_{ij} are necessary to express stress components in constitutive equations.

@Seismicisolation

$$\sigma_{11} = C_{11}\left\{u_1^{(1,0)} + 3x_1^2\ u_1^{(3,0)} + x_2^2\ u_1^{(1,2)}\right\} + C_{12}\left\{u_2^{(0,1)} + 3x_2^2\ u_2^{(0,3)} + x_1^2\ u_2^{(2,1)}\right\} + C_{13}\ \frac{\partial u_3^{(0,0)}}{\partial x_3} \qquad [7.39a]$$

$$\sigma_{22} = C_{12}\left\{u_1^{(1,0)} + 3x_1^2\ u_1^{(3,0)} + x_2^2\ u_1^{(1,2)}\right\} + C_{11}\left\{u_2^{(0,1)} + 3x_2^2\ u_2^{(0,3)} + x_1^2\ u_2^{(2,1)}\right\} + C_{13}\ \frac{\partial u_3^{(0,0)}}{\partial x_3} \qquad [7.39b]$$

$$\sigma_{33} = C_{13}\left\{u_1^{(1,0)} + 3x_1^2\ u_1^{(3,0)} + x_2^2\ u_1^{(1,2)}\right\} + C_{13}\left\{u_2^{(0,1)} + 3x_2^2\ u_2^{(0,3)} + x_1^2\ u_2^{(2,1)}\right\} + C_{33}\ \frac{\partial u_3^{(0,0)}}{\partial x_3} \qquad [7.39c]$$

$$\sigma_{12} = \left(C_{11} - C_{12}\right)\ x_1\ x_2\ \left\{u_1^{(1,2)} + u_2^{(2,1)}\right\} \qquad [7.39d]$$

$$\sigma_{13} = C_{44}\ x_1\left(\frac{\partial u_1^{(1,0)}}{\partial x_3} + x_1^2\ \frac{\partial u_1^{(3,0)}}{\partial x_3} + x_2^2\ \frac{\partial u_1^{(1,2)}}{\partial x_3}\right) \qquad [7.39e]$$

$$\sigma_{23} = C_{44}\ x_2\left(\frac{\partial u_2^{,1(0)}}{\partial x_3} + x_2^2\ \frac{\partial u_2^{(0,3)}}{\partial x_3} + x_1^2\ \frac{\partial u_2^{(2,1)}}{\partial x_3}\right) \qquad [7.39f]$$

7.6.4.3. *Boundary conditions and related stress equations*

In equation [7.37] there are seven polynomial coefficients to evaluate and include in equations of motion.

This explains the lengthy stress equations in [7.39].

Boundary conditions concerning lateral surfaces (with normal stresses set to zero), however, yield additional equations.

Equations [7.39a, b and c] are rewritten at lateral surfaces:

@Seismicisolation

$$C_{11}\left\{u_1^{(1,0)}+\frac{3h^2}{4}\,u_1^{(3,0)}+x_2^2\,u_1^{(1,2)}\right\}+C_{12}\left\{u_2^{(0,1)}+3x_2^2\,u_2^{(0,3)}+\frac{h^2}{4}\,u_2^{(2,1)}\right\}$$
$$+\,C_{13}\,\frac{\partial u_3^{(0,0)}}{\partial x_3}=0 \qquad [7.40a]$$

$$C_{12}\left\{u_1^{(1,0)}+3x_1^2\,u_1^{(3,0)}+\frac{b^2}{4}\,u_1^{(1,2)}\right\}+C_{11}\left\{u_2^{(0,1)}+\frac{3b^2}{4}\,u_2^{(0,3)}+x_1^2\,u_2^{(2,1)}\right\}$$
$$+\,C_{13}\,\frac{\partial u_3^{(0,0)}}{\partial x_3}=0 \qquad [7.40b]$$

Equations [7.40] are valid for any values of x_1 and x_2.

So setting transverse variables x_1 and x_2 to zero we obtain:

$$C_{11}\left\{u_1^{(1,0)}+\frac{3h^2}{4}\,u_1^{(3,0)}\right\}+C_{12}\left\{u_2^{(0,1)}+\frac{h^2}{4}\,u_2^{(2,1)}\right\}+C_{13}\,\frac{\partial u_3^{(0,0)}}{\partial x_3}=0 \qquad [7.41a]$$

Collecting x_2^2 terms in equation [7.40a] and setting their sum to zero:

$$C_{11}\,u_1^{(1,2)}+3\,C_{12}\,u_2^{(0,3)}=0 \qquad [7.41b]$$

Equation [7.40b] is rewritten in similar manner:

$$C_{12}\left\{u_1^{(1,0)}+\frac{h^2}{4}\,u_1^{(1,2)}\right\}+C_{11}\left\{u_2^{(0,1)}+\frac{3\,b^2}{4}\,u_2^{(0,3)}\right\}+C_{13}\,\frac{\partial u_3^{(0,0)}}{\partial x_3}=0 \qquad [7.41c]$$

$$3\,C_{12}\,u_1^{(3,0)}+C_{11}\,u_2^{(2,1)}=0 \qquad [7.41d]$$

With four equations [7.41a-d] the number of unknown independent coefficients in equation [7.37] is reduced to three.

From equation [7.41], let us write equations giving $u_1^{(1,2)}$, $u_2^{(2,1)}$, $u_1^{(3,0)}$ and $u_2^{(0,3)}$:

@Seismicisolation

$$u_1^{(1,2)} = \frac{-4C_{12}}{b^2\left(C_{12}^2 - C_{11}^2\right)}\left\{C_{12}\, u_1^{(1,0)} + C_{11}\, u_2^{(0,1)} + C_{13}\frac{\partial u_3^{(0,0)}}{\partial x_3}\right\} \qquad [7.42a]$$

$$u_2^{(2,1)} = \frac{-4C_{12}}{h^2\left(C_{12}^2 - C_{11}^2\right)}\left\{C_{11}\, u_1^{(1,0)} + C_{12}\, u_2^{(0,1)} + C_{13}\frac{\partial u_3^{(0,0)}}{\partial x_3}\right\} \qquad [7.42b]$$

$$u_1^{(3,0)} = \frac{4C_{11}}{3\,h^2\left(C_{12}^2 - C_{11}^2\right)}\left\{C_{11}\, u_1^{(1,0)} + C_{12}\, u_2^{(0,1)} + C_{13}\frac{\partial u_3^{(0,0)}}{\partial x_3}\right\} \qquad [7.42c]$$

$$u_2^{(0,3)} = \frac{4C_{11}}{3\,b^2\left(C_{12}^2 - C_{11}^2\right)}\left\{C_{12}\, u_1^{(1,0)} + C_{11}\, u_2^{(0,1)} + C_{13}\frac{\partial u_3^{(0,0)}}{\partial x_3}\right\} \qquad [7.42d]$$

7.6.4.4. *Displacement components*

The three independent coefficients for displacement components are:

$$u_1\left(x_1, x_2, x_3, t\right) = x_1\left\{\frac{4x_2^2\, C_{12}^2}{b^2\left(C_{12}^2 - C_{11}^2\right)} + \frac{4x_1^2\, C_{11}^2}{3h^2\left(C_{12}^2 - C_{11}^2\right)}\right\} u_1^{(1,0)}$$

$$+x_1\frac{C_{11}\, C_{12}}{\left(C_{12}^2 - C_{11}^2\right)}\left\{\frac{-x_2^2}{b^2} + \frac{4x_1^2}{3h^2}\right\} u_2^{(0,1)} + \frac{x_1\, C_{13}}{C_{12}^2 - C_{11}^2} \qquad [7.43a]$$

$$\bullet\left\{\frac{-4x_2^2\, C_{12}}{b^2} + \frac{4\,x_1^2\, C_{11}}{3h^2}\right\}\frac{\partial u_3^{(0,0)}}{\partial x_3}$$

$$u_2\left(x_1, x_2, x_3, t\right) = x_2\left\{1 - \frac{4x_1^2\, C_{12}^2}{h^2\left(C_{12}^2 - C_{11}^2\right)} + \frac{4x_2^2\, C_{11}^2}{3b^2\, C_{12}^2 - C_{11}^2}\right\} u_2^{(0,1)}$$

$$+\,x_2\frac{C_{11}\, C_{12}}{\left(C_{12}^2 - C_{11}^2\right)}\left\{-\frac{4x_1^2}{h^2} + \frac{4x_2^2}{3b^2}\right\} u_2^{(1,0)} + \frac{x_2\, C_{13}}{C_{12}^2 - C_{11}^2}\bullet \qquad [7.43b]$$

$$\left\{\frac{-4x_1^2\, C_{12}}{h^2} + \frac{4C_{11}\, x_2^2}{3b^2}\right\}\frac{\partial u_3^{(0,0)}}{\partial x_3}$$

@Seismicisolation

$$u_3\left(x_1, x_2, x_3, t\right) = u_3^{(0,0)}\left(x_3, t\right) \qquad [7.43c]$$

7.6.5. *Energy functionals and Hamilton's principle*

The mechanical system being conservative, equations of motion can be deduced from Hamilton's principle using variational calculus.

Hamilton's functional is:

$$\tilde{J} = \int_{t_1}^{t_2} \left[\tilde{U}_p - \tilde{U}_c + \int\int\int_{\mathcal{D}} u_i\, f_i\, dv + \int\int_{\partial\mathcal{D}} F_i\, u_i\, ds \right] dt \qquad [7.44]$$

where $\tilde{U}_c$ is reduced kinetic energy (of order < 4), $\tilde{U}_p$ is reduced potential energy (of order < 4), and $\mathcal{D}$ is the domain occupied by the rod:

$$\left[-\frac{h}{2}, \frac{h}{2}\right] x \left[-\frac{b}{2}, \frac{b}{2}\right] x \left[0, L\right]$$

f_i and F_i are volume and surface forces respectively. In the time interval (t_1, t_2), functional $\tilde{J}$ must be stationary. Kinetic energy is:

$$U_c = \frac{1}{2}\int\int\int_{\mathcal{D}} \rho \left(\frac{\partial u_i}{\partial t}, \frac{\partial u_i}{\partial t}\right) dv$$

Taking equations [7.43a-c] into account, simplified kinetic energy is:

$$\tilde{U}_c = \frac{\rho}{2}\int\int\int_{\mathcal{D}} \left\{ \begin{array}{l} x_1^2\left(\dfrac{\partial u_1^{(1,0)}}{\partial t}\right)^2 + x_2^2\left(\dfrac{\partial u_2^{(0,1)}}{\partial t}\right)^2 \\ \\ + \left(\dfrac{\partial u_3^{(0,0)}}{\partial t}\right)^2 \end{array} \right\} dx_1\, dx_2\, dx \qquad [7.45]$$

@Seismicisolation

In equation [7.45], terms of order higher than or equal to four are neglected. In the same equation, we recognize that:

$$\int\int_S x_1^2\, dx_1\, dx_2 = I_1 = \frac{h^3\, b}{12}$$

$$\int\int_S x_2^2\, dx_1\, dx_2 = I_2 = \frac{h^3\, b^3}{12} \qquad [7.46]$$

$$\int\int_S dx_1\, dx_2 = S = h\, b$$

where I_1 and I_2 are quadratic moments of the cross-section and S the section area.

7.6.5.1. *Kinetic energy*

The simplified kinetic energy for a rod of length L is:

$$\tilde{U}_c = \rho \frac{bh}{2} \left[\frac{h^3}{12} \int_0^L \left\{ \left(\frac{\partial u_1^{(1,0)}}{\partial t} \right)^2 dx + \frac{b^3}{12} \left(\frac{\partial u_2^{(0,1)}}{\partial t} \right)^2 dx_2 \right\} + \int_0^L \left(\frac{\partial u_3^{(0,0)}}{\partial t} \right)^2 dx_3 \right] \qquad [7.47]$$

7.6.5.2. *Potential energy*

Simplified potential energy is:

$$U_p = \frac{1}{2} \int\int\int_{\mathcal{D}} \sigma_{ij}\, \varepsilon_{ij}\, dv$$

$$= \frac{1}{2} \int\int\int C_{ijkl}\, \varepsilon_{ij}\, \varepsilon_{kl}\, dv \qquad [7.48]$$

The expressions of strain components in equation [7.43] are introduced in equation [7.48] after the following derivations:

@Seismicisolation

$$\varepsilon_{11}\left\{1+\frac{4C_{11}^2\ b^2-C_{12}^2\ h^2\ x_2^2}{b^2\ h^2\ \left(C_{12}^2-C_{11}^2\right)}\right\}u_1^{(1,0)}+$$

$$\frac{4C_{11}\ C_{12}\ \left(b^2\ x_1^2-h^2\ x_2^2\right)}{b^2\ h^2\ \left(c_{12}^2-\ C_{11}^2\right)}\ u_2^{(0,1)} \qquad [7.49]$$

$$4\ C_{13}\ \frac{\left(C_{11}\ b^2\ x_1^2-C_{12}\ h^2\ x_2^2\right)}{b^2\ h^2\ \left(C_{12}^2-C_{11}^2\right)}\bullet\frac{\partial u_3^{(0,0)}}{\partial x_3}$$

$$\varepsilon_{22}=\frac{4\ C_{11}\ C_{12}\ \left(h^2\ x_2^2-b^2\ x_1^2\right)}{b^2\ h^2\ \left(C_{12}^2-C_{11}^2\right)}\ u_1^{(1,0)}+\left\{1+\frac{4\ C_{11}^2\ h^2\ x_2^2-C_{12}^2\ b^2\ x_1^2}{b^2\ h^2\ \left(C_{12}^2-C_{11}^2\right)}\right\}$$

$$+\ \frac{4\ C_{13}\ \left(C_{11}\ h^2\ x_2^2-C_{12}\ b^2\ x_1^2\right)}{b^2\ h^2\ \left(C_{12}^2-C_{11}^2\right)}\ \frac{\partial u_3^{(0,0)}}{\partial x_3} \qquad [7.50]$$

$$\varepsilon_{33}=\frac{\partial u_3^{(0,0)}}{\partial x_3} \qquad [7.51]$$

$$\varepsilon_{12}=\frac{-2\ C_{12}\ x_1\ x_2}{\left(C_{12}^2-C_{11}^2\right)}\left\{\begin{array}{l}\left(\frac{4\ C_{11}}{h^2}+\frac{4\ C_{12}}{b^2}\right)u_1^{(1,0)}+\left(\frac{4\ C_{12}}{h^2}+\frac{4\ C_{11}}{b^2}\right)u_2^{(0,1)}\\ +4\ C_{13}\left(\frac{1}{h^2}+\frac{1}{b^2}\right)\frac{\partial u_3^{(0,0)}}{\partial x_3}\end{array}\right\} \qquad [7.52]$$

$$\varepsilon_{13}=x_1\left\{1+\frac{4\ C_{11}^2\ b^2\ x_1^2-12\ C_{12}\ h^2\ x_2^2}{3\ h^2\ b^2\ \left(C_{12}^2-C_{11}^2\right)}\right\}\frac{\partial u_1^{(0,0)}}{\partial x_3}$$

$$+\ x_1\left\{\frac{C_{11}\ C_{12}\ \left(4\ b^2\ x_1^2-12\ h^2\ x_2^2\right)}{3\ b^2\ h^2\ \left(C_{12}^2-C_{11}^2\right)}\ \frac{\partial u_2^{(0,1)}}{\partial x_3}\right\}$$

@Seismicisolation

$$+ x_1 \left\{ \frac{C_{13} \left(4\, C_{11}\, b^2\, x_1^2 - 12\, C_{12}\, h^2\, x_2^2\right)}{3\, h^2\, b^2\, \left(C_{12}^2 - C_{11}^2\right)} \frac{\partial^2\, u_3^{(0,0)}}{\partial x_3^2} \right\} \qquad [7.53]$$

$$\varepsilon_{22} = x_2 \left\{ \frac{C_{11}\, C_{12} \left(4\, h^2\, x_2^2 - 12\, b^2\, x_2^2\right)}{3\, b^2\, h^2\, \left(C_{12}^2 - C_{11}^2\right)} \frac{\partial u_1^{(1,0)}}{\partial x_3} \right\}$$

$$+ x_2 \left\{ 1 + \frac{4\, C_{11}\, h^2\, x_2^2 - 12\, C_{12}^2\, b^2\, x_1^2}{3\, b^2\, h^2\, \left(C_{12}^2 - C_{11}^2\right)} \right\} \frac{\partial u_2^{(0,1)}}{\partial x_3}$$

$$+ x_2 \left\{ 1 + \frac{C_{13} \left(4\, C_{11}\, h^2\, x_2^2 - 12\, C_{12}^2\, b^2\, x_1^2\right)}{3\, h^2\, b^2\, \left(C_{12}^2 - C_{11}^2\right)} \right\} \frac{\partial^2 u_3^{(0,0)}}{\partial x_3^2} \qquad [7.54]$$

Using potential energy density w*:

$$w^* = \frac{1}{2} C_{ijkl}\, \varepsilon_{ij}\, \varepsilon_{kl} \qquad [7.55]$$

Potential energy is written as:

$$\tilde{U}_p = \int \int \int_{\mathcal{D}} w^*\, dx_1\, dx_2\, dx_3$$

$$\tilde{U}_p = \frac{C_{11}\, S}{6} \int_0^L \left\{ \left[u_1^{(1,0)}\right]^2 + \left[u_2^{(0,1)}\right]^2 \right\} dx_3$$

$$+ \frac{C_{13}\, S}{3} \int_0^L \left\{ u_1^{(1,0)} \bullet \frac{\partial u_3^{(0,1)}}{\partial x_3} + u_2^{(0,1)} \frac{\partial u_3^{(0,0)}}{\partial x_3} \right\} dx_3$$

@Seismicisolation

$$+\left\{\frac{C_{13}}{2}-\frac{2C_{13}^2}{3\left(C_{11}+C_{12}\right)}\right\} S\int_0^L \left(\frac{\partial u_3^{(0,0)}}{\partial u_3}\right)^2 dx_3$$

$$+\frac{C_{12}\ S}{3}\int_0^L u_1^{(1,0)}\bullet u_2^{(0,1)}\ dx_3+q^2\left(C_{ijkl}\right)\frac{C_{44}}{2}\bullet \qquad [7.56]$$

$$\left\{I_1\int_0^L\left(\frac{\partial u_1^{(1,0)}}{\partial x_3}\right)dx_3+I_2\int_0^L\left(\frac{\partial u_2^{(0,1)}}{\partial x_3}\right)^2 dx_3\right\}$$

In equation [7.56], the correcting coefficient is introduced so as to take into account non-uniform shear stress distribution in the planes (x_1, x_3) and (x_2, x_3). q is calculated in the next paragraph so as to satisfy the asymptotic behavior of phase velocity when the wave number goes to infinity.

With expressions of $\tilde{U}_p$ in equation [7.56] and $\tilde{U}_c$ in equation [7.47] introduced in functional $\tilde{J}$ in equation [7.44], the equations of motion are obtained as are natural boundary conditions.

7.6.5.3. *Energy functional*

$$\tilde{J}=\int_{t_1}^{t_2}\frac{\rho bh}{2}\left[\begin{array}{l}\frac{h^2}{12}\int_0^L\left(\frac{\partial u_1^{(1,0)}}{\partial t}\right)^2 dx_3+\frac{b^2}{12}\int_0^L\left(\frac{\partial u_2^{(0,1)}}{\partial t}\right)^2 dx_3\\ +\int_0^L\left(\frac{\partial u_3^{(0,0)}}{\partial t}\right)^2 dx_3\end{array}\right]dt$$

$$-\int_{t_1}^{t_2}\frac{C_{11}S}{6}\int_0^L\left\{\left[u_1^{(1,0)}\right]^2+\left[u_2^{(0,1)}\right]^2\right\}dx_2\ dt-\int_{t_1}^{t_2}\frac{C_{13}S}{3}\int_0^L \qquad [7.57]$$

$$\bullet\left\{u_1^{(1,0)}\bullet\frac{\partial u_3^{(0,0)}}{\partial x_3}+u_2^{(0,1)}\ \frac{\partial u_3^{(0,0)}}{\partial x_3}\right\}dx_3\ dt$$

@Seismicisolation

$$-\int_{t_1}^{t_2} \left\{ \frac{C_{13}}{2} - \frac{2C_{13}^2}{3\left(C_{11}+C_{12}\right)} \right\} S \int_0^L \left(\frac{\partial u_3^{(0,0)}}{\partial x_3} \right) dx_3$$

$$dt - \int_{t_1}^{t_2} \frac{C_{12}\, S}{3} \bullet$$

$$\int_0^L u_1^{(1,0)} \bullet u_2^{(0,1)}\, dx_3\, dt - q^2 \frac{C_{44}}{2} \int_{t_1}^{t_2} \left\{ \begin{array}{l} I_1 \int_0^L \left(\frac{\partial u_1^{(1,0)}}{\partial x_3} \right)^2 dx_3 \\ +I_2 \int_0^L \left(\frac{\partial u_2^{(0,1)}}{\partial x_3} \right)^2 dx_3 \end{array} \right\} dt$$

$$+ \int_{t_1}^{t_2} dt \int \int \int u_i\, f_i\, dx_1\, dx_2\, dx_3 + \int_{t_1}^{t_2} dt \int \int_{\partial D} F_i\, u_i\, dx_1\, dx_2$$

[7.57 cont]

7.6.6. *Equations of motion*

Displacement field $\vec{u}$ is such that the $\tilde{J}$ functional is stationary in the time interval (t_1, t_2). In Appendix 7.D, details of variational calculation and integrations by parts are given. Coupled equations of motion are:

$$\rho \frac{h^2}{4} \frac{\partial^2 u_1^{(1,0)}}{\partial t^2} = \frac{h^2}{4} q^2 C_{44} \frac{\partial^2 u_1^{(1,0)}}{\partial x_3^2} - C_{11} u_1^{(1,0)} - C_{12} u_2^{(0,1)} - C_{13} \frac{\partial u_3^{(0,0)}}{\partial x_3}$$

$$\rho \frac{b^2}{4} \frac{\partial^2 u_2^{(0,1)}}{\partial t^2} = \frac{h^2}{4} q^2 C_{44} \frac{\partial^2 u_2^{(0,1)}}{\partial x_3^2} - C_{11} u_2^{(0,1)} - C_{12}\, u_1^{(1,0)} - C_{13} \frac{\partial u_3^{(0,0)}}{\partial x_3}$$

$$\rho \frac{\partial^2 u_3^{(0,0)}}{\partial t^2} = \left\{ C_{33} - \frac{4\, C_{13}^2}{3\left(C_{11}+C_{12}\right)} \right\} \frac{\partial^2 u_3^{(0,0)}}{\partial x_3^2} + \frac{C_{13}}{3} \left\{ \frac{\partial u_1^{(1,0)}}{\partial x_3} + \frac{\partial u_2^{(0,1)}}{\partial x_3} \right\}$$

[7.58]

@Seismicisolation

7.6.7. *Boundary equations*

$$\frac{\partial u_1^{(1,0)}}{\partial x_3} = 0 \text{ for } x_3 = 0 \text{ and } x_3 = L$$

$$\partial u_2^{(0,1)} = 0 \text{ for } x_3 = 0 \text{ and } x_3 = L$$

$$\frac{C_{13}}{3}\left\{u_1^{(1,0)} + u_2^{(0,1)}\right\} + \left\{C_{33} - \frac{4\,C_{13}^2}{3\left(C_{11} + C_{12}\right)}\right\}\frac{\partial u_3^{(0,0)}}{\partial x_3} = 0 \qquad [7.59]$$

for $x_3 = 0$ and $x_3 = L$ for the free end.

REMARK – For isotropic materials, equation [7.58] becomes Volterra equation [7.20].

7.7. Wave dispersion relationships

The following notations are introduced to simplify equation writing:

$$\chi_{ij}^2 = \frac{C_{ij}}{\rho}\ ,\ \chi^{*2} = \chi_3^2 - \frac{4\,\chi_{13}^{*4}}{3\left(\chi_{11}^2 + \chi_{12}^2\right)} = \frac{1}{\rho}\left\{C_{33} - \frac{4\,C_{13}^2}{3\left(C_{11} + C_{12}\right)}\right\} \qquad [7.60]$$

where χ_{ij} is homogenous with velocities.

$$\frac{h^2}{4}\frac{\partial^2 u_i^{(1,0)}}{\partial t^2} = \frac{h^2}{4}\,q^2\,\chi_{44}^2\,\frac{\partial^2 u_1^{(1,0)}}{\partial x_3^2} - \chi_{11}^2\,u_1^{(1,0)} - \chi_{12}^2\,u_2^{(0,1)} - \chi_{13}^2\,\frac{\partial u_3^{(0,0)}}{\partial x_3}$$

$$\frac{b^2}{4}\frac{\partial^2 u_2^{(0,1)}}{\partial t^2} = \frac{h^2}{4}\,q^2\,\chi_{44}^2\,\frac{\partial^2 u_2^{(0,1)}}{\partial x_1^2} - \chi_{11}^2\,u_2^{(0,1)} - \chi_{12}^2\,u_1^{(1,0)} - \chi_{13}^2\,\frac{\partial u_3^{(0,0)}}{\partial x_3}$$

$$\frac{\partial^2 u_3^{(0,0)}}{\partial t^2} = \chi^{*2}\,\frac{\partial^2 u_3^{(0,0)}}{\partial x_3^2} + \frac{\chi_{13}^2}{3}\left(\frac{\partial u_1^{(1,0)}}{\partial x_3} + \frac{\partial u_2^{(0,1)}}{\partial x_3}\right) \qquad [7.61]$$

@Seismicisolation

Progressive plane waves are adopted:

$$u_j^{(m,n)}\left(x_3,t\right) = A_j \exp j\,k\left(x_3 - ct\right) \qquad , k \in \mathbb{R} \qquad [7.62]$$

Bringing equation [7.62] into [7.61]:

$$\left\{\frac{h^2}{4}\,k^2\left(c^2 - q^2\,\chi_{44}^2\right) - \chi_{11}^2\right\} A_1 - \chi_{12}^2\,A_2 - j\,k\,\chi_{13}^2 A_3 = 0$$

$$-\chi_{12}^2\,A_1 + \left\{\frac{b^2k^2}{4}\left(c^2 - q^2\chi_{44}^2\right) - \chi_{11}^2\right\} A_2 - j_2\,k\,\chi_{13}^2\,A_3 = 0$$

$$j\,k\,\frac{\chi_{13}^2}{3}\,A_1 + j\,k\,\frac{\chi_{13}^2}{3}\,A_2 + k^2\left(c^2 - \chi^{*2}\right) A_3 = 0 \qquad [7.63]$$

Let us transform equation [7.63] into dimensionless equations by adopting c as phase velocity:

$$\bar{\chi}_{ij}^2 = \frac{\chi_{ij}^2}{C_3^2}, \qquad \bar{\chi}^{*2} = \frac{\chi^{*2}}{C_3^2}, \qquad \bar{c} = \frac{c}{C_3} \qquad \text{with } c_3 = \frac{E_3}{\rho}$$

$$\bar{k}_1 = k\,\frac{h}{2}, \qquad \bar{k}_2 = k\,\frac{b}{2} \qquad [7.64]$$

A dispersion relationship is obtained by setting the coefficient determinant of homogenous equations [7.63] to zero:

$$\begin{vmatrix} \bar{c}^2 - q^2\chi_{44}^2 - \dfrac{\bar{\chi}_{11}^2}{\bar{k}_1^2} & -\dfrac{\bar{\chi}_{12}^2}{\bar{k}_1^2} & -jk\,\dfrac{\bar{\chi}_{13}}{\bar{k}_1^2} \\ -\dfrac{\bar{\chi}_{12}^2}{\bar{k}_2^2} & \dfrac{c^2 - q^2\bar{\chi}_{44}^2 - \bar{\chi}_{13}^2}{\bar{k}_1^2} & -jk\,\dfrac{\bar{\chi}_{13}^2}{\bar{k}_2^2} \\ j\dfrac{\bar{\chi}_{13}^2}{3k} & j\dfrac{\bar{\chi}_{13}^3}{3k} & \bar{c}^2 - \bar{\chi}^{*2} \end{vmatrix} = 0 \qquad [7.65]$$

@Seismicisolation

In Appendix 7.E, calculations of correcting factor q (C_{ijkl}) are presented by examining the Rayleigh surface wave. Rayleigh wave velocity is obtained by equation [7.E.44] in Appendix 7.E. The equation is of sixth order.

Table 7.1 gives the q^2 for six composite materials.

For isotropic materials, Viktorov proposed an empirical relationship between correcting factor q^2 versus Poisson's number γ:

$$q^2\ (\gamma) = \left(\frac{0.87 + 1.12\ \nu}{1+\nu}\right)^2 \qquad [7.66]$$

Table 7.1 gives this curve for $0.3 < \gamma < 0.5$.

Material	Graphite epoxy	Silica-phenolic resin	Glass-fiber epoxy	Kevlar 49 epoxy	Graphite fiber-epoxy	Glass fiber-polyester
$\bar{\chi}_{44}^2$	0.03293	0.12596	0.13408	0.02400	0.02400	0.14600
$\bar{c}_R^2$	0.02725	0.10264	0.11038	0.01975	0.01387	0.12567
q^2	0.82753	0.81488	0.82327	0.82296	0.57782	0.86077
Reference	Internal reports, not published [VIN 80]					

Table 7.1. *Values of Rayleigh wave and correcting factor q^2 for various composite materials*

7.7.1. *Phase velocity in composite materials*

Developing equation [7.65], a sixth-order equation is obtained for the extensional wave velocity in a rod of rectangular cross-section.

$$\bar{c}^6 - \bar{c}^4 \left\{2q^2\ \bar{\chi}_{44}^2 + \bar{\chi}^{*2} + \bar{\chi}_{11}^2 \left(\frac{1}{\bar{k}^2} + \frac{1}{\bar{k}^2}\right)\right\}$$

@Seismicisolation

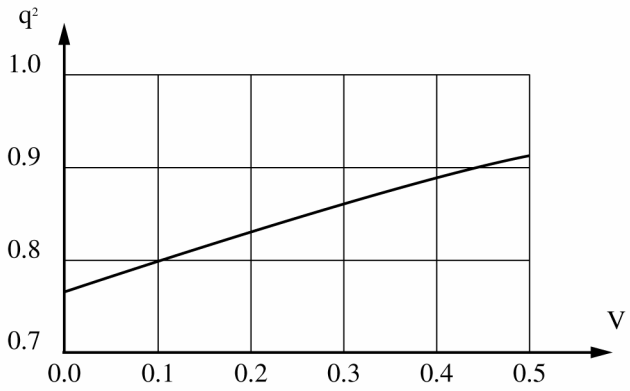

Figure 7.7. *Correcting factor q²* versus *Poisson's number, equation [7.65] after the formula given by Viktorov, which is valid for isotropic material*

$$+\bar{c}^2\left\{\begin{array}{l} q^2\ \bar{\chi}_{44}^2\ \left(q^2\bar{\chi}_{44}^2+2\bar{\chi}^{*2}\right)+ \\ \left[\left(q^2\bar{\chi}_{44}^2+\bar{\chi}^{*2}\right)\bar{\chi}_{11}^2-\dfrac{\bar{\chi}_{13}^4}{3}\right]\left(\dfrac{1}{\bar{k}_1^2}+\dfrac{1}{\bar{k}_2^2}\right)+ \\ \dfrac{\bar{\chi}_{11}^4-\bar{\chi}_{12}^4}{\bar{k}_1^2\ \bar{k}_2^2} \end{array}\right\}$$

$$+\left\{\begin{array}{l} -q^4\ \bar{\chi}_{44}^4\ \bar{\chi}^{*2}+q^2\ \bar{\chi}_{44}^2\ \left(-\bar{\chi}_{11}^2\ \bar{\chi}^{*2}+\dfrac{\bar{\chi}_{13}^4}{3}\right)\left(\dfrac{1}{\bar{k}_1^2}+\dfrac{1}{\bar{k}_2^2}\right) \\ +\left(\bar{\chi}_{11}^2-\bar{\chi}_{12}^2\right)\left[\dfrac{2\bar{\chi}_{14}^4}{3}-\bar{\chi}^{*2}\ \left(\bar{\chi}_{11}^2+\bar{\chi}_{12}^2\right)\right]\ \dfrac{1}{\bar{k}_1^2\ \bar{k}_4^2} \end{array}\right\}=0 \qquad [7.67]$$

Introducing the flatness coefficient defined as the ratio $\delta=\dfrac{\text{thickness h}}{\text{width b}}$, wave numbers $\bar{k}_1$ and $\bar{k}_2$ are related to each other by:

@Seismicisolation

$$\bar{k}_2 = k\,b = \frac{1}{\delta}\,\bar{k}_1 \qquad [7.68]$$

The dispersion equations are rewritten with δ as a parameter:

$$\bar{c}^6 - \bar{c}^4 \left\{ 2\,q^2\,\bar{\chi}^{*2} + \bar{\chi}^{*2} + \frac{\bar{\chi}_{11}^2}{\bar{k}_1^2}\left(1+\delta^2\right) \right\}$$

$$+\,\bar{c}^2 \left\{ \begin{array}{l} q^2\bar{\chi}_{44}^2\left(q^2\,\bar{\chi}_{44}^2 + 2\,\bar{\chi}^{*2}\right) + \dfrac{\left[\left(q^2\bar{\chi}_{44}^2\,\bar{\chi}^{*2}\right)\bar{\chi}_{11}^2 - \dfrac{\bar{\chi}_{13}^4}{3}\right]}{\bar{k}_1^2} \\ \bullet\left(1+\delta^2\right) + \dfrac{\bar{\chi}_{11}^4 - \bar{\chi}_{12}^4}{\bar{k}_1^4}\,\delta^2 + \left\{ \dfrac{\begin{array}{l} -q^4\,\bar{\chi}_{44}^4\,\bar{\chi}^{*2} + q^2\,\bar{\chi}_{44}^2 \bullet \\ \left(\bar{\chi}_{11}^2\,\bar{\chi}^{*2} + \dfrac{\bar{\chi}_{13}^4}{3}\right) \end{array}}{\bar{k}_1^2}\left(1+\delta^2\right) \right\} \\ + \left(\bar{\chi}_{11}^2 - \bar{\chi}_{12}^2\right)\dfrac{\left[2\,\bar{\chi}_{13}^2 - \bar{\chi}^{*2}\left(\bar{\chi}_{12}^2 + \bar{\chi}_{12}^2\right)\right]\delta^2}{\bar{k}_1^4} \end{array} \right\} = 0 \qquad [7.69]$$

This sixth-order equation is bisquared in $\bar{c}$ and has real coefficients.

Roots $\bar{c}^2$ are real and phase velocity for the three first modes of propagation can be written as [MIN 66]:

$$\bar{c}_1 = \left\{ 2\left(\frac{a_1^2}{9} - \frac{a_2}{3}\right)^{1/2} \cos\left[\frac{1}{3}\,\mathrm{Arc}\cos\frac{a_3 - \dfrac{a_1\,a_3}{3} + \dfrac{2\,a_1^3}{27}}{2\left[-\left(\dfrac{a_2}{3} - \dfrac{a_1^2}{9}\right)\right]^{1/2}} + \frac{2\,\pi}{3}\right] - \frac{a_1}{3} \right\}^{1/2}$$

@Seismicisolation

$$\bar{c}_2 = \left\{ 2\left(\frac{a_1^2}{9} - \frac{a_2}{3}\right)^{1/2} \cos\left[\frac{1}{3}\,\text{Arc}\cos\left(-\frac{a_3 - \frac{a_1\,a_2}{3} + \frac{2\,a_1^3}{27}}{2\left[-\left(\frac{a_2}{3} - \frac{a_1^2}{9}\right)^3\right]^{1/2}}\right) + \frac{4\pi}{3}\right] - \frac{a_1}{3} \right\}^{1/2}$$

$$\bar{c}_3 = \left\{ 2\left(\frac{a_1^2}{9} - \frac{a_2}{3}\right)^{1/2} \cos\left[\frac{1}{3}\,\text{Arc}\cos\left(-\frac{a_3 - \frac{a_1\,a_2}{3} + \frac{2\,a_1^3}{27}}{2\left[-\left(\frac{a_2}{3} - \frac{a_1^2}{9}\right)^3\right]^{1/2}}\right)\right] - \frac{a_1}{3} \right\}^{1/2} \qquad [7.70a]$$

with:

$$a_1 = -\left\{ 2\,q^2\,\bar{\chi}_{44}^2 + \bar{\chi}^{*2} + \frac{\bar{\chi}_{11}^2\left(1+\delta^2\right)}{\bar{k}_1^2} \right\}$$

$$a_2 = q^2\,\bar{\chi}_{44}^2\left(q^2\,\bar{\chi}_{44}^2 + 2\,\bar{\chi}^{*2}\right) + \frac{\left(q^2\,\bar{\chi}_{44}^2 + \bar{\chi}^{*2}\right)\bar{\chi}_{11}^2 - \bar{\chi}_{13}^4}{\bar{k}_1^2} \bullet \left(1+\delta^2\right) + \frac{\bar{\chi}_{11}^4 - \bar{\chi}_{12}^4}{\bar{k}_1^4}\,\delta^2$$

$$a_3 = -q^4\,\bar{\chi}_{44}^4\,\bar{\chi}^{*2} + q^2\,\bar{\chi}_{44}^2\,\frac{-\bar{\chi}_{11}^2\,\bar{\chi}^{*2} + \frac{\bar{\chi}_{13}^4}{3}}{\bar{k}_1^2}\left(1+\delta^2\right)$$

$$+ \left(\bar{\chi}_{11}^2 - \bar{\chi}_{12}^2\right)\frac{\left[\frac{2\,\bar{\chi}_{13}^4}{3} - \bar{\chi}^{*2}\left(\bar{\chi}_{11}^2 + \bar{\chi}_{12}^2\right)\right]\delta^2}{\bar{k}_1^4} \qquad [7.70b]$$

7.7.2. *Extensional waves in an anisotropic composite rod with rectangular cross-section – dispersion curves*

Elastic constants of various composite materials are experimentally evaluated. Figure 7.8 shows the curve of a dimensionless phase velocity:

@Seismicisolation

$$c/c_L \left(C_L = \sqrt{\frac{E_2}{\rho}} \right)$$

plotted against the dimensionless wave number $\bar{k} = b/2\ k$, b being the rod width.

The dispersion curves in the first elastodynamic mode are very pronounced, even at a low value of $\bar{k}$. The two important factors to take into account are Poisson's number γ_{31} in plane (1, 3), and the ratio of shear modulus G_{13}/Young's modulus E_3.

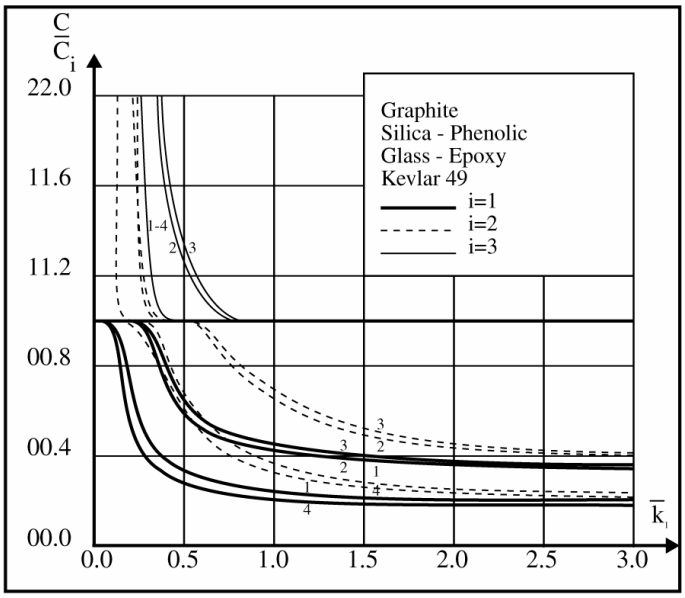

Figure 7.8. *Dispersion of extensional wave velocity in a rod with rectangular cross-section and flatness: thickness/width = δ = 0.5. Dispersion curves are very different from each other depending on the nature of composite materials. i= (1,2,3) mode rank*

7.7.2.1. *Influence of Poisson's number*

In Figure 7.9 the curves are drawn for isotropic materials with Poisson's numbers varying in the interval (0.2–0.4). For the first elastodynamic mode, and for a square section, dispersion is not pronounced in spite of the variation of γ.

@Seismicisolation

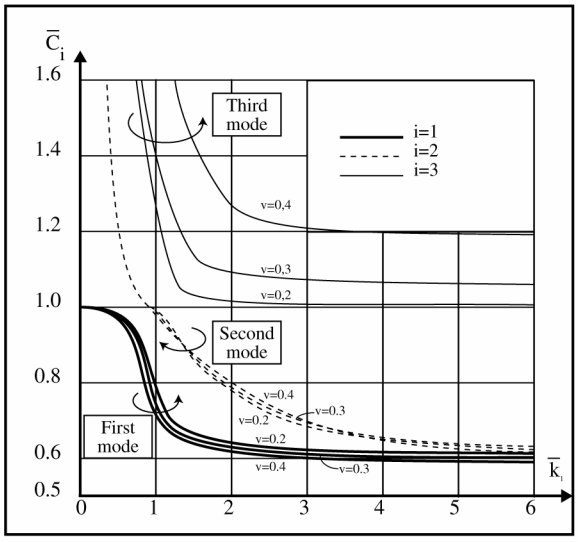

Figure 7.9. *Extensional wave dispersion in a rod with square section. Three elastodynamic modes are represented. For the first mode, dispersion phenomenon is not pronounced for the square section. The materials are isotropic*

7.7.2.2. *Combined influence of shear modulus and Poisson's number*

Poisson's number is not the only elastic constant we need to take into account when studying composite materials. In Figure 7.10 four composite materials are examined, the square section being adopted. The dispersion curves are different between one composite material and another. To understand this difference, it is worth examining the elastic constants of some composite materials, see Figure 7.11.

Note the small value of $\alpha^2 = G_{31}/E_3$ for composite materials. In the first column, the figure between brackets is the percentage of fiber in volume.

7.7.2.3. *Influence of rod flatness* $\delta = \dfrac{b}{h}$

Parameter δ is important in the trend of dispersion curves. Figure 7.12 shows the influence of rod flatness on the dispersion curve of a glass-epoxy composite. Flatness is an important parameter.

@Seismicisolation

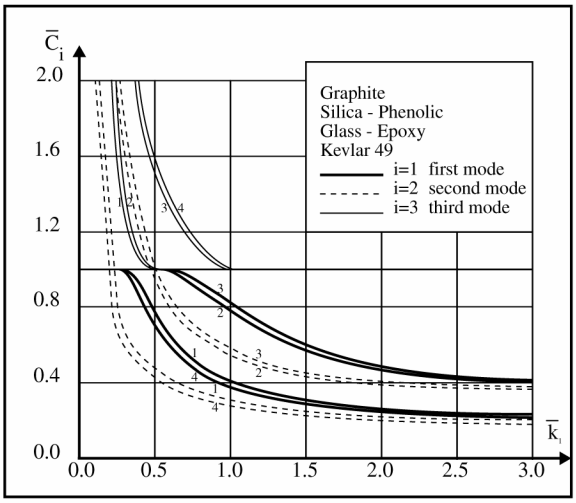

Figure 7.10. *Dispersion curves of different composite materials with square cross-section reduced extensional wave velocity* versus *reduced wave number* $\overline{k} = b/2\ k$

From a practical point of view, if an experimenter has a choice of latitude for the rod's cross-section in the evaluation of Young's modulus, it is better to adopt a square section for which the slope of the dispersion curve for small $\overline{k}$ is less pronounced, see Figure 7.10.

Even for isotropic material, the flatness parameter is important for the examination of an extensional wave, see Figure 7.11.

7.7.2.4. *Eigenvalue equation for a rod of finite length*

What is presented above concerns extensional wave dispersion in a rod of infinite length.

For a rod with finite length, we have to account for stationary waves and boundary conditions at both ends.

For ease, when further handling equations of motion and related boundary conditions it is convenient to adapt dimensionless equations by introducing rod length L.

@Seismicisolation

Material	E_3 (MPa)	G_{31} (MPa)	ν_{31}	ρ $\left(kg/m^3\right)$	C_L (m/s)	C_T (m/s)	α^2
Steel	210,000	81,000	0.3	7.8×10^3	5,100	3,225	0.385
Glass/ epoxy (60%)	45,000	5,000	0.12	1.86×10^3	4,918	1,652	0.111
Graphite/ epoxy (57%)	120,000	3,000	0.3058	1.43×10^3	9,169.5	1,448	0.025
Kevlar/ epoxy (60%)	87,800	20,000	0.204	1.34×10^3	8,085.5	3,858.6	0.227

Table 7.2. *Table of some materials and their elastic characteristics and two velocities, C_L and C_T*

The two principle spatial and temporal dimensionless variables are:

$$\eta = \frac{x_3}{L} \text{ and } \tau = \omega\, t \qquad [7.71]$$

The unknown function is $u_j^{(m,n)}$:

$$u_j^{(m,n)}\left(x_3, t\right) = \tilde{u}_j^{(m,n)}\left(\eta, \tau\right) \qquad [7.72]$$

As function $u_3^{(0,0)}$ is homogenous with a length, it is possible to write:

$$\tilde{u}_3^{(0,0)}\left(\eta, \tau\right) = L\, u_3^{*(0,0)}\left(\eta, \tau\right) \qquad [7.73]$$

Equations [7.58] become:

$$\frac{h^2}{4}\,\omega^2\,\frac{\partial^2\,\tilde{u}_1^{(1,0)}}{\partial\tau^2} = q^2\,\frac{h^2}{4}\,\frac{\chi_{44}^2}{L^2}\,\frac{\partial^2\tilde{u}_1^{(1,0)}}{\partial\eta^2}$$

@Seismicisolation

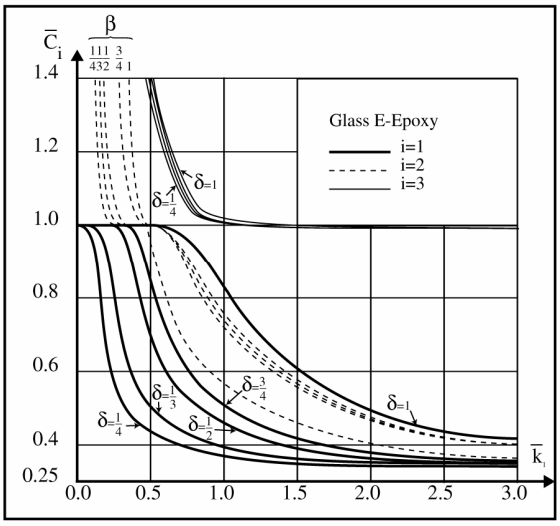

Figure 7.11. *Influence of flatness* $\delta = \frac{\text{thickness}}{\text{width}}$ *on the dispersion curves for a glass-epoxy composite.* $\bar{c}_L$ *is the reduced extensional wave velocity and* $\bar{k}$ *the reduced wave number*

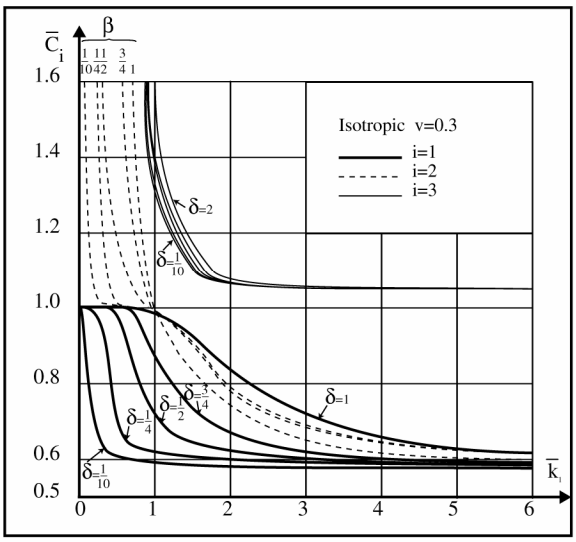

Figure 7.12. *Dispersion curves for an isotropic material with* $\gamma = 0.3$*. Three elastodynamic modes are presented for various values of flatness factor* $\delta = h/b$

@Seismicisolation

The two principle spatial and temporal dimensionless variables are:

$$\chi_{11}^2\ \tilde{u}_1^{(1,0)} - \chi_{12}^2 u_2^{(0,1)} - \chi_{13}^2 \frac{\partial u^{*(0,0)}}{\partial \eta}$$

$$\frac{b^2}{4}\ \omega^2\ \frac{\partial^2\ \tilde{u}_2^{(0,1)}}{\partial \tau^2} = q^2\ \frac{b^2}{4}\ \frac{\chi_{44}^2}{L^2}\ \frac{\partial^2 \tilde{u}^{(0,1)}_{\ 2}}{\partial \eta^2} - \chi_{11}^2\ \tilde{u}_2^{(0,1)} - \chi_{12}^2 u_1^{(1,0)} - \chi_{13}^2\ \frac{\partial u_3^{\ *(0,0)}}{\partial \eta}$$

$$L\omega^2 \frac{\partial^2\ u_3^{*(0,0)}}{\partial \tau^2} = \frac{1}{L}\left\{\chi_{33}^2 - \frac{4\ \chi_{13}^4}{3\left(\chi_{11}^2+\chi_{12}^2\right)}\right\}\frac{\partial^2 u_3^{*(0,0)}}{\partial \eta^2} + \frac{\chi_{13}^2}{3\ L}\left(\frac{\partial \tilde{u}_1^{(1,0)}}{\partial \eta} + \frac{\partial u_2^{(0,1)}}{\partial \eta}\right)$$

[7.74]

Dividing the above equations by $\frac{h^2}{4}$, $\frac{b^2}{4}$ and L respectively and multiplying the three equations member-by-member by $\frac{L^2}{\chi_{44}^2}$, the following additional dimensionless parameters are retained:

$$\alpha_1^2 = \frac{\chi_{11}^2}{\chi_{44}^2} = \frac{C_{11}}{C_{44}}$$

$$\alpha_2^2 = \frac{\chi_{12}^2}{\chi_{44}^2} = \frac{C_{12}}{C_{44}}$$

$$\alpha_3^2 = \frac{\chi_{33}^2}{\chi_{44}^2} = \frac{C_{33}}{C_{44}}$$

$$\alpha_4^2 = \frac{\chi_{13}^2}{\chi_{44}^2} = \frac{C_{13}}{C_{44}}$$

$$\gamma^2 = \frac{\omega^2\ L^2}{\chi_{44}^2} \qquad [7.75]$$

@Seismicisolation

and then:

$$\beta = \frac{h}{b}, \qquad \delta = \frac{L}{h}, \qquad \chi_{ij}^2 = \frac{C_{ij}}{\rho} \qquad [7.76]$$

In the third dimensionless equation of propagation [7.74], the coefficients of the second derivative with respect to space are written as follows:

$$\begin{aligned} \alpha'^2 &= \frac{1}{\chi_{44}^2}\left\{\chi_{33}^2 - \frac{4\,\chi_{13}^2}{3\left(\chi_{11}^2+\chi_{12}^2\right)}\right\} \\ &= \alpha_3^2 - \frac{4\,\alpha_4^4}{3\left(\alpha_1^2+\alpha_2^2\right)} \end{aligned} \qquad [7.77]$$

Finally, the dimensionless propagation equations are:

$$\gamma^2\,\frac{\partial^2 \tilde{u}_1^{(1,0)}}{\partial \tau^2} = q^2\,\frac{\partial^2 \tilde{u}_1^{(1,0)}}{\partial \eta^2} - \alpha_1^2\,\delta^2\,\tilde{u}_1^{(1,0)} - \alpha_2^2\,\delta^2\,\tilde{u}_2^{(0,1)} - \alpha_4^2\,\delta^2\,\frac{\partial u_3^{*(0,0)}}{\partial \eta}$$

$$\gamma^2\,\frac{\partial^2 \tilde{u}_2^{(0,1)}}{\partial \tau^2} = q^2\,\frac{\partial^2 \tilde{u}^{(0,1)}{}_2}{\partial \eta^2}\partial^2\,\tilde{u}_2^{(0,1)} - \alpha_1^2\,\beta^2\delta^2\,\tilde{u}_2^{(1,0)}$$

$$- \alpha_2^2\,\beta^2\delta^2\,\tilde{u}_1^{(1,0)} - \alpha_4^2\,\beta^2\,\delta^2\,\frac{\partial u_3^{*(0,0)}}{\partial \eta}$$

$$\gamma^2\,\frac{\partial^2 \tilde{u}_3^{*(0,0)}}{\partial \tau^2} = \alpha'^2\,\frac{\partial^2 u_3^{*(0,0)}}{\partial \eta^2} + \frac{\alpha_4^2}{3}\left(\frac{\partial \tilde{u}_1^{(1,0)}}{\partial \eta} + \frac{\partial \tilde{u}_2^{(0,1)}}{\partial \eta}\right) \qquad [7.78]$$

7.7.2.5. *Solutions of propagation equations*

By separation of variables, solutions of the partial differential equations [7.78] are to be found:

@Seismicisolation

$$\tilde{u}^{(m,n)}\ (\eta,\tau) = e^{j\tau}\ \tilde{U}_j^{(m,n)}\ (\eta) \qquad [7.79]$$

$$u^{*(0,0)}\ (\eta,\tau) = e^{j\tau}\ U_3^{*(0,0)}\ (\eta)$$

where $\tilde{U}_j$ and U_3^* are normal undetermined functions of the solution. Those functions satisfy the differential system:

$$q^2\ \frac{d^2\tilde{U}_1^{(1,0)}}{d\eta^2} + \left(\gamma^2 - \alpha_1^2\ \delta^2\right)\ U_1^{(1,0)} - \alpha_2^2\ \delta^2\ \tilde{U}_2^{(0,1)} - \alpha_4^2\ \delta^2\ \frac{dU_3^{*(0,0)}}{d\eta} = 0$$

$$q^2\ \frac{d^2\tilde{U}_2^{(0,1)}}{d\eta^2} + \left(\gamma^2 - \alpha_1^2\ \delta^2\ \beta^2\right)\ U_2^{(0,1)} - \alpha_2^2\ \beta^2\delta^2\ \tilde{U}_1^{(1,0)} - \alpha_4^2\ \beta^2\delta^2\ \frac{dU_3^{*(0,0)}}{d\eta} = 0$$

$$\alpha'^2\ \frac{d^2U_3^{*(0,0)}}{d\eta^2} + \gamma^2\ U_3^{*(0,0)} + \frac{\alpha_4^2}{3}\left\{\frac{dU_1^{(1,0)}}{d\eta} + \frac{dU_2^{(0,1)}}{d\eta}\right\} = 0 \qquad [7.80]$$

This differential system is linear, with constant coefficients.

Normal functions are used under the form:

$$\tilde{U}^{(m,n)}\ (\eta) = A_j\ e^{sn}\ \ j \in \{1,2\}$$

$$U_3^{*(0,0)}\ (\eta) = A_3\ e^{sn} \qquad [7.81]$$

where s can be real or complex.

Eigenvectors corresponding to eigenvalue s_i constitute a basis of vectorial space C^6 to which the solutions belong.

Eigenvalue s_j is obtained by setting the determinant formed by coefficients A_j of the linear algebraic system to zero.

@Seismicisolation

$$q^4\ \alpha'^2\ s^6 + q^2 \left\{ \left(2\ \alpha'^2 + q^2\right)\ \gamma^2 + \left(-\alpha_1^2\ \alpha'^2 + \frac{\alpha_4^3}{3}\right)\ \left(1+\beta^2\right)\ \delta^2 \right\} s^4$$

$$+ \left\{ \begin{array}{l} \left(2\ q^2 + \alpha'^2\right)\ \gamma^4 + \left[\frac{\alpha_4^4}{3} - \alpha_2^1\ \left(\alpha'^2 + q^2\right)\right]\ \left(1+\beta^2\right)\ \delta^2\ \gamma^2 \\ \\ + \left(\alpha_2^2 - \alpha_1^2\right)\ \left[\frac{2\ \alpha_4^4}{3} - \left(\alpha_1^2 + \alpha_2^2\right)\ \alpha'^2\right]\ \beta^2\ \delta^4 \end{array} \right\} s^2 \qquad [7.82]$$

$$+ \gamma^2\ \left(\left\{\gamma^4 - \alpha_1^2\ \left(1+\beta^2\right)\ \delta^2\ \gamma^2 + \left(\alpha_1^4 - \alpha_2^4\right)\ \beta^2\ \delta^4\ \right\}\right) = 0$$

This bisquared sixth-order equation has real coefficients. If this equation has an imaginary root, it has the conjugate imaginary root of this imaginary root, with the same multiplicity.

With the following notations:

$$d_1 = \left(\frac{1}{\alpha'^2} + \frac{2}{q^2}\right)\ \gamma^2 + \left(\frac{\alpha_4^4}{3\ \alpha'^2} - \alpha_1^2\right)\frac{\delta^2}{q^2}\ \left(1+\beta^2\right)$$

$$d_2 = \left(\frac{2}{\alpha'^2} + \frac{1}{q^2}\right)\ \frac{\gamma^4}{q^2} + \left\{\frac{\alpha_4^4}{3\ \alpha'^2\ q^2} - \alpha_1^2\ \left(\frac{1}{q^2} + \frac{1}{\alpha'^2}\right)\right\} \bullet \left(\frac{1+\beta^2}{q^2}\right)\ \delta^2\ \gamma^2$$

$$+ \left\{\frac{2\ \alpha_4^4}{3\ \alpha'^2} - \left(\alpha_1^2 + \alpha_2^2\right)\right\}\ \left(\alpha_2^2 - \alpha_1^2\right)\ \frac{\beta^2\ \delta^4}{q^4}$$

$$d_3 = \frac{\gamma^2}{q^4\ \alpha'^2}\ \left\{\gamma^4 - \alpha_1^2\ \delta^2\ \left(1+\beta^2\right)\ \gamma^2 + \left(\alpha_1^4 - \alpha_2^4\right)\ \beta^2\ \delta^4\right\}$$

$$s^2 = S' \qquad [7.83]$$

@Seismicisolation

by forming the following expression:

$$R' = \left[\frac{1}{3}\left(d_2 - \frac{d_1^2}{3}\right)\right]^3 + \left[\left(\frac{d_1}{3}\right)^3 - \frac{d_1\, d_2}{6} + \frac{d_3}{2}\right]^2 \qquad [7.84]$$

The equation in S′:

$$S'^3 + d_1\, S'^2 + d_2\, S' + d_3 = 0 \qquad [7.85]$$

is the contracted form of equation [7.78]. It admits real roots.

$$S_1' = 2\left\{-\frac{1}{3}\left(d_2 - \frac{d_1^3}{3}\right)\right\}^{1/2} \cos\frac{1}{3}\,\text{Arc}\cos\left\{\frac{\frac{d_1\, d_2}{3} - d_3 - \frac{d_1^3}{27}}{2\left[-\frac{1}{27}\left(d_2 - \frac{d_1^2}{3}\right)\right]^{1/2}}\right\} - \frac{d_3}{3}$$

$$S_2' = 2\left\{-\frac{1}{3}\left(d_2 - \frac{d_1^3}{3}\right)\right\}^{1/2} \cos\frac{1}{3}\left[\text{Arc}\cos\left\{\frac{\frac{d_1\, d_2}{3} - d_3 - \frac{d_1^3}{27}}{2\left[-\frac{1}{27}\left(d_2 - \frac{d_1^2}{3}\right)\right]^{1/2}}\right\} + 4\pi\right] - \frac{d_3}{3}$$

$$S_3' = 2\left\{-\frac{1}{3}\left(d_2 - \frac{d_1^3}{3}\right)\right\}^{1/2} \cos\frac{1}{3}\left[\text{Arc}\cos\left\{\frac{\frac{d_1\, d_2}{3} - d_3 - \frac{d_1^3}{27}}{2\left[-\frac{1}{27}\left(d_2 - \frac{d_1^2}{3}\right)\right]^{1/2}}\right\} + 2\pi\right] - \frac{d_3}{3}$$

[7.86]

Let us point out that in equation [7.86] the solutions S'_1, S'_2 and S'_3 are similar and differ only in $\left[\text{Arc}\cos[\quad] + \text{angle } 4\pi \text{ or } 2\pi\right]$ for the two last equations.

REMARKS ON THE SOLUTIONS TO EQUATION [7.85] – These solutions depend on the coefficients in equation [7.85] d_j, where $d_j = d_j\,(\gamma)$.

@Seismicisolation

$$0 < \gamma < \gamma_1 : d_1 < 0, \quad d_2 > 0, \quad d'_3 > 0$$

$$\gamma_1 < \gamma < \gamma_2 : d_1 < 0, \quad d_2 > 0, \quad d'_3 > 0$$

$$\gamma_2 < \gamma < \gamma_3 : d_1 < 0, \quad d_2 > 0, \quad d'_3 < 0$$

$$\gamma_3 < \gamma < \gamma_4 : d_1 > 0, \quad d_2 < 0, \quad d'_3 < 0 \qquad [7.87]$$

$$\gamma_4 < \gamma < \gamma_5 : d_1 > 0, \quad d_2 > 0, \quad d'_3 < 0$$

$$\gamma < \gamma_5 \qquad d_1 > 0 \qquad d_2 > 0 \qquad d'_3 > 0$$

with:

$$d'_3 = \frac{q^4 \ \alpha'^2}{\gamma^2} \bullet d_3$$

whereas γ_j, $1 \leq j \leq 5$ are positive roots of the three equations [7.83]:

$$d_1 \ (\gamma) = 0$$

$$d_2 \ (\gamma) = 0 \qquad [7.88]$$

$$d'_3 \ (\gamma) = 0$$

Relationships between coefficients d_j (γ) and roots S'_j enable us to obtain indications concerning the solutions to equations [7.82].

For practical cases, the following inequality is adopted:

$$d'_3 > 0 \qquad [7.89]$$

Only one root S′ is negative $(S'_3 < 0)$ and only if:

@Seismicisolation

$$d'_3 < 0$$

where two roots S′ are negative (S'_2 and S'_3).

So, when a root $S'_j < 0$, there are two imaginary conjugated roots for equation [7.82]:

$$s_j = \pm\, j\sqrt{\left|S'_j\right|} \qquad [7.90]$$

Roots s_j being distinct, general solution of the differential system will be:

$$\hat{U}_j^{(m,n)}(\eta) = \sum_{p=1}^{6} A_{jp}\, e^{s}\, p^{\eta} \qquad [7.91]$$

with:

$$\hat{U}_j = \tilde{U}_j \text{ or } U^*_j \text{ and } j \in \{1, 2, 3\}$$

This solution uses 18 arbitrary constants that are not independent. The differential system [7.82] furnishes the 12 following relationships:

$$A_{2p} = \frac{\dfrac{q^2\, s_p^2}{\delta^2} + \dfrac{a_4^4\, s_p^2}{3\left(\alpha'^2\, s_p^2 + \gamma^2\right)} + \dfrac{\gamma^2}{\delta^2} - \alpha_1^2}{\alpha_2^2 - \dfrac{\alpha_4^4\, s_p^2}{3\left(\alpha'^2\, s_p^2 + \gamma^2\right)}}\, A_{1p} \qquad [7.92]$$

and:

$$A_{3p} = -\frac{\alpha_4^2\, s_p}{3\left(\alpha'^2\, s_p^2 + \gamma^2\right)} \left\{1 + \frac{\dfrac{q^2\, s_p^2}{\delta^2} + \dfrac{\alpha_4^4\, s_p^2}{3\left(\alpha'^2\, s_p^2 + \gamma^2\right)} + \dfrac{\gamma^2}{\delta^2} - \alpha_1^2}{\alpha_2^2 - \dfrac{\alpha_4^4\, s_p^2}{3\left(\alpha'^2\, s_p^2 + \gamma^2\right)}}\right\} A_{1p} \qquad [7.93]$$

@Seismicisolation

The following calculations will be simplified with:

$$A_{2p} = \bar{K}'_p \; A_{1p} \qquad [7.94]$$

$$A_{3p} = \bar{K}'_p \; A_{1p}$$

There is no summation on the repeated indexes, A_{1p} being independent constants. The general solution to equation [7.92] is written in the form:

$$\tilde{U}_1^{(1,0)} = \sum_{p=1}^{6} A_{1p} \; e^{s_p \eta} \qquad [7.95]$$

$$\tilde{U}_2^{(0,1)} = \sum_{p=1}^{6} \bar{K}'_p \, A_{1p} \; e^{s_p \eta} \qquad [7.96]$$

$$U^{*(0,0)}_3 = \sum_{p=1}^{6} \bar{K}''_p A_{1p} \; e^{s_p \eta} \qquad [7.97]$$

7.7.3. *Natural boundary conditions*

Natural boundary conditions are obtained from functional J in equation [7.57].

The stationarity of this functional is satisfied for all variations of:

$$\delta \, u_j^{(m,n)} \left(P_j \, , t\right)$$

The boundary conditions are obtained by integration of the equation by parts. Six equations are obtained, see Appendix 7.F.

$$\rho_j \left(\frac{\partial^2 \, u_1^{(1,0)}}{\partial \, t^2} \right)_{P_j} = \varepsilon \, q^2 \, C_{44} \left(\frac{\partial \, u_1^{(1,0)}}{\partial \, x_3} \right)_{P_j}$$

@Seismicisolation

$$\rho_j \left(\frac{\partial^2 u_2^{(0,1)}}{\partial t^2} \right)_{P_j} = \varepsilon\, q^2\, C_{44} \left(\frac{\partial u_2^{(0,1)}}{\partial x_3} \right)_{P_j} \qquad [7.98]$$

$$\rho_j \left(\frac{\partial^2 u_3^{(0,0)}}{\partial t^2} \right)_{P_j} = \varepsilon \frac{C_{13}}{3} \left(u_1^{(1,0)} + u_2^{(0,1)} \right)_{P_j} + \varepsilon \left\{ C_{33} - \frac{4\, C_{13}^2}{3\, (C_{11} + C_{12})} \right\} \left(\frac{\partial u_3^{(0,0)}}{\partial x_3} \right)_{P_j}$$

with $j \in \{1,2\}$ and $\varepsilon = 1$ if $j = 1$, $\varepsilon = -1$ if $j = 2$.

7.7.4. *Various types of solutions for the equations of motion*

The equations in [7.76] are solved and give rise to a sixth-order equation in s. The closed-form expressions for the three components of displacement deserve discussion.

7.7.4.1. *First case*

S'_3 in equation [7.85] is real and negative, the two remaining roots S'_1 and S'_2 being positive.

$$S'_1 = X^2, \qquad S'_2 = Y^2, \qquad S'_3 = -Z^2 \qquad [7.99]$$

Displacement solutions are:

$$\tilde{U}_1'^{(1,0)} = A_1 \cos h\, X\, \eta + A_2 \sin h\, X\, \eta + A_3 \cos h\, Y\, \eta + A_4 \sin h\, Y\, \eta + A_5 \cos Z\, \eta + A_6 \sin Z\, \eta$$

$$\tilde{U}_2'^{(0,1)} = B_1 \cos h\, X\, \eta + B_2 \sin h\, X\, \eta + B_3 \cos h\, Y\, \eta + B_4 \sin h\, Y\, \eta + B_5 \cos Z\, \eta + B_6 \sin Z\, \eta$$

$$\tilde{U}_3'^{(0,0)} = C_1 \cos h\, X\, \eta + C_2 \sin h\, X\, \eta + C_3 \cos h\, Y\, \eta + C_4 \sin h\, Y\, \eta + C_5 \cos Z\, \eta + C_6 \sin Z\, \eta \qquad [7.100]$$

@Seismicisolation

There are 18 coefficients to determine. Fortunately, examination of equations [7.75] enables us to ascertain that, for all possible values of η, the following relationships between coefficients A_j, B_j and C_j are:

$$\begin{aligned} B_1 &= M_1\ A_1 \\ B_2 &= M_2\ A_2 \\ B_3 &= M_3\ A_3 \\ B_4 &= M_4\ A_4 \\ B_5 &= M_5\ A_5 \\ B_6 &= M_6\ A_6 \end{aligned} \qquad [7.101]$$

with:

$$M_1 = \frac{q^2\ X^2 + \gamma^2 - \alpha_1^2\ \delta^2 + \dfrac{\alpha_4^4\ \delta^2\ X^2}{3\left(\alpha'^2\ X^2 + \gamma^2\right)}}{\delta^2\left\{\alpha_2^2 - \dfrac{\alpha_4^4\ X^2}{3\left(\alpha'^2\ X^2 + \gamma^2\right)}\right\}}$$

$$M_2 = \frac{-q^2\ Z^2 + \gamma^2 - \alpha_1^2\ \delta^2 - \dfrac{\alpha_4^4\ \delta^2\ X^2}{3\left(-\alpha'^2\ Z^2 + \gamma^2\right)}}{\delta^2\left\{\alpha_2^2 + \dfrac{\alpha_4^4\ Z^2}{3\left(-\alpha'^2\ Z^2 + \gamma^2\right)}\right\}}$$

$$M_3 = \frac{-q^2\ Z^2 + \gamma^2 - \alpha_1^2\ \delta^2 - \dfrac{\alpha_4^4\ \delta^2\ Z^2}{3\left(-\alpha'^2\ Z^2 + \gamma^2\right)}}{\delta^2\left\{\alpha_2^2 + \dfrac{\alpha_4^4\ Z^2}{3\left(-\alpha'^2\ Z^2 + \gamma^2\right)}\right\}}$$

@Seismicisolation

Similar equations can be obtained for C_j and A_j:

$$C_1 = -K_1 \left(1 + M_1\right) A_2$$

$$C_2 = -K_1 \left(1 + M_1\right) A_1$$

$$C_3 = -K_2 \left(1 + M_2\right) A_4$$

$$C_4 = -K_2 \left(1 + M_2\right) A_3$$

$$C_5 = -K_3 \left(1 + M_3\right) A_6$$

$$C_6 = K_3 \left(1 + M_3\right) A_5$$

with:

$$K_1 = \frac{\alpha_4^2 X}{3\left(\alpha'^2 X^2 + \gamma^2\right)}$$

$$K_2 = \frac{\alpha_4^2 Y}{3\left(\alpha'^2 Y^2 + \gamma^2\right)}$$

$$K_3 = \frac{\alpha_4^2 Z}{3\left(-\alpha'^2 Z^2 + \gamma^2\right)}$$

7.7.4.2. *Second case*

Two roots S'_2 and S'_3 in equation [7.85] are real and negative, root S'_j being real and positive.

$$S'_1 = X^2, \qquad S'_2 = -Y^2, \qquad S'_3 = -Z^2 \qquad [7.102]$$

Closed-form expressions for displacement components are:

@Seismicisolation

$$\tilde{U}_1^{(1,0)} = A'_1 \cos h\, X\, \eta + A'_2 \sin h\, X\, \eta + A'_3 \cos Y\, \eta + A'_4 \sin Y\, \eta + A'_5 \cos Z\, \eta + A'_6 \sin Z\, \eta$$

$$\tilde{U}_2^{(0,1)} = B'_1 \cos h\, X\, \eta + B'_2 \sin h\, X\, \eta + B'_3 \cos Y\, \eta + B'_4 \sin Y\, \eta + B'_5 \cos Z\, \eta + B'_6 \sin Z\, \eta$$

$$\tilde{U}_3^{(0,0)} = C'_1 \cos h\, X\, \eta + C'_2 \sin h\, X\, \eta + C'_3 \cos Y\, \eta + C'_4 \sin Y\, \eta + C'_5 \cos Z\, \eta + C'_6 \sin Z\, \eta \qquad [7.103]$$

A'_j, B'_j and C'_j are arbitrary constants that are not independent.

As above, the relationship between them can be established:

$$B'_j = A_j\, M'_i \text{ with } I = 1, 2, 3\ ;\ j = \{1, ..., 6\}$$

$$M'_1 = M_1$$

$$M'_3 = M_3 \qquad [7.104]$$

Constants C'_j are written as:

$$\begin{aligned} C'_1 &= -K'_1\ (1 + M'_1)\ A'_2 \\ C'_2 &= -K'_1\ (1 + M'_1)\ A'_1 \\ C'_3 &= -K'_2\ (1 + M'_2)\ A'_4 \\ C'_4 &= K'_2\ (1 + M'_2)\ A'_3 \\ C'_5 &= -K'_3\ (1 + M'_3)\ A'_6 \\ C'_6 &= K'_3\ (1 + M'_3)\ A'_5 \end{aligned} \qquad [7.105a]$$

@Seismicisolation

with:

$$K'_1 = K_1, \quad K'_3 = K_3, \quad K'_2 = \frac{\alpha_4^2\ Y}{3\left(-\alpha'^2\ Y^2 + \gamma^2\right)} \qquad [7.105b]$$

7.7.4.3. *Eigenvalue equations and solutions*

Eigenvalue equations are obtained by bringing the two types of solutions for displacement components [7.100] or [7.102] obtained above, into boundary condition equations [7.98].

7.7.4.4. *Dimensionless eigenvalues equations*

Using reduced variables for displacement components (equations [7.71], [7.72] and [7.73]) the following dimensionless equations are obtained:

$$\rho_j\ \omega^2\ \frac{\partial^2\ \tilde{u}_1^{(0)}}{\partial\ t^2} = \varepsilon\ q^2\ \frac{C_{44}}{L}\ \frac{\partial\ \tilde{u}_1^{(1,0)}}{\partial\ \eta}$$

$$\rho_j\ \omega^2\ \frac{\partial^2\ \tilde{u}_2^{(0,1)}}{\partial\ t^2} = \varepsilon\ q^2\ \frac{C_{44}}{L}\ \frac{\partial\ \tilde{u}_2^{(0,1)}}{\partial\ \eta}$$

$$\rho_j\omega^2 L\frac{\partial^2\ u_3^{*(0,0)}}{\partial\ t^2} = \varepsilon\frac{C_{13}}{3}\left(\tilde{u}_1^{(1,0)}+\tilde{u}_2^{(0,1)}\right)+\varepsilon\left\{C_{33}-\frac{4\ C_{13}^2}{3\ \left(C_{11}+C_{12}\right)}\right\}\bullet\frac{\partial u_3^{*(0;0)}}{\partial\eta} \qquad [7.106]$$

$$j \in \{1, 2\}\ \varepsilon = 1 \text{ if } j = 1;\ \ \varepsilon = -1 \text{ if } j = 2, \quad \eta = 0 \text{ if } j = 1,\ \eta = 1 \text{ if } j = 2$$

The first, second, fourth and fifth equations of [7.106] are multiplied member-by-member by:

$$\frac{S\ L^2}{M}$$

whereas the third and sixth equations are multiplied by:

@Seismicisolation

$$\frac{S\,L}{M}$$

with $M = \rho\, S\, L$ [7.107]

$$\bar{m}_i = \frac{m_i}{M}$$

where m_i is additional mass at the end, and M is the rod mass.

Dividing all of the transformed equation members by χ_{44}^2 and using dimensionless notations [7.71], the six boundary equations are:

$$\bar{m}_j\, \gamma^2\, \frac{\partial^2\, \tilde{u}_1}{\partial \tau^2} - \varepsilon\, q^2\, \frac{\partial\, \tilde{u}_1}{\partial\, \eta} = 0$$

$$\bar{m}_j\, \gamma^2\, \frac{\partial^2\, \tilde{u}_1}{\partial \tau^2} - \varepsilon\, q^2\, \frac{\partial\, \tilde{u}_2}{\partial\, \eta} = 0$$

$$\bar{m}_j\, \gamma^2\, \frac{\partial^2\, \tilde{u}_3^*}{\partial \tau^2} - \varepsilon\, \frac{\alpha_4^2}{3}\, \left(\tilde{u}_1 + \tilde{u}_2\right) - \varepsilon\, \alpha'^2\, \frac{\partial u^*_3}{\partial\, \eta} = 0 \qquad [7.108]$$

$j \in \{1, 2\}$, $\varepsilon = 1$ if $j = 1$ and $\eta = 0$

$\varepsilon = -1$ if $j = 2$ and $\eta = 1$

REMARKS – If $\bar{m}_1 = \bar{m}_2 = 0$ both ends and the lateral surface are free.

The solutions for the equations in [7.106] are similar to those adopted for propagation equations [7.95]–[7.97].

$$\sum_{p=1}^{6} \left(\bar{m}_1\, \gamma^2 + q^2\, s_p\right) A_{1p} = 0$$

@Seismicisolation

$$\sum_{p=1}^{6} \left(\bar{m}_1\ \gamma^2 + q^2\ s_p\right) \bar{K}'_p\ A_{1p} = 0$$

$$\sum_{p=1}^{6} \left\{\frac{\alpha_4^2}{3}\ \left(1 + \bar{K}'_p\right) + \left(\bar{m}_1\ \gamma^2 + \alpha'^2\ s_p\right) \bar{K}''_p\right\} A_{1p} = 0$$

$$\sum_{p=1}^{6} \left(-\bar{m}_2\ \gamma^2 + q^2\ s_p\right) e^{s_p}\ A_{1p} = 0$$

$$\sum_{p=1}^{6} \left(-\bar{m}_2\ \gamma^2 + q^2\ s_p\right) \bar{K}'_p\ e^{s_p} A_{1p} = 0$$

$$\sum_{p=1}^{6} \left\{\frac{\alpha_4^2}{3}\ \left(1 + K'_p\right) + \left(-\bar{m}_2\ \gamma^2 + \alpha'^2\ s_p\right) \bar{K}''_p\right\} e^{s_p} A_{1p} = 0 \qquad [7.109]$$

The eigenvalue equation is then:

$$\text{Det}\ [M] = 0 \qquad [7.110]$$

where [M] is the square matrix with coefficients A_{1p} of the system [7.109]. The coefficients of [M] are:

$$M_{1j} = \bar{m}_1\ \gamma^2 + q^2\ s_j$$

$$M_{2j} = \left(\bar{m}_1\ \gamma^2 + q^2\ s_j\right) K'_j \qquad [7.111]$$

$$M_{3j} = \frac{\alpha_4^2}{3}\ \left(1 + \bar{K}_j\right) + \left(\bar{m}_1\ \gamma^2 + s'^2\ s_j\right) \bar{K}''_j$$

$$M_{4j} = \left(-\bar{m}_2\ \gamma^2 + q^2\ s_j\right) e^{s_j}$$

@Seismicisolation

$$M_{5j} = \left(-\bar{m}_2\ \gamma^2 + q^2\ s_j\right)\ \bar{K}'_j\ e^{s_j}$$

$$M_{6j} = \left\{\frac{\alpha_4^2}{3}\ \left(1 + \bar{K}'_j\right) + \left(-\bar{m}_2\ \gamma^2 + \alpha'\ s_j\right)\ \bar{K}''_j\right\}\ e^{s_j} \qquad [7.111\ \text{cont}]$$

with $j \in \{1, 2, 4, 5, 6\}$

$$\gamma = \gamma\ (\omega), \quad s_j = s_j\ (\omega), \quad \bar{K}'_j = \bar{K}'_j\ (\omega), \quad \bar{K}''_j = \bar{K}''_j(\omega)$$

where ω circular frequency is the unknown when the other rod characteristics are known.

Appendix 7.G presents details on the solutions of eigenvalue equations with different possible cases.

7.8. Short rod and boundary conditions

In the case of a short rod, the influence of boundary conditions is predominant. Some simplifying assumptions concerning the weight of rod which is larger than the additional weights at the free ends is not valid.

Let us find two closed-form expressions for eigenvalues in the two cases:

– elementary theory;

– Touratier's theory.

Their comparison and confrontation with experiments are interesting. It is difficult to use wave number, as for a long rod. It is more appropriate to derive eigenvalue equations.

7.8.1. *Elementary theory*

Using equations [7.7] and [7.10], variable separation is adopted:

$$w\ (z\ ,\ t) = F\ (z)\ G(t) \qquad [7.112]$$

@Seismicisolation

Bringing in equation [7.10]:

$$\frac{1}{C_3^2}\frac{\partial^2 w}{\partial t^2} = \frac{\partial^2 w}{\partial z^2} \text{ with } C_3 = \sqrt{\frac{E_z}{\rho}}$$

$$\frac{1}{C_3^2}\frac{\ddot{G}}{G} = \frac{F_{zz}}{F} \qquad [7.113]$$

$$w(z,t) = \sum_{n=1}^{\infty}\left(A_n \cos\frac{\omega_n}{c_3} z + B_n \sin\frac{\omega_n}{c_3} z\right)\left(C_n \cos\omega_n t + D_n \sin\omega_n t\right) \qquad [7.114]$$

7.8.2. *Boundary conditions*

Two masses m_1 and m_2 respectively are attached at the free ends. The stress vector at z = 0 is:

$$\vec{T}\left(P, -\vec{z}\right) = -\sigma_{zz}\left(0,t\right)\vec{z}_2 \qquad [7.115]$$

At z = 0 the boundary condition is:

$$m_1 \frac{\partial^2 w(0,t)}{\partial t^2} = ES\frac{\partial w(0,t)}{\partial z} \qquad [7.116]$$

At z = L:

$$m_2 \frac{\partial^2 w(L,t)}{\partial t^2} = ES\frac{\partial w(L,t)}{\partial z} \qquad [7.117]$$

Bringing [7.116] into [7.115]:

$$B_n = -\frac{m_1 C_z \omega_n}{SE} A_n \qquad [7.118]$$

@Seismicisolation

Equations [7.114], [7.118] and [7.117] give the eigenvalue equation:

$$\operatorname{tg} \frac{\omega_n L}{C_3} = \frac{\left(m_1 + m_2\right) \dfrac{\omega_n L}{C_3}}{\dfrac{m_1 m_2}{M} \left(\dfrac{\omega_n L}{C_3}\right)^2 - M} \qquad [7.119]$$

Letting:

$$\gamma'_n = \frac{\omega_n L}{C_3}, \qquad \bar{m}_i = \frac{m_i}{M} \qquad [7.120]$$

where $M = \rho S L$ is the rod weight, then finally equation [7.119] is rewritten as:

$$\operatorname{tg} \gamma'_n = \frac{\left(\bar{m}_1 + \bar{m}_2\right) \gamma'_n}{\bar{m}_1 \bar{m}_2 \gamma'^2_n - 1}$$

7.9. Concluding remarks about Touratier's theory

Dimensionless eigenvalues are calculated *versus* the geometrical and elastic characteristics of the rod. As the equations are more complex to handle, programs with iterative calculations must be devised in the following order:

– eigenvalue equations [7.76] are taken into account as well as the evaluation of eigenvalues [7.86];

– examination of the signs of coefficients $d'_3\ (\gamma)$ that determine the type of differential equation [7.76];

– calculation of eigenvalues γ by means of equation [7.G.3] or equation [7.G.5] in Appendix 7.G, depending on the sign of $d'_3\ (\gamma)$.

On numerical computation grounds, eigenvalues γ are evaluated by searching the pivot for the column of matrix determinants [P] and [Q] of components P_{ij} and Q_{ij}, see equations [7.G.4] and [7.G.7] of Appendix 7.G.

Jordan-Gauss reduction method is applied here.

@Seismicisolation

– extension of Volterra's theory, which is valid for isotropic and ansitropic materials by Touratier seems to be compatible with Pochhammer's theory;

– dispersion phenomenon is correctly described, at least for the first three elastodynamic modes. It is inherent to the sixth-order decoupled equation of motion. For a higher elastodynamic mode, a more elaborate theory using Reisner's variational principle is referred to[5].

7.10. Bibliography

[BIS 52] BISHOP R. E. D., "Longitudinal waves in beams", *Aeronaut Quarterly*, vol. 3, p.280, 1952.

[CHA 76] CHADWICK P., "The existence of pure surface modes in elastic materials with orthorhombic symmetry", *Journal of Sound and Vibration*, vol. 47, no. 1, p.39-52, 1976.

[CHE 10] CHEVALIER Y., VINH J. V., *Mechanical Characterization of Materials and Wave Dispersion*, ISTE, London , John Wiley, New York (in press).

[CHR 1889] CHREE C., "The equations of an isotropic elastic solid in polar and cylindrical coordinates their solutions and applications", *Trans Camb Phil Soc Math Phys*, vol. 14, p 250, 1889.

[FRA 69] FRASER W. B., "Stress wave propagation in rectangular bars", *International Journal of Solids and Structures*, vol.10, p. 63-73, 1969.

[HER 50] HERMANN G. A., MINDLIN R. D., "One dimensional theory of compressional wave in elastic rods", *Proc. 1st US National Congress Applied Mechanics*, p. 187-191, 1950.

[HET 68] HETERLENDY P., "An approximate theory governing symmetric motions of elastic rods of rectangular or square section cross section", *Journal of Applied Mechanics*, vol. 13, series E, no. 2, p. 333-341.

[KYN 57] KYNCH G. J., GREEN W.A., "Vibrations of beams – I – longitudinal modes", *Quarterly Journal of Mechanics and Applied Mathematics*, vol.10, p. 63-73, 1957.

[LOV44] LOVE A. E., *A Treatise on the Mathematical of Elasticity*, Dover Publications, New York, Re-edition, 1944.

[MED 66] MEDICK M. A., "One dimensional theory of propagation and vibration in elastic bars of rectangular cross section", *Journal of Applied Mechanics*, p. 489-495, 1966.

[MIN 60] MINDLIN R. D., NIVEN H. D. Mc, "Axially symmetric waves in elastic rods", *Journal of Applied Mechanics,* vol. 27, p. 145-151, 1960.

[MIN 66] MINEUR H., *Techniques de Calcul Numérique*, Dunod Editor, Paris, 1966.

5 See *Mechanical Characterization of Materials and Wave Dispersion* by the same authors.

@Seismicisolation

[MOR 50] MORSE R. W., "The velocity of compressional waves in rods of rectangular cross-section", *Journal of the Acoustic Society of America*, vol. 22, p. 219, 1950.

[NIG 68] NIGRO N. J., "Wave propagation in anisotropic bars of rectangular cross section", *Journal of the Acoustic Society of America*, vol. 43, no. 5, p. 958, 1968.

[POC 1876] POCHHAMMER L., "Über die Fortpflanzungsgeschwindigkeiten kleiner Schwingungen in einem übergrenzten isotropen Kreiszylinder", *J. Rein. Angew. Math.*, vol. 81, p. 324-336, 1876.

[RAO 74] RAO D. K, RAO J. S., "Free and forced vibrations of rod according to Bishop's theory", *Journal of the Acoustic Society of America*, vol. 56, no. 6, p. 1792-1800, 1974.

[RAY 45] RAYLEIGH J. W. S., *The Theory of Sound, vol. I and vol. II*, Dover Publications, New York, 1945.

[ROS 74] ROSENFELD G., KELLER J. B., "Wave propagation in elastic rods of arbitrary cross section", *Journal of the Acoustic Society of America*, vol. 55, no. 3, p. 555, 1974.

[TOU 77] TOURATIER M., On the propagation of longitudinal waves on rectangular composite rods. (Rayleigh waves, wave dispersion), Report of final studies to obtain engineer degree, Conservatoire National des arts et Métiers, Paris, 1977.

[TOU 79] TOURATIER M., About the wave propagation in transverse isotropic rod with rectangular cross-section (Utilization of Hellinger-Reissner's variational principle – Theoretical and experimental studies at higher modes), PhD thesis, University of Paris VI, 1979.

[VIK 67] VIKTOROV I. A., *Rayleigh and Lamb Waves,* Plenum Press, New York, 1967.

[VIN 80] VINH T., CHEVALIER Y., GARCEAU P., *Final Reports of Industrial Aerospace Contract*, I.S.C.M. Saint Ouen, France, 1980.

[VOL 55] VOLTERRA E., "A one dimensional theory of wave propagation in elastic rod based in the method of internal constraints", *Ing. Archi. Belin*, vol. 23, p. 410, 1955.

[VOL 65] VOLTERRA E., ZACHMANOGLOU E. C., *Dynamics of Vibrations*, Charles Merril, Columbus, Ohio, p. 551-554, 1965.

7.11. List of symbols

Latin alphabet

b	rod width
c	phase velocity
c_L	longitudinal wave velocity

@Seismicisolation

c_R	Rayleigh wave velocity
$\bar{c}_R$	dimensionless Rayleigh velocity
C_T	shear wave velocity
E, E_i	Young's modulus
F_i	components of surface force
G, G_i	shear modulus (subscripts concern anisotropic materials)
h	rod thickness
I, I_2	quadratic moment of the cross-section
$\tilde{J}$	Hamilton's functionals
k, $\bar{k}$	wave number, reduced wave number $\left(\bar{k} = \frac{2\pi b}{\Lambda}\right)$
L	rod length
M	rod mass
q (C_{ijkl})	correcting coefficient (equation [7.56])
R	radius of the circular section of a rod
r_p	radius of gyration
S	area of the cross-section
t_1, $\bar{t}$	time variable, reduced time variable
U_c	kinetic energy
U_p	potential energy
u_1, u_2, u_3	displacement components along coordinates x_1, x_2, x_3
$z = x_3$	coordinates along rod axis
$\bar{z}$	dimensionless axial coordinate

Greek alphabet

α_i	dimensionless parameter (equation [7.74])
γ	dimensionless parameter (equation [7.74])
Λ	wavelength

@Seismicisolation

ρ	density
ν, ν_{ij}	Poisson's number for isotropic and anisotropic materials respectively
$\chi_{ij} = C_{ij}/\rho$	notation introduced in equation [7.66]

7.12. Appendices

Appendix 7.A. an outline of some studies on longitudinal vibration of rods with rectangular cross-section

Here we attempt to classify studies into three groups.

7.A.1. *Rod with circular cross-section*

7.A.1.1. *Exact solution*

The geometry of the section permits us to consider the problem as a two-dimensional one (r, x_3). Cylindrical coordinates are used and from governing dynamics equations in an isotropic elastic medium.

Equations of motion are derived. The lateral boundary conditions are satisfied for an infinite rod.

These equations are recognized as being Bessel's type and Bessel's functions are utilized to obtain a closed-form expression for displacements.

This is the Pochhammer-Chree solution [CHR 89, POC 76].

7.A.1.2. *Approximate solutions*

These solutions are proposed by Hermann-Mindlin [HER 50] and Hermann-Mc Niven [MIN 60] with a radial inertia correction and second-order approximation respectively.

7.A.2. *Rod with arbitrary cross-section*

This type of rod gives rise to a three-dimensional problem that does not have an exact solution. All of the solutions are approximate.

@Seismicisolation

7.A.2.1. *Elementary equation of motion and solution*

The second-order equation of motion is popular and can be found in any text book. There is no wave dispersion at all in the context of this theory.

7.A.2.2. *Improved elementary equation with correcting terms*

Love [LOV 44] and Rayleigh [RAY 45] suggested the introduction of a lateral inertia correcting term. Bishop [BIS 52] proposed two correcting terms: the lateral inertia correction and shear correction.

Bishop's equation is adopted for low and medium frequencies. Rosenfeld and Keller [KEL 74] adopted higher-order terms for displacements. Mindlin [MIN 60] contributed to the improvement of an approximate solution.

7.A.2.3. *Rod with square or rectangular cross-section*

The various publications that can be found on this subject take into account either the flatness of the rod (ratio of thickness/width) [MOR 50] or solutions that satisfy dispersion curves at higher frequencies. In this respect, let us mention Volterra [VOL 65], whose solutions are satisfactory up to third elastodynamic vibration modes. The three components of displacement contribute to the solution.

Medick [MED 66] examined an isotropic rod and introduced weighting coefficients deduced from plate theory considerations. He examined the influence of these coefficients on phase velocity due to higher-order terms of the displacement field. Legendre polynomials were used.

Nigro [NIG 68] proposed a study of orthotropic composite materials and did not use weighting coefficients. Important numerical calculations are necessary here. This author used the displacement field with tenth-order terms to examine the convergence of phase velocity.

Heterlendy [HET 68] used Legendre polynomials in the series for displacement components. The series are truncated up to the second terms for u_1 and u_2, and four terms for u_3. The eigenvalue equation is of fifth-order and consequently permits examination up to the fifth elastodynamic mode.

Fraser [FRA 69] extrapolated Green and Kynch's solution devoted to a circular section [GRE 57] by using Cartesian coordinates and Bessel functions. Numerical computation is complicated.

@Seismicisolation

Appendix 7.B. Formulation of Bishop's equation by Hamilton's principle by Rao and Rao [RAO 74]

Bishop probably formulated his equation using the d'Alembert's principle.

Rao and Rao have reformulated this equation using Hamilton's principle. They presented homogenous natural boundary conditions as well as rod dynamic response using eigenfunctions and mode shapes.

7.B.1. *Displacement field*

The following field with three displacement components is proposed:

$$\left.\begin{aligned} u = u_x &= -\nu\, x \frac{\partial w}{\partial z} \\ v = u_y &= -\nu\, y \frac{\partial w}{\partial z} \\ u_z &= w\,(z, t) \end{aligned}\right\} \qquad [7.B.1]$$

Poisson's number is introduced in 7.B.1 to indicate the lateral contraction when the rod is submitted to a tension.

7.B.2. *Strain components*

$$\left.\begin{aligned} &\varepsilon_{11} = -\nu\, w_{,z}, \quad \varepsilon_{22} = -\nu\, w_{,z}, \quad \varepsilon_{33} = w_{,z} \\ &\gamma_{12} = 0, \quad \gamma_{13} = -\nu\, x\, w_{,zz}, \quad \gamma_{23} = -\nu\, y\, w_{,zz} \end{aligned}\right\} \qquad [7.B.2]$$

In subscript, the number of letters after the comma indicates the order of derivative with respect to this variable.

@Seismicisolation

7.B.3. *Potential energy U*

In equation [7.B.2], there are five strain components and there will be more than two terms in energy expression U. However, Rao and Rao retained three terms and neglected the others. They neglected normal stresses σ_{11} and σ_{22}. Shear stresses σ_{13} and σ_{33} contribute to expressing U:

$$U = \frac{1}{2} \int_V \sigma_{ij}\ \varepsilon_{ij}\ dv = \frac{1}{2} \int C_{ijkl}\ \varepsilon_{ij}\ \varepsilon_{kl}\ dv \qquad [7.B.3]$$

After Rao and Rao:

$$U \simeq \frac{1}{2} \int_V \left[E_3\ w_{,z}^2 + \gamma_{31}^2\ w_{,zz}^2\ \left(y^2 + x^2\right) G_{31} \right] dv$$

Bishop's equation can be extended to transversely isotropic material with symmetry material axis 3[6], which coincides with rod axis z.

Integrating from one tip z = 0 to z = L we get:

$$U = \frac{1}{2} \int \int \int_0^L \left[E_3\ w_{,z}^2 + \nu_{31}^2\ \left(x^2 + y^2\right) G_{31}\ w_{,zz}^2 \right] dx\ dy\ dz$$

$$U = \frac{1}{2} \int_0^t \left[E_z\ S\ w_{,z}^2 + \nu_{31}^2\ G_{31}\ w_{,zz}^2\ I_p \right] dz \qquad [7.B.4]$$

where S is the area of the section.

7.B.4. *Kinetic energy U_c*

$$U_c = \frac{1}{2} \rho \int_V \left[\left(\frac{\partial u}{\partial t}\right)^2 + \left(\frac{\partial v}{\partial t}\right)^2 + \left(\frac{\partial w}{\partial t}\right)^2 \right] dv \qquad [7.B.5]$$

6 In subscripts, numbers 3,1 are added to Poisson's number vand shear modulus G, the material being transverse isotropic $G_{31} = G_{32}$.

@Seismicisolation

7.B.5. *Hamilton's principle and equation of motion*

The following functional is used in variational calculus:

$$\delta\left[\int_{t_1}^{t_2}\left(U_p - U_c - W\right)dt\right] = 0 \qquad [7.B.6]$$

where W is the work of external force. Bringing equation [7.B.4] and [7.B.5] into [7.B.6] and effecting integration by parts, the equation of motion is obtained:

$$\frac{\partial^2 w}{\partial t^2} - \frac{E}{\rho}\frac{\partial^2 w}{\partial t^2} - \nu_{31}^2\, r_p^2\, \frac{\partial^4 w}{\partial z^2\, \partial t^2} + \nu_{31}^2\, G_{31}\, r_p^2\, \frac{\partial^4 w}{\partial z^4} = 0 \qquad [7.B.7]$$

where r_p is the radius of gyration of the section.

$$r_p = \frac{b\,h^3 + b^3\,h}{12\,bh} = \left(\frac{h^2 + b^2}{12}\right) \qquad [7.B.8]$$

7.B.6. *Natural boundary conditions*

The two boundary condition equations are:

$$\left(\gamma_{31}^2\, \rho\, I_p\, \frac{\partial^2 w}{\partial t^2\, \partial z} + E_3 S\, \frac{\partial w}{\partial z} - \gamma_{31}^2\, G_{31}\, I_p\, \frac{\partial^3 w}{\partial z^3}\right)\delta\, w = 0 \qquad [7.B.9]$$

$$\left(I_p\, \gamma_{31}^2\, G_{31}\, \frac{\partial^2 w}{\partial z^2}\right)\delta\left(\frac{\partial w}{\partial z}\right) = 0 \qquad [7.B.10]$$

$$I_p = \frac{b\,h^3 + h\,b^3}{12} \qquad [7.B.11]$$

There are four natural boundary conditions.

@Seismicisolation

7.B.6.1. *Physical interpretation of boundary conditions*

Consider a rod subjected to tensile axial forces P_z (L , t) and the outward forces per unit length on the lateral boundary applied at x = 0 and x = L respectively.

Equation [7.B.1]'s assumption mentions that particles at the ends w (0 , t) and w (L , t) move axially and the radial motions are portrayed by $-\nu\, x \dfrac{\partial w}{\partial z}$ and $-\nu\, y \dfrac{\partial w}{\partial z}$.

The virtual work of these forces is:

$$\delta w' = \left[\left(P_z\ \delta w \right) - \left(2\ \nu_{31}\ p_1\ S \right) \bullet \delta \left(\frac{\partial w}{\partial z} \right) \right] \qquad [7.B.12]$$

If W′ is introduced in equation [7.B.6], variational calculus yields the following non-homogenous boundary conditions:

$$\left[\nu_{31}^2\ \rho\ I_p\ \frac{\partial^3 w}{\partial z\, \partial t^2} + E\ S\ \frac{\partial w}{\partial z} - \nu_{31}^2\ G_{31}\ I_p\ \frac{\partial^3 w}{\partial z^3} - P_z \right] \bullet \delta w = 0$$

$$\left[\nu_{31}^2\ G_{31}\ I_p\ \frac{\partial^2 w}{\partial z^2} + 2\ \nu_{31}\ p_1\ S \right] \delta \left(\frac{\partial w}{\partial z} \right) = 0 \qquad [7.B.13]$$

In the above equations, the bracket in the first equation in [7.B.13] represents the axial forces applied at the ends and the second brackets in [7.B.13] are the radial forces at the same ends.

7.B.6.2. *Possible end conditions*

The equations in [7.B.13] show that setting the bracket and variation to zero is not possible. There are consequently four possible natural boundary conditions and a couple of end conditions that correspond to special situations.

Rao and Rao suggested the situation of a gripped end that does not correspond to axial force or lateral displacement u = 0 = v in [7.B.1]. These end conditions can be created by four rigid smooth cylinders fixing the rod around a cross-section.

@Seismicisolation

Appendix 7.C. Dimensionless Bishop's equations of motion and dimensionless boundary conditions

To simplify the writing of lengthy solutions, the following equations are adopted.

7.C.1. *Equations of motion*

Bishop's equation of motion [7.11] is rewritten with new set of variables, given below.

7.C.1.1. *Displacement, coordinates and time*

$$\begin{cases} \bar{t} = \dfrac{t\,v}{L}, \quad \text{with } v_L = \sqrt{\dfrac{E}{\rho}}, \quad L \text{ rod length} \\ \bar{z} = \dfrac{z}{L} \\ \bar{w} = \dfrac{w}{L} \end{cases} \qquad [7C.1]$$

7.C.1.2. *Non-dimensional factors in Bishop's equations*

Equation [7.11] is rewritten here:

$$\frac{\partial^2 w}{\partial t^2} - \frac{E}{\rho}\frac{\partial^2 w}{\partial z^2} - \gamma^2 r_p^2 \frac{\partial^4 w}{\partial z^2\,\partial t_2} + \gamma^2 r_p^2 \frac{G}{\rho}\frac{\partial^4 w}{{}_4} = 0 \qquad [7.C.2]$$

Using new variable [7.C.1], equation [7.C.2] is rewritten as:

$$\frac{\partial^2 \bar{w}}{\partial E^2} \bullet \frac{L^2 v_L^2}{L^2} - v_L^2 \frac{L^2}{L^2}\frac{\partial^2 \bar{w}}{\partial \bar{z}^2} - \frac{\gamma^2 r_p^2 \bullet L^4 v_L^2}{L^2\left(L^2 L^2\right)}\frac{\partial^4 \dot{w}}{\partial \bar{z}^2\,\partial \bar{t}^2}$$

$$+ \gamma^2 \frac{r_p^2}{L^2} \bullet \frac{L^2}{L^2} v_L^2 \alpha^2 \frac{\partial^4 \bar{w}}{\partial \bar{z}^4} = 0$$

@Seismicisolation

$$\frac{\partial^2 \overline{w}}{\partial E^2} - \frac{\partial^2 \overline{w}}{\partial \overline{z}^2} - r_1 \frac{\partial^4 \overline{w}}{\partial \overline{z}^2 \, \partial \overline{t}^2} + r_2 \frac{\partial^4 \overline{w}}{\partial \overline{z}^4} = 0 \qquad [7.C.3]$$

with:

$$r_1 = \nu^2 \frac{r_p^2}{L^2} = \nu^2 \frac{I_p}{S\,L^2} \qquad [7.C.4]$$

$$r_2 = \frac{\nu^2 \, I_p \, \alpha^2}{S^2 \, L^2}; \qquad \alpha^2 = \frac{G}{E} \qquad [7.C.5]$$

7.C.1.3. *Non-dimensional boundary condition equations*

Natural boundary conditions obtained in Appendix 7.B are rewritten here:

$$\gamma^2 \, \rho \, I_p \frac{\partial^2 w}{\partial z \, \partial t^2} + E\,S \frac{\partial w}{\partial z} - \gamma^2 \, G \, I_p \frac{\partial^3 w}{\partial z^2} = 0 \qquad [7.B.9]$$

Dividing all the numbers by ρ S:

$$\gamma^2 \frac{I_p}{S} \frac{\partial^3 w}{\partial z \, \partial t^2} + \frac{E}{\rho} \frac{\partial w}{\rho} \frac{\partial w}{\partial z} - \frac{\gamma \, G \, I_p}{\rho \, S} \frac{\partial^3 w}{\partial^3} = 0 \qquad [7.C.6]$$

Using dimensionless variables, as in equation [7.C.1], and dimensionless parameters in [7.C.4] and [7.C.5], we get:

$$\gamma^2 \frac{I_p}{L^2 \, S} \frac{L^3 \, v_L^2}{L^2 \, L^2} \frac{\partial^3 \overline{w}}{\partial \overline{z} \, \partial \overline{t}^2} + v_L^2 \frac{\partial \overline{w}}{\partial \overline{z}} - \gamma^2 \, v_L^2 \, \alpha^2 \frac{\partial^3 \overline{w}}{\partial \overline{z}^3} = 0$$

$$r_1 \frac{\partial^3 \overline{w}}{\partial \overline{z} \, \partial \overline{t}^2} + \frac{\partial \, \overline{w}}{\partial \, \overline{z}} - r_2 \frac{\partial^3 \overline{w}}{\partial \overline{z}^3} = 0 \qquad [7.C.7]$$

@Seismicisolation

The second boundary equation is:

$$\gamma^2 \, G \, I_p \, \frac{\partial^2 \, w}{\partial \, z^2} = 0$$

$$\gamma^2 \, G \, \frac{I_p}{L^2} \, \frac{\partial^2 \, \overline{w}}{\partial \, \overline{z}^2} = 0$$

$$\gamma^2 \, \frac{G \, I_p}{L^2} \, \frac{\partial^2 \, \overline{w}}{\partial \, \overline{z}^2} = 0$$

or:

$$r_2 \, \frac{\partial^2 \, \overline{w}}{\partial \, \overline{z}^2} = 0 \qquad [7.C.8]$$

The two other kinematic boundary conditions are replaced by:

$$\delta \, (w) \;\rightarrow\; \delta \, (\overline{w}) = 0 \qquad [7.C.9]$$

$$\delta \left(\frac{\partial \, w}{\partial \, \overline{z}} \right) \;\rightarrow\; \delta \left(\frac{\partial \, \overline{w}}{\partial \, \overline{z}} \right) = 0$$

7.C.1.4. *Dimensionless Bishop's equation of motion and dimensionless boundary condition equations for transversely isotropic material*

Equation [7.11] is replaced by equation [7.12]. Using the same set of dimensionless variables in equation [7.C.1], we have to replace r_1 and r_2 by:

$$r_1 = \frac{\gamma_{31}^2 \, r_p^2}{L^2} = \frac{\gamma_{31}^2 \, I_p}{S \, L^2} \qquad [7.C.10]$$

$$r_2 = \frac{\gamma_{31}^2 \, I_p^2}{S^2 \, L^2} \, \frac{G_{31}}{E_3} = \frac{\gamma_{31}^2 \, I_p^2 \, \alpha^2}{S^2 \, L^2} \quad , \quad \alpha^2 - \frac{G_{13}}{E_3} \qquad [7.C.11]$$

@Seismicisolation

The same dimensionless equation of motion can be used with the new set of r_1 and r_2 presented above.

Free (case A)	$P_z(z, t) = 0$	No axial force
	$\frac{\partial^2 w}{\partial t^2} = 0$	No lateral force
Gripped (case B)	$P_z(z, t) = 0$	No axial force
	$\frac{\partial w}{\partial z} = 0$	No lateral displacement
Fixed (case C)	$w(z, t) = 0$	No axial displacement
	$\frac{\partial^z w}{\partial z^2} = 0$	No lateral force
Centered (case D)	$w(x, t)$	No axial displacement
	$\frac{\partial^z w}{\partial z^z} = 0$	No lateral force

Table 7.B.1. *The two boundary conditions are presented. A, B, C and D designate the possible couple for each end. The table indicates the four natural end conditions*

Appendix 7.D. Touratier's equations of motion by variational calculus

From equation [7.57] let us calculate $\delta\,\tilde{J}$:

$$\delta\,\tilde{J} = \int_{t_1}^{t_2} \frac{\rho\, bh}{3} \int_0^L \left\{ \begin{array}{l} \frac{h^2}{4}\,\frac{\partial u_1^{(1,0)}}{\partial t} \bullet \frac{\partial \delta u_1^{(1,0)}}{\partial t} + \frac{b^2}{4}\,\frac{\partial u_2^{(0,1)}}{\partial t} \bullet \frac{\partial \delta u_2^{(0,1)}}{\partial t} \\ + 3\,\frac{\partial u_3^{(0,0)}}{\partial t} \bullet \frac{\partial u_3^{(0,0)}}{\partial t} \bullet \frac{\partial \delta u_3^{(0,0)}}{\partial t} \end{array} \right\}$$

$$dx_3\, dt - \int_{t_1}^{t_2} \frac{S}{3} \int_0^L \left\{ C_{11}\, u_1^{(1,0)} + C_{12}\, u_2^{(0,1)} + C_{13}\, \frac{\partial u_3^{(0,0)}}{\partial x_3} \right\} \left(\delta u_1^{(1,0)} + \delta u_2^{(0,1)} \right) \qquad [7.D.1]$$

$$\bullet\, dx_3\, dt - \int_{t_1}^{t_2} q^2\, C_{44} \int_0^L \left\{ I_p\, \frac{\partial u_1^{(1,0)}}{\partial x_3}\, \frac{\partial \delta u_1^{(1,0)}}{\partial x_3} + I_2\, \frac{\partial u_2^{(0,1)}}{\partial x_2} \right\} dx_3\, dt$$

$$- \int_{t_1}^{t_2} S \int_0^L \left\{ \frac{C_{13}}{3} \left(u_1^{(1,0)} + u_2^{(0,1)} \right) + 2 \left[\frac{C_{33}}{2} - \frac{2\, C_{13}^2}{3\, (C_{11} + C_{12})} \right] \bullet \frac{\partial u_3^{(0,0)}}{\partial x_3} \right\} \frac{\partial u_3^{(0,0)}}{\partial x_3}$$

@Seismicisolation

Variations of displacement coefficients are set to zero:

$$\delta\, u_i^{(m,n)}\left(x_3\ ,\ t_j\right) = 0\ , \qquad \forall\ x_3 \qquad [7.D.2]$$

Integration by parts, with equation [7.D.2] being accounted for, gives rise to the following equations from which natural boundary equations are obtained:

$$\int_{t_1}^{t_2}\int_{9}^{L} \frac{\partial u_i^{(m,n)}}{\partial t} \bullet \frac{\partial \delta u_i^{(m,n)}}{\partial\, t} \bullet dx_3\ dt = -\int_{t_1}^{t_2}\int_{0}^{L} \frac{\partial^2 u_i^{(m,n)}}{\partial t^2} \bullet \delta u_i^{(m,n)}$$

$$\bullet \int_{t_1}^{t_2}\int_{0}^{L} \frac{\partial u_i^{(m,n)}}{\partial x_3} \bullet \frac{\partial u_i^{(m,n)}}{\partial x_3}\ dx_3\ dt = \int_{0}^{t_2} \left[\frac{\partial u_i^{(m,n)}}{\partial x_3}\ \delta u_i^{(m,n)}\right]_{\circ}^{L} dt \qquad [7.D.3]$$

$$\int_{t_1}^{t_2}\int_{0}^{L} \frac{\partial u_i^{(m,n)}}{\partial x_l^2}\ \delta\, u_i^{(m,n)}\ dx_3\ dt \bullet \int_{t_1}^{t_2}\int_{0}^{L} \frac{\partial u_j^{(p,q)}}{\partial x_3}\ dx_3\ dt = \int_{t_1}^{t_2} \left[u_i^{(m,n)} \bullet \delta u_j^{(p,q)}\right]_0^L dt$$

$$-\int_{t_1}^{t_2}\int_{0}^{L} \frac{\partial u_i^{(m,n)}}{\partial x_3}\ \delta u_j^{(p,q)}\ dx_3\ dt$$

Using equation [7.D.3] in [7.D.2], equations [7.58] are obtained.

Appendix 7.E. Calculation of correcting factor q (C_{ijkl})

The way of reasoning for an extensional wave in a rod with rectangular cross-section is similar to Mindlin's method devoted to a bending wave in a rod.

The calculation is based on a square cross-section.

As the Rayleigh surface wave c_R occurs for a high value of wave number corresponding to a wavelength λ, which is small compared to the smallest transverse dimension of the rod, the value obtained for c_R is also valid for the rectangular cross-section.

7.E.1. *Asymptotic value of phase velocity of a Rayleigh wave*

For a square section $\overline{k}_1 = \overline{k}_2 = \overline{k} = k\ b$, equation [7.65] becomes:

@Seismicisolation

$$\begin{vmatrix} \bar{c}^2 - q^2\bar{\chi}_{44}^2 - \dfrac{\bar{\chi}_{11}^2}{\bar{k}^2} & -\dfrac{\bar{\chi}_{12}^2}{\bar{k}^2} & -jk\dfrac{\bar{\chi}_{13}^2}{\bar{k}^2} \\ -\dfrac{\bar{\chi}_{12}^2}{\bar{k}^2} & \bar{c}^2 - q^2\bar{\chi}_{44}^2 - \dfrac{\bar{\chi}_{11}^2}{\bar{k}^2} & -jk\dfrac{\bar{\chi}_{13}^2}{\bar{k}^2} \\ j\dfrac{\bar{\chi}_{13}^2}{3\bar{k}} & j\dfrac{\bar{\chi}_{13}^2}{3\bar{k}} & \bar{c}^2 - \bar{\chi}^{*2} \end{vmatrix} = 0 \qquad [7.E.1]$$

Term-by-term, it is easy to subtract the second line from the first line to obtain two zeros in the first line. The second elastodynamic mode is:

$$\bar{c}_2 = \left\{ q^2\,\bar{\chi}_{44}^2 + \frac{\bar{\chi}_{11}^2 - \bar{\chi}_{12}^2}{\bar{k}^2} \right\}^{1/2} \qquad [7.E.2]$$

The phase velocities for the first and third elastodynamic modes are related by bisquared equation:

$$\bar{c}^4 - \bar{c}^2\left\{ q^2\bar{\chi}_{44}^2 + \bar{\chi}^{*2} + \frac{\bar{\chi}_{11}^2 + \bar{\chi}_{12}^2}{\bar{k}^2} \right\} + \left\{ q^2\bar{\chi}_{44}^2\bar{\chi}^{*2} + \frac{3\bar{\chi}^{*2}\left(\bar{\chi}_{11}^2 + \bar{\chi}_{12}^2\right) - 2\,\bar{\chi}_{13}^4}{2\,\bar{k}^2} \right\} = 0 \qquad [7.E.3]$$

$$\bar{c}_j^2 = \frac{1}{2}\left\{ q^2\bar{\chi}_{44}^2 + \bar{\chi}^{*2} + \frac{\bar{\chi}_{11}^2 + \bar{\chi}_{12}^2}{\bar{k}^2} \right\} + \varepsilon \left\{ \begin{array}{l} \dfrac{\left(\bar{\chi}_{11}^2 + \bar{\chi}_{12}^2\right)^2}{4\,\bar{k}^4} + \\ \dfrac{3\left(\bar{\chi}_{11}^2 + \bar{\chi}_{12}^2\right)\left(q^2\bar{\chi}_{44}^2 - \bar{\chi}^{*2}\right) + 4\bar{\chi}_{13}^4}{6\,\bar{k}^2} \\ + \left[\dfrac{-q^2\,\bar{\chi}_{44}^2 + \bar{\chi}^{*2}}{2} \right]^2 \end{array} \right\}^{1/2} \qquad [7.E.4]$$

in which $\varepsilon = -1$ for $j = 1$ and $\varepsilon = +1$ for $j = 3$.

The asymptotic value of phase velocity of the first mode when wave number k tends to infinity must be the Rayleigh wave velocity c_R.

$$\left. \begin{array}{r} \lim \bar{c}_1 = \bar{c}_R = \dfrac{c_R}{\left(E_3/\rho\right)^{1/2}} \\ \lim \bar{c}_1 = 1 \end{array} \right\} \qquad [7.E.5]$$

@Seismicisolation

Equation [7.E.4] is rewritten for j = 1 and ε = -1 in the form:

$$\bar{c}_1^2 = \frac{A_1^*}{\bar{k}^2} + A_2^* - \sqrt{\frac{A_1^{*2}}{\bar{k}^4} + \frac{A_4^*}{\bar{k}^2} + A_5^*} \qquad [7.E.6]$$

where:

$$A_1^* = \frac{\bar{\chi}_{11}^2 + \bar{\chi}_{12}^2}{2}, \qquad A_2^* = \frac{q^2\ \bar{\chi}_{44}^2 + \bar{\chi}^{*2}}{2} \qquad [7.E.7]$$

$$A_4^* = \frac{3\left(\bar{\chi}_{11}^2 + \bar{\chi}_{12}^*\right)\left(q^2\ \bar{\chi}_{44}^2 - \bar{\chi}^{*2}\right) + 4\ \bar{\chi}_{13}^4}{6}$$

$$A_3 = \left(\frac{-q^2\ \bar{\chi}_{44}^2 + \bar{\chi}^{*2}}{2}\right)^2 \qquad [7.E.8]$$

for $\bar{k} \to 0$. Let us adopt the change of variable:

$$\bar{X} = \frac{1}{\bar{k}}$$

A MacLaurin series expansion gives:

$$\bar{c}_1^2 = \bar{X}^2 \left\{ \begin{array}{l} A_1^* + \dfrac{A_2^*}{\bar{X}^2} - A_1^* \left[1 + \dfrac{A_4^*}{2\ A_1^{*2}\ \bar{X}^2} + \dfrac{A_5^*}{2\ A_1^{*2}\ \bar{X}4}\right] \\ \\ - \dfrac{1}{8}\left(\dfrac{A_4^*}{A_1^{*2}\ \bar{X}^2} + \dfrac{A_5^*}{A_1^{*2}\ \bar{X}^4}\right)^2 + \ldots \end{array} \right\} \qquad [7.E.9]$$

$$\bar{c}_1^2 = A_2^* - \frac{A_4^*}{2\ A_1^*} + \eta\left(\frac{1}{\bar{X}^2}\right) \qquad [7.E.10]$$

@Seismicisolation

where:

$$\eta\left(\frac{1}{\overline{X}^2}\right) \rightarrow 0 \text{ when } \overline{X} \rightarrow +\infty$$

The first condition [7.E.5] is:

$$\lim \overline{c}_l^2 = A_2^* - \frac{A_4^*}{2\,A_1^*} = 1 \qquad [7.E.11]$$

The second condition [7.E.5] is:

$$\lim \overline{c}_l^2 = A_2^* - \sqrt{A_5^*} = \overline{c}_R^2 \qquad [7.E.12]$$

Condition [7.E.12] is equivalent to:

$$\frac{3\left(\overline{\chi}_{11}^2 + \overline{\chi}_{12}^2\right)}{3\,\overline{\chi}^{*2}\left(\overline{\chi}_{11}^2 + \overline{\chi}_{12}^2\right) - 2\,\overline{\chi}_{13}^4} = 1 \qquad [7.E.13]$$

Utilization of stiffness and compliance matrices [C_1] [S] permits writing $\overline{\chi}_{ij}^2$:

$$\overline{\chi}_{ij}^2 = \frac{C_{ij}}{E_3} = f\left(S_{ij}\right) = g\left(E_1, \ldots, E_3, \gamma_{12}, \ldots, \gamma_{13}, \gamma_{13}, G_{23}\right)$$

and an identity from equation [7.E.13].

7.E.2. *Phase velocity of a surface wave*

Chadwick [CHA 76] has presented a publication devoted to surface waves in orthorhombic material. In this chapter, attention is focused on a transversely isotropic rod whose axis coincides with the material's symmetry axis.

@Seismicisolation

The direction of wave propagation is colinear with the fiber axis. The sagittal plane is a symmetry plane and the displacement vector at the surface has two orthogonal components.

Rayleigh waves must simultaneously satisfy propagation in an unbounded medium and boundary conditions for a free lateral surface.

Let as adopt a displacement of the form:

$$\vec{u} = \vec{d} \exp - j \left(\frac{\omega}{c_R} p_1 x_1 \right) \exp j\omega \left(t - \frac{p_2 x_2 + p_3 x_3}{C_R} \right) \qquad [7.E.14]$$

where p_1 is an unknown of the problem, proportional to the penetration x_1 in the material; C_R phase velocity of the Rayleigh wave; $\vec{d}$ polarization vector; and p_2 and p_3 components of unit vector $\vec{p}$ of propagation direction. If $\vec{p} = \vec{x}_3$ the equation of wave motion is[7]:

$$\begin{vmatrix} \Gamma_{11} - \rho C_R^2 & 0 & \Gamma_{13} \\ 0 & \Gamma_{22} - \rho C_R^2 & 0 \\ \Gamma_{31} & 0 & \Gamma_{11} - \rho C_R^2 \end{vmatrix} = 0 \qquad [7.E.15]$$

$$\Gamma_{11} = C_{11} r^2 + C_{44}$$

$$\Gamma_{13} = \Gamma_{31} = \left(C_{44} + C_{13} \right) r \qquad [7.E.16]$$

$$\Gamma_{22} = C_{44} + C_{66} r^2$$

$$\Gamma_{33} = C_{33} + C_{44}^2$$

$$r = p_1$$

Developing equation [7.E.15], we obtain:

7 See details of Christoffel's equation in Chapter 10.

@Seismicisolation

$$\left(C_{44}+C_{66}\ r^2-\rho\ C_R^2\right)\left\{\begin{array}{l}\left(C_{11}\ r^2+C_{44}-\rho\ C_R^2\right)\\ \\ \left(C_{33}+C_{44}\ r^2-\rho\ C_R^2\right)-\left(C_{44}+C_{13}\right)^2\ r^2\end{array}\right\}=0 \qquad [7.E.17]$$

The root $r_2 = p_1^{(2)}$ of equation [7.E.17] is

$$r_2^2 = \frac{\rho\ C_R^2 - C_{44}}{C_{66}} \qquad [7.E.18]$$

This equation does not permit us to exponentially increase the amplitude of the displacement with penetration x_1 in the material.

$$r_2 = -\ j\ \left\{\frac{\rho\ c_R^2 - C_{44}}{C_{66}}\right\}^{1/2} \qquad [7.E.19]$$

The two other roots r_1 , r_3 are:

$$C_{11}\ C_{44}\ r^4 + r^2\left\{\begin{array}{l}C_{11}\ \left(C_{33}-\rho\ c_R^2\right)+C_{44}\ \left(C_{44}-\rho\ c_R^2\right)\\ \\ -\left(C_{44}+C_{13}\right)^2+\left(C_{33}-\rho\ c_R^2\right)\ \left(C_{44}-\rho\ c_R^2\right)\end{array}\right\}=0 \qquad [7.E.20]$$

Associated eigenvalues of equation [7.E.15] are such that:

$$\left(\Gamma_{11}-\rho\ c_R^2\right)\ d_1+\Gamma_{13}\ d_3=0 \qquad [7.E.21]$$

$$\left(\Gamma_{22}-\rho\ c_R^2\right)\ d_2=0 \qquad [7.E.22]$$

$$\Gamma_{11}\ d_1+\left(\Gamma_{33}-\rho\ c_R^2\right)\ d_3=0 \qquad [7.E.23]$$

The choice of equation [7.E.22] shows that component $\vec{x}_2$ of $\vec{d}^{(1)}$ and $\vec{d}^{(3)}$ is zero. The two other equations [7.E.21] and [7.E.22] give:

@Seismicisolation

$$d_1 = 1 \qquad d_3 = -\frac{\Gamma_{11} - \rho\, c_R^2}{\Gamma_{13}} \qquad [7.E.24]$$

as $r_i \neq 0$

$$d_3^{(i)} = -\frac{C_{11}\, r_i^2 + C_{44} - \rho\, c_R^2}{\left(C_{44} + C_{13}\right) r_i}; \qquad i \in \{1, 3\} \qquad [7.E.25]$$

Eigenvectors are consequently:

$$\vec{d}^{(1)} = \vec{x}_1 + d_3^{(1)}\, \vec{x}_3 \qquad [7.E.26]$$

$$\vec{d}^{(2)} = \vec{x}_2 \qquad [7.E.27]$$

$$\vec{d}^{(3)} = \vec{x}_1 + d_3^{(3)}\, \vec{x}_3 \qquad [7.E.28]$$

Rayleigh waves must satisfy boundary conditions. Only the plane $0x_2\, x_3$ with external normal $-\vec{x}_1$ is considered here.

Free boundary conditions require:

$$\left(\sigma_{i1}\right)_{x_1=0} = C_{ijkl} \left(\frac{\partial\, u_k}{\partial\, x_1}\right)_{x_1 = 0} = 0 \qquad [7.E.29]$$

As equation [7.E.17] has real coefficients and three couples of conjugate roots exist, only three roots with negative imaginary parts are acceptable. A wave with increasing amplitude is not acceptable. Value r_j is associated an eigenvector $d_j^{(1)}$ and a displacement of the form:

$$u_k^{(n)} = d_k^{(n)} \exp j\, \omega \left(t - \frac{p_1^{(n)}.x_1}{c_R}\right) \qquad [7.E.30]$$

The general solution is a linear combination of three displacements at the same velocity c_R:

@Seismicisolation

$$u_k = \sum_{n=1}^{3} A_n \, u_k^{(n)} \qquad [7.E.31]$$

Writing the boundary conditions:

$$\sum_{n=1}^{3} C_{ijkl} \, A_n \left(\frac{\partial u_k^{(n)}}{\partial x_1} \right)_{x_1=0} = \sum_{n=1}^{3} C_{ijkl} \, p_l^{(n)} \, d_k^{(n)} \, A_n = 0 \qquad [7.E.32]$$

Using a constitutive equation under matricial form for stiffness coefficients, [7.E.30] yields:

$$\sum_{n=1}^{3} \left(C_{11} \, p_1^{(n)} \, d_1^{(n)} + C_{12} \, p_2^{(n)} \, d_2^{(n)} + C_{13} \, p_3^{(n)} \, d_3^{(n)} \right) A_n = 0 \qquad [7.E.33]$$

$$\sum_{n=1}^{3} \left\{ p_1^{(n)} \, d_2^{(n)} + p_2^{(n)} \, d_1^{(n)} \right\} C_{66} \, A_n = 0 \qquad [7.E.34]$$

$$\sum_{n=1}^{3} \left(p_1^{(n)} \, d_3^{(n)} + p_3^{(n)} \, d_1^{(n)} \right) C_{44} \, A_n = 0 \qquad [7.E.35]$$

By identification:

$$p_1^{(n)} = r_n ; \quad p_2^{(n)} = 0, \quad p_3^{(n)} = 1 \qquad \forall \, n \qquad [7.E.36]$$

Bringing equation [7.E.36] into [7.E.33], [7.E.34] and [7.E.35]:

$$\left\{ C_{11} \, d_1^{(1)} \, r_1 + C_{13} \, d_3^{(1)} \right\} A_1 + \left\{ C_{11} \, d_1^{(3)} \, r_3 + C_{13} \, d_3^{(3)} \right\} A_3 = 0$$

$$\left\{ d_3^{(1)} \, r_1 + d_1^{(1)} \right\} A_1 + \left\{ d_3^{(3)} \, r_3 + d_1^{(3)} \right\} A_3 = 0 \qquad [7.E.37]$$

as $A_2 = 0$.

Equation [7.E.37] has non-trivial solutions if the coefficient determinant is zero:

@Seismicisolation

$$C_{11}\left(r_1 - r_3\right) + \frac{C_{11}\, r_1^2 + C_{44} - \rho\, c_R^2}{C_{44} + C_{13}}\left(-\frac{C_{13}}{r_1} + C_{11}\, r_3\right)$$

$$+ \frac{C_{11}\, r_3^2 + C_{44} - \rho\, c_r^2}{C_{44} + C_{13}} \bullet \left(\frac{C_{13}}{r_3} - C_{11}\, r_1\right) +$$

$$\frac{C_{13}\left(C_{11}\, r_1^2 + C_{44} - \rho\, c_R^2\right)\left(C_{11}\, r_3^2 + C_{44} - \rho\, c_R^2\right)}{\left(C_{44} + C_{13}\right)^2} \bullet \qquad [7.E.38]$$

$$\left(\frac{1}{r_1} - \frac{1}{r_3}\right) = 0$$

Rearranging equation [7.E.38], the following equation is obtained for r_1 and r_3:

$$r_1^2\, r_3^2\, C_{11}^2\, C_{44} - \left(r_1^2 + r_3^2\right) C_{11}\, C_{13}\left(C_{44} - \rho\, c_R^2\right)\left(C_{13} + \rho\, c_R^2\right)$$
$$= -\, r_1\, r_3\, C_{11}\left\{\left(C_{44} + C_{13}\right)\rho\, c_R^2\right\} \qquad [7.E.39]$$

which shows the product and the sum of roots r_1^2 and r_3^2 :

$$r_1^2\,,\, r_3^2 = \frac{\left(C_{33} - \rho\, c_R^2\, 2\right)\left(C_{44} - \rho\, c_R^2\right)}{C_{11}\, C_{44}} \qquad [7.E.40]$$

$$r_1^2 + r_2^2 = \frac{C_{11}\left(C_{33} - \rho\, c_R^2\, 2\right) + C_{44}\left(C_{44} - \rho\, c_R^2\right) - \left(C_{44} + C_{13}\right)^2}{C_{11}\, C_{44}} \qquad [7.E.41]$$

Bringing equations [7.E.40] and [7.E.41] into [7.E.39] enables us to write the first member, M of equation [7.E.39] as:

$$M = \left(C_{44} - \rho\, c_R^2\right)\left\{\begin{array}{l} C_{11}\left(1 + \dfrac{C_{13}}{C_{44}}\right)\left(C_{33} - \rho\, c_R^2\right) \\ -\dfrac{C_{13}^2}{C_{44}}\left(C_{13} + C_{44}\right) \end{array}\right\} \qquad [7.E.42]$$

@Seismicisolation

The square of the second member N is:

$$N^2 = \frac{C_{11}}{C_{44}} \left(C_{33} - \rho\, c_R^2\right) \left(C_{44} - \rho\, c_R^2\right) \left(C_{44} + C_{13}\right)^2 \rho^2\, c_R^4 \qquad [7.E.43]$$

The last step of the calculation is to write:

$$M^2 = N^2$$

$$\begin{aligned}
&\left(C_{44} - \rho\, c_R^2\right) C_{11} \left(1 + \frac{C_{13}}{C_{44}}\right) \left(C_{33} - \rho\, c_R^2\right) \\
&\left[C_{11} \left(1 + \frac{C_{13}}{C_{44}}\right) \left(C_{33} - \rho\, c_R^2\right) - \frac{2\, C_{13}^2}{C_{44}} \left(C_{13} + C_{44}\right)\right] \\
&+ \frac{C_{13}^4}{C_{44}^2} \left(C_{13} + C_{44}\right)^2 \\
&= \frac{C_{11}}{C_{44}} \left(C_{33} - \rho\, c_R^2\right) \left(C_{44} + C_{13}\right)^2 \rho\, c_R^2
\end{aligned} \qquad [7.E.44]$$

Let us transform equation [7.E.44] into a dimensionless equation with:

$$\bar{c}_R = \frac{c_R}{c_3} \qquad [7.E.45]$$

The final equation in c_R is:

$$\begin{aligned}
&\bar{c}_R^2 \left\{ \left(\bar{\chi}_{44}^2 - \bar{\chi}_{11}^2\right) \bar{\chi}_{11}^2 \right\} + \bar{c}_R^4 \left\{ \left(\bar{\chi}_{44}^2 + 2\, \bar{\chi}_{33}^2\right) \bar{\chi}_{11}^2 - \left(2\, \bar{\chi}_{13}^4 + \bar{\chi}_{33}^2\, \bar{\chi}_{44}^2\right) \right\} \\
&\bar{\chi}_{11}^2 + \bar{c}_R^2 \left\{ \bar{\chi}_{11}^2 \left(\bar{\chi}_{44}^2 + \bar{\chi}_{33}^2\right) \left(2\, \bar{\chi}_{13}^4 - \bar{\chi}_{11}^2\, \bar{\chi}_{33}^2\right) - \bar{\chi}_{11}^2\, \bar{\chi}_{33}^2\, \bar{\chi}_{44}^2 - \bar{\chi}_{13}^8 \right\} \\
&+ \bar{\chi}_{44}^2 \left\{ \bar{\chi}_{11}^2\, \bar{\chi}_{33}^2 \left(\bar{\chi}_{11}^2\, \bar{\chi}_{33}^2 - \bar{\chi}_{13}^2\right) + \bar{\chi}_{13}^8 \right\} = 0
\end{aligned} \qquad [7.E.46]$$

The positive real root for $\bar{c}_R^2$ is retained among the three roots. Equation [7.E.46] is numerically solved and correcting coefficient q is obtained.

@Seismicisolation

Appendix 7.F. Stationarity of functional $\tilde{J}$ and boundary equations

$$\delta \tilde{J} = \sum_{j=1}^{3} \int_{t_1}^{t_2} \int_{0}^{L} \left(\cdots, \frac{\partial^2 u_j^{(m,n)}}{\partial t^2}, u_j^{(m,n)}, \cdots \right) \delta u_j^{(m,n)} \, dx_3 \, dt$$

$$- \frac{C_{13} S}{3} \int_{t_1}^{t_2} \left[\left(u_1^{(1,0)} + u_2^{(0,1)} \right) \delta u_3^{(0,0)} \right]_0^L dt - S \left\{ C_{33} - \frac{4 C_{13}^2}{3 \left(C_{11} + C_{12} \right)} \right\}$$

$$\bullet \int_{t_1}^{t_2} \left[\frac{\partial u_3^{(0,0)}}{\partial x_3} \bullet \delta u_3^{(0,0)} \right]_0^L dt - q^2 C_{44} \int_{t_1}^{t_2} \left[\begin{array}{l} I_1 \dfrac{\partial u_1^{(1,0)}}{\partial x_3} \bullet \delta u_1^{(1,0)} \\ + I_2 \dfrac{\partial u_2^{(0,1)}}{\partial x_3} \bullet \delta u_2^{(0,1)} \end{array} \right] dt \qquad [7.F.1]$$

$$- \sum_{j=1}^{2} \rho_j I_1 \int_{t_1}^{t_2} \frac{\partial^2 u_1^{(1,0)}}{\partial t^2} \bullet \delta u^{(1,0)} \, dt + I_2 \int_{t_1}^{t_2} \frac{\partial^2 u_2^{(0,1)}}{\partial t^2} \bullet \delta u_2^{(0,1)} \, dt +$$

$$S \int_{t_1}^{t_2} \frac{\partial^2 u_3^{(0,0)}}{\partial t^2} \bullet \delta u_3^{(0,0)} \, dt$$

The first integral on the first line of equation [7.E.1] is written in abridged from. It concerns equations of motion.

Appendix 7.G. On the possible solutions of eigenvalue equations

With a stationary wave in a rod of finite length and using the solutions to equations [7.94] and [7.96], the boundary equations are rewritten producing three equations for each end:

$$\bar{m}_1 \gamma^2 \tilde{U}_1 (0) + q^2 \frac{d \tilde{U}_1 (0)}{d \eta} = 0$$

$$\bar{m}_1 \gamma^2 \tilde{U}_2 (0) + q^2 \frac{d \tilde{U}_1 (0)}{d \eta} = 0$$

$$\bar{m}_1 \gamma^2 U^*_3 (0) + \frac{\alpha_4^2}{3} \left[\tilde{U}_1 (0) + \tilde{U}_2 (0) \right] + \alpha^2 \frac{d U^*_3 (0)}{d \eta} = 0$$

@Seismicisolation

$$-\bar{m}_2\ \gamma^2\ \tilde{U}_1\ (1) + q^2\ \frac{d\ \tilde{U}_1\ (1)}{d\ \eta} = 0$$

$$-\bar{m}_2\ \gamma^2\ \tilde{U}_2\ (1) + q^2\ \frac{d\ \tilde{U}_2\ (1)}{d\ \eta} = 0$$

$$-\bar{m}_2\ \gamma^2\ U^*_3\ (1) + \frac{\alpha_4^2}{3}\ \left(\tilde{U}_1\ (1) + \tilde{U}_2\ (1)\right) + \alpha'^2\ \frac{d\ U^*_3\ (1)}{d\ \eta} = 0 \qquad [7.G.1]$$

7.G.1. ***First case***

$$S'_j\ \in\ \mathbb{R}\ ,\ \ S'_3 < 0\ ,\ S'_3 > 0$$

This solution is used in equation [7.100].

Bringing it into equation [7.G.1], we obtain a linear algebraic system in A_j

$$P_{ij}\ A_j = 0 \qquad [7.G.2]$$

$$i\ \in\ \{1, 2, \cdots, 6\}$$

The non-trivial solution of equation [7.G.2] requires us to set the determinant to zero:

$$\text{Det}\ [P\ ] = 0 \qquad [7.G.3]$$

with the following components:

$$P_{11} = P_{13} = P_{15} = \bar{m}_1\ \gamma^2$$

$$P_{12} = q^2\ X$$

$$P_{14} = q^2\ Y$$

$$P_{16} = q^2\ Z$$

@Seismicisolation

$$P_{21} = \bar{m}_1 \; X \; M_1$$

$$P_{22} = q^2 \; X \; M_1$$

$$P_{23} = \bar{m}_1 \; \gamma^2 \; M_2$$

$$P_{24} = q^2 \; Y \; M_2$$

$$P_{25} = \bar{m}_1 \; \gamma^2 \; M_3$$

$$P_{26} = q^2 \; Z \; M_3$$

$$P_{31} = \left(\frac{\alpha_4^2}{3} - \alpha'^2 \; K_1 \; X \right) \left(1 + M_1\right)$$

$$P_{32} = - \bar{m}_1 \; \gamma^2 \; K_1 \; \left(1 + M_1\right)$$

$$P_{33} = \left(\frac{\alpha_4^2}{3} - \alpha'^2 \; K_2 \; Y \right) \left(1 + M_2\right)$$

$$P_{34} = - \bar{m}_1 \; \gamma^2 \; K_2 \; \left(1 + M_2\right)$$

$$P_{35} = \left(\frac{\alpha_4^2}{3} + \alpha'^2 \; K_3 \; Z \right) \left(1 + M_3\right)$$

$$P_{36} = - \bar{m}_1 \; \gamma^2 \; K_3 \; \left(1 + M_3\right)$$

$$P_{41} = - \bar{m}_2 \; \gamma^2 \; \cos h \, X + q^2 \; X \sin h \, X$$

$$P_{42} = - \bar{m}_2 \; \gamma^2 \; \sin h \, X + q^2 \; X \cos h \, X$$

$$P_{43} = - \bar{m}_2 \; \gamma^2 \; \cos h \, Y + q^2 \; Y \sin h \, Y$$

@Seismicisolation

$$P_{44} = -\bar{m}_2\ \gamma^2\ \sin h\ Y + q^2\ Y \cos h\ Y$$

$$P_{45} = -\left(\bar{m}_2\ \gamma^2\ \cos h\ Z + q^2\ Z \sin h\ Z\right)$$

$$P_{46} = -\left(\bar{m}_2\ \gamma^2\ \sin\ Z + q^2\ Z \cos\ Z\right)$$

$$P_{51} = P_{41}\ M_1$$

$$P_{52} = P_{42}\ M_1$$

$$P_{53} = P_{43}\ M_2$$

$$P_{54} = P_{44}\ M_2$$

$$P_{55} = P_{45}\ M_3$$

$$P_{56} = P_{46}\ M_3$$

$$P_{61} = \left\{\bar{m}_2\ \gamma^2\ K_1\ \sin h\ X + \left(\frac{\alpha_4}{3} - \alpha'^2\ K_1\ X\right) \cosh X\right\}\ (1 + M_1)$$

$$P_{62} = \left\{\bar{m}_2\ \gamma^2\ K_1\ \cos h\ X + \frac{\alpha_4}{3} - \alpha'^2\ K_1\ X \sin h\ X\right\}\ (1 + M_1)$$

$$P_{63} = \left\{\bar{m}_2\ \gamma^2\ K_2\ \sin h\ Y + \left(\frac{\alpha_4^2}{3} - \alpha'^2\ K_2\ Y\right) \cos h\ Y\right\}\ (1 + M_2)$$

$$P_{64} = \left\{\bar{m}_2\ \gamma^2\ K_2\ \cos h\ Y + \left(\frac{\alpha_4^2}{3} - \alpha'^2\ K_2\ Y\right) \sin h\ Y\right\}\ (1 + M_2)$$

$$P_{65} = \left\{-\bar{m}_2\ \gamma^2\ K_3\ \sin\ Z + \left(\frac{\alpha_4^2}{3} + \alpha'^2\ K_3\ Z\right) \cos\ Z\right\}\ (1 + M_3)$$

@Seismicisolation

$$P_{66} = \left\{ \bar{m}_2 \ \gamma^2 \ K_2 \ \cos \ Z + \left(\frac{\alpha_4^2}{3} - \alpha'^2 \ K_3 \ 2 \right) \sin \ Z \right\} \ (1 + M_3) \qquad [7.G.4]$$

M_j and K_j are given by formulae [7.101] and [7.102].

7.G.2. ***Second case***

$$S' \in \mathbb{R}, \quad S'_1 > 0, \quad S'_2 \text{ and } S'_3 < 0$$

Solution [7.103] is brought into equation [7.G.1].

The homogenous algebraic system is:

$$Q_{ij} \quad A'_j = 0 \qquad [7.G.5]$$

where i and $j \in \{1, 2, \cdots, 5, 6\}$ and the eigenvalue equation becomes:

$$\det [\ Q\ ] = 0 \qquad [7.G.6]$$

Components Q_{ij} of the matrix [Q] are identical to those of [P] except:

$$Q_{23} = Q_{13} \ M'_2$$

$$Q_{24} = Q_{14} \ M'_2$$

$$Q_{33} = \left(\frac{\alpha_4^2}{3} + \alpha'^2 \ K'_3 \ Y \right) (1 + M'_2)$$

$$Q_{34} = - \bar{m}_1 \ \gamma^2 \ (1 + M'_2) \ K'_2$$

$$Q_{43} = - \left(\bar{m}_2 \ \gamma^2 \cos Y + q^2 \ Y \sin Y \right)$$

$$Q_{44} = - \bar{m}_2 \ \gamma^2 \sin Y + q^2 \ Y \cos Y$$

@Seismicisolation

$$Q_{53} = Q_{43}\ M'_2$$

$$Q_{54} = Q_{44}\ M'_2$$

$$Q_{63} = \left\{ -\bar{m}_2\ \gamma^2\ K'_2\ \sin Y + \left(\frac{\alpha_4^2}{3} + \alpha'^2\ K'_2\ Y \right) \cos Y \right\} \bullet \left(1 + M'_2\right)$$

$$Q_{64} = \left\{ \bar{m}_2\ \gamma^2\ K'_2\ \cos Y + \left(\frac{\alpha_4^2}{3} + \alpha'^2\ K'_2\ Y \right) \sin Y \right\} \bullet \left(1 + M'_2\right)$$

[7.G.7]

M'_j and K'_j are defined by equations [7.105b] and [7.104].

Circular frequency ω is given by:

$$\gamma = \frac{\omega\ L}{\chi_{44}} \qquad [7.G.8]$$

The values of γ are those that set the determinants [7.G.3] and [7.G.6] to zero.

For a rod of geometrical and elastic characteristics, X, Y, Z, K_j, M_j, K'_J and M'_j are functions of γ'.

@Seismicisolation

Chapter 8

Very Low Frequency Vibration of a Rod by Le Rolland-Sorin's Double Pendulum[1]

8.1. Introduction

An original material testing method at very low frequency is presented in this chapter. Le Rolland-Sorin's double pendulum is practically unknown in English-speaking countries, although Kolsky [KOL 63] has mentioned it in his book titled *Stress Waves in Solids*. A great number of apparatuses covering a large frequency range, from ultrasonic waves that nearly reach hyper-frequency to low frequency, such as a fraction of a Hertz, are available for experimenters.

8.1.1. *Frequency range*

At very low frequency range, electric exciters exist and work down some Hertz. Hydraulic exciters replace electric exciters to extend this range to a fraction of a Hertz. However these exciters are clumsy compared to other electrodynamic apparatuses working in the lower acoustic domain (from 50 to 10,000 Hertz).

Table 8.1 presents a classification of apparatuses according to working frequency. As with other methods at low and medium frequency ranges, the double pendulum method permits the elastic compliance measurement S_{ijkl}.

Chapter written by Mostefa ARCHI and Jean-Baptiste CASIMIR.

1 This chapter contains large extracts from Archi's PhD thesis [ARC 87]. Additional information is written by Jean-Baptiste Casimir.

Mechanics of Viscoelastic Materials and Wave Dispersion Edited by Yvon Chevalier and Jean Tuong Vinh
© 2010 ISTE Ltd. Published 2010 by ISTE Ltd.

@Seismicisolation

8.1.2. *Simplicity and ease*

If a comprehensive view covers the whole range of frequencies adopted for material testing, we notice that there are three classes of apparatuses in all experiments: an exciter, a mechanical system for holding the sample, and a set of electronic instruments (including transducers, amplifiers, signal processing, etc.).

In Le Rolland-Sorin's double pendulum there is *no independent external exciter at all*. The pendulums are the mechanical dynamic exciters themselves. The *measurement is reduced to a minimum* (time duration and beating period). Eventually the decreasing of pendulum oscillation amplitude permits us to evaluate the damping coefficient of viscoelastic material characterization using the well-known logarithmic decrement method.

Frequency ranges			
0.1 < f < 10 Hz Very low frequency	8 < f < 50,000 Hz Medium frequency	50 KHz < f < 10 MHz Ultrasound	f > 10 MHz Hyper-frequency
Electric exciter 0.01 < f < 5,000 Hz	Stationary waves (bending extensional, shear)	Progressive waves (dilatational, shear)	Progressive waves (non-conducting materials)
Hydraulic exciter 0.01 < f < 10 Hz			
Double pendulum 0.5 < f < 5 Hz			
Compliance S_{ijkl} $\varepsilon_{ij} = S_{ijkl}\ \sigma_{kl}$		Stiffness C_{ijkl} $\sigma_{kl} = C_{ijkl}\ \varepsilon_{kl}$	Dielectric characterization

Table 8.1. *Classification of material testing methods according to frequency ranges. Situation of double pendulum among other methods in the frequency range*

We think that the method presented here deserves attention in the domain of elastic (and/or viscoelastic) characterization of materials. It is difficult to find a simpler method. The apparatus is easy to construct and the accuracy of the measurements is comparable to those obtained by other testing methods.

@Seismicisolation

8.2. Short bibliography

The double pendulum system was presented by Le Rolland-Sorin [LER 14] as early as 1914. By using a sample rod as a *coupling mechanical element* between two identical gravity pendulums, he noticed that energy is transferred from one pendulum to the other and *vice versa*, see Figure 8.1. By appropriate launching, the pendulums do not oscillate in phase.

One pendulum has an increasing oscillation amplitude while the other's oscillations decrease and tend towards zero. The phenomenon then reverses. The beating period of each pendulum depends on the material elastic moduli (Young's or Coulomb's moduli) and increases with the stiffness of the sample [LER 34].

Attempts were made to make measurements on large and heavy structures [LER 34]. After the Second World War, Giet [GIE 59] afforded improvements on the mounting and sample holding as well as the presentation of the principle method.

Double pendulums were recognized as the simplest method experimenters and technicians could use them in industry for making elastic and viscoelastic measurements of materials at low frequency. It often only requires a simple chronometer! Archie [ARC 87] in his PhD thesis extended the applications to composite material characterization, and even the evaluation of non-diagonal components of a compliance matrix S_{ijkl} using a off-axis rod. Successful attempts have been made to extend applicability of the method to viscoelastic materials.

8.3. Flexural vibrations of a rod using coupled pendulums

Figure 8.1 represents the schematic drawing of the first version of Le Rolland-Sorin's pendulum. The rectangular cross-section sample is clamped at one end and the other end is attached to a platform bearing both pendulums.

Another version of the double pendulum is adopted by Archie [ARC 87], see Figure 8.2. The sample is clamped at both ends and is integral with a platform on which two identical pendulums are posed by their knife edge at both sides of the sample. This new version of the double pendulum is adopted in this chapter.

There are three degrees of freedom, see Figure 8.2, for the mechanical system: the oscillation angles θ_1 and θ_2 of the two pendulums and the horizontal translational motion x of the platform. Lagrange's equations of motion are calculated from the kinetic and potential energies of the sample and platform.

@Seismicisolation

8.3.1. *Lagrange equations of motion*

The kinetic U_c and potential energy U_p are:

$$U_c = \frac{1}{2}\left(m_p \dot{x}^2 + m\left(\dot{x} + l\,\dot{\theta}_1\right)^2 + m\left(\dot{x} + l\,\dot{\theta}_2\right)^2\right) \qquad [8.1]$$

$$U_p = \frac{1}{2}\left(mg\,l\,\dot{\theta}_1^2 + mg\,l\,\theta_2^2 + k\,x^2\right) \qquad [8.2]$$

with m_p being the platform mass and m pendulum mass. k is the translation sample rigidity, g the gravity acceleration, and l is the length of the pendulum[2].

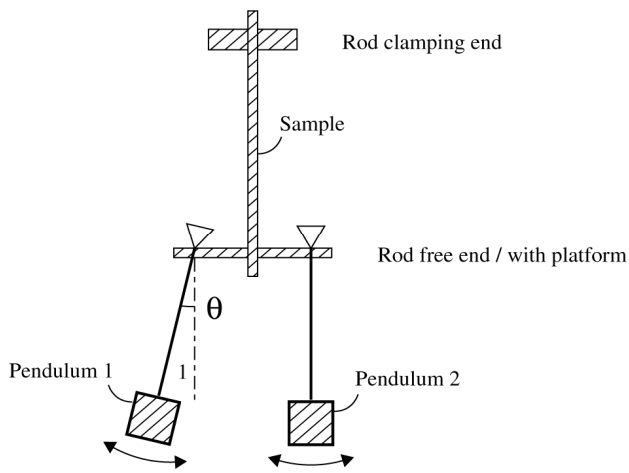

Figure 8.1. *The first version of Le Rolland-Sorin's double pendulum working with sample bending*

Lagrange's equations are deduced. The dot on the letter designates the time derivative of the corresponding variable, see Figure 8.1.

2 It is defined as the distance between the pendulum knife edge to the pendulum's center of gravity.

@Seismicisolation

$$\left.\begin{aligned} m_p\ \ddot{x}\left(\ddot{x}+l\,\ddot{\theta}_1\right)+m\left(\ddot{x}+l\,\ddot{\theta}_2\right)+k\,x=0 \\ ml\left(\ddot{x}+l\,\ddot{\theta}_1\right)+lmg\,\theta_1=0 \\ ml\left(\ddot{x}+l\,\ddot{\theta}_2\right)+lmg\,\theta_2=0 \end{aligned}\right\} \qquad [8.3]$$

after simplification this becomes:

$$\left.\begin{aligned} \ddot{x}\left(m_p+2\,m\right)\ \ddot{\theta}_1\ ml+\ddot{\theta}_2\ ml+k\,x=0 \\ \ddot{x}+l\,\ddot{\theta}_1+g\,\theta_1=0 \\ \ddot{x}+l\,\ddot{\theta}_2+g\,\theta_2=0 \end{aligned}\right\} \qquad [8.4]$$

The pendulums are supposed to be simple for the first presentation.

To obtain a non-trivial solution, the determinant of coefficients in equation [8.4] is set to zero.

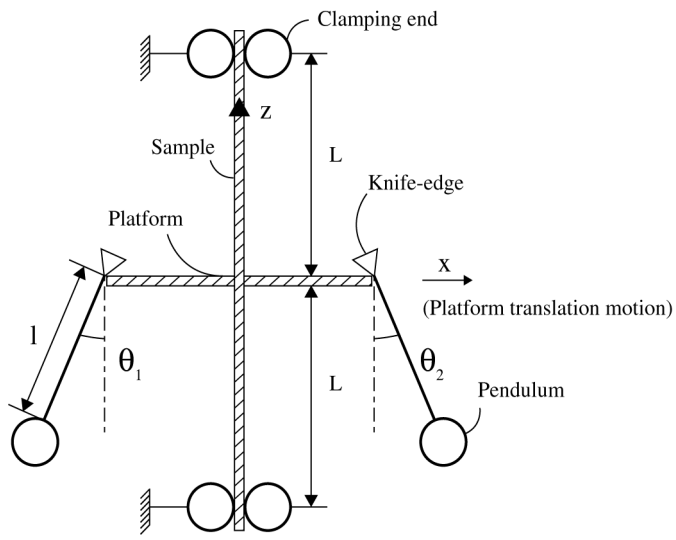

Figure 8.2. *Schematic diagram of the double pendulum with bending motion of the sample clamped at both ends. The pendulums oscillate in plane z x of the sample*

@Seismicisolation

8.3.2. *Eigenvalue equation*

$$\begin{vmatrix} k-\omega^2\left(m_p+2m\right) & -ml\omega^2 & -ml\omega^2 \\ -\omega^2 & g-l\omega^2 & 0 \\ -\omega^2 & 0 & g-l\omega^2 \end{vmatrix} = 0 \qquad [8.5]$$

By developing equation [8.5] we get:

$$\left[k-\omega^2\left(m_p+2m\right)\left(g-l\omega^2\right)-2m\,l\,\omega^4\left(g-l\,\omega^2\right)\right]=0 \qquad [8.6]$$

a solution that corresponds to $\omega_1^2 = g/l$. This gives the eigenfrequency of the pendulums ω_1.

The second factor of the developed determinant is:

$$\left[k-\omega^2\left(m_p+2m\right)\right]\left(g-l\,\omega^2\right)-2\,m\,l\,\omega^4=0 \qquad [8.7]$$

or by arranging in increasing power of ω:

$$\omega^4\left(l\,m_p\right)-\omega^2\left[k\,l+g\left(m_p+2m\right)\right]+kg=0 \qquad [8.8]$$

the two roots of [8.8] are positive.

The greatest root corresponds to motion at the highest frequency. This higher mode of vibration tends to disappear rapidly with time. The lowest mode remains and it can easily be shown that the corresponding circular frequency is lower than the pendulum eigen circular frequency.

$$\omega_2 < \omega_{pendulum} = \omega_1 \qquad [8.9]$$

In Appendix 8.A, practical considerations of the set-up are indicated so that this inequality is satisfied.

@Seismicisolation

8.3.3. *Solutions for pendulum oscillations*

The solutions $\theta_1(t)$ and $\theta_2(t)$ depend on the initial conditions adopted for the pendulums.

$$t = 0 \quad \theta_1 = \theta_0, \quad \dot{\theta}_2 = \quad \theta_2 = \dot{\theta}_1 = \dot{x} = x = 0 \qquad [8.10]$$

The platform is initially at rest, as is the second pendulum. Pendulum 1 is launched at $\theta_1 = \theta_0$ and without initial angular velocity $\dot{\theta}_1 = 0$. In Appendix 8.A, details of the calculations of $\theta_1(t)$ are presented using Laplace transform.

Taking the practical construction of the pendulums into account, we have to deal with the coupling of two mechanical oscillators of eigenfrequencies ω_1 and ω_2.

As both pendulums are identical and only the first pendulum is launched at amplitude θ_0 without initial velocity, the two pendulums oscillate in phase opposition, see Appendix 8.B.

$$\left.\begin{aligned} \theta_1(t) &= \theta_0 \cos\left(\frac{\omega_1 + \omega_2}{2}\right) t \,.\, \cos\left(\frac{\omega_1 - \omega_2}{2}\right) t \\ \theta_2(t) &= \theta_0 \sin\left(\frac{\omega_1 + \omega_2}{2}\right) t \,.\, \sin\left(\frac{\omega_1 - \omega_2}{2}\right) t \end{aligned}\right\} \qquad [8.B.19]$$

The beating of the two oscillators takes place and in equation [8.B.19] the envelope of oscillation corresponds to a beating period:

$$\tau = \frac{2\pi}{\omega_1 - \omega_2} \qquad [8.11]$$

8.3.4. *Relationship between beating period and sample stiffness k*

8.3.4.1. *Stiffness calculation*

Expanding equation [8.6] by setting $\omega_1^2 = g/l$ and $\omega_2 = \omega$, the lower circular eigenfrequency is the root of the following equation:

$$\left[k - \omega^2 \left(m_p + 2\,m\right)\right] \left(g - L\,\omega^2\right) - 2\,m\,L\,\omega^4 = 0 \qquad [8.12]$$

@Seismicisolation

or:

$$k\left(g - L\,\omega^2\right) = \omega^2\left(m_p + 2\,m\right)g - \omega^4\,m_p\,L$$

The sample stiffness is deduced as follows:

$$k = \frac{\left(m_p + 2\,m\right)\omega^2\,g}{\left(g - L\,\omega^2\right)} - \frac{\omega^4\,m_p\,L}{\left(g - L\,\omega^2\right)}$$

$$k = \frac{\left(m_p + 2\,m\right)\omega^2\,\frac{g}{L}}{\left(\frac{g}{L} - L\,\omega^2\right)} - \frac{\omega^4\,m_p}{\left(\frac{g}{L} - \omega^2\right)}$$

$$k = \frac{\left(m_p + 2\,m\right)\omega_2^2\,\omega_1^2}{\left(\omega_1^2 - \omega_2^2\right)} - \frac{\omega^4\,m_p}{\left(\omega_1^2 - \omega_2^2\right)} \qquad [8.13]$$

Using the variable δ, defined as follows, with τ being the beating period:

$$\delta = \frac{T_1}{\tau} = \frac{\omega_1 - \omega_2}{\omega_1}; \qquad \tau = \frac{2\,\pi}{\omega_1 - \omega_2} \qquad [8.14]$$

$$\omega_2 = \omega_1\,\left(1 - \delta\right) \qquad [8.15]$$

Bringing equations [8.14] and [8.15] into [8.12]:

$$k = \frac{\left(m_p + 2\,m\right)\left(1 - \delta\right)^2}{\delta\left(2 - \delta\right)}\,\omega_1^2 - \frac{\left(1 - \delta\right)^4}{\delta\left(2 - \delta\right)}\,m_p\,\omega_1^2 \qquad [8.16]$$

or

$$k = \omega_1^2\left[m_p + \frac{2\,m}{\delta\,\left(2 - \delta\right)}\right]\left(1 - \delta\right)^2 \qquad [8.17]$$

@Seismicisolation

the sample stiffness depends on the relative beating period δ in equation [8.16], m and m_p being the parameters of the pendulum system itself.

8.3.4.2. *Young's modulus calculation*

Young's modulus is related to sample stiffness by a classical formula used in the strength of material. k, the sample bending rigidity, is related to the relative beating period by [8.16] or [8.17]

$$k = \frac{48\,E\,I}{l^3} \qquad [8.18]$$

The sample is clamped at both ends and a platform is attached in its middle. As the platform is associated with the sample, some cautions are necessary for fixing the platform so it does not slide. The platform being clamped in the middle of the sample, the length of the sample consequently necessitates a correction when calculating sample elastic or viscoelstic moduli.

In equation [8.18], I is the inertia moment of the sample:

$$I = \frac{b\,h^3}{12},$$

where b is width and h thickness.

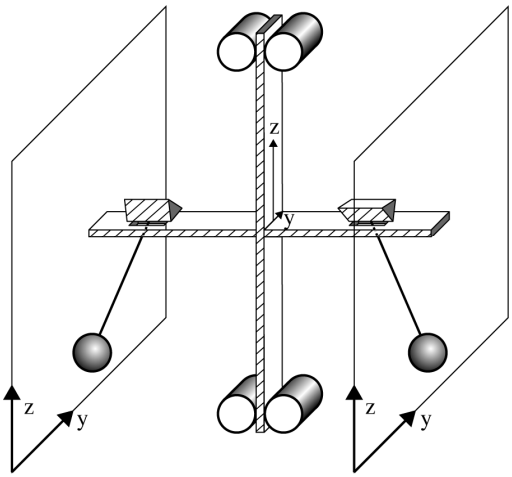

Figure 8.3. *Schematic drawing of a torsional double pendulum. The pendulums oscillate in the plane (z y)*

@Seismicisolation

8.4. Torsional vibration of a beam by double pendulum

Figure 8.3 shows a schematic drawing of the double pendulum. The knife edge of each pendulum is perpendicular to the plane z y of the beam; z being the beam axis and y the width direction. The two pendulums oscillate in plane z y and create the torsional motion of the beam. Two rectangular holes are created on the platform so as to permit the pendulum arms to move in the indicated plane.

8.4.1. *Equations of torsional motions*

Let θ_p be the rotation angle of the platform, with θ_1 and θ_2 being rotation angles of the two pendulums.

8.4.1.1. *Energy expression*

The potential and kinetic energies are:

$$U_p = \frac{1}{2}\left(C\,\theta_p^2 + m\,g\,l\,\theta_1^2 + m\,g\,l\,\theta_2^2\right)$$

$$U_c = \frac{1}{2}\left[I_p\,\dot{\theta}_p^2 + m\left(L_p\,\dot{\theta}_p + l\dot{\theta}_1\right)^2 + m\left(L_p\,\dot{\theta}_p + l\,\dot{\theta}_1\right)^2\right] \qquad [8.19]$$

(where the dot on the letter designates time derivative).

Lagrange's equations of motion are deduced:

$$\left.\begin{aligned} I_p\,\ddot{\theta}_p + m\left(L_p\,\ddot{\theta}_p + l\,\ddot{\theta}_1\right)L_p + m\left(L_p\,\ddot{\theta}_p + l\,\ddot{\theta}_2\right)L_p + C\,\theta = 0 \\ m\left(L_p\,\ddot{\theta}_p + l\,\ddot{\theta}_1\right)l + m\,g\,l\,\theta_1 = 0 \\ m\left(L_p\,\ddot{\theta}_p + l\,\ddot{\theta}_2\right)l + m\,g\,l\,\theta_2 = 0 \end{aligned}\right\} \qquad [8.20]$$

where I_p designates the inertia moment of the platform, m pendulum mass, L_p pendulum length and g gravity acceleration. In equation [8.20], C designates the

@Seismicisolation

torsional stiffness of the sample per unit length, where l is the half-length of the sample:

$$C = \frac{2\,C_T}{l_1} \qquad [8.21]$$

where C_T is torsional stiffness, as defined previously in Chapter 5, equation [5.23].

Arranging equation [8.20], we obtain the following equations:

$$\left.\begin{aligned} \left(I_p + 2\,m\,L_p^2\right)\ddot{\theta}_p + m\,l\,L_p\,\ddot{\theta}_1 + m\,l\,L_p\,\ddot{\theta}_2 + C\,\theta_p = 0 \\ L_p\,\ddot{\theta}_p + l\,\ddot{\theta}_1 + g\,\dot{\theta}_1 = 0 \\ L_p\,\ddot{\theta}_p + l\,\ddot{\theta}_2 + g\,\theta_2 = 0 \end{aligned}\right\} \qquad [8.22]$$

Comparing equation [8.22] to [8.4], we notice that the two sets of equations are similar. The solutions obtained previously for flexural vibrations can be transposed here by changing the corresponding coefficients:

$$C = \left[\frac{(1-\delta)^2}{\delta(2-\delta)}\left(I_p + 2\,m\,L_p^2\right) - \frac{(1-\delta)^4\,I_p}{\delta\,(2-\delta)}\right]\omega_1^2$$

$$C = \omega_1^2\,(1-\delta)^2\left[I_p + \frac{2\,m\,L_p^2}{\delta\,(2-\delta)}\right] \qquad [8.23]$$

$$C = 2\,\frac{C_T}{l} \qquad [8.24]$$

In Chapter 5, the torsional stiffness of a rod with rectangular section is given by the following equation:

$$C_T = b\,h^3\,G_{xz}\,\beta_T\,(c) \qquad [5.30]$$

and $\beta_T(c)$ is a function given in Chapter 5, with:

@Seismicisolation

$$c = \frac{b}{h}\sqrt{\frac{G_{yz}}{G_{xz}}}$$

b being the width, h thickness, and G_{yz} and G_{xz} shear moduli in the planes yz and xz respectively. In the case of an isotropic sample under square root radical, the ratio of two shear moduli are equal to 1. c is then reduced to b/h.

Various steps of shear modulus calculation are similar to that used previously for Young's modulus by the bending test presented above.

Figure 8.4 gives a record of one of the pendulum oscillations against time. It concerns a torsion test.

Figure 8.5 corresponds to a bending test. The beating period is larger than the one presented in Figure 8.3. This is due to the fact that the shear modulus is much smaller than Young's modulus.

In Figure 8.6, a schematic diagram gives the successive calculation operations for torsion and bending tests. The reader will notice that measurements are reduced to a minimum. The beating period of one pendulum is the only unique measurement. Often the period exceeds 5 or 10 minutes, and time measurement necessitates only a classical manual chronometer with 1/100 of second accuracy.

8.5. Complex compliance coefficient of viscoelastic materials

8.5.1. *General consideration*

Using a double pendulum, the question is: is it possible to use the amplitude decrease of one pendulum oscillation to evaluate complex compliance by using a logarithmic decrement method?

In the framework of viscoelasticity theory, the amplitude decrease, in free oscillations of the sample, is related to complex circular frequency. By evaluating logarithmic decrement of one pendulum oscillations, it is possible to measure the sample damping coefficient; on the condition that we have to deal with the damping coefficient which must be not too high to adopt such measurement method.

$\mathrm{Tan}\delta_E$ (or $\tan \delta_G$) $\leq$ The problem is to relate the imaginary part of the material viscoelastic moduli in circular frequency ω^h:

@Seismicisolation

$$\omega^* = \text{Re}\ \omega^* + j\ \text{Im}\ \omega^*$$

$$\omega^* = \omega' + j\ \omega'' \qquad [8.25]$$

in which ω^* can be calculated *versus* the complex stiffness of the sample. The complex stiffness is a function of complex circular frequency:

$$k^* = k^*(\omega^*, \text{dimensions of sample}) \qquad [8.26]$$

The condition by which we can obtain k* in equation [8.26] depends explicitly on the single complex circular frequency.

Let us recall the eigenfrequency of the set constituted by the platform and the elastic sample:

$$\omega_p^2 = \frac{k}{m}$$

The viscoelastic sample rigidity k* in equation [8.26] being complex for viscoelastic material, for the bending test we write:

$$\left(\omega_p^*\right)^2 = \frac{k^*}{m_p} = \frac{k_1 + j\,k_2}{m_p} \qquad [8.27]$$

The two square roots are:

$$\omega_p^* = \begin{cases} \omega_p' + j\ \omega_p'' \\ \omega_p' - j\ \omega_p'' \end{cases} \qquad [8.28]$$

with:

$$\omega_p' = \sqrt{\frac{k_1^2 + k_2^2}{m_p}} \bullet \text{Re}\left[e^{i\gamma}\right] \qquad [8.29]$$

@Seismicisolation

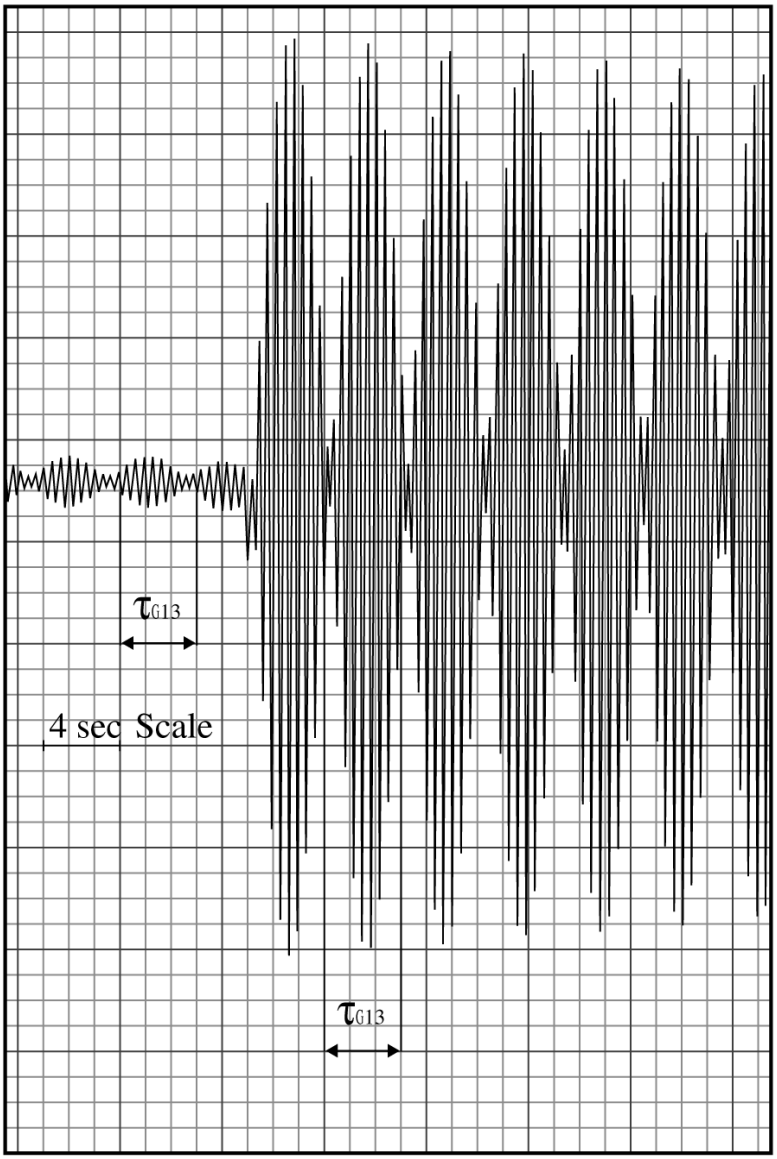

Figure 8.4. *A record of torsion oscillations of one pendulum. The first oscillations are parasitic ones. Beating periods are easy to measure by chronometer with an accuracy of 1/100 of a second*

@Seismicisolation

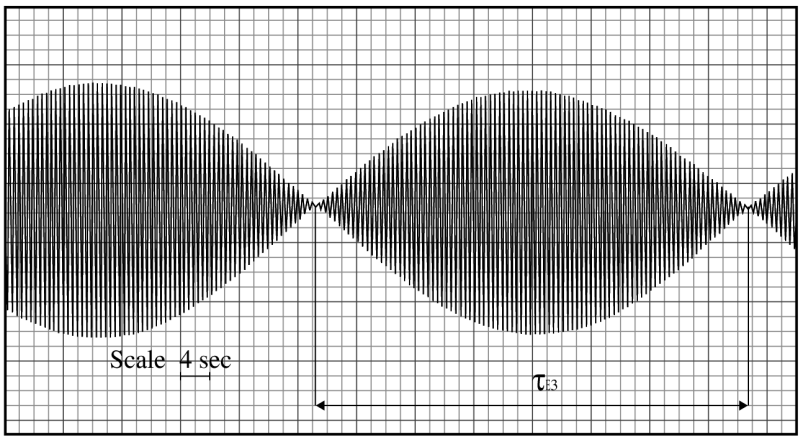

Figure 8.5. *Bending test with a double pendulum. Beating period τ is much larger than the period of each pendulum. The measurement of τ is made with accuracy*

$$\gamma = \frac{1}{2} \text{ Arc tang } \frac{k_2}{k_1} + k\,\pi\,; \qquad k = 1, 2, \ldots \qquad [8.30]$$

The two roots in equation [8.28] are complex conjugate.

8.5.2. *Expression of (ω_1-ω_2)*

The expression of oscillation amplitude of the first pendulum is shown in Appendix 8.B. The solution to equation [8.B.6] is in elastic regime:

$$\theta_1\,(t) = \left[\theta_1\,(0)\,\cos\frac{\omega_1 - \omega_2}{2}\,t\right]\cos\frac{\omega_1 + \omega_2}{2}\,t \qquad [8.B.6]$$

where ω_1 is the circular frequency of the pendulum. ω_2s the lower circular eigenfrequency of the system. Its value is given in Appendix 8.A, equation [8.A.17]:

$$\omega_2^2 = \frac{\omega_p^2}{2}\left(\frac{a}{m_p}\,\alpha^2 + 1\right)\left[1 - \left\{1 - \frac{4\,\alpha^2}{\left(1 + \frac{a}{m}\,\alpha^2\right)^2}\right\}^{0.5}\right] \qquad [8.A.17]$$

@Seismicisolation

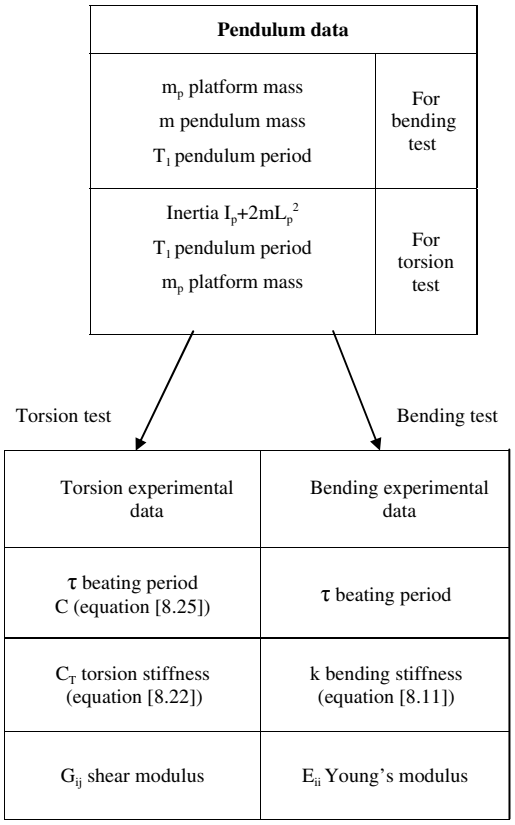

Figure 8.6. *Successive steps of calculation. Left: torsion test. Right: bending test. The measured beating period of pendulums permits the evaluation of shear modulus and Young's modulus*

$a = m_p + 2\,m$ (platform and the two pendulum masses).

$$\alpha = \frac{\omega_1}{\omega_p} << 1, \qquad \omega_p^2 = \frac{k}{m_p} \qquad [8.31]$$

Let us expand equation [8.A.17], presented in Appendix 8.A, and take equation [8.31] into account:

@Seismicisolation

$$\omega_2^2 = \frac{\omega_p^2}{2}\left(\frac{a}{m_p}\ \alpha^2 + 1\right)\left\{1-\left[1-2\ \alpha^2\ \left(1-\frac{2\,a}{m_p}\ \alpha^2\right)\right]\right\}$$

$$\omega_2^2 \simeq \frac{\omega_p^2}{2}\left(\frac{a}{m_p}\ \alpha^2 + 1\right) 2\ \alpha^2\ \left(1-\frac{2\,a}{m_p}\ \alpha^2\right) \qquad [8.32]$$

$$\omega_2 \simeq \omega_p\left(\frac{a\ \alpha^2}{2\ m_p} + 1\right)\alpha^2\ \left(1-\frac{a}{m_p}\ \alpha^2\right)$$

With limited expansion of equation [8.32] we obtain:

$$\omega_1 - \omega_2 = \omega_p\,\alpha^3(a/2m_p) = (a/2m_p)\ (\omega_1{}^3/\omega_p{}^2) \qquad [8.33]$$

8.5.3. *Utilization of correspondence principle to obtain complex sample rigidity*

Chapter 2 presents the main ideas in applied viscoelasticity. On the condition that boundary conditions remain the same, the elastic solution as well as equations of motion can be transposed in viscoelasticity.

The damping of pendulums is supposed to be weak and negligible compared to the sample damping. Then in equations [8.32] and [8.33], ω_1 the circular eigenfrequency of each pendulum remains practically real. The additional condition to be satisfied is that ratio α in equation [8.31] remains also practically real.

$$|\ \alpha^*\ | = \left|\ \frac{\omega_1}{\omega_p^*}\ \right| \cong \frac{\omega_1}{\left|\omega_p^*\right|} \cong -\frac{\omega_1}{\mathrm{Re}\ \omega^*{}_p} << 1 \qquad [8.34]$$

Damping of the sample must consequently remain weak. This condition is adopted practically to use logarithmic decrement method to evaluate the damping coefficient.

Then equation [8.34] can be transposed into viscoelasticity as follows:

$$\omega_1 - \omega^*{}_2 = \left(\frac{a}{2\ m_p}\right)\frac{\omega_1^3}{\left(\omega_p^*\right)^2} \qquad [8.35]$$

@Seismicisolation

8.5.3.1. *Expression of pendulum oscillation θ_1 (t)*

Equation [8.B.6] is rewritten for a viscoelastic sample:

$$\theta_1(t) = \theta_1(0)\cos\left[\frac{\omega_1 - \omega^*_2}{2}t\right]\cos\frac{\omega_1 + \omega_2{}^*}{2}t \qquad [8.36]$$

This equation is not easy to use. We must find a general solution for $\theta_1(t)$.

A solution under the following form is attributed to θ_1 see equation [8.A.13] in which the third term is neglected:

$$\theta_1(\tau)=[\theta_1(0)/2]\{\cos\omega_1 t + e^{-(\omega''2t)}\ (\omega'_2 t - \omega''_2 t/\omega'_2 t\ \sin\omega'_2{}'t) \qquad [8.37a]$$

This equation apparently differs from the usual expression obtained for beating phenomenon. The factor $\exp(\omega''_2 t)$ being less different from 1, the association of the first and second term in [8.37a] can give rise to the wave envelope indicated between the brackets in [8.37b].

$$\theta_1(t) \cong \theta_1(0)\ e^{-\omega''_2 t}\left\{\cos\underbrace{\left[(\omega_1 - \omega'_2)\ \frac{t}{2}\right]}_{\text{wave envelope}}\right\}\cos\omega_1 t \qquad [8.37b]$$

Retuning to [8.37a] we can see that:

$$\omega_2''= (1/nT)\ \mathrm{Ln}[2\theta_T / \boldsymbol{\theta}_1(0)]$$

Ln designates Naeperian logarithm, and n is the number of sinusoidal envelopes. That constitutes the classical definition of logarithmic decrement.

8.5.3.2. *Evaluation of complex stiffness and Young's modulus*

Equation [8.31] permits us to deduce k from the difference $\omega_1 - \omega^*_2$:

$$(\omega_1 - \omega'_2) - j\,\omega''_2 = \frac{a\,\omega_1^3}{2}\ \frac{1}{k_1 + j\,k_2}$$

$$\omega''_2 = \frac{a\,\omega_1^3}{2}\ \frac{k_2}{k_1^2 + k_2^2} \quad \text{with} \quad k_1^2 >> k_2^2$$

@Seismicisolation

$$\omega''_2 \cong \frac{a\,\omega_1^3}{2}\,\frac{k_2}{k_1^2} \quad \text{with} \quad a = m_p + 2m \qquad [8.38]$$

The real part of stiffness k_1 was evaluated previously by measuring the beating period τ, in equation [8.17].

Young's modulus can thus be calculated using equation [8.16].

8.5.3.3. *Complex shear modulus*

Equations similar to the aforementioned equations for Young's modulus can then be written.

Torsional stiffness is found in equation [8.24]. Equation [8.38] is replaced by:

$$\omega''_2 \cong \frac{a\,\omega_1^3}{2}\,\frac{C''_T}{C'^2_T} \qquad [8.39]$$

C^*_T is complex torsional stiffness:

$$C^*_T = C'_T + j\,C''_T \qquad [8.40]$$

and C^*_T complex replaces C_T in equation [8.31].

8.6. Elastic stiffness of an off-axis rod

An off-axis rod is used for anisotropic materials so as to evaluate non-diagonal compliance matrix coefficients.

In Chapter 6, when analyzing the bending vibration of rods, such off-axis rods are used.

Inevitably couplings between two (or more) vibration modes (torsional, extensional and bending) occur. The degree of differential equations of motion is expected to be higher than three. That is the price we pay for evaluating non-diagonal matrix coefficients.

@Seismicisolation

8.6.1. *Elementary equations of motion*

Here we present the first approximation of the problem of torsional or bending vibration of a rod. In the double pendulum oscillation problem, frequency range is restricted to the lowest frequency ($0.1 < f < 10$ Hz). We can ignore the dispersion problem. The dispersion problem justifies the use of nearly static theory to describe coupling between bending and torsion modes in samples.

8.6.1.1. *Practical aspects concerning measurements*

When coupling between two kinds of vibrations is to be accounted for, two kinds of measurements – for example linear and angular displacements – are desirable. On practical grounds, it might complicate the experimental set-up, at least regarding the choice of transducers.

When choice is restricted to one kind of transducer, one of the possibilities is to adopt an elementary theory of vibration. To return to Le Rolland-Sorin's double pendulum method, one elementary hypothesis consists of adopting the following ideas:

– some non-diagonal matrix coefficients intervene in the expression of sample stiffness;

– the measured displacement (torsional or flexural) is predominant. The other displacement is neglected.

8.6.1.2. *Flexural vibration of rod*

In Appendix 8.C, equation [8.C.3a] gives the Young's modulus.

$$E'_{33} = \frac{1}{s'_{33}} \qquad [8.41]$$

With [s] being the compliance matrix coefficients previously evaluated with an on-axis rod, the non-diagonal matrix coefficient s_{13} can be evaluated, α being the rotation angle. With respect to the new reference axes related to an off-axis rod; the non-diagonal compliance matrix coefficient we want to evaluate is:

$$s'_{13} = s'_{13} \left(s_{11}, s_{44}, s_{33}, \alpha\right) \qquad [8.42]$$

8.6.1.3. *Expression of bending displacement v*

Appendix 8.D gives details on the mathematical formulation of this problem. The general formula relating bending moment M to bending displacement v is proposed by Johnson [JOH 71]:

@Seismicisolation

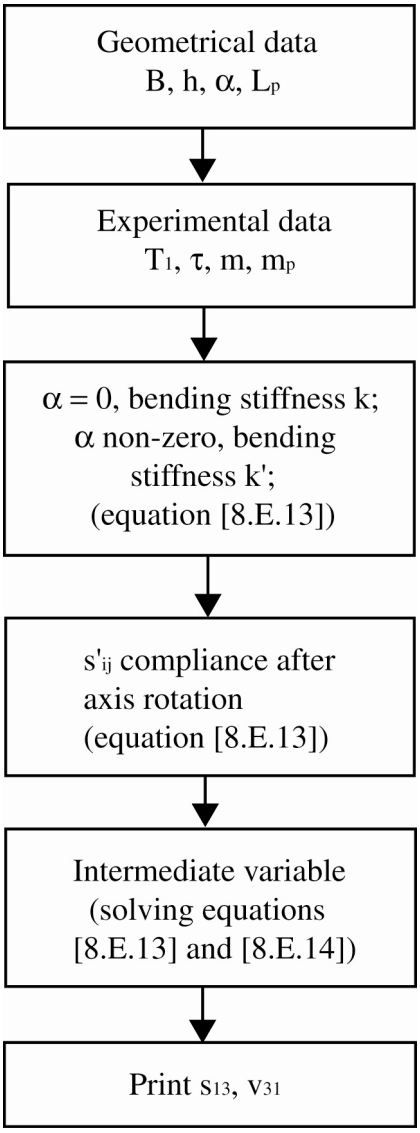

Figure 8.7. *Schematic diagram of successive steps in the calculation of s_{13} and γ_{31} from bending tests*

@Seismicisolation

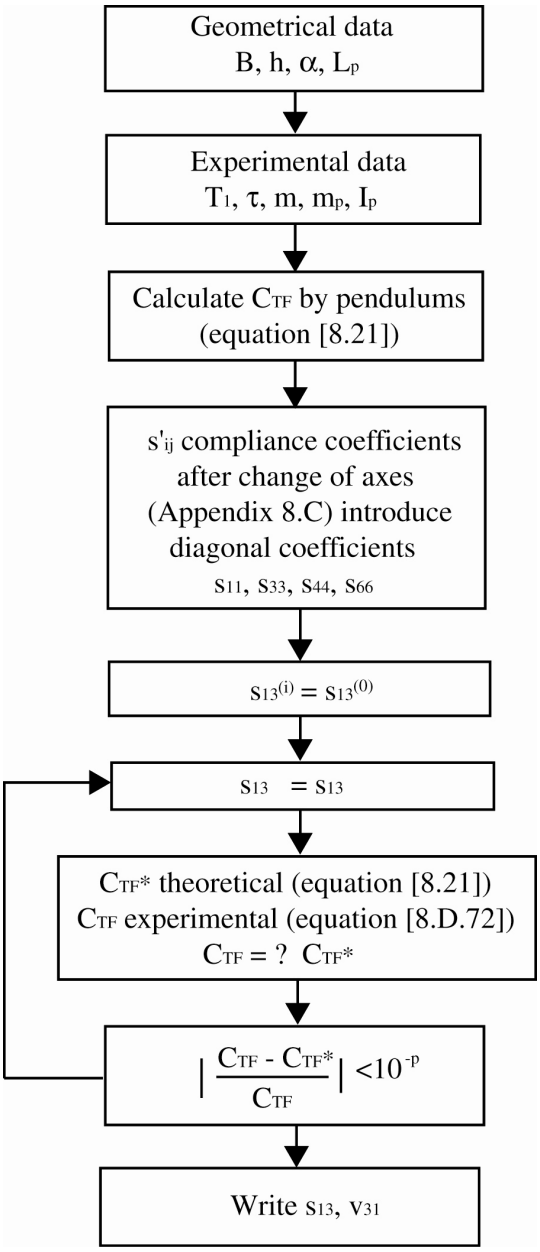

Figure 8.8. *Schematic diagram showing successive steps for calculations of s_{13}, ν_{31} by torsion tests*

@Seismicisolation

$$v = \frac{M\,L^2\,s_{33}}{8\,I\left(1 + \frac{3}{4}\,A_{35}^2\,M^*\right)} \qquad [8.43]$$

$$A_{35}^2 = \frac{s_{35}^2}{s_{33}^2},$$

where v is bending displacement, 2L the length of the sample and I the inertia moment of the section. Parameter M^* portrays the coupling bending-torsion, and M designates the bending moment applied at the support. Equation [8.43] shows that stiffness increases for an off-axis rod in the case of both ends being clamped.

Various approximate formulae for M* can be found in Appendix 8.D.

Calculation of non-diagonal coefficient s_{13} and Poisson's coefficients ν_{31} requires experimental evaluation of stiffness k and k′. k corresponds to the on-axis rod, (z = 3) and k′ to the off-axis rod. k′ depends on geometrical sample data and pendulums on one hand and, on the other hand, it depends on a set of compliance matrix coefficients s_{ij} in which non-diagonal coefficient s_{35} appears that describes the coupling between two modes of rod deformation: bending and torsion.

Details of calculations can be found in Appendix 8.E for the evaluation of s_{13} and ν_{31}. They serve to write the computer program shown in Figure 8.7.

8.6.1.4. *Torsional vibration of rod*

The torsional stiffness $C_{T\ forced}$ is given by equation [8.D.62] in Appendix 8.D.

$$C_{Tf} = \frac{b\,h^3}{4}\,\frac{M}{s'_{33}} \qquad [8.D.62]$$

M* is to be chosen from among various approximate formulae gathered in the Table 8.D.1 (Appendix 8.D). The simplest formula is:

$$M^* = M^*_1 = \frac{10}{9}\,\frac{1}{\lambda^2\,\left(A_{44} + B_{55}\right)} \qquad [8.D.70]$$

@Seismicisolation

$$A_{44} = \frac{s'_{44}}{s'_{33}}, \quad B_{55} = \frac{s'_{55}}{s'_{33}} - \left(\frac{s'_{35}}{s'_{33}}\right)^2 \qquad [8.D.68]$$

where s'_{ij} designates the coefficient of compliance matrix after a change of axis by rotation (ALPHA) around axis 3. Details of calculation of compliance:

$$s_{13} = s_{13}\left(s_{11}, s_{33}, s_{44} = s_{55}, \lambda, \gamma\right) \qquad [8.D.69]$$

using a set of intermediate variables can be found in section 8.E.1 of Appendix 8.E.

Figure 8.8 gives a synopsis of successive steps of calculations. Equations [8.42] and [8.43] suggest the evaluation of s'_{33}. Appendix 8.E contains details of the calculations of s_{13} and Poisson's number γ_{31} by torsional and bending rod vibrations (see Figure 8.7 and Figure 8.8).

8.6.2. *Higher approximation equations of motion*

The simultaneous torsional and bending displacement of the platform must both be taken into account. Let us globally evaluate the degree of differential equations of motion of the whole system constituted by: a) two pendulums; b) flexural motion; and c) torsional motion.

The items b) and c) concern Timoshenko's equations and Barr's equation respectively. Both must include coupling terms, as we have seen in Chapter 6, which are devoted to the bending vibrations of a rod. The fourth-order of the two last items with two degrees of freedom for the double pendulum leads to the equations of motion being of tenth order.

Solutions for such equations are possible but the calculations are laborious. The main difficulty in solving the inverse problem for evaluating compliance matrix coefficients resides in the fact that a set of elastic coefficients are involved in the equations of motion. The problem becomes intractable if we have to evaluate more than two compliance coefficients s'_{44} or s'_{55} [3], unless an elaborate optimization program on a computer is referred to.

3 The prime at the superscript designates compliance coefficient of off-axis rod after change of reference axes.

@Seismicisolation

The second difficulty can be met in the solution of elastic equations using an Airy stress function φ and shear stress function ψ. There are many solutions with various degrees of approximations – Rayleigh-Ritz, Kantorovich and Krylov. Johnson [JOH 71] has published a very comprehensive paper on this problem.

Abarcar and Cunniff [ABA 72] and Ritchie and Rosinger [RIT 75] have published papers analyzing transverse isotropic and orthotropic materials respectively. Nugues [NUG 76] has proposed an approximate formula, which is presented in Appendix 8.D.

On experimental grounds, if the coupling phenomenon between torsional and bending vibrations must be taken into account, measurements on pendulums need to be improved, i.e. the torsional angle and bending displacement require our attention.

Further experiments with more accurate pendulum measurements have yet to be made, although we are convinced that such research is possible.

8.7. Bibliography

[ABA 72] ABARCAR R. B., CUNIFF F. F., "The vibrations of cantilever beam of fibre reinforced materials", *Journal of Composite Materials*, vol. 6, p. 504, 1972.

[ARC 87] ARCHI M., Evaluation of elastic constants of composite material by Le Rolland-Sorin's coupled pendulum, PhD thesis, Conservatoire National des Arts et Métiers, Paris, I.S.M.C.M. Saint Ouen, France, 1987.

[GIE 59] *On the Determination of Material Elastic Constants by Forced Vibrations,* GAMI Review, 1959.

[JOH 71] JOHNSON A. F., *Bending and Torsion of Anisotropic Beams,* National Physics Laboratory, England, DNAM Report, March, 1971.

[KAN 58] KANTOROVICH L. V., KRYLOV V. I., *Approximate Methods of Higher Analysis,* Groninger, Noordhoff, Netherlands, 1958.

[KER 68] KERR A., "An extension of Kantorovich method", *Quarterly Applied Mathematics*, July, p. 219, 1968.

[KOL 63] KOLSKY H., *Stress Waves in Solids*, Dover Phoenix Editions, New York, p. 132-136, 1963.

[LER 14] LE ROLLAND P., "On the determination of the ratio of oscillation durations of two pendulums", *Comptes Rendus Académie des Sciences*, vol. 159, 1914.

[LER 33] LE ROLLAND P., *On a New Method of Evaluation of Paris*, 1933.

@Seismicisolation

[LER 34] LE ROLLAND P., *About a Method using Coupling Between two Oscillating Systems to Evaluate Mechanical Strength of Structures and Elastic Moduli,* paper no. 47, Scientific and Technical Publication of Air Force Ministry, 1934.

[LER 48] LE ROLLAND P., "About a new method for the determination of intense solid friction and the energy dissipation", *Comptes rendus Académie des Sciences*, vol. 227, p.37, 1948.

[NUG 76] NUGUES M., Study of elastostatic torsion of a beam with rectangular cross section – Dynamic torsion of anisotropic beam, Masters thesis, 1976.

[RIT 75] RITCHIE I. G., ROSINGER H. E., "Torsional rigidity of rectangular section bars of orthotropic materials", *Journal of Composite Materials*, vol. 9, p. 187-190, 1975.

8.8. List of symbols

$A_{pq} = \frac{s_{pq}}{s_{33}}$	dimensional compliance coefficient
b	width
$c = \frac{b}{h}\sqrt{\frac{G_{yz}}{G_{xz}}}$	coefficient used in [5.25]
C_T	torsional stiffness (equation [5.29b])
C^*_{Tf}	theoretical stiffness
C_{Tf}	experimental stiffness
C	torsional stiffness = $\frac{2\ _T}{l}$
E, E_{ii}	Young's modulus (i indicates the direction)
G, G_{ij}	shear modulus (ij indicates the plane where shear effect is produced
h	thickness
k	bending stiffness

@Seismicisolation

l	pendulum length
m	pendulum mass
m_p	platform mass
M	bending moment
M_t	torsional couple
M^*_i	bending-torsion coupling – i concerns the approximation degree (rank)
s_{ij}	compliance coefficient
s'_{ij}	compliance coefficient after reference axes change
T_l	natural oscillation period of each pendulum
α	angle between fiber axis and rod axis
$\delta = \frac{T_l}{\tau}$	quotient of pendulum period to beating period
τ	beating period
$\omega_l = \frac{g}{L}$	circular frequency of pendulum $= \frac{2\,T}{T_l}$
ω_2 , ω_3	eigenfrequency of the system
θ_1 , θ_2	angular displacement of pendulums
$\lambda = \frac{b}{h} = \frac{\text{thickness}}{\text{width}}$	flatness of the section

@Seismicisolation

8.9. Appendices

Appendix 8.A. Closed-form expression of θ_1 or θ_2 oscillation angles of the pendulums and practical considerations

Laplace transform is used to find θ_1 (t) or θ_2 (t). The difference between the two variables is due to the initial conditions. Let us start with equations [8.4] and [8.10]. Capital letters designate the Laplace transform:

$$X(p) = \int_0^\infty e^{-pt}\, x(t)\, dt \qquad [8.A.1]$$

$$\Theta_I(p) = \int_0^\infty e^{-pt}\, \theta_i(t)\, dt, \quad i = 1, 2 \qquad [8.A.2]$$

From equation [8.10] and with the initial conditions indicated above, Laplace transforms are presented in the second members of the following equations:

$$\frac{d^2\theta_1}{dt^2} \supset p^2\Theta_1 - \dot{\theta}_1(0) - p\,\theta_1(0) = p^2\Theta_1 - p\,\theta_1(0)$$

$$\frac{d^2\theta^2}{dt^2} \supset p^2\Theta_2 \qquad [8.A.3]$$

$$\frac{d^2X}{dt^2} \supset p^2 X(p)$$

Bringing equation [8.A.3] into [8.4] and rearranging, we get:

$$\left.\begin{aligned} &(a\,p^2 + k)\,X + (m\,L\,p^2)\,\Theta_1 + (m\,L\,p^2)\,\Theta_2 = m\,L\,p\,\theta_1(0) \\ &p^2 X + (L\,p^2 + g)\,\Theta_1 + 0 = L\,p\,\theta_1(0) \\ &p^2 X + 0 + (p^2 L + g)\,\Theta_2 = 0 \end{aligned}\right\} \qquad [8.A.4]$$

@Seismicisolation

with $a = m_{pl} + 2\,m$.

The coefficient determinant in [8.A.4] is:

$$D\,(p) = \begin{vmatrix} \left(a\,p^2 + k\right) & mLp^2 & mLp^2 \\ p^2 & \left(Lp^2 + g\right) & 0 \\ p^2 & 0 & \left(L\,p^2 + g\right) \end{vmatrix}$$

$$D\,(p) = \left(p^2\,L + g\right)^2\,\left(a\,p^2 + k\right) - 2\,m\,L\,p^4\,\left(p^2\,L + g\right) \qquad [8.A.5]$$

$$D\,(p) = L^2\,m_p\,\left(p^2 + \omega_1^2\right)\left[p^4 + \frac{p^2\,(a\,g + k\,L)}{m_p\,L} + \frac{k\,g}{m_p\,L}\right]$$

$$D\,(p) = \left(p^2\,L + g\right)\left[\left(a\,p^2 + k\right)\left(p^2\,L + g\right) - 2\,m\,L\,p^4\right]$$

$$D\,(p) = L^2\left(p^2 + \frac{g}{L}\right)m_p\left[p^4 + \frac{p^2\,(g\,a + k\,L)}{m_p\,L} + \frac{k\,g}{m_p\,L}\right] \qquad [8.A.6]$$

In the second member, the brackets represent the contribution of the two eigenvalues ω_2^2 and ω_3^2.

ω_1 is the circular eigenfrequency of the pendulums:

$$D\,(p) = m_p\,L^2\,\left(p^2 + \omega_1^2\right)\left(p^2 + \omega_2^2\right)\left(p^2 + \omega_3^2\right) \qquad [8.A.7]$$

Let us evaluate the Laplace transform of θ_1 (t):

$$\Theta_1\,(p) = \frac{N_1\,(p)}{D\,(p)} \qquad [8.A.8]$$

@Seismicisolation

with:

$$N_1\ (p) = \begin{vmatrix} \left(a\,p^2 + k\right) & m\,p\,L\,\theta_1 & m\,L\,p^2 \\ p^2 & L\,p\,\theta_1 & 0 \\ p^2 & 0 & \left(Lp^2 + g\right) \end{vmatrix}$$

$$\begin{aligned} N_1\ (p) &= \left(a\,p^2 + k\right) L\,p\,\theta_1 \left(L\,p^2 + g\right) - m\,L^2\ \theta_1\ p^5 - m\,p^3\ L\,\theta_1 \left(L\ \ p^2 + g\right) \\ &= m_p\ L^2\ \theta_1\ p^5 + \left[\theta_1\ k\,L^2 + g\,\theta_1\ L\left(m + m_p\right)\right]\ p^3 + kg\,L\,\theta_1\ p \end{aligned}$$

$$\Theta_1\ (p) = \theta_1\ \frac{m_p\ L^2\ p^5\ \left[k\,L^2 + g\,L\ \left(m + m_p\right)\right]\ p^3 + k\,g\,L\,p}{m_p\ L^2\ \left(p^2 + \omega_1^2\right)\ \left(p^2 + \omega_2^2\right)\ \left(p^2 + \omega_3^2\right)}$$

$$\Theta_1\ (p) = \theta_1\ \frac{\left[\ p^5 + \left[\frac{k}{m_p} + \frac{g}{L}\left(\frac{m + m_p}{m_p}\right)\right] p^3 + \left(\frac{k}{m_p}\ \frac{g}{L}\right)\ p\ \right]}{\left(p^2 + \omega_1^2\right)\ \left(p^2 + \omega_2^2\right)\ \left(p^2 + \omega_3^2\right)} \qquad [8.\ A.9]$$

$$\Theta_1\ (p) = \theta_1\ \frac{\left[\ p^5 + \left[\omega_p^2 + \omega_1^2\left(\frac{m + m_p}{m_p}\right)\right] p^3 + \omega_p^2\ \omega_1^2\ p\ \right]}{\left(p^2 + \omega_1^2\right)\ \left(p^2 + \omega_2^2\right)\ \left(p^2 + \omega_3^2\right)} \qquad [8.A.10]$$

Inversion of equation [8.A.10] by inverse Laplace transform is possible by decomposing Θ_1 (p) into simple elements.

$$\Theta_1\ (p) = \theta_1\ p\left[\ \frac{A}{p^2 + \omega_2^2} + \frac{B}{\left(p^2 + \omega_2^2\right)} + \frac{C}{p^2 + \omega_3^2}\right] \qquad [8.A.11]$$

@Seismicisolation

$$\left.\begin{aligned}
A &= \frac{\omega_1^4 - \left[\omega_p^2 + \omega_1^2\left(\frac{m+m_p}{m_p}\right)\right]\omega_1^2 + \omega_p^2\,\omega_1^2}{\left(-\omega_1^2+\omega_2^2\right)\left(-\omega_1^2+\omega_3^2\right)} \\
B &= \frac{\omega_2^4 - \left[\omega_p^2 + \omega_1^2\left(\frac{m+m_p}{m_p}\right)\right]\omega_2^2 + \omega_p^2\,\omega_1^2}{\left(-\omega_1^2+\omega_2^2\right)\left(-\omega_1^2+\omega_3^2\right)} \\
C &= \frac{\omega_3^4 - \left[\omega_p^2 + \omega_1^2\left(\frac{m+m_p}{m_p}\right)\right]\omega_3^2 + \omega_p^2\,\omega_1^2}{\left(-\omega_3^2+\omega_1^2\right)\left(-\omega_3^2+\omega_2^2\right)}
\end{aligned}\right\} \qquad [8.A.12]$$

Inversion by Laplace transform, term-by-term of $\Theta_1\ (p)$ is easy:

$$\mathcal{L}^{-1}\left[\Theta_1\ (p)\right] = \theta_1(t) = \theta_1(0)\left[A\cos\omega_1\ t + B\cos\omega_2\ t + C\cos\omega_3\ t\right] \qquad [8.A.13]$$

The classification of eigenfrequencies in ascending order is:

$$\omega_2 < \omega_1 < \omega_3$$

where ω_1 is the eigenfrequency of the pendulum.

The two eigenfrequencies ω_2 and ω_3 are roots of the brackets in equation [8.A.6]:

$$\omega^4 - \omega^2\ \frac{(g\,a + k\,L)}{m_p\ L} + \frac{k\,g}{m_p\ L} = 0 \qquad [8.A.14]$$

$$\left.\begin{matrix}\omega_2^2 \\ \omega_3^2\end{matrix}\right\} = +\ \frac{g\,a + k\,L}{2\,m_p\ L} \mp \frac{1}{2}\sqrt{\left(\frac{g\,a+k\,L}{m_p\ L}\right)^2 - \frac{4\,k\,g}{m_p\ L}} \qquad [8.A.15]$$

@Seismicisolation

$$\left.\begin{matrix}\omega_2^2\\ \omega_3^2\end{matrix}\right\} = \frac{1}{2}\left[\left(\frac{a}{m_p}\,\omega_l^2 + \omega_p^2\right) \mp \sqrt{\left(\omega_p^2 + \frac{a}{m_p}\,\omega_l^2\right)^2 - 4\,\omega_l^2\,\omega_p^2}\right] \qquad [8.A.16]$$

$$\omega_p^2 = \frac{k}{m_p}; \quad \omega_l^2 = \frac{g}{L}; \quad a = \left(m_p + 2\,m\right)$$

It is interesting to analyze the relative positions of eigenfrequencies ω_1, ω_2, and ω_3. For this purpose, equation [8.A.16] is rewritten as:

$$\left.\begin{matrix}\omega_2^2\\ \omega_3^2\end{matrix}\right\} = \frac{\omega_p^2}{2}\left(\frac{a}{m_p}\,\alpha^2 + 1\right)\left[1 \mp \sqrt{\frac{1-\alpha^{\;2}}{\left(1+\frac{a}{m_p}\,\alpha^2\right)^2}}\right] \qquad [8.A.17]$$

$$\alpha = \frac{\omega_l}{\omega_p} = \frac{\text{pendulum eigenfrequency}}{\text{eigenfrequency of the platform}}$$

For a sample with high stiffness, ω_p is higher than ω_1, $\alpha << 1$. In this case the highest eigenfrequency has the value:

$$\omega_3^2 \cong \omega_p^2\,; \quad \omega_2^2 \cong \omega_l^2 \text{ (pendulum eigenvalue)} \qquad [8.A.18]$$

The proximity of ω_2 and ω_1 creates *a pronounced beating phenomena* in the solution to [8.A.13]. The difference:

$$\omega_1 - \frac{2\,\pi}{\tau} \qquad \text{with} \qquad \tau >> T_1 \text{ pendulum period}$$

gives rise to a beating period τ, which is large, and each pendulum oscillates with its own period $\frac{2\,\pi}{\omega_1}$ but its amplitude $\theta_l(t)$ or $\theta_r(t)$ is such that the envelope has a long period, see Figures 8.4 and 8.5.

@Seismicisolation

For a sample with low stiffness, ω_2 is much lower than ω_1, and the beating period τ becomes smaller.

Appendix 8.B. Influence of the highest eigenfrequency ω_3 on the pendulum oscillations in the expression of θ_1 (t)

In Appendix 8.A, equation [8.A.13] gives the expression of the first pendulum oscillation.

Let us focus our attention on the amplitude of the third term, C sin ω_3t, in equation [8.A.13]. C is given by equation [8.A.12] and rewritten as:

$$C = \frac{1 - \left[\omega_p^2 + \omega_1^2 \left(\frac{m + m_p}{m}\right)\right] \frac{1}{\omega_3^2} + \frac{\omega_p^2\ \omega_1^2}{\omega_3^4}}{\left(1 - \frac{\omega_1^2}{\omega_3^2}\right)\left(\frac{\omega_2^2}{\omega_3^2}\right)} \qquad [8.B.1]$$

8.B.1. *For high stiffness of the sample*

As in Appendix 8.A, we adopt the approximation:

$$\omega_3^2 \cong \omega_p^2 \qquad [8.B.2]$$

$$C = \frac{1 - \left(\frac{\omega_1}{\omega_3}\right)^2 \left(\frac{m + m_p}{m}\right)}{\left(1 - \left(\frac{\omega_1}{\omega_3}\right)^2\right)\left(1 - \left(\frac{\omega_2}{\omega_3}\right)^2\right)} \qquad [8.B.3]$$

by construction $(\omega_1/\omega_3) << 1$. Coefficient C in equation [8.B.3] is consequently very small compared to B and C. The contribution of the third term in equation [8.A.13] is practically negligible. This equation can then be written:

$$\theta_1\ (t) = [A \cos \omega_1 t + B \cos \omega_2 t] \qquad [8.B.4]$$

@Seismicisolation

As we have shown in equation [8.A.18], the second approximation for a high sample is:

$$\omega_2^2 \cong \omega_1^2$$

The amplitudes of B and C given by equation [8.A.12] are nearly the same.

$$\theta_1(t) \cong \frac{\theta_1(0)}{2}\left[\cos\omega_1 t + \cos\omega_2 t\right] \qquad [8.B.5]$$

$$\theta_1(t) = \theta_1(0) \bullet \cos\frac{(\omega_1+\omega_2)t}{2}\cos\frac{\omega_1-\omega_2 t}{2} \qquad [8.B.6]$$

8.B.2. ***Expression of*** $\theta_2(t)$ ***for sample high stiffness***

The equalities in equation [8.A.18] are also valid.

It is possible to completely solve this equation by using the Laplace transform equation [8.A.4] to find the closed-form expression of θ_2 (t).

It can be shown that θ_2 (t) has the form:

$$\theta_2(t) = \theta_1(0)\sin\frac{(\omega_1+\omega_2)t}{2}\sin\frac{(\omega_1-\omega_2)t}{2} \qquad [8.B.7]$$

Appendix 8.C. Coefficients of a compliance matrix after a change of axes for transverse isotropic material

Figure 8.C.1 represents rod axes (x, y, z) with respect to material symmetry axes (1, 2, 3). α is the angle between z and 3. It relates to a transverse isotropic material made up of fibers imbedded in a matrix and regularly distributed in the plane (1, 2). Initially along axes (1, 2, 3), five independent elastic constants are defined, as in matrix $[s_{ij}]$ in equation [8.C.1].

@Seismicisolation

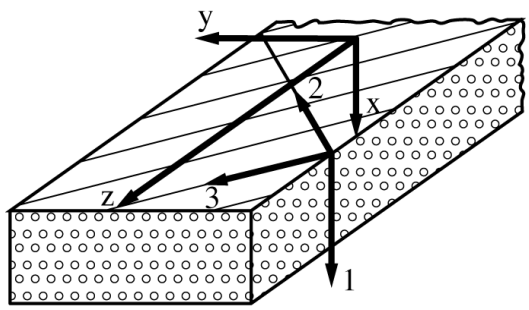

Figure 8.C.1. *Rotation α around the symmetry axis 3 of a material fiber. The material is transverse isotropic*

$$[s] = \begin{bmatrix} s_{11} & s_{12} & s_{13} & 0 & 0 & 0 \\ & s_{22} & s_{23} & 0 & 0 & 0 \\ & & s_{33} & 0 & 0 & 0 \\ & & & s_{44} & 0 & 0 \\ \text{sym} & & & & s_{55} & 0 \\ & & & & & s_{66} \end{bmatrix} \qquad [8.C.1]$$

The surrounding coefficients represent equal and independent coefficients. After a rotation α, see Figure 8.C.1, we have to deal with a monoclinic material with 13 independent elastic coefficients gathered in matrix [8.C.2]:

$$s' = \begin{bmatrix} s'_{11} & s'_{12} & s'_{13} & 0 & s'_{15} & 0 \\ & s'_{22} & s_{23} & 0 & s'_{25} & 0 \\ & & s'_{33} & 0 & s'_{35} & 0 \\ & & & s'_{44} & 0 & 0 \\ \text{sym} & & & & s'_{55} & 0 \\ & & & & & s'_{66} \end{bmatrix} \qquad [8.C.2]$$

The new set of compliance coefficients contains 13 coefficients. Only the coefficients necessary for the formulation of dynamic problem, i.e. s'_{55} and s'_{44}, s'_{55}, s'_{33} [4] are mentioned below:

4 See Chapter 1 for change of axes using matrix multiplications.

@Seismicisolation

$$s'_{33} = s_{11} \sin^4 \alpha + \left(2\, s_{13} + s_{44}\right) \sin^2 \alpha \bullet \cos^2 \alpha + s_{33}\, \alpha \qquad [8.C.3a]$$

$$s'_{35} = \sin \alpha \cos \alpha \begin{bmatrix} 2\, s_{11} \sin^2 \alpha \\ + \left(2\, s_{13} + s_{55}\right) \left(\cos^2 \alpha - \sin^2 \alpha\right) - 2\, s_{33} \cos^2 \alpha \end{bmatrix} \qquad [8.C.3b]$$

$$s'_{55} = s_{55} + 4\, \left(s_{11} + s_{33} - 2\, s_{13} - s_{55}\right) \sin^2 \alpha \cos^2 \alpha \qquad [8.C.3c]$$

$$s'_{44} = s_{66} \sin^2 \alpha + s_{44} \cos^2 \alpha \qquad [8.C.3d]^5$$

After equations [8.C.3] and [8.D.3], if compliance coefficients s_{11}, s_{44}, and s_{33} were previously evaluated with an on-axis rod an off-axis rod with known angle α would permit the calculation of s_{13}.

Coefficients s_{12} in equation [8.C.1] can be deduced from the so-called transverse isotropic relationship:

$$s_{12} = s_{11} - 2\, s_{66} \qquad [8.C.4]$$

Let us recall from Chapter 1 that Poisson's coefficients are deduced from equation [8.C.1]:

$$s_{12} = -\, \nu_{12} / E_1 \,,\; s_{13} = -\, \nu_{13} / E_1 \text{ (no summation)}$$

Appendix 8.D. Mathematical formulation of the simultaneous bending and torsion of an off-axis rectangular rod

There is abundant technical literature available on this problem. Some publications emphasize theoretical and mathematical rigor. In other publications attention is focused on applied mathematical methods. The reason for the great variety of papers devoted to this problem can be found in the nature of the mathematical problem to be solved.

The elastostatic problem is solved in successive steps. The first two steps are common to all of the proposed methods. In the first step, closed-form expressions are found for stress and strain components *versus* space coordinates x, y and z from

5 For transverse isotropic material $s_{66} = (s_{11} - s_{12})/2$

@Seismicisolation

compatibility, Saint Venant's equation and the equilibrium equation. Polynomials of the coordinate and some arbitrary functions of x, y (z is along the rod axis) make up the displacement field. Both Airy stress function φ and shear stress function ψ are referred to. In the next step, the torque and bending moment are evaluated using the aforementioned functions.

In the last step, the variational problem is solved. The functionals include one that is a sum of the space derivatives of φ and ψ. There is no exact solution to this last problem.

All the solutions are approximate and use a variety of mathematical methods, i.e.: the Rayleigh-Ritz method to evaluate coefficients of the function; with successive approximations Kantorovich-Krylov's method; Kerr's method or Saint Venant's method are extended to anisotropic material using trigonometric and hyperbolic functions.

The objective of this appendix is to present the trends of the two first steps. The last step, however, is the most interesting to users of dynamic tests. Large extracts from Nugues' masters thesis [NUG 76] are used and an attempt is made to create a comparative study of some existing methods.

8.D.1. *Mathematical formulation – elastostatic equations*

Johnson's reports [JOH 71] present a very comprehensive solution to this problem.

8.D.1.1. *Compatibility equation and equilibrium equation*

The strain components are related by:

$$\varepsilon_{ij,kl} + \varepsilon_{kl,jl} + \varepsilon_{jl,ik} = 0 \qquad [8.D.1]$$

The two subscript letters after the comma designate the second derivative with respect the two coordinates. The equilibrium equation is:

$$\sigma_{ij,j} = 0 \qquad [8D.2]$$

and strain is defined as:

$$\varepsilon_{ij} = \frac{1}{2}\left(u_{i,j} + u_{j,i}\right) \qquad [8.D.3]$$

@Seismicisolation

8.D.1.2. *Adopted hypothesis – stress and strain depend on x_1, x_2 coordinates only*

$$\sigma_{ij} = \sigma_{ij}\left(x_1, x_2\right), \qquad \varepsilon_{ij} = \varepsilon_{ij}\left(x_1, x_2\right) \qquad [8.D.4]$$

Equation [8.D.2] is rewritten as:

$$\left.\begin{aligned} \sigma_{11,1} + \sigma_{12,2} &= 0 \\ \sigma_{12,1} + \sigma_{22,2} &= 0 \\ \sigma_{13,1} + \sigma_{23,2} &= 0 \end{aligned}\right\} \qquad [8.D.5]$$

Compatibility equations become:

$$\left.\begin{aligned} \varepsilon_{11,22} + \varepsilon_{22,11} &= 2\,\varepsilon_{12,12} \\ \varepsilon_{33,11} + \varepsilon_{33,22} &= 2\,\varepsilon_{33,12} = 0 \\ \left(\varepsilon_{13,2} - \varepsilon_{23,1}\right)_{,1} &= \left(\varepsilon_{13,2} - \varepsilon_{23,1}\right)_{,2} = 0 \end{aligned}\right\} \qquad [8.D.6]$$

Integrating equation [8.D.5], the second and third of [8.D.5] respectively give:

$$\varepsilon_{33} = s_{33}\left(A\,x_1 + B\,x_2 + C\right) \qquad [8.D.7]$$

$$\varepsilon_{13,1} - \varepsilon_{23,1} = -\alpha \qquad [8.D.8]$$

where A, B, C, α are integration constants.

8.D.1.3. *Airy stress function ϕ and shear stress function ψ*

$$\left.\begin{aligned} \sigma_{11} = \phi_{,22}, \quad \sigma_{22} = \phi_{,11}, \quad \sigma_{12} = \phi_{,12} \\ \sigma_{13} = \psi_{,2}, \quad \sigma_{23} = \psi_{,1} \end{aligned}\right\} \qquad [8.D.9]$$

With [8.D.9], equilibrium equation [8.D.2] is identically satisfied.

8.D.1.4. *Constitutive equations and stress components versus φ, ψ*

$$\varepsilon_{ij} = s_{ijkl}\,\sigma_{kl} \qquad [8.D.10]$$

@Seismicisolation

In equation [8.D.10] we retain the non-zero stress components of the second member. Using matricial notation for subscripts, we get:

$$\left.\begin{aligned}
\varepsilon_{11} &= s_{11}\ \sigma_{11} + s_{12}\ \sigma_{22} + s_{13}\ \sigma_{33} + s_{15}\ \sigma_{13} \\
\varepsilon_{22} &= s_{12}\ \sigma_{11} + s_{22}\ \sigma_{22} + s_{23}\ \sigma_{33} + s_{25}\ \sigma_{13} \\
\varepsilon_{33} &= s_{12}\ \sigma_{11} + s_{23}\ \sigma_{22} + s_{33}\ \sigma_{33} + s_{35}\ \sigma_{13} \\
2\ \varepsilon_{23} &= \gamma_{23} = s_{44}\ \sigma_{23} + s_{46}\ \sigma_{12} \\
2\ \varepsilon_{31} &= \gamma_{31} = s_{15}\ \sigma_{11} + s_{25}\ \sigma_{22} + s_{35}\ \sigma_{33} + s_{55}\ \sigma_{13} \\
2\ \varepsilon_{12} &= \gamma_{12} = s_{46}\ \sigma_{23} + s_{66}\ \sigma_{12}
\end{aligned}\right\} \qquad [8.D.11]$$

Bringing equations [8.D.7] and [8.D.9] into the third equation of [8.D.11], for σ_{33} we obtain:

$$\sigma_{33} = \left(A\ x_1 + B\ x_2 + C\right) - \frac{1}{s_{33}}\ \left(s_{13}\ \phi_{,22} + s_{23}\ \phi_{,11} + s_{35}\ \psi_{,2}\right) \qquad [8.D.12]$$

This equation completes [8.D.9] and furnishes the six stress components.

To be complete, the two remaining compatibility equations [8.D.6] need to be satisfied. The first [8.D.6] and second equation [8.D.8] give the strain components. The stress functions in [8.D.9] enable us to write the compatibility equation as follows:

$$D = \left\{\left(x_1\ ,\ x_2\right)\ ;\ -\frac{b}{2} \le x_1 \le \frac{b}{2};\ -\frac{h}{b} \le x_2 \le \frac{h}{2}\right\}$$

$$b_{22}\phi_{,1111} + \left(2\ b_{12} + s_{66}\right)\phi_{,1122} + b_{11}\phi_{,2222} + \left(b_{25} + s_{46}\right)\psi_{,1112} + b_{15}\psi_{,222} = 0 \qquad [8.D.13a]$$

$$\left(b_{25} + s_{46}\right)\ \phi_{,112} + b_{15}\ \phi_{,222} + s_{44}\ \psi_{,11} + b_{55}\ \psi_{,22} = -2\ \alpha - s_{35}\ B \qquad [8.D.13b]$$

@Seismicisolation

In equations [8.D.13a] and [8.D.13b], modified compliance coefficients b_{pq} are defined *versus* s_{pq} :

$$b_{pq} = s_{pq} - \frac{a_{p3}\ a_{q3}}{s_{33}} \quad p\ ,\ q = 1, 2\ ,\ 3 \qquad [8.D.14]$$

8.D.1.5. *Displacement components of the rod* u_1, u_2, u_3

General expressions of displacement u_i are obtained by integration of equation [8.D.3] using [8.D.7]:

$$\left.\begin{aligned} u_1 &= -\frac{1}{2}\ s_{33}\ A\ x_3^2 + x_3\ \left(2\ \varepsilon_{13} - \bar{U}_{31}\right) + U_1 \\ u_2 &= -\frac{1}{2}\ s_{33}\ B\ x_3^2 + x_3\ \left(2\ \varepsilon_{23} - \bar{U}_{3,2}\right) + U_2 \\ u_3 &= s_{33}\ x_3\ \left(A\ x_1 + B\ x_2 + C\right) + U_3 \end{aligned}\right\} \qquad [8.D.15]$$

In [8.D.15], U_1, U_2 and $\bar{U}_3$ are arbitrary functions of x_1 and x_2. Substituting the displacement components defined in [8.D.15] in [8.D.3], we get:

$$\left.\begin{aligned} &\varepsilon_{11}\ \left(x_1\ ,\ x_2\right) = U_{1,1} \qquad \varepsilon_2\ \left(x_1\ ,\ x_2\right) = U_{2,2} \\ &\left(2\ \varepsilon_{13} - \bar{U}_{3,1}\right)_{,1} = \left(2\ \varepsilon_{23} + \bar{U}_{3,2}\right) = 0 \end{aligned}\right\} \qquad [8.D.16]$$

then:

$$2\ \varepsilon_{13} - \bar{U}_{3,1} = k_2\ \left(x_2\right);\ 2\ \varepsilon_{23} - \bar{U}_{3,2} = k_1\ \left(x_1\right) \qquad [8.D.17]$$

where k_1 and k_2 are two arbitrary functions. Using equations [8.D.7] and [8.D.8], for k_1 and k_2, where v'_1 and v'_2 are constants, we can obtain:

$$k_1 = \alpha\ x_1 + v_2 \qquad k_2 = \alpha\ x_2\ v'_1 \qquad [8.D.18]$$

@Seismicisolation

8.D.1.6. *Complete general expression for displacement versus coordinates x_1, x_2, x_3 and U_1, U_2, U_3*

In equation [8.D.15], ε_{23} and ε_{13} can be replaced by [8.D.17]:

$$u_1 = -\frac{1}{2} s_{33} A x_3^2 - \alpha x_2 x_3 + v'_1 x_3 + U_1 (x_1, x_2) \qquad [8.D.19]$$

$$u_2 = -\frac{1}{2} s_{33} B x_3^2 + \alpha x_1 x_3 + v'_2 x_3 + U_2 (x_1, x_2)$$

$$u_3 = s_{33} x_3 (A x_1 + B x_2 + C) - v'_1 x_1 - v'_2 x_2 + U_3 (x_1, x_2)$$

Here (U_1, U_2, U_3) satisfy the following equations:

$$\left.\begin{aligned} U_{1,1} &= s_{13}(A x_1 + B x_2 + C) + b_{12} \phi_{,11} + b_{11} \phi_{,22} + b_{15} \psi_{,2} \\ U_{2,2} &= s_{23}(A x_1 + B x_2 + C) + b_{22} \phi_{,11} + b_{12} \phi_{,22} + b_{25} \psi_{,2} \\ U_{3,2} &= -\alpha x_1 - s_{44} \psi_{,1} -_{46} \psi_{,12} \end{aligned}\right\} \qquad [8.D.20]$$

where:

$$U_3 = \bar{U}_3 + v'_1 x_1 + v'_2 x_2$$

The analysis is now reduced to the bending and torsion of the rod and the search for a solution to equation system [8.D.13] to find φ and ψ. Stress and strain components in the rod are evaluated from equations [8.D.10], [8.D.9], [8.D.14] [8.D.19] and [8.D.12].

Before going further, it is necessary to physically interpret constants A, B, C, v'_1 and v'_2 and define the boundary conditions to integrate equations [8.D.13a] and [8.D.13b].

@Seismicisolation

8.D.1.7. *Boundary conditions*

There are two groups of boundary conditions at both ends:

– displacements at the two tips;

– forces and moments on the lateral rod surface.

For a simply supported end at x = 0, x = L and $x_2 = 0, L$, we have:

$$U_1\ (0,0) = U_2\ (0,0) = U_3\ (0,0) = C = 0$$

$$v'_1 = \frac{1}{2} s_{33}\ AL \qquad [8.D.21]$$

$$v'_2 = \frac{1}{2} s_{33}\ BL$$

and the displacements are:

$$u_1 = -\frac{1}{2}\ s_{33}\ A\, x_3\ (x_3 - L) - \alpha\, x_2\ x_3 + U_1\ (x_1, x_2) \qquad [8.D.22]$$

$$u_2 = -\frac{1}{2}\ s_{33}\ B\, x_3\ (x_3 - L) + \alpha\, x_1\ x_3 + U_2\ (x_1, x_2)$$

$$u_3 = s_{33}\ A\, x_1 \left(x_3 - \frac{L}{2}\right) + s_{33}\ B\, x_2 \left(x_3 - \frac{L}{2}\right) + U_3\ (x_1, x_2)$$

If we refer to expressions for solutions concerning an isotropic elastic rod, A and B characterize the bending of a rod on axes x_1 and x_2 respectively. α is the torsional angle per unit length along axis x_3. U_3 designates the warping and U_1, U_2 the displacement of cross-section D of the beam. Lateral surfaces of the rod are free of stresses.

$$\sigma_{11} = \sigma_{12} = \sigma_{13} = 0 \ \text{ for } x_1 = \pm \frac{b}{2}$$

$$0 \le x_3 \le L$$

@Seismicisolation

$$\sigma_{12} = \sigma_{22} = \sigma_{23} = 0 \text{ for } x_2 = \pm \frac{b}{2} \qquad [8.D.23]$$

Distribution of stresses is supposed to be equivalent to bending moment M and torque T.

8.D.1.8. *Expressions of bending moment and torque*

Bending moment is given by integration in the cross-section:

$$\int_D \sigma_{33}\, x_2\, d\,D = M; \qquad \int_D \sigma_{33}\, x_1\, d\,D = 0 \qquad [8.D.24]$$

Torque has the expression:

$$T = \int_D \left(x_1\, \sigma_{23} - \sigma_{13}\, x_2\right) d\,D = T \qquad [8.D.25]$$

$$d\,D = d\,x_1\, d\,x_2$$

Utilizing equations [8.D.11], [8.D.7] and [8.D.8], the two first equations in [8.D.23] become:

$$B\, I_1 - \frac{1}{s_{33}} \int_D \left(s_{13}\, \sigma_{11} + s_{23}\, \sigma_{22} + s_{35}\, \sigma_{13}\right) x_2\, d\,D = M \qquad [8.D.26]$$

$$A\, I_2 - \frac{1}{s_{33}} \int_D \left(s_{13}\, \sigma_{11} + s_{23}\, \sigma_{22} + s_{35}\, \sigma_{13}\right) x_1\, d\,D = 0$$

Where I_2 and I_1 are defined as:

$$I_1 = \int_D x_2^2\, d\,D; \qquad I_2 = \int_D x_1^2\, d\,D \qquad [8.D.27]$$

Integrals in equations [8.D.25] and [8.D.26] can be solved using [8.D.5] and [8.D.22] and divergence theorem.

@Seismicisolation

$$\int_D \sigma_{11}\, x_1\, d\,D = \int_D \sigma_{11} \left[\frac{x_1^2}{2}\right]_{,1} d\,D = \int_D \left\{\left[\sigma_{11} \bullet \frac{x_1^2}{2}\right]_{,1} - \sigma_{11,1} \bullet \frac{x_1^2}{2}\right\} d\,D$$

$$= \int_D \left\{\left[\sigma_{11} \bullet \frac{x_1^2}{2}\right]_{,1} + \left[\sigma_{12} \bullet \frac{x_1^2}{2}\right]_{,2}\right\} d\,D$$

$$= \int_D \frac{1}{2}\, x_1^2\, \{\sigma_{11}\, x_1 + \sigma_{12}\, n_2\}\, d\,S = 0 \qquad [8.D.28]$$

d D is the contour of D and d S is the elementary arc of d D, n_1, n_2, which are components of external normal to d D. In similar manner as above we can find:

$$\int \sigma_{11} \bullet x_2\, d\,D = \int \sigma_{22}\, x_2\, d\,D = 0 \qquad [8.D.29a]$$

$$\int_D \sigma_{13}\, x_1\, d\,D = 0 \int \sigma_{13}\, x_2\, d\,D = -\frac{1}{2}\, T \qquad [8.D.29b]$$

The second equation [8.D.29b] is written as:

$$\int_D \sigma_{13}\, x_1\, d\,D = \int_D \sigma_{13} \left[\frac{x_1^2}{2}\right] d\,D = \int_D \left\{\left[\sigma_{13} \bullet \frac{x_1^2}{2}\right]_{,1} + \left[\sigma_{23} \bullet \frac{x_1^2}{2}\right]_{,2}\right\} d\,D = 0$$

$$\int_D \sigma_{13}\, x_2\, d\,D = \int \sigma_{13}\, [x_1\, x_2]_{,1}\, d\,D$$

$$= \int_D \left\{[\sigma_{13}\, x_2\, x_1]_{,1} + \sigma_{23,2} \bullet x_1\, x_2\right\} d\,D$$

$$= -\int_D \sigma_{23}\, x_1\, d\,D \qquad [8.D.30]$$

@Seismicisolation

$$T = \int_D \left(\sigma_{23}\, x_1 - \sigma_{13}\, x_2\right) d\,D \qquad [8.D.31]$$

$$-\frac{T}{2} = \int_D \sigma_{13}\, x_2\, d\,D \quad \frac{T}{2} = \int \sigma_{23}\, x_1\, d\,D$$

8.D.1.9. *Evaluation of A, B and* I_1

Equation [8.D.25] gives:

$$A = 0 \qquad B = \frac{1}{I}\left(M - \frac{s_{35}}{2\, s_{33}}\, T\right) \qquad [8.D.32]$$

$$I_1 = \frac{b\, h^3}{2} = I \quad \text{(where b is the width and h the thickness of the rod.)}$$

A, B and C are calculated from applied bending and torsional moments. The torsional angle per unit length α is to be determined.

Using equations [8.D.9] and [8.D.22] and integrating them along the contour ∂D, we obtain stress conditions.

$$\phi = \frac{\partial\, \phi}{\partial\, n} = \psi = 0 \text{ on } \partial\, D \qquad [8.D.33]$$

This equation replaces [8.D.22]. $\frac{\partial}{\partial\, n}$ designates the external normal derivative on ∂D. From equations [8.D.9], [8.D.23] and [8.D.32], and using divergence theorem, we get:

$$T = 2 \int \psi\, d\,D \qquad [8.D.34]$$

M and T are evaluated if φ and ψ are calculated from partial derivative equations [8.D.13] associated with boundary conditions [8.D.32]

@Seismicisolation

8.D.2. *Variational formulation of the problem*

The displacement and rotation of the beam can be evaluated by numerical or closed-form solution, providing the bending moment and torque are known.

Our interest resides in the inverse problem, however, in which our aim is to determine the elastic constants with a given bending moment and torque. Here it is necessary to obtain an approximate solution to the problem of compliance coefficients s_{pq}.

Variational calculus is referred to so as to facilitate an approximate solution.

8.D.2.1. *Deformation energy*

This is defined as:

$$U_p = \frac{1}{2} \int_v \sigma_{ij}\, \varepsilon_{ij}\, d\,V = \frac{1}{2}\, L \int_D \sigma_{ij}\, \varepsilon_{ij}\, d\,D \qquad [8.D.35]$$

because stress and strain components do not depend on x_3.

The volume integral is reduced to a surface integral with L being the rod length.

8.D.2.2. *Energy of stress applied at the tip of surfaces Σ*

$$U_E = \int_{\Sigma} \sigma_{ij}\, n_j\, u_i\, d \sum \qquad [8.D.36]$$

8.D.2.3. *Complementary energy*

This is defined as:

$$W = U_p - U_E \qquad [8.D.37]$$

8.D.2.4. *Minimum complementary energy theorem*

This states that W reaches an absolute minimum if a stress tensor is such that the static equilibrium of the rod is reached. It ensures that all σ_{ij} components satisfy [8.D.13] and there is no stress at lateral surfaces [8.D.22] and compatibility conditions [8.D.6] are satisfied.

@Seismicisolation

Expression of U_p in equations [8.D.6] and [8.D.7] with A = C = 0 permit us to obtain the following expression for U_c:

$$U_p = \frac{1}{2} L \begin{bmatrix} b_{11}\ \sigma_{12}^2 + b_{22}\ \sigma_{22}^2 + s_{44}\ \sigma_{23}^2 + b_{15}\ \sigma_{13}^2 \\ + s_{66}\ \sigma_{12}^2 + 2\ b_{12}\ \sigma_{11}\ \sigma_{22} + 2\ b_{15}\ \sigma_{11}\ \sigma_{13} \\ + 2\ b_{25}\ \sigma_{22}\ \sigma_{13} + 2\ s_{46}\ \sigma_{12}\ \sigma_{23} \\ + s_{33}\ B^2\ x_2^2 \end{bmatrix} d\,D \qquad [8.D.38]$$

Expression of U_e

$$\int_{\Sigma} \sigma_{ij}\ n_j\ u_i\ d\Sigma = \int_{\Sigma_L} [\sigma_{i3}\ u_i]_{x_3=L}\ d\Sigma_L - \int_{\Sigma_0} [\sigma_{i3}\ u_i]_{x_3=0}\ d\Sigma_0$$

$$= L \int_D [-\alpha\ x_2\ \sigma_{13} + \alpha\ x_1\ \sigma_{23} + \sigma_{33}\ B\ s_{33}\ x_2]\ d\,D \qquad [8.D.39]$$

Substituting σ_{33} by its given value in [8.D.12]:

$$\int_{\Sigma} \sigma_{ij}\ n_j\ u_i\ d\Sigma = L \int_D \begin{bmatrix} \alpha\ x_1\ \sigma_{23} - (\alpha + s_{35}\ B)\ x_2\ \sigma_{13} \\ + s_{33}\ B^2\ x_2^2 - B\ x_2\ (s_{23}\ \sigma_{11} + s_{23}\ \sigma_{22}) \end{bmatrix} d\,D \qquad [8.D.40]$$

8.D.2.5. *Expression of W versus φ, ψ, x_1, x_2*

In equations [8.D.39] and [8.D.37], components σ_{ij} are replaced by their expressions *versus* functions φ and ψ in equations [8.D.23] and [8.D.28]. Here we obtain:

$$W = L \int (\phi,\ \psi, x_1,\ x_2)\ d\,D \qquad [8.D.41]$$

@Seismicisolation

with:

$$F = \frac{1}{2}\, b_{11}\, \left(\phi_{,22}\right)^2 + \frac{1}{2}\, b_{22}\, \left(\phi_{,22}\right)^2 + \frac{1}{2}\, s_{66}\, \left(\phi_{,12}\right)^2 + \frac{1}{2}\, s_{44}\, \left(\psi_{,1}\right)^2$$

$$+\frac{1}{2}\, b_{55}\, \left(\psi_{,2}\right)^2 + b_{12} \bullet \phi_{,11}\, \phi_{,22} + b_{15}\, \phi_{,22}\, \psi_{,2} + s_{46}\, \phi_{,12}\, \psi_{,1} \qquad [8.D.42]$$

$$-\left(2\,\alpha + a_{35}\, B\right)\, \psi - s_{33}\, B^2\, x_2^2 + b_{25}\, \phi_{,11}\, \psi_{,2}$$

We need to minimize the set of functions ϕ and ψ, which must satisfy stress conditions:

$$\phi = \frac{\partial\, \phi}{\partial\, n} = \psi = 0 \quad \text{on } \partial\, D \qquad [8.D.43]$$

In can be proven that by variation ∂W *versus* the variations $\delta\varphi$ and $\delta\psi$ in [8.D.40], we obtain [8.D.13a] and [8.D.13b], which is Euler's equation deduced from equations [8.D.41] and [8.D.42].

8.D.2.6. *Rayleigh-Ritz method*

φ_i and ψ_i are group of functions in the domain D that satisfy equation [8.D.43] on ∂D. The following functions are adopted:

$$\phi'_m = \sum_{i=1}^{m} a_i\, \phi_i\,, \quad \psi'_m = \sum_{i=1}^{m} b_i\, \psi_i \qquad [8.D.44]$$

$$I = 1, \ldots, m \quad m \leq n$$

a_i and b_i are chosen to satisfy integral W ($a_1, \ldots, a_m, b_1, \ldots, b_m$) in such a manner that:

$$\frac{\partial\, W}{\partial\, a_i}, \quad \frac{\partial\, W}{\partial\, b_i}, \; I = 1, \ldots, m \qquad [8.D.45]$$

@Seismicisolation

If the absolute minimum of W is obtained, then $\varphi = \varphi'_m$ and $\psi = \psi'_m$ are the solutions to the variational problem. It is doubtful that such a solution will be reached, however a good approximation can be obtained when a_i and b_i are calculated to minimize W.

8.D.2.7. *Approximate solutions to the variational problem*

It is convenient to adopt a non-dimensional form for φ and ψ. Let us introduce the non-dimensional coordinates:

$$X_1 = \frac{2\,x_1}{b\ (\text{width})}; \qquad X_2 = \frac{2\,x_2}{h\ (\text{thickness})}$$

$$\Phi\ (X_1, X_2) = \frac{8\ s_{33}}{h^3\ (2\ \theta + s_{35}\ B)} \bullet \phi$$

$$\psi\ (X_1, X_2) = \frac{4\ s_{33}}{h^3\ (2\ \theta + s_{35}\ B)} \bullet \psi \qquad [8.D.46]$$

The following non-dimensional compliance is adopted:

$$A_{pq} = \frac{s_{pq}}{s_{33}} \qquad B_{pq} = \frac{b_{pq}}{s_{33}} = A_{pq} - A_{p3\,q3} \qquad [8.D.47]$$

Bringing equations [8.D.44] and [8.D.45] into [8.D.13a], [8.D.13b] and [8.D.41], we obtain the limiting values of the problem, i.e. the determination of Φ and ψ:

$$\lambda^4\ B_{22} \bullet \Phi_{,1111} + \lambda^2\ (2\ B_{12} + A_{66})\ \Phi_{,1122}$$

$$+ \lambda^2\ (B_{25} + A_{46})\ \Psi_{,112} + B_{15} \bullet \Psi_{,222} = 0$$

$$\lambda^2\ (B_{25} + A_{46})\ \Phi_{,112} + B_{15} \bullet \Phi_{,222} + \lambda^2\ A_{44} \bullet \Psi_{,11}$$

$$+ B_{55} \bullet \Psi_{,22} = -1 \qquad [8.D.48]$$

for $(X_1, X_2) \in D^*$

@Seismicisolation

$$\Phi = \frac{\partial \Phi}{\partial n} = \Psi = 0 \quad \text{for} \quad (X_1, X_2) \in D^* \qquad [8.D.49]$$

$$D^* = (X_1, X_2): -1 \leq X_1, X_2 \leq 1, \quad \lambda = \frac{h}{b}$$

$$\frac{\partial \Phi}{\partial X_i} = \Phi_{,i}$$

The complementary energy W* is non-dimensional:

$$W^* = \frac{16\, s_{33}}{b\, h^3\, L\, (2\,\theta + s_{35}\, B)^2} \left(W + \frac{1}{2}\, s_{33}\, I\, B^2\, L \right) \qquad [8.D.50]$$

Φ and Ψ minimize the functionals.

$$W^* = \int_{D^*} F^*\, d\, D^* \qquad [8.D.51]$$

with:

$$F^* = \frac{1}{2}\, B_{11}\, (\Phi_{,22})^2 + \frac{1}{2}\, \lambda^4\, B_{22} \bullet (\Phi_{,11})^2 + \frac{1}{2}\, \lambda^2\, A_{66}\, (\Phi_{,12})^2$$
$$+ \frac{1}{2}\, \lambda^2\, A_{44}\, (\Psi_{,1})^2 + \frac{1}{2}\, B_{55} \bullet (\psi_{,2})^2 + \lambda^2\, B_{12} \bullet \Phi_{,11}\, \Phi_{,22} \qquad [8.D.52]$$
$$+ B_{15}\, \Phi_{,22} \bullet \Psi_{,2} + B_{25}\, \Phi_{,11} \bullet \Psi_{,2} + \lambda^2\, A_{46}\, \Phi_{,12} \bullet \Psi_{,1} - \psi$$

associated with the conditions in equation [8.D.47].

We are not aiming to evaluate the complete stress distribution in the rod. In bending tests the central point displacement of the rod is measured when a known bending moment is applied.

In the torsion test, angular displacement θ is measured when a known torque is applied. With these practical considerations in view, we try to deduce the relationships for anisotropic rods.

@Seismicisolation

8.B.2.8. *Torque and torsional angle*

For equations [8.D.33] and [8.D.44], we can obtain the following equations for the torque:

$$M_t = T = \frac{3\,I\,(2\,\theta + s_{35}\,B)\,M^*}{2\,s_{33}} \qquad [8.D.53]$$

$$M^* = \int_{D^*} \Psi\, d\,D^* \qquad [8.D.54]$$

$$B = \frac{M - \frac{1}{2}\,A_{35}\,M_t}{I} \qquad [8.D.55]$$

8.B.2.9. *Bending moment M and bending displacement v*

From equation [8.D.15], bending rod displacement v is deduced:

$$v = u_2\left(0, -\frac{h}{2}, \frac{L}{2}\right) = \frac{1}{8}\,B\,s_{33}\,L^2 + U_2\left(0, -\frac{h}{2}\right) \qquad [8.D.56]$$

At the right side of [8.D.50], displacement v concerns the middle of the rod:

$$\left(0, 0, \frac{L}{2}\right), \quad U_2\,(0, 0) = 0 \qquad U_2\left(0, -\frac{h}{2}\right),$$

which is the correction for change of thickness when the rod is submitted to bending and torsion.

Integrating [8.D.20] we obtain:

$$U_2\left(0, -\frac{h}{2}\right) = \frac{1}{8}\,s_{23}\,B\,h^2 + b_{22}\int_0^{-b/2} \Phi_{,11}\,(0, x)\,d\,x$$
$$-b_{12}\,\phi_{,2}\,(0,0) - b_{25}\,\Psi\,(0,0)$$

Rewriting this equation under a non-dimensional form, we have:

@Seismicisolation

$$v = \frac{1}{8} B\, s_{33}\, L^2 \left(1 + \frac{h^2}{L^2} A_{23}\right)$$

$$+ \frac{1}{4} b^2 \left(2\,\theta + s_{35}\, B\right) \begin{bmatrix} \lambda^2\, B_{22} \int_0^{-1} \Phi_{,11}\left(0, X_2\right) d\, X_2 \\ +B_{12}\, \Phi_{,2}\left(0,0\right) - B_{25}\, \psi\left(0,0\right) \end{bmatrix} \qquad [8.D.57]$$

Relationships [8.D.54] and [8.D.50] will serve us in further calculations. These equations show that it is not necessary to evaluate all of the Φ and ψ. What we have to know is the expression of M* and its derivatives.

8.B.2.10. *Coupling*

Coupling exists between torsion and bending. If we have $B = \frac{1}{2} A_{33} \frac{M_t}{I}$ in a torsional test with M = 0, $M_t = T \neq 0$, then [8.D.54] gives the bending displacement, which occurs around $x_1 = x$, and the rod is submitted to a torsion around $x_3 = z$. Similarly, in a bending test with $M \neq 0$ and $M_t = T \neq 0$, equation [8.D.51] shows that the rod rotates at an angle:

$$\theta = \frac{1}{2} = s_{35} \frac{M}{I} \neq 0$$

This can be explained by the fact that $s_{35} \neq 0$ creates a coupling.

For a monoclinic rod with $a_{35} = 0$, the rotation $\alpha = 0, \frac{\pi}{2}$ with respect to the symmetry fiber axis $z = x_3$. This creates experimental difficulties in bending and torsion tests.

8.D.3. *Useful formulae for bending and torsion tests*

8.D.3.1. *Bending without torsion*

If M and $M_t = T$ are chosen so that $\theta = 0$ in equation [8.D.51] becomes:

$$M_t = T = \frac{3\, A_{35}\, M^*\, M}{2 + \frac{3}{2} A_{35}^2\, M^*} \qquad [8.D.58]$$

@Seismicisolation

and

$$B = \frac{M}{I\left(2 + \frac{3}{2} A_{35}^2 M^*\right)} \qquad [8.D.59]$$

the bending displacement becomes:

$$v = \frac{M\, s_{33}\, L^2}{8\, I\left(1 + \frac{3}{4} A_{35}^2 M^*\right)} \left[1 + \frac{h^2 N}{L^2}\right] \qquad [8.D.60]$$

Correcting term N is given by:

$$N = A_{23} + 2\, A_{35} \left[\begin{array}{l} \lambda^2 B_{22} \int_0^{-1} \Phi_{,11}(0,X_2)\, d X_2 - B_{12}\, \Phi_{,2}(0,0) \\ -B_{25}\, \psi\,(0,0) \end{array}\right] \qquad [8.D.61]$$

Equation [8.D.57] contains a particular case where the classical formula for isotropic material and $\frac{h_2 N}{L^2} << 1$:

$$v = \frac{M L^2}{8 E_3 I}, \qquad E_3 = \frac{1}{s_{33}}$$

The torque M_t given by equation [8. D.55] must be applied to the rod.

When the torsion is forbidden, Young's modulus increases with a factor $\left(1 + \frac{3}{4} A_{35}^2 M^*\right)$, with $\frac{h^2 N}{L^2}$ being negligible. It is not necessary to apply a torque M_t explicitly; M_t exists implicitly.

8.D.3.2. *Free torsion and constrained torsion*

Examining [8.D.21] for displacements A = 0 we see that if B = 0, the rod is twisted around axis $x_3 = z$.

@Seismicisolation

Terms U_i (x_1, x_2) represent the warping and the increase of section D.

Then, when B = 0, the rod does not bend and from equations [8.D.31] and [8.D.51] we obtain:

$$M_t = T = \frac{3\, I\, \theta\, M^*}{s_{33}} \qquad [8.D.62]$$

$$M = \frac{1}{2}\, A_{35}\, M_t \qquad [8.D.63]$$

Bending moment M is implicitly applied on the supports. As for the bending test discussed above, it is necessary to keep the rod straight to prevent bending.

Let us note that M* in equation [8.D.59] depends on s_{pq}. s_{33} is not an elastic constant for shear test. If the rod is allowed to bend freely, then M = 0 and from equation [8.D.51] we write:

$$M_t = T = \frac{3\, I\, \theta\, M^*}{s_{33}\left(1 + \frac{3}{4}\, A_{35}^2\, M^*\right)} \qquad [8.D.64]$$

Comparing equation [8.D.59] to [8.D.61] we see that torsional stiffness increases by a factor of $\left(1 + \frac{3}{4}\, A_{35}^2\, M^*\right)$ when the bending is suppressed.

8.D.4. *Approximation of M**

It is necessary to find a closed-form expression for M* in equations [8.D.61] and [8.D.55] for practical applications.

8.D.4.1. *First approximation $\Phi = 0$ and $\Psi = 0$*

Equation [8.D.47] shows that $\Phi = 0$ is a solution if and only if a scalar $\mathcal{B}$ exists such that:

$$B_{25} + A_{46} = \mathcal{B}\, A_{44}, \qquad B_{15} = \mathcal{B}\, B_{55} \qquad [8.B.65]$$

@Seismicisolation

This condition is not satisfied in general. However, in the special case where $\alpha = 0$ and $\frac{\pi}{2}$, the relationships giving A_{pq} and B_{pq} show that $B_{25} + A_{46} = 0$. In this case, equation [8.D.63] is identically acceptable to $\mathcal{B} = 0$.

It is reasonable to hypothesize that Φ remains small when:

$$0 < \alpha < \frac{\pi}{2}$$

For ψ we adopt the following polynomials:

$$\psi = K\left(X_1^2 - 1\right)\left(X_2^2 - 1\right) \qquad [8.D.66]$$

Bringing [8.D.64] into [8.D.50] and evaluating integral [8.D.49] we obtain:

$$W^* = \frac{16}{9} K \left[\frac{4K}{5}\left(\lambda^2 A_{44} + B_{55}\right) - 1\right] \qquad [8.D.67]$$

If W* is minimum when $\frac{\partial W^*}{\partial K} = 0$ then we obtain:

$$K = \frac{5}{8\left(\lambda^2 A_{44} + B_{55}\right)} \qquad [8.D.68]$$

Bringing [8.D.66] into [8.D.65]:

$$\Phi = 0 \qquad \Psi = \frac{5\left(X_2^2 - 1\right)\left(X_1^2 - 1\right)}{8\left(\lambda^2 A_{44} + B_{55}\right)} \qquad [8.D.69]$$

Using [8.D.52] we obtain a first approximation for M*:

$$M^* = M_1^* = \frac{10}{9}\frac{1}{\left(\lambda^2 A_{44} + B_{55}\right)} \qquad [8.D.70]$$

This is the simplest formula.

@Seismicisolation

8.D.4.2. *Second approximation with two non-zero stress functions*

Let us adopt the following functions:

$$\Phi = L_1\ X_2\ \left(X_1^2 - 1\right)\ \left(X_2^2 - 1\right); \qquad \psi = L_2\ \left(X_2^2 - 1\right)\ \left(X_1^2 - 1\right) \qquad [8.D.71]$$

Equation [8.D.68] satisfies the stress conditions in [8.D.47] and Φ is even in X_1 and odd in X_2 (see equation [8.D.46]). Bringing equation [8.D.68] into [8.D.40] and [8.D.41] we obtained $W^* = W^*\ \left(L_1, L_2\right)$.

Coefficients L_1 and L_2 in [8.D.68] are evaluated so as:

$$\frac{\partial\ W^*}{\partial\ L_1} = \frac{\partial\ W^*}{\partial\ L_2} = 0$$

$$L_1 = \frac{-5\ R}{2\ \left(4\ P\ Q - R^2\right)} \qquad L_2 = \frac{5\ P}{2\ \left(4\ P\ Q - R^2\right)} \qquad [8.D.72]$$

where:

$$P = \frac{8}{7}\left[\frac{5819}{7}\ B_{11} + \frac{256}{105}\ \lambda^2\ \left(2\ B_{12} + A_{66}\right) + \frac{3099}{55}\ \lambda^4\ B_{12}\right]$$

$$Q = \lambda^2\ A_{44} + B_{55}$$

M^*_2 is the second approximation:

$$R = \frac{32\ \lambda^2\ \left(B_{25} + A_{46}\right)}{35}$$

$$M^*_2 = \frac{40\ P}{9\ \left(4\ PQ - R^2\right)} \qquad [8.D.73]$$

@Seismicisolation

REMARK: The value M^*_2 is no different to M^*_1. The reason is that the following inequality is satisfied:

$$R^2 << P\,Q$$

so we can write:

$$M^*_2 = \frac{40\,P}{9\left(4\,P\,Q - R^2\right)} = \frac{40\,P}{36\,P\,Q} = \frac{10}{9\,Q} = M^*_1$$

8.D.4.3. *Third approximation*

$$\phi = 0 \qquad \psi = \left(X_1^2 - 1\right)\left(X_2^2 - 1\right)\left(X_2^2 - 1\right)\left(K_1 + K_2\,X_1^2 + K_3\,X_2^2\right) \qquad [8.D.74]$$

Using the Rayleigh-Ritz method, we obtain the set of coefficients:

$$K_1 = 35\left(9\,\lambda^2\,A_{44}^2 + 9\,B_{55}^2 + 130\,\lambda^2\,A_{44} \bullet B_{55}\right)/T$$

$$K_2 = 105\,B_{55}\left(\lambda^2\,A_{44}^2 + 9\,B_{55}^2\right)/T$$

$$K_3 = 105\,\lambda^2\,A_{44}\left(9\,\lambda^2\,A_{44}^2\;B_{55}^2\right)/T$$

$$\text{with } T = 16\left(\lambda^2\,A_{44} + B_{55}\right)\left(45\,\lambda^2\,A_{44}^2 + B_{55}^2\right) + 464\,\lambda^2\,A_{44} \bullet B_{55}$$

Finally the third approximation is:

$$M^*_3 = \frac{56\left(9\,\lambda^4\,A_{44}^2 + 9\,B_{55}^2 + 82\,\lambda^2\,A_{44}B_{55}\right)}{9\left(\lambda^2\,A_{44} + B_{55}\right)\left[45\left(\lambda^2\,A_{44}^2 + B_{55}^2\right) + 464\,\lambda^2\,A_{44}\,B_{55}\right]} \qquad [8.D.75]$$

Table 8.D.1 gives formulae for the calculations of stiffness in torsion and bending tests, the rod being off-axis.

@Seismicisolation

8.D.5. *Extension of Saint Venant's theory to an anisotropic and off-axis rectangular rod*

[NUG 78] suggested the extension of Saint Venant's theory to find the torsional stiffness of a monoclinic off-axis rod. [8.D.42] represents the equation relating to the non-dimensional Airy stress function Φ and shear stress function Ψ. For practical applications, Φ is to set to zero for the usual first approximation adopted for the afore-mentioned functions. Equation [8.D.42] becomes:

$$\lambda^2 \, A_{44} \, \psi_{,11} + B_{55} \, \psi_{,22} = -1 \qquad [8.D.76]$$

This is the transposition of Saint Venant's warping problem to an anisotropic material for an off-axis rod.

$$(X_1, X_2) \in D^* \text{ and } \Psi = 0, \qquad (X_1, X_2) \in \partial D^*$$

By a change of variables, we get:

$$\Psi = \zeta - \frac{X_1^2}{4 \lambda^2 A_{44}} - \frac{X_2^2}{4 B_{55}} \qquad [8.D.77]$$

Equation [8.D.73] can be rewritten as follows:

$$\lambda^2 \, A_{44} \, \zeta_{,11} + B_{55} \, \zeta_{,22} = 0 \qquad [8.D.78]$$

This biharmonic form lends itself to a solution by variable separation.

$$\left.\begin{aligned} &\zeta_{,11} + \frac{1}{\mu^2} \, \zeta_{,22} = 0 \\ &\mu^2 = \lambda^2 \, \frac{A_{44}}{B_{55}} \end{aligned}\right\} \qquad [8.D.79]$$

This equation system is equivalent to the following one:

@Seismicisolation

$$\left.\begin{aligned} & f_{,11} + \frac{1}{\mu^2} f_{,22} = 0 \\ & f_{,1} = \frac{1}{\mu^2} \zeta_{,2}, \quad -f_2 = \zeta_{,1} \end{aligned}\right\} \qquad [8.D.80]$$

By variable separation:

$$f\left(X_1, X_2\right) = g\left(X_1\right) h\left(X_2\right) \qquad [8.D.81]$$

Equation [8.D.77] has a new form:

$$\left.\begin{aligned} & \frac{g_{,11}}{g} + \frac{1}{\mu^2} \frac{h_{,22}}{h} = 0 \\ & \frac{g_{,11}}{g} = -r^2, \quad \frac{h_{,22}}{h} = r^2 \mu^2 \end{aligned}\right\} \qquad [8.D.82]$$

It is convenient to pose: $r = \frac{m \pi}{h}$, $m = 1, 2, \ldots$

$$\text{For } m = 0 \quad \begin{cases} g = p'_1 X_1 + p'_2 \\ h = q'_1 X_2 + q'_2 \end{cases} \qquad [8.D.83]$$

and $f = f_0 = p'_1 q'_1 X_1 X_2$.

For $m \neq 0$, solutions to equation [8.D.79] are:

$$\left.\begin{aligned} & g = C_m \sin \frac{m \pi X_1}{2} + C'_m \cos \frac{m \pi X_1}{2} \\ & h = D_m \sin h \frac{m \pi \mu X_2}{2} + D'_m \cos h \frac{m \pi \mu X_2}{2} \end{aligned}\right\} \qquad [8.D.84]$$

@Seismicisolation

Notation	$A_{pq} = \frac{s_{pq}}{s_{33}}, \qquad B_{pq} = A_{pq} - A_{p3}\ A_{q3}$ $\lambda = \frac{h}{b} \quad \frac{\text{thickness}}{\text{width}}$
Torsion	$M_t = \frac{3\ I\ \theta\ M^*}{s_{33}}$ equation [8.D.62] θ torsion angle, M_t torsion moment, I inertia of the section $= \frac{bh^3}{12}$
Bending	$v = \frac{M\ s_{33}\ L^2}{8\ I\left(1 + \frac{3}{4}\ A_{35}^3\ M^*\right)}\left[1 + \frac{h^2\ N}{L^2}\right]$ V, M bending displacement and moment N correcting term (equation [8.D.61] can be negligible
M^*_1 first approximation	$M^*_1 = \frac{10}{9}\ \frac{1}{\left(\lambda^2\ A_{44} + B_{55}\right)}$ equation [8.D.70]
M^*_2 second approximation	$M^*_2 = \frac{40\ P}{9\ \left(4\ P\ Q - R^2\right)}$
M^*_3 third approximation	$M^*_3 = \frac{56\ \left(9\ \lambda^4\ A_{44}^2 + 9\ B_{55}^2 + 82\ \lambda^2\ A_{44}B_{55}\right)}{9\left(\lambda^2 A_{44} + B_{55}\right)\left[45\left(\lambda^2 A_{44}^2 + B_{55}^2\right) + 464\ \lambda^2 A_{44}B_{55}\right]}$

Table 8.D.1. *Formulae for the calculation of torsional stiffness and bending stiffness of an off-axis rod. The material is monoclinic (13 elastic constants)*

Summing all the terms of the series, we get:

$$f = p'_1\ q'_1\ X_1\ X_2 + \sum_{m=1,2,3}^{\infty} \left(C_m \sin \frac{m\,\pi}{2}\ X_1 + C'_m \cos \frac{m\,\pi}{2}\ X_1\right) \left(D_m \sin h\ \frac{m\,\pi\,\mu}{2}\ X_2 + D'_m \cos h\ \frac{m\,\pi\,\mu}{2}\ X_{\acute{e}}\right) \qquad [8.D.85]$$

@Seismicisolation

Constants p′, q′, C_m, C'_m, D_m and D'_m must satisfy boundary conditions for stress [8.D.47]:

$$\sigma_{13} = \psi_{,2} = 0 \text{ for } x_1 = \pm b/2 \qquad \left.\begin{array}{l} s_{13} = \psi_{,2} = 0 \text{ for } x_1 = \pm b/2 \\ s_3 = -\psi_{,1} = 0 \text{ for } x_2 = \pm h/2 \end{array}\right\}$$

$$[\sigma_{33} = -\psi_{,2} = 0 \qquad x_2 = \pm h/2 \qquad [8.D.86]$$

$$\Psi_{,2} = 0 \quad \text{for} \quad X_1 = \pm 1, \qquad \Psi_{,1} = 0 \quad \text{for} \quad X_2 = \pm 1 \qquad [8.D.87]$$

The solution for M* includes successive steps of calculations concerning functions f, ζ and Ψ [NUG 76].

For shear stress function, Nugues proposes:

$$\psi = \frac{1}{\lambda^2 A_{44}} \left[\frac{1 - X_1^2}{2} + 16 \sum_{m=1,3,5} (-1)^{\frac{m+1}{2}} \frac{1}{m^3 \pi^3 \cosh \frac{m \pi \mu}{2}} \bullet \cos \frac{m \pi X_1}{2} \cosh \frac{m \pi \mu X_2}{2} \right] \qquad [8.D.88]$$

From equation [8.D.85], we evaluate M*:

$$M^* = \int_{-1}^{+1} \int_{-1}^{+1} \Psi \, dX_1 \, dX_2$$

$$= \frac{4}{\lambda^2 A_{44}} \left[\frac{1}{3} - \frac{64}{\pi^5} \frac{1}{\mu} \sum_{m=1,3,5}^{\infty} \frac{1}{m^5} \bullet \tanh \frac{m \pi \mu}{2} \right]$$

[8.D.89]

The interesting thing about Nugue's formulation is that the series in [8.D.86] is quickly convergent and consequently is easier to use than formulae using successive approximation methods.

@Seismicisolation

$$\left.\begin{aligned} \mu^2 &= \frac{\lambda^2\ A_{44}}{B_{55}} \\ \mu^2 &= \frac{\lambda^2\ s_{44}}{\left(s_{55} - \dfrac{s_{35}^2}{s_{33}}\right)} \\ B_{55} &= \frac{s_{55}}{s_{33}} - \frac{s_{35}^2}{s_{33}^2} \end{aligned}\right\} \qquad [8.D.90]$$

$$A_{44} = \frac{s_{44}}{s_{33}}$$

Appendix 8.E. Details on calculations of s_{35} and υ_{13} of transverse isotropic materials

Off-axis rods are used here. A change of axes is then adopted with a rotation α around fiber axis z = 3 in the plane (3, 2).

Appendix 8.C gives the formulae [8.C.3a-e] useful for expressing compliance coefficient s'_{ij} (after a change of axes) *versus* the original s'_{ij}.

8.E.1. *Torsion tests*

The following formula, see Table 8.D.1 in Appendix 8.D, is used:

$$M_t = \frac{3\ I\ \theta\ M^*}{s'_{33}} \qquad [8.D.62]$$

and we adopt the simplest approximate for M*:

$$M^* = M^*_1 = \frac{10}{9}\ \frac{1}{\left(\lambda^2\ A_{44} + B_{55}\right)} \qquad [8.D.70]$$

@Seismicisolation

in which:

$$A_{44} = \frac{s'_{44}}{s'_{33}}, \qquad B_{55} = \frac{s'_{55}}{s'_{33}} - \left(\frac{s'_{35}}{s'_{33}}\right) \qquad [8.D.68]$$

Bringing equations [8.D.68] and [8.D.67] into [8.D.61] we obtain:

$$M_T = \frac{3\ b\ h^3\ \theta}{12\ s'_{33}}\ \frac{10}{9\left(\lambda^2\ A_{44} + B_{55}\right)} \qquad [8.E.1]$$

The torsional stiffness is:

$$C_{Tf} = \frac{M_t}{\theta} = \frac{1}{\left(\lambda^2\ s'_{44} + s'_{55} - \frac{s'^2_{35}}{s'^2_{33}}\right)} \qquad [8.E.2]$$

C_{Tf} is experimentally evaluated. The right-hand side contains s'_{ij}, which is to be expressed against the original s_{ij}. Appendix 8.C gives such expressions in equation [8.C.3]. The aim of these calculations is to obtain the non-diagonal compliance coefficient:

$$s = s\left(s'_{11}, s'_{33}, s'_{44}, \lambda, C_{Tf}\right) \qquad [8.E.3]$$

in which λ is the ratio $\lambda = \frac{h}{b}\ \frac{\text{thickness}}{\text{width}}$ and C_{Tf} is measured stiffness.

The four compliance coefficients s'_{11}, s'_{33}, s'_{44} and s'_{55} are to be expressed against the original coefficients (defined in the natural symmetry axis of the material) and the rotation angle α. In Appendix 8.C equations [8.C.3a-d] give such expressions.

[8.D.70] is then to be developed and for convenience of calculation, the following set of intermediate variables is used.

$$F_1 = s_{11}\ \sin^4\ \alpha + s_{33}\ \cos^4\ \alpha \qquad [8.E.4a]$$

$$F_2 = 2\ s_{11}\ \sin^2\ \alpha - 2\ s_{33}\ \cos^2\ \alpha \qquad [8.E.4b]$$

@Seismicisolation

$$F_3 = s_{55} + 4\left(s_{11} + s_{33}\right)\sin^2\alpha\cos^2\alpha \qquad [8.E.4c]$$

$$\gamma = s_{55} + 2\,s_{13} \qquad [8.E.4d]$$

In equation [8.D.70], the following products are used and are to be expressed *versus* F_1, F_2, F_3 and γ :

$$\left.\begin{aligned} s'_{33}\,s'_{44} &= F_1\,s'_{44} + \gamma\left(\sin^2\alpha\cos^2\alpha\right)s'_{44} \\ s'_{33}\,s'_{55} &= -4\,\gamma^2\left(\sin\alpha\cos\alpha\right)^4 + F_1\,F_3 + \gamma\left(F_3 - 4\,F_1\sin^2\alpha\cos^2\alpha\right) \end{aligned}\right\}$$

$$\left.\begin{aligned} \left(s'_{35}\right)^2 &= \sin^2\alpha\cos^2\alpha\;F_2^2 + \gamma^2\left(\cos^2\alpha - \sin^2\alpha\right)^2 \\ &\quad + 2\,F_2\,\gamma\left(\cos^2\alpha - \sin^2\alpha\right) \\ s'_{33} &= F_1 + \gamma\sin^2\alpha\cos^2\alpha \end{aligned}\right\} \qquad [8.E.5]$$

Bringing [8.E.5] into [8.D.70] we obtain an equation in γ :

$$\left.\begin{aligned} &\gamma^2\left[-4\sin^4\alpha\cos^4\alpha - \sin^2\alpha\cos^2\alpha\left(\cos^2\alpha - \sin^2\alpha\right)^2\right] \\ &+ \gamma\left[\lambda^2\,s'_{44}\sin^2\alpha\cos^2\alpha - \left(F_3 - 4\,F_1\right)\sin^2\alpha\cos^2\alpha\right] \\ &-2\,F_2\left(\cos^2\alpha\right)\sin^2\alpha\cos^2\alpha - \frac{5}{18}\,\frac{bh^3}{C_{Tf}}\sin^2\alpha\cos^2\alpha \\ &+ \lambda^2\,F_1\,s'_{44} + F_1\,F_3 - F_3^2\sin^2\alpha\cos^2\alpha - \frac{5\,bh^3}{18\,C_{Tf}}\,F_1 = 0 \end{aligned}\right\} \qquad [8.E.6]$$

s'_{44} is not unknown:

@Seismicisolation

$$s'_{44} = s_{66} \sin^2 \alpha + s_{44} \cos^2 \alpha \qquad [8.E.7]$$

From equation [8.E.4] the following equation is derived:

$$\left.\begin{aligned} &\gamma^2 - \gamma \lambda^6 s'_{44} + F_3 - 4 F_1 - 2 F_2 \left(\cos^2 \alpha - \sin^2 \alpha\right) - \frac{5\, bh^3}{18\, C_{Tf}} + F_2 \\ &-\left(s_{11} \tan^2 \alpha + \frac{s_{33}}{\tan^2 \alpha}\right)\left(\lambda^2 s'_{44} + F_3 - \frac{5\, bh^3}{18\, C_{Tf}}\right) = 0 \end{aligned}\right\} \qquad [8.E.8]$$

$$\text{with } \lambda = \frac{h}{b} \quad \frac{\text{thickness}}{\text{width}}$$

Taking the negative value of [8.E.8] we obtain:

$$\gamma = \frac{\hat{B} \pm \sqrt{\Delta}}{2} = s_{55} + 2\, s_{13} \qquad [8.E.9]$$

with:

$$\left.\begin{aligned} &\hat{B} = \lambda^2 s'_{44} + F_3 - 4 F_1 - 2 F_2 \left(\cos^2 \alpha - \sin^2 \alpha\right) - \frac{5\, bh^3}{18\, C_{Tf}} \\ &\hat{A} = F_2^2 - \left(s_{11} \tan^2 \alpha + \frac{s_{33}}{\tan^2 \alpha}\right)\left(\lambda^2 s'_{44} + F_3 - \frac{5\, bh^3}{18\, C_{Tf}}\right) \end{aligned}\right\} \qquad [8.E.10]$$

Finally, γ is given by the condensed equation:

$$\gamma^2 - \gamma \hat{B} + \hat{A} = 0 \qquad [8.E.11]$$

The non-diagonal coefficient of the compliance matrix is:

$$s_{13} = \frac{\gamma - s_{55}}{2} \qquad [8.E.12]$$

@Seismicisolation

8.E.2. *Bending tests*

Equations that serve to obtain bending stiffness and non-diagonal compliance coefficient s_{13} are simpler to calculate than those used in torsion tests. The off-axis rods contribute to an increase in the bending stiffness k′ in equation [8.40]. The formula [8.D.57] in Appendix 8.D serves for this calculation.

If the slenderness is sufficient, the correcting term $\frac{h^2\ N}{L}$ can be neglected and the formula is simplified:

$$v_{\text{off-axis}} = \frac{M\ s'_{33}\ L^2}{8\ I\left(1 + \frac{3}{4}\ A_{35}^2\ M^*\right)} \qquad [8.E.13a]$$

with:

$$A_{35} = \frac{s'_{35}}{s'_{33}}; \qquad k' = \frac{M}{v_{\text{off-axis}}} \qquad [8.E.13b]$$

The corresponding stiffness k deduced from equation [8.E.10] differs from stiffness k with an on-axis rod:

$$v_{\text{on-axis}} = \frac{M\ s_{33}\ L^2}{8\ I} \qquad [8.E.14a]$$

$$k = \frac{8\ I}{L^2\ s_{33}} \qquad [8.E.14b]$$

The ratio is:

$$\frac{k'}{k} = \frac{s_{33}}{s'_{33}}\left(1 + \frac{3}{4}\ A_{35}^2\ M^*\right) \qquad [8.E.15]$$

We have to choose an approximate formula for M*. The simplest is presented in equation [8.D.67] and Figure 8.D.1:

@Seismicisolation

$$M^* = M^*_1 = \frac{10}{9}\,\frac{1}{\left(\lambda^2\,A_{44} + B_{55}\right)} \qquad [8.D.70]$$

Bringing equation [8.D.67] into [8.E.15]:

$$\frac{k'}{k} = \frac{s_{33}}{s'_{33}}\left(1 + \frac{3}{4}\frac{\left(s'_{35}\right)}{\left(s'_{33}\right)} \bullet \frac{10}{9}\,\frac{1}{\left[\frac{\left(\lambda^2\,s'_{44}\right)}{s'_{33}} + \left(\frac{s'_{55}}{s'_{33}}\right)\right]}\right)^2$$

$$\frac{k'}{k} = \frac{s_{33}}{s'_{33}}\left\{1 + \frac{5}{6}\left(\frac{s'_{35}}{s'_{33}}\right)^2 \frac{1}{\left[\lambda^2\,\frac{s'_{44}}{s'_{33}} + \left(\frac{s'_{55}}{s'_{33}}\right)^2\right]}\right\} \qquad [8.E.16]$$

The left-hand side of equation [8.E.13] is obtained by applying experimental measurements on the double pendulum. The right-hand side includes compliance s'_{ij} after a change of axis α (see equation [8.C.3] in Appendix 8.C).

The development of equation [8.E.16] enables us to obtain the equation:

$$s_{13} = s_{13}\left(\frac{k'}{k}, s_{11}, s_{44} = s_{55}, s_{33}, s_{66}, \lambda\right) \qquad [8.E.17]$$

with $\lambda = \frac{h}{b}\,\frac{\text{thickness}}{\text{width}}$.

A third-power equation of s_{13} is obtained from equations [8.E.16] and [8.E.17] and an intermediate variable γ. We then use equation [8.E.4c].

@Seismicisolation

Chapter 9

Vibrations of a Ring and Hollow Cylinder[1]

9.1. Introduction

In many applications, the experimenter has rings and hollow cylinders as at his or her disposal rather than plane and straight beams. This chapter is devoted to the vibrations of such samples. The differential equations of motion, whose degree is higher than those concerning a straight beam, are presented here using d'Alembert's principle.

In 1871 Hoppe [HOP 1871] first determined the equation of a complete circular ring and in 1888 Lamb [LAM 1888] obtained the eigenfrequency equation of motion for an incomplete ring. The equations of motion in and out of a plane are presented by Love [LOV 34] for a ring of circular cross-section. In all of the aforementioned publications, the rod is supposed to be inextensible.

Philipson [PHI 56] takes into account the extension of the neutral line in the cross-section of the plane in order to study the flexural vibration of the ring. Rotational inertia and shear effects are included in equations of motion by Kuhl [KUL 92]. Lincoln and Volterra [LIN 67] showed that, at higher frequencies, even for a thin ring, it is necessary to include the inertia and shear effects. Seidel and Erdelyi [SEI 64], Rao and Sundararajan [RAO 69] and Kirkhope [KIR 71] examined in-plane vibrations of a ring with any cross-section.

Chapter written in abridged version by Jean Tuong VINH.

1 This chapter is taken from the report presented by Bersegol [BER 77] to obtain an engineering degree from CNAM, Paris.

Mechanics of Viscoelastic Materials and Wave Dispersion Edited by Yvon Chevalier and Jean Tuong Vinh
© 2010 ISTE Ltd. Published 2010 by ISTE Ltd.

@Seismicisolation

Out-of-plane vibrations of a curved rod must take into account coupling between in-plane and out-of-plane vibrations. This problem occurs when the curved rod has a neutral plane that is not a principal inertia plane. By means of an energetic approach, Kirkhope [KIR 71] established a stiffness matrix.

In 1977, Hawkings [HAW 77] numerically solved the differential equation system using generalized displacements and forces for any cross-section.

9.2. Equations of motion of a circular ring with rectangular cross-section

9.2.1. *Generalized displacement and force*

Figure 9.1 shows the geometry of a ring with two cylinder coordinate systems, the first of which is centred on symmetry axis z and the second is the running coordinate system ($\vec{\tau}$ tangential axis, $\vec{\beta}$ parallel to $\vec{z}$, $\vec{\gamma}$ radial axis). Let $\vec{U}$ and $\vec{\omega}$ be the generalized displacement of a point M and rotation of a section respectively.

The generalized displacement has the following components:

$$\vec{U} = u\,\vec{v} + v\,\vec{\tau} \qquad [9.1]$$

$$\vec{\omega} = \omega\,\vec{\beta} \qquad [9.2]$$

The volumic force components are:

$$f(s) = p(s)\vec{v} + q(s)\,\vec{\tau} \qquad [9.3]$$

Generalized internal force has three components –N (s), T (s) and M(s):

$$\vec{\tau}(s) = N(s)\,\vec{\tau} + \vec{T}(s)\,\vec{\gamma} \qquad [9.4a]$$

where N (s) is the tension or compression force, T (s) shear force, and s is the running coordinate of point M.

$$\vec{M}(s) = M(s)\,\vec{\beta} \qquad [9.4b]$$

and M (s) designates the bending moment.

@Seismicisolation

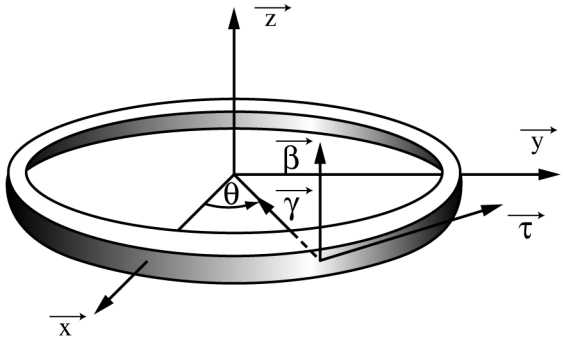

Figure 9.1. *Circular ring with rectangular cross-section. Two cylindrical coordinate systems are presented* $(\vec{x}, \vec{y}, \vec{z})$ *centred at the ring axis,* $\vec{\beta}, \vec{\tau}, \vec{\gamma}$. *Cartesian unit vectors at a running coordinates*

9.2.2. *Bending equations*

Dynamic law enables us to write:

$$p = -\mu \frac{\partial^2 u}{\partial t^2} \qquad [9.5]$$

$$q = -\mu \frac{\partial^2 v}{\partial t^2} \qquad [9.6]$$

where μ is the mass per unit length, p and q are inertia force components. With R being the ring radius, the laws of motion are:

$$\frac{\partial N}{\partial s} - \frac{T}{R} + q = 0 \qquad [9.7]$$

$$\frac{\partial T}{\partial s} + \frac{N}{R} + p = 0 \qquad [9.8]$$

$$\frac{\partial M}{\partial s} + T = 0 \qquad [9.9]$$

N and T are normal and tangential forces respectively.

@Seismicisolation

9.2.3. *Strain components*

For a curvilinear continuous medium, the following strain components are obtained:

$$\vec{\gamma} = \frac{d\,\vec{\omega}}{d\,s} \qquad [9.10]$$

$$\vec{\varepsilon} = \frac{d\,\vec{u}}{d\,s} + \vec{\tau} \wedge \vec{\omega} \qquad [9.11]$$

The constitutive equation for an isotropic ring:

– the bending moment is:

$$M\,(s) = E_1\,I\,\gamma \qquad [9.12]$$

– the normal force component is:

$$N\,(s) = E_1\,S\,\varepsilon \qquad [9.13]$$

with $E_1 = E_{\theta\theta} = E_{11}$ the longitudinal Young's modulus:

$$\vec{\gamma} = \gamma\,\vec{\beta},\ \vec{\varepsilon} = \varepsilon\,\vec{\tau} \qquad [9.14]$$

and the following unit vectors can be written:

$$\frac{d\,\vec{\tau}}{d\,\theta} = \vec{\gamma},\ \frac{\partial\,\vec{\gamma}}{\partial\,\theta} = -\vec{\tau} \qquad [9.15]$$

The three components of strain $\vec{\varepsilon}$ are:

$$\vec{\varepsilon} = \begin{Bmatrix} \dfrac{\partial\,v}{R\,\partial\,\theta} - \dfrac{u}{R} \\ \dfrac{\partial\,u}{R\,\partial\,\theta} + \dfrac{v}{R} - \omega \\ 0 \end{Bmatrix} \qquad [9.16]$$

@Seismicisolation

As $\vec{\varepsilon} = \varepsilon\,\vec{\tau}$:

$$\left.\begin{aligned} \varepsilon &= \frac{\partial V}{R\,\partial\theta} - \frac{u}{R} && \text{(a)} \\ \omega &= \frac{\partial u}{R\,\partial\theta} + \frac{v}{R} && \text{(b)} \end{aligned}\right\} \qquad [9.17]$$

From equation [9.17b], γ is:

$$\gamma = \frac{1}{R^2}\left[\frac{\partial^2 u}{\partial\theta^2} + \frac{\partial v}{\partial\theta}\right] \qquad [9.18]$$

9.2.4. *Force components*

Equation [9.9] gives rise to tangential force:

$$T = -\frac{\partial}{\partial s}\left[\frac{E\,I}{R^2}\left(\frac{\partial^2 u}{\partial\theta^2} + \frac{\partial V}{\partial\theta}\right)\right] \qquad [9.19]$$

E and I are Young's modulus and inertia moment respectively, and with $\partial s = R\,\partial\theta$, T becomes:

$$T = -\frac{E\,I}{R^3}\left(\frac{\partial^3 u}{\partial\theta^3} + \frac{\partial^2 V}{\partial\theta^2}\right) \qquad [9.20]$$

Equation [9.8] is rewritten as normal force:

$$N = R\left[\mu\,\frac{\partial^2 u}{\partial t^2} - \frac{\partial T}{\partial s}\right] \qquad [9.21]$$

Bringing equation [9.20] into [9.21]:

$$N = R\left[\mu\,\frac{\partial^2 u}{\partial t^2} + \frac{E\,I}{R^4}\left(\frac{\partial^4 u}{\partial\theta^4} + \frac{\partial^3 v}{\partial\theta^3}\right)\right] \qquad [9.22]$$

@Seismicisolation

Equation [9.7] then becomes equation [9.23], taking into account equations [9.20] and [9.21].

9.2.5. *Equations of motion*

$$\mu \frac{\partial^3 u}{\partial t^2 \partial \theta} + \frac{E I}{R^4}\left[\frac{\partial^5 u}{\partial \theta^5} + \frac{\partial^4 v}{\partial \theta^4}\right] + \frac{E I}{R^4}\left[\frac{\partial^3 u}{\partial \theta^3} + \frac{\partial^2 v}{\partial \theta^2}\right] = \mu \frac{\partial^2 v}{\partial t^2} \quad [9.23]$$

If the classical inextensibility law is admitted, we have:

$$\frac{\partial v}{\partial \theta} = u \quad [9.24]$$

Then equation [9.23] can be rewritten in the final form:

$$\mu\left[\frac{\partial^4 v}{\partial \theta^2 \partial t^2} - \frac{\partial^2 v}{\partial t^2}\right] + \frac{E I}{R^4}\left[\frac{\partial^6 v}{\partial \theta^6} + 2\frac{\partial^2 v}{\partial \theta^4} + \frac{\partial^2 v}{\partial \theta^2}\right] = 0 \quad [9.25]$$

9.2.6. *Eigenvalue equations*

The separation of variables is applied to equation [9.25]:

$$v(\theta, t) = v(\theta) \bullet f(t) \quad [9.26]$$

Bringing equation [9.26] into [9.25], we get:

$$\frac{I}{R^4}\left[\frac{d^6 v}{d\theta^6} + 2\frac{d^4 v}{d\theta^4} + \frac{d^2 v}{d\theta^3}\right] + \frac{\mu}{E}\frac{f''}{f}\left(\frac{d^2 v}{d\theta^2} - v\right) = 0 \quad [9.27]$$

$$\frac{I}{R^4}\left[\frac{v^{(6)} + 2v^{(4)} + v^{(2)}}{v - v^{(2)}}\right] - \frac{\mu}{E}\frac{f''}{f} = 0 \quad [9.28]$$

The superscript figure between brackets designates the derivative order with respect to θ. The superscript comma designates time derivative. The number of commas is the order of time derivative.

A non-trivial solution to equation [9.28] must be derived from the following equations:

@Seismicisolation

$$\frac{\mu}{E}\,\frac{f''}{f} = -m_c^{\,2} \qquad [9.29]$$

$$\frac{I}{R^4}\left[\,v^{(6)} + 2\,v^{(4)} + v^{(2)}\right] + m_c^{\,2}\left(\,v - v^{(2)}\right) = 0 \qquad [9.30]$$

with m_c being a constant. Equation [9.29] has a solution of the form:

$$f = A\cos\omega\,t + B\sin\omega\,t \qquad \text{with} \qquad \omega^2 = \frac{E\,m^2{}_c}{\mu} \qquad [9.31]$$

Let v be $v = ke^{s\theta}$ in equation [9.30]:

$$\frac{1}{R^4}\,s^2\left(s^2+1\right)^2 + m_c^{\,2}\left(1 - s^2\right) = 0 \qquad [9.32]$$

which can be rewritten as follows

$$\lambda = s^2,\quad \lambda^3 + 2\,\lambda^2 + \lambda\,(\,1 - Q\,) + Q = 0 \qquad [9.33]$$

which is the characteristic equation with $Q = m^2{}_c\,\dfrac{R^4}{I}$.

9.2.7. *Solution of characteristics equation*

Equation [9.33] includes all the powers of λ. It is possible to transform this into a simpler third-degree equation without the terms in λ^2. This canonical form is obtained by letting:

$$\lambda = X - \frac{a}{3} \qquad [9.34]$$

$$\lambda^3 + a\,\lambda^2 + b\,\lambda + c = 0 \qquad [9.35]$$

@Seismicisolation

$$X^3 + p\,X + q = 0 \qquad [9.36]$$

with:

$$p = b - \frac{a^3}{3},\ q = \frac{2\,a^3}{27} - \frac{b\,a}{3} + c$$

Identifying equations [9.35] to [9.33], we get:

$$\left.\begin{aligned} p &= -\frac{1}{3} - Q \\ q &= -\frac{2}{27} + \frac{5}{3}\,Q \end{aligned}\right\} \qquad [9.37]$$

The discriminant of equation [9.36] is:

$$\Delta = 4\,p^3 + 27\,q^2 = Q\left(-4\,Q^2 + 71\,Q - 8\right) \qquad [9.38]$$

which is equal to zero with the following values of Q:

$$\left.\begin{aligned} Q_1 &= 0 \\ Q_2 &= 0.1134 \\ Q_3 &= 17.8375 \end{aligned}\right\} \qquad [9.39]$$

9.2.8. *Equations of motion of the ring submitted to in plane forced vibrations*

Characteristics equation [9.33] is an expression with parameter Q, which can be a multiplicity of values depending on positive integer m. Equation [9.39] gives the three root values of [9.38]. Interval $0 < Q < \infty$ is then divided into three subintervals inside which the sign of Q is determined. The three subintervals are:

@Seismicisolation

$$\left.\begin{array}{l} Q \in \ ]\,0\ ,\ 0.1134\ ] \\ Q \in \ ]\,0.1134\ ,\ 17.6375\ [\\ Q \in \ [\ 17.6375\ ,\ +\infty\ [\end{array}\right\} \qquad [9.40]$$

Sign Q depends on the sign of the determinant Q. The following table gives the sign Q in each subinterval.

Q	0	0.1134	17.6375	$+\infty$
Sign of Δ	]	-]	+ [	- [
Roots λ of [9.83]	Three real negative roots	One real negative root and two complex conjugate roots		Two real positive roots One real negative root
One negative root, two double negative roots				

Table 9.1. *The nature of root λ in equation [9.33]*

Depending on the nature of the roots λ, three differential equation [9.30] solution types can be written depending on subinterval in which Q is found. Details of the various expressions of u (θ) are presented in Appendix 9.A. The three values of Q corresponding to the first three vibration modes are:

$$Q_1 = 2.56, \qquad Q_2 = 33.15, \qquad Q_3 = 147.3 \qquad [9.41]$$

For further information, see Appendix 9.A, equation [9.A.24].

9.2.9. *Expression of Young's modulus versus Q*

Let us recall the expressions of Q and ω^2:

$Q = \dfrac{m_c^{\,2}\ R^4}{I}$ where m_c is the integer positive number, I the inertia moment

@Seismicisolation

$$\omega^2 = \frac{E\, m_c^{\,2}}{\mu} \text{ where } \mu \text{ is the weight per unit length}$$

$$(\mu = \rho\, S)$$

$$E_1 = \frac{4\,\pi^2\, f_k^2\, \rho\, S\, R^4}{Q_k\, I} = \frac{2\,\pi\, f_k^2\, R^3\, M_r}{Q_k\, I} \qquad [9.42]$$

and M_r is the ring weight.

9.3. Bibliography

[BER 77] BERSEGOL J. P., *Elastic and Viscoelastic Characteristics of Pyrolitic Graphite*, Report of engineer final studies, ISMCM, 93400, Saint-Ouen, France, 1977.

[HAW 77] HAWKINGS D. L., "A generalized analysis of the vibration of circular rings", *Journal of Sound and Vibration*, vol. 54, p.67-74, 1977.

[HOP 1871] HOPPE R., "Vibrationen eines ringes in seiner ebene", *Journal für die reine und angewandte Mathematik (Crelle's)*, vol. 73, p. 158-170, 1871.

[KIR 71] KIRKHOPE J., "Vibration of system of elastically coupled concentric ring", *Journal of the Acoustical Society of America*, vol. 14, p. 371-373, 1971.

[KUH 42] KUHL W., "Messungen zu den Theorien der Eigenchwingungen von Kreisringen beliebiger Wandstärke", *Akustische Zeitschrift*, vol. 7, p. 125-152, 1942.

[LAM 1888] LAMB H., *London Mathematical Society Proceedings*, vol. 19, p. 165, 1888.

[LIN 67] LINCOLN J. W., VOLTERRA E., "Experimental and theoretical determination of Frequencies of elastic toroids", *Experimental Mechanics*, vol. 24, p. 211-217, 1967.

[LOV 34] LOVE A. E. H., *The Mathematical Theory of Elasticity*, Cambridge University Press, 1934.

[PHI 56] PHILIPSON L. L., "On the role of extension in the flexural vibrations of rings", *Journal of Applied Mechanics*, vol. 23, p. 324-336, 1956.

[RAO 69] RAO S. S., SUNDARARAJAN V., "In plane flexural vibration of circular ring", *Journal of Applied Mechanics*, vol. 91, p. 620-625, 1969.

[SEI 64] SEIDEL B. S., ERDELYI E. A., "On the vibration of a thick ring in its own plane", *Journal of Engineering for Industry,* vol. 86, p. 240-243, 1964.

@Seismicisolation

9.4. Appendices

Appendix 9.A. Expression u (θ) in the three subintervals delimited by the roots λ of equation [9.33]

9.A.1. *Solution in the subinterval* $Q \in \left]0, 0.1134\right]$

In Table 9.1, in this subinterval there are three negative roots for λ. The expression of v (θ) includes exclusively trigonometric functions.

The characteristics equation of the third order is:

$$v(\theta) = A \cos l\,\theta + B \sin l\,\theta + C \cos m\,\theta + D \sin m\,\theta + E \cos n\,\theta + F \sin n\,\theta \qquad [9.A.1]$$

where l, m and n are three roots of characteristic equation [9.33]. Displacement component u (θ) is obtained by the derivation:

$$u(\theta) = \frac{d\,v\,(\theta)}{d\,\theta} = A\,l \sin l\,\theta + B\,l \cos l\,\theta - C\,m \sin m\,\theta + D\,m \cos m\,\theta - E\,n \sin n\,\theta + F\,n \cos n\,\theta \qquad [9.A.2]$$

$$\frac{d\,u\,(\theta)}{d\,\theta} = -A\,l^2 \cos l\,\theta - B\,l^2 \sin l\,\theta - C\,m^2 \cos m\,\theta - D\,m^2 \sin m\,\theta - E\,n^2 \cos n\,\theta - F\,n^2 \sin n\,\theta \qquad [9.A.3]$$

The symmetry consideration and boundary conditions are:

$$\left.\begin{array}{lll} \theta \rightarrow -\theta & u(\theta) = u(-\theta) & v(\theta) = -v(-\theta) \\ \theta = 0 & v = 0 & \dfrac{d\,u}{d\,\theta} = 0 \\ \theta = \pi & v = 0 & \dfrac{d\,u}{d\,t} = 0 \end{array}\right\} \qquad [9.A.4]$$

Introduction of equation [9.A.4] into equations [9.A.3] and [9.A.2] gives rise to:

@Seismicisolation

$$u(\theta) = F\left[-\frac{l\sin n\pi}{\sin l\pi}\left(\frac{n^2-m^2}{l^2-m^2}\right)\cos l\theta + \frac{m\sin n\pi}{\sin m\pi}\left(\frac{n^2-l^2}{l^2-m^2}\right)\cos m\theta + n\cos n\theta\right] \quad [9.A.5]$$

It is now necessary to indicate the localization of excitation. Figure 9.A.1 shows the ring clamped between two cylinders with a circular cross-section. We can then write:

$$u(\theta,t) = u(\theta)\bullet f(t) \quad [9.A.6]$$

$$f(t) = A\cos\omega t + B\sin\omega t$$

$$u(\pi,t) = u(\pi)\left[A\cos\omega t + B\sin\omega t\right] = \Gamma\cos\omega t$$

The choice of $u(\pi,t)$ in the last equation with $B = 0$ and [9.A.5] gives:

$$A\,F = \frac{\Gamma}{-\frac{l\sin n\pi}{\mathrm{tg}\, l\pi}\left(\frac{n^2-m^2}{l^2-m^2}\right) + \frac{m\sin n\pi}{\mathrm{tg}\, n\pi}\left(\frac{n^2-l^2}{l^2-m^2}\right) + n\cos n\pi} \quad [9.A.7]$$

then:

$$u(\theta,t) = \frac{\Gamma\cos\omega t}{D}\left[\frac{\sin n\pi}{\sin l\pi}\left(\frac{n^2-m^2}{l^2-n^2}\right)\cos l\theta + \frac{m\sin n\pi}{\sin m\pi}\left(\frac{n^2-l^2}{l^2-m^2}\right)\bullet\cos m\theta + n\cos n\theta\right] \quad [9.A.8]$$

with:

$$D = -(l\sin n\pi/\mathrm{tang}\, l\pi).(m\sin n\pi/\mathrm{tang}\, m\pi)([n^2-l^2]/[l^2-m^2]) + n\cos np \quad [9.A.9]$$

@Seismicisolation

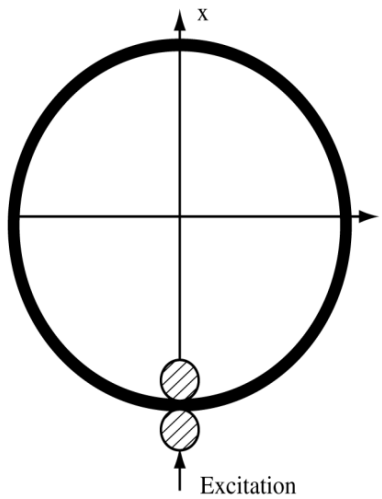

Figure 9.A.1. *Ring clamped between two cylinders. Excitation is applied to the ring at this point*

Integration of u (θ) with respect to θ gives v (θ). In the subinterval mentioned above, there is no resonance of the ring.

9.A.2. *Solution in the subinterval* $Q \in \left]0.1134\,,\,17.6375\right[$

Table 9.1 mentions one negative root and two imaginary conjugate roots. In this case, the solution has the form:

$$\begin{aligned} v\,(\theta) &= a\cos l\,\theta + b\sin l\,\theta + c\cos\eta\,\theta\cosh\xi\,\theta \\ &+ e\cos\eta\,\theta\sinh\xi\,\theta + d\sin\eta\,\theta\cosh\xi\,\theta \\ &+ f\sin\eta\,\theta\sinh\xi\,\theta \end{aligned} \qquad [9.A.10]$$

In equation [9.A.10], -1^2 is the negative real root λ. ξ the real and η the imaginary part are the square roots of the characteristic equation's complex conjugate roots λ.

@Seismicisolation

$$u(\theta) = \frac{d\,v(\theta)}{d\,\theta} = -a\,l \sin l\,\theta + b\,l \cos l\,\theta$$
$$+ c\,[\xi \sin h\,\xi\,\theta \cos n\,\theta - \eta \sin \eta\,\theta \cos h\,\xi\,\theta]$$
$$+ e\,[\xi \cos h\,\xi\,\theta \cos \eta\,\theta - \eta \sin \eta\,\theta \bullet \sin h\xi\,\theta] \qquad [9.A.11]$$
$$+ d\,[\xi \sin h\,\xi\,\theta \sin n\,\theta + \eta \cos n\,\theta \cos h\,\xi\,\theta]$$
$$+ f\,[\xi \cos h\,\xi\,\theta \bullet \sin \eta\,\theta + \eta \cos \eta\,\theta \sin h\,\xi\,\theta]$$

The same boundary conditions and symmetry consideration as in section 9.A.1. give:

$$u(\theta,t) = D\left\{\frac{2\,\xi\,\eta\,l}{\sin\,l\pi}\left[\frac{\tanh \xi\pi \cos \eta\pi \sinh \xi\pi + \sin \eta\pi \cosh \xi\pi \tan \eta\pi}{\tanh \xi\pi\left(l^2 + \xi^2 - \eta^2\right) - 2\,\xi\,\eta \tan \eta\pi}\right]\right\}\bullet$$

$$\left[\frac{\tan\,\eta\pi\left(l^2 + \xi^2 - \eta^2\right) + 2\,\xi\,\eta \tanh \xi\pi}{\tanh \xi\pi\left(l^2 + \xi^2 - \eta^2 - 2\,\xi\,\eta \tan \eta\pi\right)}\right]\left(\xi \cos h\xi\theta \cos \eta\theta - \eta \sin \eta\theta \sinh \xi\theta\right)$$

$$+ \xi \sinh \xi\,\theta \sin \eta\,\theta + \eta \cos \eta\,\theta \cosh \xi\,\theta\,\left(A\theta \cos \omega t + B \sin \omega t\right) \qquad [9.A.12]$$

As above, β is set to zero:

$$u(\theta,t) = \frac{\Gamma \cos \omega t}{D}\left\{\begin{array}{l}\dfrac{2\,\xi\,\eta\,l}{\sin l\,\pi}\left[\dfrac{\tan h\,\xi\,\pi \cos \eta\,\pi \sin h\,\xi\,\pi + \sin \eta\,\pi \cos h\,\xi\,\pi\,tg\,\eta\,\pi}{\tan h\,\xi\pi\left(l^2 + \xi^2 - \eta^2\right) - 2\,\xi\,\eta \tan \eta\,\pi}\right] \\ \bullet \cos l\,\theta - \left[\dfrac{\tan \eta\pi\left(l^2 + \xi^2 - \eta^2\right) + 2\,\xi\,\eta \tanh \xi\pi}{\tanh \xi\,\eta\left(l^2 + \xi^2 - \eta^2\right) - 2\,\xi\,\eta \tan \eta\pi}\right]\bullet \\ \left(\xi \cos h\,\xi\theta \cos \eta\,\theta - \eta \sin \eta\,\theta \sinh \xi\,\theta\right) + \xi \sin h\,\xi\,\theta \sin \eta\,\theta \\ + \eta \cos \eta\,\theta \cosh \xi\,\theta)\end{array}\right\}$$

[9.A.13]

@Seismicisolation

with the denominator D defined as:

$$D=\frac{2\,\xi\,\eta\,l}{\sin l\,\pi}\left\{\begin{array}{l}\left[\dfrac{\tanh\xi\,\pi\cos\eta\,\pi\sinh\xi\,\pi+\sin\eta\,\pi\cos h\,\xi\,\pi\tan\eta\,\pi}{\tanh\xi\,\pi\left(l^2+\xi^2-\eta^2\right)-2\,\xi\,\eta\tan\eta\,\pi}\right]\bullet \\ \cos l\,\pi-\left[\dfrac{\tan\eta\,\pi\left(l^2+\xi^2-\eta^2\right)+2\,\xi\,\eta\tanh\xi\,\pi}{\tanh\xi\,\pi\left(l^2+\xi^2-\eta^2\right)-2\,\xi\,\eta\tan\eta\,\pi}\right]\bullet \\ \left[\begin{array}{l}\xi\cos h\,\xi\,\pi\cos\eta\,\pi-\pi\sin\eta\,\pi\sinh\xi\,\pi+\xi\sinh\xi\,\pi\sin\eta\,\pi \\ +\eta\cos\eta\,\pi\cosh\xi\,\pi\end{array}\right]\end{array}\right\}$$

[9.A.14]

and v (θ, t) is obtained by integrating equation [9.A.14] with respect to θ.

To obtain resonance frequency, the denominator is set to zero. We then obtain the eigenfrequency equation:

$$0=\tan h\,\xi\,\pi\left(l^2-\xi^2-\eta^2\right)-\xi\tan\eta\,\pi\left(l^2+\xi^2+\eta^2\right)+$$

$$\tan\eta\,\pi\tan h\,\xi\,\pi\left[\begin{array}{l}\xi\tan h\,\xi\,\pi\left(l^2+\xi^2+\eta^2\right) \\ +\eta\tan\eta\,\pi\left(l^2-\eta^2-\xi^2\right)\end{array}\right]+\frac{2\,\xi\,\eta\,l}{\tan l\,\pi}\left(\tan h^2\,\xi\,\pi+\tan^2\eta\,\pi\right)$$

[9.A.15]

With $\tan h\ \pi\ \simeq\ 1$, [9.A.15] is reduced to:

$$\frac{l^2-\xi^2-\eta^2}{2\,\xi\,l}=-\frac{\sin^2\eta\,\pi}{\tan l\,\pi}$$ [9.A.16]

The value for Q at resonance frequency (see Figure 9.A.2) is:

$$Q_1=2.56$$ [9.A.17]

@Seismicisolation

Deformation shape of the ring at resonance frequency – there are two nodes (see Figure 9.A.3) situated at angles:

$$\theta = \pi = 180°$$

$$\theta = \pm\ 1.1 \text{ radian} = \pm\ 63°$$

9.A.3. *Solution in the subinterval* $Q \in [17.6375\ ,+\infty[$

Table 9.1 indicates that there are three real roots: two positive and one negative. The general solution for the differential equation [9.27] is first obtained for u (θ, t). Integration on this last function permits us to obtain v (θ, t).

As roots λ are real, v (θ, t) has the form:

$$v\ (\theta,t) = a \cosh l\theta + b \sinh l\theta + c \cosh m\theta + d \sinh m\theta + e \sin n\theta + f \cos n\theta \qquad [9.A.18]$$

l^2 and m^2 are the two real positive roots λ, whereas n^2 are negative with $l > m$.

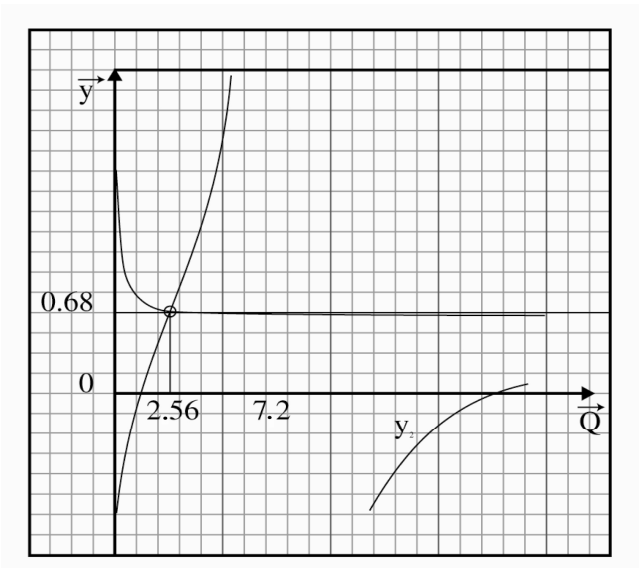

Figure 9.A.2. *Value of Q at resonance is obtained by solving a transcendental equation*

@Seismicisolation

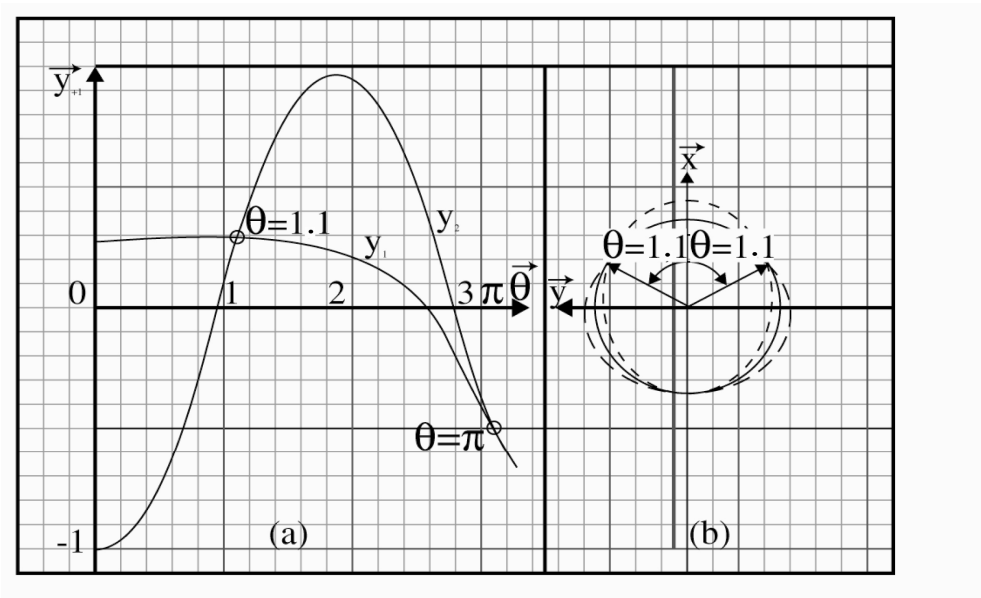

Figure 9.A.3. *a) The shape of the deformed ring is obtained by solving an indicated equation; b) position of nodes on the ring*

$$u\ (\theta,t) = \frac{d\ v\ (\theta)}{d\ \theta} = a\ l \sinh l\theta + b\ l \cosh l\ \theta + c\ m \sinh m\ \theta + d\ m \cosh m\ \theta + e\ n \cos n\theta - fn \sin n\theta \qquad [9.A.19]$$

The calculation is similar to the two aforementioned cases.

$$u\ (\theta,t) = \frac{\Gamma}{D}\left[\frac{-l \sin n\ \pi \cosh l\ \theta}{\sinh l\ \pi}\left(\frac{n^2 + m^2}{m^2 - l^2}\right) + m \cosh m\ \theta \bullet \frac{\sin n\ \pi}{\sinh m\ \pi}\left(\frac{n^2 + l^2}{m^2 - l^2}\right) + n \cos n\ \theta\right] \qquad [9.A.20]$$

$$(\ a \cos \omega\ t + b \sin \omega\ t)$$

with the same excitation as above, $\beta = 0$.

@Seismicisolation

$$u\ (\theta,t) = \cos\omega t \left[\begin{array}{l} -\dfrac{l \sin n\pi}{\sinh l\pi} \cosh l\theta \left(\dfrac{n^2 + m^2}{m - l^2} \right) \\ + m \cosh m\theta \bullet \dfrac{\sin n\pi}{\sinh m\pi} \left(\dfrac{n^2 + l^2}{m^2 - l^2} \right) \\ + n \cos n\theta \end{array} \right] \frac{\Gamma}{D} \qquad [9.A.21]$$

$$D = -l \frac{\sin n\pi}{\tanh l\pi} \left(\frac{n^2 + m^2}{m^2 - l^2} \right) + m \frac{\sin n\pi}{\tanh m\pi} \left(\frac{n^2 + l^2}{m^2 - l^2} \right) + n \cos n\pi \qquad [9.A.22]$$

Integration of equation [9.A.21] with respect to θ gives v (θ, t). The eigenvalue equation corresponds to the resonance that sets the denominator D to zero, see Figure 8.A.4. Here we obtain:

$$\tanh\ n\pi = \frac{n\ (m + l)}{m\ l - n^2} \qquad [9.A.23]$$

with $\tan h\ l\pi$ and $\tan m\pi \simeq 1$.

Figures 9.A.4 and 9.A.5 show that the first two roots are:

$Q_2 = 33.15$ and $Q_3 = 147.3$

Five vibration nodes are obtained and situated at the following angles (see Figure 9.A.6):

$\theta = \pi = 180°$

$\theta = \pm\ 0.55$ rad $= \pm\ 31°\ 30'$

$\theta = \pm\ 1.84$ rad $= \pm\ 105°\ 24'$

@Seismicisolation

9.A.3.1. *Conclusion*

The first three modes are obtained and corresponding values of Q are:

$$Q_1 = 2.58 \qquad Q_2 = 33.15 \qquad Q_3 = 147.3 \qquad [9.A.24]$$

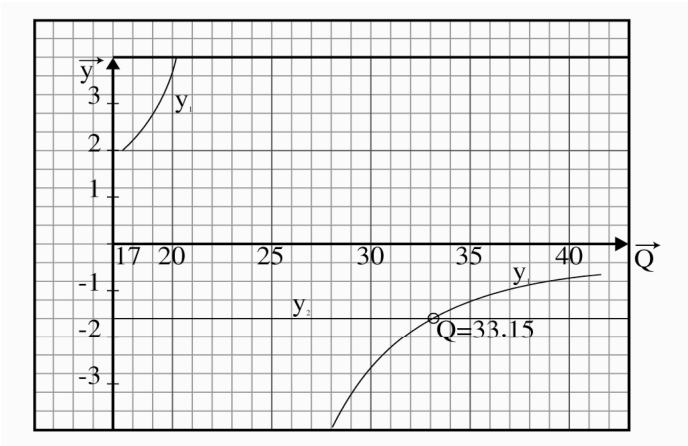

Figure 9.A.4. *Graphical representation of the solution to equation [9.A.23]. Solution for the first root*

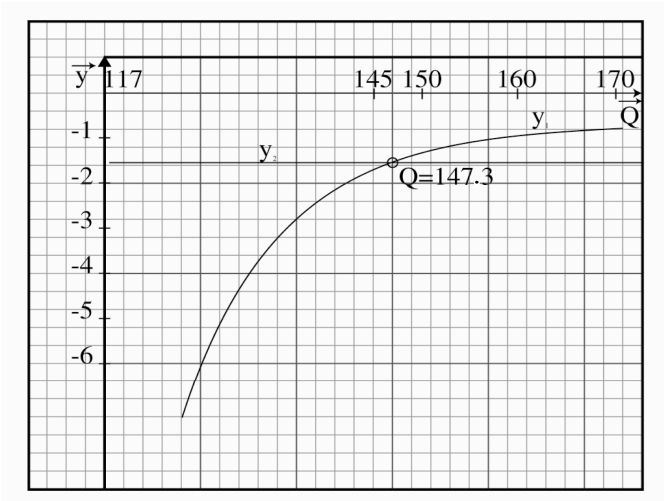

Figure 9.A.5. *Graphical representation of equation [9.A.23]. Solution for the second root*

@Seismicisolation

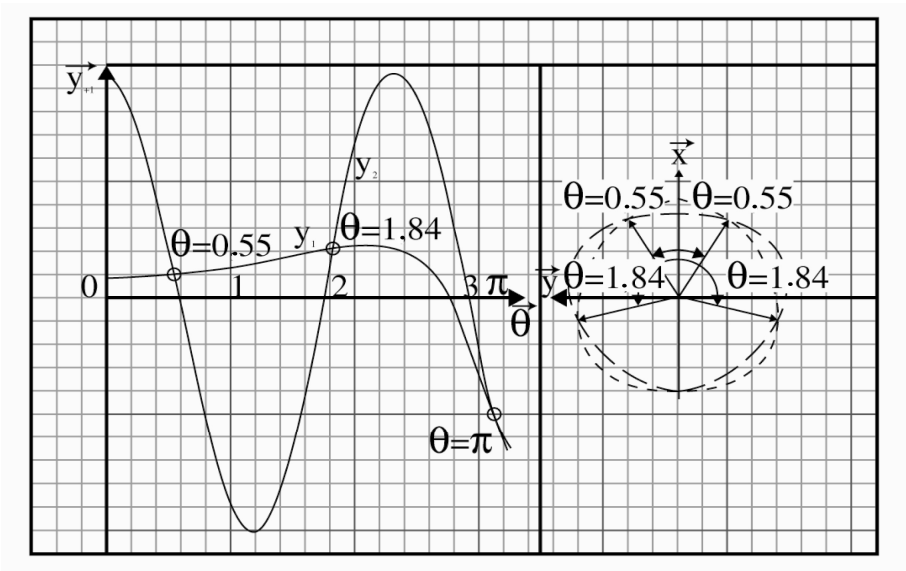

Figure 9.A.6. *Positions of the vibration nodes on the ring. Angles θ are obtained by solving the equation presented in the figure*

@Seismicisolation

Chapter 10

Characterization of Isotropic and Anisotropic Materials by Progressive Ultrasonic Waves[1]

10.1. Presentation of the method

Widespread common opinion in industry is that the applications of ultrasonic waves are essentially devoted to the non-destructive inspection of machine parts and structures. The safety of mechanical parts, such as railways, pressure vessels, ships, etc., and their longevity depends on the preventive detection of flaws and defects in the structure. Indeed it occupies the majority of industrial applications in this field. In this chapter we will examine two aspects of ultrasonic waves – theoretical and practical – for the quantitative characterization of elastic (or viscoelastic) materials.

10.1.1. *Use of ultrasonic waves*

10.1.1.1. *Theoretical aspects*

Ultrasonics constitutes a large research field in acoustics. In the domain of elastic behavior of materials at high frequency, the theory of progressive wave propagation is easy to formulate, at least in a medium that is not too dependent on boundary conditions. If caution is taken to satisfy such conditions, the medium can be considered as infinite. The equations of wave motion require only the utilization of

---

Chapter written by Patrick GARCEAU.

1 This chapter is largely extracted from Pierre Garceau's masters thesis [GAR 77]. Abridged English version is written by Jean Tuong Vinh.

Mechanics of Viscoelastic Materials and Wave Dispersion Edited by Yvon Chevalier and Jean Tuong Vinh
© 2010 ISTE Ltd. Published 2010 by ISTE Ltd.

@Seismicisolation

Christoffel's second-order tensor, which is derived from the fourth-order stiffness tensor C_{ijkl}. The evaluation of eigenvalues and eigenvectors *versus* Christoffel's tensor components is straightforward.

If we compare ultrasonic wave propagation to stationary waves in rods, rod equations of motion are more difficult to establish. Eigenvalues derived from these equations are more complicated to handle and they depend on the degree of approximation you want to adopt. This is due to boundary conditions on the lateral surfaces and at both ends.

A sophisticated mathematical solution to the problem of wave motion in a wave guide calls on a simple field of displacement using polynomials of coordinates or mixed fields of displacement and stress. Such a sophisticated formulation is not necessary for an infinite or semi-infinite medium.

Phase velocities are easy to obtain and stiffness matrix coefficients C_{ijkl} can be directly deduced. The main practical advantage in calculations made to obtain such coefficients resides in the fact they can be evaluated directly from phase velocities using Christoffel's tensor Γ_{ik}. In a propagation direction, which is not necessarily colinear with a symmetry axis of the material, we can easily obtain the following expression of Γ where P_l and P_j are direction cosines:

$$\Gamma_{ik} = C_{ijkl}\ P_l\ P_j \qquad [10.1]$$

Compared to the compliance matrix coefficient s_{ijkl} used in the equations of rod motions, the change of axes are more complicated:

$$s_{ijkl} = P_{im}\ P_{jn}\ P_{kp}\ P_{lq}\ s_{mnpq} \qquad [10.2]$$

In the framework of an inverse problem, we can obtain incomparably better accuracy when calculating C_{ijkl} in equation [10.1] compared to [10.2].

10.1.2. *Practical considerations of ultrasonic waves*

10.1.2.1. *Ultrasonic wave propagation direction*

It is easy to choose the direction in which an ultrasonic wave should be launched in a medium. It is a matter of transducer orientation and of coupling liquid between the transducer and sample. It can otherwise be determined by simply using a water immersion bench.

@Seismicisolation

10.1.2.2. *Measurements of wave phase velocities during propagation*

These two quantities are physically the most accurate measurements.

10.2. Propagation of elastic waves in an infinite medium

The equation of motion for a continuum in the absence of body force is:

$$\sigma_{ij,\,j} = \rho\, u_{i,\,tt} \qquad [10.3]$$

The index after the comma in subscript designates derivatives of the orthonormal coordinates; and t the time.

The constitutive equation is:

$$\sigma_{ij} = C_{ijkl}\ \varepsilon_{kl} \qquad [10.4]$$

with the small strain defined as:

$$\varepsilon_{kl} = \frac{1}{2}\left(u_{k,l} + u_{l,\,k}\right) \qquad [10.5]$$

To obtain the propagation equation, [10.5] is brought into [10.4] and σ_{ij} is substituted in [10.3] to get:

$$\sigma_{ij} = \frac{1}{2}\, c_{ijkl}\ \left(u_{k,\,l} + u_{l,\,k}\right) \qquad [10.6]$$

with the remark concerning symmetry:

$$c_{ijkl} = c_{klij} \qquad [10.7]$$

Equation [10.6] is then rewritten as:

$$\sigma_{ij} = \frac{1}{2}\, C_{ijkl}\ u_{k,\,l} + \frac{1}{2}\, C_{ijkl}\, u_{l,\,k} \qquad [10.8]$$

@Seismicisolation

In equation [10.8], the two terms in the second members are equal, so:

$$\sigma_{ij} = C_{ijkl}\ u_{k,\,l} \qquad [10.9]$$

Bringing [10.9] into [10.3], we get:

$$C_{ijkl}\ u_{k,\,lj} = \rho\ u_{i,\,tt} \qquad [10.10]$$

This is the relationship that will be helpful to us.

10.3. Progressive plane waves

A harmonic progressive plane wave has the following form:

$$u_k = A_k\ \exp j\ \omega \left(t - \frac{p_i\ x_i}{v} \right) \qquad [10.11]$$

where p_i is the direction cosine of the propagation direction.

$$\vec{p} = \vec{p}\ (p_1, p_2, p_3) \qquad [10.12]$$

Let us write the wave amplitude as:

$$A_k = A d_k \qquad [10.13]$$

where d_k is the unit vector that indicates the direction of particle motion.

REMARK:

– exponential is used in equation [10.11]. It is inherent to progressive waves[2].

– instead of equation [10.10], we can write:

$$u_k = A_k\ \exp j\ \omega \left(\frac{p_i\ x_i}{v} - t \right)$$

2 For stationary waves, instead of [10.10] cosine or sine wave is used.

@Seismicisolation

– we can also write u_k in the following way:

$$u_k = A_k \exp j \left(\omega t - k\, p_i\, x_i\right) \qquad [10.14]$$

$$\text{with } v = \frac{\omega}{k}\ , \qquad [10.15]$$

where k is the wave number.

10.3.1. *Christoffel's tensor*

Bringing equation [10.11] into [10.10], and with [10.13] being taken into account:

$$C_{ijkl}\, p_l\, p_j = \left(-\frac{j\,\omega}{v}\right)^2 A_k = -\rho\, A_i\, \omega^2 \qquad [10.16]$$

To simplify the calculation, let us adopt the notation:

$$\Gamma_{ik} = C_{ijkl}\, p_l\, p_j \qquad [10.17]$$

This is the second-order Christoffel's tensor. The second-order character is explained by the product of two direction cosines, p_l and p_j. Its symmetry is derived from that of stiffness tensor C_{ijkl}.

10.3.2. *Christoffel's equation*

Equation [10.15] is rearranged as follows:

$$C_{ijkl}\, p_l\, p_j\, A_k - \rho\, v^2\, A_i = 0 \qquad [10.18]$$

Let A_i be:

$$A_i = \delta_{ik}\, A_k \qquad [10.19]$$

@Seismicisolation

and δ_{ik} is Kronecker's notation. Finally the so-called Christoffel's equation is:

$$\left(\Gamma_{ik} - \rho\, v^2\, \delta_{ik}\right) A_k = 0 \qquad [10.20]$$

[10.19] is recognized as an equation that gives us the polarization $\vec{d}$, which is the direction of particle vibration and also the phase velocity v. The eigenvalues and eigenvectors of Christoffel's tensor Γ_{ik} are given by Christoffel's equation.

10.3.3. *Eigenvalues of Γ_{ik} are real*

The eigenvalues are positive and the velocity must be real:

$$\gamma = \rho\, v^2 > 0 \qquad [10.21]$$

10.3.4. *Eigenvectors of Γ_{ik} are mutually orthogonal*

The consequence is that the three plane waves propagate in the same direction $\vec{p}\,(p_1, p_2, p_3)$, with three different velocities. Polarizations of these three waves are mutually orthogonal.

10.4. Polarization of three kinds of waves

Here we examine the characteristics of waves in greater detail.

10.4.1. *Longitudinal wave*

If $\vec{p} \bullet \vec{d} = 1$, then $\vec{p}$ and $\vec{d}$ are collinear. That means that particle motion $\vec{d}$ is in the direction of propagation. We have to deal with a longitudinal (or dilatational) wave. This wave propagates with change of volume.

10.4.2. *Transverse or shear wave*

If $\vec{p} \wedge \vec{d} = 1$, wave polarization $\left(\vec{d}\right)$ is orthogonal to propagation direction $\left(\vec{p}\right)$. We also call this the non-dilatational wave, which means that the wave propagates without a change in volume.

@Seismicisolation

10.4.3. *Quasi-transverse (QT) wave*

This is neither a longitudinal or a pure transverse wave.

The two equations written above $\left(\vec{p} \wedge \vec{d} = 1\right)$ are not valid. The two unit vectors make angles $\theta \neq 0$ and $\frac{\pi}{2}$. In physical terms, this means that there is a coupling between one longitudinal wave and two transverse waves.

Then in the expression of Christoffel's tensor components, we introduce non-diagonal and non-zero stiffness coefficient C_{ijkl} ( ) see equation [10.17].

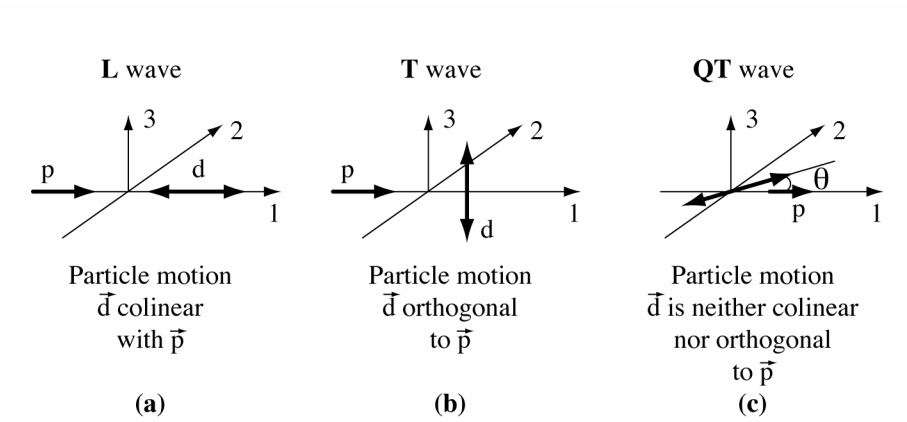

Figure 10.1. *The three kinds of waves: a) longitudinal (or extensional) wave; b) transverse (or shear) wave; c) QT (quasi-transverse) wave. The direction of wave propagation is supposed to be 1, which is a symmetry direction of the material in cases a) and b) and not in case c). The three kinds of waves are used for characterization of material. The QT wave is used in a direction of propagation that is not a symmetry axis of the material*

10.5. Propagation in privileged directions and phase velocity calculations

Christoffel's equation [10.20] has a non-trivial solution if and only if the determinant of the equation is identically set to zero.

$$\left|\Gamma_{ik} - \rho\, \upsilon^2\, \delta_{ik}\right| = 0 \qquad [10.22]$$

@Seismicisolation

Let us develop the determinant.

$$\begin{vmatrix} \left(\Gamma_{11} - \rho\, v^2\right) & \Gamma_{12} & \Gamma_{13} \\ \Gamma_{21} & \left(\Gamma_{22} - \rho\, v^2\right) & \Gamma_{23} \\ \Gamma_{31} & \Gamma_{32} & \left(\Gamma_{33} - \rho v^2\right) \end{vmatrix} = 0 \qquad [10.23]$$

To obtain a solution for [10.22], components of Christoffel's tensor need to be expressed *versus* the components C_{ijkl}. In Figure 10.2, these components are detailed. Developing [10.23] we obtain a polynomial which is cubic in v^2.

10.5.1. *Wave propagation along material symmetry axes*

Let (1, 2, 3) be the orthonormal reference axes that coincide with symmetry axes. For example, let us adopt:

$$p_1 = 1 \qquad\qquad p_2 = p_3 = 0$$

In equation [10.21], non-zero terms are reduced to the diagonal and the non-diagonal terms are zero (see Figure 10.2).

$$\begin{vmatrix} (C_{1111} - \rho v^2) & 0 & 0 \\ 0 & \left(C_{1212} - p\, v^2\right) & 0 \\ 0 & 0 & \left(C_{3131} - p\, v^2\right) \end{vmatrix} = 0 \qquad [10.24]$$

Expansion of equation [10.23] is reduced to the product of three factors:

$$\left(C_{1111} - \rho\, v^2\right)\left(C_{1212} - \rho\, v^2\right)\left(C_{3131} - \rho\, v^2\right) = 0 \qquad [10.25]$$

or separately each factor is set to zero:

$$\left.\begin{aligned} C_{1111} - \rho\, v^2 &= 0 \\ C_{1212} - \rho\, v^2 &= 0 \\ C_{3131} - \rho\, v^2 &= 0 \end{aligned}\right\} \quad \begin{aligned} &(a) \\ &(b) \\ &(c) \end{aligned} \qquad [10.26]$$

@Seismicisolation

The first equation corresponds to a wave such that:

$$v = v_1 = \sqrt{\frac{C_{1111}}{\rho}}$$

The second and third equations give rise to:

$$v = v_2 = \sqrt{\frac{C_{1212}}{\rho}}, \quad v = v_3 = \sqrt{\frac{C_{3131}}{\rho}} \text{ respectively}$$

10.5.1.1. *Particle motion direction* $\vec{d}$ *and polarization direction* $\vec{p}$

Equation [10.26] gives the velocity:

$$v = v_{1/1} = \sqrt{\frac{C_{1111}}{\rho}}\ \vec{p} \qquad [10.27]$$

where $\vec{d}$ and $\vec{p}$ are collinear and $\vec{p}$ component $p_1 = 1$. This corresponds to an extensional wave, as indicated in Figure 10.1a.

If we examine the four letters in the subscript of C_{1111}, we notice that the first two letters are related to stress components σ_{11} and the last two letters to strain component ε_{11} in the constitutive equation:

$$\sigma_{11} = C_{1111}\ \varepsilon_{11}$$

As in the case of the propagation of a wave in the direction of symmetry of the material, an interpretation of equations [10.25] and [10.26] is useful for understanding the polarization and direction of waves. We adopt tensorial writing (with four indexes) instead of matricial writing (with two indexes), which is largely adopted in vibrations of rods .

In equation [10.25] we have the product of three brackets. The first bracket is equalized to zero first:

$$(C_{11\,1l} - \rho\, v^2) = 0$$

@Seismicisolation

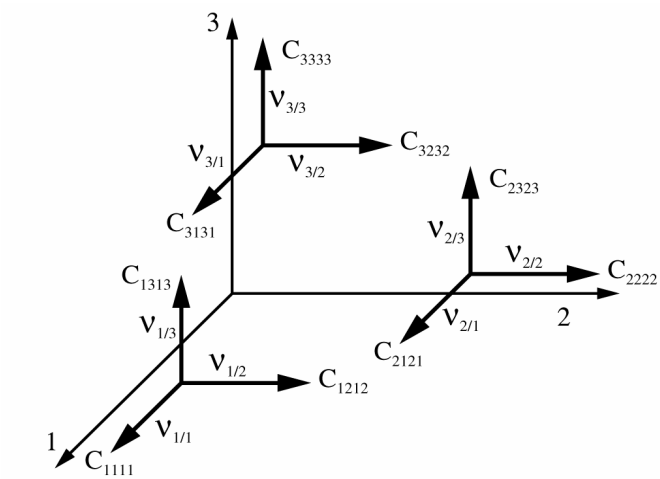

Figure 10.2. *Axes 1, 2, 3 are symmetry axes of the material along which waves can be launched, $v_{i/j}$ represents velocity C_{ijij} is stiffness coefficient deduced from $v_{i/j}$*

The first group of indexes 11 in subscript indicates that the normal stress component (direction 1 = x) is non-zero as well as the second group of indexes 11 concerning normal strain. The first figure in group 1 or 2 can designate the direction of polarization, which is colinear with abscissa x. The second figure in each group is also 1 and can designating the direction of unit polarization vector, which is also colinear with axis x. Physically we must use an extensional wave along the x axis. The measurement of the received wave is also along this axis x with an appropriate transducer.

Let us consider the second bracket in [10.25]:

$$(C_{12\,12} - \rho v^2) = 0$$

This time the two indexes in each group are different. The first figure is 1 and the second figure is 2. With the same remark as in the previous case we have: $\vec{d} = \vec{y}$, $\vec{p} = \vec{y}$, $\vec{x}$, $\vec{y}$ designate unit vectors along x and y axes respectively. We have to deal with shear waves that permit us to reach shear modulus C_{1212}.

So instead of v for the phase velocity, we can write $v_{1/1}$ for the first bracket and $v_{1/2}$ for the second bracket in which the subscript has two different figures – the first one for polarization and the second for propagation .

@Seismicisolation

We notice, however, that the convention we have adopted can be the reverse of the first figure designating propagation unit vector and the second figure of the unit of polarization. This convention gives rise to the same result, taking into account the symmetry in the writing components of stiffness tensor $C_{ij\,kl}$:

$$C_{ij\,kl} = C_{ji\,lk}$$

For the third bracket similar reasoning can be adopted as for the second bracket.

Tensorial writing is necessary, particularly when we have to deal with the general case where propagation of a wave is adopted in a direction that is not colinear with any symmetry direction of the material.

In Figure 10.3 all the components of the Christoffel's tensor are written in full. Utilization of the abridged convention with two indexes, instead of four indexes, for the stiffness tensor gives rise to the possibility of great errors in writing, if not making it impossible.

$\Gamma_{11} = C_{1111}p_1^2 + C_{1313}p_3^2 + C_{1212}p_2^2 + 2C_{1112}p_1p_2 + 2C_{1131}p_1p_3 + 2C_{3112}\,p_3p_2$	$\Gamma_{12} = C_{1112}p_1^2 + C_{2212}p_2^2 + C_{3123}p_3^2 + p_1p_2(C_{1122}+C_{1212}) + p_2p_3(C_{1223}+C_{3112}) + (C_{3112}+C_{1123})p_3p_1$	$\Gamma_{13} = C_{1131}p_1^2 + C_{1223}p_2^2 + C_{1333}p_3^2 + p_1p_2(C_{1123}+C_{1231}) + p_2p_3(C_{1233}+C_{3123}) + p_3p_1(C_{1313}+C_{1133})$
$\Gamma_{21} = C_{2111}p_1^2 + C_{2221}\,p_2^2 + C_{2331}p_3^2$ $p_1p_2(C_{2121}+C_{2221}) + p_2p_3(C_{2231}+C_{2321}) + p_3p_1(C_{3311}+C_{3131})$	$\Gamma_{22} = C_{2222}p_2^2 + C_{2323}^2p_3^2 + C_{1212}p_1^2 + 2C_{2212}p_1p_2 + 2C_{2223}p_2p_3 + 2C_{2312}p_3p_1$	$\Gamma_{23} = C_{2113}p_1^2 + C_{2223}p_2^2 + C_{2333}p_3^2 + p_1p_2(C_{2123}+C_{2213}) + p_2p_3(C_{2313}+C_{2133}) + p_3p_1(C_{2311}+C_{2133})$
$\Gamma_{31} = C_{3111}p_1^2 + C_{3221}p_2^2 + C_{3331}p_3^2 + p_1p_2(C_{3121}+C_{3211}) + p_2p_3(C_{3231}+C_{3321})$ $p_1p_3(C_{3311}+C_{3131})$	$\Gamma_{32} = C_{3112}p_1^2 + C_{3222}p_2^2 + C_{3332}p_3^2 + p_1p_2\,(C_{3122}+C_{3212}) + p_1p_3(C_{3232}+C_{3322})$ $p_3p_1(C_{3312}+C_{3132})$	$\Gamma_{33} = C_{3333}p_3^2 + C_{3131}p_1^2 + C_{3232}p_2^2 + 2C_{3132}p_1p_2 + 2C_{3323}p_3p_2 + 2C_{3331}p3_{p1}$

Figure 10.3. *Components of Christoffel's tensor* versus *components of stiffness tensor C_{ijkl}. Usually the following group of two indexes are adopted (11, 22, 33, 23, 31, 12) for stress σ_{ij} and strain components ε_{ij}. If one group is inverted, we can re-establish the order indicated above. For example C_{3121} is to be replaced by C_{3112}. We are also reminded that six components are retained for stress and strain components by consideration of symmetry*

@Seismicisolation

The long explanations presented above show that recourse to tensorial writing of tensor of four orders C_{ijkl} in an ultrasonic wave propagation problem is a necessity, not only on theoretical but also on practical grounds.

10.5.1.2. *Tensorial and matricial notations*

Here we focus on using tensorial notation C_{ijkl} .

As presented above, this notation includes an indication on vectors $\vec{d}$ (particle motion) and $\vec{p}$ (propagation direction) in the group of letters (11).

The matricial notation is a kind of shorthand with fewer letters in subscript, but the orientations of $\vec{d}$ and $\vec{p}$ are lost, as we shall see below.

10.5.1.3. $\vec{d}$ *and* $\vec{p}$ *for transverse waves*

The second factor in [10.25] gives:

$$v = v_{1/2} = \sqrt{\frac{C_{1212}}{v}} \qquad [10.28]$$

In subscript, 1 designates the direction $\vec{p}$ with $(p_1 = 1, p_2 = p_3 = 0)$ and the second letter 2 corresponds to $\vec{d}$:

$$(d_1 = 0 \qquad d_2 = 1 \qquad d_3 = 0)$$

The third factor in equation [10.25] gives:

$$v = v_{3/1} = \sqrt{\frac{C_{3131}}{\rho}} = \sqrt{\frac{C_{1313}}{\rho}} = v_{1/3} \qquad [10.29]$$

Directions 1 and 3 correspond respectively to $\vec{p}$ and $\vec{d}$:

$$\left[\ \vec{P}\ (1, 0, 0) \qquad \vec{d}\ (0, 0, 1)\right] \qquad [10.30]$$

@Seismicisolation

10.5.1.4. *Inversion of $\vec{d}$ and $\vec{p}$ in symmetry axes*

The stiffness tensor being symmetrical, in equation [10.29] the inversion of the letters in superscript is possible. That means that wave propagation after equation [10.28] is equivalent to:

$$\left[\ \vec{p}\ (0, 0, 1) \qquad \vec{d}\ (1, 0, 0)\right] \qquad [10.31]$$

10.5.2. *Elastic constants obtained with $\vec{p}$ colinear with one of the three material directions of symmetry*

Figure 10.2 represents $\vec{d}$ and $\vec{p}$, velocities $v_{i/j}$ and a possible measurement of C_{ijij}. In the material symmetry direction for propagation $\vec{p}$, nine elastic constants C_{ijij} can be obtained with three extensional waves and six shear waves. If the material satisfies symmetry directions 1, 2, 3, however, only the following coefficients are obtained:

– six elastic constants C_{1111}, C_{2222}, C_{3333n} C_{1212}, C_{2323} and C_{3131} are obtained for orthotropic materials (see Chapter 1);

– four elastic constants (C_{111} = C_{2222}), C_{3333}, C_{1212} and (C_{2323} = C_{3131}) are obtained for transverse isotropic materials, axis 3 being the transverse isotropic axis;

– diagonal stiffness matrix coefficients are only obtained in Figure 10.2. Non-diagonal coefficient evaluation requires wave propagation along a direction that does not coincide with the direction of symmetry.

10.5.3. *Wave propagation along a non-privileged direction*

It is interesting to adopt a non-privileged direction because the coupled waves occur (longitudinal and transverse waves) and the determinant in equation [10.23] is not empty in non-diagonal terms.

Let us take an example of an isotropic transverse medium. Figure 10.4 shows a long-fiber composite. In a cross-section perpendicular to fibers, the regular distribution in quincunx enables us to say that this cross-section is an isotropic plane (1, 2). We then have:

$$p_2 = 0 \qquad p_1 = \cos R, \qquad p_2 = \sin R \qquad [10.32]$$

@Seismicisolation

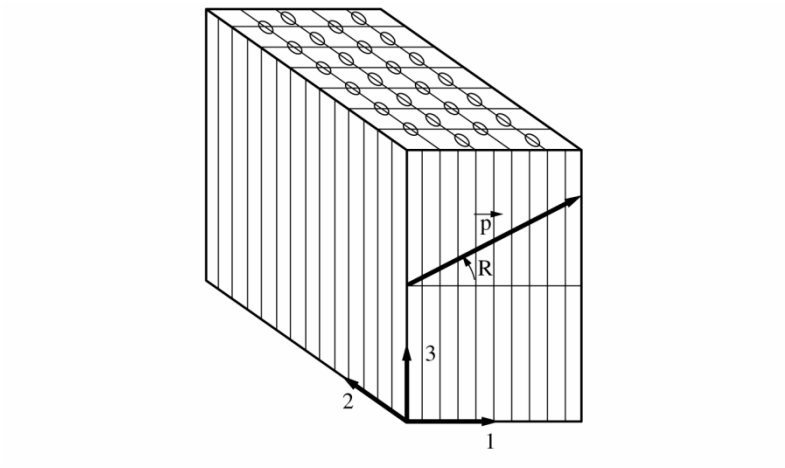

Figure 10.4. *The direction of propagation through the thickness of a transverse isotropic composite material* $\vec{p}$ *makes an angle R with symmetry direction 1 and is in the plane (1, 3). Plane 3 is symmetrical to the fiber axis*

In Figure 10.4, the components of Γ_{ik} are presented.

The six non-zero components of Christoffel's tensor, [10.32] being accounted for, are:

$$\left.\begin{aligned} \Gamma_{11} &= C_{1111}\, p_1^2 + C_{3131}\, p_3^2 && \text{(a)} \\ \Gamma_{22} &= C_{2323}\, p_3^2 + C_{1212}\, p_1^2 && \text{(b)} \\ \Gamma_{33} &= C_{3333}\, p_3^2 + C_{3131}\, p_1^2 && \text{(c)} \end{aligned}\right\}$$

$$\left.\begin{aligned} \Gamma_{12} &= \Gamma_{21} = 0 && \text{(d)} \\ \Gamma_{13} &= p_3\, p_1\, \left(C_{3131} + C_{1133}\right) = \Gamma_{31} && \text{(e)} \\ \Gamma_{23} &= \Gamma_{32} = 0 && \text{(f)} \end{aligned}\right\} \qquad [10.33]$$

Equation [10.33] being accounted for, the determinant [10.23] can be rewritten as follows:

@Seismicisolation

$$\begin{vmatrix} \left(\Gamma_{13} - v^2\right) & 0 & \Gamma_{13} \\ 0 & \left(\Gamma_{22} - \rho\, v^2\right) & 0 \\ \Gamma_{13} & 0 & \left(\Gamma_{33} - \rho\, v^2\right) \end{vmatrix} = 0 \qquad [10.34]$$

By developing [10.34], we get:

$$\left(\Gamma_{11} - \rho\, v^2\right)\left(\Gamma_{22} - \rho\, v^2\right)\left(\Gamma_{33} - \rho\, v^2\right) - \Gamma_{13}^2\left(\Gamma_{22} - \rho\, v^2\right) = 0 \qquad [10.35]$$

or

$$\left(\Gamma_{22} - \rho\, v^2\right)\left[\left(\Gamma_{11} - \rho\, v^2\right)\left(\Gamma_{33} - \rho\, v^2\right) - \Gamma_{13}^2\right] = 0 \qquad [10.36]$$

Setting the brackets to zero and developing this equation, accounting for equation [10.33]:

$$\begin{aligned} &\left(C_{1111}\, p_1^2 + C_{3131}\, p_3^2 - \rho\, v^2\right) \\ &\left(C_{3333}\, p_3^2 + C_{3131}\, p_1^2 - \rho\, v^2\right) \\ &- p_3^2\, p_1^2\, \left(C_{1313} + C_{1133}\right)^2 = 0 \end{aligned} \qquad [10.37]$$

In [10.37], all elastic constants except C_{1133} are known from previous measurements. This coefficient can be deduced from [10.37]:

$$C_{1133} = \frac{1}{p_1\, p_3}\left[\begin{matrix}\left(C_{1111}\, p_1^2 + C_{3131}\, p_3^2 - \rho\, v^2\right) \\ \left(C_{3333}\, p_3^2 + C_{3131}\, p_1^2 - \rho\, v^2\right)\end{matrix}\right]^{1/2} - C_{1313} \qquad [10.38]$$

In a more condensed form, this becomes:

@Seismicisolation

$$\left.\begin{aligned} C_{1133} &= \frac{B + A\,x + x^2}{\sin R \cos R} - C_{1313} \\ B &= \left(C_{1111}\ \omega^2\ R + C_{1313}\ \sin^2 R\right)\left(C_{3333} - \sin^2 R + C_{1313}\ \cos^2 R\right) \\ A &= C_{1111}\ \cos^2 R + C_{1313}\ \sin^2 R + C_{1313} \\ x &= \rho\ v^2 \end{aligned}\right\} \quad [10.39]$$

In [10.39], the accuracy of the measurement of C_{1133} depends upon many parameters:

– accuracies concerning C_{1111}, C_{1313} and C_{3333};

– accuracy of the angle R (direction of propagation);

– accuracy of the velocity measurement.

In equations [10.38] and [10.39], the coefficient C_{1313} (shear stiffness) plays an outstanding role in the calculation.

Figure 10.3 presents components of Christoffel's tensor in the most general case, where the direction of wave propagation has three non-zero components. What we have presented in equations [10.33] to [10.39] corresponds to the case where one direction's cosine component is zero (see Figure 10.3).

Figure 10.5 shows curves $C_{1313} = C_{13}$ compared to the angle R with $C = C_{55}$ as parameters. Ten per cent of the value of C_{1313} gives rise to C_{1113} in a large interval.

An optimization method is necessary here and the optimal value of C_{1313} is adopted so as to obtain a value of C_{1113} that is not dependent on the direction of wave propagation R.

10.6. Slowness surface and wave propagation through a separation surface

From an experimental point of view, the medium constituted by the sample is not infinite. Often it is presented as a blade with two parallel surfaces. The blade thickness h must be large compared to wavelength λ:

@Seismicisolation

$$h >> \lambda = v/f$$

where v is the phase velocity, f the frequency.

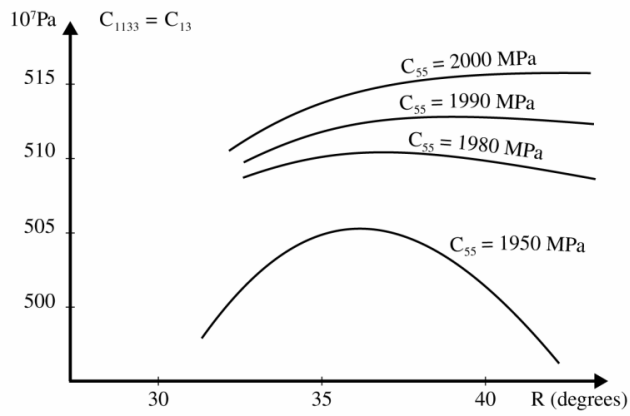

Figure 10.5. *Curve $C_{1133} = C_{35}$* versus *orientation angle R. Optimization is achieved by varying the shear stiffness coefficient C_{55} in a narrow limit of 10%. The couple of coefficients, $C_{55} = 1990$ and $C_{13} = 5140.10^6$ Pa, are obtained. The material being analyzed is composite KEVLAR [PRP 49]*

To obtain a progressive wave through the material blade, a wave is launched as a burst of a restricted number of sinusoids so that its time duration is limited[3]. Transmission of the ultrasonic wave through the separating surface between two media (the transducer or coupling liquid and material blade).

Knowledge of the transmitted and reflected waves on this surface is important when we use ultrasonic benches.

10.6.1. *Slowness surface representation*

From point 0 of the separating surface (a pole) in a given propagation direction $\vec{p}$, let us draw a vector whose amplitude is the inverse of the phase velocity 1/v. If direction $\vec{p}$ varies, the vector $\vec{p}/v$ describes a closed curve (see Figure 10.6). This curve is a circle if the material is isotropic in the exploratory plane.

3 *Mechanical Characterization of Materials and Wave Dispersion*, written by the same authors.

@Seismicisolation

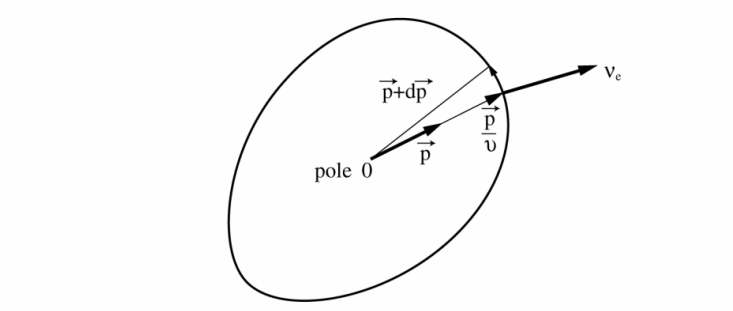

Figure 10.6. *Slowness surface, energy velocity and phase velocity*

If the material is anisotropic, the closed curve may have various shapes depending on the material symmetry itself.

The type of curve is of great interest to us. In Appendix 10.B it is shown that the energy velocity V_e is orthogonal to the slowness surface and Figure 10.6.

$$\vec{p} \bullet V_e = v \text{ (phase velocity)} \qquad [10.40]$$

10.6.1.1. *Application of slowness surface – propagation through a plane surface separating two isotropic media*

Let us take a simple example of two semi-infinite isotropic solids separated by a plane surface, see Figure 10.7.

Let an incident wave of medium *I*, be $u_{inc}{}^{I}{}_{,L}$ which makes an angle θ_0 normal to the separating surface.

We can write the displacement continuity in mediums I and II:

$$u^{I}_{inc,\,L} + u^{I}_{eef,\,L} + u^{I}_{ref,\,T} = u^{II}_{trans,\,L} + u^{II}_{trans,\,T} \qquad [10.41]$$

in which the superscript designates the medium; the subscript before the comma is the wave origin (incident = inc, reflected = ref); and subscript after the comma is the nature of the wave (L = longitudinal, T = shear wave).

For each wave, let us write the displacement of the progressive wave:

@Seismicisolation

$$u_k = A\, d_k \exp j\, \eta \quad \text{with} \quad \eta = \omega \left(t - \frac{P_i\, x_i}{v} \right) \qquad [10.42]$$

$$k = \frac{\omega}{v} \text{ the wave number}$$

Bringing equation [10.42] into [10.41], we must take caution to ensure that for:

$$\forall\, x_i \quad \text{and} \quad \forall\, t$$

we have the multiple equalities:

$$\eta^{I}_{\text{inc, L}} = \eta^{I}_{\text{ref, L}} = \eta^{I}_{\text{ref, T}} = \eta^{II}_{\text{trans, T}} \qquad [10.43]$$

For $x_2 = 0$ and $t = 0$, each η in equation [10.43] can be expressed as:

$$-\eta = \omega \left(+ \frac{P_i\, x_i}{v} \right) = \frac{\omega\, p_1\, x_1}{v} = k\, p_1\, x_1 \qquad [10.44]$$

then [10.43] rewritten, as in Figure 10.7, as:

$$k_0 \sin \theta_0 = k_1 \sin \theta_1 = k_2 \sin \theta_2 = k_3 \sin \theta_3 = k_4 \sin \theta_4 \qquad [10.45]$$

or

$$\frac{\sin \theta_0}{v^{I}_{L}} = \frac{\sin \theta_1}{v^{I}_{L}} = \frac{\sin \theta_2}{v^{I}_{T}} = \frac{\sin \theta_3}{v^{II}_{L}} = \frac{\sin \theta_4}{v^{II}_{T}} \qquad [10.46]$$

This is the well-known Snell-Descartes' law. The graphical construction of various wave directions is facilitated by using slowness surfaces; here semi-circles have a radius of $\frac{1}{v}$, v being the phase velocity. In medium I, the incident wave is supposed to be a longitudinal wave. From [10.46] we get:

$$\theta_0 = \theta_1$$

@Seismicisolation

To find θ_2 corresponding to reflected transverse wave, the equality deduced from Snell's law [10.46] is rewritten here:

$$\frac{\sin\theta_1}{v_L^I} = \frac{\sin\theta_2}{v_T^I}$$

or

$$\frac{\sin\theta_1}{\sin\theta_2} = \frac{v_L^I}{v_T^I} \qquad [10.47]$$

Angle θ_2 is obtained by a perpendicular to separating line and cutting surface of radius $\frac{1}{v_L^I}$ at point A (see Figure 10.7). Point B on the same perpendicular and at the intersection with the circle of radius $1/v_T^I$ gives the angle θ_2. Extending this perpendicular T beyond the separating line in medium II we obtain two other intersecting points, C and D, corresponding respectively to angles θ_3 and θ_4 in [10.46] and the two transmitted rays.

10.6.1.2. *Critical angle for wave transmission through the separation surface*

The condition a for a wave to be transmitted into medium II is that the perpendicular to the separating line must intersect the circle corresponding to the extensional wave (circle of radius $\frac{1}{v_L^{II}}$), or at least tangent to this circle point E. Beyond this angle (Point E):

$$\theta_0 > \theta_{I\ \text{critical}}$$

with the incident longitudinal wave with displacement amplitude u_{inc}, L is transformed into a wave propagating in the separating surface. It thus becomes Stonely's wave, confined in the frontier (OE).

In medium II, there is a shear wave in the direction OF. Adjusting the angle $\theta_{critical}$ it is possible to obtain an isolated shear wave.

The graphical construction presented above enables us to grasp the experimental set-up using an ultrasonic immersion bench. Water is considered to be the first

@Seismicisolation

medium (I) in Figure 10.7. To obtain wave propagation in a plate we can orient the incident wave in water by using a goniometer to obtain the critical angle θ_c, which only gives rise to one unique shear wave in medium II (inside the plate itself).

10.6.2. *Slowness surfaces for transverse isotropic composite material*

It is interesting to draw slowness surfaces for various (dilatational and shear) waves in two media separated by a plane surface. As before, we draw only the traces of those surfaces in plane (1, 3). For the composite material, the symmetry axis is 3.

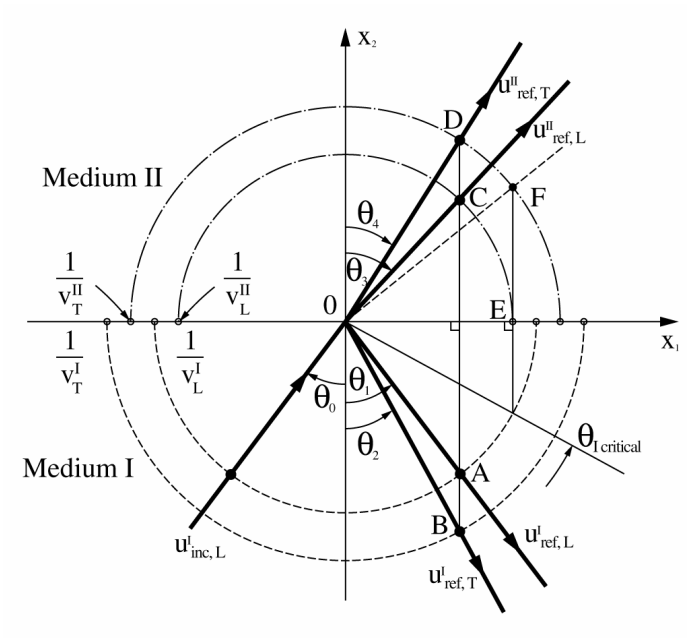

Figure 10.7. *The slowness surfaces of two isotropic media I and II separated by a plane surface. The traces of their slowness surfaces are the two halves for each medium. Geometrical construction of incident reflected and refracted propagation directions, angles θ_1, θ_2, θ_3, θ_4, is shown*

In Figure 10.8, for each medium one quadrant is reserved to a slowness surface and one quadrant to phase velocity.

@Seismicisolation

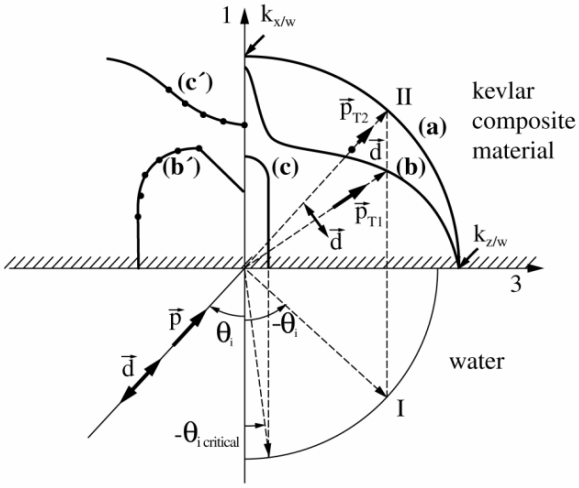

Figure 10.8. *Transmission of wave through plane interface water-composite: 1) longitudinal wave in water – the slowness surface is a circle; II) curve (a) is a circle – polarization* $\vec{p}$ *is orthogonal to plane (1, 3). This curve cannot be obtained by a wave transmitted from water to the composite glued to the interface. It can be obtained by ultrasonic emitter (with a mechanical system for variation of the angle θ incident). In curve (b), the transverse wave has its polarization in plane (1, 3). For propagation vector* $\vec{p}$ *=(0, 0, 1) the phase velocity corresponds to* C_{3131}*. For propagation vector* $\vec{p}$ *=(1, 0, 0) phase velocity to* C_{1313}*. The slowness curve does not show* $C_{1313} = C_{3131}$*. There is a lack of symmetry in the composite Kevlar-epoxy. Curve (c) corresponds to an extensional wave. Along axis 3, it is related to* C_{3333} *and for* $\vec{p}$ *=(1, 0, 0) to* C_{1111}

Figure 10.9 represents the sample. Unidirectional fibers are oriented along the x_3 axis. x_3 and x_1 are the thickness direction. Measurement techniques are examined below. For clarity, the three rays A, B and C represent transverse waves in the sample. Propagation directions $\vec{p}$ correspond respectively to the incidence angles 0°, 45°, and 90°. The double arrows on the each ray represent polarization vectors, which are all in plane (1, 3). Case A corresponds to stiffness coefficient $C_{1313} = C_{55}$. Case B corresponds to a quasi transverse wave, and case C corresponds to a stiffness coefficient $C_{3232} = C_{44}$.

If the material is really transverse isotropic:

$$C_{3233} = C_{44} = C_{3131} = C_{1313} = C_{55}$$

@Seismicisolation

In quadrant III, the radiation curves are drawn. In this polar representation, the radius is equal to the phase velocity $v = \frac{\omega}{k}$. Curves (c′) and (b′) correspond to C_{3333} and C_{1111} respectively.

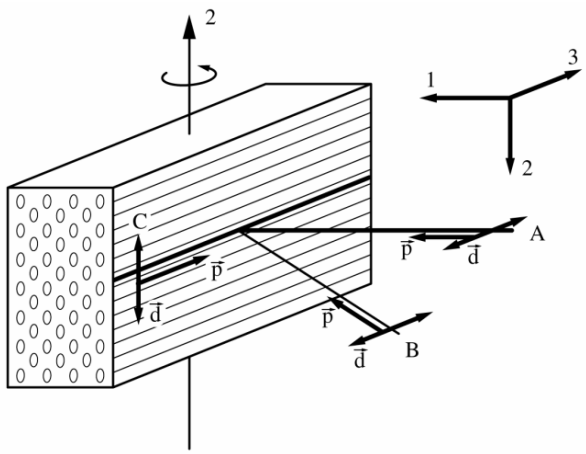

Figure 10.9. *Examination of the elastic properties of a transverse isotropic material in the plane (1,3), with 3 being the fiber direction. Rotation is around axis 2*

Let us draw your attention to the fact that beyond the incident critical angle $\theta_i = 10° \; 24'$ (for a Kevlar-epoxy composite) it is not possible to obtain information for this wave. Other methods are needed to obtain the whole curve.

The graphical method deduced from Snell's law, presented in Figure 10.9 for isotropic materials, is applicable here for slowness curves.

10.7. Propagation of an elastic wave through an anisotropic blade with two parallel faces

To launch an ultrasonic wave through an anisotropic plate, there are many possibilities, see Figure 10.10, including transmission without wave reflection and transmission with transmitted and reflected waves at the lower sample face.

Ultrasonic emitters and receivers are commonly used in the industry for non-destructive examination. Here we focus our attention on an experimental set-up that contributes to the measurement of elastic constants of an anisotropic material. The two principal devices are:

@Seismicisolation

– transducers in direct contact with the plate;

– transducers immersed in a water bench with water serving as the coupling liquid between them.

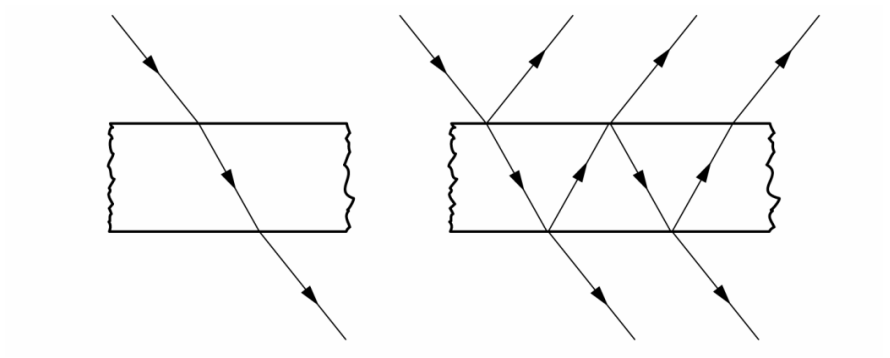

Figure 10.10. *Waves transmitted through the plate thickness with and without reflected waves*

10.7.1. *Direct transducer couplings with sample*

In Figure 10.11 the set-up is the simplest one. The normal incidence of waves is exploited. The problem is to ensure contact between the transducers and the sample. Generally an appropriate coupling fluid is used for this purpose[4]. In Figure 10.11b one transducer is used as emitter and one as a receiver.

Polarization of the wave is chosen in advance and guides the choice of transducers themselves. The transducer with polarization is orthogonal to the propagation directly and t is adopted for shear wave. The orientation of polarization vector $\vec{d}$ is adjusted by the user. The longitudinal (or extensional) wave transducer has $\vec{d}$ and $\vec{p}$ colinear. No orientation of $\vec{d}$ is necessary.

The discussion about the way ultrasonic energy propagates, and eventual correction of the ultrasonic path in the sample, has given rise to many publications. The phase velocity is evaluated as:

4 For shear wave transmission it is necessary to choose a viscous fluid. We do not use glue because it might damage the coating of the transducer directly in contact with the plate sample.

@Seismicisolation

$$v = \frac{\text{distance}}{\text{propagation time}} = \frac{d}{t} \qquad [10.48]$$

where d is the thickness of the plate. t is measured by various techniques – the usual technique is with an oscilloscope.

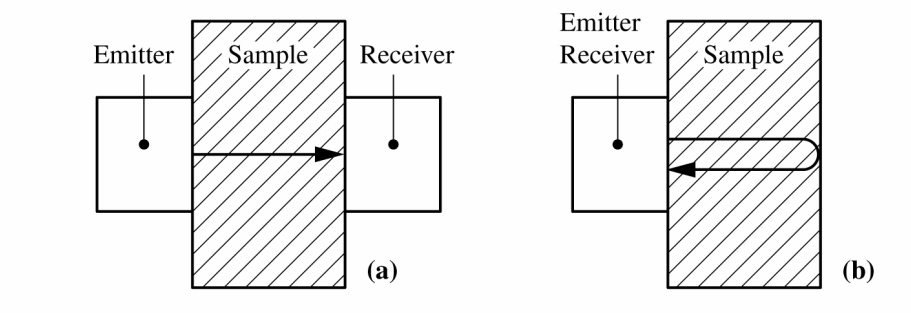

Figure 10.11. *a) One of the transducer serves as emitter, the other is a receiver; b) an emitter-receiver transducer*

10.7.2. *Water immersion bench*

The main advantages of this bench are:

– the possibility of adjusting the sample's orientation angle using a goniometer;

– that the coupling liquid does not contaminate the sample surfaces;

– it enables easy examination of waves in the sample.

Figure 10.12 shows an isolated transmitted wave[5]. We will now examine just the principle of the method and how to formulae equations to obtain phase velocities.

10.7.2.1. *Distance covered by a wave in the sample*

In the sample, the wave propagation distance is AB, which we want to measure with accuracy. i is the incident angle in water, and R the transmission angle R in the sample.

Angle (i – R) serves to evaluate AB:

5 There are two transmitted waves in the sample: longitudinal wave L and shear wave T. To facilitate understanding, we examine one wave in Figure 10.12.

@Seismicisolation

$$AB = \frac{e}{\cos\ R} \qquad [10.49]$$

where e is the thickness.

With t being the time duration and v the phase velocity we have:

$$t_{AB} = \frac{AB}{v} = \frac{e}{v \cos R} \qquad [10.50]$$

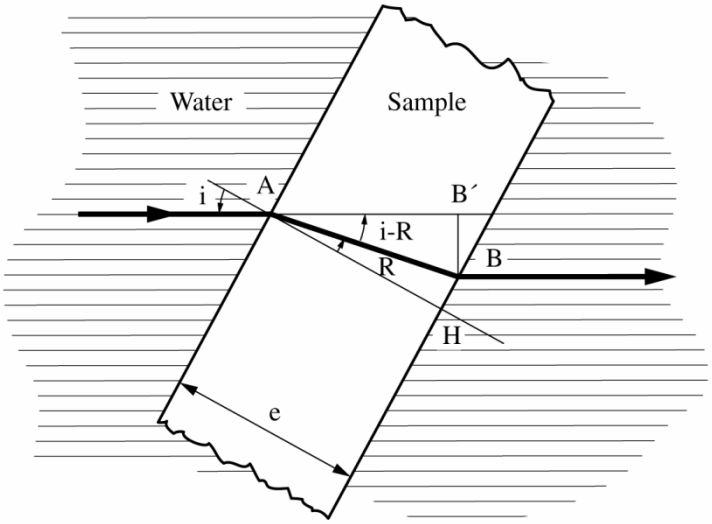

Figure 10.12. *Ultrasonic wave transmission through a plate immersed in a wave*

10.7.2.2. *Equivalent distance in water without a sample*

When the sample is taken away, the ultrasonic beam travels a distance d′:

$$d' = AB' \qquad [10.51]$$

@Seismicisolation

The travel time in water is:

$$t_{AB'} = \frac{AB'}{v_0} \qquad [10.52]$$

10.7.2.3. *Propagation time*

The difference between the two times in equations [10.49] and [10.52] is:

$$\delta t = t_{AB'} - t_{AB} = \frac{AB'}{v_0} - \frac{AB}{v'} \qquad [10.53]$$

Let n be the refraction index defined as:

$$n = \frac{v_0 \text{ water}}{v \left(\text{composite}\right)} \qquad [10.54]$$

The relationship between incidence angle i and refraction angle R is Snell's law.

$$\frac{\sin i}{v_0} = \frac{\sin R}{v}$$

or

$$\frac{\sin i}{\sin R} = n \qquad [10.55]$$

Equation [10.53] can be written as:

$$\delta t = \frac{e \cos\left(i - R\right)}{\cos R \, v_0} - \frac{e}{\cos R \, . \, v}$$

$$\delta t = \frac{e}{v_0 \cos R} \left[\cos\left(i - R\right) - n\right] \qquad [10.56]$$

and developing the brackets we get:

@Seismicisolation

$$\delta t = \frac{e}{v_0}\left(\frac{\cos i \cos R + \sin i \sin R - n}{\cos R}\right)$$

$$\delta t = \frac{e}{v_0}\left(\cos i - \sqrt{n^2 - \sin^2 i}\right) \qquad [10.57]$$

10.7.2.4. *Expression of phase velocity in the sample*

Equation [10.57] contains the measurable parameters, i.e. δt, cos i, sin i, v_0 and e. The phase velocity is contained in the refraction index. Let us extract n from [10.57]:

$$\cos i - \sqrt{n^2 - \sin^2 i} = \frac{v_0\ \delta t}{e}$$

$$n^2 = \sin^2 i = \left(\cos i - \frac{v_0\ \delta t}{e}\right)^2$$

$$n^2 = \sin^2 i + \left(\cos i - \frac{v_0\ \delta t}{e}\right)^2$$

$$v = \frac{v_0}{\left[1 + \frac{v_0\ \delta t}{e}\left(\frac{v_0\ \delta t}{e} - 2\cos i\right)\right]^{1/2}} \qquad [10.58]$$

The formula for v can be used in two manners.

10.7.2.5. *Phase velocity measurement by propagation time δt evaluation*

Propagation of sinusoid packets in the form of tone bursts can be visualized on an oscilloscope in spite of their progressive wave character, by using a given position on the oscilloscope screen. This can be obtained with repetitive wave packets. The sweeping is synchronized by the wave emitted from the generator itself. δt is measured by difference between two time durations:

$$\delta t = T_{water} - T_{sample} \qquad [10.59]$$

@Seismicisolation

T_{water} corresponds to the position of the pulse packet at the receiver without the sample and T_{sample} corresponds to the pulse packet after traveling through the sample, see Figure 10.13.

10.7.2.6. *Phase velocity evaluation without time measurements*

The second method uses the oscilloscope as an electronic bridge for detecting zero position.

If we can adjust the distance between the two transducers (emitter and receiver) by mounting one of the transducers on an adjustable micrometer platform, we can arrive at the situation represented in Figure 10.13. The distance d on micrometer is equal to, v_0 being velocity in water:

$$d = v_0 \ \delta t = l \qquad [10.60]$$

The phase velocity is then:

$$v = \frac{v_0}{\left[1 + \frac{1}{e}\left(\frac{1}{e} - 2\cos i\right)\right]^{1/2}} \qquad [10.61]$$

and l is adjusted, as in Figure 10.13, so the position of pulse packet B is moved and becomes coincident with T_{water}.

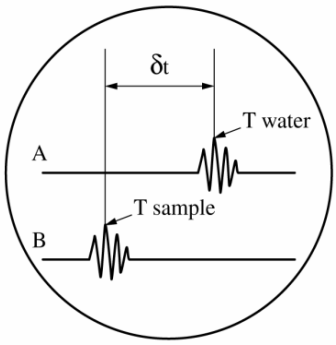

Figure 10.13. *A – pulse packet position without a sample; B – pulse packet position with a sample*

@Seismicisolation

10.7.2.7. *Measurement of longitudinal wave velocity*

In equations [10.58] or [10.61], the incident wave that is normal to the separating surface is chosen, so i = 0. The wave velocity is:

$$v_L = \frac{v_0}{\left(1 - \frac{v_0\ \delta t}{e}\right)} \qquad [10.62]$$

10.7.2.8. *Measurement of shear wave velocity*

Incidence angle i is chosen beyond the critical angle, see Figure 10.9:

$$\theta_i \geq \theta_{i\ \text{critical}} \qquad [10.63]$$

The reason for this choice is that in here only the shear wave of the sample travels.

Let us focus our attention on the following. For continuity, equation [10.41] shows that polarizations of waves in medium II must be the same as polarization of medium I (water). Polarizations of all waves (incident and transmitted) are in the incidence plane.

In water only the longitudinal wave exists. For this reason, in the sample the propagating transverse wave must have polarization $\vec{d}$ in the same plane.

10.8. Concluding remarks

Ultrasonic progressive waves constitute a convenient method by which to evaluate stiffness matrix coefficients.

Propagation of waves in the direction of symmetry of a material permits us to evaluate diagonal stiffness matrix coefficients.

Non-diagonal coefficients of a stiffness matrix are evaluated by using the direction of a wave in the sample that is not coincident with any symmetry axis. Non-diagonal coefficients give rise to coupled waves and by choosing an incident wave direction by goniometer it is possible to separate coupled waves and retain just the shear wave.

@Seismicisolation

Evaluation of non-diagonal stiffness coefficients requires optimization of the refraction wave angle and an appropriate stiffness coefficient being taken for optimization parameters. The accuracy of stiffness coefficients depends on the geometrical accuracy of the sample, particularly the width. It also depends on the propagation distance measurement.

It is not necessary to use a unique ultrasonic bench but at least two benches are needed to complete the characterization of stiffness coefficients, particularly for anisotropic materials.

It is possible to evaluate the complex stiffness coefficients of a material by using a logarithmic decrement method.

Readers must be aware that the characterization of the stiffness coefficients of materials is only possible using ultrasonic waves.

It is difficult to compare those stiffness coefficients to compliance moduli obtained by rod (or plate) vibrations. This comparison is only possible if the two following conditions are satisfied:

– the stiffness matrix must be inverted to obtain a compliance matrix on the condition that all stiffness coefficients be evaluated;

– the working frequency in dynamic tests (vibration tests and ultrasonic tests) must be the same. This is impossible. Consequently the coefficients of the stiffness matrix obtained by ultrasonic techniques must only be considered as *upper bound values at high frequency. To complete the measurement at a lower frequency we need to measure the vibration of rods and the viscoelastic characterization of the material*.

10.9. Bibliography

[ACH 73] ACHENBACH J. D., *Wave Propagation in Elastic Solids*, North Holland, American Elsevier, Amsterdam, 1973.

[AUL 77] AULD B. A., *Acoustic Field and Waves in Solids*, vol. I and II, John Wiley and Sons, New York, 1977.

[GAR 75] GARCEAU P., *Kevlar Composite, Elastic Stiffness Matrix Component Evaluation by Ultrasound*, Report at ISMCM Saint Ouen, France, in French, 1975.

[KLI 92] KLINE R. A., *Non Destructive Charaterisation of Composite Media,* Technomic Publishing & Co., Lancaster, USA, 1992. (The most comprehensive and recent publication treating the characterization of composite material.)

@Seismicisolation

[THU 74] THURSTON R. N., "Waves in solids", In: *Encyclopedia of Physics*, C. Truesdell, ed., vol. V Ia /7, p. 109-302, 1974.

[TRU 69] TRUEL R., ELBAUM C., CHICK B., *Ultrasonic Methods in Solid State Physics,* Academic Press, 1969.

10.10. List of symbols

C_{ijkl}	stiffness tensor component
d	distance
$\vec{d}$	polarization (particle motion) direction
e	thickness
f	frequency
k	wave number $= \dfrac{2\pi}{\lambda} = \dfrac{\omega}{v} \dfrac{\text{circular frequency}}{\textit{phase velocity}}$
i	incidence angle of wave
$\vec{n}$	normal unit vector
$\vec{p}$	polarization direction
$\vec{P}$	Poynting vector
p_i	direction cosine
R	refraction angle
s_{ijkl}	compliance matrix coefficient
t, T	time
u	displacement
U_c	kinetic energy

@Seismicisolation

U_p	potential energy
U_{Total}	total energy
v or v_p	phase velocity
v_g	group velocity
v_e	energy velocity
v_T	transverse wave velocity
v_L	longitudinal wave velocity
v_0	water longitudinal velocity
$v_{i/j}$	phase velocity (i: direction of propagation; j: polarization direction)
Γ_{ik}	Christoffel's tensor component
ρ	density
σ_{ij}	stress component
ε_{ij}	strain component
ω	circular frequency = $2\pi f$
λ	wavelength = $\frac{v}{f}$
θ	angle evaluated from normal to separating surface
δ_{ik}	Kronecker notation

@Seismicisolation

10.11. Appendices

Appendix 10.A. Energy velocity, group velocity, Poynting vector

10.A.1. *Phase velocity*

Phase velocity is used to characterize a wave plane that is normal to the ray vector, such that in this plane $x_i\ p_i$ = constant and P_i is the cosine of propagation direction. If the wave is *divergent* we can define a polar diagram, called the radiation surface, which means that this surface is reached by all particles being emitted by the same source centered at the origin (or pole) at the same time. On this surface, phase velocity is defined as:

$$v = \frac{\omega}{k} \qquad [10.A.1]$$

where ω is the circular frequency and k the wave number.

10.A.2. *Particle velocity*

Particle velocity is the time derivative of displacement. Let us take a displacement as:

$$u\left(x, t\right) = A \cos k\left(x - v\,t\right) \qquad [10.A.2]$$

$$\dot{u} = \frac{du}{dt} = -A\,k\,v \sin k\left(x - v\,t\right) \qquad [10.A.3]$$

The ratio $\dot{u}/v$ has a maximum value of:

$$\left.\frac{\dot{u}}{v}\right|_{max} = A\,k \qquad [10.A.4]$$

10.A.3. *Group velocity and phase velocity*

Group velocity is necessary for the study of waves with complicated shapes, such as a wave packet or wave burst constituted by an envelope of waves and a reduced number of sinusoids with various amplitudes.

@Seismicisolation

If we observe the propagation of such waves (the envelope as well as the sinusoids), we can see that they do not propagate at the same velocity. The velocity of the wave envelope is the *group velocity*. Let us take an example:

$$u = A\left[\sin\left(k, x - \omega_1\ t\right) + \sin\left(k_2\ x - \omega_2\ t\right)\right] \qquad [10.A.5]$$

$$u = 2\,A\left[\cos\left(\frac{k_1 - k_2}{2}\ x - \frac{\omega_1 - \omega_2}{2}\right) t\right]\left[\sin\ \frac{k_1 + k_2}{2}\ x + \frac{\omega_1 + \omega_2}{2}\ t\right] \qquad [10.A.6]$$

In equation [10.A.6] the envelope corresponds to the second bracket. The first bracket corresponds to the wave carrier:

$$\left(\frac{k_1 - k_2}{2} x - \frac{\omega_1 - \omega_2}{2}\ t\right) = cs\ t$$

$$\Delta\ k\ x - \Delta\ \omega\ t = 0$$

$$\frac{d\ x}{d\ t} = \frac{\Delta\ \omega}{\Delta\ k} = 1$$

For $\Delta\ k \rightarrow 0$ we obtain group velocity:

$$v_g = \frac{d\omega}{dk} \qquad [10.A.7]$$

Phase velocity is obtained by examining the second bracket:

$$v_p = \frac{\omega + \delta\omega / 2}{k + \delta k/2}$$

or

$$v_p = \frac{\omega}{k} \qquad [10.A.8]$$

@Seismicisolation

10.A.4. *Relationship between group velocity and phase velocity*

From [10.A.8] we deduce:

$$d\ \mathrm{v_p} = \frac{\mathrm{d}\,\omega}{\mathrm{k}} - \frac{\omega}{\mathrm{k}^2}\ \mathrm{d\,k}$$

then:

$$\mathrm{v_p} = \mathrm{v_p} + \mathrm{k}\ \frac{\mathrm{d\,v_p}}{\mathrm{d\,k}} \quad \text{with } \mathrm{k} = 2\pi/\lambda \quad \lambda \text{ wavelength} \qquad [10.A.9a]$$

$$\mathrm{v_g} = \mathrm{v_p} - \lambda\ \frac{\mathrm{d\,v_p}}{d\ \lambda} \qquad [10.A.9b]$$

Some wave spectra include some branches on which the dispersion is abnormal, see Figure 10.A.2.

10.A.5. *Poynting vector* $\vec{P}$

The Poynting vector is well known in electricity and radioelectricity. It is usually used to study electromagnetic wave propagation. It designates power flux density, which applies to dynamic problems. Naturally it can be applied to acoustics. Throughout this vector, energy velocity can be defined.

Let us recall the basic equation in elastodynamics:

$$\sigma_{\mathrm{ij,\,j}} + \mathrm{F} = \rho\ \frac{\partial^2\ \mathrm{u_i}}{\partial \mathrm{t}^2} \qquad [10.A.10]$$

in which F is volume force.

Let us multiply both members of [10.A.10] by velocity $\dot{u}_i$ and integrate:

@Seismicisolation

$$\int_v \sigma_{ij,j} \dot{u}_i \, dv + \int_v F \dot{u}_i \, dv = \int_v \rho \frac{\partial^2 u_i}{\partial t^2} \, dv \qquad [10.A.11]$$

Let us add the following quantity to both members:

$$\int_v \left(\sigma_{ij} \dot{u}_{i,j} \right) dV = \int \sigma_{ij} \dot{\varepsilon}_{ij} \, dv \qquad [10.A.12]$$

The volume integral can be transformed into a surface integral:

$$\int_V \left(\sigma_{ij,j} \dot{u}_i + \sigma_{i,j} \dot{u}_{i,j} \right) dv = \int_S \left(\sigma_{ij} \dot{u}_i \right) n_j \, ds \qquad [10.A.13]$$

$$\int_S \left(\sigma_{ij} \dot{u}_i \right) n_j \, ds + \int_V F \dot{u}_i \, dv = \int \rho \frac{\partial^2 u_i}{\partial t^2} \dot{u}_i \, dv + \int_V \sigma_{ij} \dot{\varepsilon}_{ij} \, dv \qquad [10.A.14]$$

Let $\vec{P}$ be the Poynting vector:

$$\vec{P} = -\sigma_{ij} \frac{\partial u_i}{\partial t} \qquad [10.A.15]$$

Equation [10.A.14] can be rewritten by appropriately assembling terms in the first and second members:

$$\int_S P_j n_j \, dS = \int_V \left(F \dot{u}_i \right) dv - \int_V \frac{\partial^2 u_i}{\partial t} \frac{\partial u_i}{\partial t} \, dv - \int_V \sigma_{ij} \dot{\varepsilon}_{ij} \, dv \qquad [10.A.16]$$

@Seismicisolation

10.A.5.1. *Physical interpretation of equation [10.A.16]*

The first member represents power flowing through a closed surface S. If a tube is chosen as the closed surface, whose lateral surface is parallel to S, the contribution of $\vec{P}$ in the corresponding surface integral is zero. Mechanical tension T is only applied to the surfaces at both ends. The second member in equation [10.A.16] represents, respectively, the power source in the volume, power due to kinetic energy and elastic power due to potential energy.

10.A.5.2. *Direction of* $\vec{P}$

This is the direction of energy transport.

10.A.5.3. *Sign of* $\vec{P}$

In the second member of equation [10.A.15], the minus sign is interpreted as follows: the power that is delivered by medium I to medium II is $\left(-v\, T\, \vec{n}\, d\, S\right)$, see Figure 10.A.1.

$\vec{P}$ is a surface power density. It has a concrete significance.

10.A.5.4. *Energy surface* V_e

In equation [10.A.16], if the power due to source (F) is neglected, in the second member we can write:

$$\int_S P_j\, r_j\, ds - \int_V \left(\dot{U}_c + \dot{U}_p\right) dv = \int_V \dot{U}_{total}\, dv \qquad [10.A.17]$$

$$U_c = \frac{1}{2}\rho\left(\frac{\partial^2 U_c}{\partial t^2}\right)^2 \text{ specific kinetic energy} \qquad [10.A.18a]$$

$$U_p = \int \sigma_{ij}\, \varepsilon_{ij}\, dv \text{ specific potential energy} \qquad [10.A.18b]$$

$$U_{total} = U_p + U_c = \text{ total specific energy or total energy density} \qquad [10.A.18c]$$

@Seismicisolation

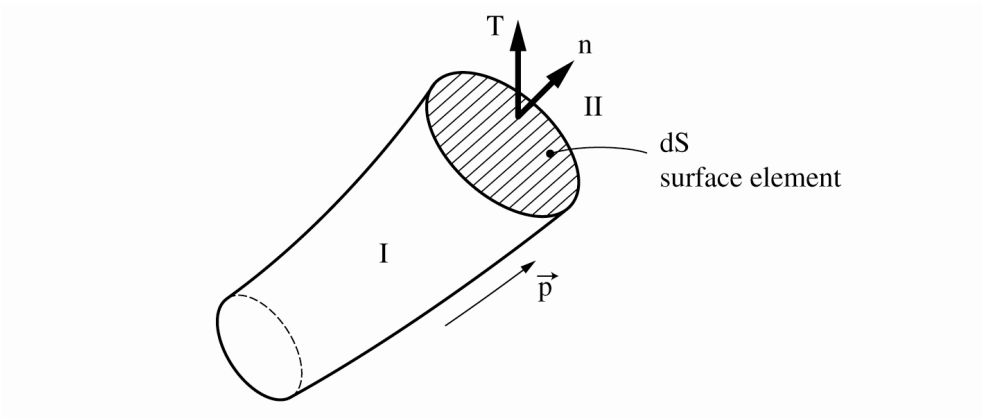

Figure 10.A.1. *Flux tube and the power of external forces*

10.A.5.5. *Energy velocity*

By definition energy velocity is defined as:

$$v_e = \frac{\vec{P}\ (\text{Poynting vector})}{U_{total}\ (\text{total energy density})} \qquad [10.A.19]$$

In elasticity, it can be shown that under the harmonic regime, kinetic energy is equal to potential energy:

$$U_c = U_p \quad \text{or} \quad U_{total} = 2\,U_c \qquad [10.A.20]$$

10.A.5.6. *Energy velocity and phase velocity*

Let us examine progressive waves that have the following form:

$$\dot{U} = v_0 \exp j\,(\omega\, t - k_\alpha\, x_\alpha), \qquad \alpha = 1, 2, 3 \qquad [10.A.21]$$

$$\sigma = \sigma_0 \exp j\,(\omega\, t - k_\alpha\, x_\alpha)$$

Equation [10.A.14] is rewritten under vectorial form, and with equation [10.A.21] being taken into account, the star designating conjugate quantity is:

@Seismicisolation

$$\int_V (v * \sigma)\, dv = 2 \int v^* \rho \frac{\partial^2 u}{\partial t^2}\, dv \qquad [10.A.22]$$

where v* = conjugate quantity of $\frac{d\,u}{d\,t} = \dot{u}\,*$,

$$j\,(-v^* k_\alpha - v^* k_\alpha) = -2\,\rho\, j\,\omega \left(\dot{u} \bullet v^*\right)$$

$$2\, v^* k_\alpha = 2\,\rho\,\omega \left| v^* \right|^2 \qquad [10.A.23]$$

$$k_\alpha \bullet \vec{P} = U_{total} \bullet \omega \quad \text{with} \quad \frac{\omega}{k} = v = v_p$$

$$\left(\frac{k_\alpha}{k}\right) \vec{P} = v\, U_{total} \qquad [10.A.24]$$

where $\frac{k_\alpha}{k} = p_\alpha$ direction is the cosine of propagation direction. Equation [10.A.24] can be rewritten:

$$p_\alpha\, \vec{P} = v\, U_{total} \qquad [10.A.25]$$

Consequently,

$$P_\alpha \bullet \frac{\vec{P}}{U_{total}} = v \qquad [10.A.26]$$

By the definition of energy velocity (equation [10.A.19]), we obtain a relationship between the two velocities v_e and v_p:

$$P_\alpha\, v_e = v = v_p \qquad [10.A.27]$$

with P_α being less than unity. [10.A.27] shows that v_p phase velocity is less than energy velocity v_e. Equation [10.A.27] also shows that the propagation direction of energy velocity is not colinear with that of phase velocity. This is important for an

@Seismicisolation

anisotropic material. The wave launched by the emitter is not necessarily orthogonal to the emitter's surface. The ultrasonic beam can have d_n energy direction, which is oblique with respect to the incidence normal to the emitter surface.

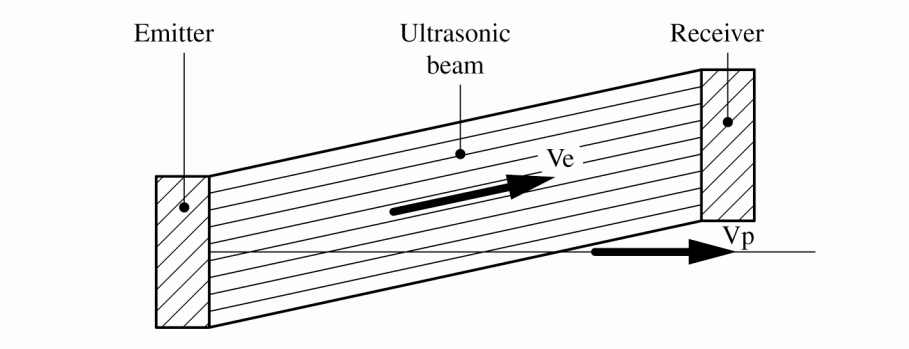

Figure 10.A.2. *Phase velocity v_p and group velocity v_e are not colinear*

10.A.5.7. *Group velocity v_g and energy velocity v_e*

It can be shown that these two velocities are identical:

$$v_g = v_e$$

Appendix 10.B. Slowness surface and energy velocity

Let:

$$L_i = \frac{p_i}{v} \qquad [10.B.1]$$

where p_i is the direction cosine and $v = v_p$ the phase velocity.

The derivative of L_i is:

$$\frac{\partial L_i}{\partial p_k} = \frac{\partial p_i}{v\,\partial p_k} - \frac{p_i}{v^2}\frac{\partial v}{\partial p_k} \qquad [10.B.2]$$

$$\frac{\partial p_i}{\partial p_k} = \delta_{ik} \text{ Kronecker notation}$$

@Seismicisolation

Let us multiply equation [10.B.1] by the component of v_e along the direction p_i:

$$v_e^i \frac{\partial L_i}{\partial p_k} = \frac{1}{v}\left(v_e^i \, \delta_{ik} - \frac{v_e^i \, p_i}{v^2} \frac{\partial v}{\partial p_k} \right) = \frac{1}{v}\left(v_e^k - \frac{p_i \, v_e^i}{v} v_g^k \right) \qquad [10.B.3]$$

We notice that:

$$\frac{\partial v}{\partial p_k} = v_g^k \qquad [10.B.4]$$

is the component of group velocity:

$$v_e^i \frac{\partial L_i}{\partial p_k} = \frac{1}{v}\left(v_e^k - v_g^k \right) = 0 \qquad [10.B.5]$$

The energy velocity is consequently orthogonal to the slowness surface.

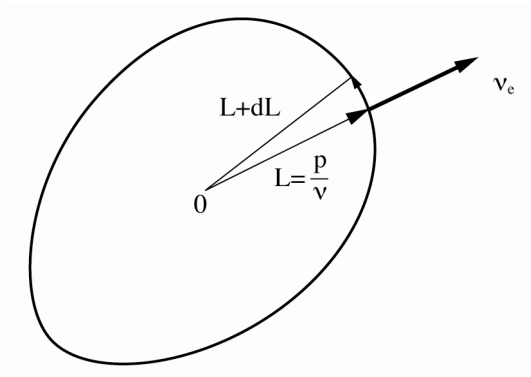

Figure 10.B.1. *Slowness surface with pole O and two adjacent radii. Energy velocity is normal to the slowness surface*

@Seismicisolation

Chapter 11

Viscoelastic Moduli of Materials Deduced from Harmonic Responses of Beams[1]

11.1. Introduction

The objective of this chapter is to present solutions to the viscoelastic problems of beam vibrations. In the framework of inverse problems where the dynamic responses of beams are known, complex moduli are to be evaluated.

11.1.1. *Trial and error method*

Trial and error method is usually referred to. Here, differences between experimental dynamic responses and calculated dynamic responses from estimated complex moduli, in a given frequency interval, need to be minimized.

There are a variety of optimization methods available that can be used and the degree of complexity of the adopted method depends on the number of unknowns (i.e. complex moduli or one complex modulus with a certain number of parameters to be adopted at the beginning).

Chapter written by Tibi BEDA, Christine ESTEOULE, Mohamed SOULA and Jean Tuong VINH.
1 This chapter features large extracts from [VIN 67, EST 87] and [BED 90, SOU 96] theses. For further information, see the bibliography at the end of this chapter.

Mechanics of Viscoelastic Materials and Wave Dispersion Edited by Yvon Chevalier and Jean Tuong Vinh
© 2010 ISTE Ltd. Published 2010 by ISTE Ltd.

@Seismicisolation

11.1.2. *Are wave dispersion phenomena to be taken into account or not?*

This problem is presented in detail in Part A. In experimental rheology, to our knowledge, this dynamic problem is often ignored by using a restricted very-low working frequency interval inside of which dispersion phenomenon can be ignored.

11.1.3. *Williams-Landel-Ferry's method*

This method, presented in Chapter 3, enables us to obtain an artificial, very large frequency interval. In practice, this artificial dilatation of frequency interval is obtained by using a large range of test temperatures. We cannot be certain that we will be operating in satisfactory experimental conditions, and suboptimum conditions might change the viscoelastic behavior of the materials themselves.

11.1.4. *Validity of elementary equations of motion*

Wave dispersion is often ignored and experimenters adopt elementary equations of motion that do not take this phenomenon into account. Experimentally speaking, the errors in the value of viscoelastic moduli are not discussed.

When the frequency range is large, e.g. three or more decades, errors can be large. This can lead to us either overestimating or underestimating complex moduli, depending on the kind of waves (bending, torsional or extensional) adopted and the governing equations of motion used.

11.1.5. *Choice of equations of motion without recourse to Williams-Landel-Ferry's method*

Some artificial and natural composite materials do not obey Williams-Landel-Ferry's method (see Chapter 3). For example, composite materials are made with long fibers periodically distributed in each layer and non-linear friction at the frontiers of layers cannot be ignored. Consequently, to experimentally characterize the viscoelastic behavior of materials, it is necessary to adopt vibration methods up to the ultrasonic frequency zone. This aspect of a problem is not purely academic as it is used in industrial and military applications of materials in the near-ultrasonic frequency zone.

@Seismicisolation

11.2. Guidelines for practicians

In this section we have tried to present useful indications for practicians and experimenters to enable them to choose appropriate equations of motion.

11.2.1. *Viscoelastic complex moduli and frequency range*

11.2.1.1. *Application domain and frequency range*

The problem to be solved might be industrially oriented, for example the building industry may use plastic or composite materials that must satisfy thermal and/or acoustic isolations. The frequency range concerning the mechanical behavior of the building can be restricted to a lower frequency (0.01 to 100 Hertz). Some materials used in construction, however, have to satisfy phonic isolation in the acoustic range of, for example, 0.1 to 10,000 Hertz. This presents us with the problem of characterizing complex moduli in four decades of frequency!

11.2.1.2. *Complex moduli to be measured*

The nature and mechanical structure symmetry of the material needs to be defined. In Chapter 1, long complements of anisotropic material are presented to enable the reader to define the material's symmetry degree and consequently evaluate the number of viscoelastic moduli (or stiffness) to be evaluated. If the material is isotropic, only two viscoelastic moduli need to be measured. The frequency range, naturally, must be defined. This helps the experimenter to choose the type of equations of motion that should be used.

If he or she adopts testing in the isothermal regime over a large frequency range (of more than two decades) equations of motion with a higher degree of approximation should be chosen. The nature of vibration depends on the viscoelastic modulus to be evaluated.

11.2.1.3. *Diagonal or non-diagonal complex compliance (or stiffness) to be evaluated*

11.2.1.3.1. Diagonal constants

In mechanical structure calculations we have to deal with diagonal components of the material's stiffness matrix (Young's moduli and shear moduli), which necessitate only pure waves (extensional, bending or torsional). Unfortunately, in the equations of motion applicable in a large frequency range, more than one viscoelastic modulus is required. This can be explained by the presence of many

@Seismicisolation

deformation mechanisms that occur in the sample, even when an on-axis sample is adopted.

We have to formulate a hypothesis on a set of additional components of viscoeleastic matrix that are unknown. Let us take an example. A popular bending test is adopted to evaluate an elastic and/or viscoelastic Young's modulus. In this case, Timoshenko's equation is preferred to Bernoulli-Euler's equation.

In Timoshenko's equation two elastic (or viscoelastic) moduli are used, i.e. Young's modulus and shear modulus. To solve the elastic problem for isotropic material we can introduce the ratio E/G (with G being shear modulus). This ratio is proved to be equal to 2 $(1 + \nu)$, with ν being Poisson's coefficient. As ν is practically constant over a large frequency range, in a first approximation, ratio E/G is supposed to be constant and the elastic (or viscoelastic) problem can be solved with one unknown.

We are not always in this favorable situation. We may have two unknown parameters to evaluate. If we can use the same sample in two different tests (for example one with a bending test and the other with a torsion test), we can deal with an optimization problem including two unknowns on the condition that information on both dynamic responses are examined at the same frequency.

11.2.1.3.2. Non-diagonal matrix constants

For non-isotropic materials, non-diagonal components of the matrix (stiffness or compliance) need to be evaluated. In Chapters 5, 6 and 7, off-axis samples are adopted. Here, intentionally coupled motions (bending-torsion, for example) are produced. This gives rise to a decoupled higher degree equation of motion (sixth or eighth).

11.3. Solution of a viscoelastic problem using the principle of correspondence

In Chapter 2, the principle of correspondence is presented.

There are two steps to solving this problem, on the condition that both the corresponding elastic and viscoelastic problems concern a sample with the same geometry and boundary conditions[2].

2 In some transient problems, boundary conditions in a viscoelastic medium might vary with time, even though in a similar elastic problem boundary conditions do not change.

@Seismicisolation

11.3.1. *First step: elastic solution*

To solve the inverse problem when evaluating elastic modulus, the choice of equation of motion is important.

11.3.1.1. *Choice of equations of motion*

There are a number of equations of motion that can be used in various circumstances, which are discussed below. These include:

– longitudinal wave;

– bending wave;

– torsion wave;

– higher-order approximations.

11.3.1.1.1. Longitudinal wave

The elementary second-order equation of motion gives rise to wave velocity, which is frequency independent. This is a serious limitation when evaluating Young's modulus from an extensional wave velocity. Comparisons of dispersion curves given by various theories should be made with caution. Here we must be sure that the velocity *versus* frequency (or wave number) used to evaluate frequency interval (from zero to maximum low frequency) – in which the trend of the dispersion curve corresponds to elementary theory – does not exceed the percentage fixed by the experimenter him- or herself (see Chapter 7, Figures 7.4 and 7.5).

11.3.1.1.2. Bending wave

Bernoulli-Euler's equation is the simplest equation of motion (see Chapter 6). Wave dispersion related to this is high even at low frequency and Young's modulus may be overestimated. The low frequency interval should be evaluated first. Comparison between various dispersion curves, see Chapter 6, enables us to choose the lowest frequency interval.

11.3.1.1.3. Torsion wave

Torsion wave is used to evaluate shear modulus. Saint Venant's theory should be referred to for a rectangular cross-section. Once again, the dispersion curve is referred to (see Chapter 5).

If a latitude of choice of rectangular rod section exists, a square section is preferred because the corresponding wave dispersion curve is less pronounced compared to other sections.

@Seismicisolation

11.3.1.1.4. Higher-order approximation equations of motion

All phenomena that appear in a sample with a large frequency range are taken into account (inertia, shear and eventually wave coupling) in higher-order approximation equations of motion. Inevitably, the degree of the equation is high and closed-form characteristic functions are cumbersome to handle.

More than one elastic modulus needs to be accounted for in the equations of motion. From a practical perspective, there are two possible classes of solution:

– elastic modulus is retained as the unknown. Other moduli give rise to a first estimation and are considered as known parameters in order to solve the equations of motion. By trial and error, the aforementioned parameters are estimated and their values introduced in the retained equation of motion in order to re-evaluate the elastic modulus;

– the second class of solution involves the optimization method, with many unknowns.

11.3.2. *Second step: estimation of dispersion curves*

When reading Chapters 5, 6 and 7 devoted to torsion, bending and extensional waves, the reader can see that wave dispersion curves depend on the geometric characteristics of a sample and also on certain mechanical parameters, such as inertia.

For a composite material, there is an important parameter – e.g. the ratio E_{ii} (Young's modulus)/G_{ij} (shear modulus) – which is much higher than 2.6 times the value obtained for isotropic materials. Wave dispersion consequently becomes very important.

In the chapters mentioned, direct problems are analyzed. All elastic moduli are supposed to be known and dispersion curves are presented with a set of geometric parameters from which one parameter is retained to enable us to draw the dispersion curve.

The problem of evaluating elastic and viscoelastic moduli is that we must resort to the inverse problem. Trial and error method is one possible way of evaluating complex moduli using characteristic functions. The other method systematically applies matrix calculation to continuous elements. This is discussed in Chapter 12.

@Seismicisolation

11.3.3. *Searching for a solution to viscoelastic moduli using characteristic functions*

11.3.3.1. *First step*

We begin with the harmonic transfer function, which relates output signals to input signals. This is often the transmissibility function in which both signals are of the same nature. The set of boundary condition equations gives the eigenvalues which are brought into the equation of motion. The elastic modulus is evaluated from the last equation of motion under closed-form expression.

11.3.3.2. *Second step*

The solution to the inverse problem begins with:

– the choice of elementary equations of motion and boundary conditions; and

– the choice of equations of motion with a higher degree of approximation.

11.3.3.2.1. Choice of elementary equations of motion and boundary conditions

Choosing elementary equations is not an easy task. Elementary equations of motion for each type of wave are presented in Chapters 5, 6 and 7.

Their utilization, however, is conditioned by restriction and validity conditions that we have to keep in mind. These restrictions give rise to the delimitation of frequency interval, which can seriously limit the curve of complex modulus *versus* frequency. Some physical effects are neglected (i.e. inertia, shear, warping of the section, etc). Consequently, application of the elementary equations of motion give rise to large errors of calculation, particularly in the higher frequency range.

The experimental boundary conditions adopted are also important and can seriously restrict frequency interval. For example, additional mass at the ends of the sample might lower the frequency range.

11.3.3.2.2. Choice of equations of motion with a higher degree approximation

In view of obtaining a complex modulus in a large frequency range, it is tempting to choose an equation with a higher degree approximation. It does, however, give rise to difficulties in numerical calculations and we have to face the problem that there is more than one unknown complex modulus that needs to be evaluated. Below we present some practical considerations in these circumstances.

@Seismicisolation

11.3.3.3. *Some preliminary practical considerations*

11.3.3.3.1. Magnitude of orders of elastic moduli

One way or another, we try to obtain an estimate for each modulus. For isotropic materials the technical literature may provide this information. Ultrasonic methods are easy to use and constitute an option. For anisotropic materials, provisional calculations are available, see Chapter 1. Ultrasonic methods are one of the possibilities for evaluating the upper bounds of stiffness constants.

11.3.3.3.2. Importance of unknown parameters

When reading the aforementioned chapters, the experimenter will observe that for a given type of wave, there are some predominant parameters in the discussion of wave dispersion *versus* frequency (or wave number). We will now examine some of these parameters according to the type of wave.

11.3.3.3.3. Extensional wave

Flatness δ = *(thickness h/width b)* has a strong influence on the trend of dispersion curve, as we can see in Chapter 7, Figures 7.8, 7.9 and 7.10. This geometrical parameter is available to the experimenter. If he or she has to choose this parameter before fabrication of the sample itself, square section is the best choice as it approaches the circular section when comparing wave dispersion curves. If we adopt a lower frequency range, the dispersion curve is "flat" in the frequency interval of interest.

Poisson's number ν plays important role, see Figure 7.9. When the two parameters are pre-evaluated, the Viktorov parameter (equation [7.70]) is calculated, see Figure 7.7. With these estimated parameter values, the next step is the calculation of the dispersion curve in non-dimensional variables.

What we have presented above concerns the choice of lowest frequency range with the objective of using the elementary second-order equation of motion, which is dispersion free.

11.3.3.3.4. Torsional wave

Flatness $\delta_{O,N}$ = *(width b/thickness h)*[3]. For a sample with circular cross-section, there is no dispersion in the whole frequency range for the first elastodynamic mode.

3 Nugues and Onobiono in Chapter 5 define flatness as the inverse of that used by Touratier in Chapter 7. To avoid confusion we add two subscripts N, O in δ as $\delta_{N,O}$ in this section.

@Seismicisolation

The problem of viscoelastic complex moduli evaluation is greatly facilitated if the experimenter is able to choose which type of section to work on.

If the experimenter has the choice confined to a rectangular section, the square section is to be preferred (see Figure 5.13, Chapter 5). For flatness $\delta_{O,N} = 1$, the dispersion curve is flat for any frequency value. In this case, the elementary second-order approximation equation of motion can be used on the condition that rod length L is large:

$$L >> b \text{ or } h$$

with b as the width and h the thickness.

Young's modulus E_z ratio on the transverse shear modulus G_{xz} or G_{yz}.is E_z /(G_{xz} or G_{yz}) For anisotropic materials, this ratio plays an important role in the dispersion curve trend. Adopting this higher approximation, equations of motion are adopted.

11.3.3.3.5. Bending wave

This wave gives rise to the simplest equation of motion if we compare it to equations corresponding to extensional and torsional waves. The degree of those last, simplest equations is of second order, but as we see above the application based on them is restrictive in spite of the fourth-order equations of motion (Bernoulli-Euler for lower frequency waves). Timoshenko-Mindlin's equation, concerning bending, is able to describe all possible mechanical phenomena occurring in the dynamic bending beam and working in the whole frequency range, from zero to ultrasonic. The parameters and elastic moduli in the equation of motion in view of Young's modulus calculation are:

Shear modulus G_{xz} or Poisson's number ν.

For isotropic materials, shear modulus combined with Young's modulus gives rise to the ratio $E/G = 2(1+\nu)$, which is practically frequency independent. This assertion is valid for isotropic materials.

The geometric parameters are:

Slenderness: L (length)/b(width)

Flatness: δ = (thickness h/width b)

@Seismicisolation

Bernoulli-Euler's equation gives rise to a strong dispersion at a higher frequency. Utilization of this equation may lead to an erroneous value for Young's modulus. Timoshenko's equation is preferred to Bernoulli's one and gives satisfactory results even at a higher frequency, on the condition of using Mindlin's coefficient, with ν being Poisson's coefficient:

$$K_M = [10(1+\nu) / (12+11\nu)]$$

which satisfies asymptotic behavior, such as the bending velocity which tends to Rayleigh surface wave velocity (see Figure 6.C.1, Chapter 6) when frequency goes to infinity. For the extension of coefficient K_M to anisotropic materials, see Chapter 1.

11.4. Viscoelastic solution of equation of motions

Using *correspondence principle*, the dynamic response of a rod to a specified stationary wave in an elastic regime is converted into a viscoelastic dynamic response, expressed in a closed-form expression. Characteristic functions are referred to here and the elastic moduli are replaced by complex moduli.

11.4.1. *Experimental dynamic responses must be available*

The excitation signal is usually force in cases where transmissibility function (with input and output signals of the same nature: displacement, velocity and acceleration) or transfer function (with input and output signals that are different in nature: inertance, receptance, etc) are used. Dynamic response is obtained directly in the frequency domain when using sinusoidal excitation. When other excitation signals are used, such as impact or white noise, the transfer function in the harmonic regime is obtained by Fourier transforms of the input and output signals.

Examples presented in this section concern the following boundary conditions:

– two additional masses m_1 and m_2 attached at both ends of the rod for longitudinal or bending vibrations;

– two additional inertias I_1 and I_2 for torsional vibrations.

Other boundary conditions can be adopted.

@Seismicisolation

m_1 and I_1 represent the additional mass or inertia of an electrodynamic exciter in translation or rotation motion. They include the mass or inertia of the transducer. m_2 and I_2 represent the additional mass or inertia of the accelerometer that furnish acceleration as an output signal. Figure 11.1 gives the three parts of the excitation system:

– electrodynamic exciter;

– sample; and

– accelerometer or displacement (linear or rotational) transducer.

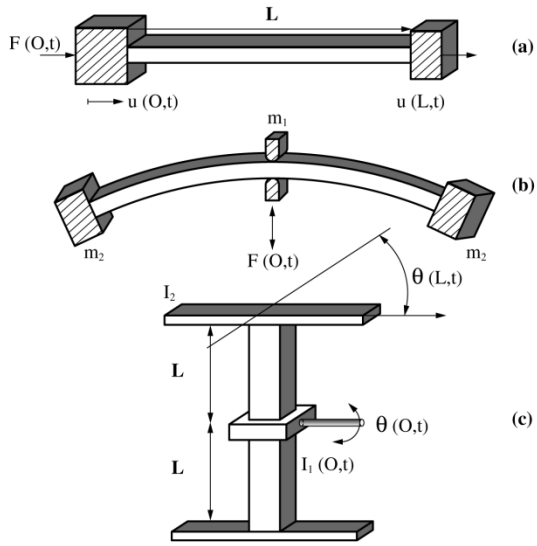

Figure 11.1. *Examples of boundary conditions are represented by two additional mass m_1 m_2 (or inertias I_1 and I_2): a) longitudinal vibration; b) bending vibration – a symmetrical mechanical system is adopted. The total length of the sample is 2L. Excitation signal is applied in the middle; c) torsional vibration – a symmetrical system is also adopted. $I_1(o,t)$ is the inertia of the excitation system*[4]

Successively, three types of transmissibility functions are presented:

– For a rod with longitudinal excitation (Figure 11.1a) and torsional excitation (Figure11.1b) elementary equations of motion are used. The two following cases will be examined in the next sections.

4 Other boundary conditions can be adopted.

@Seismicisolation

– A rod with a higher degree of approximation for equations of motion including more than one viscoelastic modulus and with a closed-form transmissibility function.

– A rod with coupled equations of motion and a numerical solution to the problem.

11.4.2. *Elementary equations of motion and closed-form expression for the transmissibility function for an extensional wave*

The longitudinal and torsional vibrations of a rod are presented with the hypothesis that wave dispersion is absent. This hypothesis is valid on the condition that, in a restricted lower frequency interval, wave dispersion is negligible, taking into account the sample's slenderness (i.e. ratio length L to width b) and the trend of dispersion *versus* wave number $k = 2\pi/\Lambda$, where Λ is the wavelength for the torsion test (see Chapter 5). In Chapter 7, Figures 7.10, 7.11 and 7.12 give the trend of wave dispersion *versus* relative wave number $k_r = 2\pi b$, where b is the width of the extensional wave. The validity of the adopted hypothesis is therefore restricted to $k_r \leq 0.2$.

11.4.2.1. *Transmissibility expression*

The elementary elastic equation of motion is:

$$E\frac{\partial^2 w}{\partial z^2} = \rho S\frac{\partial^2 w}{\partial t^2} \qquad [11.1]$$

With the boundary conditions presented in Figure 11.1a:

$$z = 0 \qquad m_1\frac{\partial^2 w}{\partial t^2} = ES\frac{\partial w(0,t)}{\partial z} + F(0,t) \qquad [11.2a]$$

$$z = L \qquad m_2\frac{\partial^2 w(L,t)}{\partial t^2} = -ES\frac{\partial w(0,t)}{\partial z} \qquad [11.2b]$$

where m_1 and m_2 designate two additional masses at the free ends and center of the rod, and S is the cross-section area of the rod.

@Seismicisolation

In Appendix 11.A, an expression of transmissibility function is presented as $H_T(\omega)$:

$$H_T(\omega) = \frac{1}{\cos\beta - \gamma\beta\sin\beta} \qquad [11.3]$$

$$\gamma = \frac{m_2}{M} = \frac{m_2 \text{ (additional mass)}}{\rho SL(\text{rod mass})}, \text{ M is the mass of half of the rod} \qquad [11.4]$$

It is convenient in the computation to adopt the inverse of transfer function $H_T(\omega)$:

$$[H_T(\omega)]^{-1} = \cos\beta - \gamma\beta\sin\beta = T(\omega) \qquad [11.5]$$

Let us recall that β is related to wave number k and angular frequency ω via the equation of motion:

$$\beta = k/L \text{ (L rod length)}, \quad \beta^2 = \rho\omega^2 L^2 / E \qquad [11.A.4]$$

11.4.2.2. *Viscoelastic transfer function*

Using the principle of correspondence from Chapters 2 and 3, with boundary conditions being the same, the inverse of the transfer function is easy to manipulate:

$$H^*(\omega) = \frac{1}{\cos\beta^* - \gamma\beta^*\sin\beta^*} = 1/T^*(\omega) \qquad [11.6]$$

with $\beta^{*2} = \rho L^2\omega^2 / E^*$ [11.7]

$$E^* = E_1(\omega) + j\,E_2(\omega) \qquad [11.8]$$

Young's modulus is complex and consequently β^* is complex. Let us mention that in equation [11.8], the imaginary part of E^* is positive and the imaginary part of β^* after equation [11.7] is negative:

@Seismicisolation

$$\beta^* = \beta_1 - j\beta_2 = L\omega = \sqrt{\frac{\rho}{E}} = L\omega\, \rho^{1/2}[E_1 + jE_2]^{-1/2} \qquad [11.9a]$$

$$\beta^* = \beta^* = \frac{L\omega}{|v|}\exp(-jd_E/2); |v| = \left[\frac{E_1^2 + E_2^2}{\rho^2}\right]^{1/4}$$

$$\tan\delta_E = E_2 / E_1 \qquad [11.9b]$$

11.4.2.3. *Newton-Raphson's method*

Developing $\cos\beta^*$ and $\sin\beta^*$ *versus* β_1 and β_2 we obtain the expression:

$$f(\beta) = T_r^* - \cos\beta^* + \frac{m_2}{M} \qquad \beta^* \sin\beta^* = 0 \qquad [11.10]$$

which is decomposed into a sum of two functions: $T_r^* = f_1(\beta_1, \beta_2) + jf_2(\beta_1, \beta_2)$.

$$f_1(\beta_1, \beta_2) = \mathscr{R}e\,(T_r^*) - \cos\beta_1 \cosh\beta_2 + \gamma_2\beta_1 \sin\beta_1 \cosh\beta_2 - \gamma_2\beta_2 \cos\beta_1 \sinh\beta_2$$

[11.11]

$$f_2(\beta_1, \beta_2) = \mathfrak{I}m\,(T_r^*) \sin\beta_1 \sinh\beta_2 - \gamma_2\beta_1 \cos\beta_1 \sinh\beta_2 - \gamma_2\beta_2 \sin\beta_1 \cosh\beta_2$$

[11.12]

$$\text{with } \gamma_2 = \frac{m_2}{M} = \frac{m_2}{\rho SL} \qquad [11.13]$$

where S is the cross-section area, ρ density, and L length.

Numerical calculation utilizes both functions f_1 and f_2 of variables β_1 and β_2. The increments $\Delta\beta_1$ and $\Delta\beta_2$ are:

@Seismicisolation

$$\Delta\beta_1 = \beta_1^{i+1} - \beta_1^{i} = [-f_1 f_{2,\beta 2} - f_2 f_{1,\beta}]/[f_{1,\beta 1} f_{2,\beta 2} - f_{2,\beta 1} f_{1,\beta 2}] \qquad [11.14a]$$

$$\Delta\beta_2 = \beta_2^{i+1} - \beta_2^{i} = [f_1 f_{2,\beta 1} + f_2 f_{1,\beta 1}]/[f_{1,\beta 1} f_{2,\beta 2} - f_{2,\beta 2}] \qquad [11.14b]$$

Appendix 11.B gives details for obtaining equations [11.14a] and [11.14b].

Subscript i designates the order of calculation step corresponding to angular frequency ω_i. The letter after the comma in subscript designates the derivative with respect to this variable:

$$f_{i,\beta q} = \partial f_i / \partial \beta q \text{ , } i = (1,2), q = (1,2) \qquad [11.15]$$

There is no summation on i and q.

11.4.2.4. *Method using a derivative of complex variable function*

This method directly uses equation [11.10] as follows:

$$f(\beta^*) = T_r^* - \cos\beta^* + \gamma_2 \beta^* \sin\beta^* \qquad [11.16]$$

Newton-Raphson's method formulae is:

$$\beta^{*(i+1)} = \beta^{*i} - = \frac{f\left(\beta^{*i}\right)}{f_{,\beta^{*i}}} \qquad [11.17]$$

with the derivative:

$$f_{,b^*i} = \frac{\partial f}{\partial \beta^{*i}} = j\frac{\partial f}{\partial \beta_2^{*i}} + j\frac{\partial f}{\partial \beta_2^{*i}} \qquad [11.18]$$

Re and Im designate the real and imaginary parts of the function. Superscript i designates the value of f at the angular frequency ω_i in equation [11.6].

11.4.2.2.1. Derivative of f with respect to β^*

Equation [11.5] shows that β^* is a function of three real variables: angular frequency ω, phase velocity v and damping angle δ. Then $\partial f/\partial\beta^*$ is written as follows:

@Seismicisolation

$$df/d\beta^* = [\partial f/\partial w][\partial w/\partial\beta^*] + [\partial f/\partial v][\partial v/\partial w][\partial w/\partial\beta^*] + [\partial f/\partial\delta][\partial\delta/\partial w][\partial w/\partial\beta^*] \quad [11.19]$$

There are three terms in equation [11.19]. The variations of velocity v and damping δ *versus* angular frequency are very low and so we can neglect them and retain just the first term in the second member of [11.19]:

$$df/d\beta^* \cong [\partial f/\partial w][\partial w/\partial\beta^*] \quad [11.20]$$

The difficulty when using equation [11.15] to find the root β^* in equation [11.10] resides in the fact that the transfer function includes maximas and minimas (resonances and antiresonances). In equation [11.20], the second factor tends to infinity when the absolute value of β^* reaches an extremum.

11.4.2.4.2. Remarks on the calculation of complex Young's modulus

Caution must be taken so that the use of Newton-Raphson's formula does not give rise to inadmissible oscillations of the curve of complex moduli E^* *versus* angular frequency after equation [11.6]. Here let us mention that the real part of E^*, or its absolute value, is a monotonous increasing function of angular frequency ω without extrema. In equations [11.14a and b], frequencies corresponding to resonances and antiresonances for E^* are discarded. At resonance frequency, the real part of T^* goes to zero and [11.11] is rewritten as:

$$-\cos\beta_1\cosh\beta_2 + \gamma_2\beta_1\sin\beta_1\cosh\beta_2 - \gamma_2\beta_2\cos\beta_1\sinh\beta_2 = 0 \quad [11.21]$$

The imaginary part reaches a maximum:

$$\Im m(T^*) = \sin\beta_1\sinh\beta_2 - \gamma_2\beta_1\cos\beta_1\sinh\beta_2 - \gamma_2\beta_2\sin\beta_1\cosh\beta_2 = \text{Max} \quad [11.22]$$

Equations [11.14a] and [11.14b] are reduced to:

$$\Delta\beta_1 = \beta_1^{i+1} - \beta_1^{i} = -f_1 f_{2,\beta 2}[f_{1,\beta 1} f_{2,\beta 2} - f_{2,\beta 1} f_{1,\beta 2}]^{-1} \quad [11.23]$$

@Seismicisolation

$$\Delta\beta_2 = \beta_2^{i+1} - \beta_2^{i} = f_1 f_{2,\beta 1}[\,-f_{2,\beta 2}\, f_{1,\beta 2}]^{-1} \qquad [11.24]$$

With the notation concerning the derivative with respect to β_i^*:

$$\frac{\partial f_k}{\partial \beta_q} = f_{k,q}; \quad \mathrm{k} = (1,2); \quad \mathrm{q} = (\beta_1, \beta_2), \text{ no summation}$$

Equations [11.23] and [11.24] allow the evaluation of root β^*_{ar} at antiresonance frequency ω_{ar}.

The calculation of complex modulus through resonance and antiresonance frequencies is possible using equation [11.17] if the frequency range is decomposed into intervals excluding resonance and antiresonance frequencies.

In such intervals, calculations based on equation [11.17] give rise to a complex modulus with reduced oscillations.

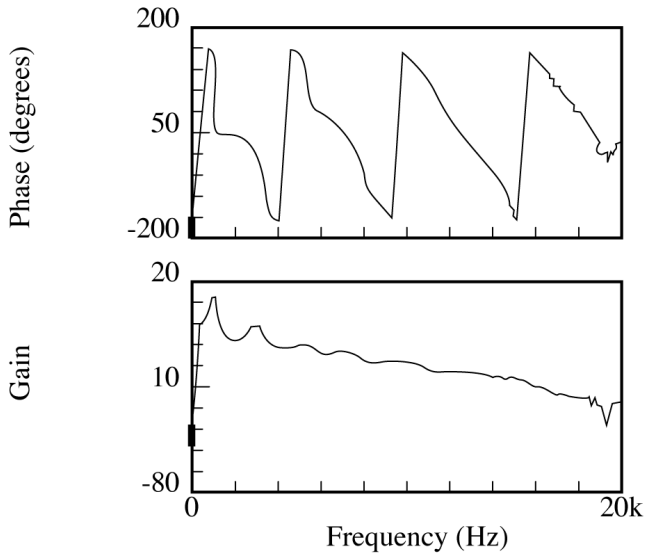

Figure 11.2. *The experimental transmissibility function $H^*(f)$ of polyamide 6 (PA6) phase and gain (circular cross-section, diameter 10.5 mm and length 200 mm, longitudinal vibration tests)*

@Seismicisolation

To illustrate the oscillating phenomenon presented above, Figure 11.2 shows the experimental complex transmissibility function $H^*(\omega)$ of a polyamide (PA6) represented in gain (absolute value of $H^*(\omega)$) and phase angle.

Figures 11.4a and 11.4b represent the two zones, including the first and second resonance of transmission response. The couple of values ($|H^*|$, Φ) are obtained experimentally for a given frequency ω and are reported on Black's chart. Interpolation permits us to obtain β_1 and β_2 from which the complex modulus is deduced using equation [11.7]. The presence of hyperbolic functions f_1 and f_2 in equations [11.11] and [11.12], makes the chart non-symmetric with respect to phase angle Φ, as can be seen in Figure 11.4.

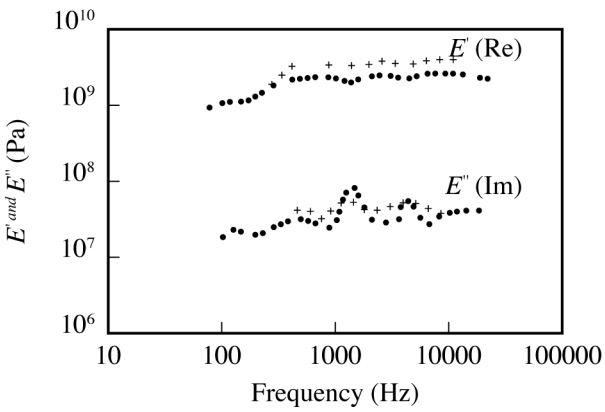

Figure 11.3. *Complex Young's modulus obtained by complex Newton-Raphson's method as in equations [11.23] and [11.24]. Parasitic oscillations are present on both curves (real and imaginary parts) ,+ + + + Odeen and Lundberg obtained similar results*

11.4.3. *Torsional vibration of a viscoelastic rod*

The elementary equation of motion[5] is presented in Chapter 5 with Saint Venant's theory for a rectangular rod section. In section 11.3.3.2, preliminary cautions and considerations are presented.

5 For a rod with circular section, there is no wave dispersion at all in the whole range of frequency. The restriction indicated above is not valid, see Chapter 5.

@Seismicisolation

When frequency interval is chosen with validity conditions taken into account, the second-order equation of motion with the boundary conditions indicated in Figure 11.1, i.e. the additional torsional inertias replace the additional masses.

11.4.3.1. *Isotropic material: circular cross-section*

$$G^* \frac{\partial^2 \alpha}{\partial z^2} = \rho \frac{\partial^2 \alpha}{\partial t^2} \qquad [11.25]$$

where α is the torsional angle, and G* complex shear modulus. The adopted boundary conditions are:

$$z = 0 \quad J_1 \partial^2 \alpha(0,t)/\partial t^2 + M_T^0(t) = C_T^* \partial \alpha(0,t)/\partial z \qquad [11.26a]$$

$$z = L \quad J_2 \partial^2 \alpha(L,t)/\partial t^2 = -C_T^* \partial \alpha(L,t)/\partial z \qquad [11.26b]$$

J_1 and J_2 are the two additional inertias at both ends. Comparing equation [11.25] and [11.26a and b] to equations [11.1] and [11.2a and b], the similarity of the equations of motion as well as boundary conditions permits us to transpose the solution obtained for extensional waves to torsional waves.

Black's chart, presented in Figure 11.4, is also applicable for the torsion test.

11.4.3.2. *Anisotropic material with a second-order equation of motion (rectangular cross-section)*

With a rod axis in coincidence with the symmetry material axis, the equation of motion is:

$$C_T^* \frac{\partial^2 \alpha}{\partial z^2} = \rho I_p \frac{\partial^2 \alpha}{\partial t^2} \qquad [11.27]$$

With $C_T^* = KG^*$, $K = bh^3\xi(c)$, b width and h thickness, ξ is a function describing warping phenomenon, see Chapter 5.

$$c = [b/h][G_{yz}/G_{xz}]^{0.5} \qquad [11.28]$$

Equation [11.28] is similar to equation [11.25], with a comparable set of boundary conditions.

@Seismicisolation

The solutions proposed in section 11.4.2 are easily transposed here with an appropriate change in the set of coefficients.

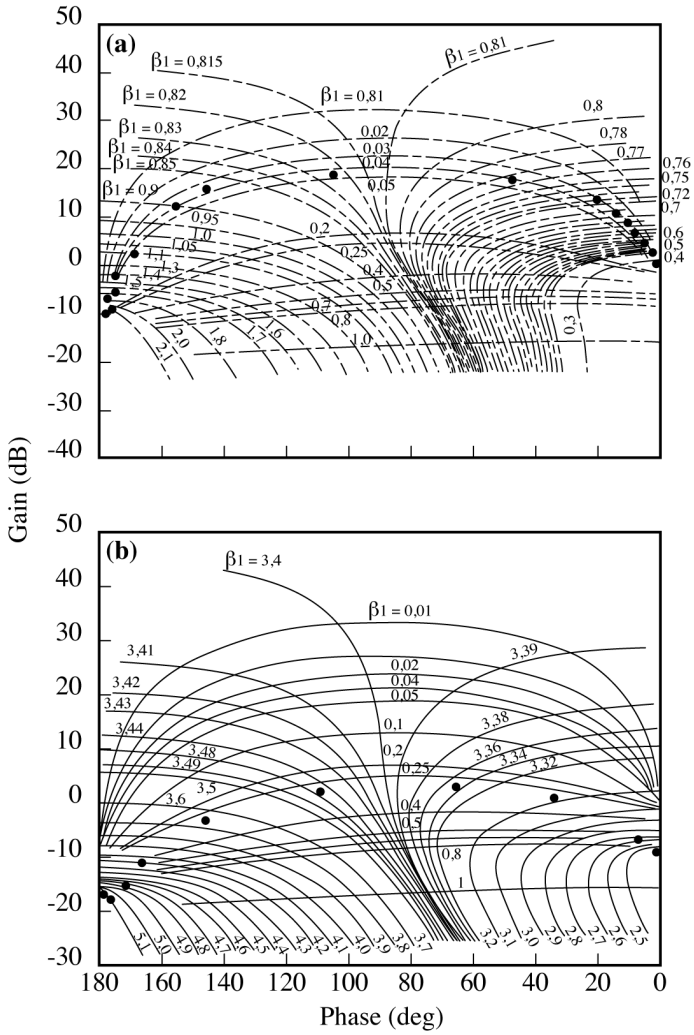

Figure 11.4. *Black's chart (gain* versus *phase), applicable to longitudinal wave and torsional wave, is drawn after equation [11.16] with two families of curves, Re[β]= β and Im[β*] =-β₂. The first mode is represented. By interpolation a couple of results (gain and phase) in the figure permits us to obtain the couple of values(β, β). Complex Young's modulus is deduced*

@Seismicisolation

11.4.3.3. *Higher-order equations of torsional motions of a rod*

In Chapter 5 the direct problem is presented in details for the rectangular section and in a higher frequency range. Saint Venant's theory of warping is completed with the extension of the rod along axis z. This phenomenon increases the degree of decoupled equation of torsional motion from two to four.

The viscoelastic solution using the principle of correspondence becomes tedious and more than one viscoelastic complex modulus must be taken into account.

11.4.4. *Bending vibration of a viscoelastic rod*

Let us recall from Chapter 6 that for an axis rod there are only two theories: Bernoulli-Euler's and Timoshenko-Mindlin's theories, which give rise to fourth-order equations of motion.

11.4.4.1. *Bernoulli-Euler's equation*

The choice of frequency interval and validity conditions are presented above. The corresponding equation [6.5] in Chapter 6 does not take inertia effects into account.

One of the simplest experimental set-ups is the clamped rod. With this experiment, the sample is clamped in the middle[6].

The equation of motion is:

$$\mathrm{EI}\,\frac{\partial^4 w}{\partial z^4} + \rho \mathrm{S}\frac{\partial^2 w}{\partial t^2} = 0 \qquad [11.29]$$

where I inertia of the cross-section with respect to neutral plane = $bh^3/12$ with: b width, h thickness, ρ density and S cross-section area.

In section 6.2.2 of Chapter 6, details of the solution to equation [11.29] with the following set of boundary conditions can be found:

6 This pseudo-clamping system has the properties of a real clamping system and does not necessitate great clamping force. Details are given in another book written by the same authors entitled: *Mechanical Characterization of Materials and Wave Dispersion*

@Seismicisolation

$z = 0 \quad w(0,t) = W_0(t)$ (displacement);

$\partial w(0,t)/\partial z = 0$ (slope); [11.30a]

$z = L \quad \partial^2 w(L,t)/\partial z^2 = 0$ (bending moment);

$\partial^3 w/\partial z^3 = 0$ (shear force) [11.30b]

For stationary waves, displacement is adopted as:

$$w(z,t) = e^{j\omega t}[A\cosh(\beta z/L) + B\sinh(\beta z/L) + C\cos(\beta z/L) + D\sin(\beta z/L)] \quad [11.31]$$

Bringing equation [11.31] into equations [11.30a] and [11.30b], we find that the solution to equation [11.29] for displacement is at z = L. Appendix 11.B presents details of these calculations. The transmissibility function that is obtained in equation [11.B.6] is:

$$H^*(\omega) = \frac{\cos\beta^* + \cosh\beta^*}{1 + \cos\beta^* \cosh\beta^*} \quad [11.32]$$

In equation [11.32], star superscripts are added to transfer function and β^* to indicate that we have to deal with a viscoelastic solution, by using correspondence principle. The viscoelastic equation of motion is:

$$E^* I \frac{\partial^4 w}{\partial z^4} + \rho S \frac{\partial^2 w}{\partial t^2} = 0 \quad [11.33]$$

β^* is related to equation [11.33] with a solution indicated in equation [11.32]:

$$E^* I \beta^{*4}/L^4 - \rho S \omega^2 = 0 \quad [11.34]$$

@Seismicisolation

$$\beta^* = \omega^{0.5}\, L \frac{\exp\left(-\frac{j\delta E}{4}\right)}{\left[\left|E^*\right| \frac{1}{\rho S}\right]^{1/4}} \qquad [11.35]$$

$$E^* = E_1 + jE_2 = |E^*|\,(1 + j\tan\delta_E) \qquad [11.36]$$

Young's modulus in equation [11.36] is expressed in polar coordinate $|E^*|$, $\Phi = \text{Arc}\tan\delta_E$, with δ_E being the damping angle.

For each angular frequency ω, from [11.32], we have to find:

$$\beta^*(\omega) = \beta_1(\omega) - j\,\beta_2(\omega) \qquad [11.37]$$

The next step is to evaluate E^* from equations [11.34] and [11.35]. The methods utilized are similar to those adopted above for longitudinal waves.

11.4.4.2. *Decomposition of complex transfer function into two functions with real variables β_1 and β_2*

Details of the calculations to obtain the two functions $f_1(\beta_1,\beta_2)$ and $f_2(\beta_1,\beta_2)$ are presented in Appendix 11.D. Increments $\Delta\beta_1$ and $\Delta\beta_2$ are given by equations [11.14a] and [11.14b]. Complex Young's modulus is deduced from equation [11.34]:

$$E^* = \rho S L^4 \omega^2 / \mathbf{I}\,\beta^{*4} \qquad [11.38]$$

$$E^* = |E^*|\,\exp(j\delta_E) = (\rho\omega^2 S L^4 / I) = \frac{\exp j4\delta_\beta}{\left|\beta^{*4}\right|} \qquad [11.39]$$

$$\delta_E = \text{Arc}\tan\frac{\text{Im}\,\beta^*}{\text{Re}\,\beta^*} \qquad [11.40]$$

@Seismicisolation

To avoid oscillations of curve E^* when the tangent of curve $|H^*|$ goes to zero, the same cautions must be taken as those for an extensional wave.

11.4.4.3. *Black's chart representing the curve $|T^*|$ versus Φ_{T*} after equation [11.32]*

Two sets of parameters β_1 and β_2 are used to draw the curve around the structural mode, see Figure 11.5. For a given couple of values, $|T^*|$ and ϕ_T, β_1 and β_2 can be evaluated by interpolations, from which E^* is deduced. Black's chart is easily extended to a higher structural mode.

11.4.4.4. *Complex Young's modulus evaluated at resonance frequency*

A simple method of evaluating complex Young's modulus at resonance frequency consists of measuring the sharpness of transmissibility curve $T^*(\omega)$ around resonance frequencies in a bandwidth of three decibels.

This method is acceptable if the damping coefficient is weak [VIN 63]:

$$\beta_2 << \beta_1 \text{ and } \beta_2/\beta_1 = \tan\delta_\beta << 1$$

This method is naturally applicable when we want to obtain just a scale of size of material damping. Let us recall that the sharpness of curve $|T^*|$ *versus* frequency evaluated with three decibels bandwidth is not necessarily the material damping angle, see equation [11.32].

A hypothesis of the weak damping of a material, however, allows the simplification of this equation by using limited series expansion.

In equation [11.31] the denominator represents the eigenvalue equation in the elastic case:

$$1 + \cos\beta \,.\, \cosh\beta = 0$$

The roots of this equation are:

$$\beta_0^1 = 1.875104 \qquad \beta_0^2 = 4.694091 \qquad \beta_0^3 = 70855 \qquad \beta_0^4 = 10.996$$

$$\beta_0^n \cong (2n-1)\pi/2 \qquad \text{with} \qquad n > 4$$

@Seismicisolation

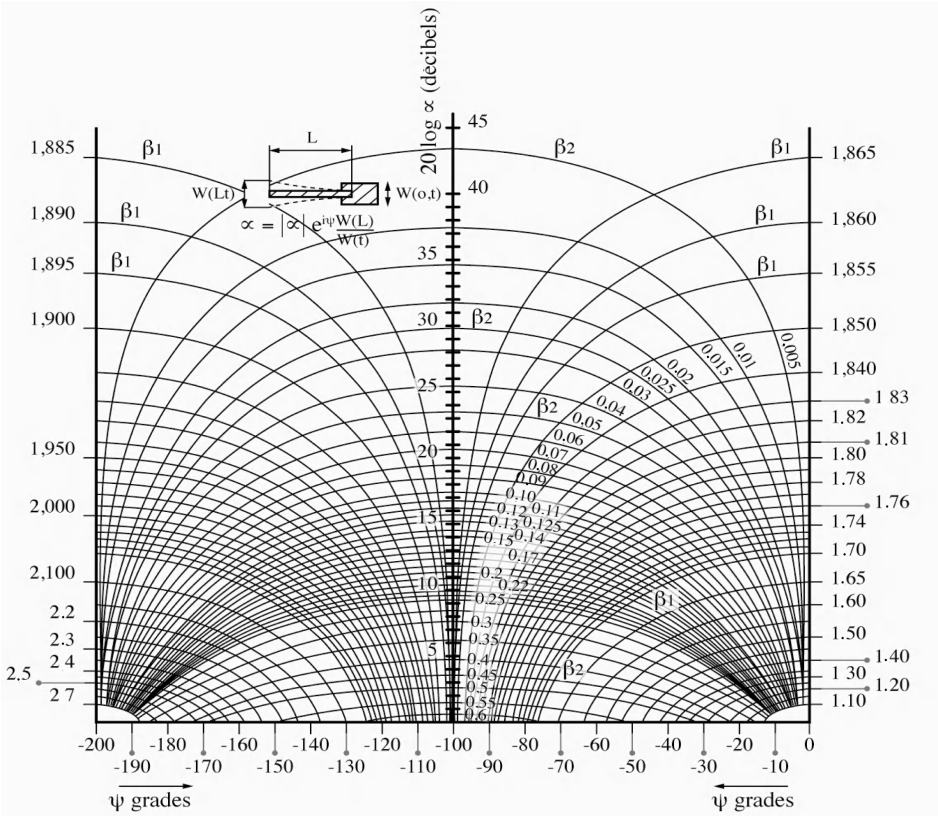

Figure 11.5. *Black's chart, concerning bending test represents the transmissibility curve in gain and phase with two parameters β_1 and β_2. Each of them is represented by a family of curves. The chart is valid around the first eigenvalue with the boundary conditions of clamped-free rod. Gain and phase being known experimentally, Black's chart permits us to obtain the couple of values (β_1, β_2) from which complex Young's modulus is evaluated*

11.5. Viscoelastic moduli using equations of higher approximation degree

In section 11.3.3.3, some mechanical effects are discussed.

In this section we try to recapitulate for each type of wave the various effects, which are:

– inertia;

– shear;

@Seismicisolation

– warping due to non-circular cross-section;

– warping due to open cross-section and called Vlasov effect;

– coupling of many types of waves due to an off-axis rod (where the rod axis is not the symmetry axis of a material).

Interia, shear and warping (due to non-circular cross-section) effects are discussed in Chapters 5, 6, 7 and we will focus our attention on these three effects. The overview presented below enables the reader to choose the adequate theory for various applications.

Warping due to Vlasov effect concerns a rod with an open cross-section. If the experimenter has a latitude of choice of sample geometry, he or she can avoid the difficulty inherent with this kind of section.

It is necessary to exploit the coupling of many wave types in order to reach some non-diagonal components of compliance matrix $[S_{ij}]$. Coupled vibrations occurring in the sample give rise to coupled equations of motion. It is possible to decouple these equations and obtain a higher degree equation. Characteristic functions can be used with lengthy mathematical manipulations.

11.5.1. *Inertia and shear effects*

Inertia and shear effects contribute to increase the degree of the decoupled equation of motion. This degree exceeds four, calculation becomes tedious and lengthy when manipulating characteristic functions. Below we present various theories in order of increasing difficulty for each wave type.

11.5.1.1. *Extensional wave*

Principle theories are presented in Chapter 7 and their main characteristics are succinctly presented below.

11.5.1.1.1. Love's theory and its main characteristics

Love's theory is a fourth-order equation with ν Poisson's number, I inertia moment, S cross-section area, ρ density and E Young's modulus:

$$\frac{\partial^2 w}{\partial t^2} - (\nu^2 \mathrm{I}/\mathrm{S})\frac{\partial^4 w}{\partial z^2 \partial t^2} - (\mathrm{E}/\rho)\frac{\partial^2 w}{\partial t^2} = 0 \qquad [11.41]$$

At higher frequencies the dispersion curve imperfectly follows the real one.

@Seismicisolation

11.5.1.1.2. Bishop's theory and its main characteristics

Bishop's theory is a fourth-order equation of motion:

$$\frac{\partial^2 w}{\partial t^2} - (\nu^2 \mathrm{I}/\mathrm{S})\frac{\partial^4 w}{\partial z^2 \partial t^2} \Big] - (\mathrm{E}/\rho)\frac{\partial^2 w}{\partial t^2} + \left[\nu^2 \mathrm{GI}/\mathrm{S}\rho\right]\frac{\partial^4 w}{\partial z^4} = 0 \qquad [11.42]$$

taking inertia and transverse shear effects into account.

The dispersion curve is satisfactory in low and medium frequency intervals, and its weakness is at higher frequencies.

11.5.1.1.3. Volterra's theory and its main characteristics

Volterra's theory uses the method of internal constraints.

It is a sixth-order equation of motion (see Chapter 7) that is valid for isotropic materials when all effects (inertia and transverse shear) are taken into account. It has a good dispersion curve trend throughout the whole frequency range.

11.5.1.1.4. Touratier's theory and its main characteristics

Touratier's theory is a sixth-order equation of motion (see Chapter 7) that is valid for anisotropic material (transverse isotropic).

It has a good dispersion curve trend throughout the whole frequency range.

11.5.2. *Torsional vibration*

11.5.2.1. *Torsion of a rod with rectangular section*

11.5.2.1.1. Barr's theory and its main characteristics

Barr's theory is a fourth-order equation of motion, valid for isotropic materials. It takes inertia and warping effects into account. For further details, see Appendix 5.C.1, Chapter 5.

Barr's correcting coefficient permits us to obtain the correct asymptotic behavior of the dispersion curve at a frequency going to infinity.

Consequently, it can be used at a higher frequency.

@Seismicisolation

11.5.2.1.2. Nugues' theory and its main characteristics (see Chapter 5)

The fourth-order equation of motion is valid for anisotropic materials. It is applicable for the first elastodynamic[7] mode.

Two or three viscoelastic complex moduli are used in the equation and this complicates the search for a viscoelastic solution. The method using characteristic functions has its own limitation. Continuous element method, see Chapter 12, is more appropriate here[8].

Some simplified assumptions, if they are valid, permit us to obtain tractable solutions. For viscoelastic and isotropic materials, for example, we can replace the coefficient E^*/G^* by $(1+2\nu)$, which we can be reasonably suppose to be real and constant.

For a second-order viscoelastic equation, the methods presented for extensional waves are applicable, taking into account the similarity of equations of motion.

11.5.3. *Bending vibration of a rod (higher order approximation)*

The two principle classes of equations of motion are Bernoulli-Euler and Timoshenko-Mindlin.

Indeed, there are many works about the bending vibration of rods [COW 66, STE 79], but the proposed equations differ slightly from Timoshenko's one only in coefficients.

It is not necessary to use a higher-order equation of motion in bending beam theory. Timoshenko's theory correctly describes wave effect in the whole frequency range.

7 For elastodynamic modes see Figures 5.7 and 5.8 and Onobiono's work in section 5.8 of Chapter 5.

8 Strictly speaking, two independent viscoelastic complex moduli must be used to characterize isotropic materials. Consequently, Poisson's number is complex. For an isotropic polymer, the constant Poisson's number is verified for this class of materials, at least in the low and medium frequency range.

@Seismicisolation

11.5.3.1. *Mindlin-Timoshenko's theory*[9]

$$\rho S \frac{\partial^4 w}{\partial t^4} + \mathrm{E}_z{}^* \mathrm{I} \frac{\partial^4 w}{\partial z^4} + (\rho^2 \mathrm{I} / KG) \frac{\partial^4 w}{\partial t^4} - (\rho I + E_z^* \rho I / KG^*) \frac{\partial^4 w}{\partial t^2 \partial z^2} = 0$$

[11.43]

This theory correctly describes wave dispersion in the whole frequency range. At higher frequencies some coefficients in equation [11.43] must be replaced by those proposed by Mindlin [MIN 51].

11.5.3.1.1. Remarks about equation [11.43]

Wave dispersion is described correctly by equation [11.43] in the whole frequency range.

The roots β^* of the equation of motion are two complex distinct values of β^*, i.e. β^{*1} and β^{*2}.

Two complex moduli E^* and G^* are taken into account in equation [11.43]. To solve this equation with one complex modulus, an additional hypothesis is necessary. For example, for an isotropic material where ratio $|E^*|/|G^*|$ is constant and equal to 2 (1 + ν), with ν being Poisson's number, which is supposed to be real and constant, on practical grounds the trends of damping curves for E^* and G^* are the same. If this hypothesis is rejected, the tests must be conducted on the same sample for bending and torsion. The solution of an inverse problem includes the search of two complex moduli using optimization techniques with two complex unknown quantities.

11.5.3.2. *Solutions of Timoshenko-Mindlin's equation*

Practicians and experimenters have various reasons for determining the characteristics of materials. Below we present some methods for improving measurements of elastic and/or viscoelastic moduli.

11.5.3.2.1. Improvement of elastic modulus values by trial and error method

For the first approximation, the ratio E/G is supposed to be constant for an isotropic material:

9 For details on notations, see Chapter 6.

@Seismicisolation

$$E_z/G_{sz} = 2(1+\nu) = \text{constant} \qquad [11.44]$$

For anisotropic material, equation [11.44] is not valid. We have to use a previsional calculus, which is presented in Chapter 1, in order to estimate the ratio E_{zz}/G_{xzw} (which largely exceeds three). Bernoulli's equation can be used to evaluate Young's modulus:

$$E \approx [\rho S\omega^2 L^4/I\beta^4]$$

where eigen value β is supposed to be real and its value depends on the structural order mode.

We can use Timoshenko's equation to improve the estimated value of E. Bringing β into equation [11.43] we obtain:

$$E = \left[\frac{\rho S\omega^2}{I\beta^4} L^4\right] . \left[\frac{1 - \frac{\rho I\omega}{GxzKS} - \frac{I\beta^2}{L^2 S}}{1 + \frac{L^4 \rho\omega^4}{\beta^4 K G_{xz}}}\right] \qquad [11.45]$$

In the second member of equation [11.45], the second factor at the numerator represents the combined effect of shear wave and inertia. The third factor at the denominator is essentially due to shear effect. The second and third factors (in the second bracket) contribute to reduce the value of Young's modulus.

This means that Bernoulli's theory overestimates wave velocity and consequently overestimates Young's modulus. The correction afforded by the second and third factors in equation [11.44] contribute to reducing the first estimated value of E by Bernoulli's equation.

We can also estimate the eigenvalues β of Timoshenko's equation. The two eigenvalues β_1 and β_2 are distinct (while Bernoulli's equation gives rise to an equal value of β), see Chapter 6, section 6.3.

@Seismicisolation

11.5.3.2.2. Transmissibility function of a clamped-free elastic Timoshenko's rod

In section 6.3, equations [6.46] and [6.47], two variables w (z, t) and ϕ (z, t) are used to determine bending and shear phenomena. Let us recall that the equation is of fourth order and provides solutions for those two variables. The solutions are:

$$\mathrm{w}(\mathrm{z},\mathrm{t}) = (\exp \mathrm{j}\omega t)[\,\mathrm{A}_1 \cosh \beta_1 z / L + B_1 \sinh \beta_1 z / L + D_1 \sin \beta_2 z / L]$$

$$\varphi(\mathrm{z},\mathrm{t}) = (\exp \mathrm{j}\omega t)[\mathrm{A}_2 \cosh \beta_1 z / L + B_2 \sinh \beta_1 z / L + C_2 \cos \beta_2 z / L + D_2 \sin \beta_2 z / L]$$

[11.46]

We have eight coefficients to evaluate and at the same time we only have four boundary equations. Fortunately, there are equations relating w (z , t) and ϕ (z , t):

$$\frac{\partial^2 w}{\partial t^2} - (\rho / KG)\frac{\partial^2 w}{\partial t^2} = \frac{\partial \varphi}{\partial t} \qquad [11.47]$$

Bringing equation [11.46] into [11.47] we obtain:

$$\mathrm{A}_2 = \mathrm{r}\mathrm{A}_1 \quad \mathrm{B}_2 = \mathrm{r}\,\mathrm{B}_1 \;\; ; \;\; \mathrm{C}_2 = \mathrm{s}\mathrm{C}_1 \quad \mathrm{D}_2 = \mathrm{s}\mathrm{D}_1 \qquad [11.48]$$

where r and s are given by equation [11.48].

Matricial solving of the boundary equations enables us to express the free end output signal w (L , t) received at the free end *versus* the input signal w (0 , t), which is applied at the clamped end.

$$\begin{pmatrix} 1 & 0 & 1 & 0 \\ 0 & \mathrm{r} & 0 & -\mathrm{s} \\ \beta_1 \mathrm{r} \cosh\beta_1 & \beta_1 \mathrm{r} \sinh\beta_1 & \beta_2 \mathrm{s} \cos\beta_2 & \\ \left(\frac{\beta_1}{L} - r\right)\sinh \beta_1 & \left(\frac{\beta_1}{L} - r\right)\cosh \beta_1 & (\frac{\beta_2}{L} + s)\sin \beta_2 & -(\frac{\beta_2}{L} + s)\cos \beta_2 \end{pmatrix} \begin{pmatrix} A_1 \\ B_1 \\ C_1 \\ D_1 \end{pmatrix} = \begin{pmatrix} W(0) \\ 0 \\ 0 \\ 0 \end{pmatrix}$$

[11.49]

@Seismicisolation

Transmissibility function is defined as:

$$H(\beta_1, \beta_2, \omega) = N_H / D_H \qquad [11.50]$$

$$N_H = (\beta_1/L - r)s\,[\beta_1 r - \beta_2 s]\cos\beta_2 + (\beta_2/L + s)r[\beta_2 s - \beta_1 r]\cosh\beta_1 \qquad [11.51]$$

$$D_H = \{[\beta_1(\beta_1/L - r) + \beta_2(\beta_2/L + s)]\,sr - [\beta_1 r^2(\beta_2/L + s) + \beta_2 s^2(\beta_1/L - r]\cosh\beta_1\cos\beta_2$$

$$[\beta_1(\beta_2/L + s) - \beta_2(\beta_1/L - r)]\,sr\sin\beta_2\sinh\beta_1\} \qquad [11.52]$$

The reader may notice that the transmissibility function H^* in equations [11.50], [11.51] and [11.52] reduce to that given by equation [11.32] corresponding to Bernoulli-Euler's theory if:

$$\beta_1 = \beta_2 \qquad s = -r$$

11.5.3.2.3. Viscoelastic transmissibility function of a clamped-free Timoshenko's rod

The expression of transmissibility given above can easily be transformed into complex function H* of two complex variables β_1^* and β_2^*. If we refer to Chapter 6, equation [6.53], we notice that there are two equations relating the two complex variables, so we can write[10]:

$$H^* = H^*[\beta_1^*, \beta_2^*, s, r, \omega] \qquad [11.53]$$

The problem then becomes difficult to handle. Complex shear modulus plays an important role. All of the methods presented above concerning the elementary equations of motion, see section 11.4.3.1, can be used with the appropriate adaptations and tedious calculations.

Figure 11.6 shows the absolute value of the transmissibility function of a Timoshenko's clamped-free rod with two damping coefficients δ_E and δ_G as parameters. Indexes E and G refer to Young's and shear moduli respectively. It shows that the shape of this function is strongly dependent on both coefficients.

10 To avoid confusion, δ_1 and δ_2^* are two distinct complex wave numbers obtained from equation [11.49] by equalizing the determinant to zero. They are not the same as in section 11.4.3.1, which is applicable for Bernoulli's rod.

@Seismicisolation

In the framework of the solution to the viscoelastic inverse problem of rod vibration, it is reasonable to call on another form of solution, such as that of using continuous methods [CAS 97], see Chapter 12. With the appropriate identification technique, complex exponentials can be extracted by manipulating the matrix in the framework of a continuous element method.

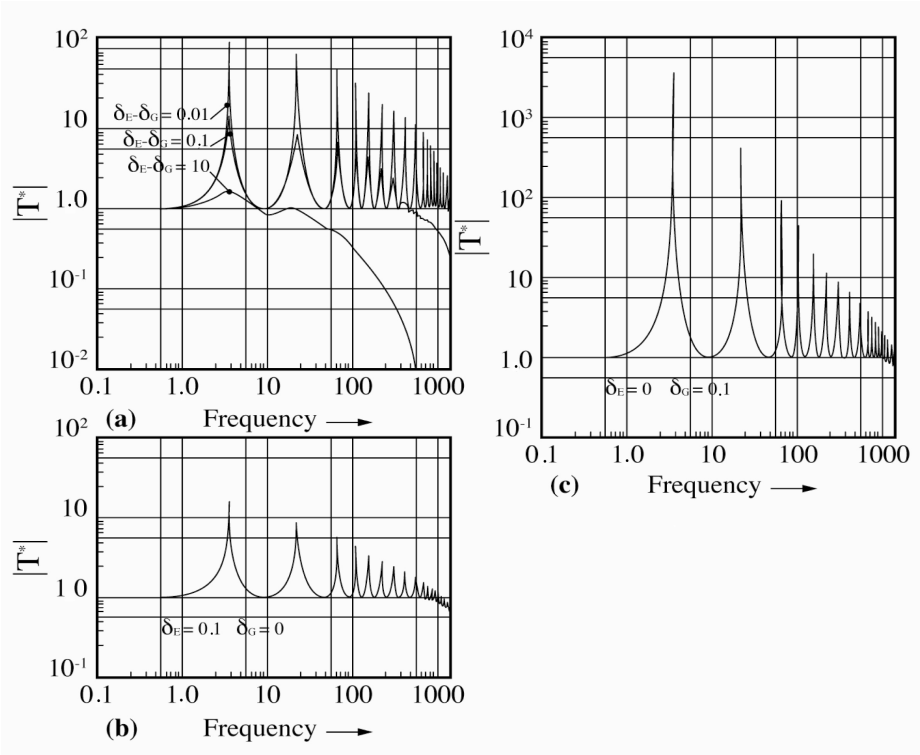

Figure 11.6. *Transmissibility function of a clamped-free Timoshenko's rod* versus *circular frequency, with damping coefficients δ_E and δ_G being two parameters*

Details of calculations for the closed-form expression of transmissibility of Timoshenko-Mindlin's rod are presented in Appendix 11.F.

Figure 11.6 presents transmissibility *versus* dimensionless angular frequency for Timoshenko's equation, after Snowdon [SNO 69].

@Seismicisolation

The curves are drawn with constant damping coefficients δ_E and δ_G as parameters in the whole frequency range.

Strictly speaking, these coefficients are frequency dependent. However, strong damping (δ_E >1) tends to suppress resonance at a higher frequency.

11.6. Bibliography

[BED 90] BEDA T., Complex moduli of viscoelastic materials by dynamic tests on rods (modernization, instrumentation and characterization), PhD thesis, Conservatoire National des Arts et Métiers, Paris, 1990.

[CAS 97] CASIMIR J. B., Rod-type continuous elements (Static and dynamic study of planar and non planar beam assemblies), PhD thesis, Conservatoire National des Arts et Métiers, Paris, 1997.

[CAS 03] CASIMIR J. B., DUFORET C., VINH T., "Dynamic behavior of structure over a large frequency range by continuous element methods", *Journal of Sound and Vibration*, vol. 267, p. 1085-1106, 2003.

[COW 66] Cowper G. R., "The shear coefficient in Timoshenko beam theory." *Journal of Applied Mechanics*, vol. 33, p. 335-340, 1966.

[EST 87] ESTEOULE C., VINH T., CHEMOUIL J. *Impact Tests on Solid Propellant,* Mémorial de l'Artillerie Française, vol 61, 3rd edition, 1987

[LUN 88] LUNDBERG B., BLANC R. H., "Determination of material properties from the two point response of an impacted linearly viscoelastic rod specimen", *Journal of Sound and Vibration*, vol. 126, no. 1, p. 97-108, 1988.

[MIN 51] MINDLIN R. D., "Influence of rotary inertia and shear on flexural motion of isotropic elastic plates", *Journal of Applied Mechanics*, vol. 18, p. 31-38, 1951.

[ODE 93] ODEEN S., LUNDBERG B., "Determination of complex modulus from measured end-point accelerations of an impacted rod specimen", *Journal of Sound*, vol. 165, no. 1, p. 1-8, 1993.

[SNO 69] SNOWDON J.S. *Vibration and Shock in Damped Mechanical System*, New York, John Wiley, 1969.

[SOU 96] SOULA M., Mechanical behavior of viscoelastic materials by fractional derivatives, PhD thesis, Conservatoire National des Arts et Métiers, Paris, 1996.

[STE 79] STEPHEN N. G. LEVINSON M., "A second order beam theory." *Journal of sound and Vibration*, vol. 67, p. 293-305, 1979.

[VEY 68] VEYSSEYRE R., VINH T., *Passage from Harmonic Regime to Transient Regime in Viscoelasticity*, Comptes rendus de l'Académie des Sciences, Paris, vol. 266, series A, 1968.

@Seismicisolation

[VIN 67] VINH T., *Interrelationship Between Harmonic Regime and Transient Regime Applications of Fractional Derivatives*, Mémorial de l'Artillerie Française, 3rd edition, 1967.

[VIN 63] VINH T., *Determination of Complex Modulus and Damping Coefficient of Viscoelastic Materials by Bending Vibration*, Mémorial de l'Artillerie Française, Fourth section, p. 980-1007, 1963.

11.7. Appendices

Appendix 11.A. Transmissibility function of a rod submitted to longitudinal vibration (elementary equation of motion)

In Chapter 7, the eigenvalue equation is given with two boundary equations:

$$E\partial^2 w/\partial z^2 = \rho\partial^2 w/\partial t^2 \qquad [11.A.1]$$

where z is coordinate along the rod axis.

The boundary conditions are additional masses at both ends and force excitation F at z=0: $P_0 = F_0\,(0,t)/\mathbf{S}$, with S being the cross-section area and m_1, m_2 additional masses:

$$z=0(\,m_1/\mathbf{S}\,)\partial^2 w(0,t)/\partial t^2 = E(\partial w(0,t)/\partial z) + P_0(t) \qquad [11.A.2a]$$

$$z=L(m_2/S)\,\partial^2 w\,(L,\,t)/\partial t^2 = -E\partial\, w(L,\,t)/\partial z \qquad [11.A.2b]$$

As we have to deal with the second-order equation of motion, the general solution in the stationary wave state is:

$$w(z,t) = \exp(j\omega t)\,[A\cos(\beta z/L) + B\sin(\beta z/L)] \qquad [11.A.3]$$

Bringing equation [11.A.3] into [11.A.1], we get:

$$E\beta^2/L^2 = \rho\omega^2 \quad \text{or} \quad \beta^2 = \rho\omega^2 L^2/E \qquad [11.A.4]$$

Bringing equation [11.A.3] into [11.A.2], the constants A and B are obtained as follows:

@Seismicisolation

$$A = \{-[ESL^2/\omega^2 m_1]\cos\beta + (m_2/m_1)(\sin\beta)P_0\} / \{(1+m_2/m_1)EL\beta\cos\beta + (E^2S\beta^2\cos\beta/\omega^2L^2m_1) - \omega^2/S)\sin\beta\} \quad [11.A.5]$$

$$B = \{(-m_2/m_1)\cos\beta + (ESL\beta/\omega^2 m_1)(\sin\beta)P_0\} / \{(1+m_2/m_1)EL\beta\cos\beta + [(E^2S\beta^2L^2/\omega m_1) - \omega^2 m_2/S)\sin\beta]\} \quad [11.A.6]$$

With equations [11.A.5] and [11.A.6] and if z = L, we can write w (L , t) and obtain the ratio w(L , t)/w(0 , t) as the transmissibility function:

$$H(\omega) = 1/[\cos\beta - \gamma\beta\sin\beta] \quad [11.A.7]$$

with $\gamma = m_2/M$ where M is the rod mass = $SL\rho$.

Appendix 11.B. Newton-Raphson's method applied to a couple of functions of two real variables β_1 and β_2 components of β

Let $f_1(x, y)$ and $f(x, y)$ be two functions of two real variables x and y. In the case of convergence towards (x_0, y_0), a Taylor expansion around this solution gives:

$$f(x, y) = f(x_0,y_0) + (x-x_0)\,\partial f(x_0, y_0)/\partial x + (y-y_0)\,\partial f(x_0,y_0)/\partial y + \ldots \quad [11.B.1]$$

With an initial estimation (x_i, y_i) we try to obtain the couple (x_i, y_i) so that the two functions f_1 and f_2 can be written as follows:

$$f_1(x_{i+1},y_{i+1}) \equiv f_1(x_i, y_i) + (x_{i+1}-x_i)\,\partial f_1(x_i, y_i)/\partial x + (y_{i+1}-y_i)\,\partial f_1(x_i, y_i)/\partial y + \ldots) \quad [11.B.2]$$

$$f_2(x_{i+1},y_{i+1}) \equiv f_2(x_i, y_i) + (x_{i+1}-x_i)\,\partial f_2(x_i, y_i)/\partial x + (y_{i+1}-y_i)\,\partial f_2(x_i, y_i)/\partial y \quad [11.B.3]$$

@Seismicisolation

The following notation is adopted:

$$f_{j,s} = \partial f_j / \partial s$$

The solutions of equations [11.B.2] and [11.B.3] are:

$$\Delta x = x_{i+1} - x_i = [\ -f_1 f_{2,y} + f_2 f_{1,y}] / [\ f_{1,x} f_{2,y} - f_{2,x} f_{1,y}] \qquad [11.B.4]$$

$$\Delta y = y_{i+1} - y_i = [\ f_1 f_{2,x} + f_2 f_{1,x}\ ] / [\ f_{1,x} f_{2,y} - f_{2,x} f_{2,y}] \qquad [11.B.5]$$

In equations [11.B.4] and [11.B.5] the two functions f_1 and f_2 are taken at the couple of variables (x_i, y_i):

$$f_1 = f_1(x_i, y_i),\ f_2 = f_2(x_i, y_i)$$

The two variables x, y are identified as β_1 and β_2:

$$\beta^* = \beta_1 - j\beta_2 \qquad \beta_1 = x \qquad \beta_2 = y \qquad [11.B.6]$$

Appendix 11.C. Transmissibility function of a clamped-free Bernoulli's rod submitted to bending vibration

The characteristic function is used here to express the displacement:

$$w(z,t) = \exp(j\omega t)[\ A\cosh(\beta z/L) + B\sinh(\beta z/L) + C\cos(\beta z/L) + D\sin(\beta z/L)] \qquad [11.C.1]$$

at $z = 0$:

$A + C = W_0$ imposed displacement (clamping end)

$B + D = 0$ slope [11.C.2]

@Seismicisolation

$$A\cosh\beta + B\sinh\beta - C\cos\beta - D\sin\beta = 0$$

bending moment (a)

at z = L [11.C.3]

$$A\sinh\beta + B\cosh\beta + C\cos\beta - D\sin\beta = 0$$

shear force (b)

The four equations presented above can be written under matricial form.

11.C.1. *Eigenvalues from equation [11.C.4]*

The determinant of this equation equalized to 0 permits obtain eigenvalue β. This determinant 4 X 4 is easily reduced to a 3 X 3 one:

$$\begin{pmatrix} 1 & 0 & 1 & 0 \\ 0 & 1 & 0 & 1 \\ \cosh\beta & \sinh\beta & -\cos\beta & -\sin\beta \\ \sinh\beta & \cosh\beta & \sin\beta & -\sin\beta \end{pmatrix} \bullet \begin{pmatrix} A \\ B \\ C \\ D \end{pmatrix} = \begin{pmatrix} W_0 \\ 0 \\ 0 \\ 0 \end{pmatrix}$$

$$\Delta = \begin{vmatrix} 0 & 1 & 1 \\ (\cosh\beta + \cos\beta) & \sinh\beta & -\sin\beta \\ (\sinh\beta - \sin\beta) & \cosh\beta & -\cos\beta \end{vmatrix} = 0 \qquad [11.C.4]$$

$$\Delta = -(2 + 2\cosh\beta.\cos\beta) = 0 \qquad [11.C.5]$$

Eigenvalues evaluated from [11.C.5] can easily be obtained numerically.

11.C.2. *Transmissibility function T(ω) = w (L, t)/w (0, t)*

The closed-form expression of T(ω) is:

$$T(\omega) = (\cosh\beta + \cos\beta)/(1+\cos\beta\cosh\beta) \qquad [11.C.6]$$

@Seismicisolation

Appendix 11.D. Complex transmissibility function of a clamped-free Bernoulli's rod and its decomposition into two functions of real variables β_1, β_2

Expression [11.C.4] is rewritten here with β^* complex according to the correspondence principle presented in Chapters 2 and 3 with:

$$\beta^* = \beta_1 - j\beta_2 \qquad [11.D.1]$$

Equation [11.C.4] is written under an appropriate form for calculation:

$$T^* [1 + \cosh \beta^* \cos \beta^*] - [\cosh \beta^* + \cos \beta^*] = 0 \qquad [11.D.2]$$

For writing simplicity let us adopt:

$$T^* = |T^*| \exp(j\Phi) \quad |T^*| = T$$

$$[T\cos\Phi + j\, T \sin\Phi\,] [\,1 + \cos\beta^* \cosh\beta^*] - [\cos\beta^* + \cosh\beta^*] = 0 \qquad [11.D.3]$$

Developing $\cos(\beta_1 - j\beta_2) = \cos\beta^*$ and $\cosh(\beta_1 - j\beta_2) = \cosh \beta^*$ with:

$$\cos j\alpha = \cosh \alpha, \ \cosh j\alpha = \cos\alpha, \sin j\alpha$$

$$= -j\sinh \alpha, \sinh j\alpha = j\sin\alpha \qquad [11.D.4]$$

Using equation [11.D.4] in the development of [11.D.3] and collecting real and imaginary terms, the real part of equation [11.D.3] is:

$$\{T\cos\phi\, [1 + \cos\beta_1 \cos\beta_2 \cosh\beta_2 \cosh\beta_1 + \sin\beta_1 \sin\beta_2 \sinh\beta_1 \sinh\beta_2$$

$$-\cos\beta_1 \cosh \beta_2 - \cos\beta_2 \cosh \beta_1]$$

$$-T\sin\phi\, [-\sin\beta_1 \sinh\beta_2 \cosh\beta_1 \cos\beta_2 + \cos\beta_1 \cosh\beta_2 \sinh\beta_1 \sinh\beta_2$$

$$+ \sin\beta_1 \sinh\beta_2 - \sinh\beta_1 \sin\beta_2]\} = 0 \qquad [11.D.5]$$

@Seismicisolation

The imaginary part of equation [11.D.3] is:

$$\{T\cos\phi\ [-\sin\beta_1 \sinh\beta_2 \cosh\beta_1 \cos\beta_2 + \cos\beta_1 \cosh\beta_2 \sinh\beta_1 \sin\beta_2$$

$$+ \sin\beta_1\ \sinh\beta_2 - \sinh\beta_1 \sin\beta_2]$$

$$+ T\sin\phi\ [1 + \cos\beta_1 \cosh\beta_2 \cos\beta_2\ \cosh\beta_1 + \sin\beta_1\ \sinh\beta_1 \sin\beta_2 \sinh\beta_2$$

$$-\cos\beta_1\ \cosh\beta_2 - \cos\beta_2\ \cosh\beta_1]\} = 0 \qquad [11.D.6]$$

Appendix 11.E. Eigenvalue equation of clamped-free Timoshenko's rod

Coefficients A, B, C and D in equation [11.47] are represented under a matricial form. Setting the determinant of the corresponding matrix at the right-hand side to zero, we obtain the closed-form eigenvalue equation of the rod:

$$\Delta = \begin{vmatrix} 1 & 0 & 1 & 0 \\ 0 & r & 0 & -s \\ \beta_1 r \cosh\beta_1 & \beta_1 \sinh\beta_1 & \beta_2\, s \cos\beta_2 & \beta_2\, s \sin\beta_2 \\ [(\beta_1 / L) - r]\sinh & [(\beta_1 / L) - & [(\beta_2 / L) & [(\beta_2 / L) +]\cos \\ \beta_1 & r]\cosh\beta_1 & +s]\sin\beta_2 & \beta \end{vmatrix} = 0$$

[11.E.1]

It is possible to reduce this 4 x 4 determinant into a 3 x 3 one by setting the first term of the third column to zero by subtracting the first column from the third column in [11.E.1] term-by-term.

The eigenvalue equation obtained by solving [11.D.1] is:

$$\Delta = s\,r\,[\beta_1[(\beta_1/L) - r] + \beta_2[(\beta_2/L) + s] - [\beta_1 r^2[(\beta_2/L) + s] + \beta_2 s^2[(\beta_1/L) - r]$$

$$\cosh\beta_1 \cos\beta_2 + \sin\beta_2 \sinh\beta_1\,[\beta_1\,(\beta_2/L + s) - \beta_2(\beta_1/L - r)]\ sr = 0 \qquad [11.E.2]$$

Timoshenko's eigenvalue equation in [11.E.2], which is valid for a clamped-free rod is naturally more difficult to manipulate than the Bernoulli's one.

@Seismicisolation

It does however include Bernoulli's eigenvalue equation as a peculiar case by setting the following in the above equation:

$$s = -r, \text{ and } \beta_1 = \beta_2$$

$$\Delta = -s^2 [\, \beta\, (\beta/L - r) + \beta(\beta/L - r) + [\beta r^2(\beta/L - r) + \beta r^2(\beta/L - r)] \cos\beta \cosh\beta$$

$$+ \sin\beta \sinh\beta\, [\beta\ (\beta/L - r) - \beta\, (\beta/L - r)](-s^2) = 0 \qquad [11.E.3]$$

$$\Delta = -2 - 2 \cosh \beta .\ \cos\beta = 0$$

or

$$1 + \cosh\beta \cos\beta = 0 \qquad [11.E.4]$$

Appendix 11.F. Transmissibility function of clamped-free Timoshenko's rod

With the same set of boundary conditions as in Appendix 11.E and Chapter 6, section 6.3, the first step is to evaluate the set of coefficients in the characteristic function that expresses displacement w (z, t) against forced displacement imposed at the clamped end, z = 0.

We can derive the closed-form expression using lengthy calculations.

Below, we present the set of coefficients A_1,B_1,C_1 and D_1 *versus* the two eigenvalues β_1 and β_2 without details.

$$W(z, \beta_1, \beta_2) = A_1 \cosh(\beta_1 z/L) + B_1 \sinh(\beta_1 z/L) +$$

$$C_1 \cos(\beta_2 z/L) + D_1 \sin(\beta_2 z/L) \qquad [11.F.1]$$

11.F.1. ***Expression of A_1***

$$A_1 = W(0)\{-\beta_2 s^2[(\beta_1/L) - r] \cosh\beta_1 \cos\beta_2 + \beta_1 rs\, [(\beta_2/L) + s]$$

$$\sinh\beta_1 \sin\beta_2 + \beta_2 rs\, \beta_2 rs\, [(\beta_2/L) + s]\} \qquad [11.F.2]$$

@Seismicisolation

11.F.2. ***Expression of B_1***

$$B_1 = W(0)s\ \{\beta_2 s[(\beta_1/L)-r]\cos\beta_2 \sinh\beta_1 - \beta_1 r\,[(\beta_2/L)+s]\cosh\beta_1 \sin\beta_2\} \qquad [11.F.3]$$

11.F.3. ***Expression of C_1***

$$C_1 = W(0)\ \{-\beta_1 sr\,[(\beta_1/L)-r]\sinh^2\beta_1 - \beta_1 r^2\,[(\beta_2/L)+s]\cosh\beta_1 \cos\beta_2 - \beta_2 rs\,[(\beta_1/L)-r]\sin\beta_2 \sinh\beta_1 + \beta_1 rs[(\beta_1/L)-r]\cosh^2\beta_1\} \qquad [11.F.4]$$

11.F.4. ***Expression of D_1***

$$D_1 = W(0)\ \{-\beta_1 r^2[(\beta_2/L)+s]\cosh\beta_1 \sin\beta_2 + \beta_2[(\beta_1/L)-r]\,sr \sinh\beta_1 \cos\beta_2\} \qquad [11.F.5]$$

11.F.5. ***Expression of transmissibility function $T(\beta_1, \beta_2)$***

Collecting A_1, B_1, C_1 and D_1 in equations [11.F.2] to [11.F.5] to express w (L) *versus* w (0) in [11.F.1], we find the transmissibility function is:

$$T(\beta_1, \beta_2, \omega) = \frac{w(L)}{w(0)} \qquad [11.F.6]$$

Collecting A_1, B_1, C_1 and D_1 in equations [11.F.1] to [11.F.4], we obtain the numerator in [11.F.6]:

$$\{\text{Real}\,[T_{exp}^*(\omega)]\ ,\ \text{Im}\,[T_{exp}^*(\omega)]\} \qquad [11.F.7]$$

$$\{\,|\,T_{exp}^*\,|\ ,\ \Phi = \arctan\,[\,\text{Im}\,(T_{exp}^*)/\text{Re}\,(T_{exp}^*)]\} \qquad [11.F.8]$$

11.F.6. ***Complex transmissibility function for viscoelastic materials $T^*(\beta_1^*, \beta_2^*)$***

Experimentally speaking, the transfer function T^*_{exp} is a complex function evaluated against the frequency either in Cartesian coordinates or in polar coordinates:

@Seismicisolation

$$\{\text{Real}\,[T_{exp}^{*}(\omega)]\,,\ \text{Im}\,[T_{exp}^{*}(\omega)]\} \qquad [11.F.9]$$

$$\{\,|\,T_{exp}^{*}\,|\,,\ \Phi = \arctan\,[\text{Im}\,(T_{exp}^{*})/\text{Re}\,(T_{exp}^{*})]\} \qquad [11.F.10]$$

We have two measurements for T^* at our disposal, circular frequency ω being known. To solve the inverse problem for evaluating complex modulus E^* in equations [11.F.6] to [11.F.8], two complex quantities are to be evaluated, i.e. β_1^* and β^*_2 (see equation [11.E.2]). The relationships between those quantities can be seen in Chapter 6 equations [6.52] and [6.53]. A trial and error computer-based method is presented. The solution to the problem is consequently tractable, although with lengthy manipulation of closed-form expressions when using Newton-Raphson's method (see Appendix 11.B).

@Seismicisolation

Chapter 12

Continuous Element Method Utilized as a Solution to Inverse Problems in Elasticity and Viscoelasticity[1]

12.1. Introduction

Finite element method is largely utilized in structural dynamics as the solution to a direct problem. When the geometrical characteristics of a structure and elastic moduli of materials are known, the dynamic response of the structure can be evaluated for a given set of input signals.

However, for acoustic applications in a higher frequency range this method requires meshing with ever smaller elements, as the frequency increases. The mesh size is chosen so that its largest dimension does not exceed the wavelength because the calculation of eigenvalues becomes cumbersome and time consuming.

Many attempts have been made to obtain the values of elastic or viscoelastic moduli of materials used in a structure. However, the results obtained are far from convincing.

Over the last 50 years, continuous elements have largely exploited the theoretical results obtained in elastodynamics. Progress has been particularly noticeable in the

---

Chapter written by Jean-Baptiste CASIMIR.

1 The first part of this chapter is a large extract from Jean-Baptiste Casimir's doctoral thesis [CAS 97]. The abridged English version has been written by Jean Tuong Vinh.

Mechanics of Viscoelastic Materials and Wave Dispersion Edited by Yvon Chevalier and Jean Tuong Vinh
© 2010 ISTE Ltd. Published 2010 by ISTE Ltd.

@Seismicisolation

domain of wave dispersion in bounded media. In the framework of this method, users have a broad choice of theories for rod or plate with a suitable degree of approximation for the equations of motion, whether or not they take various mechanical effects (inertia, shear, warping, etc.) into account. Choosing an appropriate theory of bounded medium vibration it is possible to evaluate, in the direct problem, the responses of the structure, even in higher frequency range covering the ultrasonic domain.

For this purpose, eigenfunctions are expressed as a combination of exponential functions (or trigonometric and hyperbolic functions) that are capable of describing an infinity of vibration modes. The so-called characteristic functions using a combination of the aforementioned functions are largely exploited in continuous element method ([CAS 03, KUL 89, LEU 83, LUN 93] among others).

In this chapter, attention is focused on inverse problems in elasticity and viscoelasticity. In Chapter 11, characteristic functions are exploited to evaluate the transmissibility function of a rod submitted to a vibration of any kind (extensional, bending or torsional vibration). When a refined theory is referred to, however, direct calculation of transfer functions using characteristic functions becomes more and more intractable and the degree of differential equations of motion equals or exceeds four. This complexity increased when we try to solve the viscoelastic problem. The wave numbers β_i (which determine nodal lines on the rod) become complex quantities:

$$\beta_i^* = \mathrm{Re}\,\beta_i^* + \mathrm{j}\,\mathrm{Im}\,\beta_i^*$$

and the number of unknowns are doubled.

Interest in the continuous element method resides in the use of matrix formulation. The state vector includes generalized displacement components and/or generalized force components whose number depends on the vibration theory adopted.

Various versions of matrix representations for continuous elements (transfer of generalized forces, dynamic stiffness) cover most requirements in structural dynamics.

The set of boundary conditions imposed on the bounded medium find expressions in so-called transfer matrix [T], which relates two state vectors at both ends of the rod. It consists of dividing [T] into four submatrices and, for a given set

@Seismicisolation

of boundary conditions at both ends, sets all of the components of an appropriate submatrix to zero.

When manipulating matrices, it is not necessary to know the transmissibility function in a closed-form expression. Components of the transfer matrix [T] require explicit expressions that are not difficult to evaluate.

The main use of continuous element method is in solving dynamic problems using a numerical method. The transmissibility function can be calculated against frequency with all of the eigenvalues in the chosen frequency range.

The solutions of an inverse problem are in the calculations of complex wave numbers β_i^*, from which complex viscoelastic modulus is evaluated for each frequency via the equation of rod motion.

12.2. Overview of the continuous element method

Before presenting the solution to a viscoelastic inverse problem, an overview of the continuous element method is necessary. Details of the method can be found in the bibliography of this chapter [CAS 97, CAS 03, DUF 85, LUN 83].

12.2.1. *Equilibrium equations and the force-displacement relationship*

Let $L_{s,t}(u,f)$ be a differential operator applied to displacement vector u and the internal force vector f along the beam, see Figure 12.1.

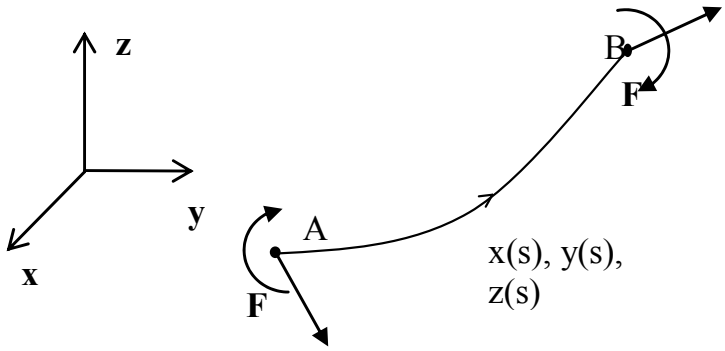

Figure 12.1. *Beam element*

@Seismicisolation

We now need to consider that:

– s is the curvilinear abscissa variable;

– t the time variable; and

– q (s, t) is the distributed load along the beam.

$$\begin{aligned} & s \in [O \quad L], t > 0 \\ & L_{s,t}(\mathrm{u},\mathrm{f}) = \mathrm{q}(s,t) \end{aligned} \qquad [12.1]$$

Equation [12.1] represents the formulation of the elementary problem in which operator $L_{s,t}$ is classified into two categories: equilibrium equations and a force-displacement relationship. Initial conditions need to be added to [12.1].

As an example, let us adopt Timoshenko's straight beam. In this instance, operator $L_{s,t}$(u,f) is of first order relative to abscissa s and second order relative to t. Operator $L_{s,t}$(u,f) is given by:

$$\begin{cases} \dfrac{\partial U_Y}{\partial s} - \dfrac{k_Y}{GS} F_Y - \Omega_Z = 0 \\[2ex] \dfrac{\partial \Omega_Z}{\partial s} - \dfrac{M_Y}{EI_Z} = 0 \\[2ex] \rho S \dfrac{\partial^2 U_Y}{\partial t^2} - \dfrac{\partial F_Y}{\partial s} = p_Y(s,t) \\[2ex] \rho I_0 \dfrac{\partial^2 \Omega_Z}{\partial t^2} - \dfrac{\partial M_Z}{\partial s} - F_Y = m_Z(s,t) \end{cases} \qquad [12.2]$$

where U_Y and Ω_Z are the vertical translation and rotation of the section respectively. S, k_Y, k_Z and I_0 are the cross-sectional area, Timoshenko's shear deflection constant, the area and polar moments of inertia respectively. E, G and ρ are Young's modulus, shear modulus and mass density respectively, in the case of an isotropic material. F_Y and M_Z are the internal shearing force and bending

@Seismicisolation

moment. p_Y and m_Z are the distributed vertical force and bending moment applied to the beam.

In a harmonic regime, the resolution of equation [12.2] is possible by removing time variable t. This leads to a differential system where circular frequency appears as a parameter.

$$\begin{cases} s \in [0 \quad L] \\ L_{s,\omega}(\mathrm{u},\mathrm{f}) = \mathrm{q}_\omega(s) \\ \mathrm{f}_\omega(0) = -\mathrm{F_A} \\ \mathrm{f}_\omega(L) = \mathrm{F_B} \end{cases} \qquad [12.3]$$

In this last expression, internal force f at a given point M(s) along the beam has been defined as the force acting on segment AM.

Vector E(s) = [u(s), f(s)] is known as a state vector. Its components are the primary unknown of the problem and depend on circular frequency ω.

12.2.2. *Explicit continuous element*

In the case of a general Timoshenko's/Saint-Venant's beam, the state vector has 12 components. From equation [12.3], it is possible to extract the differential equation satisfied by each component. In a more general case, these are 12-order equations. Where there is an absence of coupling, the order of equations of motion is reduced and explicit displacement solutions are tractable, as we have seen in preceding chapters. Displacement vector u is expressed with characteristic functions.

Displacement at both ends (s = 0, s = L) is obtained from the general solution and is given by:

$$\mathrm{U} = \begin{pmatrix} \mathrm{u}(0,\omega) \\ \mathrm{u}(L,\omega) \end{pmatrix} = \begin{pmatrix} \mathrm{U_A} \\ \mathrm{U_B} \end{pmatrix} = \begin{pmatrix} \mathrm{g}(0,\omega) \\ \mathrm{g}(L,\omega) \end{pmatrix} c + \begin{pmatrix} \mathrm{g}_0(0,\omega) \\ \mathrm{g}_0(L,\omega) \end{pmatrix} \qquad [12.4]$$

By inversion of [12.4] integration constants can be obtained:

@Seismicisolation

$$c = \begin{pmatrix} g(0,\omega) \\ g(L,\omega) \end{pmatrix}^{-1} \begin{pmatrix} U_A - g_0(0,\omega) \\ U_B - g_0(L,\omega) \end{pmatrix} \qquad [12.5]$$

The displacement field along the beam is evaluated from nodal displacement vector U. This leads to the following solution:

$$u(s,\omega) = [g(s,\omega)] \begin{pmatrix} g_0(0,\omega) \\ g(L,\omega) \end{pmatrix}^{-1} \begin{pmatrix} U_A - g_0(0,\omega) \\ U_B - g_0(L,\omega) \end{pmatrix} + g_0(s,\omega) \qquad [12.6]$$

Internal force unknowns f are deduced from the force displacement relationship [12.3], which can be written as:

$$f = [A][D]u \qquad [12.7]$$

where [D] is the differential operator and [A] a constitutive matrix built from the elastic characteristics of the material. If the linearity of operator [D] and the six components of vector $h_0(0, \omega)$ are connected with the unknown forces:

$$[h(s, \omega)] = [D]\,[g(s, \omega)] \qquad [12.8]$$

$$h_0(s, \omega) = [D]\, g_0(s, \omega)$$

then the nodal force vector is:

$$\begin{pmatrix} F_A \\ F_B \end{pmatrix} = \begin{pmatrix} -[A][h(0,\omega)] \\ [A][h(L,\omega)] \end{pmatrix} c + \begin{pmatrix} -[A]h_0(0,\omega) \\ [A]h_0(L,\omega) \end{pmatrix} \qquad [12.9]$$

Internal force fields along the beam are evaluated from the nodal displacement vector U. This leads to the following solution:

$$f(s,\omega) = [A][h(s,\omega)] \begin{pmatrix} g(0,\omega) \\ g(L,\omega) \end{pmatrix}^{-1} \begin{pmatrix} U_A - g_0(0,\omega) \\ U_B - g_0(L,\omega) \end{pmatrix} + [A]h_0(s,\omega) \qquad [12.10]$$

@Seismicisolation

12.2.3. *State vector and dynamic transfer matrix*

A differential problem can be reduced to a first-order problem using a vector variable that is composed of as many components as necessary in order to reduce the order to one. This can be achieved by using intermediate variables. In Timoshenko's beam it has been shown that the vector composed of both displacement and force components satisfies a one-order differential system. The state vector E is used:

$$E_\omega(s) = (u, f)^t \qquad [12.11]$$

Vector $E_\omega(s)$ depends on the curvilinear coordinate s and on circular frequency ω, which is subscript. U and f are the displacement and generalized force vectors respectively. The formulation of the elementary problem in a harmonic regime, according to equation [12.3], is rewritten as follows, using the state vector:

$$\frac{dE_\omega(s)}{ds} = \left[D_\omega(s)\right]E_\omega(s) \qquad [12.12]$$

where $[D_\omega(s)]$ is the differential dynamic matrix.

Figure 12.2 shows utilization of equation [12.12] to relate the state vector at the origin of a beam segment.

$$E_\omega(s) = [T(s)]\, E_\omega(0) \qquad [12.13]$$

The transfer matrix [T(s)] is defined relating the state vector at the abscissa s to the input state vector at the origin $s=0$.

According to equations [12.12] and [12.13], the first-order differential equation relates to the dynamic transfer matrix and its first derivative to:

$$[D_\omega(s)].\frac{d[T_\omega]}{ds} = [D_\omega(s)].[T_\omega(s)] \qquad [12.14]$$

with $[T_\omega(0)] = [I]$ being the identity matrix.

@Seismicisolation

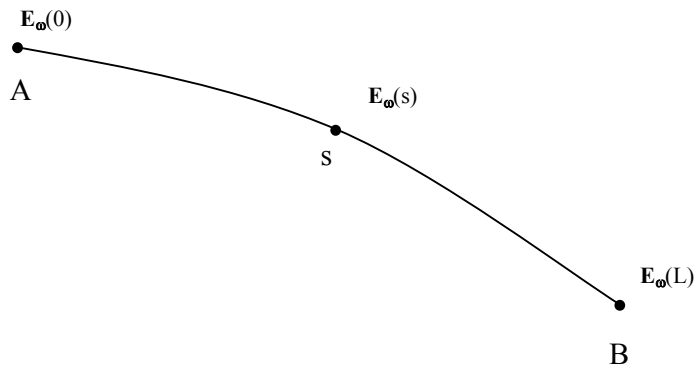

Figure 12.2. *State vector along the beam*

If the differential matrix is supposed to be independent of the abscissa s, we get the following first-order differential equation:

$$\frac{d[\mathrm{T}_\omega]}{ds} = [\mathrm{D}_\omega].[\mathrm{T}_\omega(s)] \qquad [12.15]$$

The beams satisfying this assumption are those whose section, material and curvature/tortuousness and radii are constant along the middle line. The most general example is a helical beam with constant section.

12.2.4. *Transfer matrix and dynamic stiffness presented in suitable form for matrix calculation*

Matrix exponentials are introduced here as the solution to equation [12.15] for a transfer matrix.

$$\mathrm{T}_\omega(s) = e^{[\mathrm{D}_\omega]s} \qquad [12.16]$$

The exponential matrix is given by:

$$e^{[\mathrm{X}]} = \sum_{i=0}^{+\infty} \frac{[\mathrm{X}]^i}{i!} \qquad [12.17]$$

@Seismicisolation

In the case where [D] is diagonalizable, the following decomposition is adopted:

$$[D_\omega]s = [Q][\Lambda][Q]^{-1}s \qquad [12.18]$$

in a [Q] matrix whose columns are eigenvectors of $[D_\omega]$ and $[\Lambda]$ is the eigenvalue diagonal matrix of $[D_\omega]$.

Equations [12.16] and [12.17] then enable us to obtain the following expression:

$$[T_\omega(s)] = [Q]e^{[\Lambda]s}[Q]^{-1} \qquad [12.19]$$

with

$$e^{[\Lambda]} = \begin{pmatrix} e^{\lambda_1} & & & 0 \\ & e^{\lambda_2} & & \\ & & \ddots & \\ 0 & & & e^{\lambda_n} \end{pmatrix} \qquad [12.20]$$

If $[D_\omega]$ cannot be diagonalized it is possible to come to a solution by a method using canonical Jordan form.

It is not possible to further simplify expression [12.19], $[D_\omega]$ being neither a Hermitian matrix or a symmetrical one.

Eigenvectors are consequently not orthogonal two-by-two. The inversion of $[Q_\omega]$ matrix is, however, possible using a special matrix algorithm.

12.2.5. *Eigenvalues and eigenvectors of dynamic stiffness*

The first step in this calculation is to search for eigenvalues. A QR algorithm is retained that enables us to obtain a complex set of eigenvalues or a real or complex matrix.

@Seismicisolation

The sensitivity of eigenvalues to rounding-off errors can be reduced if a balancing non-symmetric matrix is created beforehand. The eigenvectors of $[D_\omega]$ can be evaluated by using the method of matrix deflation of subspace.

12.3. Boundary conditions and their implications in the transfer matrix

Relationships connecting generalized internal forces to generalized external forces can be represented in vector form, F_A^i,= - F_A, $F_B^i = F_B$, where A and B are the rod ends and superscript I designates the internal force.

The dynamic stiffness matrix $[K_\omega]$ is obtained via the dynamic transfer matrix as follows:

$$\begin{pmatrix} F_A \\ F_B \end{pmatrix} = \begin{pmatrix} -f_A \\ f_B \end{pmatrix} = [K(\omega)] \begin{pmatrix} U_A \\ U_B \end{pmatrix} \qquad [12.21]$$

$$[K(\omega)] = \begin{pmatrix} [T_{12}(\omega)]^{-1}[T_{11}(\omega)] & -[T_{12}(\omega)]^{-1} \\ [T_{21}(\omega)] - [T_{22}(\omega)][T_{12}(\omega)]^{-1}[T_{11}(\omega)] & [T_{22}(\omega)][T_{12}(\omega)]^{-1} \end{pmatrix}$$

[12.22]

We have to deal with a linear system, in the framework of which Maxwell reciprocity theorem is valid for components of $[K_\omega]$, e.g. $k_{ij}(\omega)$. Here equation [12.22] is rewritten as:

$$[K(\omega)] = \begin{pmatrix} [T_{12}(\omega)]^{-1}[T_{11}(\omega)] & -[T_{12}(\omega)]^{-1} \\ -[T_{12}(\omega)]^{-T} & [T_{22}(\omega)][T_{12}(\omega)]^{-1} \end{pmatrix} \qquad [12.23]$$

It is worth considering submatrices $[T_{11}(\omega)]$, $[T_{12}(\omega)]$, $[T_{21}(\omega)]$ and $[T_{22}(\omega)]$, which are symmetric. This symmetry simplifies calculations.

Transfer matrix $[T(\omega)]$ can be decomposed into four submatrices:

$$[T(\omega)] = \begin{pmatrix} [T_{11}(\omega)] & [T_{12}(\omega)] \\ [T_{12}(\omega)] & [T_{22}(\omega)] \end{pmatrix} \qquad [12.24]$$

@Seismicisolation

Equation [12.13] then becomes:

$$\begin{pmatrix} U_B \\ F_B \end{pmatrix} = \begin{pmatrix} [T_{11}(\omega)] & [T_{12}(\omega)] \\ [T_{12}(\omega)] & [T_{22}(\omega)] \end{pmatrix} \begin{pmatrix} U_A \\ F_A \end{pmatrix} \qquad [12.25]$$

The four submatrices in equation [12.25] enable us to evaluate the eigenfrequencies of the beam for various sets of boundary conditions. If we set the matrix eigenfrequencies for the following submatrix determinant set to zero, it is easy to see that they correspond to the following cases:

Free-free rod: $|T_{21}(\omega)| = 0$ [12.26]

Clamped-free rod: $|T_{22}(\omega)| = 0$ [12.27]

Clamped-clamped rod: $|T_{12}(\omega)| = 0$ [12.28]

The boundary condition (free-clamped) admits the same eigenfrequencies as for the (clamped-free) condition. It is described by the following equivalence:

$$|T_{22}(\omega)| = 0 \Leftrightarrow |T_{11}(\omega)| = 0 \qquad [12.29]$$

The continuous element permits us to continue the calculation beyond the transfer matrix to evaluate the dynamic stiffness matrix $[K(\omega)]$, which is defined as follows [CAS 97]:

$$\begin{pmatrix} F_A \\ F_B \end{pmatrix} = [K(\omega)] \begin{pmatrix} U_A \\ U_B \end{pmatrix} \qquad [12.30]$$

Equation [12.26] is useful for structural dynamics.

12.4. Extensional vibration of straight beams (elementary theory)

In what follows, non-dimensional differential systems are presented for the consideration of numerical stability. This system is obtained by changing the variable of components of the state vector and curvilinear abscissa *s*.

@Seismicisolation

$$\overline{U} = \frac{U_x}{L} \text{ and } \overline{F} = \frac{F_x}{ES} \quad \bar{s} = \frac{s}{L} \qquad [12.31]$$

The differential system then becomes:

$$\begin{cases} \dfrac{d\overline{U}}{d\bar{s}} = \overline{F} \\ \\ \dfrac{d\overline{F}}{d\bar{s}} = -\dfrac{\rho L^2 \omega^2}{E}\overline{U} \end{cases} \qquad [12.32]$$

The differential dynamic matrix is as follows:

$$[D_\omega] = \begin{pmatrix} 0 & 1 \\ -n_\omega^2 L^2 & 0 \end{pmatrix} \qquad [12.33]$$

$$n_\omega = \omega\sqrt{\frac{L}{E}} \qquad [12.34]$$

and the eigenvalues of $[D_\omega]$ are:

$$\lambda_1(\omega) = j\, n_\omega L, \qquad \lambda_1(\omega) = -jn_\omega L \qquad [12.35]$$

Thanks to these eigenvalues, it is possible to predict the upper bound of the frequency interval covered by the algorithm. It also enables us to ensure the diagonalization of matrix $[D_\omega]$.

Matrices $[Q_\omega(\omega)]$ and $[Q_\omega(\omega)]^{-1}$ for chosen eigenvalues are:

$$[Q(\omega)] = \begin{pmatrix} 1 & 1 \\ jn_\omega L & -jn_\omega L \end{pmatrix}; \quad [Q(\omega)]^{-1} = \frac{1}{2}\begin{pmatrix} 1 & \dfrac{1}{jn_\omega L} \\ 1 & -\dfrac{1}{jn_\omega L} \end{pmatrix} \qquad [12.36]$$

@Seismicisolation

From equations [12.19] and [12.20], the dynamic transfer matrix can be written:

$$[\mathrm{T}(\omega)] = \begin{pmatrix} \cos n_\omega L & \dfrac{\sin n_\omega L}{n_\omega L} \\ -n_\omega L \sin n_\omega L & \cos n_\omega L \end{pmatrix} \qquad [12.37]$$

Using equation [12.23], the non-dimensional dynamic stiffness is deduced:

$$[\mathrm{K}(\omega)] = \begin{pmatrix} n_\omega L \cot n_\omega L & \dfrac{-n_\omega L}{\sin n_\omega L} \\ \dfrac{-n_\omega L}{\sin n_\omega L} & n_\omega L \cot n_\omega L \end{pmatrix} \qquad [12.38]$$

[CAS 97] presents Love's extensional rod in which inertia effect is taken into account. Figure 12.3 shows the responses of the two rods (elementary and Love's theories) in the frequency range 0 to 3.10^4 Hz in a direct problem with the constant Young's modulus of steel. It concerns a free-free rod.

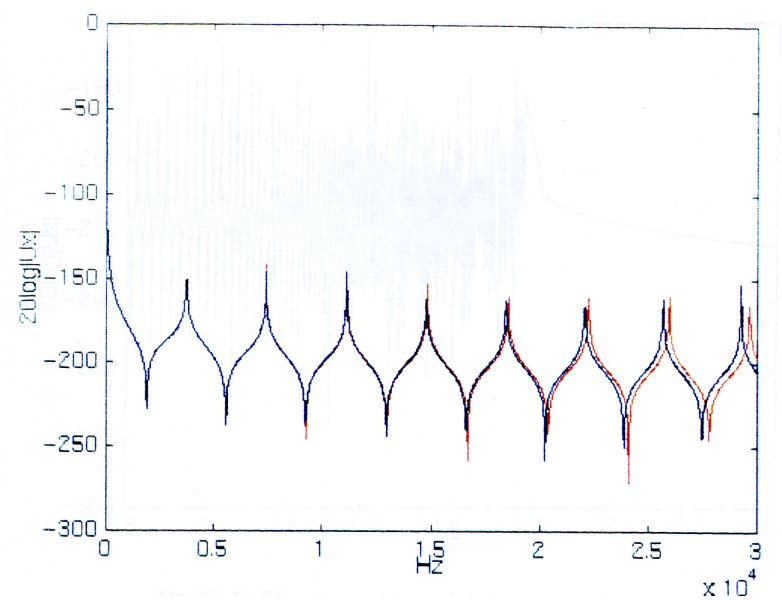

Figure 12.3. *Harmonic response for elementary and Love's theories*

@Seismicisolation

12.5. The direct problem of beams submitted to bending vibration

12.5.1. *Euler-Bernoulli's transfer matrix and dynamic stiffness matrix*

The non-dimensional differential system is obtained with the following notations:

$$\overline{V} = \frac{U_Y}{L}, \ \overline{F} = \frac{F_Y L^2}{EI}, \ \overline{\Omega} = \Omega, \ \overline{M} = \frac{LM}{EI}, =$$

$$\frac{d\overline{V}}{d\overline{s}} = \overline{\Omega_Z}$$

$$\frac{d\overline{\Omega}}{d\overline{s}} = \overline{M_Z} \qquad [12.39]$$

$$\frac{d\overline{F_Y}}{d\overline{s}} = -\frac{\rho S L^4 \omega^2}{EI}\overline{V}$$

$$\frac{d\overline{M_Z}}{d\overline{s}} = -\overline{F_Y}$$

Then the differential dynamic matrix is:

$$[\mathrm{D}_\omega] = \begin{pmatrix} 0 & 1 & 0 & 0 \\ 0 & 0 & 0 & 1 \\ -\dfrac{\rho S L^4 \omega^2}{EI_Z} & 0 & 0 & 0 \\ 0 & 0 & -1 & 0 \end{pmatrix} \qquad [12.40]$$

where [D(ω)] corresponds to the free-free beam. This matrix has four distinct non-zero eigenvalues:

$$\lambda_1 = \mathrm{j}\,\beta$$

@Seismicisolation

$\lambda_2 = -\,j\,\beta$

$\lambda_3 = \beta$

$\lambda_4 = -\beta$ [12.41]

Matrix [D (ω)] is then diagonalizable in the whole interval [0, ω_{max}], with:

$$\omega_{max} = \frac{l_{max}^{\ 2}}{L^4}\sqrt{\frac{EI_Z}{\rho S}} \qquad [12.42]$$

where l_{max} designates a maximum value compatible with numerical stability calculations with a 32-bit computer working with double precision.

The transmissibility [T_ω] is:

$$[T_\omega] = \frac{1}{2}\begin{pmatrix} C+c & \beta^{-1}(S+s) & \beta^{-3}(-S+s) & \beta^{-2}(C-c) \\ \beta(S-s) & C+c & \beta^{-2}(-C+c) & \beta^{-1}(S+s) \\ \beta^{-3}(-S-s) & \beta^{2}(-C+c) & C+c & \beta(-S+s) \\ \beta^{2}(C-c) & \beta(S-s) & \beta^{-1}(-S-s) & C+c \end{pmatrix} \qquad [12.43]$$

with C = cosh β, S = sinh β, c = cos β, and s = sin β.

For the free-free rod $|T_{21}(\omega)| = 0$, it gives rise to the classical relationship:

$1 - \cosh\beta\cos\beta = 0$ [12.44]

The dynamic stiffness is:

$$[K_\omega] = \frac{\beta}{1-cC}\begin{pmatrix} \beta^2(Cs+Sc) & \beta Ss & -\beta^2(S+s) & \beta(C-c) \\ \beta Ss & Cs-Sc & \beta(c-C) & S-s \\ -\beta^2(S+s) & \beta(c-C) & \beta^2(Cs+Sc) & -\beta Ss \\ \beta(C-c) & S-s & -\beta Ss & Cs-Sc \end{pmatrix} \qquad [12.45]$$

@Seismicisolation

12.5.2. *Numerical simulation for a free-free Bernoulli's rod*

Consider a straight beam with inertia $I = I_Z = 6.25.10^{-7}$ m^4, square cross-section area of $S = 3.10^{-3}$ m^2, length L = 0.7 m, Young's modulus $E = 210{,}000.10^6$ N/m^2 and mass density $\rho = 7{,}800$ kg/m^3. Taking into account the upper bound frequency in equation [12.42], the frequency range is $f \in]0, 3.10^7\, Hz]$.

Figure 12.4 shows the response of Bernoulli-Euler's rod. Calculations by continuous element (one element) and analytical calculation give rise to the same curve for at least 10 first bending modes. Beyond $f > 3.10^4$ Hz there is instability in the numerical computation with oscillations[2].

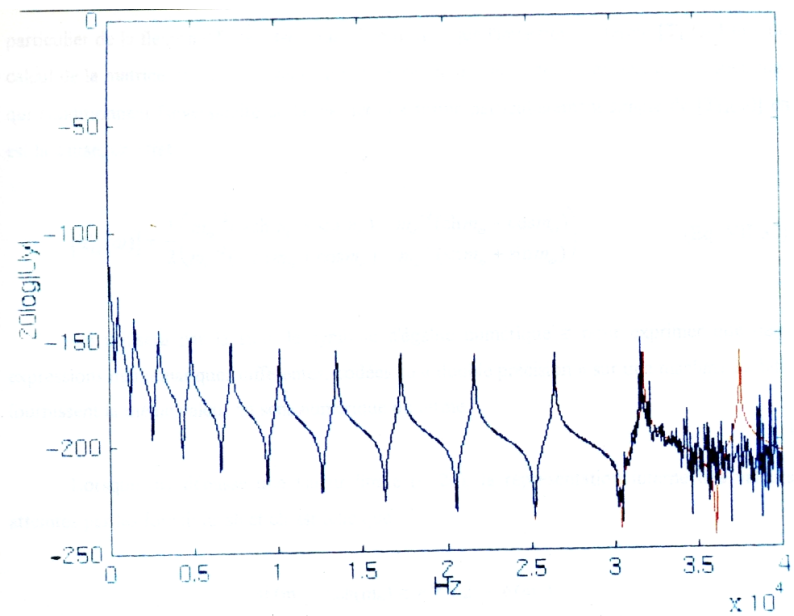

Figure 12.4. *The harmonic response for Euler-Bernoulli's bending theory*

12.5.3. *Bending vibration of a free-free Timoshenko's beam*

The differential system for an isotropic beam is:

2 This instability is attributed to the rounding-off error generated by quantities higher than 10^{11} in the transfer matrix. To overcome this difficulty, see [CAS 97].

@Seismicisolation

$$\frac{d\overline{U_Y}}{d\bar{s}} = \frac{d\overline{V}}{d\bar{s}} = \overline{\Omega_Z} + \frac{EI_Z\,\overline{F_Y}}{kL^2GS}$$

$$\frac{d\overline{\Omega}}{d\bar{s}} = \overline{M_Z}$$

$$\frac{d\overline{F_Y}}{d\bar{s}} = -\frac{\rho SL^4\omega^2}{EI}\overline{V} \qquad [12.46]$$

$$\frac{d\overline{M_Z}}{d\bar{s}} = -\overline{F_Y} - \frac{\rho L^2\omega^2}{E}\overline{V}$$

The differential dynamic matrix in this case is:

$$[\mathrm{D}_\omega] = \begin{pmatrix} 0 & 1 & \frac{EI_Z}{kGSL^2} & 0 \\ 0 & 0 & 0 & 1 \\ -\frac{\rho SL^4\omega^2}{EI_Z} & 0 & 0 & 0 \\ 0 & -\frac{\rho L^2\omega^2}{E} & -1 & 0 \end{pmatrix} \qquad [12.47]$$

Timoshenko's equation of motion [11.41] and [11.42] shows that there are four distinct wavenumbers, two of which are purely imaginary and of the opposite sign:

$$\mathrm{j}\,\beta_2, \quad -\mathrm{j}\,\beta_2$$

and two wavenumbers that can be either real or imaginary depending on the sign of the following quantity:

$$\delta_\omega = \frac{\rho I_Z}{kGS}\omega^2 - 1 \qquad [12.48]$$

@Seismicisolation

If $\delta_\omega > 0$, we obtain two imaginary wavenumbers:

$$j\,\beta_1,\ -j\,\beta_1$$

If $\delta_\omega < 0$, the real wavenumbers are obtained:

$$\beta_1,\ -\beta_1$$

$$\beta_1 = L\omega\sqrt{-\left(\frac{\rho}{2Gk}+\frac{\rho}{2E}\right)+\frac{\rho}{2E}\sqrt{\left(1-\frac{E}{kG}\right)^2+\frac{4SE}{\rho I_Z\omega^2}}} \qquad [12.49]$$

$$\beta_2 = L\omega\sqrt{-\left(\frac{\rho}{2Gk}+\frac{\rho}{2E}\right)-\frac{\rho}{2E}\sqrt{\left(1-\frac{E}{kG}\right)^2+\frac{4SE}{\rho I_Z\omega^2}}}$$

β_1 and β_2 are deduced from Timoshenko's equation of motion [11.41]. Details on the calculation can be found in Appendix 11.A.

12.5.4. *Dynamic transfer matrix for Timoshenko's beam*

For convenience, the following notations are used:

$$a_\omega = \frac{\rho S L^4 \omega^2}{E I_Z} = T$$

$$b_\omega = \frac{\rho L^2 \omega^2}{E} \qquad [12.50]$$

$$d_k = \frac{E I_Z}{k G S L^2}$$

@Seismicisolation

$$\cosh\beta_1 = C \quad \sinh\beta_1 = S$$
$$\cos\beta_2 = c \quad \sin\beta_2 = s \qquad [12.51]$$

From equation [12.48], ω_c is defined as the critical circular frequency for $\delta_\omega = 0$:

$$\omega_c = \sqrt{\frac{GkS}{\rho I_Z}} \qquad [12.52]$$

In Figure 12.5, the dynamic transfer matrix is presented in the cases where $\omega < \omega_c$ and $\omega > \omega_c$. In the dynamic transfer matrix where $\omega > \omega_c$, only trigonometric functions are present.

12.5.4.1. *Free-free beam*

The eigenvalue equation is obtained from equation [12.26].

For $\omega < \omega_c$, $(\beta_1^2 - d_k a_\omega)(\beta_1^2 - d_k a_\omega) = a_\omega$:

$$2a_\omega\left(1-\cosh\beta_1\cos\beta_2\right)-\left[\frac{\beta_2}{\beta_1}\left(\beta_2^2+d_k a_\omega\right)^2-\frac{\beta_1}{\beta_2}\left(\beta_1^2+d_k a_\omega\right)^2\right]\sinh\beta_1\sin\beta_2 = 0 \qquad [12.53]$$

Curves in Figure 12.5 are obtained in the frequency range]0, 2.10^4 Hz].

Figure 12.6 includes the dynamic response in the neighborhood of critical circular frequency ω_c. The response can be extended to the frequency 3.10^9 Hz.

12.5.4.2. *Clamped-free beam*

The transfer matrix presented in Figure 12.2 is also valid for this case. The eigenvalue equation is obtained from [12.27] by adopting $|T_{22}(\omega)| = 0$.

$$\left[\left(\beta_2^2-a_\omega d_k\right)\left(\beta_1^2-a_\omega d_k\right)-\left(\beta_1^2+a_\omega d_k\right)\left(\beta_2^2-a_\omega d_k\right)\right]$$

@Seismicisolation

$$-\cosh\beta_1\cos\beta_2\left[\left(\beta_2{}^2-a_\omega d_k\right)^2+\left(\beta_2{}^2+a_\omega d_k\right)\left(\beta_1{}^2-a_\omega d_k\right)\right]$$

$$+\sinh\beta_1\sin\beta_2\begin{bmatrix}\left(\dfrac{\beta_1}{\beta_2}a_\omega d_k-\beta_2\beta_1\right)\left(\beta_1{}^2+a_\omega d_k\right)\\ -\left(\dfrac{\beta_2}{\beta_1}a_\omega d_k+\beta_2\beta_1\right)\left(\beta_2{}^2-a_\omega d_k\right)\end{bmatrix}=0 \qquad [12.54]$$

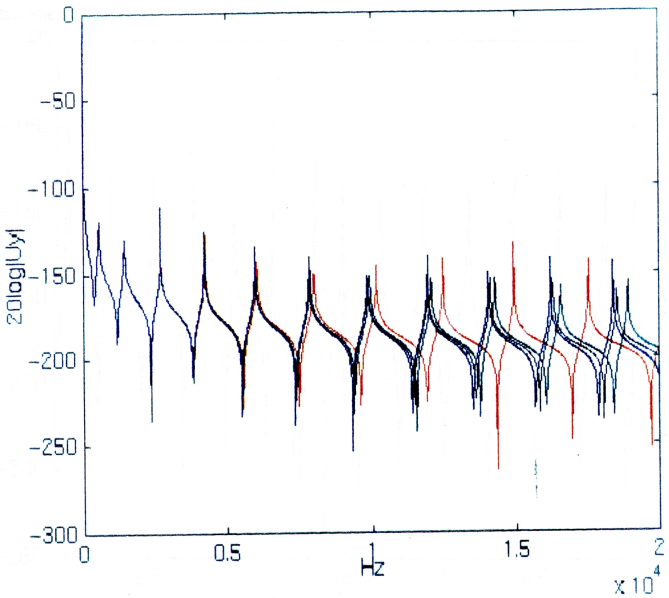

Figure 12.5. *The harmonic response for Timoshenko's bending theory for a continuous element (1) and finite element (16, 32 and 64 elements)*

It is easy to check that in this particular case, [12.54] includes the eigenvalue equation concerning Euler-Bernoulli's beam. For this purpose, we set the component describing shear effect to zero in the matrix [12.47]:

$$k=0 \Rightarrow \frac{k_Y EI_Z}{GSL^2}=0 \quad \text{or} \quad d_k=0 \qquad [12.55a]$$

@Seismicisolation

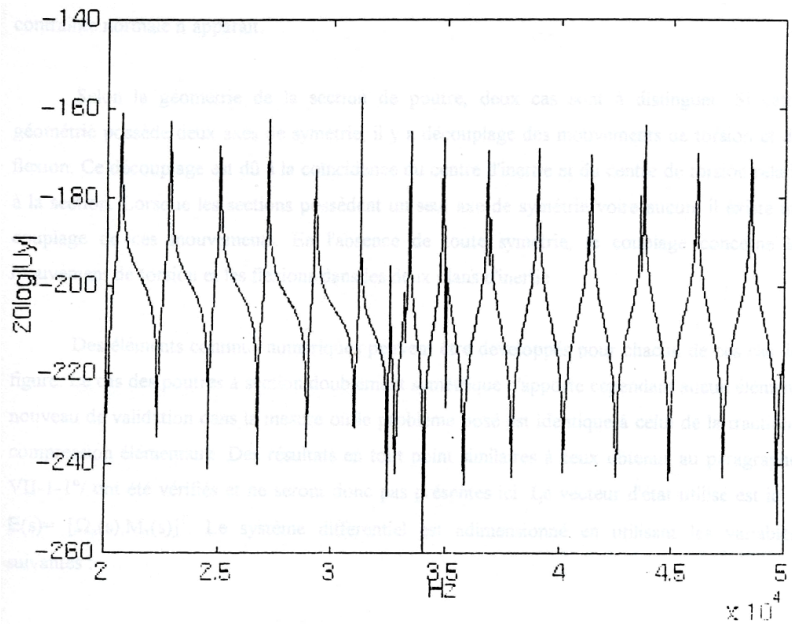

Figure 12.6. *Harmonic response in the neighborhood of critical circular frequency ω_c for Timoshenko's bending theory*

and the component:

$$\rho \frac{L^2 \omega^2}{E} = b_\omega = 0 \qquad [12.55b]$$

$$\beta_1 = \beta_2 = \beta \qquad [12.55c]$$

Bringing [12.55a] and [12.55c] into equation [12.54]:

$$-2\beta^4 - 2\beta^4 \cosh\beta \cos\beta = 0 \qquad [12.56]$$

or

$$1 + \cosh\beta \cos\beta = 0$$

@Seismicisolation

This is the eigenequation previously obtained (see Chapter 11).

12.6. Successive calculation steps to obtain a transfer matrix and simple displacement transfer function

Section 12.5 presents details on the calculation of a transfer matrix and illustrates this using examples that were analyzed in Chapter 11.

The main interest in continuous elements goes beyond simple rods. It has been shown [CAS 97, CAS 05] that this method permits calculation of the dynamic response of an assembly of rods, plates and shells in which the calculus on a vibrating rod is only an elementary element.

This book essentially focuses on the valuation of elastic and/or viscoelastic modulus. The limited space within this volume means that we are unable to present this method in greater detail. Readers wishing to study this method further should refer to [CAS 97].

12.6.1. *Eigenvalue calculations*

Successive steps in the calculation of a dynamic transfer function are presented in Figure 12.7.

The first step consists of writing a differential equation of motion that permits the adoption of the size of a state vector (number of generalized displacement components including their intermediate variables, and number of generalized force components).

The set of differential equations of motion are brought together under the form of differential matrix $[D_\omega]$.

Computer codes are then utilized to solve the matricial equation including [D] so as to obtain eigenvalues and eigenvectors in the adopted circular frequency range $]\omega_{inf}, \omega_{sup}[$. For this eigenvalue calculation, the QR Francis algorithm is adopted. It permits us to evaluate the eigenvalues of a real matrix or any complex matrix.

Its principle is based on the existence of decomposition of matrix [A] into a product [Q][R], so that [Q] is an unitary matrix and [R] a superior triangular matrix. Such decomposition is obtained using the Householder or Givens algorithm:

@Seismicisolation

Geometrical data L, b, h, ρ Elastic modulus First estimation
Type of vibration Differential equations of motion.
Differential matrix $[D_\omega]$
Eigenvalue β and eigenvector V of $[D_\omega]$
Calculation of transfer matrix [T]
Calculation of stiffness matrix [K]
Curve displacement transfer Function deduced from $[T_\omega]$. $H = \frac{w(L)}{w(0)}$

Figure 12.7. *Successive steps of calculation* $H = \frac{w(L)}{w(0)}$

$$[A_k] = [Q_k][R_k]$$
$$[A_{k+1}] = [R_k][Q_k] \qquad [12.57]$$

For each iteration a QR decomposition is created, then a matricial multiplication. Matrices $[A_k]$ are calculated so as:

@Seismicisolation

$$[A_{k+1}] = [Q_k]^{-1} [A_k] [Q_k] \qquad [12.58]$$

We have to deal with similar matrices, and their eigenvalues are those of $[A_0]$.

The number of necessary operations can be considerably reduced if the initial matrix is an Hessenberg one.

The sensitivity of eigenvalues to rounding-off errors is frequently reduced by the preliminary equilibrium of non-symmetric matrices.

12.6.2. *Eigenvector calculation of [Dω]*

The inverse iteration for this purpose is given in Figure 12.7.

The matricial equation is written as:

$$\left([D_\omega] - \lambda_i [I]\right) X_{k+1} = X_k \qquad [12.59]$$

where X_k and X_{k+1} represent two successive values obtained for the vector X by solving a successive linear system.

A Duncan Collar deflation is operated and permits us to obtain a matrix $[D_\omega]_1$, which has the same eigenvalues as $[D_\omega]$ with the exception of λ_1. This method gives the whole set of eigenvectors.

12.7. Continuous element method adapted for solving an inverse problem in elasticity and viscoelasticity

What we have presented above concerns a direct problem. In the framework of an inverse problem, the diagram for calculation is presented in Figure 12.8, with a second circuit as follows:

$$E(0) = \begin{bmatrix} U(0) \\ F(0) \end{bmatrix}$$

where $\beta_1^*, \beta_2^*, ..., \beta_n$ are complex eigenvalues that are put into the column matrix.

@Seismicisolation

The upper rectangle represents the dynamic experiment of a vibrating beam that furnishes output signal as displacement U(L) (or acceleration $-\omega^2$ U(L)) in stationary vibration. The input signal is chosen by the experimenter him- or herself – either as a displacement U(0), a force f(0) or an acceleration. By signal processing with Fourier transform we obtain a transmissibility function $H^*(\omega)$ or a stiffness function $K^*(\omega)$.

The lower rectangle corresponds to the chain of calculation. For a given circular frequency ω, a preliminary test state vector is adopted:

$$E^0(0) = \begin{bmatrix} U^0(0) \\ F^0(0) \end{bmatrix}$$

Superscript 0 designates the initial adopted value.

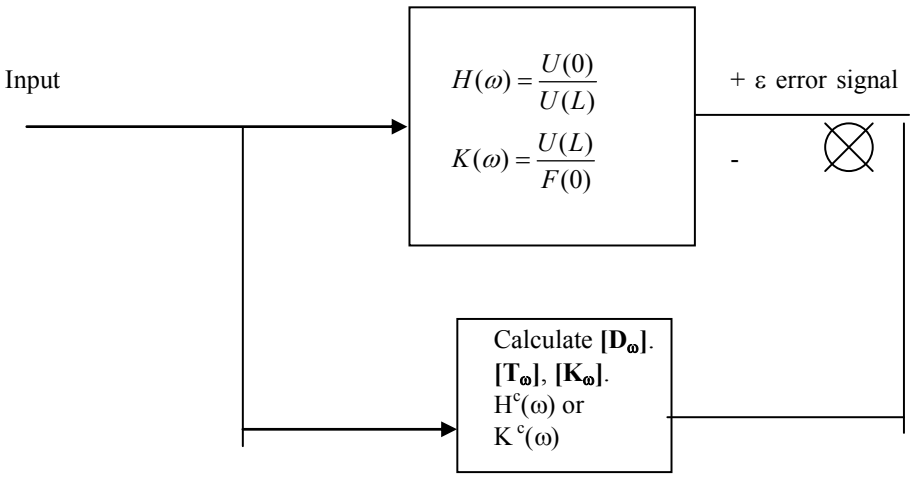

Figure 12.8. *Inverse elastic or viscoelastic problem solved by continuous element method*

An initial set of complex wavenumbers β_i^*, $i \in 1, 2, ..., n$ [3] is chosen to start the first calculations of dynamic matrix $[D_\omega]$ and transfer matrix $[T_\omega]$. Stiffness matrix

3 The number of wavenumbers depends on the degree of approximation concerning the equations of motion.

@Seismicisolation

$[K_\omega]$ (or complex stiffness function $K^*(\omega)$) is estimated and compared to the value obtained experimentally.

The error between estimated and measured values is minimized by an appropriate optimization algorithm. At the input of a computation chain, the set of complex wavenumbers are adjusted in an iteration trial and error process. When the error is below a given value fixed in advance, the value of circular frequency is changed from ω_i to ω_{i+1}. The process continues as above.

12.8. Bibliography

[CAS 97] CASIMIR J. B., Continuous beam elements – static and dynamic studies of assemblies of planar and non planar beams, PhD Thesis, Conservatoire National des Arts et Métiers, Paris, 1997.

[CAS 03] CASIMIR J. B., VINH T., DUFORET C., "Dynamic behaviour of structures in large frequency range by continuous element methods", *Journal of Sound and Vibration*, vol. 267, p. 1085-1106, 2003.

[CAS 05] CASIMIR J. B., KEVORKIAN S., VINH T., "The dynamic stiffness matrix of two dimensional elements – Application to Kirchhoff's plate continuous elements", *Journal of Sound and Vibration*, vol. 287, p. 571-589, 2005.

[DUF 85] DUFORET C., "Dynamic study of an assembling of rods in medium and higher frequency range – Computer Code ETAPE", *Third Colloquium on new Trends in Structure Calculations, Bastia, Corsica, Proceedings,* p. 229-246, 1985.

[KUL 89] KULLA P. H., "Continuous elements, some practical examples", *ESTEC Workshop, Proceedings: Modal Representation of Flexible Structures by Continuum Methods*, 1989.

[LEU 93] LEUNG A. Y. T., *Dynamic Stiffness and Substructures*, Springer, London, 1993.

[LUN 83] LUNDEN R., AKESSON B., "Damped second order Rayleigh, Timoshenko beam vibration in space – an exact complex dynamic member stiffness matrix", *International Journal for Numerical Methods in Engineering*, vol. 19, p431-449, 1983.

12.9. Appendices

Appendix 12.A. Wavenumbers β_1, β_2 deduced from Timoshenko's equation

Timoshenko's equation [6.38] is presented in Chapter 6.

Here, the expressions of wavenumbers are presented in two frequency intervals $]0, \omega_c]$ and $[\omega_c, \infty[$ separated by critical circular frequency ω_c.

@Seismicisolation

With the second member set to zero in equation [6.38], the initial Timoshenko's equation is:

$$\rho S\frac{\partial^2 w}{\partial t^2}+E_{zz}I_z\frac{\partial^4 w}{\partial x^4}+\frac{\rho^2 I}{kG_{xz}}\frac{\partial^4 w}{\partial t^4}-\left(\rho I+\frac{\rho I_z E_{zz}}{kG_{xz}}\right)\frac{\partial^4 w}{\partial t^2\partial x^2}=0 \qquad [6.38]$$

Under stationary vibration regime, the displacement is:

$$w(x,t)=\exp(j\omega t)\exp\frac{\beta z}{L} \qquad [12.A.1]$$

Bringing [12.A.1] into [6.38] and dividing all the terms by $E_{zz}I_z$, we get:

$$-\frac{\rho S}{EI}\omega^2+\frac{\beta^4}{L^4}+\frac{\rho^2}{kGE}\omega^4+\left(\frac{\rho}{E}+\frac{\rho}{kG}\right)\omega^2\frac{\beta^2}{L^2}=0 \qquad [12.A.2]$$

and rearranging in decreasing power of $\frac{\beta}{L}$:

$$\left(\frac{\beta^4}{L^4}\right)+\left(\frac{\rho}{E}+\frac{\rho}{kG}\right)\omega^2\left(\frac{\beta^2}{L^2}\right)+\left(\frac{\rho^2}{kGE}-\frac{\rho S}{EI}\omega^2\right)=0 \qquad [12.A.3]$$

For convenience when writing the equation, the subscripts for E_{zz} and G_{xz} have been dropped.

The roots of the bisquared equation in $\frac{\beta}{L}$ in [12.A.3] are:

$$\frac{\beta^2}{L^2}=\omega^2\left[-\frac{1}{2}\left(\frac{\rho}{E}+\frac{\rho}{Gk}\right)\pm\frac{\rho}{2E}\sqrt{\left(1+\frac{E}{Gk}\right)^2-4\left(\frac{E}{kG}-\frac{SE}{\rho I\omega^2}\right)}\right] \qquad [12.A.4]$$

The expression under the square root sign can be simplified as:

@Seismicisolation

$$\left(1+\frac{E}{Gk}\right)^2-4\left(\frac{E}{kG}-\frac{SE}{\rho I\omega^2}\right)=\left(1-\frac{E}{Gk}\right)^2+4\frac{SE}{\rho I\omega^2} \qquad [12.A.5]$$

then:

$$\frac{\beta^2}{L^2}=\omega^2\left[-\frac{1}{2}\left(\frac{\rho}{E}+\frac{\rho}{Gk}\right)\pm\frac{\rho}{2E}\sqrt{\left(1-\frac{E}{Gk}\right)^2+4\frac{SE}{\rho I\omega^2}}\right] \qquad [12.A.6]$$

Examining equation [12.A.3], we notice that the sum of roots β_1^* and β_2^* is:

$$\beta_1^2+\beta_2^2=-\left(\frac{\rho}{E}+\frac{\rho}{Gk}\right)<0 \qquad [12.A.7]$$

which means that the couple of wavenumbers ±j β_2 are such that:

$$|\beta_2^2|>|\beta_1^2| \qquad [12.A.8]$$

The product of roots $\beta_1^2\beta_2^2$ in (12.A.3) is positive if:

$$\frac{\rho^2\omega^4}{kGE}-\frac{\rho S}{EI}\omega^2>0$$

or

$$\frac{I\rho\omega^2}{SkG}-1>0 \qquad [12.A.9]$$

which is equation [12.54]:

$$\delta_\omega=\frac{I\rho\omega^2}{kSG}-1>0 \qquad [12.54]$$

@Seismicisolation

in the case where $\delta_\omega > 0$:

$$\omega > \omega_c = \frac{kGS}{\rho I}$$

The product of the square of a wave number is positive, which means that the two sets of wave numbers are negative and all the wave numbers are purely imaginary:

$$(\mathrm{j}\,\beta_1, -\mathrm{j}\,\beta_1), (\mathrm{j}\,\beta_2, -\mathrm{j}\,\beta_2).$$

@Seismicisolation

List of Authors

Mostefa ARCHI
University of SAAD DAHLAB
Department of Mechanics
Blida
Algeria

Tibi BEDA
École Nationale Supérieure
Polytechnique,
Department of Industrial and
Mechanical Engineering
University of Yaoundé
Cameroon

Jean-Baptiste CASIMIR
Laboratory of Mechanical
Engineering Systems and Materials
(LISMMA)
ISMEP-SUPMECA
France

Yvon CHEVALIER
Laboratory of Mechanical
Engineering Systems and Materials
(LISMMA)
ISMEP-SUPMECA
France

Christine ESTEOULE
ISMCM Engineer
Renault Industry
France

Patrick GARCEAU
ISMCM
SNECMA
Hydrogen and Combustible
Pile DPGL
France

Dominique LE NIZHERY
Laboratory of Mechanical
Engineering Systems and Materials
(LISMMA)
ISMEP-SUPMECA
France

Michel NUGUES
CNAM
ISMEP
Laboratory of Vibroacoustics
France

James ONOBIONO
Consultant
Cameroon

Mechanics of Viscoelastic Materials and Wave Dispersion Edited by Yvon Chevalier and Jean Tuong Vinh
© 2010 ISTE Ltd. Published 2010 by ISTE Ltd.

@Seismicisolation

Mohamed SOULA
Materials Engineering Research Unit
Department of Mechanical Engineering
École Nationale d'Ingénieurs de Tunis
(ENIT)
Tunisia

Maurice TOURATIER
Modeling and Mechanics Laboratory
ENSAM Paris
France

Jean Tuong VINH
Laboratory of Mechanical
Engineering Systems and Materials
(LISMMA)
ISMEP-SUPMECA
France

@Seismicisolation

Index

A

Abarcar-Cunniff formulae, 250
Ageing material, 62-63
Anisotropic dispersion curves, 223, 225, 287
Application domain, complex moduli, 557
Approximate equations, 145, 160
Asymptotic behavior, 132, 137
  bending wave, 292
  curves, 121
  value, 292, 335-337
Axes
  reference, 10-12, 27, 28, 37, 50
  change of, 15, 326-327

B

Barr's equation, 177, 178, 189, 197, 214, 257
Barr's theory, 178, 219, 221, 225
  viscoelastic moduli, 581
Basic cells, 88, 89, 92, 93, 98
Beam
  free-free, 607-611
  Timoshenko's, 602-605, 614, 616
Beating period (pendulums), 426-427, 431-436, 440-443, 451, 456, 457
Bending
  inertia force, 294
  moment, 293-295, 302, 304, 308, 314, 315, 327, 329
  rotational inertia, 292, 299, 303 311, 312, 334
  shear force, 292-308, 327, 330-304, 308, 327, 330
  Timishenko's motion, 292, 293, 309-312, 324, 325, 328
  transverse effects, 306, 311, 312
Bending motion equation,
  double pendulum, 301, 313-314
  pendulum, 429
Bending test, 558, 579
  clamped-free, 295-296, 304
  eigenvalue, 298, 308, 322
Bending wave,
  computer program, 309-310, 323, 325
  importance of, 559
Bernoulli's solution, 591-595
Bernoulli-Euler's
  equation, 558, 559, 564, 575
  theory, solution, 586
Bishop's
  equation, 339, 343-346, 400-402, 405, 407, 581
  theory, 351, 352, 397
Black's chart, 572-574, 578, 579
Bode's plot, 120

Mechanics of Viscoelastic Materials and Wave Dispersion Edited by Yvon Chevalier and Jean Tuong Vinh
© 2010 ISTE Ltd. Published 2010 by ISTE Ltd.

@Seismicisolation

Boundary conditions,
continuous element method, 598, 599, 608-609
equations, 342, 348, 355, 358, 375, 385, 394, 399, 403-407, 416
natural, 342, 385, 401, 403, 404, 406
rod ends, 340, 342, 345, 346, 349, 353, 356, 365, 375, 385, 393, 401, 404, 413
Bromwich-Wagner contour, 130, 139

C

Calculation
of phase velocity, 519, 522, 530, 532, 535-538, 541, 546of s_{35} and υ_{13}, 486, 459
Carson-Laplace transform, 74-78, 86, 89, 98, 130
inverse, 130
Change
of axes, 13, 326, 337
of reference axes, 11, 15, 326, 337
Characteristic equation ring, 499, 503, 505
Christoffel's
equation, 517, 518, 519
tensor, 514, 517-523, 526, 528
Circular section, rod, 62
Clamped-free
bending test, 295, 296, 304
solution, 305, 308, 320
Closed-form
equation of motion, 145, 163
solution, 160, 163
Coefficient
flatness, 221-225, 240-242, 246, 285-287
Poisson's, 447
stiffness, 22, 38, 40, 43-46, 529, 543
Cole-Cole diagram, 79, 80, 84, 95, 97
Comparison
between theories, 221, 225
of torsion theories, 176, 186, 246, 247
Complex
compliance, 79
function, variation, 80
stiffness, 79, 80
Young's modulus, 570-578
Complex moduli, 78, 80, 82, 92, 555-557, 560, 563, 564, 570, 582, 583
application domain, 557
diagonal coefficient, 557
non-diagonal coefficient, 557
shear, 573, 586
Compliance matrix, 8-10, 23-30, 25, 36, 427, 443-448, 458, 489
Composite
reinforced, 43, 51-54
stratified, 44, 45
Computer program
bending, 309, 310, 323, 325
trial and error method, 324
Constraints, holonomic, 146, 149
Continuous element method
boundary conditions, 598, 599, 608-609
dynamic matrix, 607, 612-615, 623
dynamic stiffness, 598, 604-611, 622
eigenvalue, 597, 599, 607-612, 620, 622
interest, 598, 620
numerical simulation, 614
successive calculation steps, 620
transfer matrix, 598, 599, 605-623
Correcting
factor, 369, 409
terms, 163

@Seismicisolation

Correspondence principle, 74-77, 82, 558, 564, 567, 575-576, 593
choice of equation of motion, 559
elastic solution, 559
solution, 558
Coulomb's moduli, 9, 22
Coupled pendulums, 427
Coupling term, 254
Creep
function, 87
test, 60-61
Curves
master, 105, 107, 108, 110, 111
relaxation, 105
rheological, 104, 112, 115

D

D'Alembert's principle, 145-148
Decoupled equation, 303, 313
Degree of approximation, 161, 163
Dimension equations of motion, 162
Dirac distribution, 66-70, 89
Dispersion
equations, 371
wave, 161-164
Dispersion curve, 344, 345, 351, 352, 355, 374, 375
bending tests, 301, 311, 334, 337
estimation, 559, 560
Double pendulum, 425-429, 433-439, 444, 448, 491
formulae, 482-487
method, 425, 444
Dynamic
experimental, 564
matrix, 605, 610-615, 623
response, 564,
stiffness, 598, 606-613, 624
transfer function, 620
transfer matrix, 616-617

E

Eigenvalue,
bending, 298, 308, 322
continuous element method, 597, 599, 607-612, 620, 622
equation, 192, 309,
progressive waves, 514, 518
Eigenvalue equation,
pendulum, 430
ring, 498, 510
torsion wave, 18
Elastic
moduli, 24
solution, 559
Elementary
equations of motion, 556, 561, 565
longitudinal theory, 559
theory, extensional vibration, 609
Energy
kinetic, 35, 53, 55, 77, 91, 151-153, 157, 165
surface, ultrasonic waves, 550
velocity, 530, 548, 551-554
Engström's theory, 176, 178, 179, 189, 207, 208, 215, 219
Equations, 37, 47, 56, 61, 66-69, 78,
boundary conditions, 342, 348, 355, 358, 375, 385, 394, 399, 403-407, 416
Christoffel's, 517-519
closed-form, 145, 163
decoupled, 303, 313
dimension, 163
dispersion, 371
eigenvalue, 298, 309,
elementary, 556, 561, 565
elementary-order, 559, 562
higher-order, 57, 558, 575, 582
Lagrange's, 149-152, 157, 427-428, 434
Love's, 580
off axis rod, 109

@Seismicisolation

practical considerations, 561-562
Rao and Rao 14, 24, 26, 43, 558-563, 583
ring, 494, 498, 500
Saint Venant's, 461
Timoshenko's, 615-616, 624-625
Timoshenko-Mindlin's, 583
torsion, 5, 15, 19, 23-30, 39, 40
validity, 161
viscoelastic solution, 564
Euler-Bernoulli's
bending theory, 614
transfer matrix, 612
Explicit continuous element, 603
Extensional
vibration, 609
wave, 347, 349, 350, 354, 369, 372-375, 377, 409

F

Fabric
reinforced, 46
Fibers
reinforced, 27, 39
Finite element method, 265
Flatness
coefficient, 221-225, 240-242, 246, 285-287
influence, 562-563
ratio, 188, 198, 200, 217
Forces, generalized, 151-156
Formula
Johnson's, 452-458, 461-469
Mindlin's, 180
Newton-Raphson's, 590
torsion stiffness, 186, 193, 207, 249
Fractional derivatives, 89, 98, 100, 115, 116, 124, 125, 129-136
Free-free beam/rod, 607-611
Frequency, 103
curve, 103, 104, 107, 109, 110, 117, 119, 121, 122, 134, 137
response curve, 119, 137
Functions,
polynomial, 116, 89, 90
relaxation, 62, 70-74, 87- 91, 95, 98, 104-107, 118, 121, 123, 131, 137, 140, 143
transmissibility, 561-572, 576, 586, 590-596
waterfall, 95

G

Generalized coordinates, 146-151, 167-168
Generalized forces, 151-156
ultrasonic waves, 546
Group velocity, 223, 279-283, 286-288
ultrasonic wave, 545-548, 553-554

H

Hamilton's
formula, 164
principle, 345, 361, 401, 403, 146, 157-159, 165-167
Harmonic regime, 83
Higher elastodynamic modes, 177, 208, 212, 242
Higher-order
approximation equations, 560
equations, 555-558, 582
Highest eigenfrequency,
pendulum, 456-457
Holonomic constraints, 146, 149
Hypergeometric series, 124, 130-142

I

Inequalities between elastic moduli, 24

@Seismicisolation

Inertia
bending force, 294
effects, 565, 573-575, 580-584,
moment, 299, 312, 327
rotational, 292, 299, 303, 312, 334
Inflexion point, 108, 119, 121, 123, 127
Influence, of flatness, 562-563
Inverse
Carson-Laplace transform, 130
Laplace transform, 121, 130, 132
problem, 162-163, 559-561, 583, 587, 597
oscillatory solution, 561
Inversion method, 121, 125, 133
Isotropic materials, 26

J

Johnson's
formulae, 461-469
static torsion, 246, 248
torsion stiffness, 452-458

K

Kinetic energy, 151-153, 157, 165, 209, 227, 230, 251, 265
formulation, 165, 168, 170

L

Lagrange's equation, 149, 152, 157, 427-428, 434
Laplace transform
inverse, 121, 130, 132
Linear viscoelastic behavior, 57, 59, 61, 62, 66, 67, 74, 80, 86-101
Loading, viscoelastic, 57, 59, 60, 71, 74
Long time response, 132, 143
Longitudinal wave,
elementary theory, 559
transmissibility, 565
Love's
equation, 580
extensional rod, 611

M

Master curve, 105, 107, 108, 110, 111
Materials
composite, 10
isotropic, 26
quasi-transverse isotropic, 10, 19-26
reinforced artificial, 20, 46
transverse isotropic, 21, 26
Matricial notations, 524
Matrix
compliance, 8-10, 23-30, 35, 36, 427, 443-448, 458, 489
dynamic, 605, 610-615, 623
dynamic transfer, 616-617
equation of torsion motion, 233
passage, 16
stiffness, 6, 10, 17, 18, 22, 24, 26, 29, 33, 36, 37, 42, 46
transfer, 598, 599, 605-620, 623
Method
finite element, 91
inversion, 121, 125, 133
Newton-Raphson's, 568-569, 590, 597
optimization, 528, 555
Rayleigh-Ritz, 461, 472, 481
trial and error method, 324
Williams-Landel-Ferry's, 104, 108, 109, 112, 136
Mindlin's formula, 180
Minimizing quadratic errors, 121, 128
Moduli
Coulomb's, 9, 22
shear, 8, 9, 22, 28, 40
Timishenko's, 558, 564

@Seismicisolation

Young's 291, 294, 298, 305, 309, 310, 324-327, 427, 433, 436, 440-444, 450, 477, 577-578,

N

Natural boundary conditions, 342, 385, 401, 403, 404, 406
Newton-Raphson's
formulae, 590
method, 568-569, 590, 597
Non-circular section rod, 339
Non-privileged propagation direction, 525
Non-trivial solutions, 297, 308, 321
Notations, matricial, 524
Nugue's theory, 242
viscoelastic moduli, 582
Numerical simulation, 614

O

Off-axis rod, 176, 177, 240, 247
equations of motion, 283
pendulums, 427, 443-447, 460, 482-484, 492
Onobiono's solution, 175, 208, 210, 212, 215, 219, 221, 242, 243, 265, 267
functional, 178, 179
Optimization
method, 555
of stiffness coefficient, 529, 543
of wave propagation, 528
Oscillatory solution, 561

P

Passage matrix, 16
Pendulums, 427, 443-460, 482, 484, 492
double pendulum, formulae, 482-487
double pendulum method, 425, 444
motion, 434, 448
off-axis rod, 427, 443-447, 460, 482-484, 492
Poisson's coefficient, 447
Saint Venant's equation, 461
Phase velocity, 190, 199, 207, 217, 223, 225, 342, 344, 345, 351, 352, 365, 368, 371, 372, 397, 400, 409, 410, 413
calculations, 519-538, 541, 546
Plane surface, 530, 533
Poisson's coefficient, 447
pendulums, 460
Poles and zeros, 116, 118, 120-123, 130, 134
Polynomial
functions, 89, 90, 116
quotients of, 115
Potential energy, 208, 229, 230, 251, 265
Poynting-Thompson model, 96-97
Practical considerations, 561-562
Principle
Hamilton, 345, 361, 401, 403, 146, 157-159, 165-167
of correspondence, 74-77, 82, 558-564, 567, 575-576, 593
Williams-Landel-Ferry, 558-567, 570-574, 577-580, 584
Privileged propagation direction, 519
Problem, inverse, 162, 163, 559-561, 583, 587, 597
Progressive extensional wave, 344, 347
Propagation, ultrasonic waves, 520, 525

@Seismicisolation

Q

Quadratic errors, minimizing, 121, 128
Quasi-transverse isotropic materials, 10, 19-26
Quotients of polynomials, 115

R

Rao and Rao's motion equation, 347-349
ratio
  E_{ij}/G_{ij}, 558-563, 583
  flatness ratio, 188, 198, 200, 217
Rayleigh-Ritz method, 461, 472, 481
Reference
  axes, 10-12, 27-28, 37, 50
  change of, 15, 326-337
Reinforced
  artificial materials, 20, 46
  composite, 43, 51-54
  fabric, 46
  fibers, 27, 39
Reissner formulation torsional vibration, 197, 208, 242, 243, 251
Relaxation
  curve, 105
  function, 62, 70-74, 87-91, 95, 98, 104-107, 118, 121, 123, 131, 137, 140, 143
  test, 60-63, 69
  time function, 116
Rheological curves, 104, 105, 110
Ring
  characteristic equation, 499, 503, 505
  eigenvalue equation, 498, 510
  Young's modulus, 496, 497, 501
Rod
  boundary conditions 340, 342, 345, 346, 349, 353, 356, 365, 375, 385, 393, 401, 404, 413
  circular section, 62, 400
  Love's extension, 611
  non-circular section, 339
Rotational inertia, bending, 292, 299, 303, 311, 312, 334

S

Saint Venant's
  equation, 461
  method, 461
  theory, off-axis rod, 482
  theory, torsion, 176, 178, 194, 197, 199, 206, 207, 223, 225, 241, 264
Satin, 46
Series
  expansion, 104, 130, 132, 137, 411, 578
  hypergeometric, 124, 130-142
Shear
  effects, 580
  bending, 306, 311-312
  bending force, 292-308, 327-330
  force, 576
  moduli, 8-9, 22, 28, 40
  properties, 160-161
Slowness surface, 528-530, 534, 553-554
Solution,
  Onobiono's, 175, 208, 210, 212, 215, 219, 221, 242, 243, 265, 267
  Timoshenko-Mindlin's, 583
  viscoelastic problem, 558, 564
State vector, 600-605, 609, 620, 623
Static torsion (Johnson), 72, 74
Stiffness
  coefficients, 22, 38, 40, 43-46
    optimization of, 529, 543
  matrix, 6, 10, 17, 18, 22, 24, 26, 29, 33, 36, 37, 42, 46
  tuft, 50
Stiffness
Stratified composite, 44, 45

@Seismicisolation

Stress components, 5, 340, 357
Successive calculation steps, 620

T

Taffeta, 20, 46-48
Temperature change, 104-105, 110
Tensor, Christoffel's, 514, 517-523, 526, 528
Tensorial notation, 521-524
Test,
  creep 60-61
  relaxation, 60-63, 69
Theory
  Euler-Bernoulli's, 612-614
  Engström's, 176, 178, 179, 189, 207, 208, 215, 219
  elementary, 559
  Nugue's 242, 582
Time
  delay, 59
  function, series expansion, 114
Timoshenko's
  beam, 602-605, 614-616
  bending motion, 292-293, 309-312, 324-328
  equation, 615-616, 624-625
  Young's modulus, 558, 564
Timoshenko-Mindlin's equation, solutions, 583
Torsion,
  dispersion, 41
  importance, 559
  St Venant's theory, 176, 178, 194, 197, 199, 206, 207, 223, 225, 241, 264
  stiffness, 186, 193, 207, 249
    test, correcting coefficient, 175, 199, 207
  wave, 191, 215, 220-225, 240, 245, 279, 280, 285, 287-289
Torsional
  motion, 434, 448
  pendulums, 435, 443-450, 478, 482, 484, 487
  stiffness, 13
  vibration (Reissner formulation), 176
Touratier's
  equation, 340, 350, 354, 408
  theory, 393, 395
Transfer function, 117
  dynamic, 618
Transfer matrix, 598-599, 605-623
Transmissibility
  function, 561, 564-572, 576, 586, 590-596
  longitudinal function, 589
  viscoelastic, 565
Transverse
  isotropic materials, 21, 26
  shear effects, 306, 311, 312
Trial and error method, 324
Tuft stiffness, 50

U

Ultrasonic immersion bench, 533
Ultrasonic waves,
  eigenvalues, 514, 518
  energy surface, 550
  energy velocity, 530, 548, 551-554
  non-privileged propagation direction, 525
  propagation of, 530, 533
  privileged propagation, 519
  slowness surface, 528-530, 534, 553, 554

V

Validity of equations of motion, 161
Variation of complex function, 80
Vector, state, 598-607, 620-623

@Seismicisolation

Velocity
group, 223, 279-283, 286-288
phase, 190, 199, 207, 217, 223, 225, 342, 344, 345, 351, 352, 365, 368, 371, 372, 397, 400, 409, 410, 413
ultrasonic wave, 525, 542
wave, 519
Vibration, torsional, 176
Viscoelastic
behavior, 57-67, 74, 80, 86-91, 95-101
loading, 57-60, 71, 74
solution, equation of motions, 564
transmissibility, 565

W

Waterfall
function, 95
modeling, 92, 96
Wave
dispersion, 161-164
extensional, 347, 349, 350, 354, 369, 372-375, 377, 409
progressive extensional, 344, 347
propagation, ultrasonic, 520, 525
torsion, 17, 41-51, 66, 71, 105-114
velocity, ultrasonic, 525, 542
Williams-Landel-Ferry's
composite materials, 112
formulation, 105
method, 104, 108-109, 112, 136
principle, 161

Y

Young's modulus,
bending, 291-298, 305, 309-310, 324-327
complex, 570-578
double pendulum, 427,
pendulums, 433, 436, 440-444, 450, 477
ring, 496, 497, 501
Timishenko's modulus, 558, 564

Z

Zener modeling, 93, 97

@Seismicisolation